STUDIES OF RUTHENIUM AND OSMIUM CARBONYL CLUSTERS WITH UNSATURATED CYCLIC HYDROCARBONS

by

Caroline M. Martin

A thesis presented for the Degree of Doctor of Philosophy
The University of Edinburgh
1995

Declaration

The research described herein was conducted by the author at The Department of Chemistry, The University of Edinburgh, between the dates of October 1991 and July 1994. It is the author's original work unless specific reference is made to the contrary. None of the work described herein has been submitted for a degree at any other institution.

Caroline M. Martin

Acknowledgements

Spending three years in the Chemistry Department at Edinburgh having a lot of fun and playing with some interesting chemistry leaves a lot of scope for saying thank-you. Although in the interest of brevity this list of acknowledgements is short, between the lines lie the names of everyone I have known and worked with, who have contributed into making my time at Edinburgh so memorable and rewarding.

First and foremost, my most sincere gratitude goes to my supervisor, Prof. Brian Johnson, for his constant advice and encouragement, and for his enthusiastic approach towards chemistry....I hope some of it has rubbed off! I would also like to thank my industrial supervisor, Dr. David Parker, for all the interest he has shown in my work and for making my trips to ICI (Wilton) so enjoyable.

During my research I have been privileged to call upon the expertise of many skilled crystallographers, who seemed to be capable of obtaining a structure from almost any material I gave them. In this respect, my thanks go to Drs. Sandy Blake and Scott Ingham at Edinburgh, as well as to Prof. Dario Braga and Dr. Fabrizia Grepioni and their group in Bologna, who are also acknowledged for their warm hospitality during my lengthy trips to Italy. I am also very grateful to Dr. David Reed for not only running the intricate NMR studies described in this thesis, but also for taking the trouble to explain them to me, and to all the technical support staff at Edinburgh, in particular Janet Heyes.

The members of the 'Johnson' group must not be forgotten from this list of thank-yous, especially those who made life in Lab 86 so much fun, namely; Anke, Dave, Doug, Jack and Ruth. In particular, a special thank-you is due to Dr. Paul Dyson for his excellent proof reading of this thesis, and also for all his help, patience and support; particularly in recent months during the preparation of this manuscript.

I would like to take this opportunity to thank Dr. Brian Piggott for not only introducing me to the delights of organometallic chemistry, but also for encouraging me to pursue a Ph.D., and for his continued interest in my progress. Finally, my parents can never be thanked enough for all the love and support that they have provided during the three years of my Ph.D., and in the twenty-two years leading up to it.

To my parents
and of course to Paul

Table of Contents

Chapter 3: Reactions of $Ru_3(CO)_{12}$ with Cyclic C_6 Alkenes

Chapter 4: [2.2]Paracyclophane Clusters of Ruthenium

Chapter 5: The Reactivity of Some [2.2]Paracyclophane Clusters of Ruthenium

Glossary of Abbreviations

PSEPT	polyhedral skeletal electron pair theory
EAN	effective atomic number
HOMO	highest occupied molecular orbital
LUMO	lowest unoccupied molecular orbital
AO	atomic orbital
MO	molecular orbital

IR	infrared
v	very
w	weak
m	medium
s	strong
br	broad
sh	shoulder

MS	mass spectroscopy
FAB	fast atom bombardment
EI	electron impact
amu	atomic mass units

NMR	nuclear magnetic resonance
s	singlet
d	doublet
t	triplet
q	quartet
m	multiplet
δ	chemical shift
ppm	parts per million
J	coupling constant

UV	ultraviolet
esd	estimated standard deviation
RT	room temperature
t.l.c.	thin layer chromatography

Et	ethyl
Me	methyl
Ph	phenyl
thf	tetrahydrofuran
DBU	1,8-diazabicyclo[5.4.0]undeca-7-ene

Numbering of Compounds

Chapter One

The Surface-Cluster Analogy

This chapter outlines the role of organometallic transition metal clusters as models for chemisorption in surface chemistry. The factors which govern the applicability of the so-called 'surface-cluster analogy' are examined, and structural comparisons between organic species chemisorbed on the metal surface and similar ligands bound to metal clusters are used to develop these ideas. In an extension of the analogy beyond structure and bonding, a number of examples are presented which imply that the reactivities of certain organic molecules are also similar in both the surface and cluster regimes. Particular reference is made to chemisorbed carbon monoxide and benzene, since these molecules are of most relevance to subsequent chapters. Finally, the synthetic procedures used in the preparation of some of these model arene carbonyl clusters are discussed.

1.1   An Introduction

The middle transition metals exhibit a propensity to agglomerate into clusters when in low oxidation states and in combination with π-acid ligands, especially carbon monoxide. The study of such compounds has been evolving for the past thirty years, and our knowledge and understanding of these systems is now well established. A vast number of clusters have been prepared over the years, containing a wide range of metal polyhedra. Cluster chemistry, however, has long since passed the point where only new metal geometries are of primary importance, and recently a number of specific areas have emerged within this field; one prominent example being the interaction of metal clusters with small organic molecules. The need to understand the role of both homogeneous and heterogeneous catalysts used in a variety of industrial chemical processes has stimulated research into this area of cluster chemistry since analogies may be drawn between organic species chemisorbed on the metal surface and similar ligands coordinated to metal clusters.

The study of the interactions between organic molecules and transition metal clusters has enhanced our understanding of the chemistry involved in processes such as hydrogenation, dehydrogenation, isomerisation, polymerisation, fragmentation and re-formation, which are very important to the chemical industry. These studies involve the synthesis and full chemical and structural characterisation of a wide and diverse range of cluster complexes bearing organic ligands, and also an investigation into the chemical and dynamical behaviour that such ligands display when attached to the cluster unit. The chemistry of numerous organic compounds has been investigated in this manner, and the

research described herein describes that of some unsaturated cyclic hydrocarbons, namely cyclohexene, cyclohexa-1,3-diene, benzene and other, more complex, arenes.

1.2   Concepts of the Surface-Cluster Analogy

In 1975 Muetterties proposed that discrete, molecular transition metal clusters may serve as reasonable models of the metal surface in the processes of chemisorption and catalysis, and speculated that cluster complexes would be found to act as catalysts with novel properties.[1] Heterogeneous catalysis forms the basis of many industrial chemical processes, yet the actual surface chemistry occurring at the molecular level is a long way from being fully understood.[2] Therefore the idea of modelling such processes using molecular systems in which the chemical reactions are more easily followed appeared an attractive hypothesis.

The main arguments behind this proposal stem from the fact that metal clusters have reactivities which differ from those of mononuclear complexes and, in some cases, approach those of the surface.[3] One of the most important differences between clusters and mononuclear complexes is in the spatial arrangement of the available coordination sites. For example, adjacent coordination sites in an octahedral mononuclear metal complex will always be perpendicular to one another, and although the same arrangement of sites can be found on a single metal atom in a cluster complex, there is an alternative parallel array formed by the combination of sites on adjacent metal atoms. It is this latter arrangement of sites that distinguishes the cluster from the mononuclear complex, and at the same time presents similarities to those found on the metal surface.[2] The parallel arrangements of sites on neighbouring metal centres in clusters can lead to ligand activation by mechanisms that are markedly different from those occurring at single metal sites, and may be comparable to those taking place on the metal surface.

A few years after his original proposition, Muetterties published a detailed quantitative assessment of the analogy between metal clusters and metal surfaces with respect to the chemisorption process.[4] This article suggested that certain critical factors should be taken into account when making such a comparison. These factors include size, coordination number, structure and stereochemistry, thermodynamics and ligand mobility, and a brief description of each follows.

1.2.1 Size

If the largest of the discrete molecular clusters are only submicroscopic fragments of a metal surface, then does it seem possible that small clusters, *i.e.* those with nuclearities between three and ten, may act as models of the metallic surface? A hypothetical metal cluster must be huge, probably hundreds of metal atoms, for it to truly possess the properties of a metal.

Calculations, based on extended Hückel molecular orbital theory, indicate that clusters should start to become metal-like at nuclearities ranging from between twenty-five and fifty (depending on the metal), therefore illustrating that small clusters are far from metal-like in their properties.[5] However, the supposed surface-cluster model is not based on this type of comparison but rather on a comparison between a discrete molecular cluster with a polyhedral metal core and a periphery of ligands and a metal surface with a similar set of chemisorbed ligands.[4] This suggests that there is no fundamental difference between the valence electron properties of the metal-ligand bond in the two regimes, therefore allowing a 'surface molecule' concept to be employed which assumes that adsorbed molecules interact strongly with only a limited number of surface metal atoms. It appears that a minimum of three to four metal atoms are required to describe the cluster-like surface chemical bond, as not only the metal atoms on the surface provide bonding but also the metal atoms in the second layer under the surface appear to be important in the formation of the surface cluster bond.[6]

1.2.2 Coordination Number

Metal-metal coordination numbers are uniformly higher for surface atoms in the bulk metal than for surface atoms in clusters. For example, the surface metal atoms in a close-packed array have a maximum metal atom coordination number of nine, which may be reduced to seven and six at certain surface sites such as steps and kinks. In comparison, the connectivity between metal atoms in clusters is relatively low; two in triangular, three in tetrahedra, four in octahedra, five in some of the larger polyhedra such as $[Rh_{13}(CO)_{24}H_3]^{2-}$,[7] and a maximum of seven in clusters like $[Rh_{14}(CO)_{25}]^{4-}$ and $[Rh_{15}(CO)_{27}]^{3-}$.[8,9] In contrast, the metal-ligand connectivity is frequently larger in cluster compounds where coordination numbers of three to five are commonly found, whereas for surface metal atoms the connectivities are small; one or less on average. The number of metal-ligand connections in clusters is dependent on both the metal and the cluster size, and only for the late transition metals are the electronic demands satisfied by low ligand-to-metal ratios; the cluster $[Pt_{19}(CO)_{12}]^{4-}$ representing a rare example where this ratio is less than one.[10] These differences in connectivities between the two regimes represent a breakdown in the analogy for small clusters (*i.e.* those with nuclearities between three and ten), but not for some of the larger ones. However, it is difficult to assess whether these variances are likely to cause a significant effect on the structural features or the binding energies of the ligand on the metal cluster and on the metal surface.

1.2.3 Structure

The single crystal metallic surface is generally regarded as an approximately close-packed, planar array of spherical atoms extending infinitely in a two dimensional lattice, and it is

from this geometrical viewpoint that clusters and the surface bear the closest similarities.[4] However, one consequence of this long range periodicity is that local atomic and electronic structure will be influenced by more distant atoms in both the surface and, if the close-packed lattice is extended into a three-dimensional network, the bulk of the metal.[11] Since small clusters contain only surface atoms, any analogy made between cluster species and the bulk metallic interface must be done so with caution. Modelling adsorption processes *via* small clusters invokes a greater degree of localisation of the substrate-metal interaction than a metal surface, and this constraint must also be taken into account when making comparisons between the two regimes.

Surface crystallography may range from the almost atomically flat, high density planes associated with low Miller indices, to the irregular arrangements characterised by highly defined rows, ridges, steps and kinks which require complex Miller indices for their exact depiction.[12] In comparison, the metal skeletons of high nuclearity carbonyl clusters are often structurally comparable to fragments of the bulk metallic lattice; for example, $[Rh_{13}(CO)_{24}H_3]^{2-}$,[7] $[Os_{10}C(CO)_{24}]^{2-}$,[13] and $[Rh_{14}(CO)_{25}]^{4-}$,[8] may be recognised as fragments of hexagonal close-packed (h.c.p.), cubic close-packed (c.c.p.), and body-centred cubic (b.c.c.) structures, respectively (see Figure 1.2.3). The series of osmium clusters based on four, ten, twenty and thirty-five metal atoms, $Os_4(\mu-H)_4(CO)_{12}$, $[Os_{10}C(CO)_{24}]^{2-}$, $[Os_{20}(CO)_{40}]^{2-}$, and $[Os_{35}(CO)_{56}]^{2-}$ follow the cubic close-packing growth sequence precisely, and it is significant that, in the dianion $[Os_{10}C(CO)_{24}]^{2-}$, the faces of the cluster correspond directly to the metal (111) surface. The cluster units observed in the smaller carbonyl clusters are typically deltahedra and their metal core configurations may, in general, be regarded as microscopic fragments of a typical close-

(a) $[Rh_{13}(CO)_{24}H_3]^{2-}$ (b) $[Os_{10}C(CO)_{24}]^{2-}$ (c) $[Rh_{14}(CO)_{25}]^{4-}$

h.c.p.   c.c.p.   b.c.c.
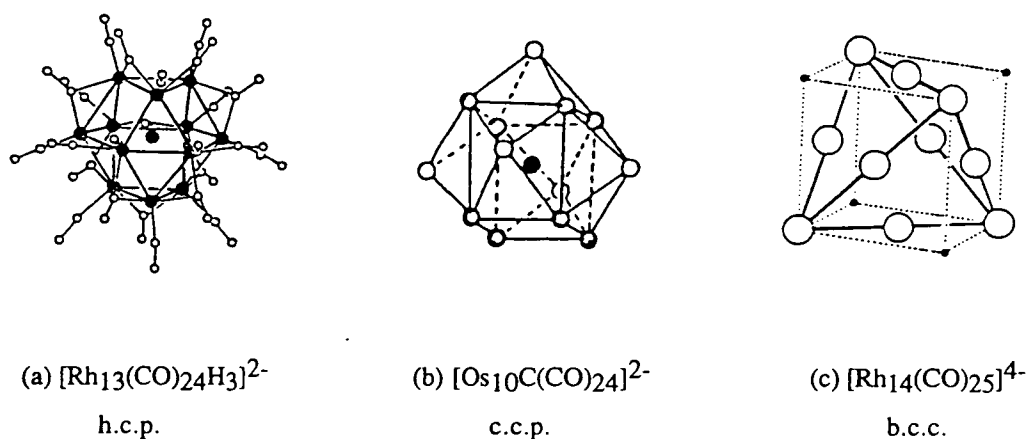
Figure 1.2.3: Relationship between the metal cores of certain high nuclearity clusters and fragments of close packing arrays.

packed lattice. The role of the ligand sphere in stabilising these bulk-like geometries should be appreciated, as should the ease in which they undergo geometrical transformation so as to modify their overall electron count *e.g.* monocapped trigonal bipyramid in $Os_6(CO)_{18}$ (84e) to octahedral in $[Os_6(CO)_{18}]^{2-}$ (86e).[14]

It would appear that structural comparisons between the chemisorbed state and ligated metal clusters are best made when there is correspondence in the metal, the ligands, and the ligand coverage.[4] The problem as to whether a flat or nearly flat surface can be modelled by a spherical or nearly spherical cluster with triangular (or a mixture of triangular and square) faces must be emphasised. This disjointed crystallographic feature will always remain between the two regimes, but experimental surface study techniques may reduce this gap. If cluster crystallography is compared to that of chemisorbed molecules on high Miller index planes, where not only is the metal-metal coordination number for surface atoms dramatically less than on low Miller index planes where there is close packing, but also where irregular features, namely steps and kinks, may develop, then the difference between the two regimes is reduced. However, as the surface becomes more complex, the characterisation techniques become less reliable, making definitive structural analysis of the chemisorbed state less precise.[4]

Perhaps the most important feature regarding the structure and stereochemistry in clusters is that many ligands exhibit multicentre metal atom interactions. In mononuclear complexes most of these ligands are unidentate with two-centre, two-electron bonds, and therefore if the structure and bonding of such simplistic ligands is altered so dramatically on passing from mononuclear transition metal chemistry to the cluster regime, then one may reasonably expect similar multicentre interactions on the metallic surface. This is precisely the behaviour that has been observed for the chemisorbed species, and there are many organic groups whose surface bonding can be viewed as being identical to that of organometallic clusters.[15] The spectroscopic properties of the organic moiety in the two regimes are also frequently comparable, and these features will be illustrated with relevant examples in due course.

1.2.4 Thermodynamics

Thermochemical data for metal-metal interactions in clusters and metal surfaces are not easily accessible by experiment. Calorimetric data for the bond energies in the two regimes are frequently in close agreement,[16,17] yet associated uncertainties, such as the assumption that surface metal-metal bond energies are equal to those calculated in the bulk, make meaningful quantitative comparisons impossible.[4,18] These metal-metal bond energies are, however, low when compared to the metal-ligand bond energies of the two systems; a feature which accounts for the general structural instability of cluster frameworks (the underlying bulk of a metal crystal generally acts as a rigid template thus conferring stability

on the surface atoms).[4] The metal-ligand bond energies in the two regimes are far more easily probed, and the values obtained are much more reliable. For example, with respect to the carbonyl ligand, energies are typically 30-50% smaller for the chemisorbed state, but increase as the crystallography is varied from densely packed to more open planes, *i.e.* as the metal connectivity approaches that of the cluster regime.[19]

1.2.5 Ligand Mobility

Studies of metal clusters and surfaces have demonstrated, on many occasions, that the ligands and chemisorbed molecules are not stationary.[4,19] Two possible mechanisms have been invoked to explain these non-stationary states. Firstly, a dissociation process in which all the bonds between the cluster framework and ligand, or metal surface and chemisorbed species are broken, or alternatively, a non-dissociative process in which the molecule migrates about the periphery of the cluster or surface. Fluxionality in clusters is a well established phenomenon with both the ligand and metal shells capable of undergoing motion.[14] Migration of an organic moiety on a metal surface is also well established and is undoubtedly of considerable importance with respect to catalysis. Ligand fluxionality in metal clusters falls within the NMR timescale, whilst mobility on the metal surface may be detected by field emission microscopy. Ligand mobility on metal surfaces that have less than monolayer coverage cannot be simulated in metal clusters because virtually all known clusters are coordinatively saturated, therefore making a localised and nonconcerted ligand migration between two metal atoms in the cluster unfavourable. At full monolayer coverage, ligand migration rates decrease markedly since a concerted motion of ligands is required, however, this idealised limit for metal surfaces is then more closely analogous to the typically saturated metal cluster.[4]

The general conclusion to be drawn from this assessment of the surface-cluster analogy is that discrete molecular metal clusters appear to have a valid contribution to make as models of the chemisorbed state in terms of structure and bonding.[1,4,10,20-25] In many cases the interactions of surface fragments are strikingly similar to those of hydrocarbon ligands in multinuclear organometallic clusters, and chemisorption can often be described as being localised, *i.e.* through a 'cluster-like' bonding of the substrate to the surface.[6,15,26] A wide range of ligands have been identified on metal surfaces and for virtually every organic surface species observed thus far there is a cluster equivalent that has been synthesised by the organometallic chemist.[26] The ability to classify these coordination modes precisely within the cluster, and to determine their spectroscopic properties has proven to be a most valuable tool in the characterisation of the chemisorbed state.

The anticipated use of metal clusters as catalysts, however, has not emerged,[27] and the few known examples are neither well understood nor of practical commercial

importance. Since this innovative report in 1979, a general consensus has arisen that the surface-cluster analogy, although imperfect, is valid in terms of structure and bonding, but is limited when extended to reactivity and catalysis.[28]

1.2.6 Structural Characterisation of the Chemisorbed State

Structural characterisation of the chemisorbed state represents a formidable challenge since the physical techniques of X-ray diffraction and NMR spectroscopy, used routinely by molecular chemists to define the essential stereochemical features of a molecule, are not generally applicable to highly ordered surfaces.[2] Even widely employed techniques such as IR or Raman spectroscopy must be exercised with caution. A wide range of ultra-high vacuum, surface analysis techniques have been developed which have helped in these characterisations.[6,29] For example, low energy electron diffraction (LEED), angle-resolved UV photoelectron spectroscopy (ARUPS), high resolution electron energy loss spectroscopy (HREELS) and Auger electron spectroscopy (AES) are among the techniques employed by surface scientists to define the crystallography of chemisorbed atoms and molecules on extended surfaces. These methods do not offer the precision available in molecular structural analysis, however, and the experimental and theoretical details of their implementation are by no means trivial.[19] It is therefore apparent that cluster systems, which are readily studied by the usual vibrational spectroscopic techniques and diffraction methods, may enable a clearer understanding of the associated surface chemistry, and these ideas have led to the synthesis of a range of comparatively 'simple' model cluster compounds.

Whatever the limitations of the surface-cluster analogy, surface scientists generally compare the vibrational spectra of adsorbed species with those of molecular metal clusters characterised by crystallography, as the basis for determining structures of adsorbates on metal surfaces.[30] Thus, the merging of organometallic chemistry and surface chemistry is well underway.[28]

1.3   The Surface and Cluster Chemistry of Carbon Monoxide and Benzene

Interest in arene carbonyl clusters was originally stimulated by the chance discovery of the hexaruthenium arene complexes, $Ru_6C(CO)_{14}(\eta^6\text{-}C_6H_{6-n}Me_n)$ [n = 0,1,2,3],[31] and the subsequent synthesis of the *bis*(benzene) derivative, $Ru_6C(CO)_{11}(\eta^6\text{-}C_6H_6)(\mu_3\text{-}\eta^2:\eta^2:\eta^2\text{-}C_6H_6)$.[32] The observation that the benzene ligands in this latter complex adopted not only the familiar η^6 terminal bonding mode found in *e.g.* $Cr(\eta^6\text{-}C_6H_6)_2$,[33] but also the then highly unusual μ_3 face-capping mode, caused the chemistry of arene-clusters to be investigated in more detail.

The research described in the chapters that follow is primarily concerned with the synthesis and characterisation of ruthenium and osmium arene carbonyl clusters. It has been found that both the arene and carbonyl ligands in these clusters are capable of adopting multicentre bonding interactions, and it is evident that the analogous bonding modes are possible when such molecules are chemisorbed on metal surfaces. Hence, an illustration of the surface-cluster analogy in terms of structure and bonding, and reactivity follows with attention focused on the carbon monoxide and benzene ligands.

1.3.1 Molecular Models for CO - Metal Surface Chemistry

The chemisorption of carbon monoxide on various transition metal surfaces is the most intensively studied of all adsorption systems, and has provided a model for how surface studies can reveal the nature of the surface-chemical bond.[15,34] A combination of techniques such as vibrational spectroscopy, LEED and ARUPS studies have been used in accomplishing this. For example, UV photoemission studies have compared the energy distribution of photoelectrons from CO chemisorbed on the (100) crystal face of iridium, with that from iridium carbonyl, $Ir_4(CO)_{12}$. The photoelectron spectra reveal that the concentration of electrons in the various occupied states are very similar in both cases, indicating that the electron-energy distribution in their chemical bonds is virtually identical; thus, the surface chemical bond of CO on iridium appears to be cluster-like.[15] Excellent agreement has also been found in metrical parameters derived from diffraction experiments of the two regimes,[18,35,36] and comparisons between the carbonyl stretching frequencies of analogously coordinated CO ligands in metal cluster complexes and on the surface are again remarkably close.[18,36,37] These latter observations provide further evidence to suggest that the chemisorption interaction may be adequately described in terms of a localised bonding between the adsorbate and neighbouring surface atoms, and can be readily modelled by cluster molecules.

The carbon monoxide ligand exhibits a large number of coordination modes in molecular transition metal chemistry; a subject which has been frequently discussed in the literature.[38,39] Although this area is too large in cover in any depth, these CO-metal interactions can generally be divided into three groups, and some relevant examples of each are illustrated in Figure 1.3.1i.

Carbon monoxide is known to bind to a metal surface in an upright manner, perpendicular to the surface, and may occupy a 1-fold site as on Pt(111), a 2-fold bridging site as on Pd(100), or a 3-fold site as on Pd(111).[40] In analogy with the molecular chemistry of the carbonyl ligand, these represent the two-centre or terminal (η^1) mode, which is by far the most frequently encountered coordination mode for CO in metal cluster complexes; the three-centre or edge-bridging (μ_2-η^1) mode; and the four-centre or triangular face-bridging (μ_3-η^1) mode, respectively.[38] These are all examples of the η^1-(C)
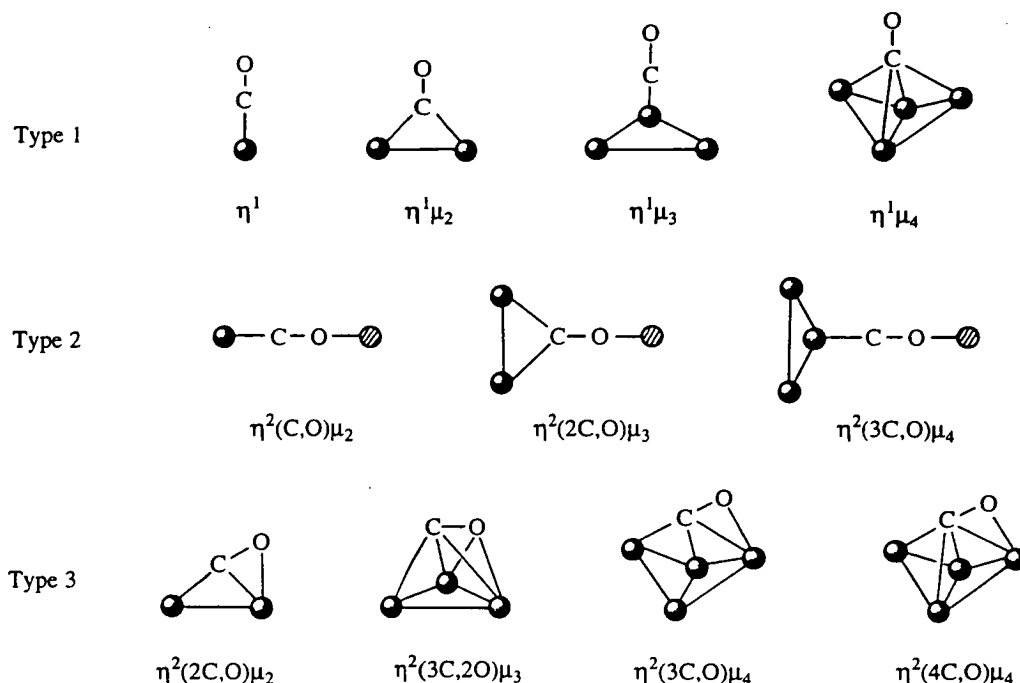
Figure 1.3.1i: Some of the CO coordination modes found in transition metal chemistry; the η^1 modes form the basis from which the *di*-hapto ligands of types 2 and 3 are derived.

bonding mode shown in Figure 1.3.1i (Type 1), and the tetrahedral cluster dianion $[Fe_4(CO)_{13}]^{2-}$ provides an example where all three types of interaction are present in the same molecule [see Figure 1.3.1ii (a)].[41] The (μ_4-η^1) coordination mode for CO in cluster complexes is far less common, however one such example has been observed in the butterfly cluster $Cp_4Mo_2Ni_2S_2CO$ [see Figure 1.3.1ii (b)].[42] The preference for the site of chemisorption on a metal surface is determined by the relative energy of the d band of the metal. The higher the energy of the d band, the greater the degree of metal-to-CO π^* back-bonding which favours bridging coordination.[34] This situation is similar to that found in cluster systems, although in clusters steric as well as electronic factors can dictate the coordination mode adopted by the carbonyl ligand.

One reason for the numerous experimental and theoretical investigations into the chemisorption and activation of carbon monoxide on transition metal surfaces stems from their importance in catalytic reactions such as carbon monoxide hydrogenation (*i.e.* the Fischer Tropsch reaction).[43] It was speculated that in order for CO dissociation to occur, a molecular intermediate should exist containing a bonding configuration in which both carbon and oxygen atoms coordinate to the metal surface.[4,44] This 'side-on' coordination mode would stretch and weaken the C-O bond, thus making it prone to cleavage. The presence of such an intermediate has since been observed from vibrational studies (based

9
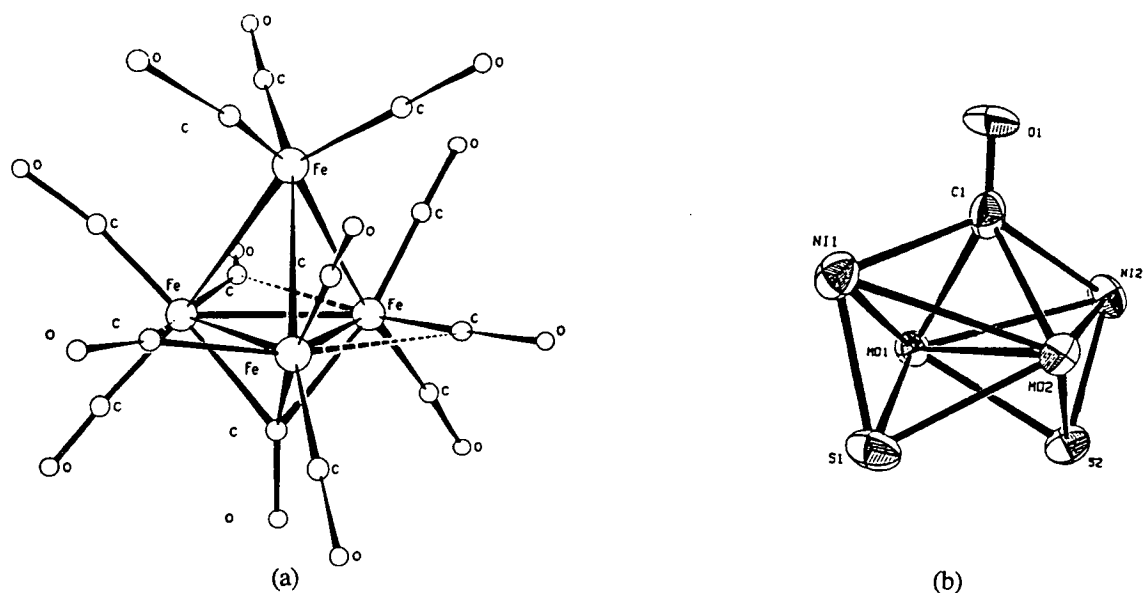
Figure 1.3.1ii: The molecular structures of (a) $[Fe_4(CO)_{13}]^{2-}$ and (b) $Cp_4Mo_2Ni_2S_2CO$.

on the observation of unusually low C-O vibrational frequencies, *i.e.* values of υ_{CO} between 1500 and 1000 cm^{-1}), and examples of metal surfaces accommodating carbon monoxide in a side-on manner now include $Cr(110)$,[45] $Fe(100)$,[46] and $Mo(100)$.[47] Similar observations have also been made on several promoted surfaces, *e.g.* potassium-promoted $Ru(001)$.[48] In these examples the d band behaves as both an electron donor to the CO π^* MOs and as an acceptor from the filled π MO of carbon monoxide. The dissociation of CO into surface bound carbide and oxide atoms has some obvious parallels in metal carbonyl cluster chemistry where, upon pyrolysis, CO_2 is evolved and carbide ligands are generated.[40] This carbide formation process is described in further detail in Chapter four.
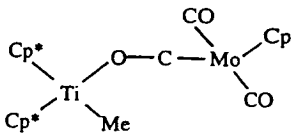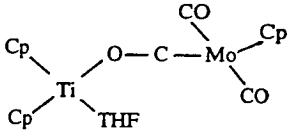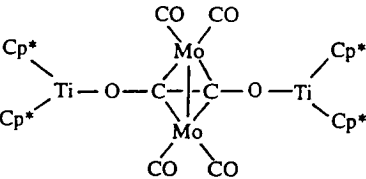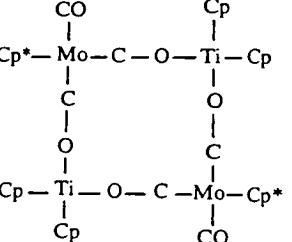
In cluster complexes, this type of 'side-on' carbonyl interaction can be illustrated by the *di*-hapto ligands found in molecules of Type 3 (see Figure 1.3.1i), *i.e.* those which contain a certain degree of interaction between the CO π orbitals and the metal framework, in addition to the usual dπ-pπ interaction. This mode of carbonyl coordination is rare in cluster compounds, especially when one considers the number of compounds containing η^1 ligands. The (μ_4-η^2) class of π-CO ligands are the most commonly observed of this type; the first and most well known example being found in the anion, $[Fe_4(CO)_{13}H]^-$.[49] The μ_4-η^2 carbonyl ligand in this complex coordinates to all four of the iron atoms which are arranged in a butterfly configuration, and the bonding mode is best described as face-bridging one triangular butterfly 'wing' *via* a μ_3 interaction through the carbon, and bonding to the fourth iron atom in an η^2 manner. The C-O distance of this ligand is relatively long [1.26(3) Å] and has a reported IR vibrational frequency (υ_{CO}) of 1415 cm^{-1}, illustrating the degree in which the C-O bond has been weakened. Upon protonation, this

C-O bond is cleaved with the loss of water and the generation of a carbido-atom, and this complex provides an excellent model for the coordination and activation of carbon monoxide on a metal surface, particularly at a step or kink site.[4,41,50]

The second type of *di*-hapto carbonyl ligand found in cluster compounds (Type 2, Figure 1.3.1i) is based on an essentially end-on array, with the η^2 interaction of the carbonyl bridging two metals which are otherwise unconnected. This class of carbonyl ligand is often described as 'end-on' or 'isocarbonyl', although true isocarbonyls which are bonded solely through the oxygen atom are not known; a fact which illustrates the increase in basicity at the O-atom upon coordination of the ligand through the C-atom.[38] The interaction of Lewis acids with the oxygen atom of a metal-bound carbonyl ligand is well-known,[39,51] and the capacity of these oxygen atoms to coordinate to Lewis acids by use of their 'lone pair' electrons will clearly increase with the accumulation of negative charge on the ligand. Accordingly, triply-bridging carbonyl ligands are expected to be more basic than doubly-bridged CO, which in turn should be more basic than terminal carbonyl ligands.[39] M-CO-M' systems of this type usually exist when both early oxophilic and late electron-rich transition metals are present, *e.g.* $Cp*_2(Me)Ti(\mu-\eta^1:\eta^1-OC)Mo(CO)_2Cp$ (see Table 1.3.1).[52] This coordination mode is again of importance with respect to activating carbon monoxide,[1,4] and interest in these complexes has arisen because such metal pairings combine the Lewis acidity of the early metals with the known ability of the late-metal centres to activate hydrogen, thus offering a potential for CO bond activation and reduction.[53] Table 1.3.1 illustrates the structural and spectroscopic data of a few carbonyl bridged Ti/Mo complexes. In each example the bridging C-O bond distances are long (> 1.20 Å) and the C-O stretching frequencies are low (≤ 1710 cm^{-1}), both of which reflect the substantial C-O bond activation arising from the interaction of the carbonyl group with the titanium atom. The Ti(IV)/Mo species, $Cp*_2(Me)Ti(\mu-\eta^1:\eta^1-OC)Mo(CO)_2Cp$, exhibits a marginally longer C-O bond distance and lower C-O stretching frequency than the Ti(III)/Mo species, $Cp_2(THF)Ti(\mu-\eta^1:\eta^1-OC)Mo(CO)_2Cp$,[53,54] and these values are further enhanced in the complex $[Cp*_2Ti(\mu-OC)Mo(CO)Cp]_2$, where the carbonyl bound to Ti bridges two Mo centres,[55] thus suggesting that the C-O bond activation is increased by both back-donation from the two Mo centres and the interaction with the Lewis acidic Ti(III) centre.

Infrared spectroscopy is the technique most frequently employed in the identification of carbonyl ligands in unusual coordination or adsorption environments. This is because the frequency of the υ_{CO} mode is very sensitive to the small changes in C-O bond order that are induced by a modification of electron density in the π^* orbitals or donation of electrons from the π-bonding orbitals. Assignments of CO coordination modes

11

Table 1.3.1: Structural and Spectroscopic Data for Carbonyl-Bridged Ti/Mo Complexes; the structural and spectral data given refer to the bridging carbonyl moieties.

Compound	μ-C-O, Å	υ_{CO}, cm^{-1}	Ref.
Cp*₂(Me)Ti–O–C(Mo(CO)₂Cp)	1.212(5)	1627	51
Cp₂(THF)Ti–O–C(Mo(CO)₂Cp)	1.205(5)	1657	53, 54
Cp*₂Ti–O–C(Mo₂(CO)₄)–C–O–TiCp*₂	1.271(7)	1351	55
Cp*Mo(Cp)Ti bridged cluster	1.208(7)	1710	56

are, however, not always unambiguous from vibrational spectroscopic data, and whereas in the majority of cluster examples X-ray crystallographic studies are undertaken to clearly elucidate the bonding mode present, this technique is not as readily available for the metal surface. As a result, characterisation of the chemisorbed species is often based on the coordination mode found in an analogous cluster system.

For example, the Mo(110) surface contains CO chemisorbed in at least four different environments (depending on experimental conditions such as CO coverage, crystal temperature, and coadsorbed atoms), all with distinct υ_{CO} vibrational frequencies.[43] In addition to the modes observed between 2055-1920 cm^{-1}, which may be readily assigned to the conventional terminal and bridge bonded CO, three unusually low υ_{CO} modes are observed at *ca.* 1500, 1345 and 1130 cm^{-1}. These low frequencies cannot be attributed to a CO molecule that is perpendicularly bonded to the metal surface only through carbon, and it is suggested that, as for other transition metals,[45-47] such frequencies can only occur if the molecular axis of the CO is tilted away from the surface normal, allowing a greater overlap

between the CO-$2\pi^*$ antibonding orbitals and the local density of electronic states of the metal substrate.

The CO species with a υ_{CO} of 1500 cm^{-1} may be correlated to a carbonyl ligand found in the organometallic complex, $(C_5H_5)_3NbMo(CO)_3$ [see Figure 1.3.1iii (a)], which gives rise to a stretch at 1560 cm^{-1}.[57] This compound possesses a bridging, 4-electron donating, carbonyl ligand which is σ-bonded through the C-atom to the molybdenum atom, and further coordinates to the niobium atom through a π-interaction involving both the carbon and oxygen atoms. This η^2 coordination mode results in a relatively long C-O bond length of 1.22 Å.

(a)   (b)
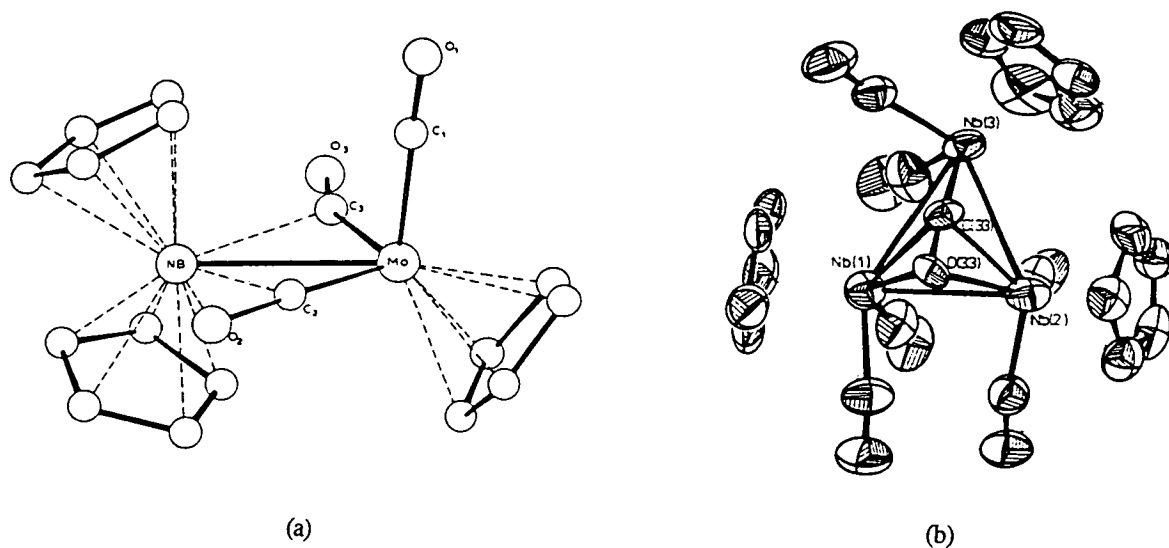
Figure 1.3.1iii: The molecular structures of (a) $(C_5H_5)_3NbMo(CO)_3$ and (b) $(C_5H_5)_3Nb_3(CO)_7$.

The carbon monoxide species on the Mo(110) surface responsible for the vibration at 1345 cm^{-1} is thought to resemble a carbonyl ligand observed in the cluster $(C_5H_5)_3Nb_3(CO)_7$.[58] One of the seven CO ligands in this molecule acts as an η^2 (μ_3-C, μ_2-O) bridge which is bonded carbon-end down to a single niobium atom as well as to each of the remaining niobium atoms *via* π-interactions [see Figure 1.3.1iii (b)]. This mode of coordination causes a considerable elongation of the C-O bond [1.30 Å], which is accompanied by a υ_{CO} absorption frequency of 1330 cm^{-1}. This carbonyl ligand acts as a 6-electron donor, providing two electrons to each Nb atom (through one σ- and two π-bonds).

Although the species giving rise to the peak at 1130 cm^{-1} has yet to be correlated with an organometallic complex, it may be considered as consisting of a carbon monoxide unit bonded to the molybdenum surface again through both the carbon and oxygen ends in a 'side-on' manner. In fact a CO group responsible for a υ_{CO} mode at 1130 cm^{-1} may be described as having a bond order of one, as predicted from the relationship of υ_{CO} *vs.* CO

bond order for metal cluster complexes.[38] Upon heating there is a decrease in the intensity of this 1130 cm^{-1} mode and a simultaneous intensity increase in the atomic υ_{Mo-C} and υ_{Mo-O} modes, thus suggesting that such a carbonyl species is a stable intermediate in the dissociation of CO to 'C' and 'O' on the Mo(110) surface.[43] The possible bonding orientations for these three low-frequency υ_{CO} modes are illustrated in Figure 1.3.1iv.

$\upsilon_{CO} = 1130$ cm^{-1}

$\upsilon_{CO} = 1345$ cm^{-1}

$\upsilon_{CO} = \sim 1500$ cm^{-1}
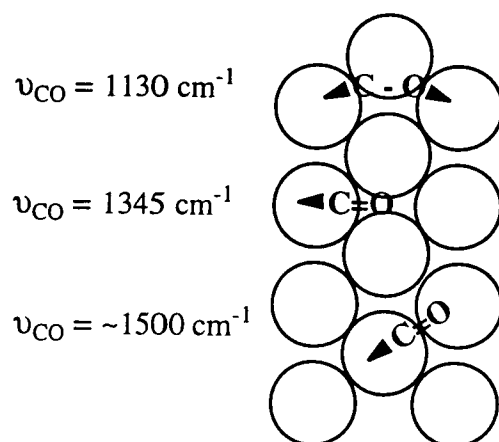
Figure 1.3.1iv: Schematic of the possible bonding orientations for the three low-frequency υ_{CO} modes observed on the Mo(110) surface.

1.3.2 Molecular Models for Benzene - Metal Surface Chemistry

There is a rich chemistry associated with the arene ligand in *mono* and *bi*nuclear species; an area which has been reviewed in several prominent articles.[59,60] Complexes of virtually every transition metal have been prepared, and a wide range of elementary and bridging coordination modes observed (*e.g.* η^1,[61] η^2,[62] η^3,[63] η^4,[64] η^6,[65] μ_2-η^2:η^2,[66] μ_2-η^3:η^3,[67] μ_2-η^4:η^4,[67,68] μ_2-η^6:η^6).[67,69] Arene cluster complexes are less well developed, but nonetheless reports are becoming increasingly frequent in the literature, and this area has also recently been comprehensively reviewed.[70] The cluster geometries produced in such molecules are diverse, and three different arene coordination modes [η^2, η^6 (terminal or apical) and μ_3-η^2:η^2:η^2 (face-capping)] have been established by X-ray crystallography.

The η^2 arene coordination mode is rare, with the only known example being found in the mixed-metal species Cu$_2$Ru$_6$(CO)$_{18}$(η^2-C$_6$H$_5$Me)$_2$.[71] The η^6 terminal bonding mode is far more commonly observed, with examples known for clusters with nuclearities ranging from three to eight. This coordination mode appears to be independent of the metal-metal connectivities within the clusters, being bound to metal atoms with connectivities of *two* in Os$_3$(CO)$_7$(R$_2$C$_2$)(η^6-C$_6$H$_6$)[72] and Ru$_3$(CO)$_7$(RC$_2$R'CO)(η^6-C$_6$H$_6$),[73] *three* in Os$_4$(μ-H)$_2$(CO)$_{10}$(η^6-C$_6$H$_6$),[74] Co$_4$(CO)$_9$(η^6-C$_6$H$_6$)[75] and Ru$_5$C(CO)$_{12}$(η^6-C$_6$H$_6$),[76] and

four in $Ru_6C(CO)_{14}(\eta^6-C_6H_6)^{31}$ and $Os_5(\mu-H)_4(CO)_{11}(\eta^6-C_6H_6).^{77}$ The $\mu_3-\eta^2:\eta^2:\eta^2$ (face-capping) bonding mode was first being observed in 1985 in the cluster complexes, $Os_3(CO)_9(\mu_3-\eta^2:\eta^2:\eta^2-C_6H_6)$ and $Ru_6C(CO)_{11}(\eta^6-C_6H_6)(\mu_3-\eta^2:\eta^2:\eta^2-C_6H_6).^{32}$ Since the initial synthesis of these prototype molecules, the facial-arene moiety has been observed in a number of other complexes based on the M_3 (M = Ru,[78] Co,[79] and Rh[80]), $Ru_5C,^{76}$ and Os_6^{81} systems. A number of interesting features have emerged from the study of arene carbonyl clusters, but the factors which govern the bonding mode adopted by the arene ligand on the cluster surface still remain a long way from being fully understood.

Benzene readily adsorbs associatively onto most transition-metal surfaces, and only decomposes (as opposed to desorbing molecularly) when heated to temperatures generally above 350 K.[23,82] It is therefore easily studied at room temperature.

The surface vibrational spectrum of chemisorbed benzene implies that adsorption is molecular, with the plane of the benzene ring parallel to the metal surface.[82,83] This bonding orientation is supported by LEED studies, which also imply that chemisorbed benzene is distorted from its equilibrium gas-phase geometry due to the metal-adsorbate interaction.[83] Large organic molecules frequently exhibit distortions of this type when adsorbed on metal surfaces and, in general, the stronger this interaction, the larger the distortion.[6] There are at least five possible sites that chemisorbed benzene may adopt on a close packed, atomically flat metal surface (see Figure 1.3.2i),[60] and advances in the dynamic theory of LEED have led to the structural characterisation of benzene in each environment. These are the so-called 'on-top' site which has sixfold symmetry (C_{6v}), *e.g.* Rh(111)/C_6H_6,[84] Pd(111)/C_6H_6;[85] the 'hollow' site with threefold local symmetry [$C_{3v}(\sigma_d)$] *e.g.* Os(0001)/C_6H_6,[86] Rh(111)/C_6H_6/CO,[87] and Pd(111)/C_6H_6/2CO;[88,89] and the 'bridge' site with twofold local symmetry (C_{2v}) *e.g.* Pt(111)/2C_6H_6/4CO.[90,91] The eclipsed conformation of M_3 and C_6 rings [$C_{3v}(\sigma_v)$, 'hollow' site symmetry], which is

C_{3v} $\qquad$ C_{6v} $\qquad$ C_{2v}
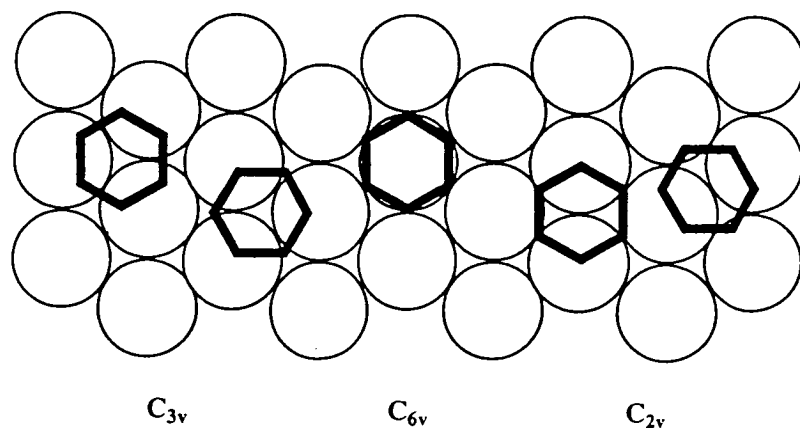
Figure 1.3.2i: Possible adsorption sites for benzene on a close-packed metal surface.

considered to be a transition state in arene rotation on the metal surface, can be stabilised by coadsorption of sodium on a Rh(111) surface.[92]

Some examples of benzene chemisorbed on the Pd(111), Rh(111) and Pt(111) surfaces are illustrated in Figure 1.3.2ii. Since metal surfaces are electron deficient there is a considerable transfer of charge from the adsorbed benzene to the metal resulting in an elongation of the benzene C-C bonds and a ring expansion with respect to its gas-phase geometry.[15,93] The symmetry of the benzene ring expansion is dependent on the adsorption site; this is twofold for the bridge site on Pt(111),[90,91] and threefold for the hollow sites on Rh(111)[87,89,91] and Pd(111).[88,89] There is even evidence to suggest that on adsorption the benzene ring may buckle to assume a boat-like configuration with two of the carbon atoms (*para* to one another) being closer to the metal surface than the remaining four. This latter situation is observed when benzene is chemisorbed without long-range order (*i.e.* in the absence of CO) on bridge sites of the Pt(111) surface, and is depicted in Figure 1.3.2iii.[6,82] It is also worthy to note that benzene has been found chemisorbed in both bridge[94] and on top sites of the Rh(111) surface,[84] however, the coadsorption of carbon monoxide is believed to force the benzene molecules into hollow, three-fold adsorption sites, thereby forming a more ordered structure.[88,91,94,95] Like most organic molecules, benzene is a strong electron donor to metal surfaces, and the presence of both electron acceptor and donor interactions apparently induces long-range ordering together with the formation of surface structures containing both benzene and carbon monoxide molecules in the same unit cell.[96]
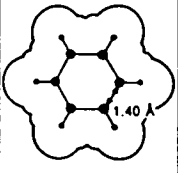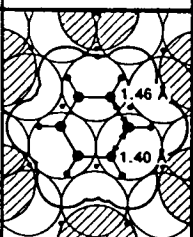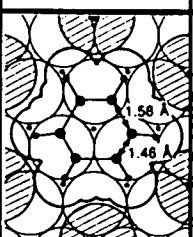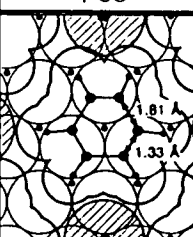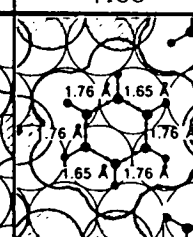
Substrate	(Gas Phase)	Pd(111)	Rh(111)		Pt(111)
Surface Structure		(3x3)-C_6H_6 + 2CO	(3x3)-C_6H_6 + 2CO	c(2$\sqrt{3}$x4)rect-C_6H_6 + CO	(2$\sqrt{3}$x4)rect-2C_6H_6 +4CO
The Structure of Benzene		1.46 Å / 1.40	1.58 Å / 1.46 Å	1.81 Å / 1.33 Å	1.76 Å 1.65 Å / 1.76 Å / 1.65 Å 1.76 Å
C_6 Ring Radius (Å)	1.40	1.43±0.10	1.51±0.15	1.65±0.15	1.72±0.15
d_{M-C}(Å)	-	2.39±0.05	2.30±0.05	2.35±0.05	2.25±0.05
γ_{CH}(cm^{-1})*	670	720-770	780-810		830-860

Figure 1.3.2ii: The surface structures of benzene on the Pd(111), Rh(111), and Pt(111) crystal faces when coadsorbed with CO which induces ordering. The gas-phase benzene molecular structure is shown for comparative purposes.
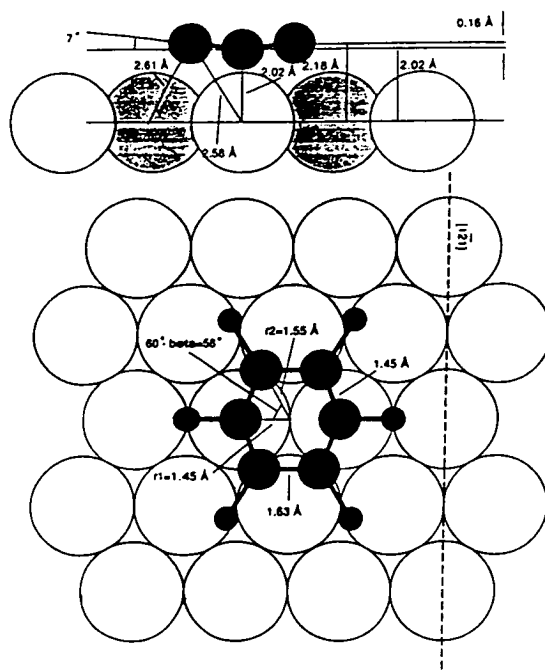
Figure 1.3.2iii: The surface structure of benzene in a disordered monolayer on Pt(111). The chemisorbed benzene monolayer remains disordered in the absence of coadsorbed CO. Note the bending of the benzene molecule into a boat-like surface structure.

On examination of these structures in more detail it becomes apparent that in $Rh(111)/C_6H_6/2CO$[89,91] and $Pd(111)/C_6H_6/2CO$[88,89] the distortion of the chemisorbed benzene is not significant [d_{C-C} = 1.46(15) and 1.58(15) Å, and 1.40(10) and 1.46(10) Å, respectively]. The same is true for benzene adsorbed at a C_{2v} site in $Pt(111)/2C_6H_6/4CO$ [two C-C bonds have d_{C-C} = 1.65(15), and four have d_{C-C} = 1.76(15) Å].[90,91] However, in the structure of $Rh(111)/C_6H_6/CO$ a substantial in-plane Kekulé-type distortion is evident with alternating 'long' [1.81(15) Å] and 'short' [1.33(15) Å] C-C bond lengths; the short bonds lying directly above the metal atoms.[87] The benzene molecule in this example appears almost as though it were three acetylene units, although the expected Van der Waals separation between two acetylenes is in the order of 2.8 Å,[26] thus indicating that this adsorbate is still very much a distorted benzene molecule. The carbon ring radius has also considerably increased with respect to gas phase benzene [1.65 *vs.* 1.40 Å].

Reports on the interaction of benzene with the Rh(111) surface, both in the presence of CO and in its absence, by Somorjai and co-workers coincided with the discovery of the benzene-clusters $Os_3(CO)_9(\mu_3\text{-}\eta^2\text{:}\eta^2\text{:}\eta^2\text{-}C_6H_6)$ and $Ru_6C(CO)_{11}(\eta^6\text{-}C_6H_6)(\mu_3\text{-}\eta^2\text{:}\eta^2\text{:}\eta^2\text{-}C_6H_6)$.[32] These novel clusters have been fully characterised by single-crystal X-ray diffraction analyses and their $\mu_3\text{-}\eta^2\text{:}\eta^2\text{:}\eta^2$ benzene moieties bear a striking resemblance to that found in the $Rh(111)/C_6H_6/CO$ surface structure.[87] In both cluster examples the benzene ligand symmetrically caps a trimetallic face, showing trigonal

distortions towards the hypothetical 1,3,5-cyclohexatriene, and it therefore appears that a clear relationship exists between the benzene-carbonyl-cluster and the benzene-carbonyl-surface interaction. Thus, the cluster-like bonding model also appears to be valid for chemisorbed benzene.[15]

The triruthenium cluster analogue, $Ru_3(CO)_9(\mu_3\text{-}\eta^2\text{:}\eta^2\text{:}\eta^2\text{-}C_6H_6)$, has since been prepared, and the high quality data obtained from the single-crystal X-ray diffraction analysis has enabled an unambiguous description of the bonding between the benzene ligand and the metal frame together with the direct location of all H atoms.[78] This complex features long and short C-C bonds [mean 1.45(1) *vs.* 1.40(2) Å] which alternate within the benzene ligand, the short bonds being those interacting directly with the ruthenium atoms. This apparent Kekulé distortion may be traced to an internal mixing of the benzene π-system which leads to an increased overlap in the three C-C bonds eclipsing the metal atoms, at the expense of the alternate non-eclipsing bonds which consequently become elongated.[14, 97] Mixing between the highest occupied and the lowest unoccupied benzene π-orbitals has also been recognised in models of the C_{3v} Rh(111)-benzene surface complex,[98] and is believed to account for the small but significant trigonal distortions found in η^6 arene complexes such as $M(CO)_3(\eta^6\text{-}C_6H_6)$ [M= Cr, Mo].[99,100]

A comparison of the benzene bonding geometries in the two regimes is displayed in Figure 1.3.2iv. The Rh(surface)-C(benzene) bond distance of 2.35(5) Å is in agreement with the mean Ru-C bond length of 2.33(1) found in $Ru_3(CO)_9(\mu_3\text{-}\eta^2\text{:}\eta^2\text{:}\eta^2\text{-}C_6H_6)$. Furthermore, theoretical modelling of the Rh(111) surface predicts that a major adsorption effect involves the symmetrical bending of all six hydrogen atoms out of the plane of the benzene ring, away from the metal.[98] This is precisely the behaviour observed in the

Rh — 1.81(15) Å

1.33(15) Å

Surface

(a)

Ru — 1.45(1) Å

1.40(2) Å

Cluster

(b)
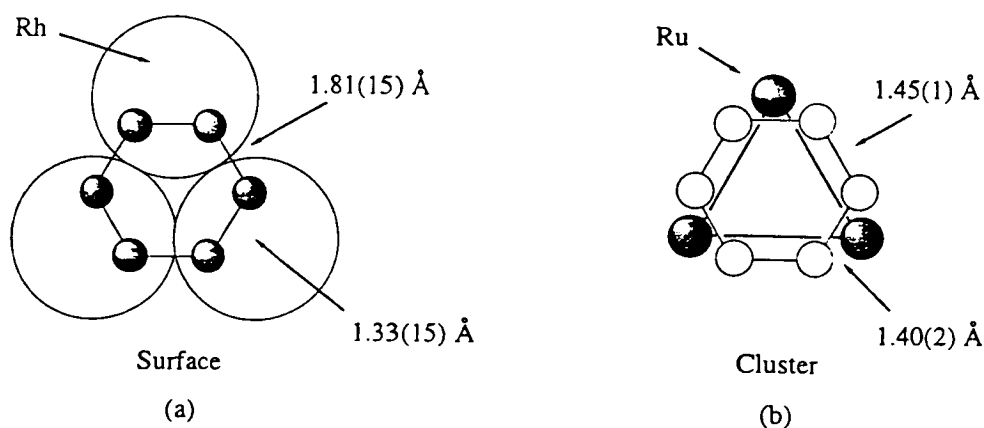
Figure 1.3.2iv: A comparison of the bonding geometries for benzene on (a) the Rh(111) metal surface and (b) the triruthenium cluster, $Ru_3(CO)_9(\mu_3\text{-}\eta^2\text{:}\eta^2\text{:}\eta^2\text{-}C_6H_6)$.

cluster species; an out of plane bending angle of 20° was predicted for the Rh(111) surface which is in excellent agreement with the value of 21.5° observed for the Ru$_3$ cluster. This C-H bending effect has been explored in organometallic compounds by Hoffman *et. al.* who found that a rehybridisation (sp^2 → sp^3) of the benzene π molecular orbitals is necessary for maximised overlap with metal orbitals.[101]

An appreciation of the way in which the interaction of the arene moiety varies as the metal substrate undergoes a change in both size and structure is fundamental to the understanding of the bonding of arenes to clusters, small metal particles or indeed the bulk metallic lattice. One of the major areas of conflict between the cluster and surface regime is size, with the anomaly being as to how a seemingly microscopic fragment of a surface, *i.e.* a cluster, can accurately model the bulk metal. The evidence available to date suggests that the nature of the benzene-metal substrate interaction is not size dependant (since the bonding displayed in the two regimes is very similar), although the subsequent distortions resulting from such interactions are closely related to the number of atoms in the metal substrate; the extent of localisation on the surface being larger than that found in cluster systems. For the face-capping bonding mode, interaction with three metal atoms obviously remains constant on the surface and in a metallic cluster. Here the concern lies in whether the additional metal atoms affect the nature of the μ$_3$-interaction. In the surface structure of Rh(111)/C$_6$H$_6$/CO,[87] C-C bond distances alternate between 1.33(15) and 1.81(15) Å, the difference being 0.48 Å (although the errors associated with these values are large). In the triruthenium cluster, Ru$_3$(CO)$_9$(μ$_3$-η^2:η^2:η^2-C$_6$H$_6$),[78] this difference is 0.04 Å, which increases to Δ = 0.08 Å in Ru$_5$C(CO)$_{12}$(μ$_3$-η^2:η^2:η^2-C$_6$H$_6$),[76] and for the hexaruthenium cluster, Ru$_6$C(CO)$_{11}$(η^6-C$_6$H$_6$)(μ$_3$-η^2:η^2:η^2-C$_6$H$_6$), the difference in bond length is 0.09 Å.[32] Although these observations are confined to a limited number of cases and the differences lie close to experimental errors, there is a clear trend showing that as the nuclearity increases, the Kekulé distortion in the ring increases accordingly. Clearly, crystallographic studies of face-capping benzene rings attached to larger clusters would be beneficial in confirming this pattern, and as long as surface scientist take this relationship into account, then analogies can be made between the surface and cluster regimes.

1.3.3 Reactivity

As already outlined, the surface-cluster analogy, whilst being valid for structure and bonding, is not generally proven in terms of reactivity, and the predicted use of metal clusters as catalysts has not materialised (their prospects usually being limited by their relative lack of stability).[27] However, there are a few examples in the literature which may argue this point, suggesting that the analogy does extend beyond structure and bonding.[25,102]

One such example demonstrates that the reactivity of a carbonyl group bridging metal atoms in an alkoxidotetratungsten cluster of the type $W_4(CO)(OR)_{12}$[40] is analogous to that of a CO molecule chemisorbed on a sparsely covered Mo(110) surface.[43] Both species react with dissociation to give carbido and oxido ligands bonded to neighbouring metal centres; a step which is important in the Fischer-Tropsch reaction catalysed by metal surfaces (see Scheme 1.3.3).[28] The evidence for this reactivity in molecular metal clusters is based upon NMR spectroscopy and crystallographic data; with the cluster $W_4(\mu_4\text{-}C)(\mu\text{-}O)(O i Pr)_{12}$ containing a carbido ligand bonded to four tungsten atoms arranged in a butterfly configuration and an oxo ligand bonded to two tungsten atoms. The species on the Mo(110) surface are characterised by vibrational (electron energy loss) spectroscopy.

Scheme 1.3.3: The dissociation of a bridging CO molecule.

On an atomically flat metal surface at ambient temperatures, benzene is chemisorbed molecularly, *i.e.* the hydrogen atoms are not involved in the attachment. In the vicinity of a step, however, the dissociative chemisorption of benzene is favoured (see Figure 1.3.3i).[6,23,83] It is therefore likely that the planar coordination of the arene parallel to one terrace of the surface allows for a close approach of its hydrogen atoms to the step atoms of a second terrace. This would facilitate C-H bond cleavage and, hence, enhance the likelihood of dehydrogenation of the chemisorbed benzene molecule.[23] An attractive cluster model for this process is provided by the μ_5-benzyne complex, $Ru_5(CO)_{13}(\mu_4\text{-}PPh)(\mu_5\text{-}C_6H_4)$,[103] since the five metal atoms mimic a step-site on a (111) surface (see Figure 1.3.3ii), where Ru(3), Ru(4) and Ru(5) are in one terrace and Ru(1) and Ru(2) are step atoms in the first row of the next. It can therefore be envisaged that the approach of

(a)   Metal crystal face   (b)
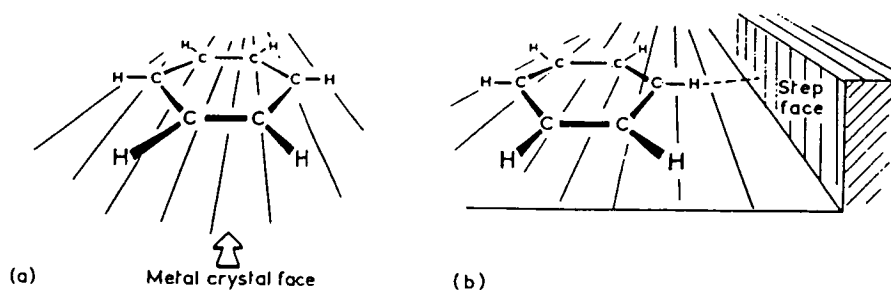
Figure 1.3.3i: Representations of the geometrical configurations of a benzene molecule chemisorbed (a) on a perfect crystal face, and (b) on a terrace in the vicinity of a step.

benzene across a terrace of a (111) surface towards exposed, low-coordinate, step atoms would result in the activation of two *ortho*-C-H bonds, generating an analogous chemisorbed benzyne species.
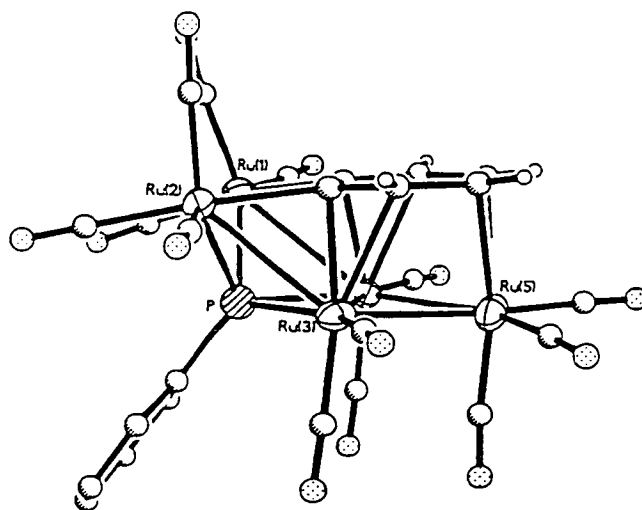
Figure 1.3.3ii: Molecular structure of $Ru_5(CO)_{13}(\mu_4\text{-PPh})(\mu_5\text{-}C_6H_4)$.

While the concept of benzene C-H bond activation at a step-site is attractive, it is possible that C-H activation can also occur at other sites on the metal surface.[103] A molecular example of this situation is provided by the triosmium benzene complex, $Os_3(CO)_9(\mu_3\text{-}\eta^2:\eta^2:\eta^2\text{-}C_6H_6)$, which undergoes photochemically induced isomerisation to afford $Os_3(\mu\text{-H})_2(CO)_9(\mu_3\text{-}\eta^1:\eta^2:\eta^1\text{-}C_6H_4)$.[104] This latter complex contains a μ_3-benzyne ligand and indicates that a triangular surface site may also be capable of inducing C-H bond activation. It is thought that the photolytic process generates a vacant site at osmium which mimics the inherent coordinative unsaturation of a metal surface, and this transformation therefore offers a cluster analogue for the interconversion of associatively and dissociatively chemisorbed states of benzene on surface planes or step sites of a metallic lattice.[104]

In contrast to the case of benzene, alkyl-substituted arenes such as toluene are chemisorbed dissociatively. The parallel coordination of the aromatic ring places the methyl hydrogens in close proximity to adjacent surface atoms, thus facilitating C-H bond cleavage.[23,105,106] A similar situation arises in the high nuclearity ruthenium clusters, $HRu_6(\eta^2\text{-}\mu_4\text{-CO})(CO)_{13}(\mu_2\text{-}\eta^1:\eta^6\text{-}C_6H_3Me_2CH_2)$,[107] and $Ru_8(\mu_8\text{-P})(CO)_{19}(\mu_2\text{-}\eta^1:\eta^6\text{-}CH_2C_6H_5)$,[108] whereby C-H bond cleavage has occurred with simultaneous Ru-C σ bond formation at the methyl C-atom of the mesitylene and toluene ligands, respectively.

From these few examples it is apparent that the behaviour and reactivity of certain organic molecules (namely CO and benzene) are similar whether coordinated to a metal

cluster or chemisorbed on a metal surface. It is important to note, however, that even in these examples there are distinct differences between the two regimes. The rate of a reaction induced by a molecular cluster is usually less than that induced by a sparsely covered surface of the same metal.[18,40] The initial step in the bonding of a ligand to a cluster requires coordinative unsaturation, and since most stable metal clusters are coordinatively saturated, reaction steps such as dissociation of a ligand or reaction of a pair of bound ligands with each other to free a coordination site are prerequisites. In contrast, relatively clean surfaces present arrays of rigid, stable, coordinatively unsaturated sites where ligands can readily bond and be activated. Thus, although the reaction pathway of a molecule may sometimes appear similar in the two regimes, the catalytic activity of a molecular metal cluster is usually expected to be less than that of a surface with a comparable arrangement of metal atoms.[28]

1.3.4 Benzene Migration and Displacement/Decomposition Pathways

The migration of benzene across a metal surface is important with respect to catalysis,[6,26] however, little is known about the mechanisms involved in such processes. Results on a number of cluster systems have demonstrated the ease with which arene migration can occur over the cluster surface, from an η^6 site to a μ_3-η^2:η^2:η^2 coordination site or *vice-versa*,[73,76,109] and there is evidence to suggest that this migration proceeds *via* a non-dissociative mechanism, possibly involving a bridging μ_2-η^3:η^3 or μ_2-η^4:η^2 intermediate. It is therefore likely that the motion of benzene over the metal surface is similar, especially when one considers that both the cluster and surface systems also require a simultaneous migration of carbonyl groups.

Once chemisorbed, the complete molecular desorption of benzene from a metal surface is not possible by thermal methods. Benzene molecules remain intact on the metal surface at temperatures up to 400 K, and it is significant that as the temperature is raised, benzene is far more likely to decompose than it is to desorb molecularly.[6,23] Thermal desorption and molecular displacement reactions of benzene have been studied in detail on both flat and stepped Pt and Ni surfaces.[23,110] No benzene chemisorption state is fully thermally reversible on either of these surfaces, and thermal desorption experiments show competing reactions between benzene desorption and decomposition; the molecular desorption / decomposition ratio being dependant on both the metal and on the surface coverage. On heating, thermally excited states of chemisorbed benzene apparently provide a close approach of the C-H hydrogen atoms to the metal surface, thus causing the irreversible cleavage of C-H bonds with the desorption of H_2 and the formation of carbon-contaminated surfaces. It is possible, however, to readily displace benzene from flat Ni(111) and Pt(111) surfaces by strong donor ligands such as phosphines; this phosphine

displacement of benzene is quantitative for the nickel and 90% complete for the platinum surface at 298K. When chemisorbed on a stepped surface [*e.g.* Ni 9(111)x(111) or Pt 6(111)x(111)] irreversible chemisorption is increased significantly, and in the case of the stepped Pt surface at less than 0.33 of a monolayer coverage, benzene displacement by trimethylphosphine is completely inhibited. This behaviour is rationalised by the topographical or electronic features (or both) intrinsic to the stepped surface which allows a more facile irreversible C-H bond breaking process for chemisorbed benzene,[23] thus reducing the likelihood of molecular displacement.

The thermal decomposition of benzene follows a different course on the Rh(111) surface to that observed for Pt and Ni, and it is intriguing to consider whether the observed distortion of the chemisorbed benzene molecule correlates with its subsequent decomposition pathway. Deuterium labelling studies of benzene on the Rh(111) surface have shown no evidence for C-H bond cleavage, suggesting that C-C bond scission initiates the decomposition process. The decomposition fragments, as determined by HREELS, may be compared to those observed for ethylene; the first stable decomposition intermediates being identified as CH and C_2H in each case. It therefore appears that, consistent with the threefold distortion determined by LEED, benzene decomposes *via* three acetylene units which are unstable at the decomposition temperature and immediately dehydrogenate to CH and C_2H.[111] There is no evidence to suggest that the μ_3-η^2:η^2:η^2 benzene ligand in cluster complexes undergoes a similar reaction. Instead it is thought that the cluster core is more likely to breakdown or rearrange upon heating than the benzene is to decompose. The reasons for this difference in behaviour are probably a combination of the relative instability of the cluster unit when compared to the bulk metallic surface, and the far smaller Kekulé distortion exhibited by benzene in a cluster complex when compared to that chemisorbed on a metal surface (*vide supra*). In this regard it is interesting to note that the Pd(111) surface, which induces the least distortion in chemisorbed benzene (see Fig. 1.3.2ii), is an active surface for the reverse cyclotrimerisation of acetylene to benzene.[112] Hence, the mechanisms of benzene-acetylene interconversion reactions on metal surface catalysts can be related to the strong distortion of the benzene ring found in these systems.[113] This cyclotrimerisation process of acetylenes to arenes may also be catalysed by numerous molecular organometallic compounds,[114a] and has appeared favourable in some triosmium cluster chemistry.[114b]

The preceding sections have illustrated the appeal of arene carbonyl clusters to the organometallic chemist, and has served as a general introduction into the work which is to follow. Apart from providing models of the metal surface, the cluster complexes described in subsequent chapters are interesting in their own right, with a vast range of metal geometries and ligand coordination modes being established. However, before

commencing with the main bulk of the thesis it is worth briefly considering the general synthetic routes employed in the preparation of such molecules.

1.4   Synthetic Routes to Arene Carbonyl Clusters

All early examples of arene carbonyl clusters were prepared similarly, from the direct thermal reaction of a metal carbonyl with the appropriate arene solvent.[31] While this route is still widely employed, newer techniques have been developed which tend to be far more selective. It is not a straightforward task to classify these synthetic procedures, but distinction may be drawn between reactions in which the arene is added directly, and those employing indirect methods whereby other reagents are initially coordinated to the cluster unit and are chemically modified to yield the arene at a later stage in the synthesis. There are advantages and disadvantages for both types of reaction; in the former, the direct addition of the arene is beneficial in terms of the simplicity of the reaction and the number of arene ligands that are commercially available for direct use. However, these reactions are generally initiated by either thermolytic or photolytic means and often result in several products in low yield, most of which have undergone a change in cluster nuclearity, which therefore limits the scope of mechanistic information available from the reaction. On the other hand, the latter method employs chemical activation of the cluster and is a far more selective route. The reaction is easier to monitor with the cluster core usually remaining intact and hence, the mechanistic appreciation of the reaction is enhanced. The main disadvantage of this route is that an activated form of the arene ligand is generally required (*e.g.* cyclohexa-1,3-diene is used as a source of benzene) and such compounds are not always readily available. Also, difficulties may be encountered when trying to convert the coordinated ligand into the arene moiety during the final stage of the synthesis. Despite the wide range of synthetic routes available, trial and error is often required to find that most suited to the specific cluster and arene system under examination.

The chemical activation route to substituted carbonyl clusters uses the oxidative decarbonylation reagent trimethylamine *N*-oxide (Me$_3$NO). The use of amine oxides to remove coordinated carbon monoxide was first reported by Shvo and Hazum,[115] and since this initial report the method has been used extensively for both mononuclear and cluster carbonyl complexes. Carbonyl dissociation is thought to occur *via* nucleophilic addition of the amine oxide on a coordinated carbonyl ligand, thus generating a coordinatively unsaturated intermediate. This vacant coordination site may then be partially stabilised by the trimethylamine (formed when the carbonyl ligand is removed as CO$_2$) before

coordination of an incoming 2-electron donor ligand generates the coordinatively saturated product.

This procedure generally involves the dropwise addition of Me_3NO, in acetonitrile, to a solution of the appropriate cluster in a dichloromethane-acetonitrile solvent mixture under ambient conditions.[116] This results in the substitution of one or two carbonyl ligands, depending on the stoichiometry of the reagent added, by acetonitrile. Subsequent reaction of the activated acetonitrile derivative with an appropriate ligand results in substitution of the relatively labile acetonitrile group(s). For example, the preparation of the triruthenium benzene cluster $Ru_3(CO)_9(\mu_3-\eta^2:\eta^2:\eta^2-C_6H_6)$ commences with the activated species $Ru_3(CO)_{10}(MeCN)_2$, prepared by the method outlined above.[117] On reaction with cyclohexa-1,3-diene, the acetonitrile ligands are displaced affording the cyclohexadienyl complex, $HRu_3(CO)_9(\mu_3-\eta^1:\eta^2:\eta^2-C_6H_7)$, which can then be converted to the aforementioned benzene cluster.[78]

An alternative strategy may be applied in the preparation of substituted carbonyl clusters which by-passes the acetonitrile intermediate. This pathway involves the direct activation of the cluster towards the incoming ligand. An appropriate solvent is chosen so as not to play an active role in the reaction, and again the number of carbonyls removed is dependant on the stoichiometry of the Me_3NO added. For example, if the pentaruthenium cluster, $Ru_5C(CO)_{15}$, is activated using two molecular equivalents of Me_3NO in the presence of cyclohexadiene, the cluster complex $Ru_5C(CO)_{13}(\mu_2-\eta^2:\eta^2-C_6H_8)$ results in which two carbonyl ligands have been replaced by the diene moiety.[76] The benzene clusters $Ru_5C(CO)_{12}(\mu_3-\eta^2:\eta^2:\eta^2-C_6H_6)$ and $Ru_5C(CO)_{12}(\eta^6-C_6H_6)$ may subsequently be generated from this diene cluster by the *formal* dehydrogenation of the cyclohexadiene ring. This direct route is generally employed when the activated acetonitrile intermediates are very unstable and hence cause cluster decomposition, or, as in the case of $Ru_5C(CO)_{15}$, when the presence of acetonitrile has an affect on the cluster framework. The square-pyramidal metal core in $Ru_5C(CO)_{15}$ modifies almost instantaneously upon contact with small nucleophiles, including acetonitrile.[118] Cleavage of a metal-metal bond takes place with the formation of the bridged-butterfly species, $Ru_5C(CO)_{15}(MeCN)$, and attempts to activate this complex further result in extensive decomposition.

1.5   Concluding Remarks

The use of molecular clusters as models of the metallic surface in terms of structure, bonding and reactivity has been evaluated, as have the factors which should be considered when making a direct comparison between the cluster and surface regimes. The most important and deciding factor which stems from this assessment of the surface-cluster

analogy is the relatively small size of the molecular clusters under examination when compared to the bulk of the metallic lattice. In general, the analogy seems to be more valid for the larger cluster systems, which therefore presents a problem since it is the smaller clusters that have a far more developed organometallic chemistry and are of most significance to surface scientists. Despite this discrepancy, the nature of the organic species-metal substrate interaction does not appear to be size dependant, with the bonding displayed in the two regimes being very similar. However, it is possible that the distortions of the organic molecule which result from such an interaction are dependant on size, and there seems to be a direct relationship between the number of metal atoms present in the substrate and the magnitude of the distortion found in the attached organic ligand/adsorbate. If this relationship is taken into account, then analogies can be made between the surface and even the smallest of clusters.

The surface-cluster analogy has been illustrated with particular attention paid to benzene and carbon monoxide, since these are the ligands of most pertinence to subsequent chapters of this thesis. Whilst there are distinct similarities in the coordination modes adopted by these molecules in the two regimes, there is also evidence to suggest that their reaction pathways are comparable. This observation is significant because although the analogy is generally proven in terms of structure and bonding, the number of valid examples when extended to reactivity are quite limited.

Despite the limitations of the surface-cluster analogy, there is no doubt that comparisons between molecular clusters and metal surfaces has led to a much clearer understanding of the bonding modes adopted by a variety of chemisorbed species on the metal surface, and has shed light on some of the surface chemistry that such adsorbates undergo. The preceding discussion of the surface-cluster analogy should enhance ones understanding of the arguments presented in future chapters, and help to place cluster chemistry in context with surface chemistry. In order to extend the analogy further, with respect to arenes and carbon monoxide, some important challenges need to be addressed. For example: the synthesis of clusters that contain arenes and/or carbon monoxide in bonding modes related to those that have been postulated to exist on the surface; the investigation of the changes in electronic character and coordination mode of the ligand as the number and type of metal atoms change, as well as the monitoring of related changes in bonding as a function of ligand type; and the exploration of the migratory patterns that exist on the cluster surface and their relationship to motion in the bulk metallic regime. The remainder of this thesis describes some of the efforts made in response to these challenges.

1.6 References

1. Muetterties, E.L.; *Bull. Soc. Chim. Belg.*, **1975**, *84*, 959.
2. Johnson, B.F.G.; Lewis, J.; Gallop, M.A.; Martinelli, M.; *Faraday Discuss.*, **1991**, *92*, 241.
3. Adams, R.D.; Horvath, I.T.; *Prog. Inorg. Chem.*, **1985**, *33*, 127.
4. Muetterties, E.L.; Rhodin, T.N.; Band, E.; Brucker, C.; Pretzer, H.; *Chem. Rev.*, **1979**, *79*, 91.
5. Baetzold, R.; *Adv. Catal.*, **1976**, *25*, 1.
6. Somorjai, G.A.; *J. Phys. Chem.*, **1990**, *94*, 1013.
7. Albano, V.G.; Ceriotto, A.; Chini, P.; Ciani, G.; Martinego, S.; Anker, W.M.; *J. Chem. Soc., Chem. Comm.*, **1975**, 859.
8. Ciani, G.; Sironi, A.; Martinengo, S.; *J. Chem. Soc., Dalton Trans.*, **1982**, 1099.
9. Chini, P.; *J. Organomet. Chem.*, **1980**, *200*, 37.
10. For example: (a) Vargas, M.D.; Nicholls, J.N.; *Adv. Inorg. Chem. Radiochem.*, **1986**, *30*, 123; (b) Chini, P.; Longoni, G.; Albano, V.G.; *Adv. Organomet. Chem.*, **1976**, *14*, 285.
11. Grimley, T.B.; in *Electronic Structure and Reactivity of Metal Surfaces*, Ed. Derouane, E.; Lucas, A.; Plenum, New York, **1970**, vol. B16.
12. Campbell, I.M.; in *Catalysis at Surfaces*, Chapman & Hall, London, **1988**.
13. Jackson, P.F.; Johnson, B.F.G.; Lewis, J.; Nelson, W.J.H.; McPartlin, M.; *J. Chem. Soc., Dalton Trans.*, **1982**, 2099.
14. Johnson, B.F.G.; Gallop, M.; Roberts, Y.V.; *J. Mol. Cat.*; **1994**, *86*, 51.
15. Somorjai, G.A.; in *Introduction to Surface Chemistry and Catalysis*, Wiley, New York, **1994**, Ch. 6, 402.
16. Connor, J.A.; *Top. Curr. Chem.*, **1977**, *71*, 71.
17. Brewer, L.; *Science*, **1968**, *161*, 115.
18. Ertl, G.; in *Metal Clusters in Catalysis*, Ed. Gates, B.C.; Guczi, L.; Knozinger, H.; Elsevier, Amsterdam, **1986**.
19. Ertl, G.; in *The Nature of the Surface Chemical Bond*, Ed. Rhodin, T.N.; Ertl, G.; North-Holland, Amsterdam, **1979**.
20. Muetterties, E.L.; *Angew. Chem. Int. Ed. Engl.*, **1978**, *17*, 545.
21. Muetterties, E.L.; *Pure Appl. Chem.*, **1978**, *50*, 941.
22. Muetterties, E.L.; *Science*, **1979**, *196*, 839.
23. Muetterties, E.L.; *Pure Appl. Chem.*, **1982**, *54*, 83.
24. Moskovits, M.; *Acc. Chem. Res.*, **1979**, *12*, 229.
25. Evans, J.; *Chem. Soc. Rev.*, **1981**, *10*, 159.
26. Somorjai, G.A.; Bent, B.E.; *Adv. Colloid Interface Sci.*, **1989**, *29*, 223.
27. Gladfelter, W.L.; Rosselet, K.J.; in *The Chemistry of Metal Cluster Complexes*, Ed. Shriver, D.F.; Kaesz, H.D.; Adams, R.D.; VCH, Weinheim, **1990**, 329.
28. Gates, B.C.; *Angew. Chem. Int. Ed. Engl.*, **1993**, *32*, 228.
29. Woodruff, D.P.; Delchar, T.A.; in *Modern Techniques in Surface Science*, Cambridge University Press, Cambridge, U.K., **1986**.
30. Somorjai, G.A.; in *Perspectives in Catalysis*, Ed. Thomas, J.M.; Zamaraev, K.I.; Blackwell, London, **1992**, 147.
31. (a) Johnson B.F.G.; Johnston, R.D.; Lewis, J.; *J. Chem. Soc., Chem. Comm.*, **1967**, 1057; (b) Johnson B.F.G.; Johnston, R.D.; Lewis, J.; *J. Chem. Soc. (A)*, **1968**, 2866; (c) Eady, C.R.; Johnson, B.F.G.; Lewis, J.; *J. Chem. Soc., Dalton Trans.*, **1975**, 2606.
32. Gomez-Sal, M.P.; Johnson, B.F.G.; Lewis, J.; Raithby, P.R.; Wright, A.H.; *J. Chem. Soc., Chem. Comm.*, **1985**, 1682.
33. Fischer, E.O.; Hafner, W.; *Z. Naturforsch*, **1955**, B10, 665.

34. For general features of the coordination of CO to metal surfaces and the theory of bonding see: Albert, M.R.; Yates, J.T.; in *A Surface Scientists Guide to Organometallic Chemistry*, Am. Chem. Soc., Washington, **1987**.

35. Koestner, R.J.; Van Hove, M.A.; Somorjai, G.A.; *Surf. Sci.*, **1981**, *107*, 439.

36. Koel, B.E.; Somorjai, G.A.; in *Catalysis, Science and Technology*, Ed. Anderson, J.R.; Boudart, M.; **1984**, 7, Ch. 3, and references cited therein.

37. (a) Dubois, L.H.; Somorjai, G.A.; *Surf. Sci.*, **1980**, *91*, 514; (b) Cromwell, J.E.; Somorjai, G.A.; *Appl. Surf. Sci.*, **1984**, *19*, 73.

38. Horwitz, C.P.; Shriver, D.F.; *Adv. Organomet. Chem.*, **1984**, *23*, 219.

39. Wade, K.; in *Transition Metal Clusters*, Ed. Johnson, B.F.G.; Wiley, **1980**, 193.

40. Chisholm, M.H.; Hammond, C.E.; Johnston, V.J.; Streib, W.E.; Huffman, J.C.; *J. Am. Chem. Soc.*, **1992**, *114*, 7056.

41. Dahl, L.F.; Doedens, R.J.; *J. Am. Chem. Soc.*, **1966**, *88*, 4847.

42. Li, P.; Curtis, D.; *J. Am. Chem. Soc.*, **1989**, *111*, 8279.

43. Colaianni, M.L.; Chen, J.G.; Weinberg, W.H.; Yates, J.T.; *J. Am. Chem. Soc.*, **1992**, *114*, 3735.

44. (a) Anderson, A.B.; Onwood, D.P.; *Surf. Sci.*, **1985**, *154*, 261; (b) Rong, C.; Satoko, C.; *Surf. Sci.*, **1989**, *223*, 101.

45. (a) Shinn, N.D.; Madey, T.E.; *J. Phys. Chem.*, **1985**, *83*, 5928; (b) Shinn, N.D.; Madey, T.E.; *Phys. Rev. Lett.*, **1984**, *53*, 2481.

46. (a) Benndorf, C.; Krüger, B.; Thieme, F.; *Surf. Sci.*, **1985**, *163*, 675; (b) Lu, J.-P.; Albert, M.R.; Bernasek, S.L.; *Surf. Sci.*, **1989**, *217*, 55.

47. Zaera, F.; Kollin, E.; Gland, J.L.; *Chem. Phys. Lett.*, **1985**, *121*, 464.

48. Hoffmann, F.M.; De Paola, R.A.; *Phys. Rev. Lett.*, **1984**, *52*, 1697.

49. Manssero, M.; Sansoni, M.; Longoni, G.; *J. Chem. Soc., Chem. Comm.*, **1976**, 919.

50. (a) Whitmire, K.H.; Shriver, D.F.; *J. Am. Chem. Soc.*, **1980**, *102*, 1456; (b) Tachikawa, M.; Muetterties, E.L.; *J. Am. Chem. Soc.*, **1980**, *102*, 4541.

51. See for example: (a) Shriver, D.F.; Alich, A.; *Coord. Chem. Rev.*, **1972**, *8*, 15; (b) Darensbourg, M.Y.; Darensbourg, D.J.; Burns, D.; Drew, D.A.; *J. Am. Chem. Soc.*, **1976**, *98*, 3127.

52. Hamilton, D.M.; Willis, W.S.; Stucky, G.D.; *J. Am. Chem. Soc.*, **1981**, *103*, 4255.

53. Dick, D.G.; Stephan, D.W.; *Organometallics*, **1990**, *9*, 1910.

54. Merola, J.S.; Gentile, R.A.; Ansell, G.B.; Modrick, M.A.; Zentz, S.; *Organometallics*, **1982**, *1*, 1731.

55. De Boer, E.J.M.; De With, J.; Orpen, A.G.; *J. Chem. Soc., Chem. Comm.*, **1985**, 1666.

56. Merola, J.S.; Campos, K.S.; Gentile, R.A.; Modrick, M.A.; Zentz, S.; *Organometallics*, **1984**, *3*, 334.

57. Pasynskii, A.A.; Skripkin, Y.V.; Eremenko, I.L.; Kalinnikov, V.T.; Aleksandrov, G.G.; Andrianov, V.G.; Struchkov, Y.T.; *J. Organomet. Chem.*, **1979**, *165*, 49.

58. Herrmann, W.A.; Biersack, H.; Ziegler, M.L.; Weidenhammer, K.; Siegel, R.; Rehder, D.; *J. Am. Chem. Soc.*, **1981**, *103*, 1692.

59. (a) Zeiss, H.; Wheatley, P.J.; Winkler, H.J.S.; *Benzenoid Metal Complexes*, Ronald Press Co., New York, **1966**; (b) Silverthorn, W.E.; *Adv. Organomet. Chem.*, **1975**, *13*, 47; (c) Muetterties, E.L.; Bleeke, J.R.; Wucherer, E.J.; Albright, T.A.; *Chem. Rev.*, **1982**, *82*, 499.

60. Wadepohl, H.; *Angew. Chem. Int. Ed. Engl.*, **1992**, *31*, 247.

61. Shelly, K.; Finster, D.C.; Lee, Y.L.; Scheidt, W.R.; Reed, C.A.; *J. Am. Chem. Soc.*, **1985**, *107*, 5955.

62. Van der Heijden, H.; Orpen, A.G.; Pasman, P.; *J. Chem. Soc., Chem. Comm.*, **1985**, 1576.

63. Keasey, A.; Bailey, P.M.; Maitlis, P.M.; *J. Chem. Soc., Chem. Comm.*, **1978**, 142.

64. Bandy, J.A.; Green, M.L.H.; O'Hare, D.; Prout, K.; *J. Chem. Soc., Chem. Comm.*, **1984**, 1402.

65. Le Bozec, H.; Touchard, D.; Dixneuf, P.H.; *Adv. Organomet. Chem.*, **1991**, *29*, 163 and references cited therein.

66. (a) Harman, W.D.; Taube, H.; *J. Am. Chem. Soc.*, **1987**, *109*, 1883; (b) Omori, H.; Suzuki, H.; Take, Y.; Moro-oka, Y.; *Organometallics*, **1989**, *8*, 2270.

67. Jonas, K.; Koepe, G.; Schieferstein, L.; Mynott, R.; Krüger, C.; Tsai, Y.H.; *Angew. Chem. Int. Ed. Engl.*, **1983**, *22*, 620.

68. Jonas, K.; Wiskamp, V.; Tsai, Y.H.; Krüger, C.; *J. Am. Chem. Soc.*, **1983**, *105*, 5480.

69. Lamanna, W.M.; Gleason, W.B.; Britton, D.; *Organometallics*, **1987**, *6*, 1583.

70. Braga, D.; Dyson, P.J.; Grepioni, F.; Johnson, B.F.G.; *Chem. Rev.*, **1990**, *94*, 1585.

71. Ansell, G.B.; Modrick, M.A.; Bradley, J.S.; *Acta Cryst.*, **1984**, *C40*, 365.

72. Braga, D.; Grepioni, F.; Johnson, B.F.G.; Lewis, J.; Martinelli, M.; Gallop, M.A.; *J. Chem. Soc., Chem. Comm.*, **1990**, 53.

73. Braga, D.; Grepioni, F.; Johnson, B.F.G.; Parisini, E.; Martinelli, M.; Gallop, M.A.; Lewis, J.; *J. Chem. Soc., Dalton Trans.*, **1992**, 807.

74. Chen, H.; Johnson, B.F.G.; Lewis, J.; Braga, D.; Grepioni, F.; Parisini, E.; *J. Chem. Soc., Dalton Trans.*, **1991**, 215.

75. (a) Khand, I.U.; Knox, G.R.; Pauson, P.L.; Watts, W.E.; *J. Chem. Soc., Perkin 1*, **1973**, 975; (b) Bird, P.H.; Fraser, A.R.; *J. Organomet. Chem.*, **1974**, *73*, 103; (c) Gancarz, R.A.; Blount, J.F.; Mislow, K.; *Organometallics*, **1985**, *4*, 2028.

76. Braga, D.; Grepioni, F.; Sabatino, P.; Dyson, P.J.; Johnson, B.F.G.; Lewis, J.; Bailey, P.J.; *J. Chem. Soc., Dalton Trans.*, **1993**, 985.

77. Lewis, J.; Li, C.K.; Ramirez de Arellano, M.C.; Raithby, P.R.; Wong, W.T.; *J. Chem. Soc., Dalton Trans.*, **1993**, 1359.

78. (a) Johnson, B.F.G.; Lewis, J.; Martinelli, M.; Wright, A.H.; Braga, D.; Grepioni, F.; *J. Chem. Soc., Chem. Comm.*, **1990**, 364; (b) Braga, D.; Grepioni, F.; Johnson, B.F.G.; Lewis, J.; Housecroft, C.E.; Martinelli, M.; *Organometallics*, **1991**, *10*, 1260.

79. (a) Wadepohl, H.; Büchner, K.; Herrmann, M.; Pritzkow, H.; *Organometallics*, **1991**, *10*, 861; (b) Wadepohl, H.; Büchner, K.; Pritzkow, H.; *Organometallics*, **1989**, *8*, 2745.

80. Müller, J.; Gaede, P.E.; Qiao, K.; *Angew. Chem. Int. Ed. Engl.*, **1993**, *32*, 1697.

81. Lewis, J.; Li, C.K.; Raithby, P.R.; Wong, W.T.; *J. Chem. Soc., Dalton Trans.*, **1993**, 999.

82. Somorjai, G.A.; in *Introduction to Surface Chemistry and Catalysis*, Wiley, New York, **1994**, Ch. 2, 67.

83. Johnson, A.L.; Muetterties, E.L.; Stöhr, J.; *J. Am. Chem. Soc.*, **1983**, *105*, 7183.

84. (a) Neumann, M.; Mack, J.U.; Bertel, E.; Netzer, F.P.; *Surf. Sci.*, **1985**, *155*, 629; (b) Netzer, F.P.; Rosina, G.; Bertel, E.; *Surf. Sci.*, **1987**, *184*, L397.

85. Netzer, F.P.; Mack, J.U.; *J. Chem. Phys.*, **1983**, *79*, 1017.

86. Netzer, F.P.; Graen, H.H.; Kuhlenbeck, H.; Neumann, M.; *Chem. Phys. Lett.*, **1987**, *133*, 49.

87. Van Hove, M.A.; Lin, R.F.; Somorjai, G.A.; *J. Am. Chem. Soc.*, **1986**, *108*, 2532.

88. Somorjai, G.A.; *Pure Appl. Chem.*, **1988**, *60*, 1499 and references cited therein.

89. Barbieri, A.; Van Hove, M.A.; Somorjai, G.A.; *Surf. Sci.*, **1994**, *306*, 261.

90. Ogletree, D.F.; Van Hove, M.A.; Somorjai, G.A.; *Surf. Sci.*, **1987**, *183*, 1.

91. Lin, R.F.; Blackman, G.S.; Van Hove, M.A.; Somorjai, G.A.; *Acta Cryst., Sect. B.*, **1987**, *43*, 368.

92. Rosina, G.; Rangelov, G.; Bertel, E.; Saalfeld, H.; Netzer, F.P.; *Chem. Phys. Lett.*, **1987**, *140*, 200.

93. Anderson, A.B.; McDevitt, M.R.; Urbach, F.L.; *Surf. Sci.*, **1984**, *146*, 80.

94. Mate, C.M.; Somorjai, G.A.; *Surf. Sci.*, **1985**, *160*, 542.

95. Ohtani, H.; Wilson, R.J.; Chiang, S.; Mate, C.M.; *Phys. Rev. Lett.*, **1988**, *60*, 2398.

96. Somorjai, G.A.; Ohtani, H.; Van Hove, M.A.; *Appl. Surf. Sci.*, **1988**, *33*, 254.

97. Gallop, M.A.; Gomez-Sal, M.P.; Housecroft, C.E.; Johnson, B.F.G.; Lewis, J.; Owen, S.M.; Raithby, P.R.; Wright, A.H.; *J. Am. Chem. Soc.*, **1992**, *114*, 2502.
98. Garfunkel, E.L.; Minot, C.; Gavezzotti, A.; Simonetta, M.; *Surf. Sci.*, **1986**, *176*, 177.
99. Kok, R.A.; Hall, M.B.; *J. Am. Chem. Soc.*, **1985**, *107*, 2599.
100. Byers, B.P.; Hall, M.B.; *Organometallics*, **1987**, *6*, 2319.
101. Elian, M.; Chen, M.M.L.; Mingos, D.M.P.; Hoffmann, R.; *Inorg. Chem.*, **1976**, *15*, 1148.
102. See for example: Cabeza, J.A.; Fernández-Collins, J.M.; Llamazares, A.; Riera, V.; *Organometallics*, **1993**, *12*, 4141.
103. (a) Knox, S.A.R.; Lloyd, B.R.; Orpen, A.G.; Vinas, J.M.; Weber, M.; *J. Chem. Soc., Chem. Comm.*, **1987**, 1498; (b) Knox, S.A.R.; Lloyd, B.R.; Morton, D.A.V.; Nicholls, S.M.; Orpen, A.G.; Vinas, J.M.; Weber, M.; Williams, G.K.; *J. Organomet. Chem.*, **1990**, *394*, 385.
104. Gallop, M.A.; Johnson, B.F.G.; Lewis, J.; McCamley, A.; Perutz, R.N.; *J. Chem. Soc., Chem. Comm.*, **1988**, 1071.
105. Tsai, M.C.; Muetterties, E.L.; *J. Phys. Chem.*, **1982**, *86*, 5067.
106. Avery, N.R.; *J. Chem. Soc., Chem. Comm.*, **1988**, 153.
107. Anson, C.E.; Bailey, P.J.; Conole, G.; Johnson, B.F.G.; Lewis, J.; McPartlin, M.; Powell, H.R.; *J. Chem. Soc., Chem. Comm.*, **1989**, 442.
108. (a) Bullock, L.M.; Field, J.S.; Haines, R.J.; Minshall, E.; Smit, D.N.; *J. Organomet. Chem.*, **1986**, *310*, C47; (b) Bullock, L.M.; Field, J.S.; Haines, R.J.; Minshall, E.; Moore, M.H.; Mulla, F.; Smit, D.N.; Steer, L.M.; *J. Organomet. Chem.*, **1990**, *381*, 429.
109. Dyson, P.J.; Johnson, B.F.G.; Braga, D.; *Inorg. Chim. Acta*, **1994**, *222*, 229.
110. (a) Tsai, M.C.; Muetterties, E.L.; *J. Am. Chem. Soc.*, **1982**, 104, 2534; (b) Tsai, M.C.; Friend, C.M.; Muetterties, E.L.; *J. Am. Chem. Soc.*, **1982**, *104*, 2539.
111. Koel, B.E.; Crowell, J.E.; Bent, B.E.; Mate, C.M.; Somorjai, G.A.; *J. Phys. Chem.*, **1986**, *90*, 2949.
112. (a) Rucker, T.G.; Logan, M.A.; Gentle, T.M.; Muetterties, E.L.; Somorjai, G.A.; *J. Phys. Chem.*, **1986**, *90*, 2703; (b) Gentle, T.M.; Muetterties, E.L.; *J. Phys. Chem.*, **1983**, *87*, 2469.
113. Parker, W.L.; Hexter, R.M.; *J. Am. Chem. Soc.*, **1985**, *107*, 4584.
114. (a) Colquhoun, H.M.; Holton, J.; Thompson, D.J.; Twigg, M.V.; in *New Pathways for Organic Synthesis*, Plenum Press, New York, **1984**, 105; (b) Deeming, A.J.; *Adv. Organomet. Chem.*, **1986**, *26*, 1 and references cited therein.
115. Shvo, V.; Hazum, E.; *J. Chem. Soc., Chem. Comm.*, **1974**, 336.
116. See for example: Johnson, B.F.G.; Lewis, J.; Pippard, D.A.; *J. Chem. Soc., Dalton Trans.*, **1981**, 407.
117. Foulds, G.A.; Johnson, B.F.G.; Lewis, J.; *J. Organomet. Chem.*, **1985**, *296*, 147.
118. Johnson, B.F.G.; Lewis, J.; Nicholls, J.N.; Puga, J.; Raithby, P.R.; Rosales, M.J.; McPartlin, M.; Clegg, W.; *J. Chem. Soc., Dalton Trans.*, **1983**, 277.

Chapter Two

The Systematic Synthesis of Some C_6 Ring Derivatives of $Os_4(\mu\text{-}H)_4(CO)_{12}$

This chapter is primarily concerned with metal cluster induced C-H bond activation, rearrangement and formation. It commences with a brief introduction illustrating this subject with relevant examples that emphasise how such transformations are more prevalent in cluster complexes than in related monometallic systems. Following this section, a detailed description of the reactivity of the tetranuclear hydrido cluster, $Os_4(\mu\text{-}H)_4(CO)_{12}$, and its activated derivative, $Os_4(\mu\text{-}H)_4(CO)_{10}(MeCN)_2$, towards cyclohexa-1,3-diene is provided. A series of organometallic derivatives containing six membered rings have been produced which interact with the cluster framework in a variety of coordination modes. The majority of the C_6 rings in these complexes have undergone C-H bond activation, such that rearrangement or aromatisation of the ring has taken place, however, hydrogenation is also found to occur resulting in complexes with C_6H_9 ligands. Inferences are drawn from these transformations and possible reaction mechanisms are postulated. The reactivity of the tetraosmium hydrido benzene cluster, $Os_4(\mu\text{-}H)_2(CO)_{10}(\eta^6\text{-}C_6H_6)$, is discussed in terms of the synthesis of more highly substituted derivatives and the exchange of the benzene unit for other arenes or π-ligands. Lastly, the synthesis of high nuclearity osmium-benzene clusters is briefly considered.

2.1 An Introduction

Polynuclear coordination may induce reactivity into a ligand that is very different to that produced by mononuclear coordination.[1] In a mononuclear complex, potential coordination sites must be either perpendicular or opposite to one another. However, in polynuclear complexes, *i.e.* clusters, there is also the possibility that they may be on adjacent metal atoms and parallel, thus allowing an unsaturated substrate molecule to bridge two or more sites, or even coordinate at one metal centre and undergo reaction at another. The cleavage of C-H bonds is a very important area in the oxidative-addition reactions of alkanes, alkenes and arenes, and the activation of C-H bonds in these molecules has been demonstrated in a number of cluster systems.

C-H Activation in CH_x Ligands:
The activation of alkyl C-H bonds has been observed in mononuclear metal complexes on numerous occasions, however the process appears to occur far more readily in cluster

compounds which is probably a direct consequence of the interaction of the affected C-H bond with a metal atom adjacent to the primary coordination site.[2] An example of a metal carbonyl cluster containing an alkyl ligand is Os$_3$(μ-H)(CO)$_{10}$(CH$_3$).[3] This complex has a formal electron count of 46 and is therefore deficient by two electrons according to the Effective Atomic Number (EAN) electron counting rules. The structure of Os$_3$(μ-H)(CO)$_{10}$(CH$_3$) has not been confirmed by X-ray crystallographic methods, but spectroscopic evidence suggests a significant interaction of at least one C-H bond with an adjacent metal atom, and a structure similar to that illustrated in Scheme 2.1.1 (species II) has been proposed.[4] An interaction of this type has been found in the binuclear complex, [Fe$_2$(μ-CH$_3$)(μ-CO)(Ph$_2$PCH$_2$PPh$_2$)(η^5-C$_5$H$_5$)$_2$]$^+$, for which structural characterisation in the solid-state has revealed the presence of an asymmetric bridging methyl ligand containing a strong interaction of one of the methyl hydrogen atoms to one of the iron atoms.[5] The structure can be viewed as the first step in the cleavage of the C-H bond and indeed Os$_3$(μ-H)(CO)$_{10}$(CH$_3$) smoothly converts into the methylene compound Os$_3$(μ-H)$_2$(CO)$_{10}$(μ-CH$_2$) (species III in Scheme 2.1.1) which contains a bridging CH$_2$ ligand and two bridging hydride ligands on an Os$_3$ triangle.[6] This C-H bond cleavage is reversible, and the two compounds exist in equilibrium in solution,[3] as evidenced by NMR spectroscopy. It has been proposed that the activation of a C-H bond on a bridging CH$_2$ unit can occur by interaction with a third metal atom, yielding a stable triply bridging methylidyne ligand.[2] No examples of the partially activated intermediate (species IV) have been reported, but the methylene complex is transformed into the methylidyne complex Os$_3$(μ-H)$_3$(CO)$_9$(μ_3-CH) upon decarbonylation (species V).[3]
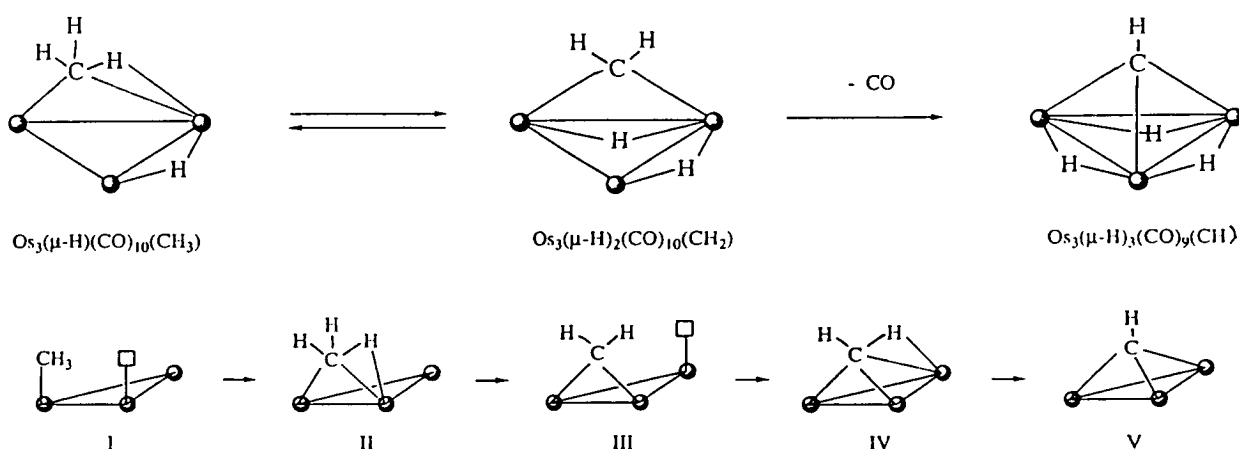
Scheme 2.1.1: The series of C-H bond activations which transform the alkyl cluster Os$_3$(μ-H)(CO)$_{10}$(CH$_3$) into the methylidyne complex Os$_3$(μ-H)$_3$(CO)$_9$(μ_3-CH).

Activation of Olefinic C-H Bonds:

Activation of C-H bonds in aromatic and alkane moieties by mononuclear metal complexes has been observed in a number of cases, however the activation of olefinic C-H bonds in alkenes is quite rare and seems to be achieved most effectively by cluster compounds.[2] The triosmium cluster compound, $Os_3(CO)_{11}(C_2H_4)$, which contains a π-coordinated ethylene ligand,[7] loses CO when heated and is converted into the vinylidene complex $Os_3(\mu\text{-}H)_2(CO)_9(\mu_3\text{-}C=CH_2)$,[8] *via* a sequence of 1,1 diactivations which almost certainly traverse the σ,π-vinyl complex $Os_3(\mu\text{-}H)(CO)_{10}(\mu\text{-}C_2H_3)$[9] (see Scheme 2.1.2). This latter complex is produced from the reaction between $Os_3(CO)_{10}(MeCN)_2$ and C_2H_4,[10] probably *via* a reaction sequence involving olefin complexation to one metal atom and C-H activation at an adjacent metal site, and undergoes transformation into $Os_3(\mu\text{-}H)_2(CO)_9(\mu_3\text{-}C=CH_2)$ on heating.[11]
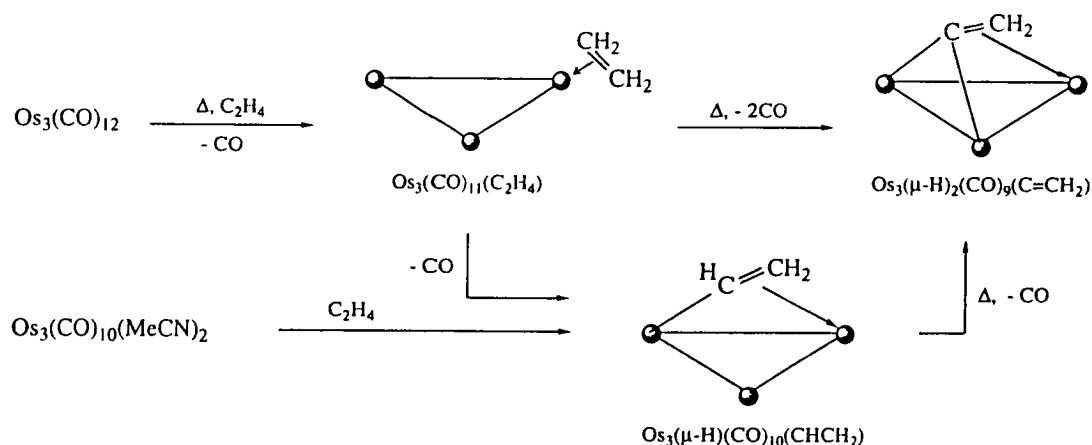
Scheme 2.1.2: The reaction of $Os_3(CO)_{12}$ with C_2H_4 at 125°C.

Activation of Aryl C-H Bonds and Orthometallation Reactions:

The activation of C-H bonds in arenes by both mononuclear and cluster complexes has been documented on a number of occasions.[12] An example of the latter situation is the formation of the triosmium benzyne complex, $Os_3(\mu\text{-}H)_2(CO)_9(\mu_3\text{-}C_6H_4)$, from the reaction of benzene with $Os_3(CO)_{12}$ at 463K,[11] or alternatively, with the activated cluster $Os_3(CO)_{10}(MeCN)_2$ under more moderate conditions.[13] The mechanism involves a 1,2 diactivation, and the cluster complex has been shown crystallographically to contain a triply bridging C_6H_4 benzyne ligand. The same benzyne derivative may also be produced upon irradiation or thermolysis in toluene of the face-capping benzene cluster, $Os_3(CO)_9(\mu_3\text{-}\eta^2:\eta^2:\eta^2\text{-}C_6H_6)$, which readily isomerises by the activation of two ring C-H bonds with transfer of the H-atoms to the metal core.[14,15] It has been further established that the

prolonged thermolysis of the phosphine substituted μ_3 benzene complexes, $Os_3(CO)_{9-n}(PPh_3)_n(\mu_3\text{-}\eta^2{:}\eta^2{:}\eta^2\text{-}C_6H_6)$ (n = 0, 1, 2), in toluene results in conversion to the corresponding μ_3 benzyne compounds, $Os_3(\mu\text{-}H)_2(CO)_{9-n}(PPh_3)_n(\mu_3\text{-}\eta^1{:}\eta^2{:}\eta^1\text{-}C_6H_4)$, and that the rate of the *intra*molecular oxidative-addition increases with phosphine substitution (*i.e.* with increasing electron richness of the cluster unit).[15]

Cluster complexes containing aryl-substituted ligands readily undergo orthometallation reactions that frequently involve the use of two or more metal atoms.[2] For example, the pyrolysis of $Os_3(CO)_{10}(PPh_3)_2$ and of $Os_3(CO)_{12}$ with triphenylphosphine has yielded the complexes, $Os_3(CO)_8(\mu\text{-}Ph)(\mu\text{-}PPh_2)(\mu_3\text{-}PPhC_6H_4)$, $Os_3(\mu\text{-}H)(CO)_8(PPh_3)(\mu_3\text{-}PPh_2C_6H_4)$, and $Os_3(\mu\text{-}H)(CO)_9(PPh_3)(\mu\text{-}PPh_2C_6H_4)$, as well as the benzyne derivatives $Os_3(CO)_7(\mu\text{-}PPh_2)_2(\mu_3\text{-}C_6H_4)$ and $Os_3(\mu\text{-}H)(CO)_7(PPh_3)(\mu\text{-}PPh_2)(\mu_3\text{-}C_6H_4)$,[16] suggesting that the orthometallation step precedes the P-C cleavage of the phenyl ring from the phosphine unit to produce the benzyne moiety. The former complex contains a triply bridging $PPhC_6H_4$ ligand in which the phosphorous atom bridges two osmium atoms and the orthometallated phenyl ring is bonded to the third osmium atom. It also contains an unusual $\mu\text{-}\eta^1\text{-}C_6H_5$ ring that was apparently cleaved from the PPh_3 ligand. The complex $Os_3(\mu\text{-}H)(CO)_8(PPh_3)(\mu_3\text{-}PPh_2C_6H_4)$ contains a triply bridging $PPh_2C_6H_4$ unit in which the metallated carbon atom bridges two osmium atoms, and in $Os_3(\mu\text{-}H)(CO)_9(PPh_3)(\mu\text{-}PPh_2C_6H_4)$ the orthometallated $PPh_2C_6H_4$ ligand bridges only two metal atoms. In the final two complexes the C_6H_4 ligand serves as a triple bridge in the μ_3- coordination mode.

Clearly, C-H bond activation is one of the predominant reactions that hydrocarbon ligands undergo when coordinated to metal clusters. This chapter describes a series of reactions between cyclohexa-1,3-diene and the tetrahedral osmium cluster $Os_4(\mu\text{-}H)_2(CO)_{12}$ **1**, which illustrate that, once coordinated to the cluster unit, the diene ligand can undergo a number of transformations such as hydrogenation, isomerisation, and C-H bond activation with dehydrogenation, resulting ultimately in benzene products.

2.2 Intermediates in the Synthesis of $Os_4(\mu\text{-}H)_2(CO)_{10}(\eta^6\text{-}C_6H_6)$ 6

The activated tetranuclear cluster $Os_4(\mu\text{-}H)_4(CO)_{10}(MeCN)_2$ **2**, may be prepared from the reaction of $Os_4(\mu\text{-}H)_4(CO)_{12}$ **1** with Me_3NO in acetonitrile at room temperature. Treatment of this highly reactive cluster with cyclohexa-1,3-diene in dichloromethane at room temperature for 6 hours, or alternatively the direct reaction of a dichloromethane solution of **1** with Me_3NO in the presence of cyclohexa-1,3-diene at -78°C, yields several products. Four major compounds have been isolated from the reaction mixture after chromatographic

separation using a dichloromethane-hexane solution (1:3, v/v) as eluent. These products have been identified on the basis of their spectroscopic properties and crystal structure determinations as, $Os_4(\mu-H)_3(CO)_{11}(\mu_2-\eta^1:\eta^2-C_6H_9)$ **3**, $Os_4(\mu-H)_2(CO)_{12}(\eta^2-C_6H_8)$ **4**, $Os_4(\mu-H)_2(CO)_{11}(\eta^4-C_6H_8)$ **5** and $Os_4(\mu-H)_2(CO)_{10}(\eta^6-C_6H_6)$ **6**. The remaining products from these reactions are obtained in such low yields that characterisation has not been possible. However, if the reaction is subjected to slightly more forcing conditions, *i.e.* by heating a dichloromethane solution of $Os_4(\mu_2-H)_4(CO)_{10}(MeCN)_2$ **2** to reflux in the presence of cyclohexa-1,3-diene for an 18 hour period, the yields of these additional products are enhanced, thus allowing their isolation and identification (see Section 2.4). A series of separate experiments have further established that upon heating, the η^2 diene complex **4** undergoes conversion to the η^4 diene cluster **5**, which is subsequently converted to the benzene complex **6**. These conversions are by no means quantitative and only occur in low yield, with the thermolysis at higher temperatures leading to further cluster decomposition rather than enhanced yields. This series of reactions is illustrated in Scheme 2.2.1.

$Os_4(\mu-H)_4(CO)_{12}$ **1**   or $Os_4(\mu-H)_4(CO)_{10}(MeCN)_2$ **2**
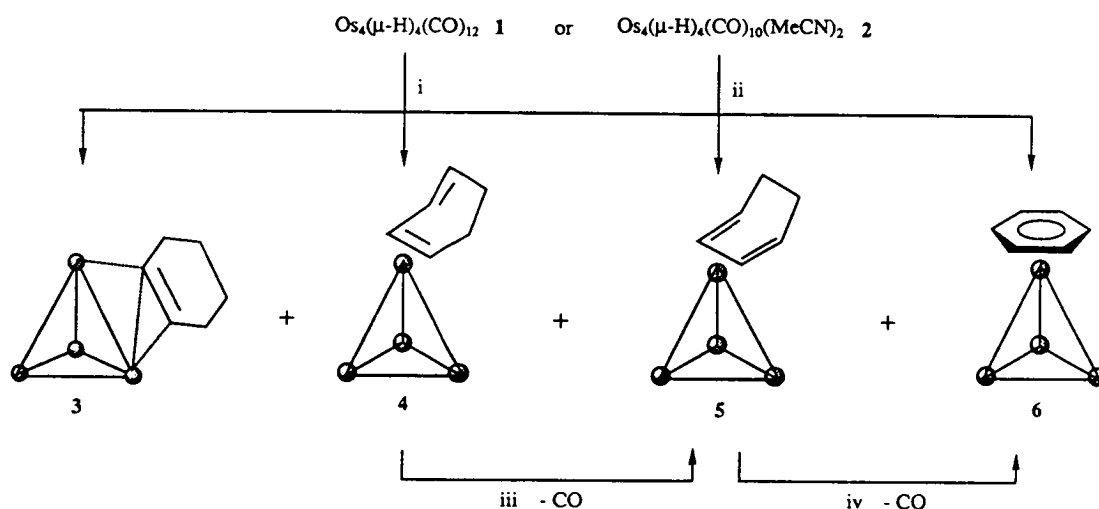
Scheme 2.2.1: The Synthesis of Clusters **3**, **4**, **5** and **6**: (i) 3 mol. equiv. $Me_3NO/1,3-C_6H_8/$ $CH_2Cl_2/-78°C$, (ii) $1,3-C_6H_8/CH_2Cl_2/RT.$, (iii) and (iv) Δ, hexane.

Compound **3** was characterised as $Os_4(\mu-H)_3(CO)_{11}(\mu_2-\eta^1:\eta^2-C_6H_9)$ from a comparison of its infrared spectrum with that reported in the literature.[17] Its formulation was confirmed by mass spectroscopy, with the spectrum exhibiting a parent peak at 1154 (calc. 1153) amu, followed by peaks corresponding to the sequential loss of several carbonyl groups. The tetraosmium cyclohexenyl cluster **3** has been previously observed, in low yield, from the photolysis of a benzene solution of $Os_4(\mu-H)_4(CO)_{12}$ **1** containing excess cyclohexene.[17] Its molecular structure has been determined by a single crystal X-ray

analysis, and Figure 2.2.1 shows that the four osmium atoms define a tetrahedron, with the cyclohexene ring bridging a M-M edge *via* a σ-interaction with one metal atom, and a π-interaction with the other, thereby contributing three electrons to the cluster framework. This type of olefin coordination mode is the same as that observed in the related triosmium clusters $Os_3(\mu\text{-}H)(CO)_{10}(HC=CH_2)$[9] and $Os_3(\mu\text{-}H)(CO)_{10}(HC=CHEt)$.[18]
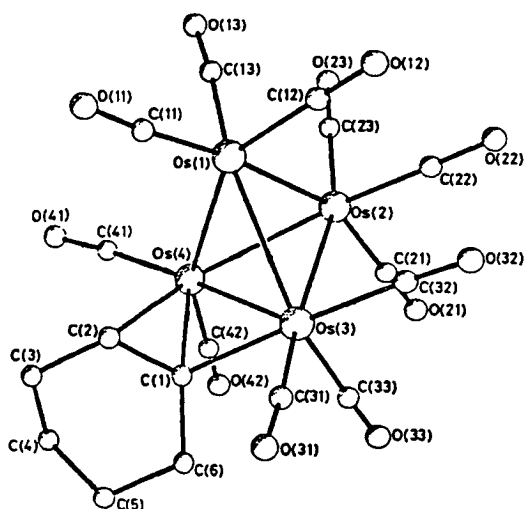
Figure 2.2.1: The molecular structure of $Os_4(\mu\text{-}H)_3(CO)_{11}(\mu_2\text{-}\eta^1{:}\eta^2\text{-}C_6H_9)$ **3**.

The molecular formula of $Os_4(\mu\text{-}H)_2(CO)_{12}(\eta^2\text{-}C_6H_8)$ **4** was initially proposed on evidence provided by the customary spectroscopic techniques. The infrared spectrum shows peaks between 2080 and 1956 cm^{-1} that are typical of terminally bonded CO, and also a weak band at 1880 cm^{-1} which suggests the presence of a bridging carbonyl ligand. The mass spectrum exhibits a strong parent peak at 1179 (calc. 1178) amu, followed by peaks corresponding to the successive loss of twelve carbonyl groups. The ^{1}H NMR spectrum of **4**, recorded in CDCl$_3$, exhibits seven multiplet resonances at δ values of 4.95 (2H), 3.26 (1H), 3.06 (1H), 2.45 (1H), 1.82 (1H), 1.28 (1H) and 1.11 (1H) ppm, and also a broad singlet at δ -19.62 (2H) ppm. Whilst the spectrum has not been subjected to a detailed analysis, the following assignments appear to be quite reasonable; the signal at δ 4.95 ppm may be attributed to the two olefinic protons on the free double bond of the η^2 cyclohexadiene moiety, whilst the resonances at δ 3.26 and 3.06 ppm represent those olefinic protons of the double bond involved in the interaction with the cluster. The four signals between δ 2.45 and 1.11 ppm may be assigned to the aliphatic protons of the cyclohexadiene, and the final resonance at δ -19.62 ppm is typical of bridging hydrides, with its integral suggesting the presence of two such ligands.

Attempts were made to characterise **4** in the solid-state by X-ray diffraction, but the crystal (grown from a toluene solution at -25°C) was found to be affected by disorder that could not be fully modelled, hence preventing a complete interpretation of the system.

However, despite the disorder, the information available from the crystallographic study suggests the structure proposed from spectroscopic data, *i.e.* a tetrahedron of osmium atoms containing eleven terminal and one bridging carbonyl group and an η^2 coordinated diene ligand, as illustrated in Figure 2.2.2.
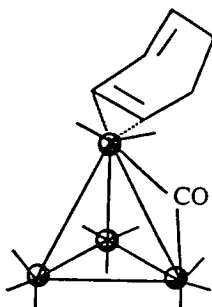
Figure 2.2.2: The proposed molecular structure of $Os_4(\mu-H)_2(CO)_{12}(\eta^2-C_6H_8)$ **4**.

The infrared spectrum of **5** contains peaks in the carbonyl stretching region between 2092 and 1842 cm^{-1}, indicating the presence of both terminal and bridging carbonyl ligands. The mass spectrum exhibits a parent peak at 1150 (calc. 1151) amu followed by peaks corresponding to the subsequent loss of eleven CO groups, suggesting that the molecular formula of cluster **5** is $Os_4(H)_2(CO)_{11}(C_6H_8)$. The ^1H NMR spectrum corroborates such a formulation containing a broad singlet resonance at δ -19.70 ppm (2H) which is typical of bridging hydride ligands, in addition to three multiplet resonances at δ 5.58, 3.96 and 2.02 ppm with relative intensities 2: 2: 4. This signal pattern is typical of a coordinated η^4 cyclohexadiene moiety, in which the former two signals can be assigned to the olefinic protons of the diene, and the latter to the four aliphatic ring protons.

Crystals of $Os_4(\mu-H)_2(CO)_{11}(\eta^4-C_6H_8)$ **5**, suitable for single crystal X-ray analysis, were grown from a toluene solution at -25°C. The solid-state molecular structure of **5** is shown in Figure 2.2.3 together with relevant structural parameters and, as anticipated from spectroscopic data, the compound consists of an Os_4 tetrahedron containing a cyclohexa-1,3-diene ligand bonded to a single osmium atom *via* its two unsaturated bonds.

The Os-Os distances within the tetrahedral metal atom framework of $Os_4(\mu-H)_2(CO)_{11}(\eta^4-C_6H_8)$ **5** range from 2.8069(7) to 2.9354(7) Å. The cyclohexadiene ligand is terminally bound to a single osmium atom [Os(3)] of the cluster polyhedron in an η^4 manner similar to that observed in the related triosmium cluster $Os_3(CO)_{10}(\eta^4-C_6H_8)$.[20] This type of coordination mode has also been observed in a number of the ruthenium and osmium cluster complexes that shall be discussed in subsequent chapters. The Os-C(diene) bonding distances in $Os_4(\mu-H)_2(CO)_{11}(\eta^4-C_6H_8)$ **5** range from 2.191(13) to 2.248(13) Å,
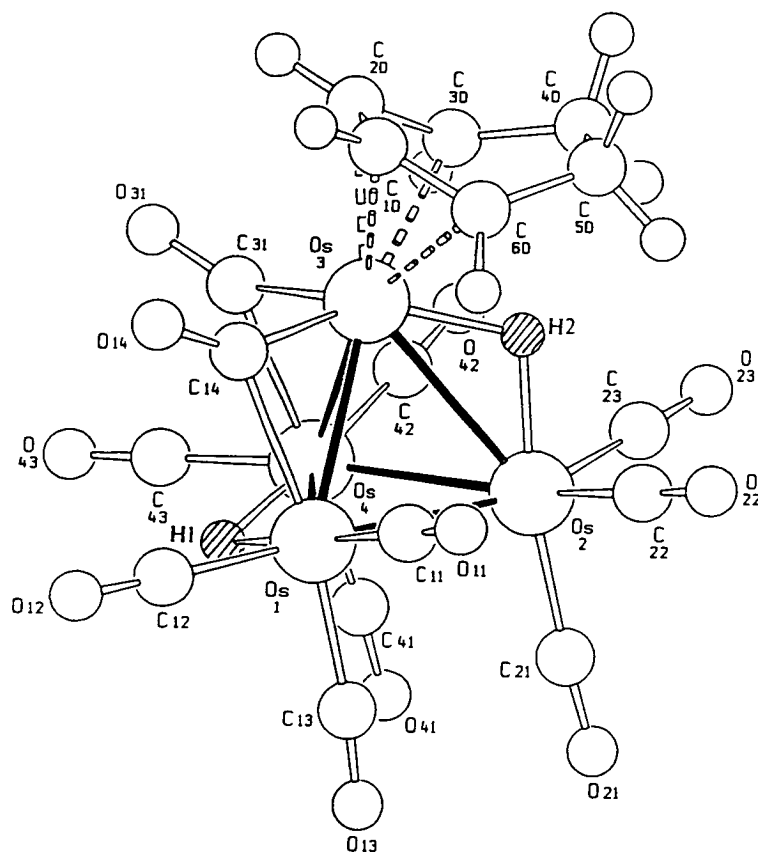
Figure 2.2.3: The molecular structure of Os₄(μ-H)₂(CO)₁₁(η⁴-C₆H₈) 5 in the solid-state showing the atomic labelling scheme. The C-atoms of the CO ligands bear the same numbering as the corresponding O-atoms. The H (hydride) positions were determined by XHYDEX,[19] and correspond to niches in the ligand envelope. Relevant bond distances (Å) include: Os(1)-Os(2) 2.8277(8), Os(1)-Os(3) 2.8295(8), Os(1)-Os(4) 2.9354(7), Os(2)-Os(3) 2.9009(8), Os(2)-Os(4) 2.8113(7), Os(3)-Os(4) 2.8069(7), mean Os-C(CO_terminal) 1.912(14), mean C-O(CO_terminal) 1.137(18), Os(3)-C(14) 1.933(13), Os(1)···C(14) 2.326(13), C(14)-O(14) 1.172(16), Os(3)-C(31) 1.913(14), Os(4)···C(31) 2.311(14), C(31)-O(31) 1.179(17), Os(3)-C(1D) 2.200(13), Os(3)-C(2D) 2.191(13), Os(3)-C(3D) 2.226(13), Os(3)-C(6D) 2.248(13), C(1D)-C(2D) 1.442(18), C(1D)-C(6D) 1.357(18), C(2D)-C(3D) 1.449(18), C(3D)-C(4D) 1.525(19), C(4D)-C(5D) 1.502(19), C(5D)-C(6D) 1.477(18).

and within the diene ring three C-C bonds are short (those involved in an interaction with the ruthenium atoms) and the other three are longer [mean 1.41(2) *vs.* 1.50(2) Å] suggesting that the diene contains a delocalised C₄ section. The cyclohexa-1,3-diene ligand is positioned with the -CH₂-CH₂- section of the ring bent away from the cluster core. There are eleven CO ligands, nine of which are coordinated in a terminal mode, three on each of the osmium atoms not involved in bonding with the C₆H₈ ligand, and the remaining two carbonyls are in asymmetric bridging positions along the Os(1)-Os(3) and Os(3)-Os(4) edges with shorter distances from the diene bound Os-atom, *i.e.* Os(3) [Os(3)-C(14) 1.933(13), Os(3)-C(31) 1.913(14) Å *vs.* Os(1)-C(14) 2.326(13), Os(4)-C(31) 2.311(14) Å].

The H(hydride) atoms in **5** could not be located experimentally, however a close analysis of the molecular space filling diagram revealed the presence of two large cavities in the ligand envelope along the Os(1)-Os(4) and Os(2)-Os(3) edges. These niches are accompanied by a pronounced distortion of the CO ligands, which are bent away from the metal-metal bonds as illustrated in Figure 2.2.4 with respect to the Os(1)-Os(4) edge. The hydride ligands are thought to be situated in bridging positions along these edges on the basis of the least energetic steric interactions with the surrounding ligands, and it is worth noting that these two Os-Os bonds are also the longest observed in the molecule [2.9354(7) and 2.9009(8) Å, respectively]. The position of these hydrides has been verified using the program XHYDEX.[19] A distance of 1.83 Å was chosen for the Os-H interaction, and the results of these calculations are in total agreement with the supposedly preferred location of the hydrides within the largest cavities of the ligand envelope.
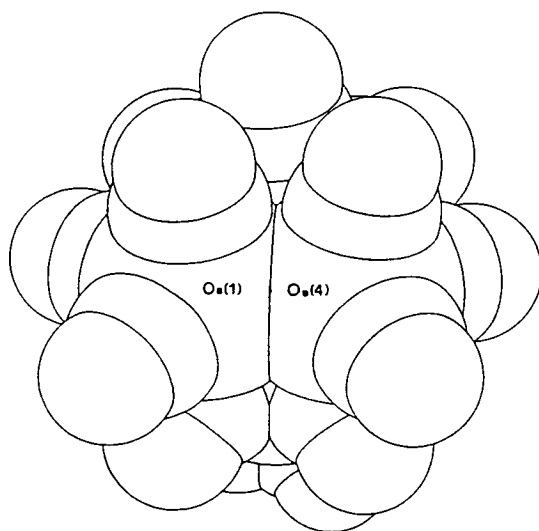
Figure 2.2.4: Space filling representation of the structure of **5** along the Os(1)-Os(4) edge, showing a large niche in the ligand envelope corresponding to the XHYDEX location of a hydride ligand.

The tetraosmium benzene cluster, $Os_4(\mu\text{-}H)_2(CO)_{10}(\eta^6\text{-}C_6H_6)$ **6**, has been previously observed from a reaction similar to that described above, using slightly more forcing conditions, and was therefore easily identified by infrared spectroscopy.[21] The molecular structure of **6** has been determined by a single crystal X-ray diffraction analysis and shows that the benzene ligand is coordinated to a single osmium atom of the tetrahedron in an η^6 fashion (see Figure 2.2.5). As described in the introductory chapter, the terminal coordination mode observed in this complex is that most frequently adopted by arenes in cluster compounds, and there are examples of tri,[22] tetra,[23] penta,[24] hexa,[25] hepta,[26] and octanuclear [27] clusters of ruthenium and osmium containing η^6 benzene ligands.
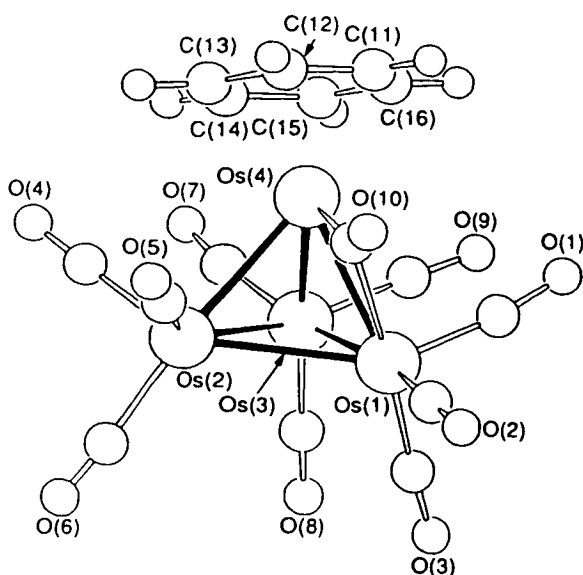
Figure 2.2.5: The molecular structure of $Os_4(\mu\text{-}H)_2(CO)_{10}(\eta^6\text{-}C_6H_6)$ **6**.

Compounds **4, 5** and **6** emerge as a closely related series; as a CO ligand is lost, additional electron-pair donation from the C_6 organic fragment is observed, paralleling the change from an η^2 to an η^4 and then to an η^6 bonding configuration. The conversion from **5** to **6** not only requires the loss of a CO ligand, but also the elimination of dihydrogen and aromatisation of the ring *via* the activation of two C-H bonds. This conversion has also been found to proceed smoothly upon irradiation,[28] and it is therefore possible that a similar process, *viz.* CO-ejection, is the primary step for both the thermal and photolytic reactions. The coordinatively unsaturated intermediate compounds generated by CO expulsion may then gain the two electrons required to stabilise the cluster by interacting with the second unsaturated C-C bond of the diene (**4→5**), or by causing ring aromatisation (**5→6**).

The precise mechanism by which these reactions occur is unclear. However, since the formation of $Os_4(\mu\text{-}H)_3(CO)_{11}(\mu_2\text{-}\eta^1:\eta^2\text{-}C_6H_9)$ **3** involves both the hydrogenation and isomerisation of coordinated cyclohexa-1,3-diene, and the formation of $Os_4(\mu\text{-}H)_2(CO)_{10}(\eta^6\text{-}C_6H_6)$ **6** involves dehydrogenation of the same diene, it would appear that the reaction sequence requires the presence of both a 'sacrificial' and a 'benefactor' molecule of cyclohexa-1,3-diene. Thus, a mechanistic pathway similar to that shown in Scheme 2.2.2 may be involved. The product $Os_4(\mu\text{-}H)_3(CO)_{11}(\mu_2\text{-}\eta^1:\eta^2\text{-}C_6H_9)$ **3** is commonly observed under all reaction conditions studied, and it is easy to envisage its formation from either the C_6H_{10} produced during the mechanism outlined in Scheme 2.2.2 (possibly *via* a sequence involving olefin complexation at one metal atom followed by C-H activation at an adjacent one), or directly from cyclohexa-1,3-diene *via* partial hydrogenation and C-H bond formation, together with C-H cleavage and Os-C σ-bond formation. This species does not seem to be an active intermediate in the formation of

clusters **4, 5** and **6**, instead it appears to be an intermediate on route to the formation of a μ_3-η^1:η^2:η^1 alkyne-type complex (see Section 2.4).

$Os_4(\mu\text{-}H)_4(CO)_{12}$ **1**
60 e

$-H_2$
$+C_6H_8$

$Os_4(\mu\text{-}H)_2(CO)_{12}(C_6H_8)$ **4**
60 e

$-CO$

$Os_4(\mu\text{-}H)_2(CO)_{11}(C_6H_8)$ **5**
60 e

$-CO$

$Os_4(\mu\text{-}H)_2(CO)_{10}(C_6H_8)$
58 e

$+C_6H_8$

$Os_4(\mu\text{-}H)_2(CO)_{10}(C_6H_6)$ **6**
60 e

$-C_6H_{10}$
C-H bond cleavage,
H-migration

$Os_4(CO)_{10}(C_6H_8)(C_6H_{10})$
58 e

H-migration
C-H bond formation

$Os_4(\mu\text{-}H)_2(CO)_{10}(C_6H_8)_2$
60 e
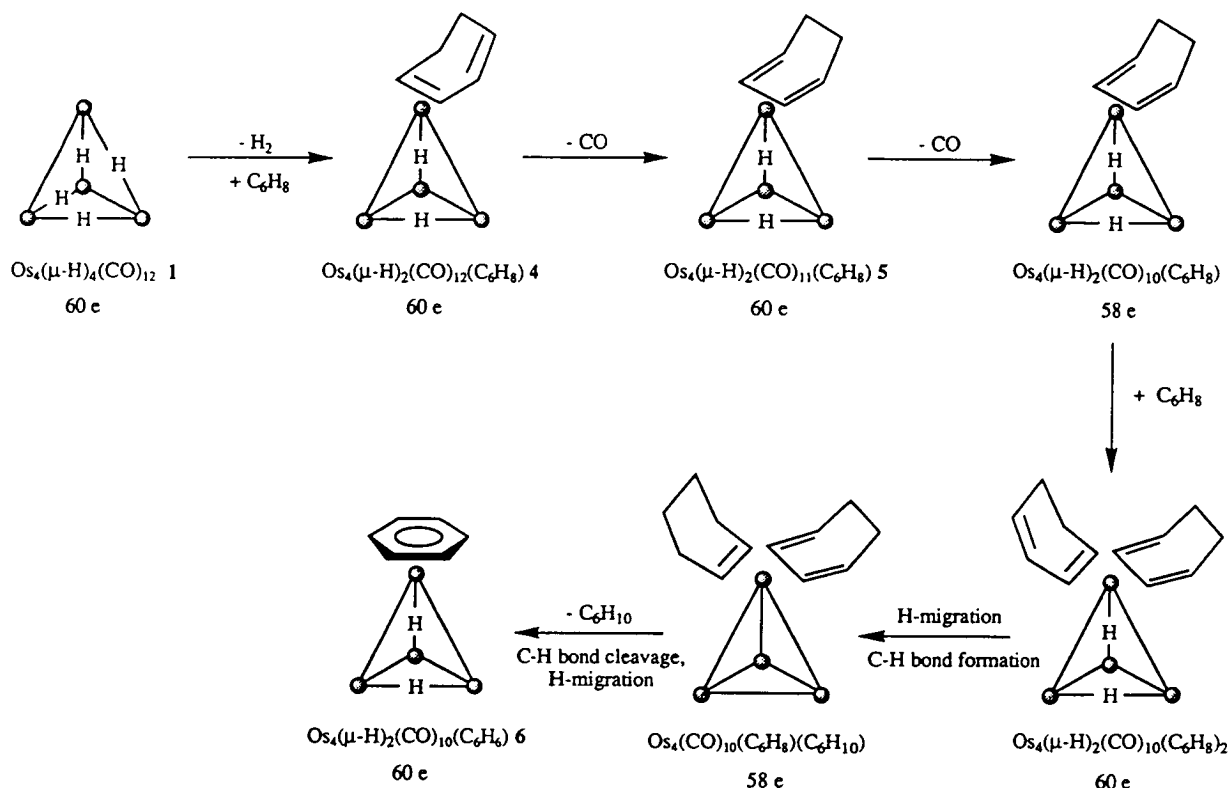
Scheme 2.2.2: A possible mechanism for the reaction of $Os_4(\mu\text{-}H)_4(CO)_{12}$ **1** with 1,3-C_6H_8.

It is apparent from the synthetic route outlined above that, in this tetraosmium system, the cyclohexa-1,3-diene moiety bonds to the cluster framework firstly through a single double bond and then, on the removal of CO, through the 1,3-diene unit, before dehydrogenation *via* the cleavage of two C-H bonds occurs with the formation of the benzene product. A similar reaction pathway has been paralleled by the triosmium benzene cluster, $Os_3(CO)_9(\mu_3\text{-}\eta^2:\eta^2:\eta^2\text{-}C_6H_6)$, which reacts with Me_3NO and cyclohexa-1,3-diene to produce a benzene-diene cluster containing an η^2 coordinated diene ligand, *viz.* $Os_3(CO)_8(\eta^2\text{-}C_6H_8)(\mu_3\text{-}\eta^2:\eta^2:\eta^2\text{-}C_6H_6)$.[29] This reacts with a further aliquot of Me_3NO to form the η^4 diene complex, $Os_3(CO)_7(\eta^4\text{-}C_6H_8)(\mu_3\text{-}\eta^2:\eta^2:\eta^2\text{-}C_6H_6)$, which in turn readily produces the *bis*(benzene) species, $Os_3(CO)_6(\eta^6\text{-}C_6H_6)(\mu_3\text{-}\eta^2:\eta^2:\eta^2\text{-}C_6H_6)$, on reaction with trityl tetrafluoroborate followed by treatment with DBU (diazabicyclo[5.4.0]undeca-7-ene) or simply upon thermolysis in dichloromethane. However, the coordination mode of the cyclohexadiene moiety in these examples, and its subsequent conversion to benzene, is not the same for all cluster systems. For example, the triosmium-diene cluster, $Os_3(CO)_{10}(\eta^4\text{-}C_6H_8)$,[20] contains the cyclohexa-1,3-diene unit

coordinated in a similar manner to that observed in the tetranuclear species, $Os_4(\mu\text{-}H)_2(CO)_{10}(\eta^6\text{-}C_6H_6)$ **5**, and the triosmium benzene-diene species $Os_3(CO)_7(\eta^4\text{-}C_6H_8)(\mu_3\text{-}\eta^2\text{:}\eta^2\text{:}\eta^2\text{-}C_6H_6)$, however, this compound is reluctant to undergo conversion to the benzene derivative, $Os_3(CO)_9(\mu_3\text{-}\eta^2\text{:}\eta^2\text{:}\eta^2\text{-}C_6H_6)$, which contains the benzene moiety in a face-capping mode. This observation indicates that whilst an η^4 diene ligand can be converted into a terminal benzene group, it is far more difficult to convert into a facial benzene ligand. In clusters of higher nuclearity, such as derivatives of the penta- and hexaruthenium clusters $Ru_5C(CO)_{15}$ and $Ru_6C(CO)_{17}$, the diene is found to bridge an edge of the cluster polyhedron in a $\mu_2\text{-}\eta^2\text{:}\eta^2$ fashion.[24a,25a] Treatment with Me_3NO or thermolysis, results in the smooth conversion of these compounds into their corresponding benzene derivatives, in which the benzene may adopt either a facial or terminal coordination mode. This suggests that C-H bond cleavage leading to a face-capping benzene moiety is probably assisted by a multiple interaction between the diene and the central cluster unit.

2.3 The Reactivity of $Os_4(\mu\text{-}H)_2(CO)_{10}(\eta^6\text{-}C_6H_6)$ 6

In an extension to the synthetic route described for the preparation of the benzene cluster, $Os_4(\mu\text{-}H)_2(CO)_{10}(\eta^6\text{-}C_6H_6)$ **6**, from $Os_4(\mu\text{-}H)_4(CO)_{12}$ **1**, complex **6** can itself undergo further reaction with three molecular equivalents of Me_3NO in dichloromethane in the presence of cyclohexa-1,3-diene to yield two new products. These products can be separated from the reaction mixture by t.l.c. using a dichloromethane-hexane (1:3, v/v) solution as eluent, and have been characterised as the benzene-diene complexes $Os_4(CO)_9(\eta^4\text{-}C_6H_8)(\eta^6\text{-}C_6H_6)$ **7** and $Os_4(\mu\text{-}H)_2(CO)_8(\eta^4\text{-}C_6H_8)(\eta^6\text{-}C_6H_6)$ **8**.

Compound **7** was identified as $Os_4(CO)_9(\eta^4\text{-}C_6H_8)(\eta^6\text{-}C_6H_6)$ from a comparison of its infrared spectrum with that previously reported, and its formulation verified by mass spectroscopy. As with the benzene complex, $Os_4(\mu\text{-}H)_2(CO)_{10}(\eta^6\text{-}C_6H_6)$ **6**, compound **7** has been previously reported as a product from the reaction of $Os_4(\mu\text{-}H)_4(CO)_{10}(MeCN)_2$ with cyclohexa-1,3-diene under more vigorous conditions.[21] Its molecular structure has been confirmed by a single crystal X-ray diffraction analysis, which shows that both the benzene and the cyclohexadiene ligands are bonded to single metal atoms of the tetrahedral framework in η^6 and η^4 coordination modes, respectively (see Figure 2.3.1).

Formulation of the second compound as $Os_4(\mu\text{-}H)_2(CO)_8(\eta^4\text{-}C_6H_8)(\eta^6\text{-}C_6H_6)$ **8** was initially based upon evidence provided by spectroscopic techniques, and was later confirmed by an X-ray diffraction analysis using a crystal grown from the slow evaporation of a $CDCl_3$ solution at room temperature. The infrared spectrum of **8** displays
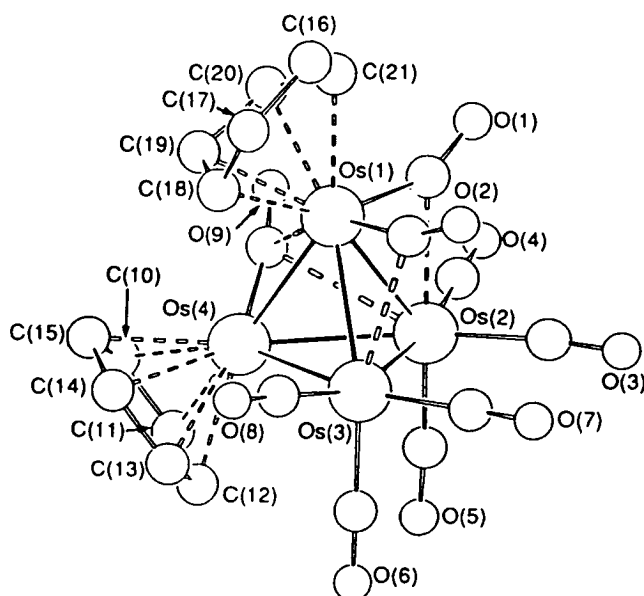
Figure 2.3.1: The molecular structure of $Os_4(CO)_9(\eta^4-C_6H_8)(\eta^6-C_6H_6)$ **7**.

peaks between 2068 and 1845 cm^{-1}, suggesting the presence of both terminal and bridging carbonyl ligands. Its mass spectrum contains a strong parent peak at 1144 (calc. 1145) amu, which is followed by the successive loss of eight CO groups. At room temperature the ^{1}H NMR spectrum of **8** exhibits two broad resonances in the hydride region at δ -15.72 and -19.44 ppm. A singlet resonance is observed at δ 5.74 ppm with a relative intensity of 6 which is consistent with a terminally bound benzene ligand, and the diene gives rise to four broad signals at δ 5.04, 3.55, 2.16 and 1.67 ppm with equal relative intensities. The former two signals are probably derived from the olefinic protons and the latter two from the aliphatic ring protons. On cooling, these broad signals are each resolved into a series of multiplet resonances. The low temperature spectrum is very complicated and has not been fully resolved, however, the change in broadness of the spectrum with temperature does indicate a degree of fluxionality. Inspection of the crystal structure indicates that each proton of the diene ring should be chemically inequivalent, and therefore give eight signals. Clearly this is not the case and rapid rotation/flexing of the ring in solution may be responsible for this.

The solid-state molecular structure of $Os_4(\mu-H)_2(CO)_8(\eta^4-C_6H_8)(\eta^6-C_6H_6)$ **8** is shown in Figure 2.3.2, together with some relevant structural parameters. The molecule possesses the customary tetrahedral arrangement of the four metal atoms. The Os-Os distances range from 2.7462(10) to 2.9001(10) Å, with the shortest edge corresponding to that connecting the two osmium atoms bearing the diene and benzene ligands [Os(1)-Os(2)], and the longest being that between the two remaining osmium atoms [Os(3)-Os(4)]. The former edge also bears an asymmetrical bridging carbonyl group, while the latter edge is thought to carry one of the two hydride ligands. The C_6H_8 moiety is

terminally bound to one osmium atom of the polyhedron [Os(1)] *via* an η^4 type interaction which is similar to that observed in the diene and benzene-diene species $Os_4(\mu$-$H)_2(CO)_{11}(\eta^4$-$C_6H_8)$ **5** and $Os_4(CO)_9(\eta^4$-$C_6H_8)(\eta^6$-$C_6H_6)$ **7**. Three of the Os-C(C6H8) bonding distances in complex **8** are almost equivalent [Os(1)-C(2D) 2.182(21), Os(1)-C(3D) 2.202(22), Os(1)-C(4D) 2.191(23) Å] and one is long [Os(1)-C(1D) 2.278(20) Å], and the conformation of the C_6H_8 ligand is again such that the C_4H_4 section of the ring interacts with the osmium-atoms while the -CH2-CH2- section bends away from the cluster core. The complex $Os_4(\mu$-$H)_2(CO)_8(\eta^4$-$C_6H_8)(\eta^6$-$C_6H_6)$ **8** also carries an η^6-bound benzene ligand as in **7**. The Os-C(benzene) distances in **8** lie in the range 2.20(2) - 2.29(2) Å, which are the same as those observed in **7** [2.20(1) - 2.29(1) Å].
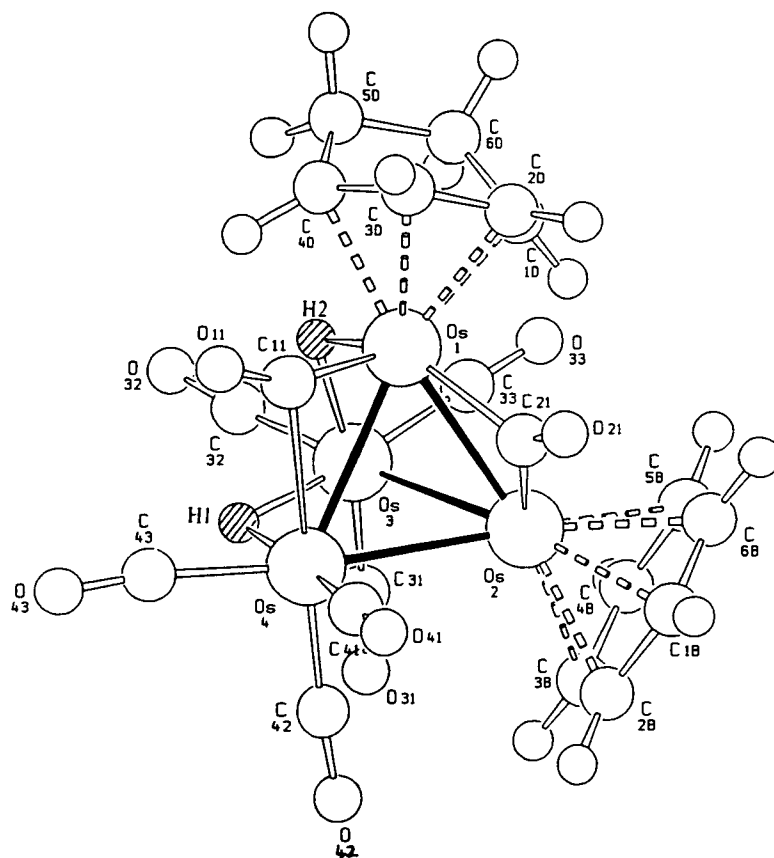
Figure 2.3.2: The molecular structure of $Os_4(\mu$-$H)_2(CO)_8(\eta^4$-$C_6H_8)(\eta^6$-$C_6H_6)$ **8** in the solid-state showing the atomic labelling scheme. The C-atoms of the CO ligands bear the same numbering as the corresponding O-atoms. The H (hydride) positions are those determined by XHYDEX,[19] and correspond to niches in the ligand coverage. Relevant bond distances (Å) include: Os(1)-Os(2) 2.7462(10), Os(1)-Os(3) 2.8628(10), Os(1)-Os(4) 2.8815(10), Os(2)-Os(3) 2.8191(10), Os(2)-Os(4) 2.7754(10), Os(3)-Os(4) 2.9001(10), mean Os-C(CO_terminal) 1.89(2), mean C-O(CO_terminal) 1.15(3), Os(1)-C(11) 1.89(2), Os(4)··C(11) 2.52(2), C(11)-O(11) 1.16(3), Os(1)-C(21) 2.11(2), Os(2)-C(21) 2.03(2), C(21)-O(21) 1.15(2), Os(2)-C(1B) 2.20(2), Os(2)-C(2B) 2.25(2), Os(2)-C(3B) 2.26(2), Os(2)-C(4B) 2.29(2), Os(2)-C(5B) 2.25(2), Os(2)-C(6B) 2.21(2), C(1B)-C(2B) 1.40(4), C(1B)-C(6B) 1.37(3), C(2B)-C(3B) 1.44(3), C(3B)-C(4B) 1.42(3), C(4B)-C(5B) 1.37(3), C(5B)-C(6B) 1.35(3), Os(1)-C(1D) 2.28(2), Os(1)-C(2D) 2.18(2), Os(1)-C(3D) 2.20(2), Os(1)-C(4D) 2.19(2), C(1D)-C(2D) 1.43(3), C(1D)-C(6D) 1.49(3), C(2D)-C(3D) 1.37(3), C(3D)-C(4D) 1.42(3), C(4D)-C(5D) 1.47(3), C(5D)-C(6D) 1.56(3).

The distribution of the eight CO-ligands in **8** can be easily derived from those observed in the complex $Os_4(\mu\text{-H})_2(CO)_{11}(\eta^4\text{-C}_6\text{H}_8)$ **5**; the Os-atom to which the C_6H_8 ligand is attached is involved in two asymmetric bridging interactions as in **5**, and the benzene ligand is substituted for the three terminally bound carbonyls of a neighbouring Os-atom. The relationship with the structure of $Os_4(CO)_9(\eta^4\text{-C}_6\text{H}_8)(\eta^6\text{-C}_6\text{H}_6)$ **7** can also be appreciated; the ninth carbonyl group in **7** [which has been replaced by two H(hydride) ligands in the structure of **8**] is in a near triply-bridging position over the metal core generating a far more congested steric situation than in **8**. The congestion is thought to be less in **8** because the H(hydride) atoms not only provide two electrons to the cluster by occupying less-demanding edge-bridging positions than the carbonyl, but also help to reduce the ligand crowding over the cluster surface by enlarging the metal framework slightly.

The two H(hydride) atoms in **8** could not be located experimentally and, as a result, a molecular space filling diagram was analysed in order to establish their most likely positions (see Figure 2.3.3). As for complex **5**, the presence of two large niches within the ligand envelope was used as a first indication of the likely positions of the two missing H atoms. One hydride is thought to be spanning the Os(3)-Os(4) edge, occupying a cavity formed by four carbonyl ligands [CO(31), CO(32), CO(42) and CO(43)], whilst the second is considered to bridge the Os(1)-Os(3) bond and is accommodated in the hollow of the diene and two carbonyls [CO(32), CO(33)]. The Os(3)-Os(4) bond is the longest [2.9001(10) Å] in the complex, while the edge-bridging location of the second hydride,

Figure 2.3.3: Space filling representation of the structure of **8** along the Os(3)-Os(4) edge, showing a large niche in the ligand envelope corresponding to the XHYDEX location of a hydride ligand.

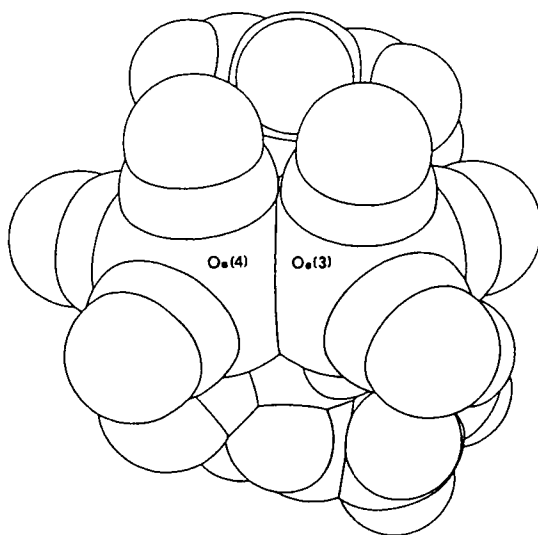Os(1)-Os(3), does not result in an equally noticeable lengthening with respect to the other M-M bonds of the molecule. Again the results of a series of XHYDEX[19] calculations, run on all the edges of the tetrahedron, were in complete agreement with the positions of the hydrides estimated from the largest cavities in the ligands envelope. As with **5**, complex **8** contains 60 valence electrons and is therefore in accordance with the PSEPT electron counting rules.

The benzene cluster, $Os_4(\mu-H)_2(CO)_{10}(\eta^6-C_6H_6)$ **6**, has also been found to react with Me_3NO in a solvent mixture of dichloromethane-acetone (6:1, v/v) in the presence of benzene instead of cyclohexa-1,3-diene, resulting in a new product which has been tentatively characterised as $Os_4(CO)_8(\eta^6-C_6H_6)_2$ **9**. Compound **9** may be isolated from the reaction mixture by t.l.c., eluting with a dichloromethane-hexane (3:7, v/v) solution, and has been characterised on the basis of its spectroscopic properties only. The infrared spectrum suggests that the molecule contains both bridging and terminal carbonyl ligands. A molecular ion is observed at 1140 (calc. 1140) amu in the mass spectrum, followed by the sequential loss of eight carbonyl ligands, and the ^1H NMR of **9** in $CDCl_3$ is very simple revealing just one signal, a singlet resonance, at δ 5.75 ppm. This is thought to correspond to the twelve protons of two apically bound benzene ligands in chemically equivalent environments, and its value is comparable to that observed in related compounds such as **6** (δ 5.95 ppm), **7** (δ 5.75 ppm), and **8** (δ 5.74 ppm). The presence of a single benzene resonance requires a plane of symmetry in the molecule (or some benzene movement to generate a plane of symmetry) and, as expected, the benzene must undergo free rotation. Unfortunately, verification of the proposed formula by X-ray crystallography has not been possible, as crystals suitable for this purpose have not been obtained.

The synthesis of compound **9** using Me_3NO directly with benzene, as opposed to cyclohexa-1,3-diene, is not unique and a similar procedure has been employed to introduce other arenes, which are not readily available in the corresponding dihydroarene form, into cluster systems. For example, a dichloromethane-acetone-xylene solution of the *mono*-xylene species $Ru_6C(CO)_{14}(\eta^6-C_6H_4Me_2)$ can be treated with 3 molar equivalents of Me_3NO, added dropwise in dichloromethane, to produce the *bis*-xylene complex $Ru_6C(CO)_{11}(\eta^6-C_6H_4Me_2)_2$.[30] The presence of acetone in these reactions is thought to weakly stabilise any coordinatively unsaturated cluster intermediates formed during the course of the reaction. It should be noted that the arene clusters are produced from these reactions in far smaller yields than is generally observed from the analogous reactions employing the corresponding dienes. This is likely to be due to the presence of localised double bonds in the diene molecules which are readily available for π-acid bonding, compared with the delocalised nature of the π-electrons in the arenes which are less prone to coordinate in the first instance. It is also worth noting that whereas the diene complex

$Os_4(\mu\text{-}H)_2(CO)_{11}(\eta^4\text{-}C_6H_8)$ **5** can be converted into the benzene cluster **6**, *albeit* in low yield, there is no evidence to suggest that either benzene-diene product **7** or **8**, can undergo conversion to the *bis*(benzene) species **9**, despite repeated attempts.
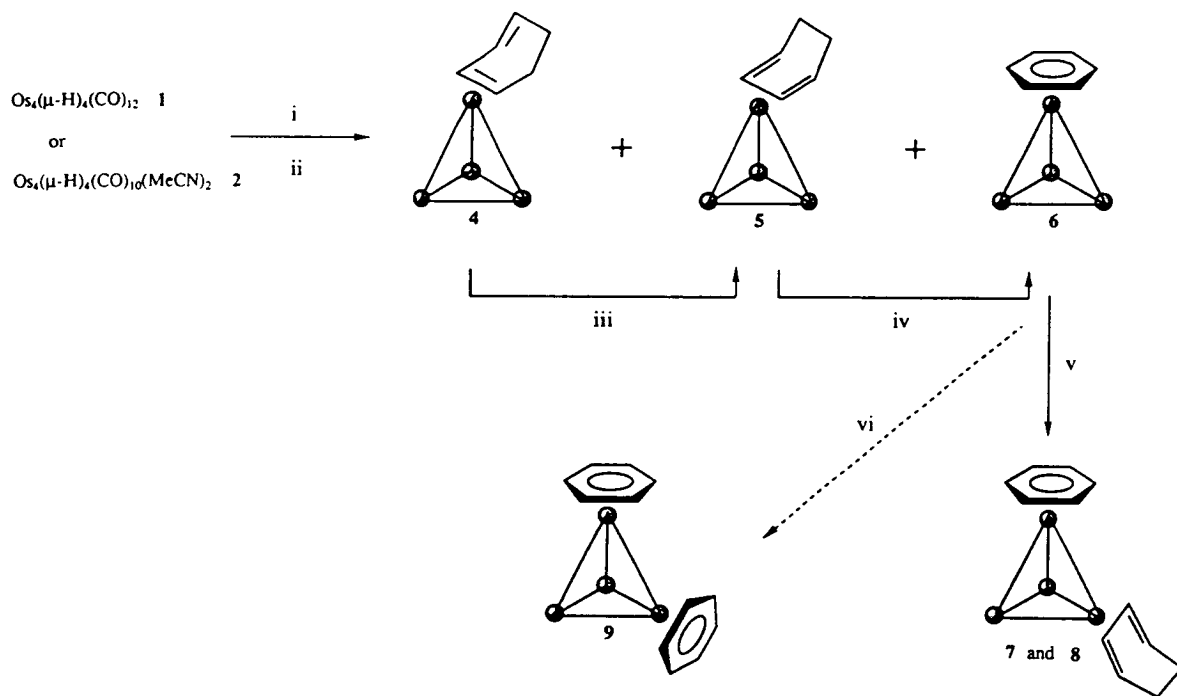
Scheme 2.3: The Sequential Formation of Clusters **4, 5, 6, 7, 8** and **9**, (i) 3.2 equiv. $Me_3NO/CH_2Cl_2/1,3\text{-}C_6H_8$; (ii) $CH_2Cl_2/1,3\text{-}C_6H_8/RT.$; (iii) and (iv) Δ, Hexane; (v) 3.2 equiv. $Me_3NO/CH_2Cl_2/1,3\text{-}C_6H_8$; (vi) 3.2 equiv. $Me_3NO/CH_2Cl_2/acetone/benzene.$

The range of diene and benzene derivatives of $Os_4(\mu\text{-}H)_4(CO)_{12}$ described in Sections 2.2 and 2.3 are summarised in Scheme 2.3. In this system the cyclohexa-1,3-diene moiety always bonds to a single osmium atom, and the benzene ligand is only observed in the η^6 terminal coordination mode. There is no evidence at any stage of the reaction to suggest the formation of the face-capping benzene moiety which prevails in other cluster systems. Similar behaviour is also displayed by the tetrahedral Co_4 cluster system, where again only the η^6 bonding mode for benzene has been observed.[31]

A feature of these Co_4 and Os_4 tetrahedral systems is the relative ease with which the terminally coordinated benzene moiety undergoes exchange with an uncoordinated arene, and for both the Co_4 and Os_4 systems this exchange provides a highly convenient route for producing different arene-cluster derivatives. The tetranuclear cobalt cluster, $Co_4(CO)_9(\eta^6\text{-}C_6H_6)$, readily undergoes arene exchange with C_6H_5Me, $C_6H_4Me_2$ and $C_6H_3Me_3$,[31] and it has been shown that upon heating $Os_4(\mu\text{-}H)_2(CO)_{10}(\eta^6\text{-}C_6H_6)$ **6** in

toluene, the cluster $Os_4(\mu\text{-}H)_2(CO)_{10}(\eta^6\text{-}C_6H_5Me)$ is produced, and by heating **6** in an octane-xylene solution the cluster $Os_4(\mu\text{-}H)_2(CO)_{10}(\eta^6\text{-}C_6H_4Me_2)$ is slowly formed.[32] Both osmium complexes have been identified by the usual spectroscopic methods and their molecular structures confirmed by single crystal X-ray diffraction studies. There is no evidence to suggest that these substitutions are reversible and, as with other η^6 arene-metal complexes,[33] the stability or displacement series for the arene ligand seems to follow the order $C_6H_4Me_2 > C_6H_5Me > C_6H_6$. The lability of the benzene ligand in $Os_4(\mu\text{-}H)_2(CO)_{10}(\eta^6\text{-}C_6H_6)$ **6** is also evident from its reaction with diphenylacetylene in the presence of $Me_3NO\text{-}MeCN$. The benzene ligand is displaced, resulting in the formation of $Os_4(\mu\text{-}H)_2(CO)_9(Ph_2C_2)_2$ which contains one of the diphenylacetylene ligands coordinated to the cluster face in a customary $\mu_3\text{-}\eta^2$ mode, and the other bonded to a single osmium atom in an η^2 manner.[34]

In contrast, it would appear from information currently available that the face-capping benzene moieties found in clusters based on Ru_3, Os_3, Ru_5C, Ru_6C, and Os_6 units are far more tightly bound to the cluster core, and are thus resistant to exchange, even though their migration to terminal sites has been observed.[15]

2.4 Further Products from the Reaction of $Os_4(\mu\text{-}H)_4(CO)_{10}(MeCN)_2$ 2 with Cyclohexa-1,3-diene

The activated cluster $Os_4(\mu\text{-}H)_4(CO)_{10}(MeCN)_2$ **2** has been shown to afford a similar range of products as $Os_4(\mu\text{-}H)_4(CO)_{12}$ **1** when treated with cyclohexa-1,3-diene at room temperature. However, reaction of the *bis*(acetonitrile) complex **2** with cyclohexa-1,3-diene under more forcing conditions leads to the isolation of some new complexes in addition to the full range previously described.

The thermolysis of $Os_4(\mu\text{-}H)_4(CO)_{10}(MeCN)_2$ **2** in dichloromethane containing excess cyclohexa-1,3-diene over an 18 hour period has previously been shown to yield the benzene and benzene-diene clusters $Os_4(\mu\text{-}H)_2(CO)_{10}(\eta^6\text{-}C_6H_6)$ **6** and $Os_4(\mu\text{-}H)_2(CO)_{10}(\eta^4\text{-}C_6H_8)(\eta^6\text{-}C_6H_6)$ **7**.[21] A reinvestigation into this reaction has revealed that the full range of derivatives **3 - 7** can infact be produced in varying yields, together with three previously unobserved compounds. These products can be separated from the reaction mixture by t.l.c., eluting with a dichloromethane-hexane (1:3, v/v) solution, and the new complexes have been fully characterised both in solution and the solid-state as $Os_4(\mu\text{-}H)(CO)_{10}(\mu_3\text{-}\eta^1{:}\eta^2{:}\eta^1\text{-}C_6H_8)(\eta^3\text{-}C_6H_9)$ **10**, $Os_4(\mu\text{-}H)_2(CO)_{10}(\eta^6\text{-}C_6H_5C_6H_9)$ **11** and $Os_5(\mu\text{-}H)_2(CO)_{13}(\eta^4\text{-}C_6H_8)$ **12** (see Scheme 2.4).

$$Os_4(\mu\text{-}H)_4(CO)_{10}(MeCN)_2 \quad \mathbf{2}$$

$$\Delta, CH_2Cl_2 / 1,3\text{-}C_6H_8$$

3, 4, 5, 6, 7 +

10

+

11

+

12
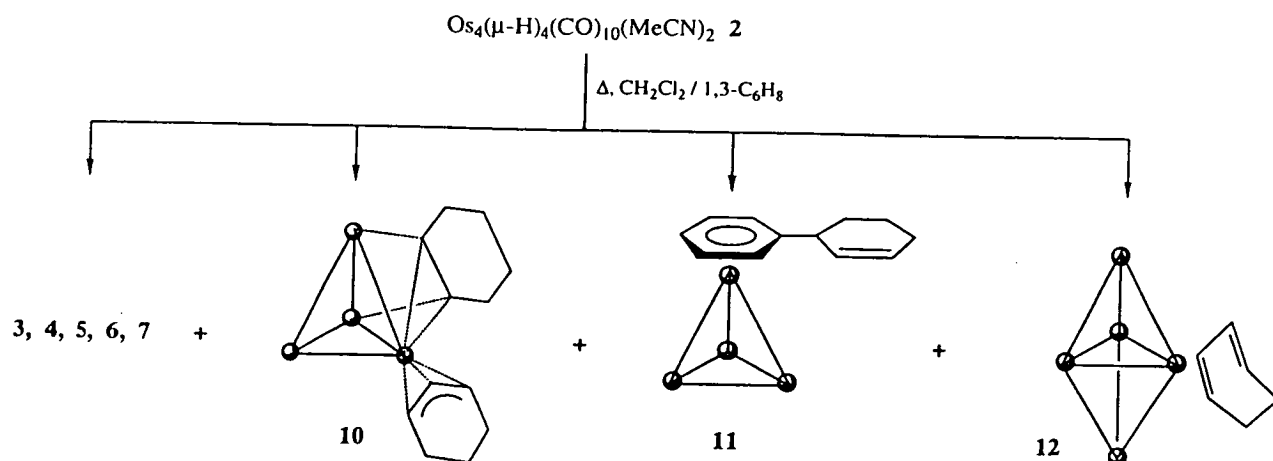
Scheme 2.4: The range of products isolated from the 18 hour thermolysis of Os4(µ-H)4(CO)10(MeCN)2 **2** with cyclohexa-1,3-diene in dichloromethane.

2.4.1: Characterisation of $Os_4(\mu\text{-}H)(CO)_{10}(\mu_3\text{-}\eta^1\text{:}\eta^2\text{:}\eta^1\text{-}C_6H_8)(\eta^3\text{-}C_6H_9)$ 10

The infrared spectrum (υ_{CO}) of compound **10** contains peaks between 2098 and 1966 cm^{-1} which are indicative of terminal carbonyl ligands. The mass spectrum exhibits a molecular ion at 1202 (calc. 1203) amu, which is followed by the most intense peak at 1121 amu corresponding to the loss of the C_6H_9 moiety. The loss of several CO groups in succession are also apparent. The ^1H NMR spectrum of compound **10** is rather complicated and comprises of a series of multiplet resonances which integrate to a total of 17 protons, and a singlet resonance at low frequency which can be attributed to the metal hydride. Before commencing with a detailed discussion of the NMR spectrum, the molecular structure will be described.

Crystals of **10** suitable for single crystal X-ray analysis were grown from a toluene solution at -25°C. The molecular structure of **10** is illustrated in Figure 2.4.1i together with the atomic labelling scheme, and relevant structural parameters. The metal atom framework of compound **10** constitutes a distorted Os4 tetrahedron, with Os-Os distances ranging from 2.6529(13) to 2.8912(13) Å, the longest edge being that thought to be bridged by the hydride ligand [Os(1)-Os(2)]. The molecule contains two C_6 ring systems, one of which is a C_6H_9 ring that coordinates to a tetrahedron apex [Os(3)] in an η^3 allylic manner, and the other is a C_6H_8 cyclohexyne-type ligand which bridges a triangular face of the cluster *via* two σ and one π- interaction. The C_6H_9 moiety donates three electrons to the metal framework by coordinating to Os(3) through one 'short' and two 'long' interactions [Os(3)-C(20) 2.12(4) *vs.* Os(3)-C(19) 2.34(4) and Os(3)-C(21) 2.29(4) Å] and the C-C bonds within the ring also vary in length quite considerably. The allylic C-C bonds involved in interactions with the osmium atom are the shortest [C(19)-C(20) 1.415(10) and

C(20)-C(21) 1.412(10) Å], the two adjacent to these are slightly longer [C(18)-C(19) 1.431(10) and C(21)-C(22) 1.436(10) Å], whilst those directly opposite are significantly longer [C(17)-C(18) 1.517(10) and C(17)-C(22) 1.518(10) Å].
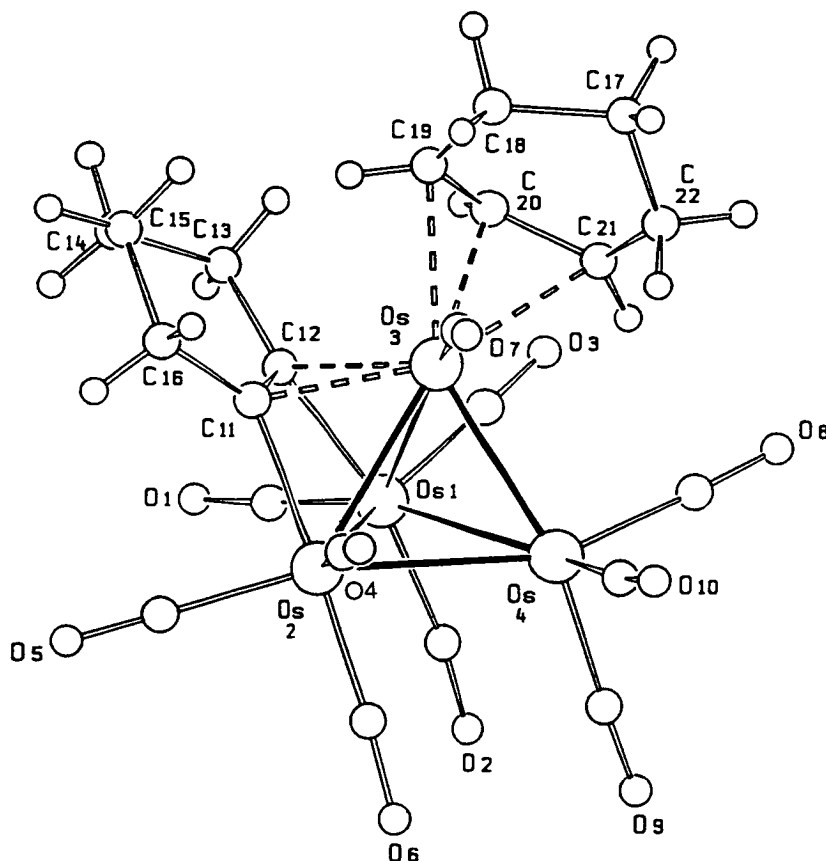
Figure 2.4.1i: The molecular structure of $Os_4(\mu\text{-H})(CO)_{10}(\mu_3\text{-}\eta^1\text{:}\eta^2\text{:}\eta^1\text{-}C_6H_8)(\eta^3\text{-}C_6H_9)$ **10** in the solid-state showing the atomic labelling scheme. The C-atoms of the CO ligands bear the same numbering as the corresponding O-atoms. Relevant bond distances (Å) include: Os(1)-Os(2) 2.8912(13), Os(1)-Os(3) 2.7936(13), Os(1)-Os(4) 2.8680(14), Os(2)-Os(3) 2.7956(12), Os(2)-Os(4) 2.8518(13), Os(3)-Os(4) 2.6529(13), mean Os-C(CO) 1.90(3), mean C-O(CO) 1.15(4), Os(1)-C(12) 2.18(3), Os(2)-C(11) 2.17(2), Os(3)-C(11) 2.19(2), Os(3)-C(12) 2.23(3), C(11)-C(12) 1.40(4), C(11)-C(16) 1.50(3), C(12)-C(13) 1.55(4), C(13)-C(14) 1.510(10), C(14)-C(15) 1.505(10), C(15)-C(16) 1.507(10), Os(3)-C(19) 2.34(4), Os(3)-C(20) 2.12(4), Os(3)-C(21) 2.29(4), C(17)-C(18) 1.517(10), C(17)-C(22) 1.518(10), C(18)-C(19) 1.431(10), C(19)-C(20) 1.415(10), C(20)-C(21) 1.412(10), C(21)-C(22) 1.436(10).

The multiple bond, C(11)-C(12), of the C_6H_8 ligand straddles the Os(1)-Os(2)-Os(3) triangular face in a manner typically observed by alkynes,[35] and this bond is short when compared to the remaining C-C bond lengths of the ring [1.40(4) *vs.* mean 1.52(4) Å]. The cyclohexyne moiety donates four electrons to the cluster *via* two σ-bonds [Os(1)-C(12) 2.18(3) and Os(2)-C(11) 2.17(2) Å] and a π-interaction with the osmium atom bearing the C_6H_9 ring [Os(3)-C(11) 2.19(2) and Os(3)-C(12) 2.23(3) Å]. There are ten

carbonyl ligands all of which are bonded in a terminal manner, three are distributed on Os(1), Os(2) and Os(4), and the remaining carbonyl is situated on the osmium atom bearing the allylic ligand, *i.e.* Os(3).

The H(hydride) atom in **10** could not be located directly, however as with compounds Os$_4$(μ-H)$_2$(CO)$_{11}$(η^4-C$_6$H$_8$) **5** and Os$_4$(μ-H)$_2$(CO)$_8$(η^4-C$_6$H$_8$)(η^6-C$_6$H$_6$) **8**, the molecular space filling diagram revealed the presence of a large niche in the ligand envelope along the Os(1)-Os(2) edge, suggesting its likely position (see Figure 2.4.1ii). The Os(1)-Os(2) bond is the longest [2.8912(13) Å] in the complex, and the results of a series of XHYDEX [19] calculations concur with observations made from the space filling diagram, suggesting that the hydride atom does infact bridge this M-M edge. The tetrahedral complex, Os$_4$(μ-H)(CO)$_{10}$(μ_3-η^1:η^2:η^1-C$_6$H$_8$)(η^3-C$_6$H$_9$) **10**, contains a total of 60 valence electrons and is therefore consistent with PSEPT electron counting rules.
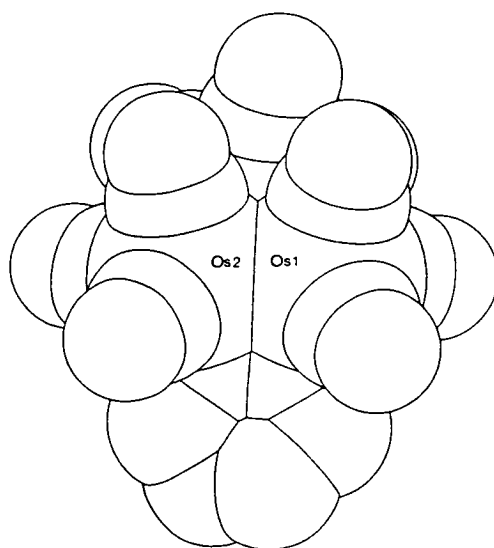
Figure 2.4.1ii: Space filling representation of the structure of **10** showing a large niche in the ligand envelope along the Os(1)-Os(2) edge corresponding to the XHYDEX location of the H(hydride) atom.

The ^{1}H NMR spectrum of Os$_4$(μ-H)(CO)$_{10}$(μ_3-η^1:η^2:η^1-C$_6$H$_8$)(η^3-C$_6$H$_9$) **10** is shown in Figure 2.4.1iii, and comprises of a complex series of signals, labelled A - S, many of which overlap [see the Experimental section (6.2) for the actual chemical shift values]. In addition, a signal ascribable to a metal hydride is found at *ca.* δ -22 ppm. The C$_6$H$_8$ and C$_6$H$_9$ rings should give rise to a total of 17 resonances, which, from the integral trace of the spectrum, appears to be the case. However, a more conclusive proof was obtained by performing a TOCSY experiment (TOtal Correlation SpectroscopY). This type of experiment provides a two-dimensional plot in which all the signals from the
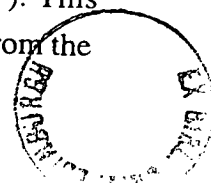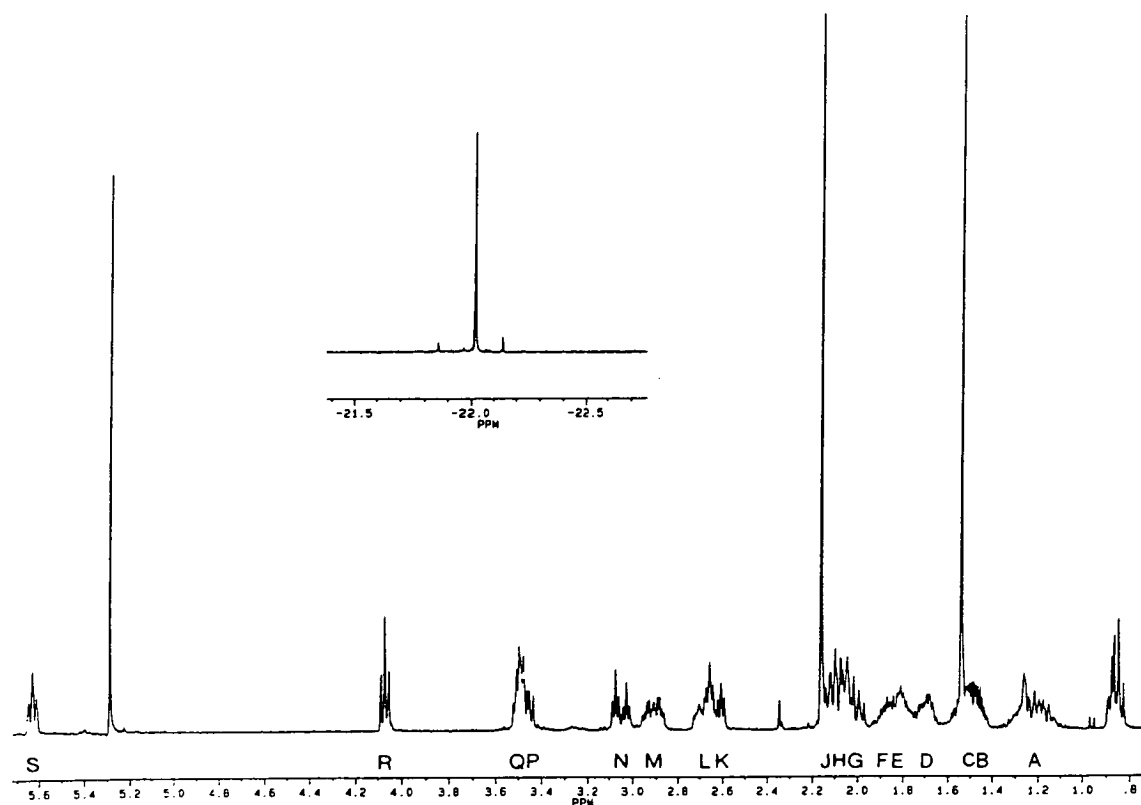
Figure 2.4.1iii: The ^{1}H NMR spectrum of $Os_4(\mu\text{-H})(CO)_{10}(\mu_3\text{-}\eta^1\text{:}\eta^2\text{:}\eta^1\text{-}C_6H_8)(\eta^3\text{-}C_6H_9)$ **10**.

Figure 2.4.1iv: The TOCSY ^{1}H NMR spectrum of **10**.

normal 1D spectrum are displayed by diagonal responses, with all the H signals from a given spin system (*e.g.* one of the six-membered ring systems in this case) being linked by cross peaks. The TOCSY experiment as performed on complex **10** is shown in Figure 2.4.1iv, and reveals that signals A, B, G, H, L, M, Q, R and S belong to one spin system, while signals C, D, E, F, J, K, N and P belong to the other. Figure 2.4.1v presents the basic ^{1}H spectrum along with cross sections as indicated on the plot of the TOCSY experiment, and clearly shows nine signals assignable to one ring and eight to the other.
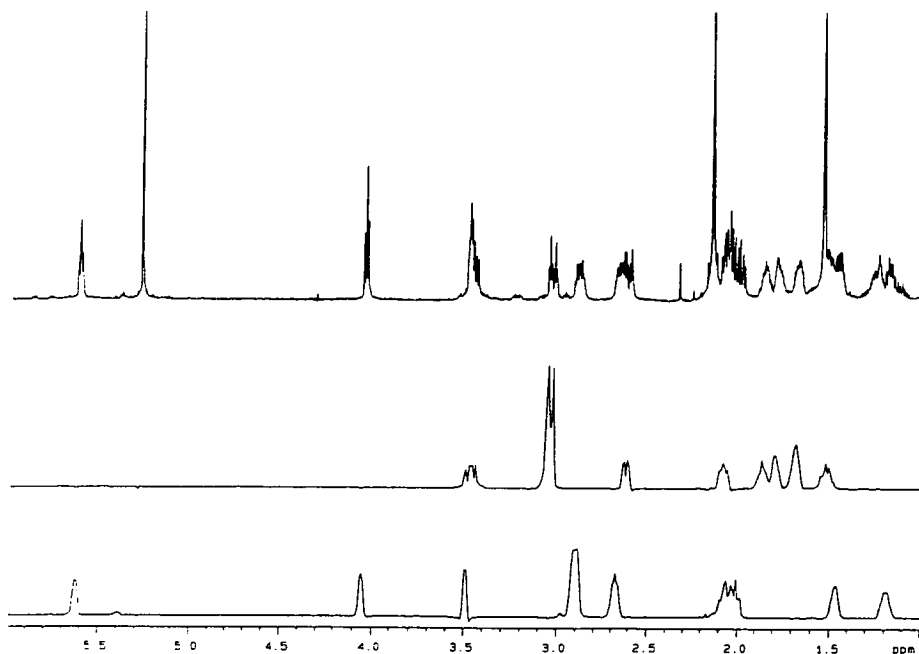
Figure 2.4.1v: The ^{1}H NMR spectrum of **10** together with cross-sections of the TOCSY experiment.

The molecule has also been analysed using a combination of homonuclear ^{1}H COSY/decoupling and NOESY experiments, which suggests that the pairs of signals C/D, E/F, J/K and N/P arise from the geminal protons of the C6H8 ring system, with A/B, G/L and H/M being attributed to those of the other ring system. These assumptions were based upon the size of coupling constants and the magnitude of nOe responses, both of which are typically large for geminal protons in six membered rings. This leaves signals Q, R and S which are associated with the allyl unit [*viz.* C(19)-C(20)-C(21)] of the C6H9 ring. Signal R appears to couple to both S and Q, and is hence assigned to H(20). The assignments of S and Q to either H(19) or H(21) is open to speculation. The ^{1}H spectrum indicates they are in markedly different environments, but it is unclear from the crystallographically obtained structure why this should be so, as the Os(3)-C(19) and Os(3)-C(21) distances are very similar within experimental error [2.34(4) and 2.29(4) Å, respectively]. As signals Q and L couple together, as do signals S and M, it would seem that the G/L protons derive from the same side of the ring as the Q proton, and the H/M protons are on the same side as the S

proton. This places the A/B protons on C(17). The data are not sufficiently conclusive to permit a full characterisation, however Table 2.4.1 summarises the probable assignments of the protons on the two rings.

Table 2.4.1: Partial assignment of the ^{1}H NMR spectrum of **10**.

Protons on C(13)	J/K or N/P
Protons on C(14)	C/D or E/F
Protons on C(15)	C/D or E/F
Protons on C(16)	J/K or N/P
Protons on C(17)	A/B
Protons on C(18)	G/L or H/M
H(19)	S or Q
H(20)	R
H(21)	S or Q
Protons on C(22)	G/L or H/M

The complex, $Os_4(\mu\text{-}H)(CO)_{10}(\mu_3\text{-}\eta^1{:}\eta^2{:}\eta^1\text{-}C_6H_8)(\eta^3\text{-}C_6H_9)$ **10**, is thought to be derived from the cyclohexenyl complex $Os_4(\mu\text{-}H)_3(CO)_{11}(\mu_2\text{-}\eta^1{:}\eta^2\text{-}C_6H_9)$ **3**, which is also isolated from the same reaction. As described earlier, cluster **3** does not appear to be an active intermediate in the formation of clusters $Os_4(\mu\text{-}H)_2(CO)_{12}(\eta^2\text{-}C_6H_8)$ **4**, $Os_4(\mu\text{-}H)_2(CO)_{11}(\eta^4\text{-}C_6H_8)$ **5** and $Os_4(\mu\text{-}H)_2(CO)_{10}(\eta^6\text{-}C_6H_6)$ **6**, but instead a second reaction mechanism can be envisaged whereby complex **3** represents an intermediate on route to the formation of a $\mu_3\text{-}\eta^1{:}\eta^2\text{-}\eta^1$ alkyne-type moiety, similar to that observed in complex **10**. These ideas will be developed further in due course.

2.4.2: Characterisation of $Os_4(\mu\text{-}H)_2(CO)_{10}(\eta^6\text{-}C_6H_5C_6H_9)$ 11

Compound **11** has been fully characterised as $Os_4(\mu\text{-}H)_2(CO)_{10}(\eta^6\text{-}C_6H_5C_6H_9)$ by spectroscopic techniques and by a single crystal X-ray diffraction analysis using a crystal grown from a toluene solution at -25°C. The profile of the infrared spectrum of **11** (υ_{CO}) is almost identical in both symmetry and wavenumber to that of the closely related benzene cluster, $Os_4(\mu\text{-}H)_2(CO)_{10}(\eta^6\text{-}C_6H_6)$ **6**, with peaks suggesting the presence of both terminal and bridging carbonyl ligands. The mass spectrum exhibits a parent peak at 1202 (calc. 1201) amu together with peaks corresponding to the subsequent loss of ten CO groups. The ^{1}H NMR spectrum at room temperature comprises of three complex multiplet signals centred at δ 5.84, 3.58 and 1.99 ppm with relative intensities 5:2:7, plus two singlet resonances at δ -19.09 and -20.45 ppm. The former signal can be attributed to the

five aromatic ring protons of the arene moiety, with the chemical shift value of 5.84 ppm being typical of η^6 coordination, while the resonances at δ 3.58 and 1.99 ppm are associated with the two olefinic and the seven aliphatic protons of the cyclohexene section of the ring system, respectively. The two signals at very low frequency may be attributed to two inequivalent hydride ligands.
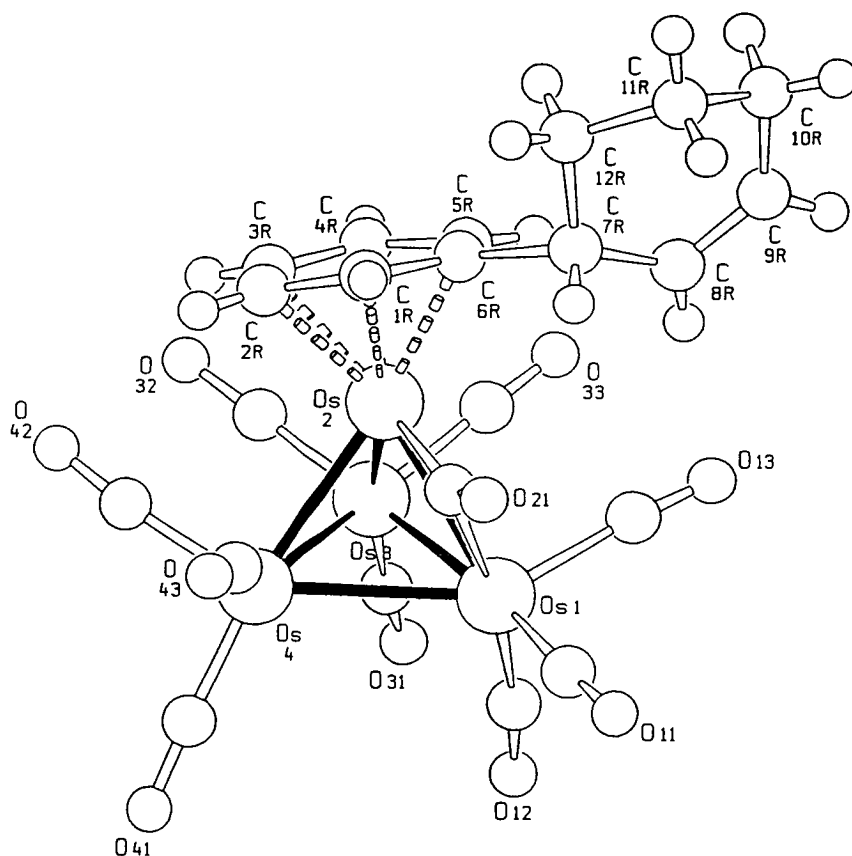
Figure 2.4.2i: The molecular structure of $Os_4(\mu\text{-}H)_2(CO)_{10}(\eta^6\text{-}C_6H_5C_6H_9)$ **11** in the solid-state showing the atomic labelling scheme. The C-atoms of the CO ligands bear the same numbering as the corresponding O-atoms. Relevant bond distances (Å) and angles (°) include: Os(1)-Os(2) 2.811(2), Os(1)-Os(3) 2.766(2), Os(1)-Os(4) 2.951(2), Os(2)-Os(3) 2.7811(14), Os(2)-Os(4) 2.7883(14), Os(3)-Os(4) 2.879(2), mean Os-C(CO_terminal) 1.90(4), mean C-O(CO_terminal) 1.15(4), Os(1)··C(21) 2.40(3), Os(2)-C(21) 1.95(2), C(21)-O(21) 1.11(3), Os(2)-C(1R) 2.25(3), Os(2)-C(2R) 2.22(3), Os(2)-C(3R) 2.22(2), Os(2)-C(4R) 2.29(2), Os(2)-C(5R) 2.25(2), Os(2)-C(6R) 2.21(3), C(1R)-C(2R) 1.43(4), C(1R)-C(6R) 1.37(4), C(2R)-C(3R) 1.46(5), C(3R)-C(4R) 1.37(5), C(4R)-C(5R) 1.41(5), C(5R)-C(6R) 1.34(4), C(6R)-C(7R) 1.62(4), C(7R)-C(8R) 1.46(5), C(7R)-C(12R) 1.55(5), C(8R)-C(9R) 1.36(6), C(9R)-C(10R) 1.46(6), C(10R)-C(11R) 1.53(7), C(11R)-C(12R) 1.54(1), C(1R)-C(2R)-C(3R) 115(3), C(1R)-C(6R)-C(5R) 126(3), C(1R)-C(6R)-C(7R) 117(3), C(2R)-C(1R)-C(6R) 119(3), C(2R)-C(3R)-C(4R) 121(3), C(3R)-C(4R)-C(5R) 121(3), C(4R)-C(5R)-C(6R) 116(3), C(5R)-C(6R)-C(7R) 117(3), C(6R)-C(7R)-C(8R) 115(3), C(6R)-C(7R)-C(12R) 103(3), C(7R)-C(8R)-C(9R) 117(4), C(7R)-C(12R)-C(11R) 110(3), C(8R)-C(7R)-C(12R) 115(3), C(8R)-C(9R)-C(10R) 129(4), C(9R)-C(10R)-C(11R) 108(4), C(10R)-C(11R)-C(12R) 108(4).

The solid-state structure of $Os_4(\mu\text{-H})_2(CO)_{10}(\eta^6\text{-}C_6H_5C_6H_9)$ **11** is shown in Figure 2.4.2i together with relevant structural parameters. As anticipated from infrared spectroscopy, in terms of the metal framework and carbonyl distribution the structure is very similar to that of $Os_4(\mu\text{-H})_2(CO)_{10}(\eta^6\text{-}C_6H_6)$ **6**, differing only in the nature of the η^6 coordinated ligand; the benzene moiety in **6** being replaced by a cyclohexenylbenzene group in **11**.

The metal framework of $Os_4(\mu\text{-H})_2(CO)_{10}(\eta^6\text{-}C_6H_5C_6H_9)$ **11** consists of a tetrahedral arrangement of the four osmium atoms with Os-Os distances ranging from 2.766(2) to 2.951(2) Å [*cf.* 2.758(1) to 2.979(1) Å in the benzene cluster **6**]. Both species **11** and **6** bear an η^6 arene ligand with the same average Os-C bond distance of 2.24(3) Å. This value is also directly comparable to the mean Os-C(benzene) distances found in the clusters $Os_4(CO)_9(\eta^4\text{-}C_6H_8)(\eta^6\text{-}C_6H_6)$ **7** [2.25(1) Å] and $Os_4(\mu\text{-H})_2(CO)_8(\eta^4\text{-}C_6H_8)(\eta^6\text{-}C_6H_6)$ **8** [2.24(2) Å]. In both **11** and **6** the arene-bound Os atom also bears a single CO ligand which appears to be forced into a semi-bridging position [Os(1)··C(21) 2.40(3), Os(2)-C(21) 1.95(2) Å for **11**, and Os(1)··C(10) 2.35(2), Os(4)-C(10) 1.91(1) Å for **6**] and the other three osmium atoms on each cluster also carry three terminal carbonyl groups. From an inspection of the CO ligand displacements in compound **11** the two H(hydride) ligands are believed to bridge the two longest Os-Os edges of the molecule, *i.e.* Os(1)-Os(4) and Os(3)-Os(4), and these positions have been further established by a series of XHYDEX[19] calculations. The location of these hydride atoms also corresponds to those edges of compound **6** which are thought to accommodate the bridging hydride ligands.
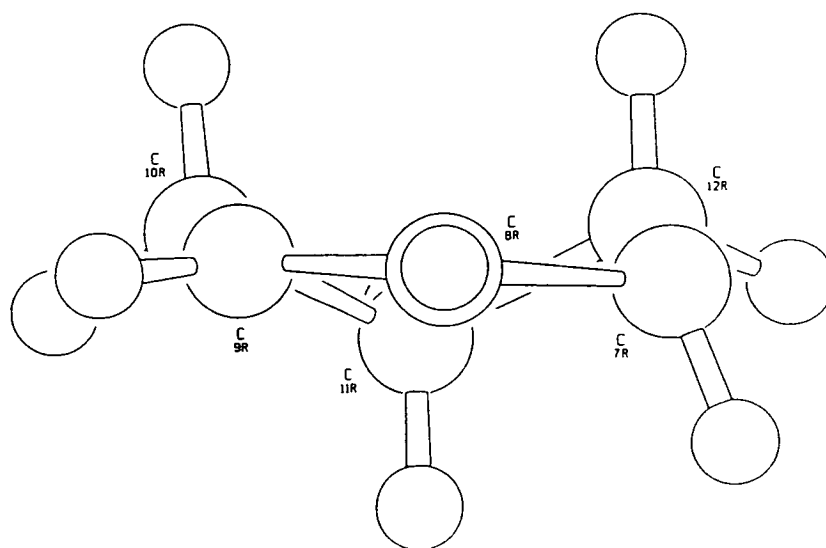

Figure 2.4.2ii: The C_6H_9 section of the cyclohexenylbenzene ligand in the complex $Os_4(\mu\text{-H})_2(CO)_{10}(\eta^6\text{-}C_6H_5C_6H_9)$ **11**.

The cyclohexenylbenzene ligand in complex **11** is rather unusual and deserves further comment. It comprises of two ring systems (benzene and cyclohexene) connected *via* a C-C single bond, with the aromatic ring coordinating to a single osmium atom [Os(2)] of the cluster framework in an η^6 manner. All C-C bonds within the benzene ring are approximately equal [mean 1.40(5) Å], and the ring is essentially planar. The cyclohexene section of the ligand is shown in Figure 2.4.2ii, illustrating that C(8R)-C(9R) represents the C-C double bond of the ring. These two carbon atoms may be considered as sp² hybridised, and the bond length of 1.36(6) Å is shorter than the remaining C-C bond distances of the C_6H_9 ring [mean 1.51(6) Å]. The two ring systems are connected by the C(6R)-C(7R) single bond, which has a length of 1.62(4) Å.

2.4.3: Characterisation of Os₅(μ-H)₂(CO)₁₃(η⁴-C₆H₈) 12

The final product to be isolated from the reaction between $Os_4(\mu\text{-}H)_4(CO)_{10}(MeCN)_2$ **2** and cyclohexa-1,3-diene was characterised as $Os_5(\mu\text{-}H)_2(CO)_{13}(\eta^4\text{-}C_6H_8)$ **12** in the first instance from mass spectroscopic evidence. The mass spectrum of **12** contains a strong parent peak at 1397 (calc. 1397) amu, together with peaks corresponding to the loss of several carbonyl groups in succession. Unfortunately a ¹H NMR of this compound has not been recorded due to the lack of crystalline material required for a clean spectrum, however, a single crystal X-ray structural analysis has been carried out using a crystal grown by vapour diffusion from dichloromethane-pentane at room temperature, which confirms the formulation proposed from mass spectroscopy.

The molecular structure of **12** is depicted in Figure 2.4.3, accompanied by principal bond lengths. Two independent molecules are present in the asymmetric unit of compound **12**. The molecular structure is not of high quality owing to the poor crystals obtained after repeated attempts, and the errors associated with the bond lengths and angles are large, especially for the lighter atoms. As a result, caution should be applied in the interpretation of the bond lengths obtained, although the gross features of the structure are worth describing.

The metal core of $Os_5(\mu\text{-}H)_2(CO)_{13}(\eta^4\text{-}C_6H_8)$ **12** comprises of a trigonal bipyramidal array of the five osmium atoms, with Os-Os bond lengths ranging from 2.763(4) to 3.004(4) and from 2.764(4) to 3.037(4) Å for the two independent molecules, respectively. The cyclohexa-1,3-diene moiety coordinates in the η^4 fashion to an equatorial osmium atom [Os(2)] having a metal connectivity of four (as opposed to an apical osmium atom which has a connectivity of three), and this osmium atom also carries a terminal carbonyl ligand. The remaining twelve carbonyl groups are all terminal and are divided equally among the four osmium atoms not involved in coordination to the diene ligand. The two hydride ligands are believed to bridge the two longest edges of each independent

molecule, *i.e.* Os(1)-Os(2) and Os(2)-Os(4), as indicated from a series of XHYDEX calculations run on all edges of the metal polyhedra.[19] In terms of simple electron counting arguments, a trigonal bipyramidal structure should contain 72 valence shell electrons, which is the number observed in compound **12**.
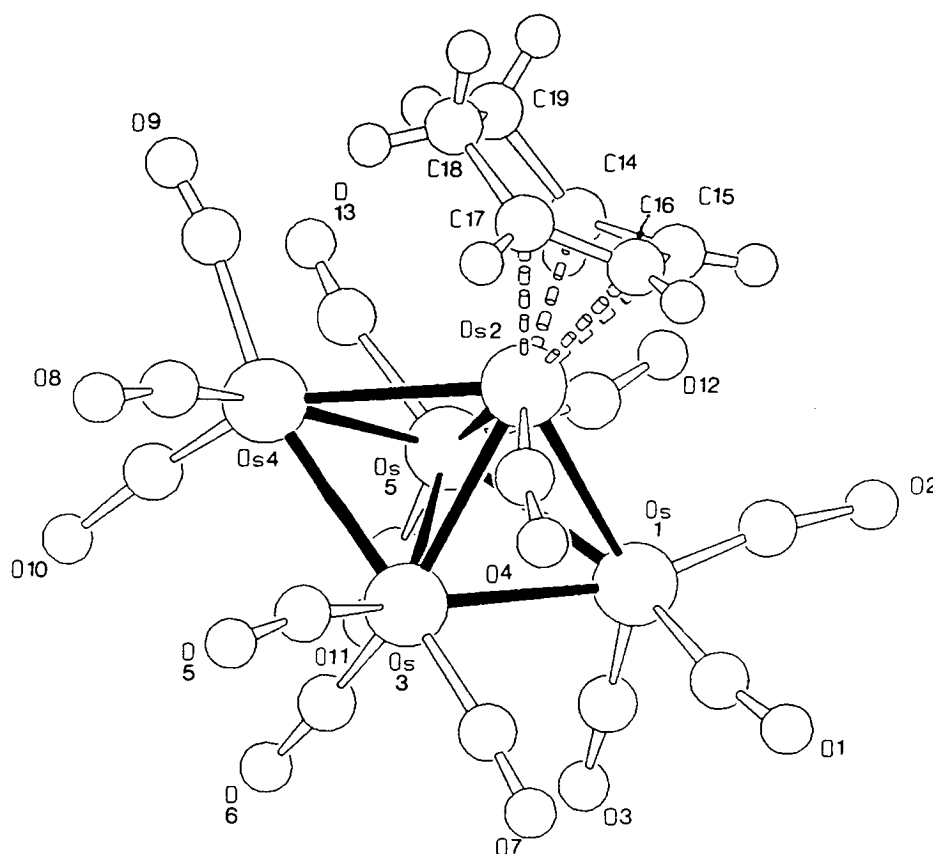

Figure 2.4.3: The molecular structure of Os$_5$(μ-H)$_2$(CO)$_{13}$(η^4-C$_6$H$_8$) **12** in the solid-state showing the atomic labelling scheme. The C-atoms of the CO ligands bear the same numbering as the corresponding O-atoms. Relevant bond distances (Å) for the two independent molecules include: Os(1)-Os(2) 3.004(4) 3.037(4), Os(1)-Os(3) 2.766(4) 2.797(3), Os(1)-Os(5) 2.811(4) 2.770(4), Os(2)-Os(3) 2.836(3) 2.827(4), Os(2)-Os(4) 2.981(4) 2.987(3), Os(2)-Os(5) 2.824(4) 2.821(4), Os(3)-Os(4) 2.763(4) 2.813(4), Os(3)-Os(5) 2.767(3) 2.789(4), Os(4)-Os(5) 2.790(4) 2.764(3), mean Os-C(CO) 1.93(12) 1.87(8), mean C-O(CO) 1.13(13) 1.18(9), Os(2)-C(14) 2.16(6) 2.32(8), Os(2)-C(15) 2.18(8) 2.26(6), Os(2)-C(16) 2.20(8) 2.18(7), Os(2)-C(17) 2.35(5) 2.30(9), C(14)-C(15) 1.40(10) 1.51(9), C(14)-C(19) 1.30(10) 1.58(10), C(15)-C(16) 1.42(11) 1.55(9), C(16)-C(17) 1.40(10) 1.34(10), C(17)-C(18) 1.70(20) 1.49(11), C(18)-C(19) 1.49(14) 1.58(9).

The formation of Os$_5$(μ-H)$_2$(CO)$_{13}$(η^4-C$_6$H$_8$) **12** from Os$_4$(μ-H)$_4$(CO)$_{10}$(MeCN)$_2$ **2** involves an increase in cluster nuclearity. It is well established that the thermal loss of CO from Os$_3$(CO)$_{12}$, for example, may result in a range of higher nuclearity clusters with between four and twenty metal atoms,[36] however, it is unusual for osmium clusters to build-up under such ambient reaction conditions as those employed during this reaction. In Chapter five a similar scenario is described whereby the action of trimethylamine *N*-oxide

on a triruthenium cluster in the presence of cyclohexa-1,3-diene, results in an increase in cluster nuclearity to a tetranuclear species under mild conditions. If this latter reaction is carried out in the absence of cyclohexa-1,3-diene, cluster degradation occurs with the formation of dinuclear complexes, therefore illustrating that condensation reactions may also be possible resulting in the formation of larger clusters. However, it is known that metal-metal bonds are stronger for heavier elements in a given group of the periodic table,[37] and it is therefore expected that osmium would be less prone to these types of reaction than ruthenium. Also Me$_3$NO is not employed in the reaction currently under investigation. Nonetheless, this reaction does involve the *bis*(acetonitrile) complex, Os$_4$(μ-H)$_4$(CO)$_{10}$(MeCN)$_2$ **2**, which is highly reactive and is quite unstable and prone to breakdown. Thus, the formation of Os$_5$(μ-H)$_2$(CO)$_{13}$(η^4-C$_6$H$_8$) **12** is at least feasible if fragments produced during breakdown are able to recombine and form clusters with different nuclearities from that of the starting material.

2.5 The Reactivity of Os$_4$(μ-H)$_3$(CO)$_{11}$(μ_2-η^1:η^2-C$_6$H$_9$) 3

An investigation into the reactivity of Os$_4$(μ-H)$_3$(CO)$_{11}$(μ_2-η^1:η^2-C$_6$H$_9$) **3** has revealed that it is likely to be an intermediate product on route to the formation of a μ_3-η^1:η^2-η^1 alkyne-type complex, similar to that observed in the cyclohexyne-allyl compound Os$_4$(μ-H)(CO)$_{10}$(μ_3-η^1:η^2:η^1-C$_6$H$_8$)(η^3-C$_6$H$_9$) **10**. The thermolysis of an octane solution of Os$_4$(μ-H)$_3$(CO)$_{11}$(μ_2-η^1:η^2-C$_6$H$_9$) **3** over a period of two hours appears to result in dehydrogenation of the C$_6$H$_9$ ring with the formation, in low yield, of a compound which has been tentatively formulated as the cyclohexyne complex Os$_4$(μ-H)$_2$(CO)$_{11}$(μ_3-η^1:η^2:η^1-C$_6$H$_8$) **13**. The reaction mixture consists mainly of decomposition products and unreacted starting material as well as the new product, **13**, which can be isolated by t.l.c. using a dichloromethane-hexane solution (1:3, v/v) as eluent.

The infrared spectrum (υ_{CO}) of **13** is comparable to those observed for the related acyclic alkyne complexes Os$_4$(μ-H)$_2$(CO)$_{11}$(μ_3-η^1:η^2:η^1-RC=CR') (R = H, R' = H, Ph, CMe$_3$; R = R' = Ph).[17] Its mass spectrum exhibits a parent peak at 1151 (calc. 1151) amu, after which peaks corresponding to the successive loss of several CO groups are observed. Since compound **13** is only produced in low yield, the ^{1}H NMR spectrum, recorded in CDCl$_3$, is not particularly clear owing to a low frequency to noise ratio. Nonetheless, four signals are observed at δ 3.18, 1.76, -10.46 and -21.53 ppm with relative intensities of 4:4:1:1; the two former signals are multiplet resonances which may be attributed to the four sets of geminal protons of the cyclohexyne ring, with the signal at lower frequency being associated with the two pairs nearest the cluster and that centred at δ 3.18 ppm representing those protons furthest from the metal core. The two signals at low frequency are singlet

resonances which can be attributed to two hydride ligands. Even though the spectrum is of poor quality, it is clear that the signal derived from the vinylic proton in compound **3** is no longer present. Also, only two resonances are exhibited at negative frequencies, suggesting the presence of two hydride ligands as opposed to the three found in complex **3**. This spectroscopic evidence suggests that dehydrogenation of compound **3** does infact occur and leads to the proposed formulation of compound **13** as Os$_4$(μ-H)$_2$(CO)$_{11}$(μ$_3$-η^1:η^2:η^1-C$_6$H$_8$), which is believed to contain the C$_6$H$_8$ fragment bound *via* two σ and one π bond to a triangular face of the Os$_4$ cluster unit.

The elimination of dihydrogen from σ,π-vinyl complexes of this type to yield the corresponding dihydrido alkyne products has previously been observed in the parent cluster system, Os$_4$(μ-H)$_4$(CO)$_{12}$, which undergoes reaction with the acyclic alkenes CH$_2$=CH$_2$, CH$_2$=CHPh, CH$_2$=CHCMe$_3$ and *cis*-CHPh=CHPh to give a range of complexes of formula, Os$_4$(μ-H)$_3$(CO)$_{11}$(alkene-H), containing the alkene ligand bonded to the cluster in the same manner as that observed in complex **3**.[17] These clusters loose H$_2$ upon heating, resulting in the formation of the dihydrido-complexes, Os$_4$(μ-H)$_2$(CO)$_{11}$(RC≡CR'), which contain the RC≡CR' unit coordinated to a triangular face of the Os$_4$ cluster *via* two σ and one π interaction. The conversion of an edge-bridging σ,π-vinyl complex into a face-capping alkyne-type complex has also been observed in a similar triosmium cluster system, although in this example CO is lost rather than dihydrogen. For example, Os$_3$(μ-H)(CO)$_{10}$(μ-η^1:η^2-C$_2$H$_3$) is produced from the reaction between Os$_3$(CO)$_{10}$(MeCN)$_2$ and C$_2$H$_4$ under mild conditions. On heating, this complex is transformed into the 1,1-Os$_3$(μ-H)$_2$(CO)$_9$(μ$_3$-η^1:η^1:η^2-C=CH$_2$) derivative, however, when cyclic or terminal alkenes are employed a competing sequence of 1,2-diactivations may also lead to complexes of the type Os$_3$(μ-H)$_2$(CO)$_9$(μ$_3$-η^1:η^2:η^1-RCCR).[2]

It can be speculated that the formation of the cyclohexenyl derivative, Os$_4$(μ-H)$_3$(CO)$_{11}$(μ$_2$-η^1:η^2-C$_6$H$_9$) **3**, may occur *via* a sequence involving olefin complexation of the ligand at one metal atom in an η^2 manner, followed by C-H activation at an adjacent one. On heating, this product appears to undergo a second C-H bond cleavage to form the 'yne' derivative, Os$_4$(μ-H)$_2$(CO)$_{11}$(μ$_3$-η^1:η^2:η^1-C$_6$H$_8$) **13**, in which the C$_6$H$_8$ moiety spans the tetrahedral Os$_4$ face. It is possible that this dehydrogenation process may occur firstly by proton transfer from the vinylic group to the Os$_4$ core, and then by H$_2$ ejection from the Os$_4$H$_4$ unit. The complex Os$_4$(μ-H)(CO)$_{10}$(μ$_3$-η^1:η^2:η^1-C$_6$H$_8$)(η^3-C$_6$H$_9$) **10** may be derived from Os$_4$(μ-H)$_2$(CO)$_{11}$(μ$_3$-η^1:η^2:η^1-C$_6$H$_8$) **13** by the loss of CO and coordination of a second C$_6$H$_8$ unit to the metal cluster, again *via* an η^2 interaction. Hydrogen migration from the cluster framework may follow, with C-H bond formation at an olefinic C atom of the uncoordinated diene double bond resulting in the η^3 allyl moiety.

This sequence of reactions is illustrated in Scheme 2.5; the $Os_4(\mu\text{-}H)_2(CO)_{10}(\mu_3\text{-}\eta^1{:}\eta^2{:}\eta^1\text{-}C_6H_8)(\eta^2\text{-}C_6H_8)$ complex postulated as a reaction intermediate has not been observed to date.

$Os_4(\mu\text{-}H)_2(CO)_{10}(C_6H_8)(\eta^2\text{-}C_6H_8)$
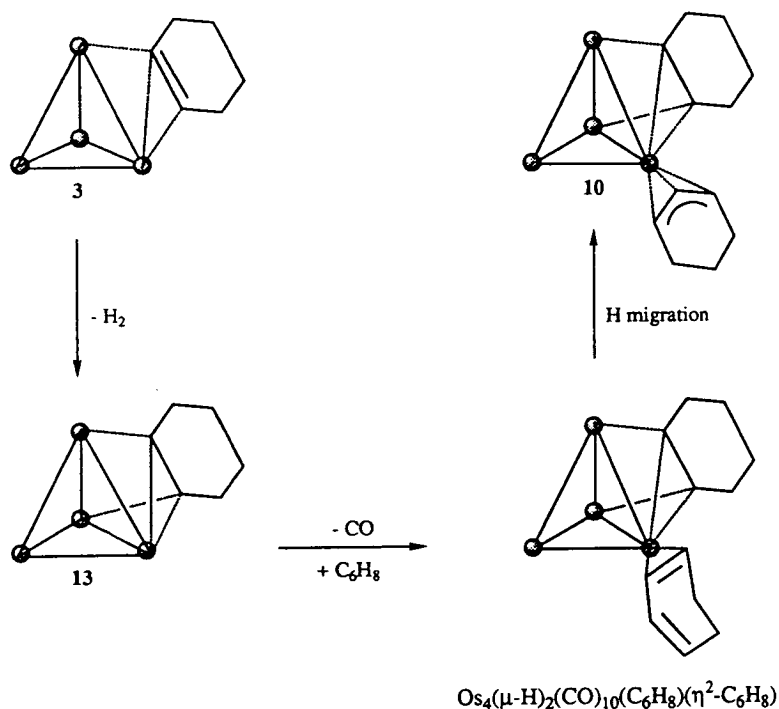
Scheme 2.5: A possible sequence of reactions for the formation of **10** from **3**.

2.6   High Nuclearity Osmium Benzene Clusters

A number of higher nuclearity benzene clusters of osmium (high nuclearity referring to clusters with five or more metal atoms, since this is where the effective atomic number rule tends to breakdown) have recently been reported in the literature,[24b-26] some of which are illustrated in Figure 2.6. The general method by which these osmium complexes are prepared involves the ionic condensation of an appropriate dianionic cluster unit with the dicationic osmium-benzene fragment, $[Os(\eta^6\text{-}C_6H_6)(MeCN)_3]^{2+}$.[38] For example, the reduction of $Os_4(\mu\text{-}H)_4(CO)_{12}$ using excess potassium-benzophenone in tetrahydrofuran yields the dianion $[Os_4(\mu\text{-}H)_4(CO)_{11}]^{2-}$, which on treatment with the capping fragment affords the pentanuclear clusters $Os_5(\mu\text{-}H)_4(CO)_{11}(\eta^6\text{-}C_6H_6)$ and $Os_5(\mu\text{-}H)_4(CO)_{12}(\eta^6\text{-}C_6H_6)$ in moderate yield.[24b] The former complex is based on a trigonal bipyramidal arrangement of osmium atoms, whilst the metal disposition of the latter species is that of an edge-bridged tetrahedron, and both complexes contain benzene in the η^6 terminal coordination mode. Alternatively, the treatment of a dichloromethane solution of $Os_4(\mu$-
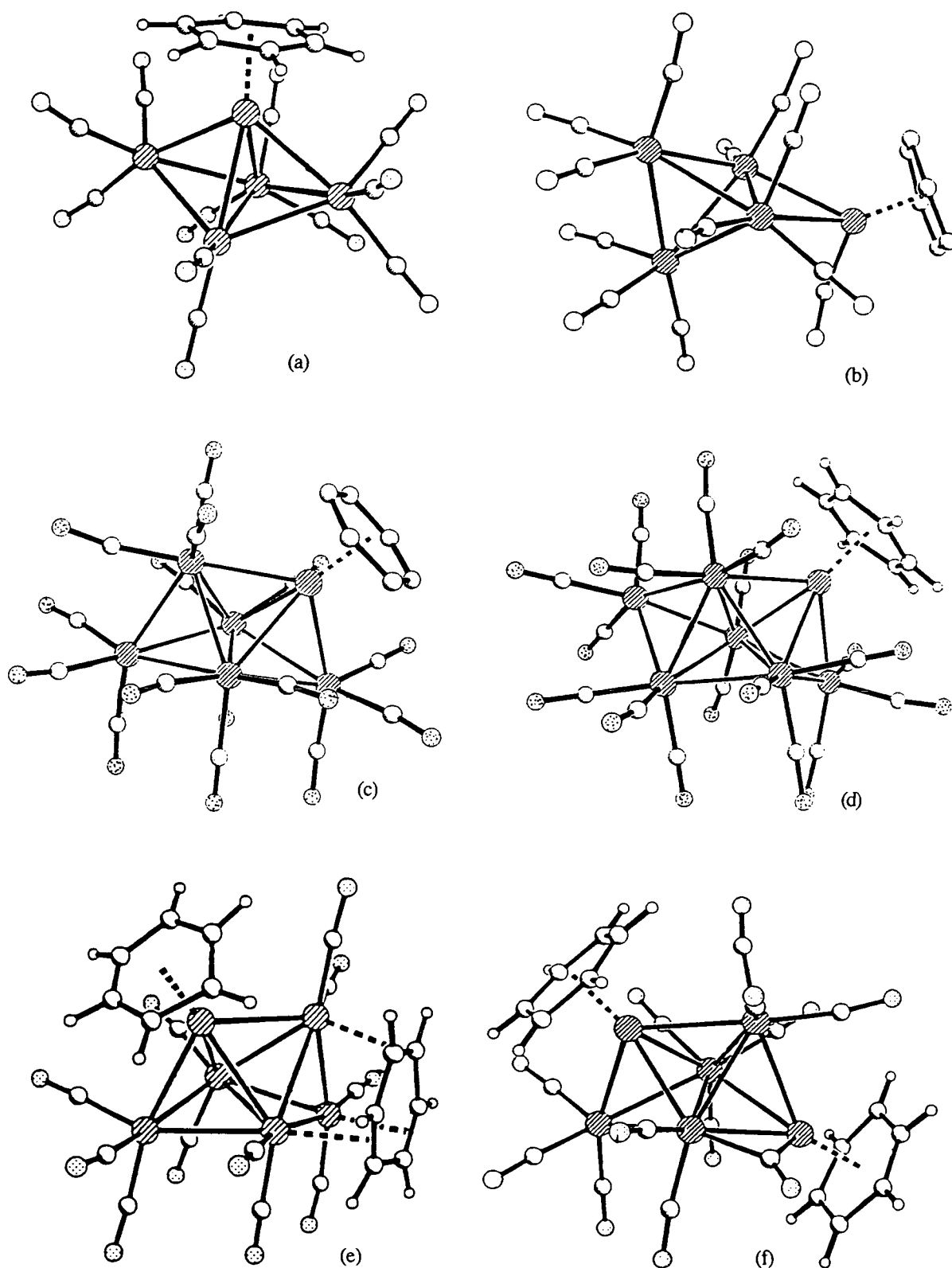
Figure 2.6: The molecular structures of (a) $Os_5(\mu-H)_4(CO)_{11}(\eta^6-C_6H_6)$, (b) $Os_5(\mu-H)_4(CO)_{12}(\eta^6-C_6H_6)$, (c) $Os_6(CO)_{15}(\eta^6-C_6H_6)$, (d) $Os_7(CO)_{17}(\eta^6-C_6H_6)$, (e) $Os_6(\mu-H)_2(CO)_{11}(\eta^6-C_6H_6)(\mu_3-\eta^2:\eta^2:\eta^2-C_6H_6)$, and (f) $Os_6(CO)_{12}(\eta^6-C_6H_6)_2$.

H)$_4$(CO)$_{12}$ with an excess of DBU (1,8-diazabicyclo[5.4.0]undeca-7-ene) affords the dianionic species [Os$_4$(μ-H)$_2$(CO)$_{12}$]$^{2-}$, which reacts with the same capping fragment to yield the cluster complex, Os$_5$(μ-H)$_2$(CO)$_{12}$(η^6-C$_6$H$_6$), which also comprises of a trigonal bipyramidal cluster framework.[25c]

In a similar manner, this cluster build-up reaction may be used in the preparation of hexa- and heptaosmium benzene-substituted clusters; the reaction of the cluster dianion [Os$_5$(CO)$_{15}$]$^{2-}$ with [Os(η^6-C$_6$H$_6$)(MeCN)$_3$]$^{2+}$ produces Os$_6$(CO)$_{15}$(η^6-C$_6$H$_6$) in good yield, whilst treatment of the hexaosmium dianionic species, [Os$_6$(CO)$_{17}$]$^{2-}$, with the capping fragment results in the heptanuclear cluster Os$_7$(CO)$_{17}$(η^6-C$_6$H$_6$).[26] In the hexanuclear cluster the metal framework geometry may be described as a bicapped tetrahedron, and that in the heptaosmium cluster can be derived from a bicapped tetrahedron with the seventh metal capping one of the two caps to give a chain of four fused tetrahedra. The η^6 benzene ligand, in each case, occupies a site on the central tetrahedron.

This capping technique may also be extended to introduce a second benzene ligand onto the cluster unit. For example, the reduction of Os$_5$(μ-H)$_4$(CO)$_{11}$(η^6-C$_6$H$_6$) with DBU affords the dianionic cluster, [Os$_5$(μ-H)$_2$(CO)$_{11}$(η^6-C$_6$H$_6$)]$^{2-}$, which can react with the capping fragment [Os(η^6-C$_6$H$_6$)(MeCN)$_3$]$^{2+}$ to produce the hexanuclear *bis*(benzene) species Os$_6$(μ-H)$_2$(CO)$_{11}$(η^6-C$_6$H$_6$)(μ_3-η^2:η^2:η^2-C$_6$H$_6$),[25b] in which the metal core comprises of a bicapped tetrahedron, and the benzene ligands adopt both the facial and terminal coordination modes. Similarly, the reaction of [Os$_5$(CO)$_{12}$(η^6-C$_6$H$_6$)]$^{2-}$ with the osmium fragment yields Os$_6$(CO)$_{12}$(η^6-C$_6$H$_6$)$_2$,[25c] although in this case both benzene groups bond to the cluster *via* η^6 interactions.

2.7   Concluding Remarks

This work has demonstrated that upon coordination to a tetraosmium cluster the cyclohexa-1,3-diene moiety may undergo hydrogenation and isomerisation producing cyclohexenyl, cyclohexyne or allylic complexes. Alternatively, C-H bond activation and dehydrogenation may occur yielding benzene derivatives. The former observations may be compared to those previously noted in the related reactions of the triosmium cluster, Os$_3$(CO)$_{10}$(MeCN)$_2$, with C$_2$H$_4$,[10] whilst the latter are thought to involve a mechanism which requires the co-operative interaction of two cyclohexa-1,3-diene molecules. Mechanistic schemes for both reaction sequences have been proposed.

It has also been shown that a terminally bonded η^6 benzene ligand may undergo arene exchange or be displaced by ligands such as acetylenes, and this behaviour is in contrast to that shown by the μ_3-η^2:η^2:η^2 coordinated form. Significantly, in virtually all the reactions described throughout this chapter the tetrahedral Os$_4$ cluster unit is maintained. This is in contrast to the general behaviour exhibited by the analogous

ruthenium cluster Ru$_4$(μ-H)$_4$(CO)$_{12}$ which undergoes M-M bond cleavage to produce both triangular and butterfly Ru$_4$ derivatives, presumably because of the weaker Ru-Ru bonds.[39] The following chapter describes how related studies on a similar ruthenium system have led to the isolation of a series of complexes based on the Ru$_4$(CO)$_{12}$(C$_6$H$_8$) cluster where the 'yne'-like unit straddles a Ru$_4$ butterfly arrangement.

2.8   References

1.   Muetterties, E.L.; *Bull. Soc. Chim. Belg.*, **1976**, *85*, 451.

2.   Adams, R.D.; Horvath, I.T.; *Prog. Inorg. Chem.*, **1985**, *33*, 127.

3.   Calvert, R.B.; Shapley, J.R.; *J. Am. Chem. Soc.*, **1977**, *99*, 5225.

4.   Calvert, R.B.; Shapley, J.R.; *J. Am. Chem. Soc.*, **1978**, *100*, 7726.

5.   Dawkins, G.M.; Green, M.; Orpen, A.G.; Stone, F.G.A.; *J. Chem. Soc., Chem. Comm.*, **1982**, 41.

6.   Shultz, A.J.; Williams, J.M.; Calvert, R.B.; Shapely, J.R.; Stucky, G.D.; *Inorg. Chem.*, **1979**, *18*, 319.

7.   Johnson, B.F.G.; Lewis, J.; Pippard, D.A.; *J. Chem. Soc., Dalton Trans.*, **1981**, 407.

8.   Lewis, J.; Johnson, B.F.G.; *Gazz. Chim. Ital.*, **1979**, *109*, 271.

9.   Orpen, A.G.; Pippard, D.; Sheldrick, G.M.; Rouse, K.D.; *Acta Cryst. (B)*, **1978**, *34*, 2466.

10.   Tachikawa, M.; Shapely, J.R.; *J. Organomet. Chem.*, **1977**, *124*, C19.

11.   Deeming A.J.; Underhill, M.; *J. Chem. Soc., Dalton Trans.*, **1974**, 1415.

12.   (a) Janowicz, A.H.; Bergman, R.G.; *J. Am. Chem. Soc.*, **1982**, *104*, 352; (b) Jones, W.D.; Fehner, F.J.; *J. Am. Chem. Soc.*, **1982**, *104*, 4240; (c) Sweet, J.R.; Graham, W.A.G.; *J. Am. Chem. Soc.*, **1983**, *105*, 305.

13.   Goudsmit, R.J.; Johnson, B.F.G.; Lewis, J.; Raithby, P.R.; Rosales, M.J.; *J. Chem. Soc., Dalton Trans.*, **1983**, 2257.

14.   Gallop, M.A.; Johnson, B.F.G.; Lewis, J.; McCamley, A.; Perutz, R.N.; *J. Chem. Soc., Chem Comm.*, **1988**, 1071.

15.   Johnson, B.F.G.; *J. Organomet. Chem.*, **1994**, *475*, 31, and references cited therein.

16.   (a) Bradford, C.W.; Nyholm, R.S.; Gainsford, G.J.; Guss, J.M.; Ireland, P.R.; Mason, R.; *J. Chem. Soc., Chem. Comm.*, **1972**, 87; (b) Gainsford, G.J.; Guss, J.M.; Ireland, P.R.; Mason, R.; Bradford, C.W.; Nyholm, R.S.; *J. Organomet. Chem.*, **1972**, *40*, C70.

17.   Bhaduri, S.; Johnson, B.F.G.; Kelland, J.W.; Lewis, J.; Raithby, P.R.; Rehani, S.; Sheldrick, G.M.; Wong, K.; McPartlin, M.; *J. Chem. Soc., Dalton Trans.*, **1979**, 562.

18.   Guy, J.J.; Reichert, B.E.; Sheldrick, G.M.; *Acta Cryst.*, **1976**, *B32*, 3319.

19.   Orpen, A.G.; XHYDEX, A Program for Locating Hydrides, Bristol University, **1980**; see also Orpen, A.G.; *J. Chem. Soc., Dalton Trans.*, **1980**, 2509.

20.   Blake, A.J.; Dyson, P.J.; Johnson, B.F.G.; Martin, C.M.; Nairn, J.G.M.; Parisini, E.; Lewis, J.; *J. Chem. Soc., Dalton Trans.*, **1993**, 981.

21.   Chen, H.; Johnson, B.F.G.; Lewis, J.; Braga, D.; Grepioni, F.; Parisini, E.; *J. Chem. Soc., Dalton Trans.*, **1991**, 215.

22.   Braga, D.; Grepioni, F.; Johnson, B.F.G.; Parisini, E.; Martinelli, M.; Gallop, M.A.; Lewis, J.; *J. Chem. Soc., Dalton Trans.*, **1992**, 807.

23.   (a) Chen, H.; Johnson, B.F.G.; Lewis, J.; Li, C.K.; Morewood, C.A.; Raithby P.R.; Ramirez de Arellano, M.C.; Wong, W.T.; *Inorg. Chim. Acta*, **1993**, 213, 177; (b) Aime, S.; Milone, L.; Osella, D.; Vaglio, G.A.; Valle, M.; Tiripicchio, A.; Tiripicchio Camellini, M.; *Inorg. Chim. Acta*, **1979**, *34*, 49.

24.   (a) Braga, D.; Grepioni, F.; Sabatino, P.; Dyson, P.J.; Johnson, B.F.G.; Lewis, J.; Bailey, P.J.; Raithby, P.R.; Stalke, D.; *J. Chem. Soc., Dalton Trans.*, **1993**, 985; (b) Braga, D.; Sabatino, P.; Dyson, P.J.; Blake, A.J.; Johnson, B.F.G.; *J. Chem. Soc., Dalton Trans.*, **1994**, 393; (c) Lewis, J.; Li, C.K.; Ramirez de Arellano, M.C.; Raithby, P.R.; Wong, W.T.; *J. Chem. Soc., Dalton Trans.*, **1993**, 1359.

25.   (a) Dyson, P.J.; Johnson, B.F.G.; Lewis, J.; Martinelli, M.; Braga, D.; Grepioni, F.; *J. Am. Chem. Soc.*, **1993**, *115*, 9062; (b) Lewis, J.; Li, C.K.; Raithby, P.R.; Wong, W.T.; *J. Chem.*

Soc., Dalton Trans., **1993**, 999; (c) Lewis, J.; Li, C.K.; Al-Mandhary, M.R.A.; Raithby, P.R.; *J. Chem. Soc., Dalton Trans.*, **1993**, 1915.

26.   Lewis, J.; Li, C.K.; Morewood, C.A.; Ramirez de Arellano, M.C.; Raithby, P.R.; Wong, W.T.; *J. Chem. Soc., Dalton Trans.*, **1994**, 2159.

27.   Johnson, B.F.G.; Martin, C.M.; Braga, D.; Grepioni, F.; Parisini, E.; *J. Chem. Soc., Chem. Comm.*, **1994**, 1253.

28.   Chen, H.; PhD Thesis, The University of Cambridge, **1990**.

29.   Johnson, B.F.G.; Nairn, J.G.M.; The University of Edinburgh, **1994**, *unpublished results*.

30.   Braga, D.; Grepioni, F.; Martin, C.M.; Parisini, E.; Dyson, P.J.; Johnson, B.F.G.; *Organometallics*, **1994**, *13*, 2170.

31.   (a) Khand, I.U.; Knox, G.R.; Pauson, P.L.; Watts, W.E.; *J. Chem. Soc., Perkin Trans.*, **1973**, *1*, 975; Kaganovich, V.S.; Rybinskaya, M.I.; *J. Organomet. Chem.*, **1988**, *344*, 383; (b) Bird, P.H.; Fraser A.R.; *J. Organomet. Chem.*, **1974**, *73*, 103; (c) Johnson, B.F.G.; Mallors, R.L.; The University of Edinburgh, **1994**, *unpublished results*.

32.   Braga, D.; Grepioni, F.; Johnson, B.F.G.; Chen, H.; Lewis, J.; *J. Chem. Soc., Dalton Trans.*, **1991**, 2559.

33.   Muetterties, E.L.; Bleeke, J.R.; Sievert, A.C.; *J. Organomet. Chem.*, **1979**, *178*, 197.

34.   Chen, H.; Johnson, B.F.G.; Lewis, J.; Braga, D.; Grepioni, F.; Sabatino, P.; *J. Organomet. Chem.*, **1991**, *405*, C22.

35.   Raithby, P.R.; Rosales, M.J.; *Adv. Inorg. Chem. & Radiochem.*, **1985**, *29*, 169.

36.   (a) Eady, C.R.; Johnson, B.F.G.; Lewis, J.; *J. Chem. Soc., Dalton Trans.*, **1975**, 2606; (b) Gade, L.H.; Johnson, B.F.G.; Lewis, J.; McPartlin, M.; Powell, H.H.; Raithby, P.R.; Wong, W.T.; *J. Chem. Soc., Dalton Trans.*, **1994**, 521 and references cited therein.

37.   Quicksall, C.O.; Spiro, T.G.; *Inorg. Chem.*, **1968**, *7*, 2365.

38.   Hung, Y.; Kung, W.J.; Taube, H.; *Inorg. Chem.*, **1981**, *20*, 457.

39.   (a) Johnson, B.F.G.; Lewis, J.; *Pure & Applied Chem.*, **1975**, *44*, 43; (b) Johnson, B.F.G.; Lewis, J.; Schorpp, K.T.; *J. Organomet. Chem.*, **1975**, *91*, C13.

Chapter Three

Reactions of $Ru_3(CO)_{12}$ with Cyclic C_6 Alkenes

This chapter commences with a description of some general butterfly cluster compounds, giving reasons for their attraction to the organometallic chemist. This is followed by a detailed discussion of the preparation and full chemical and structural characterisation of a number of such tetraruthenium compounds. A feature of these butterfly clusters is that they contain ligands derived from the dehydrogenation and/or isomerisation of cyclic C_6 alkenes (*i.e.* C_6H_8 and C_6H_{10}), showing that C-H bond activation is a dominant reaction pathway in these systems. The formation of a cluster containing a methyl-cyclopentadienyl moiety also suggests that the cluster unit may bring about C-C bond cleavage and ring contraction; a process which is comparable to the phenomena observed on the metal surface. An octanuclear-benzene cluster has also been isolated, allowing the study of benzene-cluster interactions to be extended to nuclearities greater than six. Reaction mechanisms for the interconversion of two isomeric butterfly clusters and also for the ring contraction process have been postulated, and finally, an analysis of the crystal packing displayed by a number of complexes described throughout the chapter has been undertaken.

3.1 An Introduction

A number of factors have contributed to the current interest in butterfly clusters, and this area is the subject of a recent review article.[1] The tetranuclear butterfly framework represents an intermediate structure between the tetrahedral and square planar or 'spiked' triangular clusters, and the geometry may also be regarded as a model for the chemisorption of small molecules on the step site of a metal surface,[2] this latter relationship being illustrated in Figure 3.1.1. The M_4 butterfly clusters contain an open polyhedral framework of metal atoms and are therefore structurally versatile units, with a wide variation in structural geometry being accommodated within their general descriptions. Dihedral angles between the two butterfly wings can range from 90°, for those clusters approaching a tetrahedral framework, to nearly 180° for planar systems, and within the two deltahedral fragments metal-metal interactions may also vary considerably in strength. A number of factors including the electronic structure and skeletal electron count of the butterfly, steric effects, and coordinating properties of the constituent ligands are expected to influence these geometrical features of the M_4 skeleton. It is also apparent that small ligands (such as carbido atoms) coordinated within the cavity of a butterfly framework may exhibit unusual

patterns of chemical reactivity, and it is uncertain whether the particular coordination environment of the ligand or the malleability of the cluster is responsible for this reactivity.
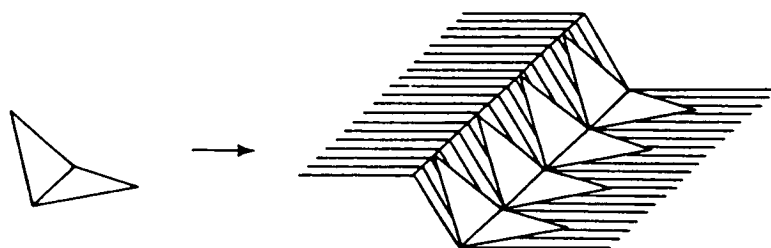

Figure 3.1.1: An idealised relationship between the butterfly cluster and superficial 'steps' on a metal surface.

In the conventional EAN rule derivation of the butterfly framework, the addition of an electron pair to a closed 60-electron tetrahedron causes M-M bond rupture, presumably *via* population of an antibonding molecular orbital with respect to the skeleton. If this argument is extended, the addition of a second electron pair should result in a transformation of the butterfly to a square or spiked triangular geometry containing four M-M bonds. Thus, in terms of simple electron counting arguments, the butterfly configuration is associated with 62 metal-plus-ligand electrons and the square or spiked triangle with 64 valence electrons.[1] However, whereas M-M bond rupture on the two electron reduction of (or donor ligand addition to) a metal cluster is a well accepted principle,[3] the consecutive ligand addition leading to the precise structural changes outlined above is quite rare. One such example is the series of clusters $Os_4(CO)_{14}$, $Os_4(CO)_{15}$ and $Os_4(CO)_{16}$, that contain 60, 62 and 64-electron counts respectively, and whose corresponding structures are tetrahedral, planar butterfly and square.[4]

In terms of the polyhedral skeletal electron pair theory (PSEPT),[5] a 60-electron tetrahedron is represented as a *nido* cluster based on a trigonal bipyramid with one missing vertex, and therefore the 62-electron butterfly may be described as an *arachno* cluster derived from an octahedron (see Figure 3.1.2). An alternative view of generating the butterfly configuration, based on skeletal electron pair theory, is by edge-bridging a closed 48-electron triangular cluster with a $M(CO)_4$ fragment.[6] This would produce the same total number of skeletal bonding MO's and an electron count of 62 (48 + 14) as required.

The formation of butterfly clusters containing cyclohexyne and benzene ligands derived from cyclic C₆ alkenes demonstrates that C-H bond activation is a prominent reaction taking place in the presence of these ruthenium clusters. The factors controlling the activation of C-H bonds by such clusters are difficult to define, however they are thought to be of considerable significance. The catalytic transformation of C₆ and C₈ cyclic
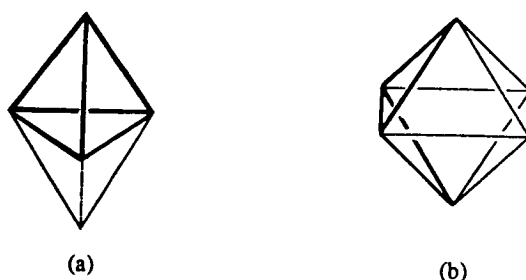
Figure 3.1.2: PSEPT view of (a) the 60-electron, *nido* (6 skeletal pairs, 4 vertices) tetrahedron, and (b) the 62-electron, *arachno* (7 skeletal pairs, 4 vertices) butterfly clusters.

hydrocarbons is of great importance, and it is known that metals such as platinum are highly effective in activating both C-H and C-C bonds within these organic molecules.[7,8] Studies of the adsorption and subsequent reactions of hydrocarbons such as cyclohexane, cyclohexene and cyclohexadiene on the Pt(111) or Ni(111) surface have revealed that the dominating chemistry is their dehydrogenation to benzene.[7] The initial interaction between an alkene and the surface atoms involves the π and π^* orbitals of the molecule, such that the unsaturated C-C bond lies almost parallel to the surface plane. If the alkene is cyclohexene or cyclohexadiene, the hydrogen atoms of the C-H bonds closely approach the metal surface and are therefore susceptible to facile bond cleavage.[7] This behaviour appears to be mimicked by related cluster compounds and it is therefore likely that a similar dehydrogenation process occurs on the surface of deltahedral clusters of ruthenium. Model compounds corresponding to the adsorption and successive dehydrogenation of cyclohexene and cyclohexadiene are described throughout this chapter, thus indicating that the cleavage of both saturated and unsaturated C-H bonds can occur. It is also apparent that coordinated cyclohexene may be converted to a methylcyclopentadienyl moiety which not only requires the activation of C-H bonds but also the activation of a C-C bond within the C_6 hydrocarbon.

3.2 Reaction of Ru₃(CO)₁₂ 14 with Cyclohexa-1,3-diene: The Molecular Structures of Ru₄(CO)₁₂(μ_4-η^1:η^1:η^2:η^2-C₆H₈) 15 and the Isomeric Pair, Ru₄(CO)₉(μ_4-η^1:η^1:η^2:η^2-C₆H₈)(η^6-C₆H₆) 16 and 17

The thermolysis of Ru₃(CO)₁₂ 14 in octane containing an excess of cyclohexa-1,3-diene affords a range of products which may be isolated from the reaction mixture by chromatographic separation on silica using a dichloromethane-hexane solution (3:7, v/v) as eluent. A total of four compounds have been characterised which include two major

products, *viz.* the tetranuclear cluster $Ru_4(CO)_{12}(\mu_4-\eta^1:\eta^1:\eta^2:\eta^2-C_6H_8)$ **15** and the hexanuclear-carbido benzene species $Ru_6C(CO)_{14}(\eta^6-C_6H_6)$ **18**, together with two isomeric compounds with the formula $Ru_4(CO)_9(\mu_4-\eta^1:\eta^1:\eta^2:\eta^2-C_6H_8)(\eta^6-C_6H_6)$ **16** and **17**, which are produced in moderate and low yields, respectively. This reaction is illustrated by Scheme 3.2.
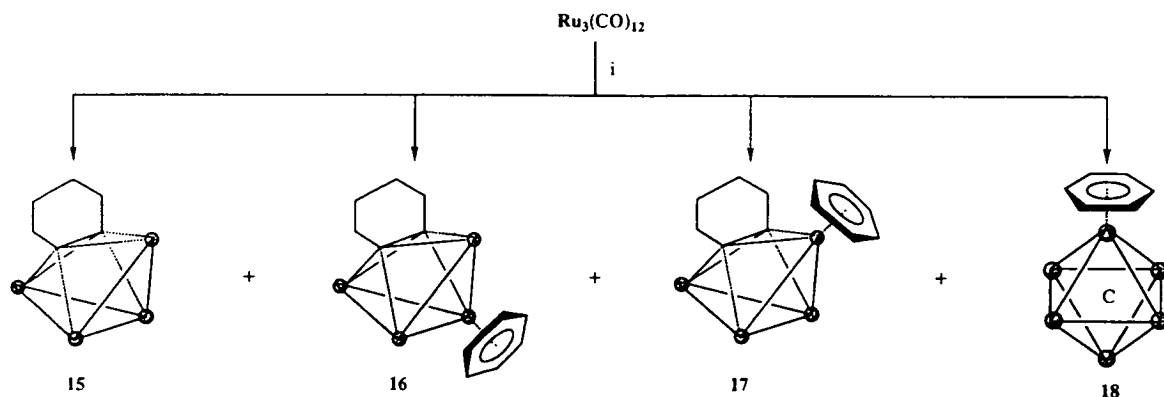
Scheme 3.2: The reaction of $Ru_3(CO)_{12}$ **14** with cyclohexa-1,3-diene. (i) Δ, octane/1,3-C_6H_8.

The molecular formula of **15** was initially proposed by a comparison of its infrared spectrum (υ_{CO}) with those recorded for the related alkyne compounds $Ru_4(CO)_{12}(\mu_4-\eta^1:\eta^1:\eta^2:\eta^2-C_2Ph_2)$ [9] and $Ru_4(CO)_{12}(\mu_4-\eta^1:\eta^1:\eta^2:\eta^2-C_2Me_2)$.[10] The three spectra are very similar, both in profile and wavenumber, and hence formulation of **15** as $Ru_4(CO)_{12}(\mu_4-\eta^1:\eta^1:\eta^2:\eta^2-C_6H_8)$ appeared reasonable. The molecular formula was further substantiated on evidence provided by mass and ^{1}H NMR spectroscopy. The mass spectrum of **15** exhibits a parent peak at m/z 821 (calc. 821) followed by the loss of twelve distinct carbonyl groups in succession, and the ^{1}H NMR spectrum, in CDCl₃, contains two multiplet resonances of equal relative intensity at δ 3.35 and 1.82 ppm which may be readily assigned to the eight aliphatic ring protons of the cyclohexyne moiety.

The molecular structure of $Ru_4(CO)_{12}(\mu_4-\eta^1:\eta^1:\eta^2:\eta^2-C_6H_8)$ **15**, as determined by X-ray diffraction methods on a crystal grown from a toluene solution at -25°C, is shown in Figure 3.2.1 together with some relevant structural parameters. The Ru₄ skeleton of the cyclohexyne cluster, $Ru_4(CO)_{12}(\mu_4-\eta^1:\eta^1:\eta^2:\eta^2-C_6H_8)$ **15**, takes the form of a butterfly. However, two carbon atoms of the cyclohexyne ligand occupy the vacant sites of the *arachno* structure described above, leading to a *pseudo closo*-octahedral description for the skeletal framework of this molecule. The cyclohexyne moiety is trapped between the two wings, with the alkyne C-C bond disposed parallel to the hinge of the Ru₄ butterfly. This ligand, derived from the isomerisation of cyclohexa-1,3-diene, bonds to all four metal
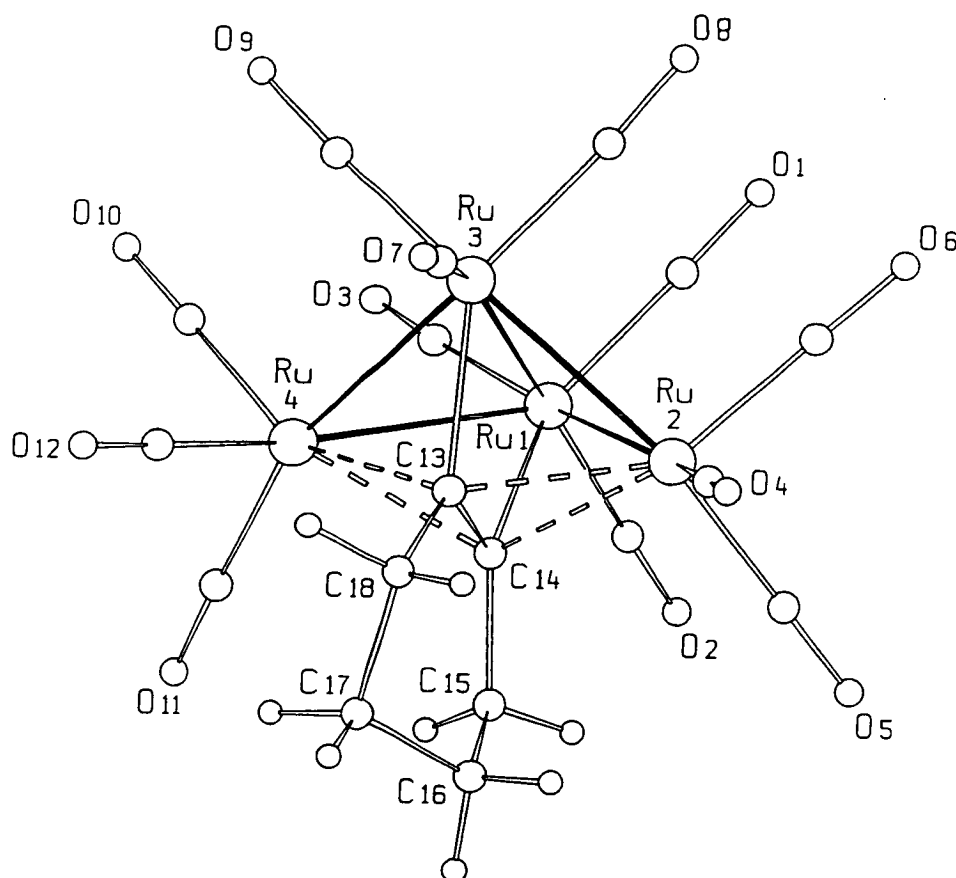
Figure 3.2.1: The molecular structure of $Ru_4(CO)_{12}(\mu_4\text{-}\eta^1{:}\eta^1{:}\eta^2{:}\eta^2\text{-}C_6H_8)$ **15** in the solid-state showing the atomic labelling scheme. The C-atoms of the CO ligands bear the same numbering as the corresponding O-atoms. Relevant bond distances (Å) and angles (°) include: Ru(1)-Ru(2) 2.743(2), Ru(1)-Ru(3) 2.849(3), Ru(1)-Ru(4) 2.725(2), Ru(2)-Ru(3) 2.727(2), Ru(3)-Ru(4) 2.721(2), mean Ru-C(CO) 1.912(5), mean C-O 1.136(6), Ru(1)-C(14) 2.123(5), Ru(2)-C(13) 2.243(5), Ru(2)-C(14) 2.244(4), Ru(3)-C(13) 2.146(4), Ru(4)-C(13) 2.234(5), Ru(4)-C(14) 2.246(5), C(13)-C(14) 1.455(7), C(13)-C(18) 1.521(7), C(14)-C(15) 1.534(6), C(15)-C(16) 1.525(7), C(16)-C(17) 1.505(7), C(17)-C(18) 1.543(6), C(13)-C(14)-C(15) 121.4(4), C(14)-C(15)-C(16) 112.2(4), C(15)-C(16)-C(17) 110.9(4), C(16)-C(17)-C(18) 111.2(4), C(17)-C(18)-C(13) 110.4(4), C(18)-C(13)-C(14) 121.5(4). Angle between planes defined by Ru(1)-Ru(2)-Ru(3) and Ru(1)-Ru(3)-Ru(4) 115.8°.

atoms and donates a total of six electrons to the cluster framework *via* two σ-interactions with the hinge atoms and two π-interactions with the wing-tip atoms. The electron count is therefore in accordance with Wade's system, with a total of 62 electrons corresponding to an 'ideal' butterfly or a 14-electron *closo*-octahedron (N = 7). The electron donation from the acetylenic bond to the cluster unit results in a lengthening of the C-C bond [C(13)-C(14) 1.455(7) Å], and the conformation of the cyclic ligand is that of a half chair due to the bonding and steric requirements of the metal cluster. The two Ru-C σ-bonds formed by

carbon atoms C(13) and C(14) with the two hinge atoms of the cluster [Ru(1)-C(14) 2.123(5) and Ru(3)-C(13) 2.146(4) Å] are shorter than the two π-bonds formed with the wing-tip atoms [Ru(2)-C(13) 2.243(5), Ru(2)-C(14) 2.244(4) and Ru(4)-C(13) 2.234(5), Ru(4)-C(14) 2.246(5) Å], and the C(13)-C(14) bond is positioned almost equidistant from Ru(2) and Ru(4). The cyclohexyne ligand in this molecule is captured between the butterfly wings in a manner very similar that observed in a number of acetylenic or cyclooctadieneic cluster complexes, for example; $Ru_4(CO)_{12}(C_2Ph_2)$,[9] $Ru_4(CO)_{12}(C_2Me_2)$,[10] $Ru_4(CO)_{11}(C_8H_{10})$,[11,12] $Ru_4(CO)_{12}(C_8H_{10})$,[11] $Ru_4(CO)_{12}(C_8H_{12})$,[11] and $Co_4(CO)_{10}(C_2Et_2)$.[13] A few M_4C_3 pentagonal bipyramidal cores are also known, and in these an allylic ligand coordinates to the butterfly cluster in a similar fashion [*e.g.* $Ru_4(CO)_{10}(C_{12}H_{16})$].[14]

In common with other butterfly structures of ruthenium, the hinge of the cluster [Ru(1)-Ru(3)] is significantly longer than the other four edges [2.849(3) *vs.* range 2.721(2) - 2.743(2) Å, mean 2.729(2) Å]. The dihedral angle between the two planes containing Ru(1)-Ru(2)-Ru(3) and Ru(1)-Ru(3)-Ru(4) is 115.8°, this angle lying in the narrow range (112-118°) that is commonly observed for these M_4C_2 systems and is thought to arise from the steric restrictions imposed on the M_4 framework by the coordinated alkyne. Each ruthenium atom also bears three terminal carbonyl groups, with an average Ru-C(CO) bond distance of 1.912(5) Å.

The two isomeric compounds of formula $Ru_4(CO)_9(\mu_4-\eta^1{:}\eta^1{:}\eta^2{:}\eta^2-C_6H_8)(\eta^6-C_6H_6)$, **16** and **17**, differ in the relative location of the benzene ring. They were characterised in the first instance by a combination of infrared, mass and ^1H NMR spectroscopic techniques. The infrared spectra of the two isomers show peaks in the terminal carbonyl region only (between 2060 - 1924 and 2065 - 1958 cm^{-1} for **16** and **17**, respectively), with the spectrum of **16** being almost identical to that of a similar compound reported previously by Milone *et al*,[15] (*vide infra*). The mass spectra of **16** and **17** exhibit parent ions at 815 and 816 (calc. 815) amu respectively, which are followed by peaks corresponding to the sequential loss of several carbonyl groups. The ^1H NMR spectra are also very similar with both complexes displaying three resonances; a singlet and two multiplets with relative intensities of 3:2:2, corresponding to the six protons of the benzene ring and the eight protons of the cyclohexyne moiety [**16**: δ 5.52 (s, 6H), 3.27 (m, 4H), 1.82 (m, 4H) ppm; **17**: δ 5.67 (s, 6H), 3.37 (m, 4H), 1.80 (m, 4H) ppm]. The singlet resonances at δ 5.52 and 5.67 ppm for **16** and **17**, respectively, are consistent with the presence of benzene coordinated in an η^6 mode, and the multiplet resonances, attributed to the cyclohexyne protons, have chemical shifts in keeping with those observed for the cyclohexyne unit in $Ru_4(CO)_{12}(\mu_4-\eta^1{:}\eta^1{:}\eta^2{:}\eta^2-C_6H_8)$ **15**.
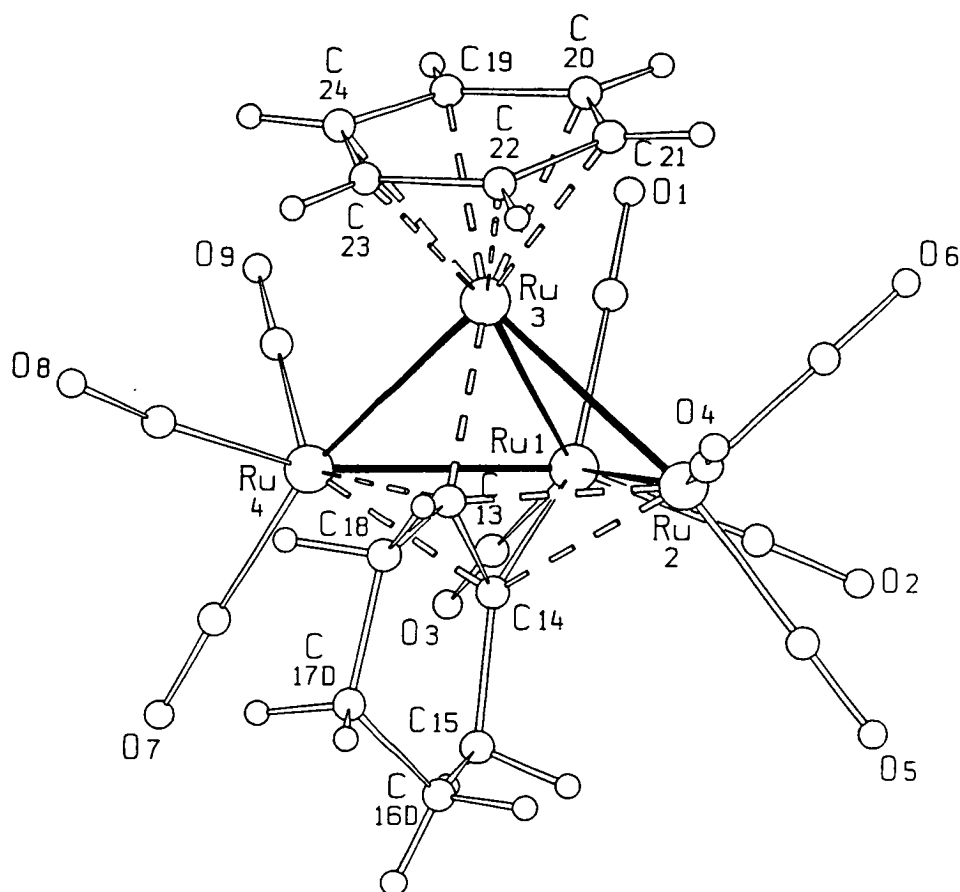
Figure 3.2.2: The molecular structure of Ru$_4$(CO)$_9$(μ_4-η^1:η^1:η^2:η^2-C$_6$H$_8$)(η^6-C$_6$H$_6$) **16** in the solid-state showing the atomic labelling scheme. The C-atoms of the CO ligands bear the same numbering as the corresponding O-atoms. Relevant bond distances (Å) and angles (°) include: Ru(1)-Ru(2) 2.7057(8), Ru(1)-Ru(3) 2.8105(8), Ru(1)-Ru(4) 2.6940(8), Ru(2)-Ru(3) 2.6476(7), Ru(3)-Ru(4) 2.6579(5), mean Ru-C(CO) 1.897(7), mean C-O 1.136(9), Ru(1)-C(14) 2.170(5), Ru(2)-C(13) 2.223(5), Ru(2)-C(14) 2.245(5), Ru(3)-C(13) 2.073(5), Ru(4)-C(13) 2.251(5), Ru(4)-C(14) 2.272(5), C(13)-C(14) 1.43(1), C(13)-C(18) 1.54(1), C(14)-C(15) 1.52(1), C(15)-C(16) 1.52(1), C(15)-C(16D) 1.49(1), C(16)-C(17) 1.53(2), C(16)-C(17D) 1.46(2), C(17)-C(18) 1.51(1), C(17D)-C(18) 1.51(2), Ru(3)-C(19) 2.207(7), Ru(3)-C(20) 2.239(6), Ru(3)-C(21) 2.260(7), Ru(3)-C(22) 2.208(6), Ru(3)-C(23) 2.184(7), Ru(3)-C(24) 2.225(7), C(13)-C(14)-C(15) 122(1), C(14)-C(15)-C(16) 110(1), C(14)-C(15)-C(16D) 115(1), C(15)-C(16)-C(17) 110(1), C(15)-C(16D)-C(17D) 113(2), C(16)-C(17)-C(18) 109(1), C(16D)-C(17D)-C(18) 118(2), C(17)-C(18)-C(13) 112(1), C(18)-C(13)-C(14) 121(1). Angle between planes defined by Ru(1)-Ru(2)-Ru(3) and Ru(1)-Ru(3)-Ru(4) 118.5°.

The molecular structures of Ru$_4$(CO)$_9$(μ_4-η^1:η^1:η^2:η^2-C$_6$H$_8$)(η^6-C$_6$H$_6$) **16** and **17** have been determined by X-ray diffraction methods on crystals grown from toluene at -25°C for **16**, and from the slow-evaporation of a dichloromethane-hexane solution for **17**,

and are shown in Figures 3.2.2 and 3.2.3, respectively, accompanied by selected bond lengths and angles. Two independent molecules are present in the asymmetric unit of compound **17**. In each case the established structure is in agreement with that derived from spectroscopic techniques. The two isomeric forms of $Ru_4(CO)_9(\mu_4\text{-}\eta^1\text{:}\eta^1\text{:}\eta^2\text{:}\eta^2\text{-}C_6H_8)(\eta^6\text{-}C_6H_6)$ **16** and **17**, contain the same structural features as $Ru_4(CO)_{12}(\mu_4\text{-}\eta^1\text{:}\eta^1\text{:}\eta^2\text{:}\eta^2\text{-}C_6H_8)$ **15**, however in **16**, three carbonyls on a 'hinge' ruthenium atom have been substituted by a benzene moiety, whereas in **17** the benzene replaces a tricarbonyl unit on a wing-tip ruthenium atom.

The same basic structural features observed in $Ru_4(CO)_{12}(\mu_4\text{-}\eta^1\text{:}\eta^1\text{:}\eta^2\text{:}\eta^2\text{-}C_6H_8)$ **15** are retained upon replacement of three terminal carbonyl groups by a benzene ligand. Figure 3.2.2 shows that in **16** the benzene coordinates to a hinge ruthenium atom [Ru(3)] of the butterfly framework in an η^6 fashion. The cyclohexyne unit in this structure is disordered showing two orientations of the outer part of the ring. These two different possibilities for ring orientation are in fact equivalent by idealised molecular symmetry and are equally occupied in the solid-state. Since ring-flipping in the solid-state is a well established phenomenon,[16] it was thought that the disorder in **16** may arise from a dynamic process. The flipping of the C_6H_8 ring from one conformation to the other was simulated *via* a rotation of the $H_2C(16)\text{-}C(17)H_2$ unit about the axis passing through the midpoint of the C(13)-C(14) bond, with the *inter*molecular atom-atom potential energy being recalculated at 10° rotational steps for a full 360° rotation. Similar procedures have previously been successfully applied to the rationalisation of several dynamic processes occurring in the solid-state.[16] Although the model is admittedly crude, it allows for a comparison between the two conformations. The barrier to interconversion is estimated to be very low (*ca.* 3.4 kJmol⁻¹) which allows the assumption that the disorder in the crystal structure of **16** is likely to be dynamic in origin to be made with some degree of confidence.

A slight difference is seen in the average metal-metal bond distance of $Ru_4(CO)_9(\mu_4\text{-}\eta^1\text{:}\eta^1\text{:}\eta^2\text{:}\eta^2\text{-}C_6H_8)(\eta^6\text{-}C_6H_6)$ **16** when compared to that of its precursor, $Ru_4(CO)_{12}(\mu_4\text{-}\eta^1\text{:}\eta^1\text{:}\eta^2\text{:}\eta^2\text{-}C_6H_8)$ **15**, [2.7031(8) *vs.* 2.753(2)]. As in the structure of **15**, the hinge Ru-Ru bond is longer [2.8105(8) Å] than the remaining four Ru-Ru distances. However, in contrast to the structure of **15**, the two Ru-Ru edges that link the hinge atom bearing the benzene moiety [Ru(3)] to the two wing-tip ruthenium atoms are notably shorter than the remaining two edges [Ru(2)-Ru(3) 2.6476(7), Ru(3)-Ru(4) 2.6579(5) *vs.* Ru(1)-Ru(2) 2.7057(8), Ru(1)-Ru(4) 2.6940(8) Å]. It is possible that these overall bond 'shrinkages' may be attributed to the less efficient π-accepting capability of the benzene ligand with respect to three carbonyl groups, hence resulting in a slight increase of bonding electron density over the metal framework, which is localised especially on Ru(3).

The cyclohexyne ligand lies between the wings of the butterfly in a manner reminiscent of that observed in Ru$_4$(CO)$_{12}$(μ_4-η^1:η^1:η^2:η^2-C$_6$H$_8$) **15**; its alkyne bond interacts with all four metal atoms and donates six electrons to the cluster *via* two σ- and two π-interactions, thus giving rise to a total electron count of 62. However whereas in **15** the cyclohexyne moiety sits approximately central with respect to the hinge ruthenium atoms, in **16** the ligand is slightly displaced towards Ru(3), as evidenced by a shorter hinge-to-ring distance [Ru(3)-C(13) 2.073(5) *vs.* Ru(1)-C(14) 2.170(5) Å]. This situation can be likened to that observed in hexaruthenium clusters of the type Ru$_6$C(CO)$_{14}$(η^6-arene), in which the carbide atom is always slightly displaced towards the Ru-atom bearing the arene ligand.[17]

Prior to this structure determination, a polymorphic modification of compound **16** had been reported by Milone *et al.*[15] In terms of molecular geometry, this previous structure is very similar to that reported here with the average Ru-Ru and Ru-C(CO) bond lengths of 2.704(3) and 1.88(1) Å being directly comparable to those observed in **16**. However, although the interaction of the C$_6$H$_8$ ligand at the metal centre is the same in both cases, in the previously reported structure this ligand does not show disorder.

The structure of Ru$_4$(CO)$_9$(μ_4-η^1:η^1:η^2:η^2-C$_6$H$_8$)(η^6-C$_6$H$_6$) **17** can again be derived from Ru$_4$(CO)$_{12}$(μ_4-η^1:η^1:η^2:η^2-C$_6$H$_8$) **15** by substituting three terminal carbonyls coordinated to a wing-tip ruthenium atom [in this case Ru(4)] for a benzene ligand (see Figure 3.2.3). The same general features found in the structures of compounds **15** and **16** are once again observed, however the shortening of the bond lengths seen on passing from **15** to **16** are not as significant on going from **15** to **17** [mean Ru-Ru and Ru-C(CO) bond lengths are 2.741(2) and 1.92(2), respectively]. As in structures **15** and **16**, the hinge bond length of 2.812(2) Å is longer than the remaining Ru-Ru bond distances [which range from 2.706(2) to 2.740(2) Å over the two independent molecules]. The cyclohexyne ligand lies parallel to the hinge of the butterfly cluster and interacts with all four metal atoms in the usual manner. The C-C alkyne bond is slightly displaced towards the ruthenium atom bearing the benzene ring [mean Ru-C(cyclohexyne) 2.17(2) *vs.* 2.25(2) Å, for Ru(4) and Ru(2) respectively] an effect previously noted in the structure of **16**. The asymmetric unit of the crystal cell contains two independent molecules which differ essentially in a slight variation in the orientation of the 'half chair' of the cyclohexyne moiety, indicating the probability of dynamical processes in the solid-state (*vide infra*). Once again the cluster contains a total of 62 valence electrons, which may be rationalised in terms of the EAN rule and PSEPT.
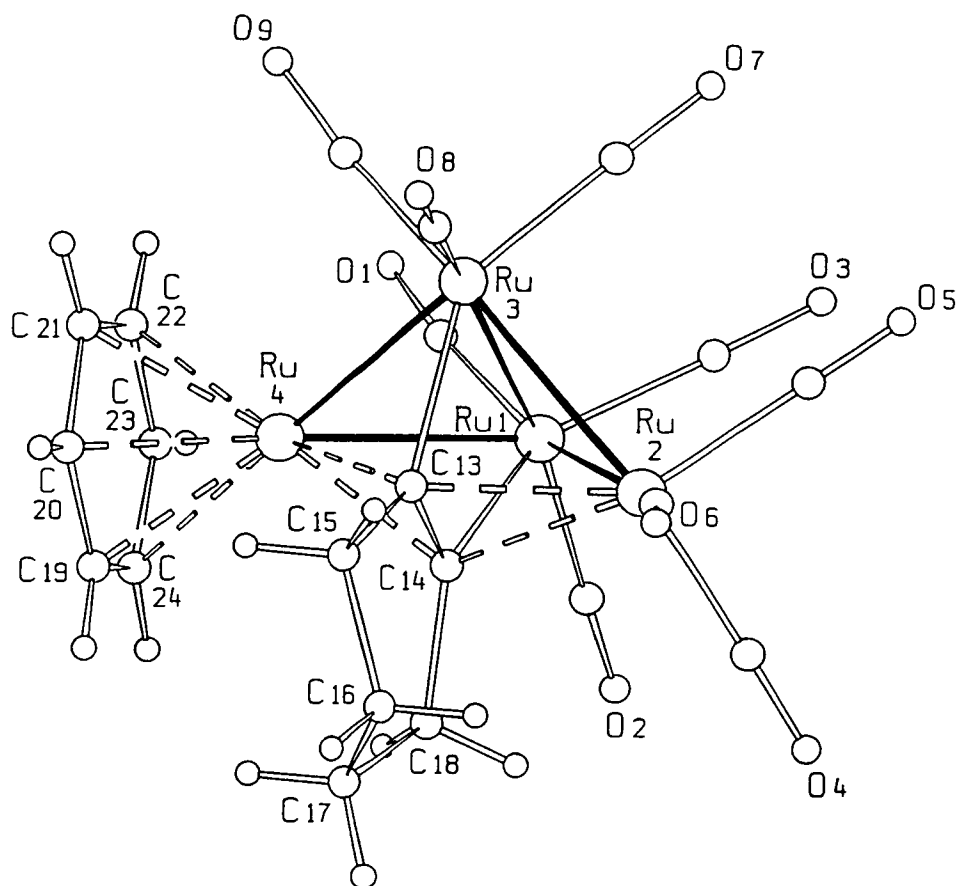
Figure 3.2.3: The molecular structure of Ru₄(CO)₉(μ₄-η¹:η¹:η²:η²-C₆H₈)(η⁶-C₆H₆) **17** in the solid-state showing the atomic labelling scheme. The C-atoms of the CO ligands bear the same numbering as the corresponding O-atoms. Relevant bond distances (Å) and angles (°) for the two independent molecules include: Ru(1)-Ru(2) 2.733(2) 2.731(2), Ru(1)-Ru(3) 2.812(2) 2.812(2), Ru(1)-Ru(4) 2.728(2) 2.708(2), Ru(2)-Ru(3) 2.722(2) 2.729(2), Ru(3)-Ru(4) 2.715(2) 2.716(2), mean Ru-C(CO) 1.92(2) 1.92(2), mean C-O 1.14(3) 1.12(3), Ru(1)-C(14) 2.11(2) 2.18(2), Ru(2)-C(13) 2.21(2) 2.29(2), Ru(2)-C(14) 2.26(2) 2.25(2), Ru(3)-C(13) 2.15(2) 2.16(2), Ru(4)-C(13) 2.18(2) 2.14(2), Ru(4)-C(14) 2.16(2) 2.20(2), C(13)-C(14) 1.45(3) 1.48(3), C(13)-C(18) 1.57(3) 1.53(3), C(14)-C(15) 1.57(3) 1.52(3), C(15)-C(16) 1.60(3) 1.53(3), C(16)-C(17) 1.56(3) 1.51(3), C(17)-C(18) 1.50(3) 1.56(3), Ru(4)-C(19) 2.21(2) 2.19(2), Ru(4)-C(20) 2.23(2) 2.19(2), Ru(4)-C(21) 2.23(2) 2.22(2), Ru(4)-C(22) 2.19(2) 2.19(2), Ru(4)-C(23) 2.19(2) 2.18(2), Ru(4)-C(24) 2.23(2) 2.19(2), C(13)-C(14)-C(15) 123(2) 123(2), C(14)-C(15)-C(16) 113(2) 110(2), C(15)-C(16)-C(17) 111(2) 112(2), C(16)-C(17)-C(18) 113(2) 115(2), C(17)-C(18)-C(13) 112(2) 110(2), C(18)-C(13)-C(14) 120(2) 122(2). Angle between planes defined by Ru(1)-Ru(2)-Ru(3) and Ru(1)-Ru(3)-Ru(4) 113.0 and 112.6°.

The final product from the reaction, **18**, was identified as Ru₆C(CO)₁₄(η⁶-C₆H₆) by a comparison of its infrared spectrum with the literature values, and the formula was substantiated by mass and ¹H NMR spectroscopic analysis. The hexanuclear-carbido cluster Ru₆C(CO)₁₄(η⁶-C₆H₆) **18** has been previously observed on numerous occasions and its molecular structure determined by a single crystal X-ray analysis.[18]

3.3 Interconversion of Isomers and Mechanistic Proposals

A series of separate experiments have established that the hinge isomer, **16**, is the major product obtained from the thermolysis of Ru$_4$(CO)$_{12}$(μ_4-η^1:η^1:η^2:η^2-C$_6$H$_8$) **15** in octane containing cyclohexa-1,3-diene, whilst reaction of **15** with Me$_3$NO in the presence of cyclohexa-1,3-diene at low temperature affords mainly the alternative wing-tip isomer **17**. Furthermore, compound **17** can be converted quantitatively into **16** by heating to reflux in octane, although when the heat is removed the hinge isomer **16** slowly reverts back into **17**, the wing-tip isomer. It has also been established that the process by which **16** is transformed back into **17** can be accelerated by exposing a hexane solution to Pyrex-filtered (> 300 nm) broad band radiation, with a photolysis period of just ten minutes resulting in its quantitative conversion. This series of reactions are summarised in Scheme 3.3.1.
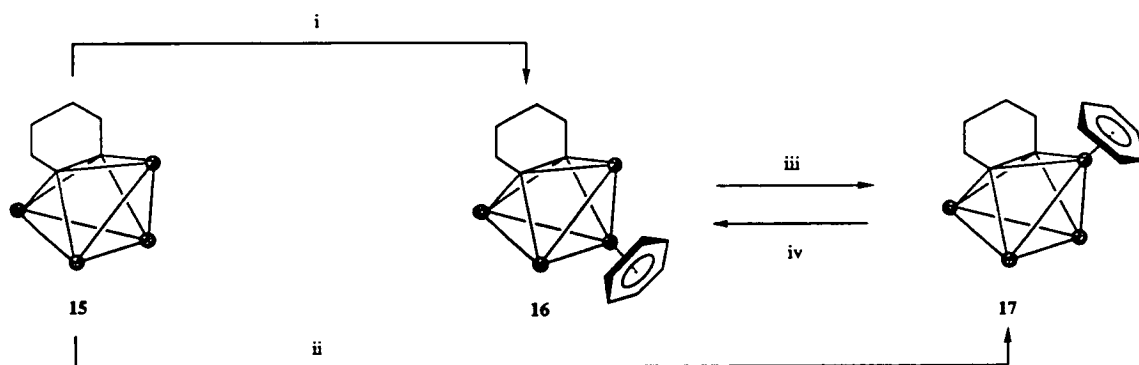
Scheme 3.3.1: The reaction of Ru$_4$(CO)$_{12}$(μ_4-η^1:η^1:η^2:η^2-C$_6$H$_8$) **15** with cyclohexa-1,3-diene, and the interconversion of the resulting products. (i) Δ, octane/1,3-C$_6$H$_8$, (ii) 3.2 equiv. Me$_3$NO/CH$_2$Cl$_2$/1,3-C$_6$H$_8$, -78°C, (iii) Δ, octane, (iv) Hexane, R.T., or hυ.

It is believed that two distinctly different mechanisms operate in the interconversion of the two isomeric forms of Ru$_4$(CO)$_9$(μ_4-η^1:η^1:η^2:η^2-C$_6$H$_8$)(η^6-C$_6$H$_6$) **16** and **17**. The migration of the benzene ligand from a hinge position to a wing-tip ruthenium atom is thought to involve the slippage of the benzene moiety over the cluster framework, possibly *via* the intermediacy of an edge-bridged (μ_2-η^3:η^3) arene molecule (see Scheme 3.3.2). This is considered to be a low energy process and therefore occurs at ambient temperatures, although it can be accelerated upon photolysis. Arene migration, either from a facial to a terminal site or from one η^6 site to another, in carbonyl clusters of ruthenium has been thought to occur *via* this type of mechanism on several occasions.[19] A cluster complex

containing an arene ligand in the edge-bridging (μ_2-η^3:η^3) coordination mode has yet to be isolated, however such a bonding mode has been observed in a dinuclear complex, and is discussed in further detail in chapter five.
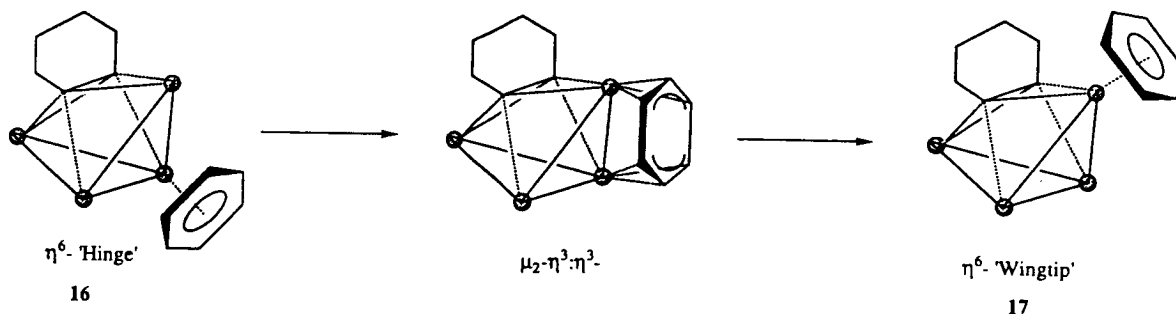

Scheme 3.3.2: A possible mechanism for the conversion of **16** to **17** under ambient conditions.

The second mechanism, in which the benzene ligand migrates from the wing-tip to a hinge position, takes place under more forcing conditions and is thought to occur by a polyhedral rearrangement of the *quasi*-octahedral Ru₄C₂ central cluster unit, *via* a trigonal prismatic complementary geometry (see Scheme 3.3.3). In an alternative view of this process the Ru₄ butterfly arrangement may be considered to form a square plane (by cleavage of the hinge Ru-Ru bond) whilst the organo-bridge rotates about the four Ru atoms. Intuitively these mechanisms would be viewed as relatively high energy processes, therefore requiring the rather more vigorous conditions employed. A combination of these two mechanisms produces the cyclic process illustrated in Scheme 3.3.4.
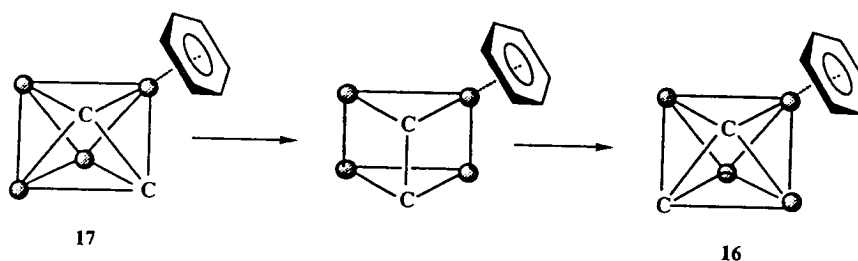
Scheme 3.3.3: A possible mechanism for the conversion of **17** to **16** under more vigorous conditions.

This behaviour is comparable to that found in a related Ru₅C system in which a different isomerisation pattern occurs upon irradiation in a polymer film to that observed in solution under thermal conditions.[20] The irradiation of the square-based pyramidal cluster,
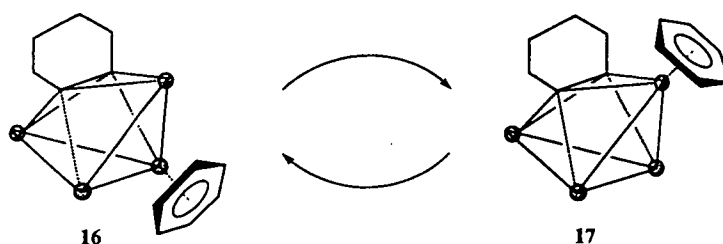
Scheme 3.3.4: The cyclic process that takes place between **16** and **17** from a combination of the two mechanisms outlined in Schemes 3.3.2 and 3.3.3.

Ru$_5$C(CO)$_{12}$(η^6-C$_6$H$_6$), (containing benzene coordinated to a basal metal atom) embedded within a polymethylmethacrylate (PMMA) film, leads to the formation of the η^6 apical isomer. However, this process is reversed upon heating in solution, and conversion of the η^6 apical to η^6 basal isomer is observed. Both isomerisations are thought to occur *via* a polyhedral rearrangement of the Ru$_5$ square-pyramidal cage, a process which involves firstly (Ru$_{apex}$-Ru$_{basal}$) edge cleavage to generate an intermediate with a bridged-butterfly structure, and then the formation of a new edge to regenerate the square pyramidal structure. This isomerisation has the effect of *apparently* transferring the benzene from the η^6-apical to the η^6-basal position and *vice-versa*, although in reality the benzene remains attached to the same Ru-atom throughout the process and so does not correspond to a migration in the 'real' sense. Even though both processes appear to proceed *via* a similar mechanistic approach, *i.e.* isomerisation by Ru-Ru edge cleavage to bring about the correct rearrangement, the thermal and photolytic reactions must almost certainly be different. It has therefore been suggested that in the thermal process the bridged-butterfly intermediate may be brought about by the *heterolytic* fission of the Ru-Ru bond to generate one 16-electron and one 18-electron metal centre, which would allow easy CO addition. In contrast, the photolytic process is more likely to proceed *via homolytic* fission and the formation of a *diradical* intermediate.

It is also worthy to note that the action of Me$_3$NO on Ru$_4$(CO)$_{12}$(μ_4-η^1:η^1:η^2:η^2-C$_6$H$_8$) **15**, results mainly in the wing-tip benzene isomer Ru$_4$(CO)$_9$(μ_4-η^1:η^1:η^2:η^2-C$_6$H$_8$)(η^6-C$_6$H$_6$) **17**, and it therefore appears that attack occurs preferentially at the wing-tip Ru(CO)$_3$ unit. The reasons for this behaviour are unclear, but may be either electronic or steric in origin; either the carbonyl groups at this site are more prone to nucleophilic attack, or due to the lower connectivity of the wing-tip ruthenium atom there is more room to accommodate the incoming ligand.

The isomeric butterfly clusters described above are comparable to a series of Ru$_5$ and Ru$_6$ cluster units which differ either in the bonding mode adopted by the arene (η^6

terminal or μ_3 face bridging) or in the site of attachment.[18,21] Extended Hückel calculations have contributed to the rationalisation of the relative stabilities of the various isomeric forms showing in the case of the *bis*(benzene) species $Ru_6C(CO)_{11}(C_6H_6)_2$, for which three isomeric forms have been observed [*viz. cis*-$Ru_6C(CO)_{11}(\eta^6$-$C_6H_6)_2$, $Ru_6C(CO)_{11}(\eta^6$-$C_6H_6)(\mu_3$-η^2:η^2:η^2-$C_6H_6)$ and *trans*-$Ru_6C(CO)_{11}(\eta^6$-$C_6H_6)_2$], that the most stable isomer is that carrying two η^6 benzene ligands in *cis*-positions on adjacent ruthenium atoms, and that the apical-facial isomer which is formed first in these reactions, does so mainly for kinetic reasons.[22] This behaviour is in accordance with the interconversion reactions observed in solution. In each of these examples, the molecular structures and their relative stabilities have also been examined in light of their intermolecular arrangements in the crystal lattice. Crystal packing forces have been shown to stabilise the less favourable isomers since their energy differences are small and comparable to those of *inter*molecular interactions.[22] The tetranuclear butterfly isomers **16** and **17** have not been analysed by extended Hückel calculations, however their crystal structures have been examined and compared with that of $Ru_4(CO)_{12}(\mu_4$-η^1:η^1:η^2:η^2-$C_6H_8)$ **15** (see Section 3.6).

3.4 Towards Higher Substituted Butterfly Clusters: The Molecular Structure of $Ru_4(CO)_8(\mu_4$-η^1:η^1:η^2:η^2-$C_6H_8)(\eta^4$-$C_6H_8)_2$ 19

It has been established that the reaction between $Ru_4(CO)_{12}(\mu_4$-η^1:η^1:η^2:η^2-$C_6H_8)$ **15** and cyclohexa-1,3-diene affords $Ru_4(CO)_9(\mu_4$-η^1:η^1:η^2:η^2-$C_6H_8)(\eta^6$-$C_6H_6)$ **16** and **17**. When carried out in refluxing octane, this reaction proceeds in low yield with the formation of the hinge-benzene isomer **16** only. However, when a dichloromethane solution of $Ru_4(CO)_{12}(\mu_4$-η^1:η^1:η^2:η^2-$C_6H_8)$ **15** is treated with three equivalents of Me_3NO in the presence of cyclohexa-1,3-diene at -78°C, a range of products are obtained which can be separated from the reaction mixture by t.l.c. using a dichloromethane-hexane (3:7, v/v) solution as eluent. The major product from this reaction is the wing-tip isomer **17**, however, three other products may be isolated in lower yield including the hinge isomer **16**, the *bis*(cyclohexadiene) butterfly cluster $Ru_4(CO)_8(\mu_4$-η^1:η^1:η^2:η^2-$C_6H_8)(\eta^4$-$C_6H_8)_2$ **19**, and the trinuclear complex $Ru_3(CO)_8(\mu_3$-η^1:η^2:η^1-$C_6H_8)(\eta^4$-$C_6H_8)$ **20**. This reaction is illustrated in Scheme 3.4.1.

The molecular formula of **19** was initially proposed as $Ru_4(CO)_8(\mu_4$-η^1:η^1:η^2:η^2-$C_6H_8)(\eta^4$-$C_6H_8)_2$ on evidence provided by infrared, mass and ^1H NMR spectroscopy. The infrared spectrum shows peaks in the terminal carbonyl region (between 2055 and 1979 cm^{-1}) and also a very strong peak at 1838 cm^{-1} that corresponds to edge-bridging carbonyl ligands. The mass spectrum exhibits a parent peak at 868 (calc. 869) amu followed by the loss of eight carbonyl groups in succession. The ^1H NMR spectrum in
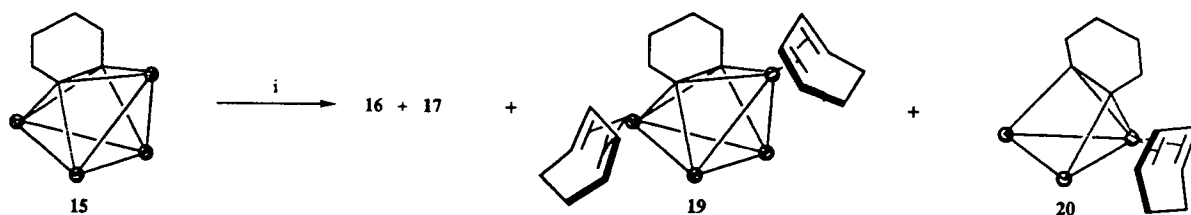
Scheme 3.4.1: The reaction of $Ru_4(CO)_{12}(\mu_4\text{-}\eta^1\text{:}\eta^1\text{:}\eta^2\text{:}\eta^2\text{-}C_6H_8)$ **15** with trimethylamine *N*-oxide in the presence of cyclohexa-1,3-diene. (i) 3.2 equiv. $Me_3NO/CH_2Cl_2/1,3\text{-}C_6H_8$, -78°C.

$CDCl_3$ exhibits six signals of equal relative intensities at δ 5.02 (m, 4H), 3.40 (m, 4H), 2.54 (br s, 4H), 2.31 (d; J = 11.5 Hz, 4H), 1.54 (d; J = 11.5 Hz, 4H) and 1.24 (br s, 4H) ppm. A series of selective decoupling experiments have facilitated an assignment of these signals and those at δ 5.02, 3.40, 2.31 and 1.54 ppm may be attributed to the two η^4 cyclohexadiene moieties; the former two signals being assigned to the olefinic protons of the diene and the latter two to the aliphatic ring protons. These latter signals are basically doublet in character and possess a coupling constant of *ca.* 11.5 Hz. The resolution of the signals is insufficiently clear for smaller coupling constants to be established. The two remaining resonances at δ 2.54 and 1.24 ppm may be attributed to the eight aliphatic ring protons of the cyclohexyne ligand, and although they show very fine couplings these signals are of essentially singlet character.

The formulation of $Ru_4(CO)_8(\mu_4\text{-}\eta^1\text{:}\eta^1\text{:}\eta^2\text{:}\eta^2\text{-}C_6H_8)(\eta^4\text{-}C_6H_8)_2$ **19** from spectroscopic data was verified by a single crystal X-ray analysis, as was the precise location of the C_6H_8 rings on the butterfly unit (*i.e.* wing-tip *vs.* hinge). Crystals of **19** were grown from the slow evaporation of a dichloromethane-hexane solution at room temperature, and the solid-state structure is shown in Figure 3.4, accompanied by some relevant bond lengths. In a similar scenario to that already described, the same general features observed for the structure of $Ru_4(CO)_{12}(\mu_4\text{-}\eta^1\text{:}\eta^1\text{:}\eta^2\text{:}\eta^2\text{-}C_6H_8)$ **15** are retained upon the substitution of four terminal carbonyl groups by two cyclohexa-1,3-diene ligands. Each diene moiety is coordinated to the butterfly cluster framework *via* an η^4 interaction with a wing-tip ruthenium atom, and the cyclohexyne unit is trapped between the butterfly wings and bonds to all four ruthenium atoms in the customary $\mu_4\text{-}\eta^1\text{:}\eta^1\text{:}\eta^2\text{:}\eta^2$ manner.

The Ru-Ru bond lengths in $Ru_4(CO)_8(\mu_4\text{-}\eta^1\text{:}\eta^1\text{:}\eta^2\text{:}\eta^2\text{-}C_6H_8)(\eta^4\text{-}C_6H_8)_2$ **19** range from 2.7218(7) to 2.8444(9) Å, with the Ru-Ru edge connecting the two hinge atoms [Ru(2)-Ru(3)] being significantly longer than the remaining four edges [2.8444(9) *vs.* a mean value of 2.7386(13) Å]. The M-M bond lengths in **19** are comparable to those found in the precursor material $Ru_4(CO)_{12}(\mu_4\text{-}\eta^1\text{:}\eta^1\text{:}\eta^2\text{:}\eta^2\text{-}C_6H_8)$ **15** [2.849(3) and 2.729(2) Å, respectively]. The cyclohexyne unit lies between the wings of the butterfly with its alkyne
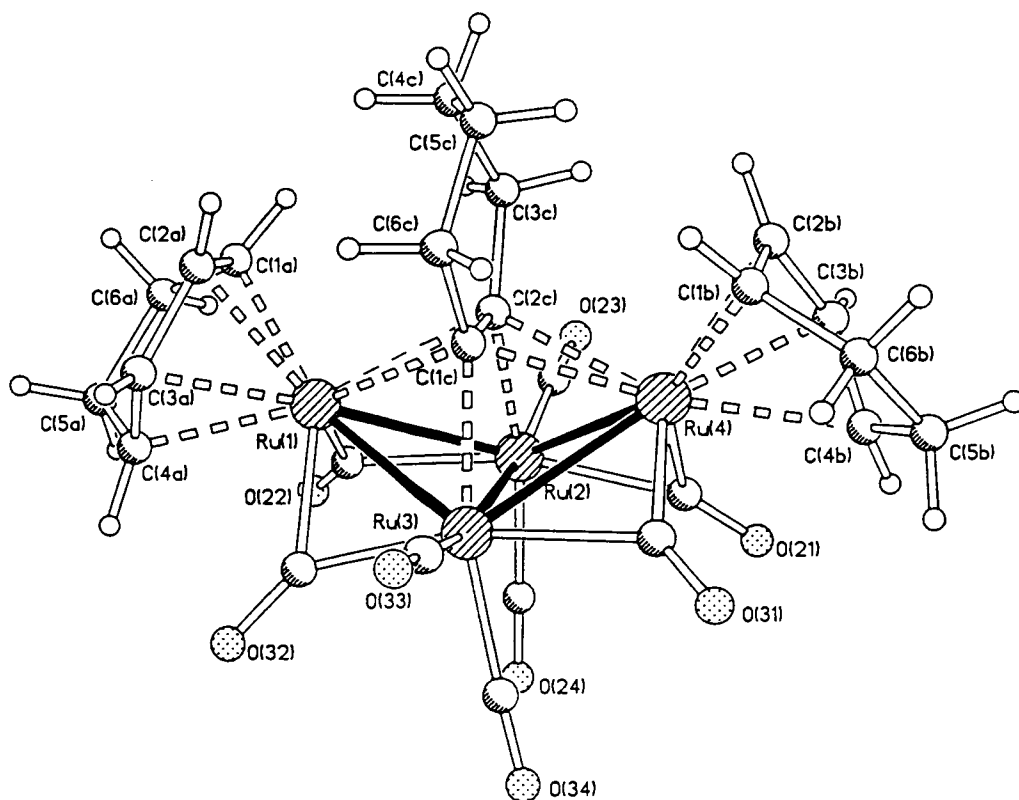
Figure 3.4: The molecular structure of $Ru_4(CO)_8(\mu_4\text{-}\eta^1\text{:}\eta^1\text{:}\eta^2\text{:}\eta^2\text{-}C_6H_8)(\eta^4\text{-}C_6H_8)_2$ **19** in the solid-state showing the atomic labelling scheme. The C-atoms of the CO ligands bear the same numbering as the corresponding O-atoms. Relevant bond distances (Å) include: Ru(1)-Ru(2) 2.7340(8), Ru(1)-Ru(3) 2.7429(12), Ru(2)-Ru(3) 2.8444(9), Ru(2)-Ru(4) 2.7557(13), Ru(3)-Ru(4) 2.7218(7), mean Ru-$C(CO_{terminal})$ 1.920(4), mean $C\text{-}O(CO_{terminal})$ 1.136(5), Ru(1)-C(22) 1.954(4), Ru(1)-C(32) 2.114(4), Ru(2)-C(21) 2.033(4), Ru(2)-C(22) 2.202(4), Ru(3)-C(31) 2.183(4), Ru(3)-C(32) 2.032(4), Ru(4)-C(21) 2.112(4), Ru(4)-C(31) 1.958(4), mean $C\text{-}O(CO_{bridging})$ 1.164(5), Ru(1)-C(1a) 2.212(4), Ru(1)-C(2a) 2.156(4), Ru(1)-C(3a) 2.154(4), Ru(1)-C(4a) 2.217(4), C(1a)-C(2a) 1.420(6), C(1a)-C(6a) 1.505(6), C(2a)-C(3a) 1.421(6), C(3a)-C(4a) 1.430(6), C(4a)-C(5a) 1.518(6), C(5a)-C(6a) 1.531(6), Ru(4)-C(1b) 2.217(4), Ru(4)-C(2b) 2.158(4), Ru(4)-C(3b) 2.146(4), Ru(4)-C(4b) 2.221(4), C(1b)-C(2b) 1.417(6), C(1b)-C(6b) 1.517(6), C(2b)-C(3b) 1.417(7), C(3b)-C(4b) 1.419(6), C(4b)-C(5b) 1.506(7), C(5b)-C(6b) 1.519(7), Ru(1)-C(1c) 2.358(4), Ru(1)-C(2c) 2.336(4), Ru(2)-C(2c) 2.136(4), Ru(3)-C(1c) 2.141(4), Ru(4)-C(1c) 2.326(4), Ru(4)-C(2c) 2.364(4), C(1c)-C(2c) 1.392(5), C(1c)-C(6c) 1.526(5), C(2c)-C(3c) 1.529(5), C(3c)-C(4c) 1.542(5), C(4c)-C(5c) 1.532(6), C(5c)-C(6c) 1.534(5).

C-C bond situated approximately parallel to the butterfly hinge and interacting with all four metal atoms. The alkyne ligand donates six electrons to the cluster framework *via* two σ-interactions with the hinge atoms and two π-interactions with the wing-tip rutheniums, and this causes a reduction in bond order of the acetylenic C(1c)-C(2c) bond [1.392(5) Å]. The two Ru-C σ-bonds formed between the cyclohexyne moiety and the two hinge atoms of the cluster are approximately equal and are considerably shorter than the two π-bonds formed

with the atoms of the wing-tips [mean values of 2.139(4) and 2.346(4) Å, respectively]. These two π-bonds are also very similar in length and hence, the C(1c)-C(2c) bond of the alkyne is positioned centrally with respect to the hinge ruthenium atoms [Ru(2) and Ru(3)] and almost equidistant from the two wing-tips [Ru(1) and Ru(4)]. This centralisation of the alkyne reflects the symmetrical substitution pattern found in this molecule when compared to the two benzene isomers Ru$_4$(CO)$_9$(μ_4-η^1:η^1:η^2:η^2-C$_6$H$_8$)(η^6-C$_6$H$_6$) **16** and **17** in which a shift of the C-C alkyne bond towards the ruthenium atom carrying the benzene ligand is observed.

Each cyclohexa-1,3-diene moiety is bound to a wing-tip ruthenium atom of the butterfly cluster in an η^4 coordination mode, which is that most commonly observed in tri and tetranuclear carbonyl clusters of ruthenium and osmium.[23] The C$_6$H$_8$ ligands each form two comparatively short and two long interactions with the metal [mean 2.154(4) *vs.* 2.217(4) Å, over the two ligands], presumably due to steric influences which cause the unattached -CH$_2$CH$_2$- section of the diene to move as far from the cluster core as possible. Within each of the diene units, three of the C-C distances are short, whilst the remaining three are longer [mean 1.421(7) *vs.* 1.516(7) Å]; the short bonds being those between the four C atoms that interact with the metal centres. There are eight carbonyl ligands in **19**, four of which are bonded in a terminal manner with two on each of the hinge ruthenium atoms. The remaining carbonyl ligands are either in symmetric or asymmetric bridging positions along the four hinge-wing-tip Ru-Ru edges. Two carbonyls symmetrically bridge the Ru(1)-Ru(3) and Ru(2)-Ru(4) edges [mean Ru-C(CO) 2.073(4) Å] while the other two are in asymmetric bridging positions along the Ru(1)-Ru(2) and Ru(3)-Ru(4) edges, with shorter distances from the wing-tip atoms in each case [mean 1.956(4) *vs.* 2.193(4) Å].

It has been noted that the substitution of three carbonyl groups in Ru$_4$(CO)$_{12}$(μ_4-η^1:η^1:η^2:η^2-C$_6$H$_8$) **15** for a benzene ligand results in a slight shrinkage of the overall cluster framework, which is thought to be due to the less efficient π-accepting capability of the benzene ligand, when compared to a tricarbonyl unit. This shrinkage is not apparent in the *bis*(diene) complex, Ru$_4$(CO)$_8$(μ_4-η^1:η^1:η^2:η^2-C$_6$H$_8$)(η^4-C$_6$H$_8$)$_2$ **19**, which may possibly be due to the presence of four bridging carbonyl ligands which can accommodate the additional electron density to a greater extent than when bonded in a terminal manner.

The molecular formula of complex **20** has been tentatively proposed as Ru$_3$(CO)$_8$(μ_3-η^1:η^2:η^1-C$_6$H$_8$)(η^4-C$_6$H$_8$) from spectroscopic data. The infrared spectrum of **20** is quite complicated, with several peaks lying in the terminal CO stretching region (between 2077 and 1987 cm^{-1}) and also two strong peaks in the bridging region (1878 and 1839 cm^{-1}). The mass spectrum exhibits a distinct parent ion peak at 688 (calc. 688) amu, followed by peaks corresponding to the sequential loss of eight carbonyl ligands, therefore suggesting a complex with the general formula Ru$_3$(CO)$_8$(C$_6$H$_8$)$_2$. The ^{1}H NMR spectrum

of **20** is of poor quality owing to the lack of crystalline material required for a clean spectrum. The signals have a low signal to noise ratio and interpretation of the spectrum has been based on comparisons with spectra of related compounds. For example, two clear multiplet resonances of equal relative intensity are observed at δ values of 4.91(m, 2H) and 3.34 (m, 2H) ppm, which are indicative (in these systems) of the four olefinic protons of an η^4 cyclohexadiene moiety. The remainder of the spectrum comprises of several multiplet signals between δ 2.83 and 1.73 ppm which integrate, in total, to twelve protons. Although the individual signals cannot be assigned, it is possible that they represent the four aliphatic protons of an η^4 cyclohexadiene ligand, and the eight aliphatic protons of a cyclohexyne ligand, which may be coordinated to the face of the metal triangle in a μ_3-η^1:η^2:η^1 manner, similar to that observed in the cluster complex $Os_4(\mu$-H)(CO)$_{10}(\mu_3$-η^1:η^2:η^1-$C_6H_8)(\eta^3$-$C_6H_9)$ **10** (see Chapter two).

Unfortunately, crystals of **20** suitable for an X-ray diffraction analysis have been unattainable, even after repeated efforts, and therefore its formulation can only be speculative. Scheme 3.4.2 illustrates how **20** may be derived from $Ru_4(CO)_8(\mu_4$-η^1:η^1:η^2:η^2-$C_6H_8)(\eta^4$-$C_6H_8)_2$ **19** by the loss of a $Ru(\eta^4$-$C_6H_8)$ fragment, and suggests that the remaining η^4 diene ligand stays coordinated to the Ru atom to which the cyclohexyne ligand is π-bonded [this is a similar situation to that observed in $Os_4(\mu$-H)(CO)$_{10}(\mu_3$-η^1:η^2:η^1-$C_6H_8)(\eta^3$-$C_6H_9)$ **10**, whereby the cyclohexyne moiety is π-bonded to the Os atom bearing the C_6H_9 group]. Such a structural formula would also contain two bridging carbonyl ligands which is in agreement with the IR spectrum, and the cluster would contain a total of 48 valence electrons and therefore be consistent with electron counting arguments. If the proposed formula is correct, it would appear that during the reaction of $Ru_4(CO)_{12}(\mu_4$-η^1:η^1:η^2:η^2-$C_6H_8)$ **15** with Me_3NO and cyclohexa-1,3-diene, cluster degradation has taken place in addition to the more usual ligand substitution reactions described earlier. This type of reaction is not totally unexpected, and similar reactions have been observed where the action of Me_3NO has caused a hexaruthenium cluster to breakdown into a trinuclear one, which likewise undergoes degradation to produce a dinuclear complex (see Chapter five). It is thought that the nucleophilic attack of trimethylamine *N*-oxide removes CO consecutively from the same metal atom (a wing-tip ruthenium in this situation), thus forming a highly unstable, unsaturated intermediate, which brings about degradation of the cluster and the formation of a lower nuclearity complex.

Attempts to prepare benzene-diene or *bis*(benzene) derivatives with the formulae $Ru_4(CO)_7(\mu_4$-η^1:η^1:η^2:η^2-$C_6H_8)(\eta^4$-$C_6H_8)(\eta^6$-$C_6H_6)$ and $Ru_4(CO)_6(\mu_4$-η^1:η^1:η^2:η^2-$C_6H_8)(\eta^6$-$C_6H_6)_2$ from the action of Me_3NO and cyclohexa-1,3-diene on either of the isomeric benzene species $Ru_4(CO)_9(\mu_4$-η^1:η^1:η^2:η^2-$C_6H_8)(\eta^6$-$C_6H_6)$ **16** and **17** have
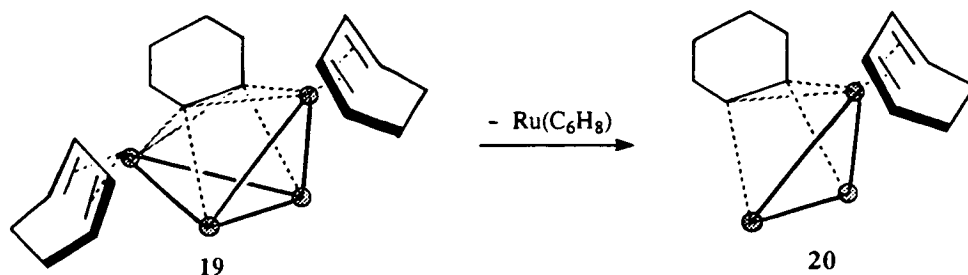
Scheme 3.4.2: The relationship between $Ru_4(CO)_8(\mu_4\text{-}\eta^1{:}\eta^1{:}\eta^2{:}\eta^2\text{-}C_6H_8)(\eta^4\text{-}C_6H_8)_2$ **19** and $Ru_3(CO)_8(\mu_3\text{-}\eta^1{:}\eta^2{:}\eta^1\text{-}C_6H_8)(\eta^4\text{-}C_6H_8)$ **20**.

been unsuccessful, resulting only in cluster breakdown and recovery of the starting material. This suggests that the butterfly cluster $Ru_4(CO)_8(\mu_4\text{-}\eta^1{:}\eta^1{:}\eta^2{:}\eta^2\text{-}C_6H_8)(\eta^4\text{-}C_6H_8)_2$ **19** may represent a saturation point where the maximum number of carbonyl ligands have been replaced by the poorer π-acid benzene and diene ligands, and therefore removal of one further carbonyl would render the cluster unstable and hence result in cluster degradation or decomposition. However, this may not be the case, and it may simply be that as more electron density is dispersed onto the remaining carbonyls (with increasing substitution), they become less susceptible to nucleophilic attack and hence Me_3NO becomes less effective at decarbonylating the cluster. Therefore an alternative synthetic method may prove to be more rewarding.

3.5 Reaction of $Ru_3(CO)_{12}$ with Cyclohexene

The six hour thermolysis of $Ru_3(CO)_{12}$ **14** in octane containing excess cyclohexene (C_6H_{10}) affords a variety of products with nuclearities ranging from four to eight, which may be separated from the reaction mixture by t.l.c. eluting with a dichloromethane-hexane solution (3:7, v/v). Four of the products are the same as those previously observed from the reaction with cyclohexa-1,3-diene, *viz.* $Ru_4(CO)_{12}(\mu_4\text{-}\eta^1{:}\eta^1{:}\eta^2{:}\eta^2\text{-}C_6H_8)$ **15**, $Ru_4(CO)_9(\mu_4\text{-}\eta^1{:}\eta^1{:}\eta^2{:}\eta^2\text{-}C_6H_8)(\eta^6\text{-}C_6H_6)$ **16** and **17**, and $Ru_6C(CO)_{14}(\eta^6\text{-}C_6H_6)$ **18**, however two new compounds, $Ru_6(\mu_3\text{-}H)(\mu_4\text{-}\eta^2\text{-}CO)_2(CO)_{13}(\eta^5\text{-}C_5H_4Me)$ **21** and $Ru_8(\mu\text{-}H)_4(CO)_{18}(\eta^6\text{-}C_6H_6)$ **22**, are also produced in moderate yields (see Scheme 3.5).
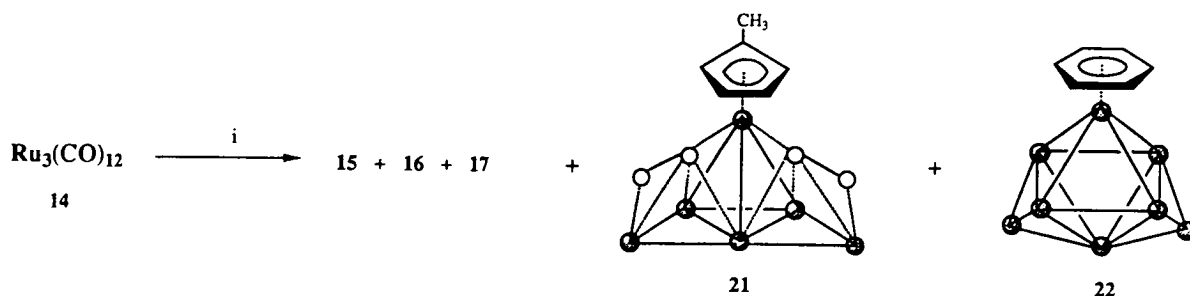
Scheme 3.5: The thermolysis of Ru3(CO)12 **14** with cyclohexene (C6H10)
in octane. (i) Δ, octane/C6H10.

3.5.1 Characterisation and Molecular Structure of $Ru_6(\mu_3\text{-}H)(\mu_4\text{-}\eta^2\text{-}CO)_2(CO)_{13}(\eta^5\text{-}C_5H_4Me)$ 21 - an Example of Cluster Mediated Ring Contraction

Most products from thermolysis reactions of this type contain hydrocarbon ligands in which the integrity of the C_6 ring has been retained. However, the isolation of the hexaruthenium cluster, $Ru_6(\mu_3\text{-}H)(\mu_4\text{-}\eta^2\text{-}CO)_2(CO)_{13}(\eta^5\text{-}C_5H_4Me)$ **21**, reveals that cleavage of a C-C bond has occurred, resulting in rearrangement and formation of a substituted five membered ring.

Compound **21** has been fully characterised as $Ru_6(\mu_3\text{-}H)(\mu_4\text{-}\eta^2\text{-}CO)_2(CO)_{13}(\eta^5\text{-}C_5H_4Me)$ both in solution by the usual spectroscopic procedures, and in the solid phase by a single crystal X-ray diffraction analysis using a crystal grown from a toluene solution at -25°C. The solution infrared spectrum only shows peaks in the C-O stretching region between 2093 and 1920 cm^{-1} that are typical of terminally bonded CO. However, the spectrum of **21** recorded in KBr reveals two bands at 1431 and 1388 cm^{-1} of medium and strong intensities, respectively, which may be assigned to the anti-symmetric and symmetric stretching modes of the two ($\mu_4\text{-}\eta^2\text{-}CO$) carbonyl ligands. The mass spectrum exhibits a strong parent ion peak at 1106 (calc. 1107) amu, which is followed by peaks corresponding to the sequential loss of several carbonyl groups. The ^1H NMR of **21** in CDCl₃ is quite simple, displaying four signals at δ 5.44, 5.31, 2.10 and −17.81 ppm, with relative intensities of 2:2:3:1. The former two resonances are multiplets which may be attributed to the four aromatic protons of the cyclopentadienyl ring, the signal at δ 2.10 ppm is a singlet which is confidently assigned to the three aliphatic protons of the methyl group, and the final singlet at δ -17.81 ppm is typical of that observed for a face-bridging hydride ligand.

The solid-state structure of $Ru_6(\mu_3\text{-}H)(\mu_4\text{-}\eta^2\text{-}CO)_2(CO)_{13}(\eta^5\text{-}C_5H_4Me)$ **21** is shown in Figure 3.5.1 together with some relevant structural parameters. The metal

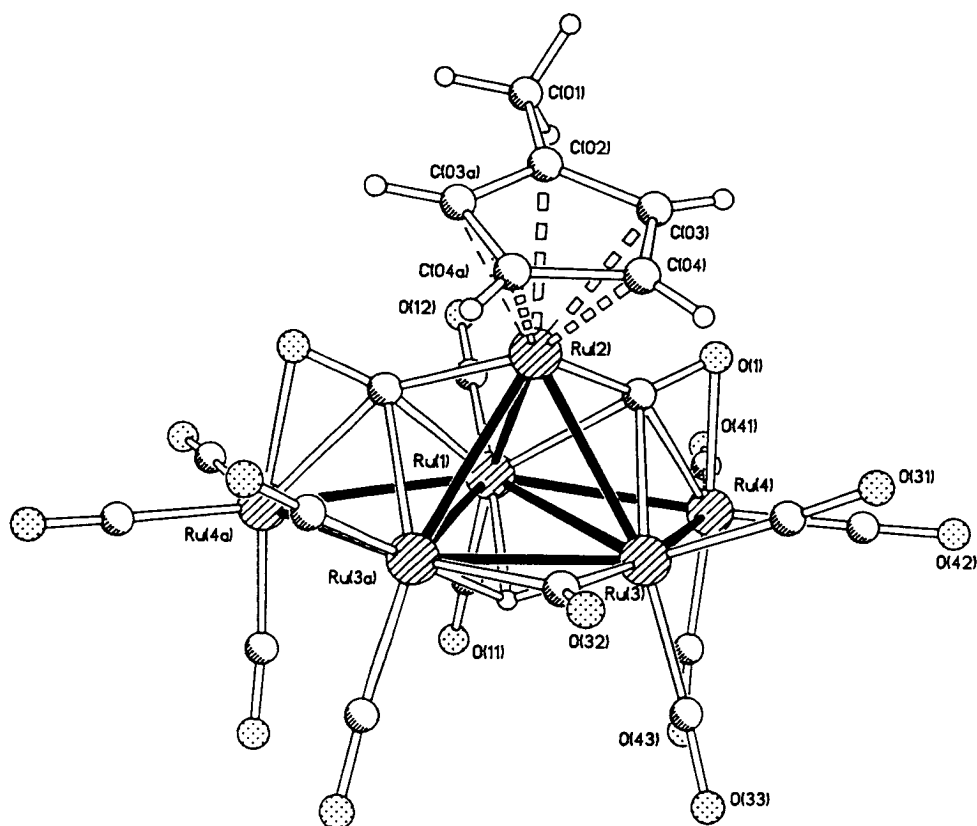**Figure 3.5.1:** Molecular structure of $Ru_6(\mu_3\text{-}H)(\mu_4\text{-}\eta^2\text{-}CO)_2(CO)_{13}(\eta^5\text{-}C_5H_4Me)$ **21**, showing the atomic labelling scheme; the C atoms of the CO groups bear the same numbering as the corresponding O atoms. Principal bond distances (Å) are: Ru(1)-Ru(2) 2.759(2), Ru(1)-Ru(3) 2.8440(13), Ru(1)-Ru(4) 2.8433(10), Ru(2)-Ru(3) 2.7798(11), Ru(3)-Ru(3a) 2.717(2), Ru(3)-Ru(4) 2.7666(12), mean Ru-C(CO_terminal) 1.899(13), mean C-O(CO_terminal) 1.137(20), Ru(3)-C(32) 2.126(10), C(32)-O(32) 1.14(2), Ru(1)-C(1) 2.219(9), Ru(2)-C(1) 1.936(9), Ru(3)-C(1) 2.267(8), Ru(4)-C(1) 2.290(8), Ru(4)-O(1) 2.139(5), C(1)-O(1) 1.232(10), Ru(2)-C(02) 2.216(11), Ru(2)-C(03) 2.204(7), Ru(2)-C(04) 2.251(8), C(01)-C(02) 1.50(2), C(02)-C(03) 1.404(12), C(03)-C(04) 1.413(13), C(04)-C(04a) 1.43(2), mean Ru-H(μ₃) 1.88(5).

framework of **21** consists of a tetrahedral Ru_4 arrangement bridged by two additional metal atoms on two edges sharing a common vertex. The Ru-Ru bond distances range from 2.717(2) to 2.8440(13) Å, with the longest edges being those of the tetrahedron that are bridged by the two ruthenium atoms [*i.e.* the *pseudo*-hinge bonds Ru(1)-Ru(3) and Ru(1)-Ru(3a)], and the shortest being the unique basal edge that is spanned by a symmetrically bridging (μ₂) carbonyl ligand [Ru(3)-Ru(3a)]. This metal core geometry has previously only been observed for the related mesitylene and hexamethylbenzene clusters $Ru_6(\mu_4\text{-}\eta^2\text{-}CO)_2(CO)_{13}(\eta^6\text{-}C_6H_3Me_3)$,[24] and $Ru_6(\mu_4\text{-}\eta^2\text{-}CO)_2(CO)_{13}(\eta^6\text{-}C_6Me_6)$,[25] and all three compounds contain 88 valence shell electrons and are hence consistent with the PSEPT. The methylcyclopentadienyl ligand in **21** adopts a conventional η^5 terminal coordination

mode and is bonded to the only tetrahedron vertex not associated with the bridged edges [mean Ru(2)-C(ring) 2.225(11) Å]. There are two, four-electron donating, π-bonded (μ_4-η^2) carbonyl ligands situated in the two *pseudo*-Ru₄ 'butterflies' created by the bridging Ru atoms and the appropriate faces of the metal tetrahedron. The C-atom bonds to four Ru-atoms [Ru(1)-C(1) 2.219(9), Ru(2)-C(1) 1.936(9), Ru(3)-C(1) 2.267(9), Ru(4)-C(1) 2.290(8) Å] with the shortest bond corresponding to that interacting with the ruthenium atom bearing the MeCp ligand, and the O-atom bonds solely to Ru(4) [2.139(5) Å]. The C-O bond lengths of the η^2 bonded carbonyl ligands are considerably lengthened with respect to the terminally coordinated ligands [1.232(10) *vs.* a mean value of 1.137(20) Å for the remaining CO ligands] and are comparable to those observed in the closely related complexes Ru₆(μ_4-η^2-CO)₂(CO)₁₃(η^6-C₆H₃Me₃) and Ru₆(μ_4-η^2-CO)₂(CO)₁₃(η^6-C₆Me₆) [*cf.* 1.245(11), 1.265(9)[24] and 1.267(7) Å,[25] respectively]. This lengthening may be attributed to electron donation from the C-O π-bond, and increased electron density in the C-O π^* orbital due to the d_π - p_π bonding from three metals. The remaining twelve carbonyls are all terminal and are situated with three on each bridging ruthenium atom and two on the remaining metal atoms that are not involved in coordination to the MeCp ligand. The triply bridging (μ_3) hydride atom has been located experimentally and is found beneath the basal plane of the central Ru tetrahedron [Ru(1)-Ru(3)-Ru(3a)].

The structure of compound **21** is closely related to the mesitylene complex, Ru₆(μ_4-η^2-CO)₂(CO)₁₃(η^6-C₆H₃Me₃), which is formed together with Ru₆(μ_3-H)(μ_4-η^2-CO)(CO)₁₃(μ_2-η^7-C₆H₃Me₂CH₂) and Ru₆C(CO)₁₄(η^6-C₆H₃Me₃) from the thermolysis of Ru₃(CO)₁₂ with mesitylene in heptane.[24] It has been further established that the thermolysis of Ru₆(μ_4-η^2-CO)₂(CO)₁₃(η^6-C₆H₃Me₃) in mesitylene results in the formation of the latter two complexes in approximately equal yield. Carbon dioxide is detected as a by-product from the reaction, thus demonstrating that Ru₆(μ_4-η^2-CO)₂(CO)₁₃(η^6-C₆H₃Me₃) is an intermediate in the formation of the hexaruthenium carbido-cluster Ru₆C(CO)₁₄(η^6-C₆H₃Me₃) from Ru₃(CO)₁₂. Experiments involving ¹³C labelling have demonstrated that the carbido-atom in Ru₆C(CO)₁₄(η^6-C₆H₃Me₃) is derived from a carbonyl ligand and it therefore seems likely that the transformation of Ru₆(μ_4-η^2-CO)₂(CO)₁₃(η^6-C₆H₃Me₃) to the carbido-cluster occurs *via* the thermally induced cleavage of one of the activated μ_4-η^2 carbonyl ligands. However, since this transformation involves the ejection of CO₂ it does not seem likely to proceed *via* an *intra*molecular process, as this would result in a cluster containing only thirteen carbonyl ligands. Instead, a mechanism has been proposed in which two activated carbonyl ligands, one on each of two molecules of Ru₆(μ_4-η^2-CO)₂(CO)₁₃(η^6-C₆H₃Me₃), undergo an *inter*molecular electronic rearrangement such that a molecule of CO₂ is formed and liberated, leaving a carbido atom coordinated to one of the cluster molecules. This

intermediate would then rearrange to form the most stable structure, *i.e.* $Ru_6C(CO)_{14}(\eta^6$-$C_6H_3Me_3)$. The other half of the reacting pair, having lost an η^2 bonded carbonyl ligand, is coordinatively unsaturated and this facilitates both the formation of a Ru-Ru bond across the cavity where the carbonyl ligand was located, and metallation at one of the methyl groups on the mesitylene ligand, with the hydride ligand migrating to the metal framework. This process results in the formation of the observed complex $Ru_6(\mu_3$-H)$(\mu_4$-η^2-CO)(CO)$_{13}(\mu_2$-η^7-$C_6H_3Me_2CH_2)$, and this reaction is summarised in Scheme 3.5.1i.

Repeated attempts to bring about an analogous thermolytic reaction and thus convert compound **21** into the *closo*-octahedral carbido cluster $HRu_6C(CO)_{14}(\eta^5$-$C_5H_4Me)$ have been unsuccessful, resulting only in extensive decomposition of the cluster. The reasons for this behaviour upon thermolysis are unclear, however similar cluster breakdown is also observed in the thermolysis of the isostructural hexamethylbenzene cluster, $Ru_6(\mu_4$-η^2-CO)$_2$(CO)$_{13}(\eta^6$-$C_6Me_6)$.[25]
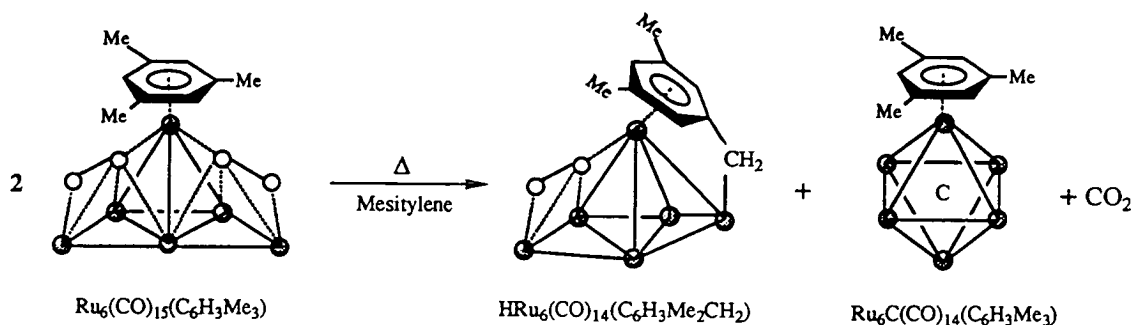
Scheme 3.5.1i: The formation of the hexaruthenium carbido cluster $Ru_6C(CO)_{14}(\eta^6$-$C_6H_3Me_3)$ from $Ru_6(\mu_4$-η^2-CO)$_2$(CO)$_{13}(\eta^6$-$C_6H_3Me_3)$.

The mechanism by which the C_6H_{10} moiety undergoes ring contraction to form the MeCp unit in $Ru_6(\mu_3$-H)$(\mu_4$-η^2-CO)$_2$(CO)$_{13}(\eta^5$-$C_5H_4Me)$ **21** is not fully understood. A possible explanation may be speculated (illustrated in Scheme 3.5.1ii) which involves the initial dehydrogenation of the cyclohexene moiety to a cyclohexa-1,3-diene ligand. A hydride shift may then occur from the C_6H_8 ligand to the metal framework resulting in a cluster stabilised cyclohexadienyl (C_6H_7) fragment. Transannular addition may follow, which, if closely pursued by hydrogen transfer, would lead to the formation of the observed methylcyclopentadienyl unit. Related cluster complexes containing the C_6H_8,[23] and C_6H_7[26] fragments described in stages (II) and (III) of this mechanism have been observed and fully characterised in other work, however a derivative representing stage (IV) has yet to be isolated.
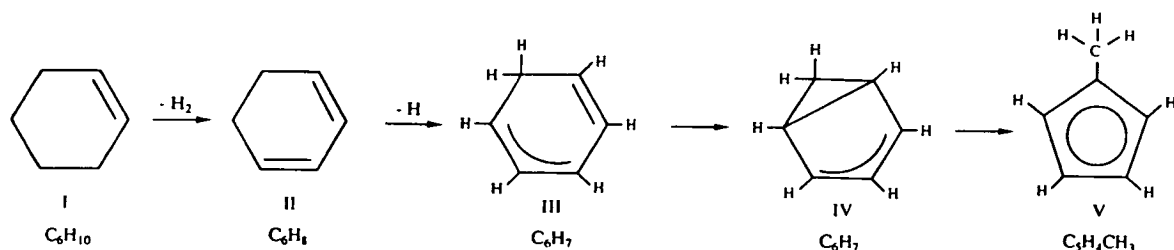
Scheme 3.5.1ii: A proposed ring contraction mechanism.

This reaction is thought to be the first example of a cluster mediated ring contraction. Although this precise behaviour has not been observed on a metal surface, ring contraction is not an uncommon phenomenon in surface science and the adsorption of cyclic C_8 alkenes on a platinum surface is known to bring about the formation of benzene and acetylene.[8] When unsaturated hydrocarbons such as cyclooctene, cycloocta-1,3-diene, and cycloocta-1,5-diene are chemisorbed on a Pt(111) surface, dehydrogenation readily occurs forming cyclooctatetraene (COT), which initially binds to the surface in a tub-shaped η^4 fashion and is converted to a planar η^8 structure at higher temperatures. The formation of this η^8 COT intermediate is apparently a necessary prerequisite for its subsequent conversion to benzene, which follows thereafter. This process has been shown to occur *via* an *intra*molecular mechanism, demonstrating that the transformation does not take place *via* dissociation of the COT into four molecules of acetylene, which then cyclotrimerise to form benzene. Instead it has been proposed that the fragmentation of COT to benzene occurs *via* a two-step process involving the contraction of the cyclooctatetraene ring to form bicyclo[4.2.0]octa-1,3,5-triene, which then undergoes a retro[2+2] cyclisation to form benzene and acetylene (Scheme 3.5.1iii). The benzene desorbs and the acetylene is dehydrogenated firstly to a surface ethynyl and then to a surface carbide overlayer.
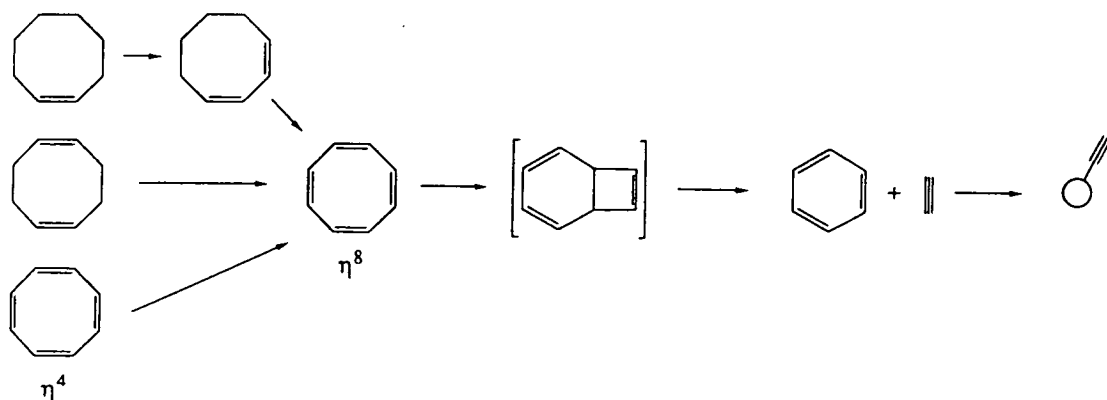
Scheme 3.5.1iii: Adsorption Reactions of cyclic C_8 alkenes on the Pt(111) metal surface.

3.5.2 Characterisation and Molecular Structure of $Ru_8(\mu\text{-}H)_4(CO)_{18}(\eta^6\text{-}C_6H_6)$ 22

The reaction of $Ru_3(CO)_{12}$ **14** with cyclohexene also results in the formation of the octaruthenium-benzene cluster $Ru_8(\mu\text{-}H)_4(CO)_{18}(\eta^6\text{-}C_6H_6)$ **22**. The infrared spectrum of compound **22** is quite simple, displaying peaks in both the terminal (2091-1922 cm⁻¹) and bridging carbonyl stretching regions (*ca.* 1823 cm⁻¹). The mass spectrum contains a parent ion at 1394 (calc. 1394) amu, followed by peaks corresponding to the sequential loss of a number of carbonyl ligands, after which the fragmentation pattern becomes too complicated to identify other specific mass ions. The ^{1}H NMR spectrum of **22** exhibits three singlet resonances at δ 5.40, -17.80, and -19.26 ppm with relative intensities 3:1:1. The former signal is readily assigned to the C-H protons of the benzene ring, whilst the two singlets at very low frequency correspond to the four hydride ligands. A total electron count of 110 is required for an octanuclear cluster with the metal atom topology observed in the solid-state structure (see below), and apart from the eighteen CO ligands and six-electron donating benzene group, an additional four electrons are required which are formally donated by these hydride ligands.

The formulation of $Ru_8(\mu\text{-}H)_4(CO)_{18}(\eta^6\text{-}C_6H_6)$ **22** from spectroscopic data has been verified by a single crystal X-ray diffraction analysis, using a crystal grown from the slow evaporation of a dichloromethane-hexane solution at room temperature. The solid-state molecular structure of **22** is shown in Figure 3.5.2i together with some relevant structural parameters. The ruthenium cluster can be described in terms of an octahedron capped by two additional metal atoms on two triangular faces sharing a common vertex, *viz.* the metal atom framework is a *cis*-bicapped octahedron. The metal core geometry can also be formally derived, by the removal of two capping atoms, from that of the tetracapped octahedral metal frameworks shared by $[HRu_{10}C(CO)_{24}]^-$ [27,28] and $[Ru_{10}C(CO)_{24}]^{2-}$ [27,29] which is also observed in a number of osmium derivatives.[30] The *cis*-bicapped octahedral core of compound **22** has been previously observed only for the osmium cluster anion $[Os_8(CO)_{22}]^{2-}$ [31] and for the mixed neutral cluster $Os_6Pt_2(CO)_{17}(C_8H_{12})_2$.[32] These compounds all share the same number of valence shell electrons (*i.e.* 110).

The Ru-Ru bond distances in $Ru_8(\mu\text{-}H)_4(CO)_{18}(\eta^6\text{-}C_6H_6)$ **22** range from 2.746(1) to 3.057(1) Å. The benzene ligand is bound in an η^6 mode to the only octahedron vertex not belonging to the capped triangular faces [mean Ru-C(ring) 2.208(5) Å]. Two symmetrically bridging CO ligands span the two opposite Ru edges that connect the capped triangles, and the remaining 16 COs are terminally bound, with three on each Ru cap and two on all of the other Ru atoms not involved in the arene substitution. Only two of the four hydride atoms could be experimentally located [H(1) and H(2)], and these were found triply bridging the Ru triangular faces adjacent to those capped. Their position was verified using the program XHYDEX,[33] which also gave an indication that a third hydride was
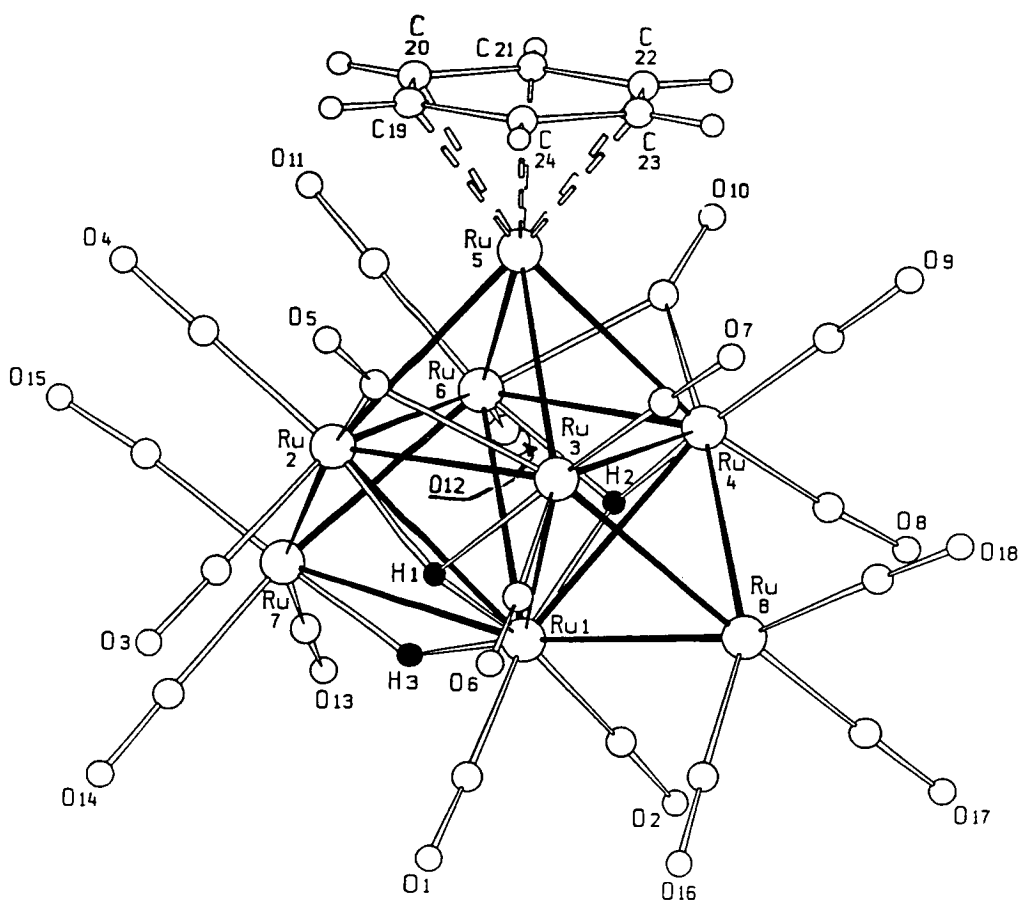
Figure 3.5.2i: Molecular structure of Ru$_8$(μ-H)$_4$(CO)$_{18}$(η^6-C$_6$H$_6$) **22**, showing the atomic labelling scheme; the C atoms of the CO groups bear the same numbering as the corresponding O atoms. Relevant bond distances (Å) are: Ru(1)-Ru(2) 3.025(1), Ru(1)-Ru(3) 3.001(1), Ru(1)-Ru(4) 2.963(1), Ru(1)-Ru(6) 3.057(1), Ru(1)-Ru(7) 3.056(1), Ru(1)-Ru(8) 2.818(1), Ru(2)-Ru(3) 2.808(1), Ru(2)-Ru(5) 2.855(1), Ru(2)-Ru(6) 2.870(1), Ru(2)-Ru(7) 2.785(1), Ru(3)-Ru(4) 2.912(1), Ru(3)-Ru(5) 2.861(1), Ru(3)-Ru(8) 2.746(1), Ru(4)-Ru(5) 2.885(1), Ru(4)-Ru(6) 2.796(1), Ru(4)-Ru(8) 2.757(1), Ru(5)-Ru(6) 2.861(1), Ru(6)-Ru(7) 2.770(1), mean Ru-C(CO$_{terminal}$) 1.882(5), mean Ru-C(CO$_{bridging}$) 2.139(5), mean C-O 1.136(6), Ru(5)-C(19) 2.201(5), Ru(5)-C(20) 2.225(5), Ru(5)-C(21) 2.198(5), Ru(5)-C(22) 2.206(5), Ru(5)-C(23) 2.212(5), Ru(5)-C(24) 2.207(5), C(19)-C(20) 1.388(8), C(19)-C(24) 1.398(7), C(20)-C(21) 1.394(8), C(21)-C(22) 1.402(8), C(22)-C(23) 1.401(7), C(23)-C(24) 1.394(8), mean H(1)-Ru 1.84(1)[a], mean H(2)-Ru 1.82(1)[a], H(3)-Ru(1) 1.62(1)[b], H(3)-Ru(7) 1.69(1)[b]. a Experimental value; b hydride position calculated with XHYDEX.[33]

bridging one of the longest Ru-Ru edges [Ru(1)-Ru(7)]. The position of this hydride could also be inferred by the presence of a large niche in the ligand envelope accompanied by a pronounced distortion of the CO ligands, which bend away from the metal-metal bond as illustrated by Figure 3.5.2ii. The location of the fourth hydride is less certain due to the absence of preferential cavities in the ligand coverage and of a clear-cut potential energy

minimum on the cluster surface, and it is thought that this atom is probably disordered over different cluster sites. A similarly complicated distribution of the hydrides has been observed in the neutron diffraction study at 20 K of the dianion $[H_4Os_{10}(CO)_{24}]^{2-}$,[34] where the hydride ligands were located on the cluster surface, two in μ_3 and two in μ_2 sites.
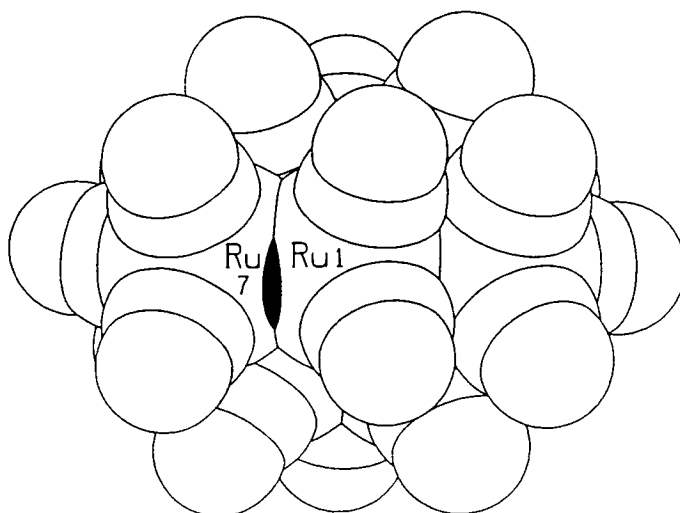
Figure 3.5.2ii: The niche in the ligand envelope of **22** which is believed to accommodate one of the H(hydride) ligands. Note how the carbonyls bend away from the metal-metal bond.

Despite the growing interest in the synthesis, structure and theoretical aspects of arene cluster compounds, those with nuclearities greater than six have been poorly developed, and relatively few arene cluster derivatives have been structurally characterised in the solid-state. The heptaruthenium complex $Ru_7(CO)_{15}(\mu_4$-$PPh)_2(\eta^6$-$C_6H_5Me)$ has been reported as a minor product from the thermolysis of $Ru_3(CO)_{12}$ with $PPhH_2$ in toluene;[35] the seven ruthenium atoms define a condensed polyhedron consisting of two square pyramidal Ru_5 units sharing a triangular face, with the two basal planes capped by μ_4-PPh ligands and the toluene ligand coordinated in an η^6 mode to one basal Ru-atom. Similarly, when $Ru_3(CO)_{12}$ is reacted with PPh_2H in refluxing toluene, the octaruthenium complex $Ru_8(CO)_{19}(\mu_8$-$P)(\mu_2$-η^1:η^6-$C_6H_5CH_2)$ is isolated as a minor product.[36] The metal framework of this complex constitutes a square-antiprism in which a P(phosphide) atom occupies the interstitial site, and the benzyl group is coordinated to two ruthenium atoms *via* a direct σ-interaction with the methylenic carbon atom and an η^6 coordinated C_6 ring. The dropwise addition of $Ru_3(CO)_{10}(\mu_3$-$S)$ in toluene to a similar solution of $Ru_3(CO)_{12}$ heated to reflux, yields the octaruthenium complex $Ru_8(CO)_{17}(\mu_4$-$S)_2(\eta^6$-$C_6H_5Me)$ in which the central metal unit contains two fused square-pyramids of ruthenium atoms, each bridged by a S-atom, and the toluene ligand is again coordinated in an η^6

terminal manner.[37] The final example of an octametallic arene cluster is found in the mixed-metal species Cu$_2$Ru$_6$(CO)$_{18}$(η^2-C$_6$H$_5$Me)$_2$ which has been prepared from the reaction of [Ru$_6$(CO)$_{18}$]$^{2-}$ with [Cu(MeCN)$_4$]$^-$ in acetone.[38] In this mixed-metal cluster an octahedral ruthenium core is capped on opposite faces by two copper atoms, *viz.* a *trans*-bicapped octahedron, and each copper bears a toluene ligand bound in an η^2 fashion. These toluene groups are apparently introduced into the system during the crystallisation of Cu$_2$Ru$_6$(CO)$_{18}$(MeCN)$_2$.

Chapter one described the relevance of arene-cluster compounds as models for the interaction of benzene on metal surfaces.[39] Although the benzene-clusters observed to date have served as reasonable models, until the isolation of Ru$_8$(μ-H)$_4$(CO)$_{18}$(η^6-C$_6$H$_6$) **22** studies on ruthenium clusters bearing only carbonyls and hydrides in addition to the benzene ligand had been limited to nuclearities between three and six.[40] Since larger clusters are considered to be more representative of the bulk metal, there is a need to explore the interactions of benzene and other arenes with clusters of higher nuclearities, which may more reasonably be considered to approach the bulk metallic regime. It has already been established that the Kekulé distortions present in the benzene molecule, when bonded to a trimetallic cluster face in the μ_3-η^2:η^2:η^2 coordination mode, increase with cluster nuclearity (*vide supra*). Although the benzene ligand in the octaruthenium cluster **22** is bound in an η^6 fashion, and is therefore not directly comparable to the above example, it has been found to exhibit properties consistent with a change in the nature of the benzene as the number of the metal atoms increases.

In order to make a meaningful comparison between benzene clusters of differing nuclearity it is important that the compounds in question are compatible. This new cluster clearly extends the sequence already observed for high nuclearity clusters since it is neutral, it contains only carbonyls and hydrides in addition to the benzene ligand, and the metal atom to which the benzene bonds has a connectivity of four. It was proposed that as the nuclearity of a cluster increased and hence became more like a bulk metal, the shielding of the benzene ligand in such a molecule would also increase, thus causing the signals attributed to the aromatic ring protons in the ^{1}H NMR to be shifted to lower frequency. This initial prediction has now been confirmed by experiment, with Ru$_5$C(CO)$_{12}$(η^6-C$_6$H$_6$) exhibiting a ^{1}H NMR singlet resonance at δ 5.93 ppm,[21a] Ru$_6$C(CO)$_{14}$(η^6-C$_6$H$_6$) at δ 5.56 ppm,[21c] and the complex Ru$_8$(μ-H)$_4$(CO)$_{18}$(η^6-C$_6$H$_6$) **22** giving rise to a singlet resonance at δ 5.40 ppm. It therefore appears that the nature of the benzene-cluster interaction may be followed quite readily as a function of cluster size, and one reason for these differences in chemical shift may be due to a greater π-accepting capability of the cluster unit as its nuclearity is increased.

3.6 Molecular Organisation in the Solid-State: The Crystal Structures of 15, 16, 17 and 22

Neutral transition metal cluster molecules aggregate in the solid-state in a typical van der Waals fashion, with their molecular shapes, sizes and polarities controlling the way in which they interlock and generate crystal structures.[41,42] Furthermore, it is well established that packing forces affect the molecular structure observed in the solid-state, although the relationship between the structure of the individual molecular entity and that of its crystal is often difficult to understand.[43] Packing forces are often invoked to account for relevant deviations from the idealised (gas phase) molecular structure or for unexpected structural features, and effects of this type have been recognised in a large number of crystalline organometallic *mono-* and *poly*nuclear complexes.[30,42] Although much progress has been made in recent years regarding the understanding of the crystal packing of molecules, the nature of these forces is far from being understood, particularly when dealing with *flexible* organometallic molecules that possess an extensive degree of structural freedom.[16] The molecular structure of these non rigid molecules in the solid-state is not necessarily identical to that in solution or in the gas phase since crystal forces, *i.e. inter*molecular bonding, can compensate for partial loss of *intra*molecular energy and hence, stabilise less stable conformations. Arene clusters are highly fluxional molecules, with arene reorientation combining with CO scrambling over the cluster framework to yield extremely flexible structural systems. In these examples, the environment, whether constituted of the same molecule packed in an ordered way throughout the crystal lattice or by rapidly tumbling solvent molecules in solution, can have a major effect on the structural features that are observed by both spectroscopic and crystallographic techniques.[40]

The approach used in the analysis of the crystal structures of $Ru_4(CO)_{12}(\mu_4-\eta^1:\eta^1:\eta^2:\eta^2-C_6H_8)$ **15**, $Ru_4(CO)_9(\mu_4-\eta^1:\eta^1:\eta^2:\eta^2-C_6H_8)(\eta^6-C_6H_6)$, **16, 17** (and that reported previously by Milone *et al.* **16a**)[15], and $Ru_8(\mu-H)_4(CO)_{18}(\eta^6-C_6H_6)$ **22** has been previously employed in the investigation of the crystal structures of numerous organometallic materials.[43] The crystal structure is 'decoded' by studying the distribution and *inter*molecular interactions between one molecule, arbitrarily chosen as a reference, and those forming the immediate surroundings which enclose this reference molecule. Methods based on empirical packing potential energy calculations within the pairwise atom-atom approach,[44] or packing analyses based on graphical methods [45] are used to identify these first neighbouring molecules (*i.e.* those forming a so-called enclosure shell), and to study the number, distribution and interactions between these molecules. These procedures have been shown to yield an accurate knowledge of the immediate molecular environment and of the *inter*molecular interlocking.[43]

Arene clusters are particularly well suited for studying the relationship between molecular and crystal structure because of the presence of both flat and cylindrical ligands on the same molecule (*viz.* the arenes and the carbonyl groups). These two different atomic groupings, with their specific spacial requirements, pose problems in the optimisation of the *inter*molecular interlocking that controls crystal cohesion and stability. Crystalline arene-clusters have been shown to pack according to only a few, well-defined, packing motifs, which are dictated by the need to maximise this *inter*molecular locking of the arene fragments with the carbonyl ligands. The basic packing motifs observed in these crystalline materials are: (i) arene-arene interactions of the graphitic type, *i.e.* with benzene or other arenes belonging to neighbouring molecules facing each other at a separation of *ca.* 3.5 Å; [40,43] (ii) carbonyl-carbonyl interactions, which are based on the intimate locking of tricarbonyl or tetracarbonyl units; [40,43] and (iii) carbonyl-arene interactions, which are most often based on intricate networks of C-H··O hydrogen bonds.[46]

The packing motifs displayed by arene cluster compounds have been explored in most detail for the tetraosmium species, $Os_4(\mu$-$H)_2(CO)_{10}(\eta^6$-arene) (arene = C_6H_6 and C_6H_5Me), discussed in Chapter two,[47] and also for a range of *mono* and *bis*(arene) hexaruthenium-carbido clusters, $Ru_6C(CO)_{14}(\eta^6$-arene) and $Ru_6C(CO)_{11}(arene)_2$.[40,43] In the tetraosmium clusters it is apparent that despite the presence of different arene ligands, both complexes pack in essentially the same way. The arene ligands form ribbons generated by the interlocking of two rows of arene fragments in a chevron like fashion as shown in Figure 3.6.1(a), and the relative orientation of these arene ribbons is of the 'herring bone' type, which is similar to that observed in benzene itself. This packing feature is also found in the crystal structure of $Ru_6C(CO)_{14}(\eta^6$-arene) (arene = C_6H_5Me and $C_6H_3Me_3$), despite the rather different molecular geometry and size of the cluster, with the toluene and mesitylene ligands forming ribbons throughout the crystal lattice [see Figure 3.6.1 (b)]. It is worth noting at this stage that all *mono*(arene) hexaruthenium cluster derivatives exhibit another fundamental interaction whereby the unique bridging carbonyl group of one molecule interlocks into the tetragonal cavity generated by four terminal ligands of a neighbouring molecule.[40,43] Molecular rows are therefore generated in which the individual clusters are linked *via* this kind of 'key-keyhole' interaction, and Figure 3.6.1(c) illustrates this type of molecular organisation with reference to the benzene adduct, $Ru_6C(CO)_{14}(\eta^6$-$C_6H_6)$.

While the arene fragments of *mono*(arene) clusters establish herring-bone patterns, this is not the case for most *bis*(arene) derivatives. The most representative example of this latter case is given by the isomeric pair of *bis*(benzene) clusters $Ru_6C(CO)_{11}(\eta^6$-$C_6H_6)(\mu_3$-η^2:η^2:η^2-$C_6H_6)$ and $Ru_6C(CO)_{11}(\eta^6$-$C_6H_6)_2$.[43,47] In both crystals the benzene ligands face each other in graphitic-type arrangements forming molecular chains; the former are

(b)

(a)

(c)

RM

B

A

μ_3

η^6 μ_3

η^6

η^6
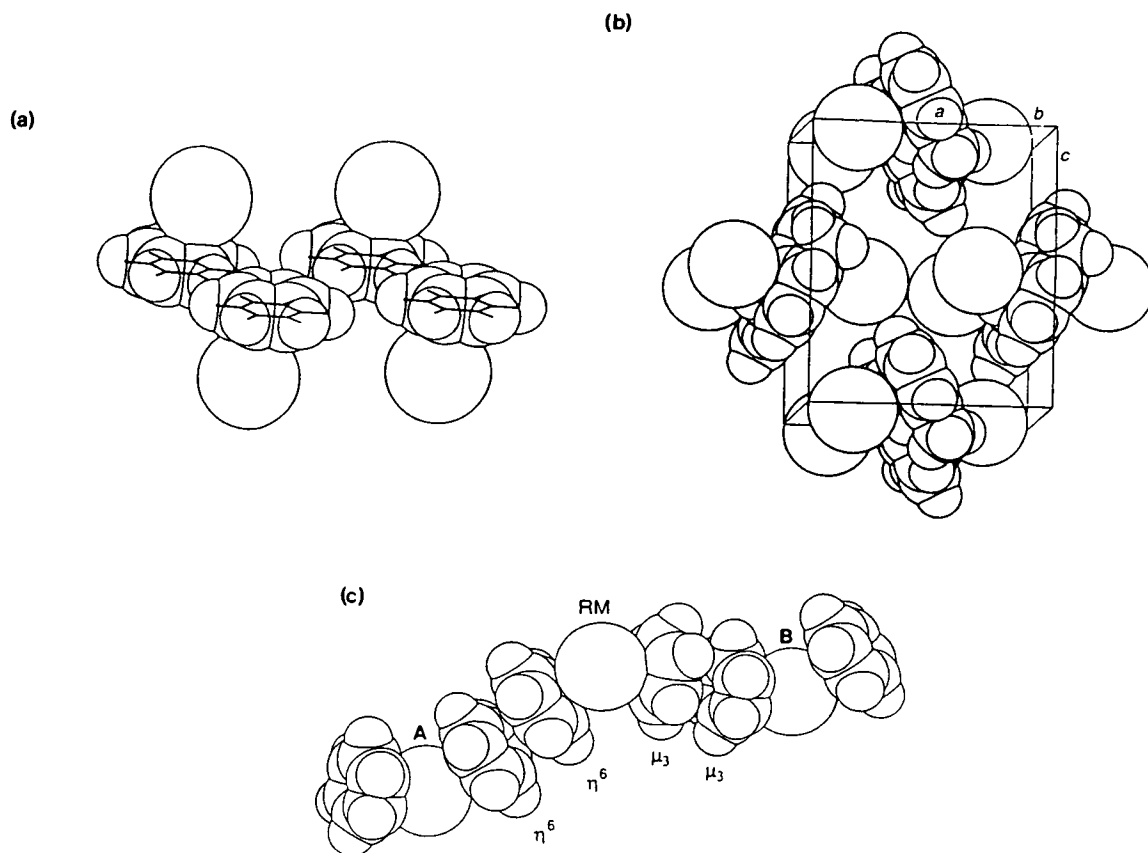
Figure 3.6.1: Schematic representations of the molecular organisation in crystalline (a) $Os_4(\mu\text{-}H)_2(CO)_{10}(\eta^6\text{-}C_6H_6)$ and (b) $Ru_6C(CO)_{14}(\eta^6\text{-}C_6H_5Me)$, showing the ribbon-like distribution of the arene fragments; the metal frameworks and the carbonyl ligands are represented by spheres for clarity. Diagram (c) shows the 'head-to-tail' interaction present in all the *mono*(arene) clusters based on the hexaruthenium-carbido carbonyl cluster, and is illustrated by $Ru_6C(CO)_{14}(\eta^6\text{-}C_6H_6)$.

crinkled ('snakes') while the latter are linear ('rods'), as shown in Figures 3.6.2(a) and (b). In the case of $Ru_6C(CO)_{11}(\eta^6\text{-}C_6H_6)(\mu_3\text{-}\eta^2:\eta^2:\eta^2\text{-}C_6H_6)$ the interaction between the reference molecule and its two next-neighbouring molecules involves a pairing of the benzene ligands almost face-to-face, with the benzene-benzene sequence being η^6/η^6 - μ_3/μ_3 - η^6/η^6 - μ_3/μ_3, *etc.* The separation between the carbon rings is 3.29 and 3.56 Å for the η^6/η^6 and μ_3/μ_3 interactions, respectively, which is very similar to the separation found in graphite itself. In crystalline *trans*-$Ru_6C(CO)_{11}(\eta^6\text{-}C_6H_6)_2$, the benzene fragments belonging to next neighbouring molecules along a row adopt a near staggered orientation at a distance of 3.52 Å. The crystal is therefore composed of parallel molecular rods, each formed by a sequence of molecules linked together *via* benzene-benzene *inter*molecular interactions. This type of behaviour is not confined to the *bis*(benzene) cluster, and has also been observed in a number of other *bis*(arene) derivatives.[40,43]

(a)

(b)
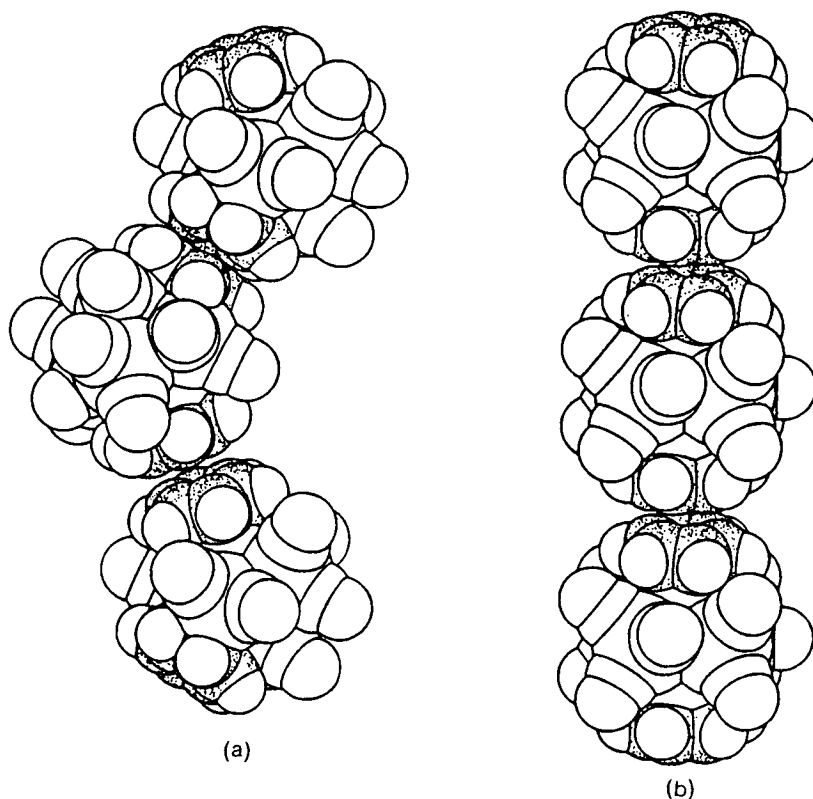
Figure 3.6.2: A comparison of the benzene-benzene interactions observed in crystalline (a) $Ru_6C(CO)_{11}(\eta^6\text{-}C_6H_6)(\mu_3\text{-}\eta^2{:}\eta^2{:}\eta^2\text{-}C_6H_6)$ and (b) *trans*-$Ru_6C(CO)_{11}(\eta^6\text{-}C_6H_6)_2$.

The above examples illustrate two out of the three basic packing motifs observed in crystalline arene carbonyl clusters, *i.e.* arene-arene interactions and carbonyl-carbonyl interactions. The third packing motif involves carbonyl-arene interactions which are usually based on intricate networks of C-H··O hydrogen bonds. This type of *inter*molecular hydrogen bonding network has previously been observed in the crystal structure of the cyclohexadienyl species, $Ru_3(\mu\text{-}H)(CO)_9(\mu_3\text{-}\eta^2{:}\eta^1{:}\eta^2\text{-}C_6H_7)$,[26] and is also detected between the C_6 organic ligands and the CO-groups in crystalline $Ru_4(CO)_{12}(\mu_4\text{-}\eta^1{:}\eta^1{:}\eta^2{:}\eta^2\text{-}C_6H_8)$ **15**, and $Ru_4(CO)_9(\mu_4\text{-}\eta^1{:}\eta^1{:}\eta^2{:}\eta^2\text{-}C_6H_8)(\eta^6\text{-}C_6H_6)$ **16, 16a, 17**.

Table 3.6.1 shows that the efficiency of packing is much higher in crystalline **15** than in the crystals of the two benzene derivatives **16** and **17** [packing coefficient (p.c.) 73.7 % *vs. ca.* 64.5%]. This difference is very large and is rarely encountered in classes of related compounds, therefore implying that the substitution of a flat benzene ligand for the conical tricarbonyl unit causes a loss of packing efficiency, very probably by reducing the extent of *inter*molecular penetration. The difference in packing efficiency is also reflected

by the values of the packing potential energy (p.p.e.), with the crystal structure of **15** being far more cohesive than that of **16**, **16a** and **17** [-317.3 *vs. ca.* -286 kJmol^{-1}]. It is well known that most molecules can (at least in principle) crystallise in different polymorphic modifications depending on the crystallisation conditions,[48] and another aspect of interest is related to the two polymorphic hinge-isomers (**16** and **16a**). The disordered structure **16** appears to achieve a slightly less efficient packing than **16a**, the reason for which is not immediately obvious, however, the loose packing in **16** is almost certainly responsible for the presence of two disordered orientations of the cyclohexyne ligand.

Table 3.6.1: OPEC energy calculations comparing **15**, **16**, **16a** and **17**.

	$Ru_4(CO)_{12}(C_6H_8)$	$Ru_4(CO)_9(C_6H_8)(C_6H_6)$		
	15	**16**	**16a**	**17**
p.c.	73.7%	63.5%	64.2%	65.7%
p.p.e.	-317.3 kJmol^{-1}	-276.7	-283.4	-296.4
Volume	402.3	379.1	381.5	383.3

p.c. = packing coefficient, p.p.e. = packing potential energy.

The molecular packing in crystalline **15** consists of a stacking of the C₆H₈ rings to give a carbon-carbon type interaction within each layer (see Figure 3.6.3). There is also one relatively short CH··OC hydrogen bonding interaction between the C₆H₈ ligands and the CO ligands of a neighbouring molecule [atom O(8) and H(16A)] (see Figure 3.6.4). Structure **16** contains a much clearer pattern of CH··O hydrogen bonding interactions between the carbonyl ligands and the H-atoms of both the C₆H₈ and C₆H₆ ligands which link the surrounding molecules. This situation is illustrated in Figure 3.6.5, and it is noted that four of the six benzene hydrogens are involved in CH··O interactions (lying in the range 2.37 - 2.67 Å). A similar distribution of CH··O interactions is also present in the crystal structures of **16a** and **17**, and the geometrical features of these hydrogen bonding interactions are reported in Table 3.6.2.

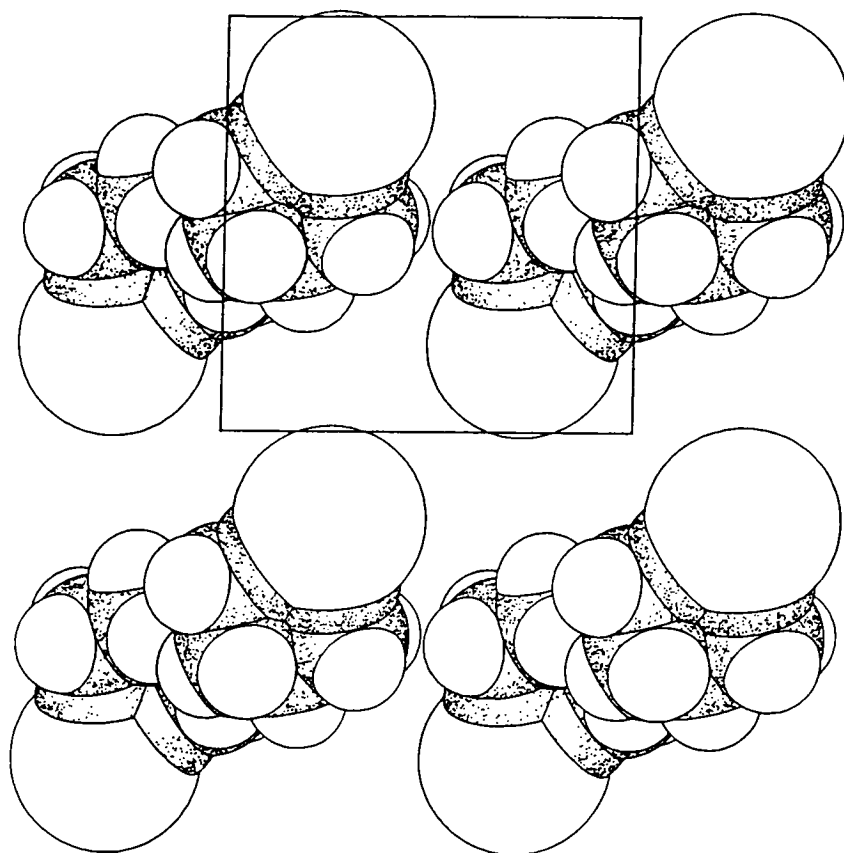**Figure 3.6.3:** The molecular organisation in crystalline $Ru_4(CO)_{12}(C_6H_8)$ **15**. Large spheres represent the centre of mass of the metal frame, and CO ligands are omitted for clarity.
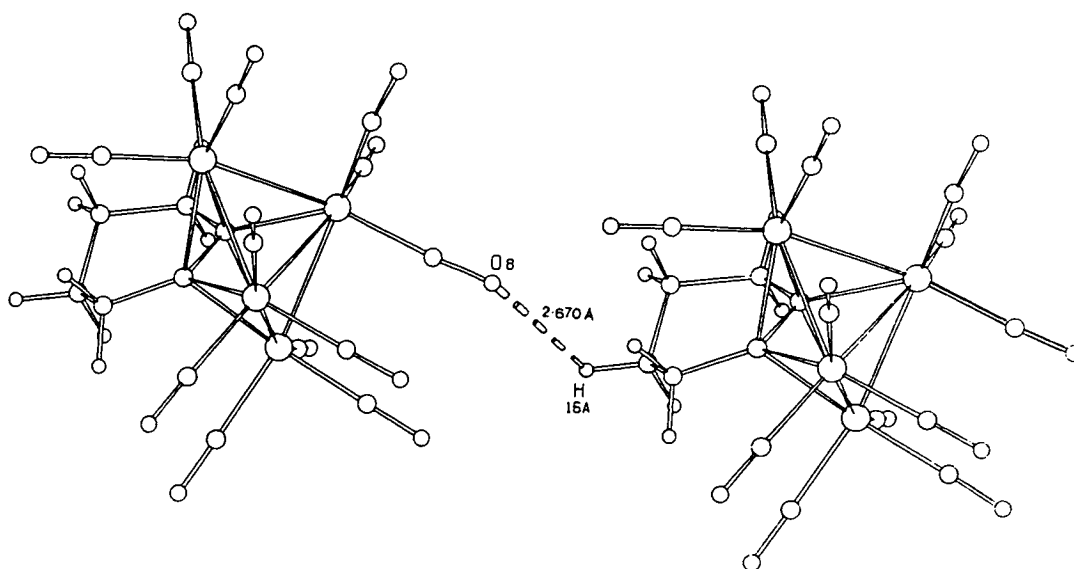
Figure 3.6.4: The C-H··O hydrogen bonding interaction in crystalline $Ru_4(CO)_{12}(C_6H_8)$ **15**.

Table 3.6.2: Analysis of Potential Hydrogen Bonds.

	C⋯O Å	H⋯O Å	CH⋯O °
Ru₄(CO)₁₂(C₆H₈) **15**			
C(16) - H(161) -- O(8)	3.35	2.67	120.5
Ru₄(CO)₉(C₆H₈)(C₆H₆) **16**			
C(19) - H(19) -- O(5)	3.65	2.58	171.1
C(22) - H(22) -- O(9)	3.30	2.42	137.1
C(24) - H(24) -- O(4)	3.52	2.45	174.2
C(17D) - H(17E) -- O(2)	3.34	2.37	147.7
C(21) - H(21) -- O(3)	3.64	2.62	156.0
C(16D) - H(16E) -- O(1)	3.72	2.67	166.5
Ru₄(CO)₉(C₆H₈)(C₆H₆) **16a**			
C(12) - H(121) -- O(5)	3.39	2.56	133.1
C(16) - H(161) -- O(6)	3.49	2.49	153.0
C(18) - H(181)-- O(7)	3.49	2.44	163.3
C(19) - H(191) - O(1)	3.73	2.67	165.6
Ru₄(CO)₉(C₆H₈)(C₆H₆) **17**			
C(19) - H(19) -- O(32)	3.38	2.56	131.3
C(22) - H(22) -- O(5)	5.53	2.47	166.1
C(24) - H(24) -- O(8)	3.26	2.49	126.9
C(50) - H(50) -- O(3)	3.33	2.54	129.0
C(50) - H(50) -- O(7)	3.36	2.49	136.3
C(45) - H(45B) -- O(2)	3.40	2.57	133.0
C(47) - H(47A) -- O(39)	3.63	2.66	149.2
C(21) - H(21) -- O(33)	3.34	2.70	117.4
C(46) - H(46B) -- O(34)	3.71	2.70	157.2
C(52) - H(52) -- O(37)	3.62	2.67	147.0

The overall *inter*molecular assembly in the two polymorphic structures, **16** and **16a**, is very similar. The space-filling projections are depicted in Figures 3.6.6 (a) and (b) for species **16** and **16a**, respectively, and they show that the interaction between the cyclohexyne rings observed in crystalline **15** is no longer present; instead there is a stacking of the benzene units on top of a tricarbonyl unit in a neighbouring molecule (this is also apparent in the crystal structure of **17**). While the benzene ligands are parallel to each other in crystalline **16**, in **16a** there are alternate rows of molecules in which the benzene units are *ca.* 90° to one another. Apart from the different relative orientations of the molecules, the molecular distribution is very similar thus accounting for the close similarity of the two crystalline cells.
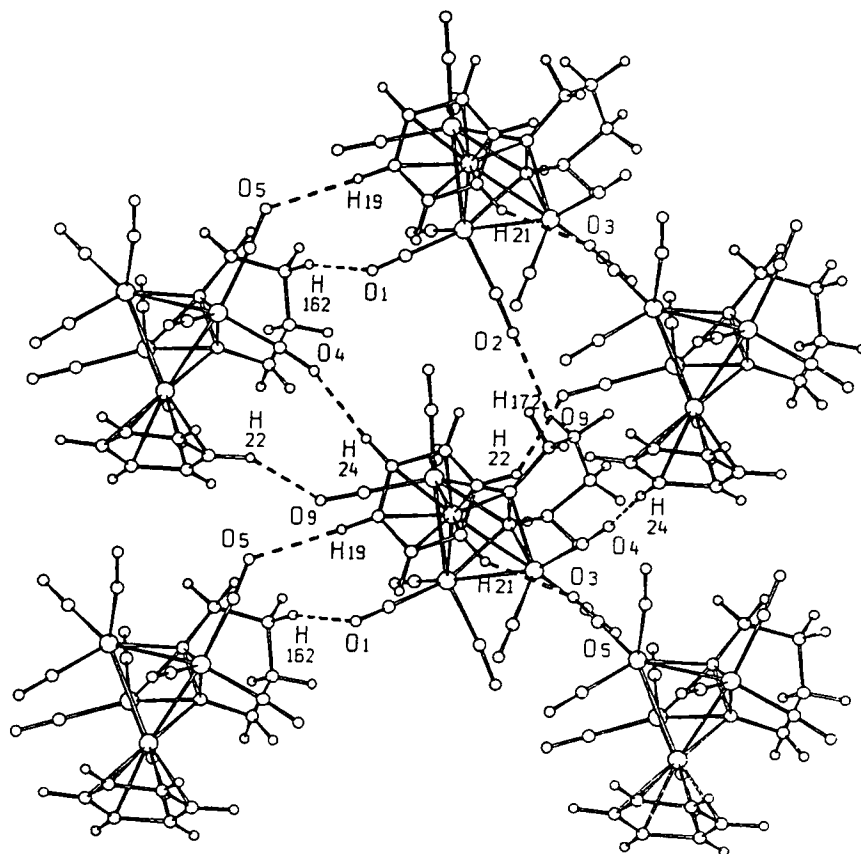
Figure 3.6.5: The pattern of C-H··O hydrogen bonding interactions in crystalline Ru$_4$(CO)$_{12}$(C$_6$H$_8$)(C$_6$H$_6$) **16**.

(a)

(b)
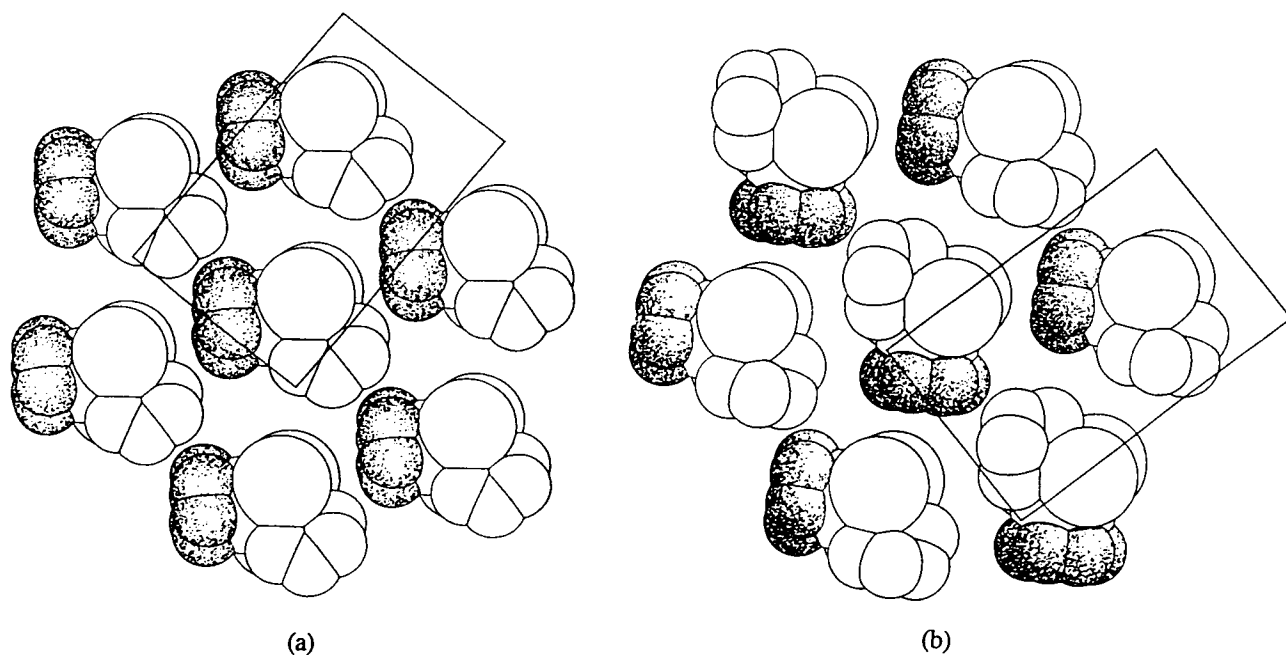
Figure 3.6.6: Comparison of the molecular organisation in crystalline Ru$_4$(CO)$_9$(C$_6$H$_8$)(C$_6$H$_6$) **16** (a) and **16a** (b). Note how, although the molecules are distributed in a very similar way, the benzene ligands (shaded) are parallel to each other in crystalline **16**, and at *ca.* 90° to one another in alternate rows of molecules in crystalline **16a**.

Finally, in spite of the size and complexity of the octanuclear cluster, $Ru_8(\mu\text{-}H)_4(CO)_{18}(\eta^6\text{-}C_6H_6)$ **22**, the molecules arrange themselves in pairs throughout the crystal lattice (see Figure 3.6.7) with the benzene ligands facing each other in a graphitic fashion (distance between the ring planes 3.32 Å), as is observed in a number of related arene transition metal clusters.[40,43] On the opposite side of the cluster with respect to the benzene moiety, the six carbonyl ligands that are terminally bound to the long Ru(7)-Ru(1)-Ru(8) 'edge' interlock in a parallel fashion with the same edge of a neighbouring molecule which has been generated by an inversion centre (see Figure 3.6.8). This latter interaction is similar to that observed for one of the 'tetrahedron' edges in $Os_{10}(\mu\text{-}H)_2C(CO)_{24}$.[49]
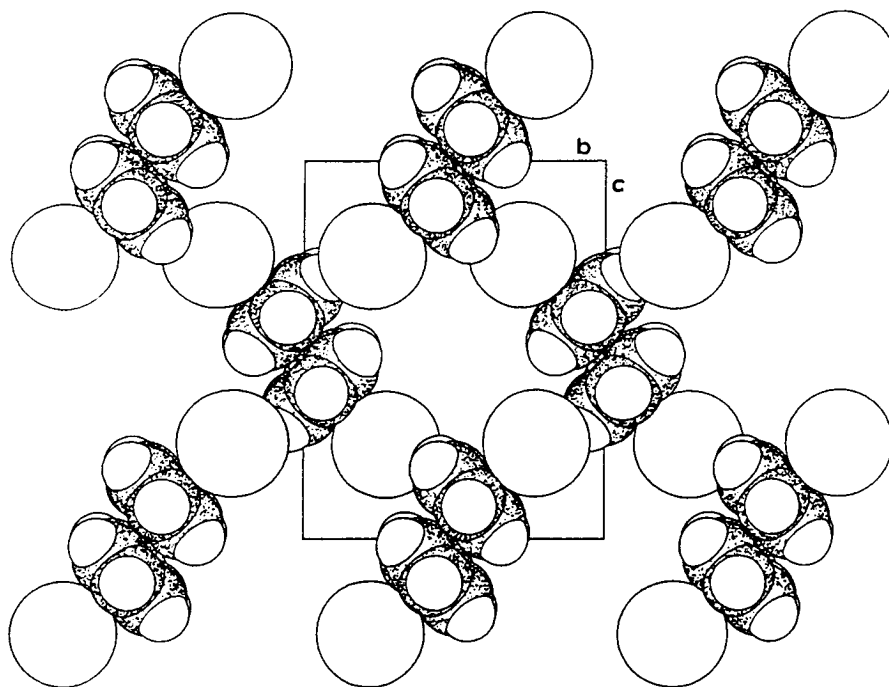
Figure 3.6.7: Crystal packing of the complex $Ru_8(\mu\text{-}H)_4(CO)_{18}(\eta^6\text{-}C_6H_6)$ **22** along the a-axis. CO ligands are omitted for clarity. Large spheres represent the centre of mass of the metal frame.

3.7 Concluding Remarks

The previous chapter outlined a detailed and systematic study of the reactions between $Os_4(\mu\text{-}H)_4(CO)_{12}$ **1** and cyclohexa-1,3-diene, which resulted in the formation of cyclohexadiene and benzene derivatives based on the Os_4 tetrahedral cluster unit. In contrast, it is now found that the tetrahedral unit is not observed in the related ruthenium chemistry, and in its place is the formation of tetranuclear cyclohexyne butterfly clusters
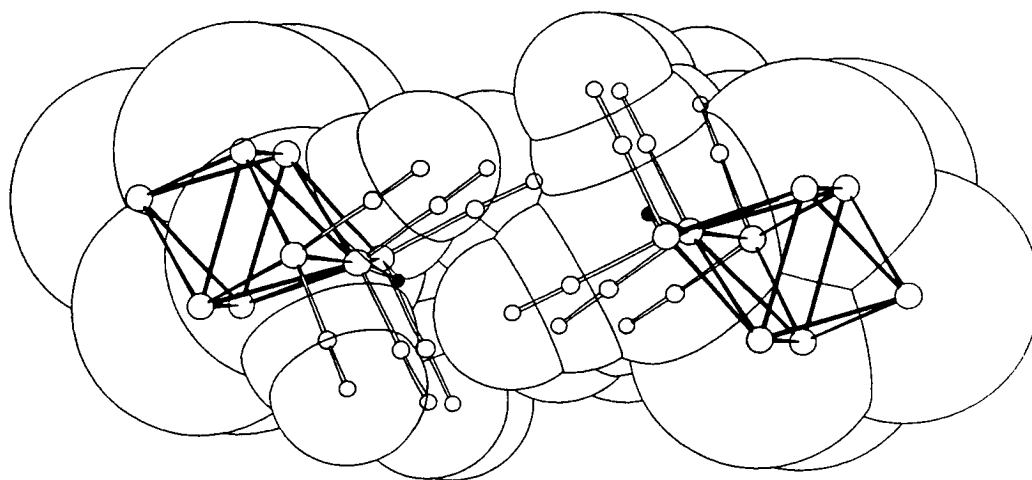
Figure 3.6.8: Interlocking of the CO ligands bound to the long Ru(7)-Ru(1)-Ru(8) 'edges' in crystalline **22**. The two molecules are related by a crystallographic centre of inversion. The benzene ligand and the remaining CO groups are omitted for clarity.

containing a *closo*-Ru$_4$C$_2$ octahedral core. The Ru$_4$ butterfly arrangement within this core closely resembles the step-site of a metal surface, and it is tempting to associate or relate its chemistry with that observed at these sites. The activation of C-H bonds appears to be an important reaction in these systems, resulting in the isomerisation and dehydrogenation of cyclohexa-1,3-diene to form the clusters Ru$_4$(CO)$_{12}$(μ_4-η^1:η^1:η^2:η^2-C$_6$H$_8$) **15** and Ru$_4$(CO)$_9$(μ_4-η^1:η^1:η^2:η^2-C$_6$H$_8$)(η^6-C$_6$H$_6$) **16, 17** which contain both cyclohexyne and benzene ligands. An unusual and reversible isomerisation process has also been found to occur between the hinge and wing-tip benzene products **16** and **17**, which is considered to involve a polytopal rearrangement of the cluster atom geometry at higher temperatures, whilst ligand migration takes place under more ambient conditions.

The reaction of Ru$_3$(CO)$_{12}$ **14** with cyclohexene also leads primarily to dehydrogenation, with products containing C$_6$H$_8$ and C$_6$H$_6$ moieties. However, the formation of the cluster complex, Ru$_6$(μ_3-H)(μ_4-η^2-CO)$_2$(CO)$_{13}$(η^5-C$_5$H$_4$Me) **21**, has revealed that C-C bond activation and ring contraction is also a significant reaction pathway. This has some relevance to surface science and is comparable with the dehydrogenation and ring contraction of C$_8$ cyclic alkenes on a Pt(111) metal surface. The isolation of Ru$_8$(μ-H)$_4$(CO)$_{18}$(η^6-C$_6$H$_6$) **22** from this same reaction has also demonstrated that the preparation of arene clusters which, in the past, has been mostly restricted to complexes with nuclearities between three and six, can be extended to the formation of higher nuclearity clusters. The octaruthenium cluster has enabled a comparative study of the interactions of benzene with clusters as their nuclearity is increased, and its ^{1}H NMR spectrum has shown that the benzene-cluster interaction may be followed quite readily as a

function of cluster size. If extended, this observation may shed further light on the complex nature of the interaction of benzene with the bulk metallic surface.

Lastly, crystal packing analyses have indicated that the packing motif displayed in the crystal structures of arene clusters is governed by the need to optimise the intermixing of the flat arene fragments and the cylindrical CO-ligands that protrude from the cluster surface. By grouping the arene fragments together in ribbons, snakes or layers, optimum CO··CO interlocking is preserved. This tendency is maintained on changing the arene type, and the arene coordination mode. With *mono*(arene) derivatives, packing optimisation is achieved by forming arene ribbons or layers through the crystal lattice, whereas with *bis*(arenes) this is achieved more effectively by placing the ligands face to face. The comparative analysis of the crystal and molecular structures of Ru$_4$(CO)$_{12}$(μ_4-η^1:η^1:η^2:η^2-C$_6$H$_8$) **15** and Ru$_4$(CO)$_9$(μ_4-η^1:η^1:η^2:η^2-C$_6$H$_8$)(η^6-C$_6$H$_6$) **16** and **17** has allowed an insight into some of the factors controlling the structural choice of flexible organometallic molecules in the solid-state, and the disorder observed in crystalline **16** has been shown to originate from a dynamical process which does not occur in the denser crystal structure of the second polymorph **16a**.

3.8 References

1. Sapa, S.; Tiripicchio, A.; Carty, A.J.; Toogood, G.E.; *Prog. Inorg. Chem.*, **1987**, *35*, 437 and references cited therein.

2. Muetterties, E.L.; Rhodin, T.N.; Band, E.; Bruker, C.F.; Pretzer, W.R.; *Chem. Rev.*, **1979**, *79*, 91.

3. Vahrenkamp, H.; *Adv. Organomet. Chem.*, **1983**, *22*, 169.

4. Pomeroy, R.K.; *J. Organomet. Chem.*, **1990**, *383*, 387.

5. (a) Wade, K.; *Adv. Inorg. Chem. Radiochem.*, **1976**, *18*, 1; (b) Mingos, D.M.P.; *Acc. Chem. Res.*, **1984**, *17*, 311; (c) Owen, S.M.; *Polyhedron*, **1988**, *7*, 253.

6. Evans, D.G.; Mingos, D.M.P.; *Organometallics*, **1983**, *2*, 435.

7. Muetterties, E.L.; *Pure & Appl. Chem.*, **1982**, *54*, 83.

8. (a) Hostetler, M.J.; Dubois, L.H.; Nuzzo, R.G.; Girolami, G.S.; *J. Am. Chem. Soc.*, **1993**, *115*, 2044; (b) Hostetler, M.J.; Nuzzo, R.G.; Girolami, G.S.; Dubois, L.H.; *J. Phys. Chem.*, **1994**, *98*, 2952.

9. (a) Johnson, B.F.G.; Lewis, J.; Reichert, B.; Schorpp, K.T.; Sheldrick, G.M.; *J. Chem. Soc., Dalton Trans.*, **1977**, 1417; (b) Johnson, B.F.G.; Lewis, J.; Schorpp, K.T.; *J. Organomet. Chem.*, **1975**, *91*, C13.

10. Jackson, P.F.; Johnson, B.F.G.; Lewis, J.; Raithby, P.R.; Will, G.J.; McPartlin, M.; Nelson, W.J.H.; *J. Chem. Soc., Chem. Comm.*, **1980**, 1190.

11. Carty, A.J.; Domingos, A.J.P.; Johnson, B.F.G.; Lewis, J.; *J. Chem. Soc., Dalton Trans.*, **1973**, 2056.

12. Mason, R.; Thomas, K.M.; *J. Organomet. Chem.*, **1972**, *43*, C39.

13. Dahl, L.F.; Smith, D.L.; *J. Am. Chem. Soc.*, **1962**, *84*, 2450.

14. Belford, R.; Taylor, H.P.; Woodward, P.; *J. Chem. Soc., Dalton Trans.*, **1972**, 2425.

15. Aime, S.; Milone, L.; Osella, D.; Vaglio, G.A.; Valle, M.; Tiripicchio, A.; Tiripicchio Camellini, M.; *Inorg. Chim. Acta*, **1979**, *34*, 49.

16. Braga, D.; *Chem. Rev.*, **1992**, *92*, 633.

17. (a) Braga, D.; Grepioni, F.; Righi, S.; Dyson, P.J.; Johnson, B.F.G.; Bailey, P.J.; Lewis, J.; *Organometallics*, **1992**, *11*, 4042; (b) Dyson, P.J.; Johnson, B.F.G.; Reed, D.; Braga, D.; Grepioni, F.; Parisini, E.; *J. Chem. Soc., Dalton Trans.*, **1993**, 2817; (c) Braga, D.; Grepioni, F.; Johnson, B.F.G.; Chen, H.; Lewis, J.; *J. Chem. Soc., Dalton Trans.*, **1991**, 2559, and references cited therein.

18. Dyson, P.J.; Johnson, B.F.G.; Lewis, J.; Martinelli, M.; Braga, D.; Grepioni, F.; *J. Am. Chem. Soc.*, **1993**, *115*, 9602.

19. Dyson, P.J.; Johnson, B.F.G.; Braga, D.; *Inorg. Chim. Acta*, **1994**, *222*, 299.

20. Brown, D.B.; Dyson, P.J.; Johnson, B.F.G.; Parker, D.; *J. Organomet. Chem.*, submitted for publication.

21. (a) Braga, D.; Grepioni, F.; Sabatino, P.; Dyson, P.J.; Johnson, B.F.G.; Lewis, J.; Bailey, P.J.; Raithby, P.R.; Stalke, D.; *J. Chem. Soc., Dalton Trans.*, **1993**, 985; (b) Braga, D.; Sabatino, P.; Dyson, P.J.; Blake, A.J.; Johnson, B.F.G.; *J. Chem. Soc., Dalton Trans.*, **1994**, 393.

22. Braga, D.; Dyson, P.J.; Grepioni, F.; Johnson, B.F.G.; Calhorda, M.J.; *Inorg. Chem.*, **1994**, *33*, 3218.

23. See for example: (a) Blake, A.J.; Dyson, P.J.; Johnson, B.F.G.; Martin, C.M.; Nairn, J.G.M.; Parisini, E.; Lewis, J.; *J. Chem. Soc., Dalton Trans.*, **1993**, 981; (b) Johnson, B.F.G.; Blake, A.J.; Martin, C.M.; Braga, D.; Parisini, E.; Chen, H.; *J. Chem. Soc., Dalton Trans.*, **1994**, 2167.

24. (a) Anson, C.E.; Bailey, P.J.; Conole, G.; Johnson, B.F.G.; Lewis, J.; McPartlin, M.; Powell, H.R.; *J. Chem. Soc., Chem. Comm.*, **1989**, 442; (b) Bailey, P.J.; Duer, M.J.; Johnson, B.F.G.;

Lewis, J.; Conole, G.; McPartlin, M.; Powell, H.R.; Anson, C.E.; *J. Organomet. Chem.*, **1990**, *383*, 441.

25. Blake, A.J.; Dyson, P.J.; Ingham, S.L.; Johnson, B.F.G.; Martin, C.M.; *Inorg. Chim. Acta*, in press.

26. Braga, D.; Grepioni, F.; Parisini, E.; Johnson, B.F.G.; Martin, C.M.; Nairn, J.G.M.; Lewis, J.; Martinelli, M.; *J. Chem. Soc., Dalton Trans.*, **1993**, 1891.

27. Bailey, P.J.; Johnson, B.F.G.; Lewis, J.; McPartlin, M.; Powell, H.R.; *J. Organomet. Chem.*, **1989**, *377*, C17.

28. Cifuentes, M.P.; Humphrey, M.G.; *Organometallics*, **1993**, *12*, 4272.

29. Chihara, T.; Komoto, R.; Kobayashi, K.; Yamazaki, H.; Matsuura, Y.; *Inorg. Chem.*, **1989**, *28*, 9643.

30. Braga, D.; Grepioni, F.; *Organometallics*, **1992**, *11*, 1256, and references cited therein.

31. Jackson, P.F.; Johnson, B.F.G.; Lewis, J.; Raithby, P.R.; *J. Chem. Soc., Chem. Comm.*, **1980**, 60.

32. Couture, C.; Farrar, D.H.; Goudsmit, R.J.; *Inorg. Chim. Acta*, **1984**, *89*, L29.

33. Orpen, A.G.; XHYDEX, *A Program for Locating Hydrides*, Bristol University, **1980**; Orpen, A.G.; *J. Chem. Soc., Dalton Trans.*, **1980**, 2509.

34. Bashall, A.; Gade, L.H.; Johnson, B.F.G.; Lewis, J.; McIntyre, G.; McPartlin, M.; *Angew. Chem. Int. Ed. Engl.*, **1991**, *30*, 1164.

35. Edwards, K.J.; Field, J.S.; Haines, R.J.; Mulla, F.; *J. Organomet. Chem.*, **1991**, *402*, 113.

36. (a) Bullock, L.M.; Field, J.S.; Haines, R.J.; Minshall, E.; Smit, D.N.; *J. Organomet. Chem.*, **1986**, *310*, C47; (b) Bullock, L.M.; Field, J.S.; Haines, R.J.; Minshall, E.; Moore, M.H.; Mulla, F.; Smit, D.N.; Steer, L.M.; *J. Organomet. Chem.*, **1990**, *381*, 429.

37. Adams, R.D.; Babin, J.E.; Tasi, M.; *Inorg. Chem.*; **1986**, *25*, 4461.

38. Ansell, G.B.; Modrick, M.A.; Bradley, J.S.; *Acta Cryst.*, **1984**, *C40*, 365.

39. See for example: (a) Van Hove, M.A.; Lin, R.F.; Somorjai, G.A.; *J. Am. Chem. Soc.*, **1986**, *108*, 2532; (b) Lin, R.F.; Blackman, G.S.; Van Hove, M.A.; Somorjai, G.A.; *Acta Cryst., Sect. B*, **1987**, *43*, 368, and references cited therein.

40. Braga, D.; Dyson, P.J.; Grepioni, F.; Johnson, B.F.G.; *Chem. Rev.*, **1994**, *94*, 1585.

41. Braga, D.; Grepioni, F.; *Acta Cryst., Sect. B.*, **1989**, *B45*, 378.

42. Braga, D.; Grepioni, F.; *Organometallics*, **1991**, *10*, 1254.

43. Braga, D.; Grepioni, F.; Dyson, P.J.; Johnson, B.F.G.; *J. Cluster Science*, **1992**, *3*, 297, and references cited therein.

44. (a) Gavezzotti, A.; Simonetta, M.; *Chem. Rev.*, **1981**, *82*, 1; (b) *Organic Solid State Chemistry*, Desiraju, G.R.; Ed.; Elsevier, Amsterdam, **1987**; (c) Kitaigorodsky, A.I.; *"Molecular Crystals and Molecules"*; Academic Press; New York, **1973**.

45. Keller, E.; SCHAKAL93, *Graphical Representation of Molecular Models*, University of Freiberg, Germany, **1993**.

46. Braga, D.; Grepioni, F.; *Acc. Chem. Res.*, **1994**, *27*, 51.

47. Braga, D.; Grepioni, F.; Chen, H.; Johnson, B.F.G.; Lewis, J.; *J. Chem. Soc., Dalton Trans.*, **1991**, 2559.

48. Braga, D.; Grepioni, F.; Dyson, P.J.; Johnson, B.F.G.; Frediani, P.; Bianchi, M.; Piacenti, F.; *J. Chem. Soc., Dalton Trans.*, **1992**, 2565.

49. Braga, D.; Grepioni, F.; Righi, S.; Johnson, B.F.G.; Frediani, P.; Bianchi, M.; Piacenti, F.; Lewis, J.; *Organometallics*, **1991**, *10*, 706.

Chapter Four

[2.2]Paracyclophane Clusters of Ruthenium

This chapter commences with an historic introduction concerning the key developments in the chemistry of the highly strained class of compounds known as the cyclophanes, with particular emphasis directed towards their interactions with transition metal atoms. This is followed by a detailed analysis of a series of cyclophane-cluster compounds, with nuclearities ranging from three to eight, obtained from the thermal reaction between $Ru_3(CO)_{12}$ and [2.2]paracyclophane. The intimate relationships between these compounds is examined, one of which is thought to be a key intermediate on route to a *closo*-octahedral carbido-cluster thus shedding light on the mechanisms involved in carbide formation. Clusters with unique metal polyhedra have been isolated, and a new bridging (μ_6-η^2) coordination mode for CO has been established which contains an extremely long C-O bond. Finally, the ^1H NMR spectra of the cyclophane moieties are critically discussed as potential electronic probes for the evaluation of the electron density associated with a cluster surface.

4.1 An Introduction to Cyclophane Chemistry

The cyclophane era is generally regarded as having begun in 1949 when Brown and Farthing reported the isolation of di-*p*-xylene from the high temperature pyrolysis (900°C) of *p*-xylene.[1] Since it was not possible, at that time, to prepare the compound by a more conventional route, the authors concluded that the ring-strain evidently present in the molecule could only be overcome by the extreme conditions of the pyrolysis reaction. These initial inferences were proved to be incorrect just two years later by Cram and Steinberg who, whilst looking at the bonding, strain energies and transannular π-electron interactions within rigid molecules of known geometry, prepared di-*p*-xylene by design using a Wurtz-coupling reaction of α,α'-dibromo-*p*-xylene.[2] Cram and Steinberg also introduced the cyclophane nomenclature which was later reinforced by Vögtle,[3] and is now commonly used for this class of compound. By this nomenclature, the term cyclophane describes any molecule containing a bridged aromatic ring. Each bridge is indicated by a number which corresponds to the number of bridge members, placed in a bracket before the name. The position of attachment of the bridges on the aromatic ring can be designated by the usual names of *ortho*, *meta* and *para* or by numbers in parentheses, and the stem of the name results from a contraction of *cyclo*, *phenyl* and alk*ane*.[4] According to this nomenclature, the first cyclophane molecule, di-*p*-xylene, can be referred to as [2.2]paracyclophane or [2.2](1,4)cyclophane.

In this innovative publication,[2] Cram not only laid the basis for the synthesis of a whole new group of aromatic compounds, but also outlined most of the reasons why cyclophane chemistry is, even today more than forty years later, an exciting and much studied area of research. Cyclophane molecules containing benzene are among those most investigated and show considerable cofacial π-π repulsions which result in the distortion of the benzene ring from planarity towards either boat or chair conformations. They therefore provide excellent models for the study of molecular strain and its relationship to reactivity, with the question "How bent can a benzene be ?" representing a challenge in itself, both in terms of molecular design (*i.e.* in predicting what extremes of deformity might be incorporated into an organic structure before molecular collapse or fragmentation occurs) and in organic synthesis.[5] The conformational simplicity and unique geometry of these cyclophane molecules also provide a means of investigating the transannular steric and electronic interactions between the aromatic rings, and therefore raises the question as to whether and how the electronic effects of substituents in one ring are transferred to the second ring, and whether these interactions are a function of bridge length.

In the years following Cram's initial study a large number of cyclophane molecules were prepared,[6] with most of the work being centred around the [2n]cyclophanes (aromatic compounds containing two benzene rings connected by n ethano bridges). Throughout the period 1950 - 1970, the original procedures of 1,6-eliminations and Wurtz-coupling reactions were still being used as general routes to cyclophanes, however in 1969 the introduction of the dithiacyclophane - sulphur extrusion approach greatly facilitated the syntheses of these compounds and created the chance of preparing multibridged [2n]cyclophanes,[7] as illustrated by the synthesis of [2$_3$](1,3,5)cyclophane; the first cyclophane with more than two bridges.[8] The possibility of constructing additional bridges by the stepwise manipulation of the known [2.2]cyclophanes was exploited in the synthesis of the [2$_3$](1,2,4) and [2$_4$](1,2,4,5)cyclophanes.[9,10] Furthermore, throughout the 1970's Hopf and co-workers developed a very convenient method for synthesising multisubstituted [2.2]paracyclophanes, and then used the substituents as anchor points for creating additional bridges. By this route the [2$_4$](1,2,3,5) and [2$_4$](1,2,3,4)cyclophanes were prepared.[11,12]

These preparative routes were becoming rather complicated and required several synthetic steps, hence, further elaboration to produce the remaining highly-bridged, highly-strained members of the series seemed a tedious and difficult task, especially if they were to be made in sufficient quantities for adequate chemical studies. Therefore an alternative approach was required, and in 1979 Boekelheide established that a combination of the thermal elimination of hydrogen chloride from *o*-chloromethyltoluenes to give aromatic cyclobutenes, together with the pyrolytic dimerization of appropriate derivatives of such

aromatic cyclobutenes appeared to be a synthetic method of general utility.[6] He proved its convenience and efficiency in preparing multibridged cyclophanes by the synthesis of [2$_3$](1,2,3)cyclophane,[6] [2$_5$](1,2,3,4,5)cyclophane[13] and the ultimate member of the series [2$_6$](1,2,3,4,5,6)cyclophane, often referred to as 'superphane'.[14] Therefore, by 1980, the development in synthetic methods had made it possible to prepare all twelve of the 'symmetrical' [2n]cyclophanes, *i.e.* those in which the bridges are aligned parallel and are anchored to identical positions of both aromatic nuclei (see Figure 4.1), and had opened the door for the synthesis of a whole range of cyclophanes in which all types of aromatic subunits could be bridged not only by polymethylene chains, but also by functionalised bridging units (*vide infra*).
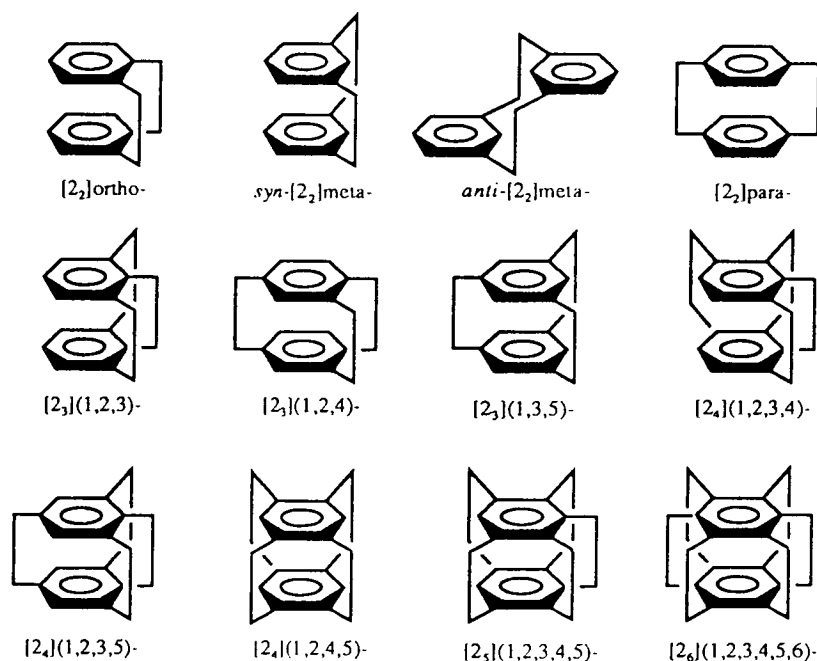
Figure 4.1: The 'symmetrical' [2n]cyclophanes.

The [2n]cyclophanes have been studied primarily from a structural and reactivity viewpoint. Structurally these hydrocarbons are of interest since their inter-ring distances are decidedly smaller than the distance between the layers of graphite, and it is therefore of interest to examine how changes in geometry and in the distance between decks can affect the properties of these molecules. The chemical behaviour of the [2n]cyclophanes is determined on the one hand by the π-electron interaction between the benzene decks, which is sufficiently strong to cause the molecules to behave as one overall π-electron system, and on the other by the internal strain of these polycyclic systems, which make them far more

reactive than conventional nonannelated aromatics; the driving force of most reactions being a reduction of this strain energy. When compared to classical arenes, their most distinct chemical property is the ease with which they undergo addition reactions such as Diels-Alder additions, hydrogenations and ionic additions.[4] However, the typical regenerative behaviour of aromatic molecules is not fully suppressed in the [2n]cyclophanes, typified by their ability to undergo electrophilic substitution reactions such as bromination, Friedel-Crafts acylation, and nitration. Besides these reactions in which the aromaticity is either destroyed or retained, reactions at, and with, the ethano bridges, *e.g.* their cleavage, isomerisation, and functionalisation can also occur.[4]

Since detailed molecular structure and strain energies are necessary to understand the physical and chemical properties of the [2n]cyclophanes, it is worth briefly addressing these topics in more detail. Particular emphasis is directed towards the [2.2]paracyclophane molecule as this is of most pertinence to subsequent discussions.

4.1.1 Structure and Strain

There has been considerable interest in the structure and properties of the unusually strained hydrocarbon, [2.2]paracyclophane. The crystal structure has been established on three separate occasions,[15-17] with a significant variance between each set of results. It is generally considered that the observed differences arise from the poor quality of the data available at the time, and a later reinvestigation by Bernstein and Trueblood has led to the apodictic molecular structure and enabled an analysis of the observed thermal motion.[18] The two benzene rings in [2.2]paracyclophane are not exactly aligned relative to one another, and the apparent slight twist is thought to relieve the repulsive interactions which are at a maximum when the rings are exactly aligned. This twist, however, introduces other strains within the molecule which act as restoring forces, either forcing the rings closer together, or stretching the C-C bridge bond (or a combination of both) and hence, bond angles are also deformed from ideality. The potential function of these restoring forces is at a minimum at the eclipsed position, but rises as the angle of twist increases. These opposite effects cause the molecule to exist near the extremes of its motion for most of the time at room temperature, and hence the crystal structure is disordered.

Even though disordered, the molecular structure shows several noteworthy structural features. The aromatic rings are deformed into boat-shaped conformations with the *para* bridgehead carbon atoms bent 12.6° out of the plane that passes through the remaining four carbon atoms. This deviation from planarity is thought to arise from a combination of two opposite effects, *viz.* the π-electron repulsion between the two rings and the strain imposed on the bridging CH_2-CH_2 units. The former is present because the distance between the two parallel parts of the ring [3.09 Å] is markedly shorter than the normal *inter*molecular distance of 3.40 Å found in graphite, and the latter because the

bridge distance of 1.562 Å is elongated when compared to an average C-C single-bond distance of 1.541 Å. Figure 4.1.1 illustrates the molecular profile of the carbon skeleton found in [2.2]paracyclophane. The hydrogen atoms substituted on the aromatic ring are also slightly displaced inwards from the least-squares plane of the four essentially coplanar atoms to which they are bonded. This structural feature probably also reflects the strong π-π repulsion between the two benzene rings which results in an increased π-electron density on the outside faces of the benzene rings, and so the molecule adjusts somewhat by a rehybridisation of the aromatic carbons to increase the p character of their σ- bonds.[6,18]
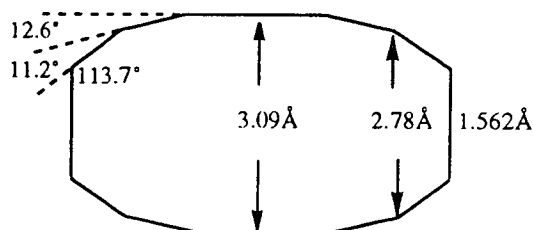
Figure 4.1.1: Molecular profile of the carbon skeleton of [2.2]paracyclophane.

The crystal structures of a large number of multibridged [2n] and longer bridged [m.n]cyclophane molecules have been established, and their respective strain energies calculated and compared with those of [2.2]paracyclophane. A couple of examples shall be briefly described in order to illustrate the consequences that a change in the proximity of the benzene rings with respect to one another (such as an increase in bridge length or a greater number of bridges) can have on the molecular structure and strain.

In the molecular structure of [3.3]paracyclophane,[19] the benzene rings still deviate from planarity towards the boat-shaped conformation, however, the out of plane bending is reduced from 12.6° in [2.2]paracyclophane to 6.4°. The distance between benzene decks is increased from 3.09 Å in the parent molecule to 3.31 Å, and the benzene rings are also considerably displaced from the centred position found in the more rigid [2.2]paracyclophane. This latter type of distortion reflects the molecules ability to overcome some of the cofacial π-π electronic interaction between its rings by maximising its asymmetry. Therefore the addition of one extra CH_2 linkage in the cyclophane bridges can reduce the strain within the molecule quite substantially. The strain energies of these compounds have also been determined,[20] and their values correlate nicely with the information obtained from crystallography: for [2.2]paracyclophane, E = 134 kJmol[-1]; for [3.3]paracyclophane, E = 52 kJmol[-1]; and for [6.6]paracyclophane, E = 9 kJmol[-1]. Clearly

[2.2]paracyclophane has the highest strain energy, whereas [6.6]paracyclophane has the characteristics of an open-chain molecule.[5]

One of the most interesting features of the multibridged [2n]cyclophanes is the reduction in the distance between the benzene decks as additional bridges are added. In [2.2]paracyclophane this distance is 3.093 Å,[18] whereas for [2_3](1,3,5)cyclophane it is 2.801 Å,[21] for [2_4](1,2,4,5)cyclophane 2.688 Å,[22] for [2_5](1,2,3,4,5)cyclophane 2.650 Å,[6] and for [2_6](1,2,3,4,5,6)cyclophane 2.624 Å.[23] Superphane is a highly symmetrical molecule with each of the benzene rings being a perfectly planar, regular hexagon, and the distance of 2.624 Å between the two aromatic rings is the closest observed thus far in a stable compound. The most surprising feature of superphane is the distortion of the sp^2-sp^3 C-C bond angles out of planarity with the benzene ring and towards the interior by 20.3°. Thus, the π-orbitals in superphane are not perpendicular to the ring plane but are deflected giving the contour representation of the π-cloud a bowl shape. Strain energies of the [2n]cyclophanes have been calculated and the data confirms that both thermal stability and strain energy increase with the number of ethano bridges: thus, for [2.2]paracyclophane, E = 134 kJmol^{-1};[20] for [2_3](1,2,4)cyclophane, E = 159 kJmol^{-1};[24] for [2_4](1,2,3,5)-cyclophane, E = 193 kJmol^{-1};[24] for [2_5](1,2,3,4,5)cyclophane, E = 331 kJmol^{-1};[24] and for [2_6](1,2,3,4,5,6)cyclophane, E = 342 kJmol^{-1}, superphane exhibiting the greatest total strain energy of any of the [2n]cyclophanes.[23]

The π-base strengths of the [m.n]paracyclophanes have also been measured [by equilibrium constants (K) in their π-salt formation with tetracyanoethylene (TCNE)] and are found to decrease in the order: [3.3] > [2.2] > [4.4] > [6.6] ~ open-chain model.[25] With the exception of [2.2]paracyclophane, the order correlates with the distance of the two benzene rings from one another; the closer the two rings, the greater the π-base strength (the non-bound benzene ring releasing electrons to the bound ring). The relaxation of internal strain in passing from π-base to π-salt is another factor affecting the base strength of the cyclophane ligand and explains why [3.3] is a stronger π-base than [2.2]paracyclophane. As previously described, the π-π repulsive interactions between the benzene rings in [3.3]paracyclophane cause them to be displaced from a central position, which in turn causes distortions in most of the bond angles throughout the molecule. These π-π repulsions are probably strongest when each benzene ring is electronically equivalent, as in the non-complexed state. However, when one ring interacts with a TCNE molecule, that ring becomes slightly electron-deficient, the π-π repulsions between the rings decrease, the rings become more centred and the bond angle strain is reduced. This effect does not occur in [2.2]paracyclophane since its more rigid structure does not possess the same initial distortions.

4.1.2 More Complex Cyclophane Molecules

Although the discussion so far has centred on the relatively simple [m.n]paracyclophanes and the 'symmetrical' [2n]cyclophanes, there exists a multitude of more complex, highly distorted, phane molecules in which all types of aromatic sub-units, such as naphthalene, anthracene, and cyclopentadienyl or heteroaromatic moieties such as pyridine or thiophene, are bridged by polymethylene chains and also by functionalised bridging units.[26] The methods by which these [2n]cyclophanes are prepared are quite general, and slight modifications of these techniques can lead to the synthesis of some remarkable compounds.

A large number of *unsymmetrical* or *skewed* [2n]cyclophanes with different substitution patterns of the two benzene rings are conceivable, but only a few are known; probably owing to the difficulty in the synthesis of such 'internally tortured' molecules. For example [2.2]metaparacyclophane,[27] [2.2]orthometacyclophane,[28] [2₃](1,2,4)(1,3,5) and [2₃](1,2,4)(1,2,5)cyclophane [27] have all been synthesised, and very recently the last and most strained of the three unsymmetrical [2.2]cyclophane isomers, [2.2]orthopara-cyclophane, has also been prepared.[29] These skewed cyclophanes are currently under investigation due to their increased reactivity which results from an increase in internal strain.

As far as the parent systems are concerned, *i.e.* those cyclophanes containing benzene decks and ethano/propano bridges only, work has mainly focused on multi-layered,[30] multistepped[31] and [2n]para[32] cyclophanes (see Figure 4.1.2i).

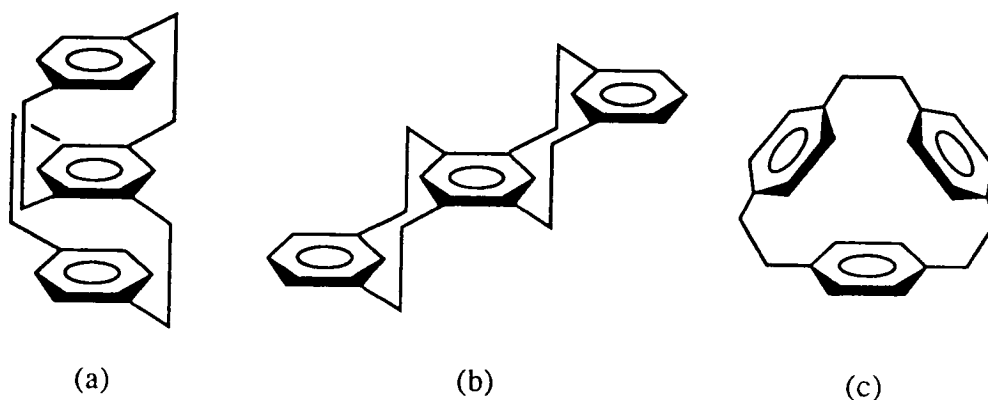**Figure 4.1.2i:** (a) Triple-layered, (b) Triple-stepped and (c) [2₃]para- Cyclophanes.

In multilayered cyclophanes the benzene rings are stacked in such a fashion that the molecules behave as single π-electron systems, with their columnar structures allowing electronic interactions over unusually large distances. Therefore, if a polymer molecule consisting of a huge pillar of multilayered cyclophane could be prepared, it should have a

single π-electron system delocalised over the whole of the molecule. Such a molecule could be expected to have interesting properties with potential practical value.[30,33] The relatively flexible multistepped cyclophanes are studied principally because of their dynamic properties,[31] and the [2n]paracyclophanes are structurally remarkable since they possess a *hollow* molecular cavity. These latter cyclophanes, in which three or more arene units are incorporated into medium or large rings, are studied for a number of reasons, including their ability to form inclusion compounds with a wide variety of substrates.[32b,34] Because the spatial shape of the [2₃]paracyclophane molecule shows a rigid prismatic arrangement of the three benzene nuclei it has been named a 'π-prismand'.[32b]

A rigid molecular framework is highly desirable in order to explore this host-guest relationship and the interaction of the π-electron system, and one method of introducing greater rigidity into a cyclophane molecule is by additional bridging. In 1985, Boekelheide prepared [2₆](1,2,4,5)cyclophane (Deltaphane), and showed that the molecule was rigid, highly symmetrical, and contained three benzene rings held face-to-face at a relatively short distance from one another with a simultaneous π-electron delocalisation among the three rings.[34] The rigid geometry of deltaphane with its internal cavity circumscribed by three benzene rings seems ideal for metal ion complexation of the 'π-prismand' type, however, the preparation of complexes where a metal ion is lodged in the cyclophane cavity has yet to be realised, even though stable silver complexes have been produced with the silver ion complexed to the exterior of the deltaphane moiety.[34] The following member of this class would be a rigid cyclophane with four benzene rings, and examination of molecular models indicate that the cavity in such a molecule would be large enough not only to accommodate metal ions, but also small, rod-like molecules such as dicyanoacetylene which form charge-transfer complexes with arenes.[34]

Host compounds with cyclophane skeletons have made an important contribution to the rapid development of supramolecular chemistry (*i.e.* chemistry predominantly involved in the study of weak *inter*molecular interactions which result in the association and self-organisation of several components to form larger aggregates) since their aromatic structural units ensure the necessary rigidity of the molecular structures and thereby improve the preorganisation of the coordination sites for the cooperative binding of their guests. A number of these synthetic hosts and their interactions with guest molecules have been studied extensively in some recent review articles,[35] and this region of chemistry is an active area of current research.

Many cyclophane compounds with funtionalised bridges are also known today, and recently several compounds have been described in which the benzene rings are held in strict orthogonality by molecular bridges. Such compounds include 1,2:7,8-dibenzo[2.2]paracyclophane,[36,37] its tetraphenyl derivative,[37] and the trimer of [2.2]-

paracyclophane with an ethyno-bridge (which is given the trivial name trifoliaphane).[38] These molecules are illustrated in Figure 4.1.2ii(a)-(c), respectively, and are all expected to exhibit interesting chemical and physical properties as well as serving as new types of ligands for metal complexation. A final example where a novel bridge, consisting of a condensed aromatic system, is used to hold two aromatic sub-units in a perpendicular arrangement is in the molecule 4,13-(9',10'-Phenanthreno)[2.2]paracyclophane[39] [see Figure 4.1.2ii(d)].
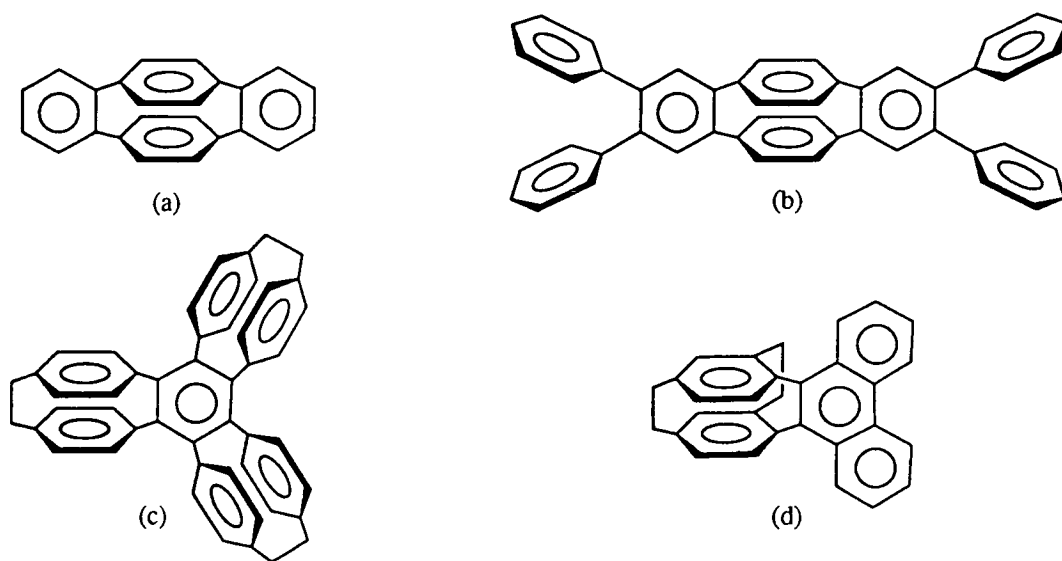

Figure 4.1.2ii: (a) Dibenzo[2.2]paracyclophane, (b) Tetraphenyldibenzo[2.2]paracyclophane, (c) Trifoliaphane and (d) Phenanthreno[2.2]paracyclophane.

Finally, in the early 1980's Sakuri and co-workers were interested in the synthesis of cyclophanes containing Si-Si bridges instead of C-C units, and prepared octamethyltetrasila[2.2]paracyclophane; the first [2.2]paracyclophane to be bridged by heteroatoms.[40] This molecule shows properties resulting from a strong σ-π mixing between the Si-Si σ bonds and the aromatic π-systems, and when compared with [2.2]paracyclophane displays a far smaller through-space and a larger through-bond interaction.[41] The X-ray crystal structure of octamethyltetrasila[2.2]paracyclophane[40] shows that it is a rather less distorted molecule than the parent [2.2]paracyclophane,[18] probably because the Si-Si bonds are longer than the corresponding C-C bridges (2.376 vs. 1.562 Å). The two benzene rings are completely eclipsed, the bridgehead carbon atoms are only slightly displaced out of the plane of the other four atoms towards a boat conformation (degree of displacement is 4.3° compared to 12.6° in [2.2]paracyclophane), and the distance between the aromatic planes of 3.458 Å is similar to that observed in graphite (3.40 Å), and longer than that in [2.2]paracyclophane (3.09 Å). Sakuri then went on to prepare 1,2,9,10,17,18-hexasila[2_3](1,3,5)cyclophane, a cage-like phane containing three Si_2Me_4 units,[42] and its X-ray diffraction analysis shows that, as with the

multibridged [2n]cyclophanes, the additional bridge has the effect of increasing the rigidity of the molecule and reducing the distance between the aromatic rings (3.32 Å). Additional members of this cyclophane class are still under investigation owing to their unique properties resulting from the through-bond interaction of the Si-Si σ bonds with the aromatic π-systems.

4.1.3 Transition Metal Complexes of [2.2]paracyclophane

The first transition metal complexes of the [m.n]paracyclophanes, *viz.* (η^6-[m.n] paracyclophane)tricarbonylchromium, were prepared by Cram and Wilkinson in 1960 from the thermolysis of chromium hexacarbonyl and the respective cyclophane in a high boiling ether.[43] A number of [m.n]paracyclophanes, ranging from [2.2] to [6.6], were employed in this initial study in order to establish whether they would complex with one or two equivalents of tricarbonylchromium. It was proposed that the lower homologues would form *mono*(complexes) and the higher ones *bis*(complexes), thereby providing evidence for transannular electronic interactions between the two rings. It was also hoped that the *mono*(complexes) could be induced to lose three moles of CO, thus forming organometallic compounds with chromium sandwiched between the two rings.

The results of these experiments demonstrated that all cyclophanes formed *mono*(tricarbonylchromium) complexes [see Fig. 4.1.3i(a)] and that only the [4.5] and [6.6]paracyclophanes formed *bis*(complexes). Also the *mono*(complexes) showed little inclination to react with additional chromium hexacarbonyl, particularly those homologues in which *m* and *n* were 4 or less. This led to the conclusion that the electron-withdrawing character of the Cr(CO)$_3$ group exerts its influence both on the aromatic ring to which it is coordinated and on the second aromatic unit. The electronic interaction between the two benzene rings is reduced with a lengthening of the methylene bridges, and therefore the rings need to be far apart as in the [4.5] and [6.6] species before they can behave as independent units and form *bis*(complexes). These observations provide strong evidence for transannular electron release from one benzene to the second, when the second is bound to an electron-withdrawing group. The solid-state molecular structure of Cr(CO)$_3$(η^6-[2.2]paracyclophane) has been established by single crystal X-ray analysis,[44] and the main feature to be noted is that upon coordination of the electron-withdrawing Cr(CO)$_3$ unit, the π-electron repulsion between the two benzene rings is reduced, as indicated by the shortened inter-ring distance of 3.017(2) Å (*cf.* free [2.2]paracyclophane 3.093(2) Å).[18]

Cram's initial attempts to eliminate CO from the *mono*(complexes) of the [4.4], [5.5] and [6.6]paracyclophanes to give compounds with the chromium atom in the centre of the cyclophane cavity were unsuccessful. These compounds were feasible in steric terms, with the estimated distance between the two benzene decks being larger than that estimated for Cr(η^6-C$_6$H$_6$)$_2$ [3.7 Å for [4.4]paracyclophane *vs.* < 3.4 Å for

bis(benzene)chromium].[43] However, the formation of these molecules required rotation of the complexed benzene ring through 180° about the axis of the bonds extending from its 1,4-position (a process which is possible for the free ligands themselves), and it therefore appeared that the additional bulk of the chromium atom attached to one face of the benzene ring provided considerable steric resistance, thus preventing such a rotation. Since cyclophane chemistry was an expanding field of research at this time it was not surprising, in view of the existence of *bis*(benzene)chromium, that further efforts were made to place a metal atom inside the cyclophane skeleton, and in 1978, Elschenbroich discovered that by co-condensing [2.2]paracyclophane with chromium atoms, the first species of this class, (η^{12}-[2.2]paracyclophane)chromium, could be prepared along with the *bis*(η^6-[2.2]paracyclophane)chromium complex [see Figures 4.1.3i(b) and (c), respectively].[45]
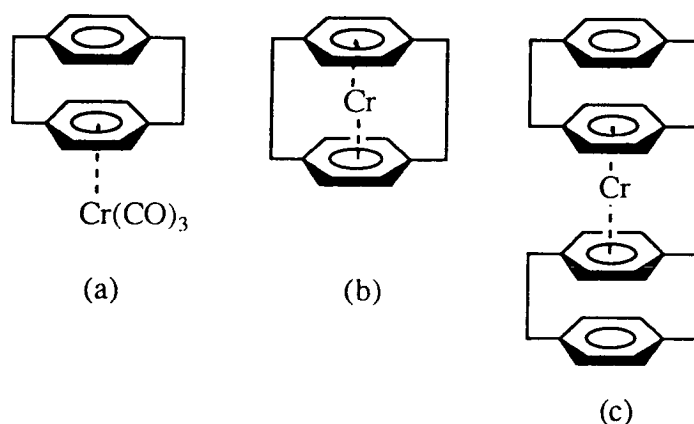

Figure 4.1.3i: (a) Cr(CO)$_3$(η^6-[2.2]paracyclophane), (b) Cr(η^{12}-[2.2]paracyclophane), (c) Cr(η^6-[2.2] paracyclophane)$_2$.

These two complexes were of interest because the former was expected to be kinetically inert and to display a change from the *intra*molecular π-π repulsion present in the free ligand to a bonding η-arene-metal interaction in the complex, whilst the latter was considered a potential precursor for polymeric structures of the composition [(η-cyclophane)-metal]$_n$. A comparison of the X-ray structural data of [2.2]paracyclophane (inter-ring C-C distance of 3.09 Å)[18] with that of Cr(η^6-C$_6$H$_6$)$_2$ (Cr-ring plane distance of 1.61 Å)[46] suggests that Cr(η^{12}-[2.2]paracyclophane) represents a compressed sandwich complex. This complex is stable in terms of solvolytic metal-ligand cleavage and is even unaffected by strong acids over a prolonged period, whereas Cr(η^6-[2.2]paracyclophane)$_2$ slowly releases its ligands when dissolved in methanol at room temperature. The difference in stability between the two complexes can be explained in steric terms; the concave sides of the non-planar benzene rings, functioning as a chelate ligand, are oriented towards the

central metal in $Cr(\eta^{12}$-[2.2]paracyclophane) thus shielding it from solvolytic attack, whereas in the case of $Cr(\eta^6$-[2.2]paracyclophane)$_2$ attack is easier because coordination *via* the convex sides of the non-planar benzene rings leaves the central metal atom exposed to attack by the solvent.

The complex $Cr(\eta^{12}$-[3.3]paracyclophane) has also been prepared,[47] and like $Cr(\eta^{12}$-[2.2]paracyclophane) it is air-sensitive and characterisation by means of X-ray analysis has yet to be achieved. However, the I_3^- and PF_6^- salts of the $[Cr(\eta^{12}$-[3.3]paracyclophane)]$^+$ complex are air stable, and their solid-state structures have been determined by X-ray crystallography.[48] The I_3^- salt gave the most accurate structure determination illustrating that, as in the uncomplexed [3.3]paracyclophane ligand,[19] the aromatic rings are bent out of the plane towards a boat-shaped conformation, however the angle of deformation is less in the complexed molecule (5.60 *vs.* 6.40°) and the aromatic rings are almost eclipsed. The distance of the Cr atom from the benzene planes are 1.58 Å to the two bridgehead carbon atoms and 1.61 Å to the remaining four coplanar carbon atoms, and therefore the distance between the two aromatic rings (3.16 and 3.22 Å) is directly comparable to the values found in $Cr(\eta^6$-$C_6H_6)_2$ (3.22 Å),[46] $[Cr(\eta^6$-$C_6H_6)_2]$ $[I_3]$ (3.18 Å),[49] and the free ligand (3.27 Å).

Since the crystal structure of octamethyltetrasila[2.2]paracyclophane had revealed that the inter-ring distance was longer than that observed in $Cr(\eta^6$-$C_6H_6)_2$ (3.46 *vs.* 3.22 Å),[40,46] and that a chromium atom had been introduced into the cavity of [2.2]paracyclophane,[45] which has an inter-ring distance markedly shorter than in $Cr(\eta^6$-$C_6H_6)_2$ (3.09 Å),[18] it was assumed that *endo* coordination of a transition metal into the octamethyltetrasila[2.2]paracyclophane cavity would be relatively facile. This led to the metal atom ligand-vapour co-condensation technique being used in the preparation of $Cr(\eta^{12}$-Me_8Si_4-[2.2]paracyclophane).[50] The molecular structure of this complex, as

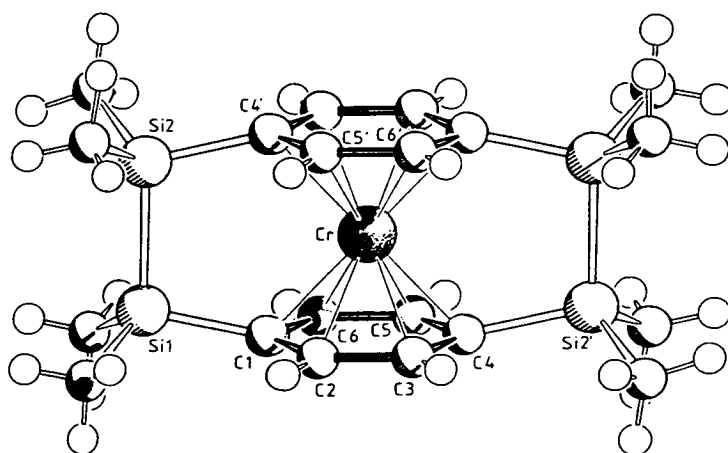**Figure 4.1.3ii:** The molecular structure of $Cr(\eta^{12}$-Me_8Si_4-[2.2]paracyclophane).

characterised by X-ray crystallography, shows that the distance between the 'best ring planes' has been reduced to 3.24 Å, which approaches that of $Cr(\eta^6\text{-}C_6H_6)_2$ (see Figure 4.1.3ii). The boat-shaped deformation of the rings is also strongly reduced (interplane angle is 2.3° *cf.* 4.3° in the free ligand), although the Si-Si bond distance is not significantly shorter than that found in the free ligand [2.361(4) *vs.* 2.376(4) Å].

An extension of Cram's original work on *mono-* and *bis*(tricarbonylchromium)-paracyclophane complexes was undertaken by Misumi and coworkers using multilayered [2.2]paracyclophanes, in an attempt to further pursue the interactions between their benzene rings.[51] By using more forcing conditions (*i.e.* by treating the corresponding cyclophanes with chromium hexacarbonyl in diglyme at 140-150°C for 2-3 hours) they managed to isolate the *mono* and *bis*(tricarbonylchromium) complexes of [2.2]paracyclophane, as well as the analogous triply- and quadruply-layered compounds [See Figure 4.1.3iii (a)-(c)]. The preparation of $\{Cr(CO)_3\}_2(\eta^6\text{-}\eta^6\text{-}[2.2]$paracyclophane) contradicted Cram's initial conclusions, which suggested that the *bis*(complex) could not be formed due to deactivation of the non-complexed benzene ring in the *mono*(complex) by the electronic-withdrawing character of the $Cr(CO)_3$ group. However, it was only produced in very small amounts, with the *bis*-complexes of the triply and quadruply layered cyclophanes being formed in far greater yields, thus indicating that the first attached $Cr(CO)_3$ group exerts a smaller transpacial electronic interaction on the uncoordinated benzene ring as the layer number is increased; a concept which formed the basis of Cram's original argument.[43] The molecular structure of the $Cr(CO)_3$(triple-layered[2.2]paracyclophane) complex shows that both the upper and lower benzene rings adopt a boat-shaped conformation, with the two bridgehead carbon atoms positioned 11.0° and 11.8°, respectively, out of the plane of the other four coplanar carbon atoms.[52] The middle layer benzene ring is twisted by 13.4° along the line passing through the two carbon atoms which are not linked by $-CH_2\text{-}CH_2\text{-}$ bridges, and the three benzene rings are not in the eclipsed position, but are mutually rotated in a slight helical manner. The interlayer distance between the base plane of the upper-layer benzene ring coordinated to the $Cr(CO)_3$ group and the least squares plane of the middle-layer is shorter than the corresponding distance between the middle and lower-layer benzene rings (2.979 *vs.* 3.057 Å), reinforcing the effect that the electron-withdrawing $Cr(CO)_3$ group has on reducing cofacial $\pi\text{-}\pi$ repulsion.

This pioneering work on chromium-cyclophane complexes demonstrated the exciting potential that cyclophanes had to offer organometallic chemistry as a new class of π-ligand, and since the early 1980's the number of publications concerning systems of this type has increased quite considerably. The outstanding characteristic of the [2n]cyclophanes, for the organometallic chemist, is the interaction of their two aromatic
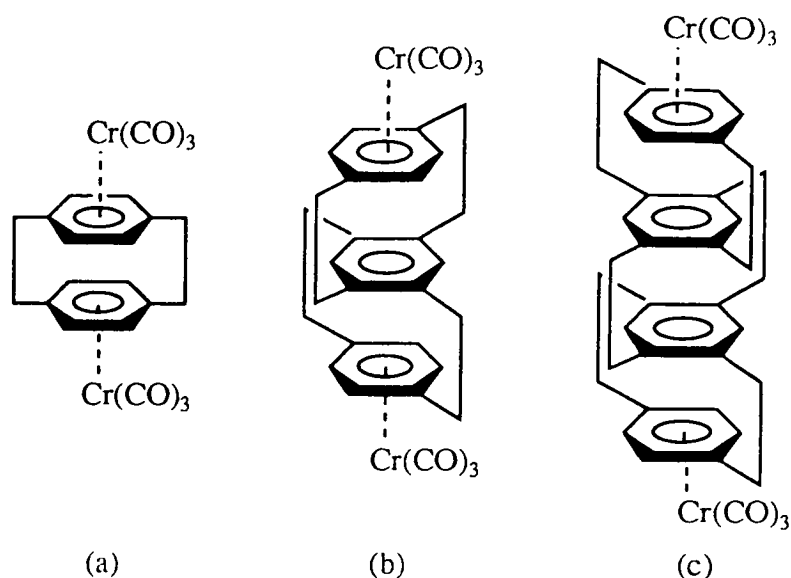
Figure 4.1.3iii: (a) {Cr(CO)3}2(η^6-η^6-[2.2]paracyclophane) and its analogous (b) triple layered and (c) quadruple layered complexes.

decks to give one overall π-electron system. This, combined with the possibility for metal complexation at both of the arene decks, raised the question as to whether oligomers and polymers of transition metal complexes of the [2n]cyclophanes might have π-electron systems extending over the whole of the macromolecular framework. Furthermore, if the molecules were designed so that the transition metal atoms along the polymer chain differed in their formal oxidation states, this may provide the electron holes necessary for a conduction band and the polymer should show properties of a unidimensional, electrical conductor, [see Figure 4.1.3iv].[33]

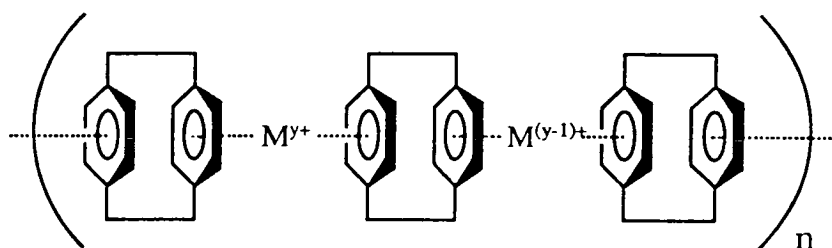**Figure 4.1.3iv:** A potential metal-cyclophane polymer.

In order to test the extent to which π-electron delocalisation would occur in these polymers Boekelheide set about the synthesis of appropriate model subunits, with a view to examine their mixed valence properties.[33,53] The traditional methods of preparing chromium complexes of the [2n]cyclophanes had severe limitations in this respect. The

reaction of cyclophanes with $Cr(CO)_6$ to give both the *mono* and *bis*(tricarbonylchromium)-cyclophane complexes could not be used, since no useful method for removing the carbonyls from such complexes to make multilayered oligomers had evolved. Similarly, the metal atom technique used in the synthesis of $Cr(\eta^{12}$-[2.2]paracyclophane) and $Cr(\eta^6$-[2.2]paracyclophane)$_2$, could not be applied in the preparation of oligomers or polymers of transition metal-cyclophane complexes. Fortunately, around this time, Bennett and his colleagues had reported a convenient method for preparing *bis*(arene)-ruthenium(II) complexes,[54] and by substituting [2.2]paracyclophane for the second arene, Boekelheide *et al* produced double and triple layered arene-[2.2]paracyclophane-ruthenium(II) complexes in excellent yield [see Figures 4.1.3v (a) and (b)].
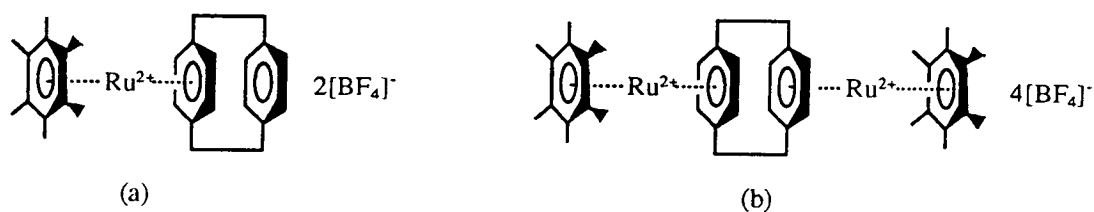

Figure 4.1.3v: (a) Double and (b) Triple layered arene-[2.2]paracyclophane-ruthenium(II) complexes.

Bennett's procedure therefore proved useful in the synthesis of arene-capped [2n]cyclophane complexes, however, it was not as successful in the preparation of *bis*(η^6-[2n]cyclophane)Ru(II) derivatives; the difficulty being in finding a way to prepare the (η^6-[2n]cyclophane)Ru(II) solvates. Boekelheide overcame this problem by removing the arene cap from an arene-capped ruthenium-[2n]cyclophane complex by hydride reduction, which if followed by treatment with acid gave the (η^6-[2n]cyclophane)Ru(II) solvate.[53] This ruthenium solvate could then be used to cap another [2n]cyclophane molecule, so forming a *bis*(η^6-[2n]cyclophane)Ru(II) derivative, [see Figure 4.1.3vi (a)]. In order to extend the chain length of the [Ru(η^6-[2.2]paracyclophane)$_2$][BF$_4$]$_2$ complex, and so form a specific oligomer containing purely [2.2]paracyclophane, the preparation of a *tris*(trifluoroacetate) solvate of [Ru(η^6-[2.2]paracyclophane)][BF$_4$]$_2$ was required which could be used to cap [Ru(η^6-[2.2]paracyclophane)$_2$]$^{2+}$ 2[BF$_4^-$] in trifluoroacetic acid, thus producing the desired *tris*(η^6-[2.2]paracyclophane)diruthenium derivative in low yield [see Figure 4.1.3vi (b)].[53] Such *bis* and *tris*-derivatives are potential key model sub-units for the synthesis of oligomers and polymers, and are of particular interest with respect to their electrochemical

reduction and the possibility of observing electron-transfer between the ruthenium atoms in their corresponding mixed-valence ions.
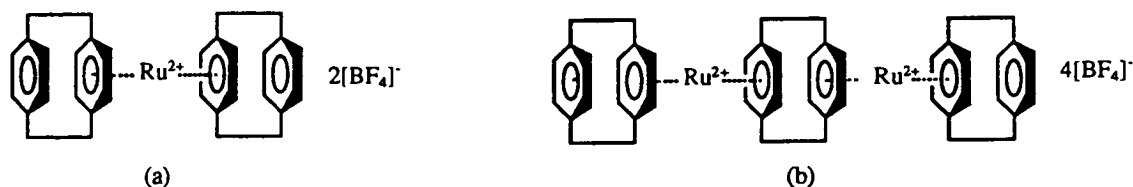

Figure 4.1.3vi: (a) [Ru(η^6-[2.2]paracyclophane)$_2$][BF$_4$]$_2$ and
(b)[Ru$_2$(η^6-[2.2]paracyclophane)$_3$][BF$_4$]$_4$.

In reduced *bis*(arene)ruthenium(0) complexes the ruthenium atom requires one less electron pair from the ligands, and this is achieved by one of the arenes adopting an η^4-bonding mode which results in it distorting to a boat-shaped geometry.[56] Similarly, for a series of (η^6-hexamethylbenzene)(η^6-[2n]cyclophane)ruthenium(II) complexes, it is found that the predominant factor influencing their reduction potential is the geometry of the cyclophane decks; the cyclophanes having boat-shaped decks (presumably well suited for η^4 complexation), being most readily reduced.[57] Thus, [Ru(η^6-C$_6$Me$_6$)(η^6-[2$_6$](1,2,3,4,5,6)cyclophane)]$^{2+}$ is the most difficult member of the series to reduce [E$_{1/2}$ (*vs.* SCE) = -0.95 V] since its extremely rigid framework does not allow distortion to provide a suitable η^4 geometry. On the other hand, free [2$_4$](1,2,4,5)cyclophane already has boat-shaped benzene decks which are well suited for η^4 bonding, and therefore [Ru(η^6-C$_6$Me$_6$)(η^6-[2$_4$](1,2,4,5)cyclophane)]$^{2+}$ is the most accessible member to reduction [E$_{1/2}$ = -0.50 V].[53] The analogous [2.2]paracyclophane-ruthenium(II) complex is also reduced quite readily [E$_{1/2}$ = -0.69 V]. Although free [2.2]paracyclophane has boat-shaped benzene decks, the prow and stern of these decks are directed away from the complexed ruthenium(II) ion and so do not seem to be well suited for η^4 bonding. However, an extensive ^{1}H NMR analysis suggests that the [2.2]paracyclophane does bond in an η^4 manner, with the geometry shown in Figure 4.1.3vii.[53] Although this geometry appears unusual, examination of molecular models suggests that it is easily attained by a simple twisting motion around the axes of the C(4)-C(5) and C(7)-C(8) bonds. These model experiments also suggest that simultaneous twisting of both benzene decks in this fashion would be exceedingly difficult, if not impossible, thus indicating that there would be a significant energy barrier for simultaneous η^4 bonding to ruthenium at each face of the [2.2]paracyclophane molecule. This is an important inference with respect to the properties

of oligomers of [2.2]paracyclophane-ruthenium complexes where the cyclophane ligand is bound to two ruthenium atoms.
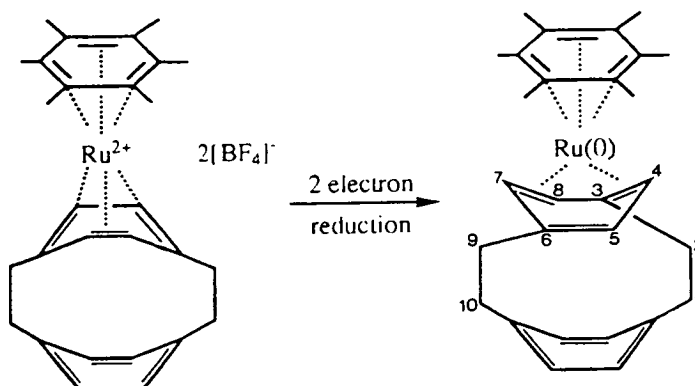

Figure 4.1.3vii: The geometry adopted by an η^4 coordinated [2.2]paracyclophane moiety.

The reduction of the *bis* and *tris* complexes shown in Figure 4.1.3vi (a) and (b) are somewhat more complicated, and the possibility of preparing and isolating a mixed-valence ion derived from the diruthenium complex is a topic still under investigation. However, the reduction of the [Ru$_2$(η^6-C$_6$Me$_6$)$_2$(η^6,η^6-[2$_4$](1,2,4,5)cyclophane)][BF$_4$]$_4$ complex and its [2.2]paracyclophane analogue to their corresponding dicationic ions and neutral species has been studied quite extensively, and results show that the two complexes behave quite differently.[58,59] The reduction of [Ru$_2$(η^6-C$_6$Me$_6$)$_2$(η^6,η^6-[2$_4$](1,2,4,5)cyclophane)]$^{4+}$ is illustrated in Scheme 4.1.3,[58] and a study of the dicationic ion shows it to be a mixed-valence ion (class II), exhibiting a net two-electron intervalence transfer. Although the ^{1}H and ^{13}C NMR spectra are symmetrical at room temperature, indicating the same environment for each of the two ruthenium atoms and thus a Ru(I)-Ru(I) system, cooling of these NMR solutions leads to a coalescence of signals, and below 228K the two ruthenium atoms have different environments indicating both a ruthenium(II) and a ruthenium(0) site. The interpretation of this behaviour is given by the equilibrium between (a) and (b) [see Scheme 4.1.3], and this system was the first example of a *net*, two-electron intervalence transfer in a discrete, mixed-valence organometallic complex.[58]

When this work is extended to the [2.2]paracyclophane diruthenium(II,II) complex,[59] the two-electron reduction of the tetracation leads to the corresponding dication which on examination of its ^{1}H and ^{13}C NMR spectra and X-ray photoelectron spectrum shows, in contrast to that just described, only one type of ruthenium ion environment. This corresponds to a Ru(II) site attached to a ligand which is a somewhat better electron donor than the benzene decks in the aforementioned dication. On the basis of the ^{1}H NMR
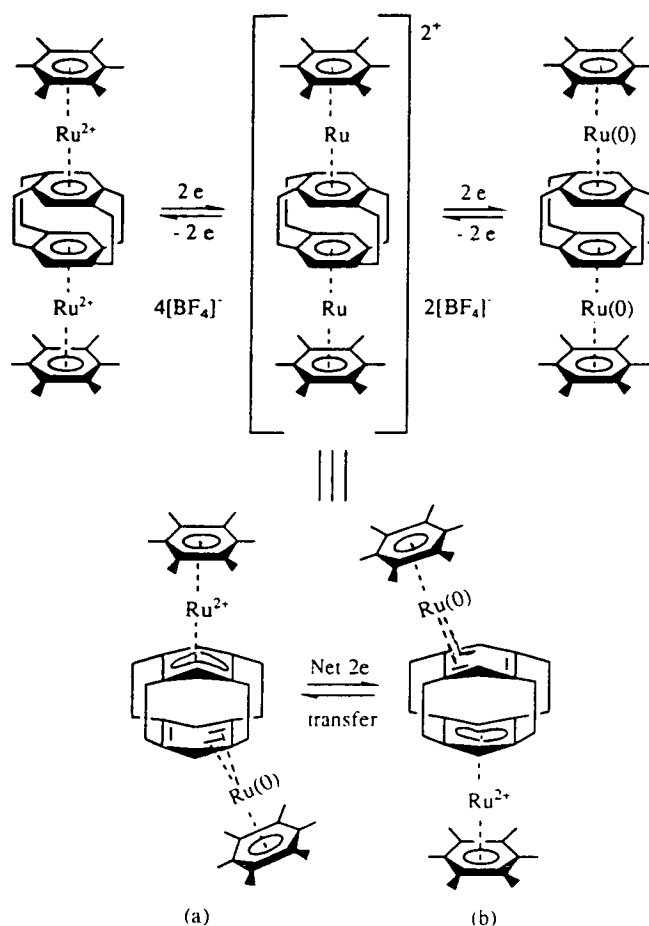
Scheme 4.1.3: The reduction of $[Ru_2(\eta^6\text{-}C_6Me_6)_2(\eta^6,\eta^6\text{-}[2_4](1,2,4,5)cyclophane)]$ $4[BF_4]$.

chemical shift pattern, the decks of the cyclophane ligand in this dication are assigned 'open' cyclohexadienyl anion structures. The chemical behaviour and NMR spectral properties of this dicationic diruthenium[2.2]paracyclophane complex strongly suggest that the complex is diamagnetic, and for this reason it is thought that a carbon-carbon bond connects the two cyclohexadienyl anion decks. This has been confirmed by a single crystal X-ray analysis,[59] which shows that the geometry of the cyclophane ligand is appreciably distorted from that of the free hydrocarbon.[18] The cyclohexadienyl-anion character is apparent and although the decks are still slightly boat-shaped, they are flattened and closer together than in [2.2]paracyclophane itself, with the C-C bond connecting the two decks being 1.96(3) Å; possibly the longest carbon-to-carbon bond length ever measured by X-ray diffraction analysis, (See Figure 4.1.3viii). The [2.2]meta- and the $[2_3](1,3,5)$-cyclophanes also undergo the same general reduction procedures. The short distance between the cyclohexadienyl anion decks and the strong interaction evident between the two ruthenium atoms in these molecules makes the possibility of preparing a stacked

metallocene polymer based on monomer units of this type an extremely attractive goal and the subject of on-going research.
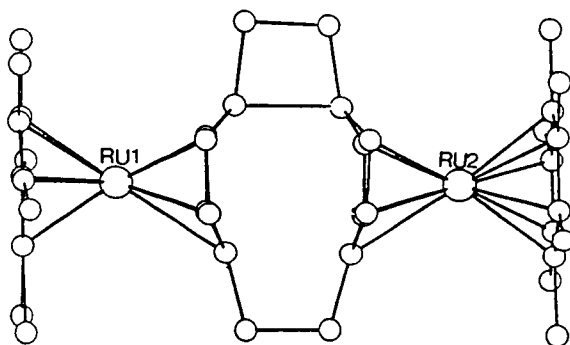
Figure 4.1.3viii: The molecular structure of [Ru$_2$(η^6-C$_6$Me$_6$)$_2$([2.2]paracyclophane)]$^{2+}$, showing that the cyclophane ligand now has two cyclohexadienyl anion decks connected by a carbon-carbon bond.

Other more recent developments in transition metal-cyclophane chemistry include the synthesis of a {Fe(CO)$_3$}$_2$(η^4-η^4-C$_{12}$H$_{12}$) complex, which represents a small cyclophane containing iron-stabilised anti-aromatic decks of cyclobutadiene.[60] This complex is again of interest as a potential precursor for polymers which have desirable electrical or magnetic properties [see Figure 4.1.3ix (a)]. Also the first typical metallaphanes, *i.e.* the 18, 20, and 22-membered diosma[7.7]cyclophanes, have been prepared,[61] and the incorporation of transition metal complex fragments into a cyclophane framework gives rise to new structural elements and reactive centres, and may form the basis for the synthesis of further cyclophanes [see Figure 4.1.3ix (b)].

(a) (b)
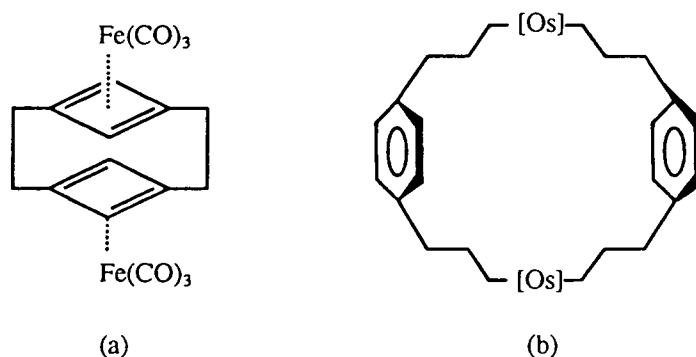
Figure 4.1.3ix: (a) {Fe(CO)$_3$}$_2$(η^4-η^4-C$_{12}$H$_{12}$) and (b) Diosma[7.7]paracyclophane.

126

This introduction has illustrated the multitude of different cyclophanes that now exist, due to progress in synthetic organic chemistry, and also the potential they have as π-acid ligands with their π-electron systems readily interacting with transition metal centres (notably with a reduction in internal strain energy). Since the discovery of ferrocene,[62] metal sandwich compounds have become the symbol of modern organometallic chemistry, and it is therefore surprising that an alternative series of polymetallic sandwich compounds has not gained the same attention. Owing to our current interest and knowledge of arene carbonyl clusters, cyclophanes were chosen as an alternative class of arene ligand for a number of reasons. Firstly, most of the chemistry outlined for a single transition metal fragment should be repeatable for a metal cluster and it is therefore of interest to see if an increase in the number of metal atoms coordinated to the cyclophane has any effect on its π-electron nature. Secondly, whilst in mononuclear arene complexes the simple η^6 bonding mode predominates, with clusters (as with surfaces) more elaborate multicentre coordination patterns are available,[63] and it is therefore intriguing to consider the potential structural diversity of the cyclophane as a bridging ligand. Lastly, as with the mononuclear complexes, the cyclophane ligand has the potential to link metal cluster units *via* the two arene decks, thereby forming, in the first instance, sandwich complexes, and eventually precursor sub-units for the first potential organometallic-cluster polymers.

These possibilities led to the following investigations concerning the reactions between $Ru_3(CO)_{12}$ and [2.2]paracyclophane. The ligand [2.2]paracyclophane was chosen owing mainly to its commercial availability, but also due to the abundance of information available in the literature for comparisons with our results.

4.2 The Reaction of $Ru_3(CO)_{12}$ with [2.2]paracyclophane

The first carbonyl clusters of ruthenium incorporating arene ligands [*viz.* $Ru_6C(CO)_{14}(\eta^6\text{-}C_6H_{6-n}Me_n)$, $n = 1,2,3$] were achieved by the thermolytic action of $Ru_3(CO)_{12}$ **14** in the appropriate arene solvent.[64] Since [2.2]paracyclophane is a solid at room temperature, with a relatively high melting point ($286°$), a direct reaction with $Ru_3(CO)_{12}$ **14** was undertaken by thermolysing with an excess of the ligand in octane. The reaction was maintained at vigorous reflux for a period of three hours, during which the colour of the reaction mixture darkened substantially, and both the infrared spectrum and spot t.l.c. indicated that a considerable change from the starting material had occurred. A range of products, with nuclearities ranging from three to eight, were isolated from the reaction mixture after chromatographic separation using a dichloromethane-hexane solution (3:7, v/v) as eluent. These products have been identified as $Ru_3(CO)_9(\mu_3\text{-}\eta^2\text{:}\eta^2\text{:}\eta^2\text{-}C_{16}H_{16})$ **23**,

$Ru_6C(CO)_{15}(\mu_3-\eta^1:\eta^2:\eta^2-C_{16}H_{16}-\mu_2-O)$ **24**, $Ru_6C(CO)_{14}(\mu_3-\eta^2:\eta^2:\eta^2-C_{16}H_{16})$ **25**, $Ru_6C(CO)_{11}(\mu_3-\eta^2:\eta^2:\eta^2-C_{16}H_{16})(\eta^6-C_{16}H_{16})$ **26**, and $Ru_8(\mu-H)_4(CO)_{18}(\eta^6-C_{16}H_{16})$ **27** (see Scheme 4.2). The distribution of products may be optimised by controlling the reaction time; a period of one hour yields mostly the trinuclear derivative **23**, whereas three hours yields mostly **25**, and as the time is lengthened beyond three hours, increased quantities of **26** and **27** are produced.
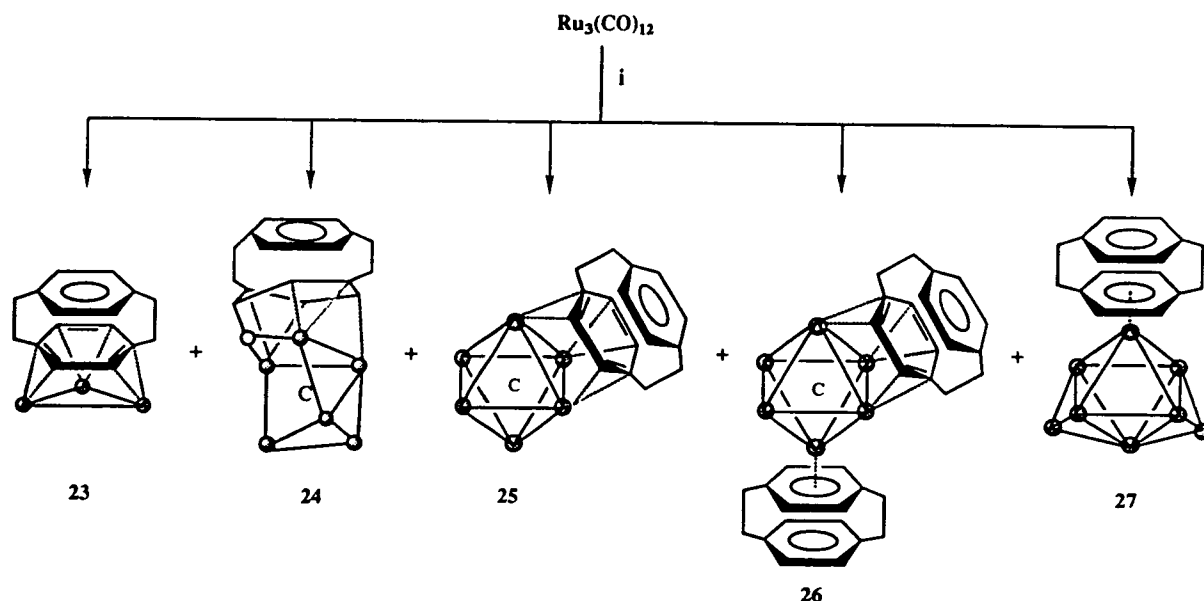
Scheme 4.2: The reaction of $Ru_3(CO)_{12}$ **14** with [2.2]paracyclophane; (i) Δ, octane/$C_{16}H_{16}$.

4.2.1 Characterisation of $Ru_3(CO)_9(\mu_3-\eta^2:\eta^2:\eta^2-C_{16}H_{16})$ 23

Complex **23** was initially identified as $Ru_3(CO)_9(\mu_3-\eta^2:\eta^2:\eta^2-C_{16}H_{16})$ from a comparison of its infrared spectrum with that observed for the benzene analogue, $Ru_3(CO)_9(\mu_3-\eta^2:\eta^2:\eta^2-C_6H_6)$, which has been fully characterised by X-ray crystallography.[65] The profile in the υ_{CO} region of **23** is virtually identical to that of the triruthenium μ_3 benzene cluster, the only difference being that the peaks in **23** occur at slightly lower wavenumbers. It is possible that this shift in υ_{CO} values may indicate a slight increase in the π-donor capabilities of the cyclophane when compared to benzene, however it may not be of any real significance. Further evidence for the molecular formula of **23** was provided by mass and ^1H NMR spectroscopy. The mass spectrum exhibits a strong parent peak at 763 (calc. 764) amu, together with peaks corresponding to the successive loss of nine CO groups. The ^1H NMR spectrum in $CDCl_3$ comprises of four signals, all with equal relative

intensity. Two singlet resonances are observed at δ 7.22 and δ 3.76 ppm which may be attributed to the four aromatic C-H protons of the unattached and coordinated rings, respectively. The frequency at which this latter resonance occurs is very low and indicative of a face-capping moiety [*cf.* aromatic proton shift in the ^{1}H NMR spectrum of $Ru_3(CO)_9(\mu_3-\eta^2:\eta^2:\eta^2-C_6H_6)$ which appears at δ 4.56 ppm]. The other two resonances, observed at δ 3.23 and 2.67 ppm, are multiplets showing typical AA'BB' couplings and may be associated with the bridging CH_2 protons. This ^{1}H NMR spectrum deserves further comment and is shown in Figure 4.2.1. There is excess [2.2]paracyclophane present in the sample which gives rise to two singlet resonances at δ 6.47 and 3.07 ppm, for the aromatic C-H and the bridge CH_2 protons, respectively. It is therefore evident that upon coordination to the metal cluster the aromatic C-H signal of the free ligand loses its degeneracy, with the proton resonance of the bound ring moving to a significantly lower
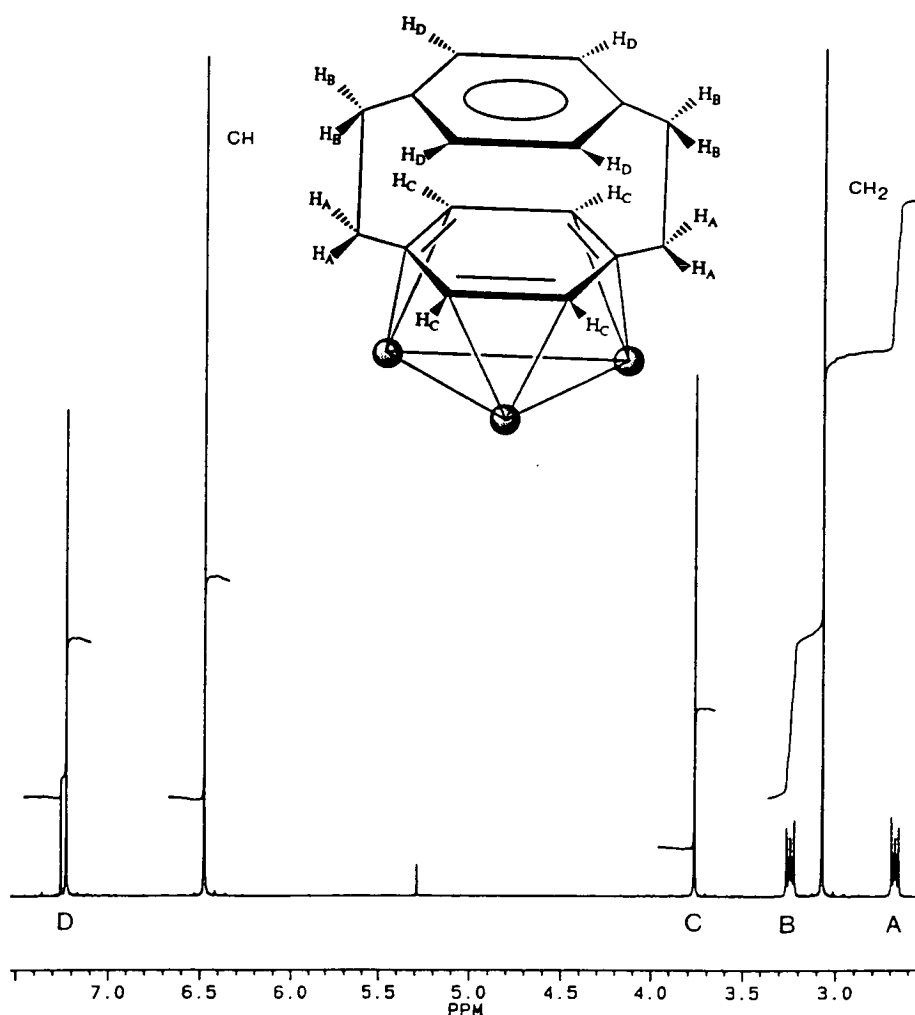
Figure 4.2.1: ^{1}H NMR of $Ru_3(CO)_9(\mu_3-\eta^2:\eta^2:\eta^2-C_{16}H_{16})$ 23, and the assignment of protons on the cyclophane moiety. The signals labelled CH and CH_2 at δ 6.47 and 3.07 ppm represent the aromatic C-H and bridge CH_2 protons of the free [2.2]paracyclophane ligand.

frequency and that of the unattached ring shifting in the opposite direction. This observation may be taken to indicate that when coordinated to one ring of the cyclophane moiety, the cluster unit exerts a transpacial electronic interaction on the other, uncoordinated ring, therefore emphasising the presence of a single π-electron system within cyclophane molecules of this type. This subject, and its relationship to NMR shifts will be discussed in more detail later in the chapter (see Section 4.6).

Since all attempts to grow crystals of **23** suitable for an X-ray diffraction study have been unsuccessful, further characterisation has been achieved using ^{13}C NMR spectroscopy. The ^{13}C NMR spectrum of **23**, in $CDCl_3$, is entirely consistent with a molecular formula of $Ru_3(CO)_9(\mu_3-\eta^2:\eta^2:\eta^2-C_{16}H_{16})$, and seven resonances are observed. A singlet resonance at δ 197.6 ppm may be attributed to the nine carbonyl groups of **23**; it indicates total fluxionality on the NMR timescale, and does not alter even on cooling to 183 K. This is followed by two signals from the unattached ring at δ 138.5 (quaternary C) and 132.1 ppm (C-H). The coordinated ring carbon signals occur at δ 76.0 and 54.7 ppm for the quaternary and C-H carbons, respectively, and lastly, the $-CH_2-CH_2-$ linkages give rise to two signals at δ 40.7 and 35.2 ppm, for the C-atoms neighbouring the bonded ring and furthest from this ring, respectively. These assignments were made with assistance from a C, H correlation spectrum.

All spectroscopic evidence leads to the assumption that $Ru_3(CO)_9(\mu_3-\eta^2:\eta^2:\eta^2-C_{16}H_{16})$ **23** is isostructural with the analogous benzene cluster, $Ru_3(CO)_9(\mu_3-\eta^2:\eta^2:\eta^2-C_6H_6)$. It is therefore considered that one ring of the cyclophane ligand straddles the triruthenium face with two carbon atoms interacting with each metal centre in a $\mu_3-\eta^2:\eta^2:\eta^2$ fashion, thus donating six electrons to the cluster framework. Each ruthenium atom also bears a tricarbonyl unit constituted of two equatorial and one axial CO ligand, and the proposed structure is consistent with the Effective Atomic Number (EAN) rule, having a total electron count of 48.

4.2.2 Characterisation of $Ru_6C(CO)_{15}(\mu_3-\eta^1:\eta^2:\eta^2-C_{16}H_{16}-\mu_2-O)$ 24

Compound **24** has been fully characterised in solution by ^1H and ^{13}C NMR studies, and in the solid phase by a single crystal X-ray diffraction analysis. The infrared spectrum shows typical terminal carbonyl stretches between 2085 and 1968 cm^{-1}, and a bridging CO stretch at 1866 cm^{-1}. Microanalysis is in reasonable agreement with a proposed molecular formula of $Ru_6C(CO)_{15}(\mu_3-\eta^1:\eta^2:\eta^2-C_{16}H_{16}-\mu_2-O)$ [Found (Calc.): C, 30.03 (30.43); H, 1.32 (1.28%)], as is the mass spectrum which exhibits a parent peak at 1262 (calc. 1263) amu, followed by the sequential loss of fifteen CO groups. The ^1H and ^{13}C NMR spectra of **24** are rather complicated and will be described after a discussion of the molecular structure. It is, however, worth noting at this stage that this spectroscopic technique indicates the

presence of two closely related isomers in solution, which are not revealed by either infrared or mass spectroscopy.

Crystals of **24**, suitable for single crystal X-ray analysis were grown from a toluene solution at -25°C. The molecular structure of **24** is illustrated in Figure 4.2.2i, together
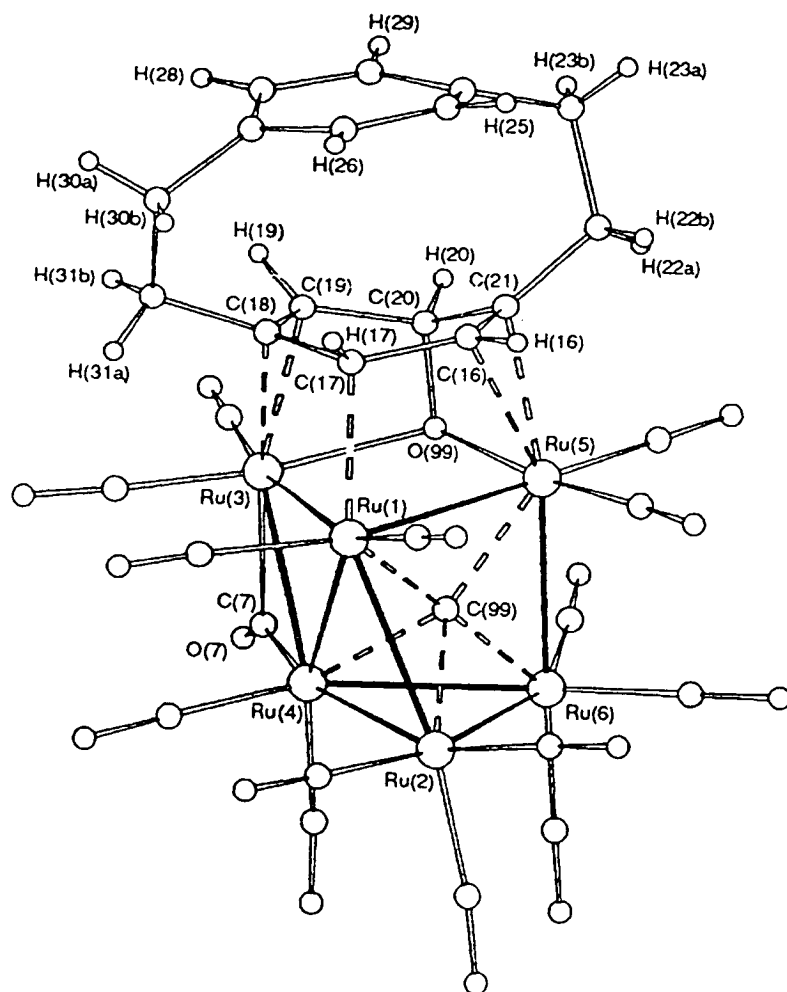
Figure 4.2.2i: The solid-state molecular structure of $Ru_6C(CO)_{15}(\mu_3\text{-}\eta^1\text{:}\eta^2\text{:}\eta^2\text{-}C_{16}H_{16}\text{-}\mu_2\text{-}O)$ **24**, showing the atomic labelling scheme; the C atoms of the CO groups bear the same numbering as the corresponding O atoms. Relevant bond distances (Å): Ru(1)-Ru(2) 2.868(3), Ru(1)-Ru(3) 2.913(3), Ru(1)-Ru(4) 2.817(3), Ru(1)-Ru(5) 2.847(3), Ru(2)-Ru(4) 2.707(3), Ru(2)-Ru(6) 2.864(3), Ru(3)-Ru(4) 2.782(3), Ru(4)-Ru(6) 2.933(3), Ru(5)-Ru(6) 2.846(3), Ru(1)-C 1.94(2), Ru(2)-C 2.17(2), Ru(4)-C 2.09(2), Ru(5)-C 2.04(2), Ru(6)-C 1.97(2), Ru(3)-O 2.14(2), Ru(5)-O 2.06(2), O-C(20) 1.40(3), Ru-C(7) mean 2.15(3), C(7)-O(7) 1.13(3), Ru-C(mean CO terminal) 1.90(3), C-O(mean CO terminal) 1.14(3), Ru(1)-C(17) 2.22(2), Ru(3)-C(18) 2.60(2), Ru(3)-C(19) 2.20(2), Ru(3)-C(20) 2.70(2), Ru(5)-C(16) 2.38(2), Ru(5)-C(20) 2.67(2), Ru(5)-C(21) 2.23(2), C(16)-C(17) 1.48(3), C(16)-C(21) 1.34(3), C(17)-C(18) 1.38(3), C(18)-C(19) 1.49(3), C(18)-C(31) 1.52(3), C(19)-C(20) 1.54(3), C(20)-C(21) 1.56(3), C(21)-C(22) 1.53(3), C(22)-C(23) 1.55(3), C(23)-C(24) 1.52(4), C(24)-C(25) 1.39(3), C(24)-C(29) 1.37(3), C(25)-C(26) 1.38(3), C(26)-C(27) 1.37(3), C(27)-C(28) 1.44(3), C(27)-C(30) 1.51(3), C(28)-C(29) 1.36(4), C(30)-C(31) 1.55(3).

with the atomic labelling scheme and relevant structural parameters. Compound **24** can be described as having an 'open' octahedral metal framework, with the reference structure being that of $Ru_6C(CO)_{17}$,[66] or of any face-capped derivative of this molecule, in particular $Ru_6C(CO)_{14}(\mu_3-\eta^2:\eta^2:\eta^2-C_{16}H_{16})$ **25** (*vide infra*). Three of the Ru-Ru edges are open when compared to a closed octahedral metal core, and the open edge between Ru(3) and Ru(5) is spanned by a bridging O-atom. The interstitial carbido-atom lies in the centre of a cavity formed by Ru atoms (1), (2), (4), (5) and (6), whereas Ru(3) is beyond that of a bonding interaction. There are a total of 15 CO ligands in this compound; Ru(2) and Ru(6) each carry three terminal CO's, the other basal atom, Ru(4), carries two terminal and one bridging carbonyl which asymmetrically spans the Ru(3)-Ru(4) edge, and the three metal atoms which interact with the paracyclophane moiety [Ru(1), Ru(3) and Ru(5)] carry two terminal CO's each, with Ru(3) also being involved in the aforementioned CO-bridge.

The interstitial carbido-atom sits in the middle of a bridged-butterfly sub-system defined by Ru(1) and Ru(6) (wing-tip atoms) and Ru(2) and Ru(4) (hinge atoms); the wing-tips being bridged by Ru(5). The distances between the carbido-atom and the wing-tip ruthenium atoms [1.94(2), 1.97(2) Å] are shorter than those from the bridging atom [Ru(5)-C 2.04(2) Å], and from the hinge atoms [2.09(2) and 2.17(2) Å]. Ru(3) is too far from the interstitial carbido-atom to interact [Ru(3)-C 3.11 Å].

The paracyclophane ligand interacts with three metal atoms of the cluster [Ru(1), Ru(3) and Ru(5)]. While the outer unattached C_6-ring, although severely distorted, clearly shows the presence of a delocalised bonding pattern, the coordinated ring can be regarded as comprising of a 1,3-diene unit. The two C=C double bonds are located between C(17) and C(18) [1.38(3) Å] and C(16) and C(21) [1.34(3) Å], however, these two unsaturated systems do not exhibit the same type of interaction with the cluster framework. C(16)-C(21) establishes a 'conventional' π-interaction by both C atoms being at a bonding distance from Ru(5) [Ru(5)-C(16) 2.38(2), Ru(5)-C(21) 2.23(2) Å], and the second short C=C bond, instead of eclipsing a Ru-atom, is *quasi*-parallel to the bond, with only one C-atom C(17) interacting with Ru(1) [Ru(1)-C(17) 2.22(2) Å]. A fourth interaction is between C(19) and Ru(3) [2.20(2) Å], and C(18) also interacts with Ru(3) but at a greater distance of 2.60(2) Å. The distribution of bond lengths and angles around the coordinated ring is in agreement with the assignment of an sp^3 hybridisation to atom C(20) which forms a σ-bond with the O-atom (*vide infra*). The other five atoms are each considered to have an sp^2 hybridisation. The paracyclophane moiety therefore contributes a total of five electrons to the cluster framework and can be represented more adequately with the delocalised π-allyl and π-ene type bonding shown in Figure 4.2.2ii.

The bridging O-atom is pyramidal; the C-O distance of 1.40(3) Å is in agreement with a C-O single bond, and the two Ru-O interactions differ slightly in length [Ru(3)-O 2.14(2), Ru(5)-O 2.06(2) Å] with an inner angle at the O-atom of 117.2(7)°. The O-atom is
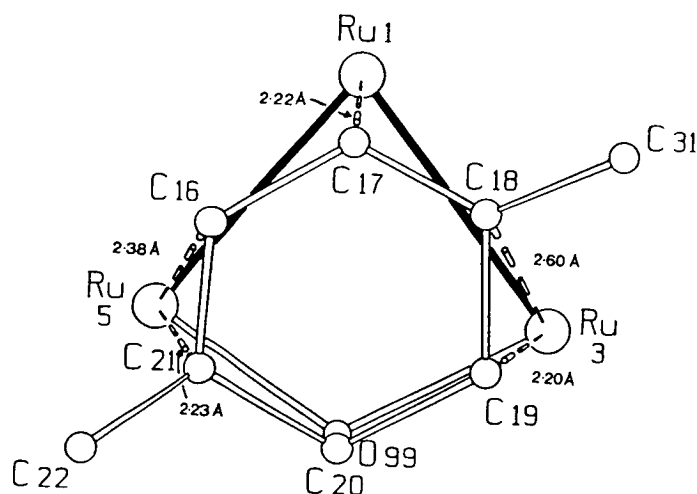
Figure 4.2.2ii: Projection of the bound paracyclophane ring over the three Ru atoms in **24**.

required to contribute three electrons to the cluster framework, leaving one 'unused' lone-pair, and giving **24** a total electron count of 90. Figure 4.2.2iii shows a space-filling representation of the structure of **24**, and it appears that the O-atom is deeply embedded within the ligand shell formed by the carbonyl ligands and the paracyclophane moiety. It is clear that the lone pair resident on the O-atom occupies the 'niche' in the ligand envelope and is therefore available on the cluster surface for electrophilic attack and further reaction.
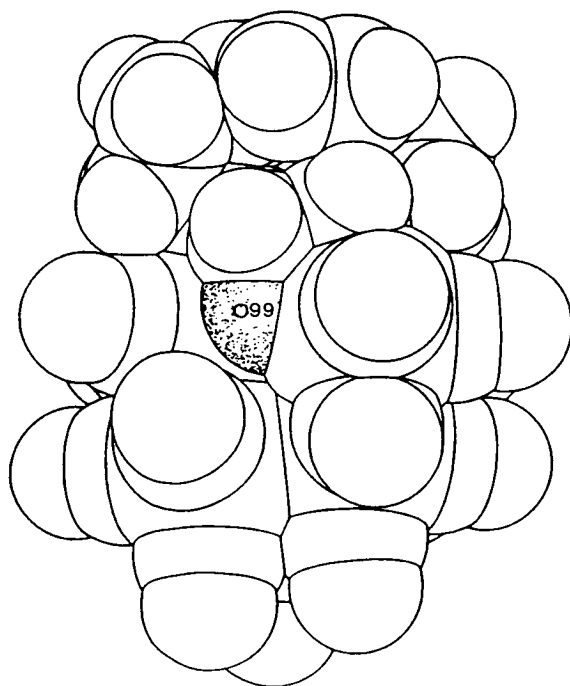
Figure 4.2.2iii: Space filling representation of the structure of **24** showing the O-atom embedded in the ligand envelope.

It is also interesting to observe how the two CO-ligands on both sides of the O-atom are repelled from the centre of the bridging system; this effect being similar to that observed for bridging H-atoms.

The situation described is reminiscent of the bonding found in $Ru_3(\mu\text{-}H)(CO)_9(\mu_3\text{-}\eta^1:\eta^2:\eta^2\text{-}C_6H_7)$, where the ligand lies nearly parallel to the metal triangle and contributes a total of five electrons to the cluster.[65a,67] In this latter case, however, the $CH\text{-}CH_2\text{-}CH$ portion of the cyclohexadienyl ligand spans the H(bridged) Ru-Ru bond, whereas in the present case the sp^3 C-atom interacts with the bridging O-atom.

The ^1H NMR spectrum of compound **24** is shown in Figure 4.2.2iv. It comprises of several multiplets which, for convenience, are labelled A-Q. Some of these resonances overlap, with three protons giving rise to the group of signals labelled D-F, two protons giving rise to signal B, and two giving rise to signal N/P. The spectrum is consistent with a [2.2]paracyclophane group asymmetrically bound to the metal cluster. Signal assignment has been achieved from a series of homonuclear decoupling and nOe experiments, using the premise that signal L corresponds to H(20) [the proton bound to the carbon atom on which the oxygen is attached], and that signals M-Q arise from the protons associated with the 'remote' non-bonded aromatic ring.
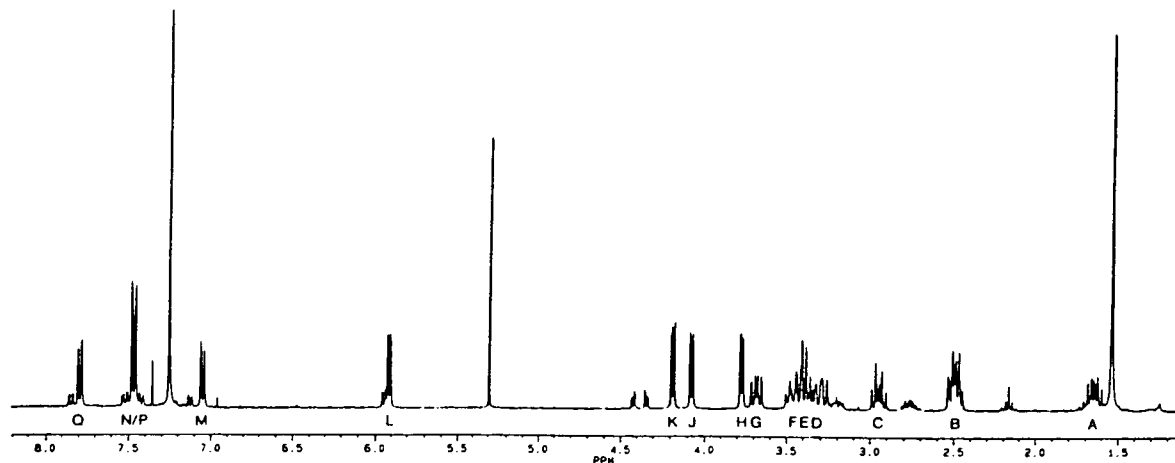
Figure 4.2.2iv: The ^1H NMR spectrum of **24**.

Decoupling of signal L results in the loss of a 6.2 Hz coupling from signal J, and a 2.1 Hz coupling from signal H. Hence J arises from H(19), with H(16) producing signal H, and it therefore follows that signal K arises from H(17); this has been confirmed from a decoupling experiment which links it to H(16). The signal labelled N/P has been shown to arise from two different protons by observing the effects of decoupling at both M and Q,

respectively; decoupling at either site causes one of the N/P pair to lose a 7.9 Hz coupling and the other to lose a 1.6 Hz coupling. Hence, M and Q do not couple with each other and are therefore *para* to each other on the aromatic ring.

The results of a series of nOe experiments performed on **24** are summarised in Table 4.2.2i, and show that interactions between protons on the two aromatic ring systems may also be detected; thus permitting a complete assignment of the spectrum. Saturation of signal H [H(16)] results in enhancements of A, K and N/P, allowing them to be assigned to protons H(22a), H(17) and H(25), respectively, and the saturation of K [H(17)] enhances signals G, H and M, confirming G as arising from H(31a), and M from H(26). It therefore follows that the assignments given in Table 4.2.2ii may be derived with confidence, and Figure 4.2.2v illustrates the corresponding H positions. In all cases, the nOe results are consistent with the proposed assignment.

Table 4.2.2i: Results of a series of nOe experiments performed on **24**, % enhancements are indicated.

Irradiation Site

	A	B	C	D	E	F	G	H	J	K	L	M	N/P	Q
A								4						
B	10.5			2			10.5		2		2			
C				18			4				5			
D			19											
E														2.5
F	1													
G			3							2				
H	7.5									11		2		
J											11			
K			2				6	13			4			
L									11					7.5
M			8							4				
N/P				3			6	3.5			5			5
Q											4			

Percentage Enhancement

The ^{1}H NMR spectrum of **24** also shows evidence for the presence of a second isomeric form; named **24a** for convenience. Isolation of this second isomer and spectroscopic analysis (infrared and mass spectroscopy) reveal that it is very similar to **24**, and suggest that it differs only in the interaction of the $C_{16}H_{16}O$ moiety with the Ru_6C cluster unit.

The ^{1}H NMR spectrum of this minor isomer, **24a**, is also very similar to that of **24**, and can be seen in Figure 4.2.2vi. Signal M is consistent with a proton attached to an oxygen-bearing carbon (*cf.* signal L from isomer **24**), and the signals N-R are consistent with those from an uncoordinated ring of a cyclophane moiety bound to a metal cluster. The

Table 4.2.2ii: Assignments of the ^{1}H NMR spectrum signals with regard to the
H positions in the solid-state structure.

H position	^{1}H signal	δ (^{1}H)	Multiplicity and J (H-H) (Hz)
H(16)	H	3.78	d,d; 5.8, 2.1
H(17)	K	4.18	d,d; 5.8, 1.6
H(19)	J	4.08	d,d; 6.2, 1.6
H(20)	L	5.91	d,d; 6.2, 2.1
H(22a)	A	1.64	d,d,d; 13.8, 9.7, 7.8
H(22b)	B	2.4 - 2.55	overlapping multiplet
H(23a)	F	3.2 - 3.5	overlapping multiplet
H(23b)	E	3.2 - 3.5	overlapping multiplet
H(25)	N/P	7.46	d,d; 7.9, 1.6
H(26)	M	7.05	d,d; 7.9, 1.6
H(28)	N/P	7.46	d,d; 7.9, 1.6
H(29)	Q	7.79	d,d; 7.9, 1.6
H(30a)	C	2.95	d,t; 13.6, 8.6
H(30b)	D	3.2 - 3.5	overlapping multiplet
H(31a)	G	3.68	d,d,d; 14.0, 8.8, 1.6
H(31b)	B	2.4 - 2.55	overlapping multiplet
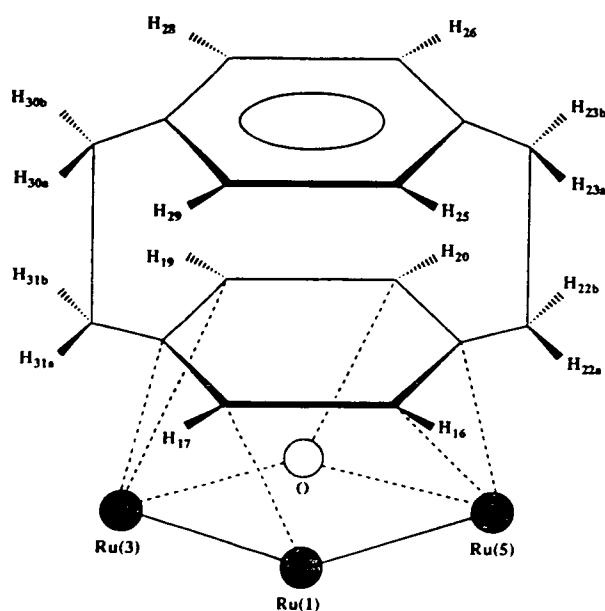
Figure 4.2.2v: Diagram showing the complexed paracyclophane ligand with appropriately labelled H's.

primary differences between the spectra of the two isomers lay in the δ values of the
protons associated with the bound aromatic ring. The assignments of the relevant protons in

136

24a were determined *via* the decoupling of signal M, and the comparative δ values are listed in Table 4.2.2iii, with the same numbering scheme used for **24a** as for **24**. The δ values corresponding to H(16) and H(19) indicate that these protons show the most difference between the two isomers.
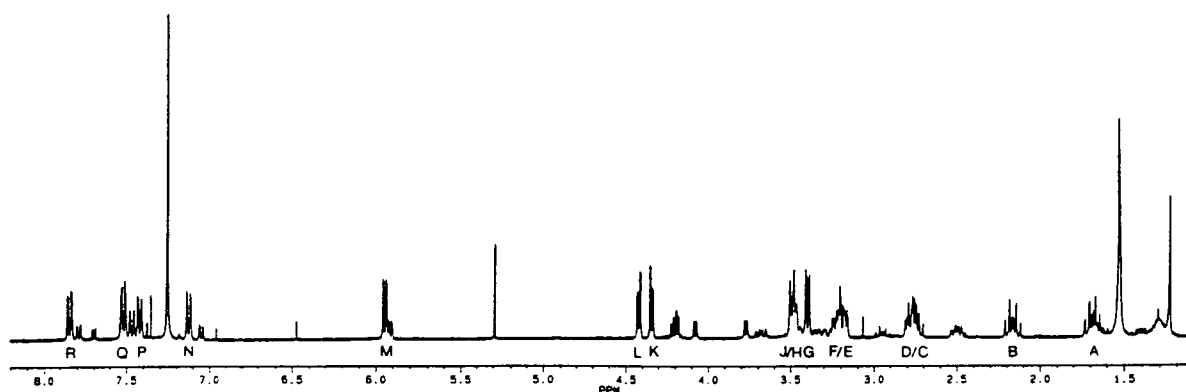
Figure 4.2.2vi: The ^{1}H NMR spectrum of **24a**.

Table 4.2.2iii: Comparative δ values for the ^{1}H signals of the coordinated aromatic rings in **24** and **24a**.

Assigned H position	δ (^{1}H) Isomer **24**	δ (^{1}H) Isomer **24a**
16	3.78	4.42
17	4.18	4.35
19	4.08	3.40
20	5.91	5.94

The relatively low yields of $Ru_6C(CO)_{15}(\mu_3-\eta^1:\eta^2:\eta^2-C_{16}H_{16}-\mu_2-O)$ **24** produced during the reaction, have prevented a detailed ^{13}C NMR study, and a C, H correlation spectrum has not been attained. A full assignment is therefore not possible, although a combination of the weak spectrum obtained and a DEPT pulse sequence has enabled the signals to be assigned as quaternary (q), CH or CH_2. Sixteen signals are observed between δ 138.2 and 21.6 ppm, as would be expected for the sixteen inequivalent carbon atoms of the paracyclophane ligand, with those corresponding to the upper, uncoordinated ring being at higher frequency [δ 138.2(q), 136.9(q), 133.8(CH), 133.6(CH), 133.4(CH), 130.1(CH) ppm] than those of the lower, bound ring [δ 109.2(q), 88.3(CH), 74.4(CH), 65.1(q), 47.4(CH), 21.6(CH) ppm]. Since the signals for the two quaternary carbons of the lower ring appear at very different frequencies, it is safe to assume that the resonance at

δ 109.2 ppm corresponds to C(18), which sits at a distance of 2.60(2) Å from Ru(3), while that at δ 65.1 ppm is associated with C(21), which has a far stronger interaction with a metal centre [C(21)-Ru(5) 2.23(2) Å]. Resonances corresponding to the four bridging (CH$_2$) carbons are found at δ 39.8, 35.8, 34.6 and 34.3 ppm, and a number of carbonyl signals with a low frequency to noise ratio are observed between δ 210 and 185 ppm. The ^{13}C NMR also shows evidence for the second isomer **24a**, although no precise details are available due to the poor quality of the spectrum.

4.2.3 Characterisation of Ru$_6$C(CO)$_{14}$(μ_3-η^2:η^2:η^2-C$_{16}$H$_{16}$) 25

Compound **25** is not immediately identifiable from a comparison of its infrared spectrum with those of other *mono*(arene) derivatives based on the hexaruthenium cluster system, *viz.* Ru$_6$C(CO)$_{14}$(η^6-arene) (arene = C$_6$H$_{6-n}$Me$_n$, n = 0,1,2,3),[64,68] although the wavenumbers of the strongest absorptions are compatible. The mass spectrum clearly corresponds to the formulation Ru$_6$C(CO)$_{14}$(C$_{16}$H$_{16}$), with a parent peak exhibited at 1219 (calc. 1219) amu, followed by the loss of several carbonyl groups in succession, and it would therefore appear that the paracyclophane group is present in **25**, although not attached to the cluster unit in the usual η^6 coordination mode found in this system. This feature is also apparent from the ^{1}H NMR spectrum, which is very similar to that described for Ru$_3$(CO)$_9$(μ_3-η^2:η^2:η^2-C$_{16}$H$_{16}$) **23**. Two singlet resonances are observed at δ values of 7.44 and 3.40 ppm, which arise from the aromatic protons of the unattached and coordinated rings, respectively, and two multiplet resonances corresponding to the CH$_2$ bridge protons occur at δ 3.43 and 2.98 ppm; all four signals having equal relative intensity. The value of δ 3.40 ppm for the coordinated ring protons is exceedingly low and is indicative of the ligand adopting a facial (μ_3-η^2:η^2:η^2) coordination mode. It is also worthy to note that the difference between the signals for the uncoordinated and bound ring protons in this hexaruthenium cluster is greater than that observed in the trinuclear complex Ru$_3$(CO)$_9$(μ_3-η^2:η^2:η^2-C$_{16}$H$_{16}$) **23** [4.04 *vs.* 3.46 ppm], and this behaviour may result from an increase in the electron withdrawing ability of the cluster as its nuclearity is increased. A similar concept was introduced in Chapter three, and will be considered in more detail later in the chapter.

In order to fully establish the molecular structure of **25** and thus confirm the facial coordination mode of the paracyclophane moiety, a single crystal X-ray diffraction study was undertaken using a crystal grown from a dichloromethane-hexane solution by slow evaporation at room temperature. The structure is shown in Figure 4.2.3, together with some relevant bond distances and angles.

Complex **25** is based upon an octahedral framework of ruthenium atoms encapsulating a central C(carbido) atom. The metal-metal bond lengths range from 2.794(1) to 2.990(1) Å; the shortest bond corresponding to the edge bridged by the μ_2-CO ligand
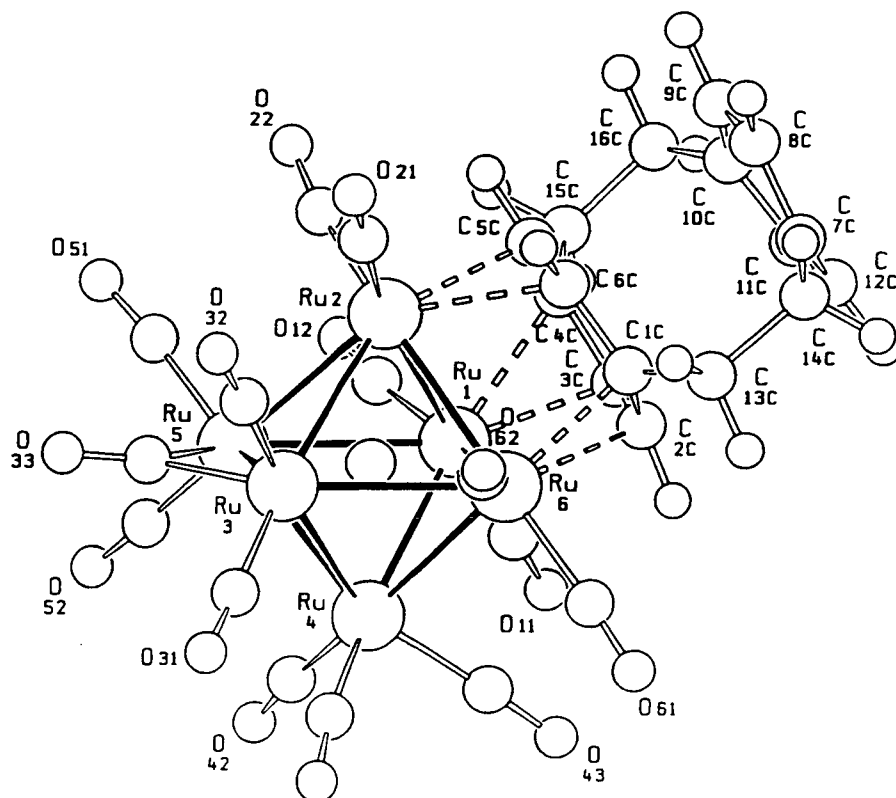
Figure 4.2.3: The solid-state molecular structure of $Ru_6C(CO)_{14}(\mu_3\text{-}\eta^2\text{:}\eta^2\text{:}\eta^2\text{-}C_{16}H_{16})$ **25**, showing the atomic labelling scheme; the C atoms of the CO groups bear the same numbering as the corresponding O atoms. Relevant bond distances (Å) and angles (°): Ru(1)-Ru(2) 2.819(1), Ru(1)-Ru(4) 2.832(1), Ru(1)-Ru(5) 2.981(1), Ru(1)-Ru(6) 2.933(1), Ru(2)-Ru(3) 2.945(1), Ru(2)-Ru(5) 2.922(1), Ru(2)-Ru(6) 2.863(1), Ru(3)-Ru(4) 2.990(1), Ru(3)-Ru(5) 2.794(1), Ru(3)-Ru(6) 2.935(1), Ru(4)-Ru(5) 2.938(1), Ru(4)-Ru(6) 2.869(1), Ru(1)-C 2.039(8), Ru(2)-C 2.001(8), Ru(3)-C 2.080(8), Ru(4)-C 2.070(8), Ru(5)-C 2.068(8), Ru(6)-C 2.050(8), Ru(3)-C(33) 2.056(9), Ru(5)-C(33) 2.054(9), C(33)-O(33) 1.167(12), Ru(1)-C(3C) 2.205(9), Ru(1)-C(4C) 2.359(9), Ru(2)-C(5C) 2.212(9), Ru(2)-C(6C) 2.375(9), Ru(6)-C(2C) 2.365(8), Ru(6)-C(1C) 2.195(9), C(1C)-C(2C) 1.44(1), C(2C)-C(3C) 1.43(1), C(3C)-C(4C) 1.40(1), C(4C)-C(5C) 1.45(1), C(5C)-C(6C) 1.46(1), C(1C)-C(6C) 1.42(1), C(1C)-C(13C) 1.44(1), C(13C)-C(14C) 1.58(1), C(4C)-C(15C) 1.53(1), C(15C)-C(16C) 1.58(1), C(10C)-C(16C) 1.51(1), C(14C)-C(7C) 1.48(1), C(7C)-C(8C) 1.40(1), C(8C)-C(9C) 1.40(1), C(9C)-C(10C) 1.39(1), C(10C)-C(11C) 1.37(1), C(11C)-C(12C) 1.42(1), C(12C)-C(7C) 1.41(1), C(1C)-C(13C)-C(14C) 114.7(8), C(4C)-C(15C)-C(16C) 115.9(8), C(7C)-C(14C)-C(13C) 113.6(8), C(15C)-C(16C)-C(10C) 111.4.

[Ru(3)-Ru(5)]. The [2.2]paracyclophane ligand has replaced three carbonyl groups, with respect to the reference molecule $Ru_6C(CO)_{17}$,[66] and one of its C_6 rings adopts a μ_3-η^2:η^2:η^2 bonding configuration. This coordination mode is similar to that of benzene in $Ru_3(CO)_9(\mu_3\text{-}\eta^2\text{:}\eta^2\text{:}\eta^2\text{-}C_6H_6)$,[65] although in **25** the mid-points of alternating C-C bonds around the ring do not eclipse the Ru atoms exactly; instead they are slightly staggered, as reflected by the alternating 'long' and 'short' Ru-C(ring) bond distances [mean 2.366(9) *vs.* 2.204(9) Å] observed in the molecule. Alternation of the ring carbon-carbon bonds is

also generally observed in face-capping benzene ligands, with 'long' and 'short' bonds lying between and directly above the Ru atoms, respectively, however, this pattern is not observed in **25** either, and the C-C bonds in the coordinated ring range between 1.40(1) and 1.46(1) Å with no clear pattern. The interaction of the cyclophane moiety with three metal atoms causes the coordinated ring to flatten somewhat and become more planar, whereas the uncoordinated ring maintains the boat-shaped geometry present in the free ligand.[18] The distance between the four coplanar atoms of the unattached ring and the least squares plane of the coordinated ring has been measured as 3.00 Å, which is slightly less than that observed in the free ligand (3.09 Å), suggesting that the cofacial repulsion between the two rings is reduced upon coordination to the electron withdrawing cluster unit. The strain in the molecule is, however, still detectable with the $C(ring)-CH_2-CH_2$ sp^3 angles [111.4(8)-115.9(8)°] being greater than 109°. These values are comparable with those of free paracyclophane (113.7°), although the angles involving the face-capping ligand are slightly larger on average than those involving the unattached ring [115.3(8) *vs.* 112.5(8)]. The CO ligand distribution in **25** is reminiscent of that observed for most arene derivatives of this family, *i.e.* with one bridging carbonyl group lying opposite to the triruthenium face involved in the interaction with the capping ligand. The remaining thirteen CO ligands range from being semi-bridging to essentially linear and are distributed with Ru(4), the only octahedral vertex not involved in either cyclophane coordination or the CO bridge, carrying three carbonyls, and the remaining five metal atoms carrying two carbonyl ligands each. The structure is consistent with the Polyhedral Skeletal Electron Pair Theory (PSEPT) of electron counting for a hexanuclear cluster,[69] having a total of 86 valence electrons.

$Ru_6C(CO)_{14}(\mu_3-\eta^2:\eta^2:\eta^2-C_{16}H_{16})$ **25** provides the first example of a *mono*(arene)-substituted derivative of $Ru_6C(CO)_{17}$ in which the arene is observed in a $\mu_3-\eta^2:\eta^2:\eta^2$ coordination mode. In fact, in all other face-capped arene derivatives previously characterised, namely $Ru_6C(CO)_{11}(\eta^6-arene)(\mu_3-\eta^2:\eta^2:\eta^2-C_6H_6)$ [arene = C_6H_6, C_6H_5Me or $C_6H_4Me_2$-1,3] and $Ru_6C(CO)_{11}(\eta^6-C_6H_5Me)(\mu_3-\eta^2:\eta^2:\eta^2-C_6H_5Me)$, face-capping only occurs in the presence of an η^6 bonded arene.[70] Although the specific factors which govern the bonding modes adopted by arenes on the cluster surface are still a long way from being fully understood, a possible reason for the unusual behaviour observed in **25** is that paracyclophane contains non-planar benzene rings. Independent of the type and degree of deformation, the overlap of the six p-orbitals in a non-planar ring cannot be as effective as in benzene itself, and this is thought to be why the distinct chemical property of cyclophanes is their ability to participate in the normally strongly disfavoured addition reactions; this behaviour being termed cyclohexatrienoid.[4] As aforementioned, the facial coordination of benzene in $Ru_3(CO)_9(\mu_3-\eta^2:\eta^2:\eta^2-C_6H_6)$ results in an alternation of bond

lengths around the C_6 ring. This apparent bond localisation represents a Kekulé-type distortion of the ring towards the hypothetical cyclohexatriene. Since free paracyclophane appears to be more olefinic in nature than, for example, benzene, a smaller rehybridisation within the ring would be required upon coordination, and it is possible that the π-orbitals are directed outwards slightly so that the appropriate overlap with the orbitals from a single metal atom in a cluster are less efficient than over a trimetal face, [it should be noted, however, that paracyclophane can also bond to a metal cluster in a terminal fashion (*vide infra*)]. It has also been observed that the driving force for many cyclophane reactions is a reduction in the internal strain energy caused from the π-electron repulsion between the two cofacial benzene rings. ^{1}H NMR studies indicate that interaction with a trimetallic face results in a greater removal of π-electron density from a coordinated arene than when bonded to a single metal atom. Therefore coordination of the [2.2]paracyclophane moiety in a facial manner should reduce the cofacial repulsion between the rings to a larger extent than when bonded in a terminal manner and, hence, result in a lower strain energy in the resulting complex. These factors, as well as the cyclophanes ability to act as a single π-electron system thereby allowing the enhanced electronic effects of the trimetallic unit to be felt by the uncoordinated ring as well as the bound ring, may account for the tendency of [2.2]paracyclophane to adopt a facial coordination site in this hexaruthenium system.

All attempts to affect the motion of this ligand to an η^6 site, a common phenomenon for facially-bound arenes,[71] have been unsuccessful, and the photolysis or thermolysis of **25** in solvents such as octane, heptane or hexane result only in the recovery of the starting compound and inextractable decomposition material.

4.2.4 Characterisation of $Ru_6C(CO)_{11}(\mu_3\text{-}\eta^2\!:\!\eta^2\!:\!\eta^2\text{-}C_{16}H_{16})(\eta^6\text{-}C_{16}H_{16})$ 26

The infrared spectrum (υ_{co}) of compound **26** is very similar to that of the *bis*(benzene) cluster, $Ru_6C(CO)_{11}(\eta^6\text{-}C_6H_6)(\mu_3\text{-}\eta^2\!:\!\eta^2\!:\!\eta^2\text{-}C_6H_6)$.[70a] The profiles of the two spectra are virtually identical, with the only difference being a shift of the main bands by about 6 cm^{-1} to lower wavenumbers for **26**; a feature that was earlier observed for $Ru_3(CO)_9(\mu_3\text{-}\eta^2\!:\!\eta^2\!:\!\eta^2\text{-}C_6H_6)$ **23**. Since $Ru_6C(CO)_{11}(\eta^6\text{-}C_6H_6)(\mu_3\text{-}\eta^2\!:\!\eta^2\!:\!\eta^2\text{-}C_6H_6)$ contains one terminal and one face-capping benzene moiety, an analogous bonding scheme can be predicted for **26**, *viz.* $Ru_6C(CO)_{11}(\eta^6\text{-}C_{16}H_{16})(\mu_3\text{-}\eta^2\!:\!\eta^2\!:\!\eta^2\text{-}C_{16}H_{16})$. The mass spectrum is in agreement with such a formulation, with a parent peak observed at 1344 (calc. 1343) amu. The ^{1}H NMR spectrum of this compound has not been recorded due to the poor solubility of crystalline material required for a clean spectrum, however, a single crystal X-ray structural analysis has been carried out using a crystal grown from the slow evaporation

141

of a dichloromethane-hexane solution at room temperature, and confirms the formulation proposed by infrared spectroscopic 'finger-printing'.

The molecular structure of **26** is depicted in Figure 4.2.4, together with some principal bond lengths. It is reminiscent of the structure of the *bis*(benzene) derivative,
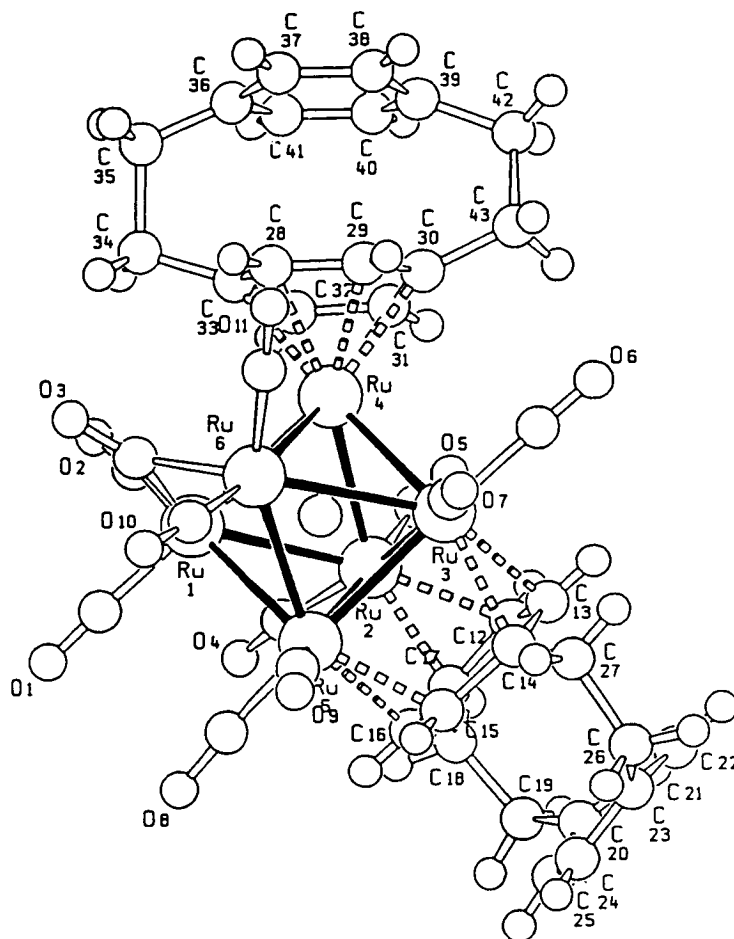

Figure 4.2.4: The solid-state molecular structure of $Ru_6C(CO)_{11}(\eta^6\text{-}C_{16}H_{16})(\mu_3\text{-}\eta^2:\eta^2:\eta^2\text{-}C_{16}H_{16})$ **26**, showing the atomic labelling scheme; the C atoms of the CO groups bear the same numbering as the corresponding O atoms. Relevant bond distances (Å): Ru(1)-Ru(2) 2.884(2), Ru(1)-Ru(4) 2.853(2), Ru(1)-Ru(5) 2.957(2), Ru(1)-Ru(6) 2.827(2), Ru(2)-Ru(3) 2.909(2), Ru(2)-Ru(4) 2.908(2), Ru(2)-Ru(5) 2.857(2), Ru(3)-Ru(4) 2.847(2), Ru(3)-Ru(5) 2.835(2), Ru(3)-Ru(6) 3.045(2), Ru(4)-Ru(6) 2.879(2), Ru(5)-Ru(6) 2.871(2), Ru(1)-C 2.08(2), Ru(2)-C 2.05(2), Ru(3)-C 2.04(2), Ru(4)-C 1.93(2), Ru(5)-C 2.08(2), Ru(6)-C 2.09(2), Ru-C(mean CO) 1.89(2), C-O(mean) 1.14(2), Ru(1)-C(3) 2.07(2), Ru(6)-C(3) 2.09(2), C(3)-O(3) 1.14(2), Ru(2)-C(12) 2.33(2), Ru(2)-C(17) 2.20(2), Ru(3)-C(13) 2.26(2), Ru(3)-C(14) 2.34(2), Ru(5)-C(15) 2.23(2), Ru(5)-C(16) 2.34(2), C(12)-C(13) 1.42(2), C(12)-C(17) 1.43(2), C(13)-C(14) 1.43(2), C(14)-C(15) 1.49(2), C(14)-C(27) 1.53(3), C(15)-C(16) 1.41(3), C(16)-C(17) 1.49(2), C(17)-C(18) 1.54(2), C(18)-C(19) 1.56(3), C(19)-C(20) 1.55(3), C(20)-C(21) 1.37(3), C(20)-C(25) 1.33(3), C(21)-C(22) 1.36(3), C(22)-C(23) 1.43(3), C(23)-C(24) 1.37(3), C(23)-C(26) 1.49(3), C(24)-C(25) 1.37(3), C(26)-C(27) 1.57(3), Ru(4)-C(28) 2.22(2), Ru(4)-C(29) 2.20(2), Ru(4)-C(30) 2.38(2), Ru(4)-C(31) 2.22(2), Ru(4)-C(32) 2.22(2), Ru(4)-C(33) 2.39(2), C(28)-C(29) 1.40(2), C(28)-C(33) 1.45(3), C(29)-C(30) 1.43(2), C(30)-C(31) 1.37(3), C(30)-C(43) 1.55(2), C(31)-C(32) 1.41(3), C(32)-C(33) 1.41(3), C(33)-C(34) 1.51(3), C(34)-C(35) 1.64(3), C(35)-C(36) 1.48(3), C(36)-C(37) 1.37(3), C(36)-C(41) 1.33(3), C(37)-C(38) 1.42(3), C(38)-C(39) 1.32(3), C(39)-C(40) 1.35(3), C(39)-C(42) 1.59(3), C(40)-C(41) 1.38(3), C(42)-C(43) 1.57(3).

$Ru_6C(CO)_{11}(\eta^6\text{-}C_6H_6)(\mu_3\text{-}\eta^2:\eta^2:\eta^2\text{-}C_6H_6)$, in that one paracyclophane ligand is apically bound while the second caps a triangular face as in $Ru_6C(CO)_{14}(\mu_3\text{-}\eta^2:\eta^2:\eta^2\text{-}C_6H_6)$ **25**. As with **25**, the metal core, comprises of an octahedral array of ruthenium atoms encapsulating a C(carbido) atom. The metal-metal bond lengths range from 2.827(2) to 3.045(2) Å; the shortest bond, again, corresponding to the edge carrying the bridging CO ligand [Ru(1)-Ru(6)]. The C(carbido) atom roughly occupies the centre of the octahedral cavity, although a slight carbide 'drift' towards the Ru atom bearing the apical ligand is observed [Ru(4)-C 1.93(2) Å *vs.* the range 2.04(2)-2.09(2) Å for the other five Ru-C distances]. This effect is invariably observed when an apical tricarbonyl unit is substituted by an apical arene, which is a poorer π-acceptor ligand. The 'free' ring in both paracyclophane moieties keeps the boat-shaped geometry found in the free ligand, and this geometry is also retained in the bound ring of the apically coordinated ligand, thus giving rise to two 'long' and four 'short' Ru-C(ring) interactions [Ru(4)-C(30) 2.38(2), Ru(4)-C(33) 2.39(2) Å *vs.* an average of 2.22(2) Å for the remaining four Ru-C bond distances]. As with **25**, the bound ring of the facially coordinated ligand tends to be more planar, with alternating 'long' and 'short' Ru-C(ring) bonds [mean 2.34(2) *vs.* 2.23(2) Å] again indicating that the mid-points of alternate C-C bonds around the ring are not truly eclipsed with respect to the underlying ruthenium atoms [as is seen in $Ru_6C(CO)_{11}(\eta^6\text{-}C_6H_6)(\mu_3\text{-}\eta^2:\eta^2:\eta^2\text{-}C_6H_6)$]. The mean C-C bond lengths for the η^6 and μ_3 coordinated rings [1.41(3) and 1.45(3) Å, respectively] are both slightly longer than in free paracyclophane [1.385 Å], whereas those for the unattached rings are both slightly shorter [1.36(3) and 1.37(3) Å, respectively] and, as with **25**, no C-C bond length alternation is observed within the face-capping ring. Of the eleven CO ligands, one bridges the Ru-Ru edge opposite the face involved in the interaction with the face-capping ligand [Ru(1)-Ru(6)], and the other ten are essentially linear and distributed evenly amongst the five metal atoms not involved in coordination with the apical cyclophane ligand. $Ru_6C(CO)_{11}(\eta^6\text{-}C_{16}H_{16})(\mu_3\text{-}\eta^2:\eta^2:\eta^2\text{-}C_{16}H_{16})$ **26** has a total electron count of 86, which, like **25**, is in accordance with PSEPT.

4.2.5 Characterisation of $Ru_8(\mu\text{-}H)_4(CO)_{18}(\eta^6\text{-}C_{16}H_{16})$ 27

The identification of compound **27** as $Ru_8(\mu\text{-}H)_4(CO)_{18}(\eta^6\text{-}C_{16}H_{16})$ was based, initially, on a comparison of its infrared spectrum with that of the benzene analogue, $Ru_8(\mu\text{-}H)_4(CO)_{18}(\eta^6\text{-}C_6H_6)$ **22**. The two spectra are very similar, with the profile of the CO stretches being almost identical and those belonging to **27** occurring at slightly lower wavenumbers; a feature that appears to be quite general for all paracyclophane derivatives discussed so far. The mass spectrum of **27** shows a molecular ion peak at 1524 (calc. 1525) amu, followed by peaks corresponding to the sequential loss of several carbonyl ligands. The ^1H NMR spectrum of **27** exhibits six resonances at δ 6.78, 4.51, 3.18, 2.85, -17.80 and -19.40 ppm, with relative intensities of 2:2:2:2:1:1, respectively. The signals at

δ 6.78 and 4.51 ppm are singlet resonances and correspond to the ring protons of the unattached and coordinated rings, respectively. These resonances again arise either side of the degenerate aromatic ring proton signal found in the spectrum of the free ligand [δ 6.47 ppm], however, the difference between signals [2.27 ppm] is not as great as that observed when the ligand is coordinated facially. The resonance assigned to the coordinated ring protons appears at a remarkably low frequency for an arene in a terminal bonding mode [δ 4.51 ppm], and as for $Ru_8(\mu\text{-}H)_4(CO)_{18}(\eta^6\text{-}C_6H_6)$ **22**, this is thought to reflect an increase in the π-accepting capability of the cluster unit as its nuclearity is increased. The multiple resonances at δ 3.18 and 2.85 ppm may be attributed to the protons in the $-CH_2CH_2-$ linkages; the former resulting from those neighbouring the unbound ring, and the latter from those nearest to the coordinated ring, and the two signals at low frequency [δ -17.80 and -19.40 ppm] are singlet resonances corresponding to the four hydridic protons.

The solid-state structure of **27** has been established by X-ray diffraction methods using a crystal grown from toluene at -25°C, and is shown in Figure 4.2.5i accompanied by relevant structural parameters.

The molecular structure of **27** shares the same fundamental structural features that were found in its benzene analogue, $Ru_8(\mu\text{-}H)_4(CO)_{18}(\eta^6\text{-}C_6H_6)$ **22** (see Chapter three). The octaruthenium cluster can be described as an octahedron capped by two additional metal atoms on two triangular faces sharing a common vertex, *i.e.* the metal atom framework is a *cis*-bicapped octahedron. The Ru-Ru bond distances range from 2.748(3) to 3.059(3) Å, and the paracyclophane moiety is η^6 bound to the only octahedron vertex not involved in bonding with the two capping ruthenium atoms [Ru(5)]. Sixteen out of the eighteen carbonyl ligands are terminally bound; with three on each capping ruthenium atom and two on each ruthenium atom of the octahedron except that involved in coordination with the cyclophane ligand. The other two carbonyls form symmetrical bridging interactions which span the two opposite Ru edges that connect the capped triangles. The boat-shaped geometry of free paracyclophane is maintained upon η^6 coordination to the cluster unit, as illustrated in the pattern of Ru-C(ring) bond lengths; the Ru(5)-C(21) and Ru(5)-C(24) bond lengths of 2.40(2) and 2.37(2) Å, respectively, are longer than the remaining four distances which range from 2.20(1) to 2.27(2) Å. Two out of the four hydride ligands have been located experimentally, showing that H(3) bridges the Ru(1)-Ru(7) edge, while H(1) is μ_3 bound to the Ru(1)-Ru(2)-Ru(3) triangular face of the octahedron. A graphical examination of the outer cluster surface, and potential energy calculations using the program XHYDEX,[72] have suggested suitable positions for the remaining two hydride atoms; H(2) triply bridges the opposite triangular face with respect to H(1) *i.e.* Ru(1)-Ru(4)-Ru(6), while H(4) is likely to be located on the Ru(3)-Ru(4)-Ru(5) metal triangle. The hydride distribution on the metal frame is consistent with the
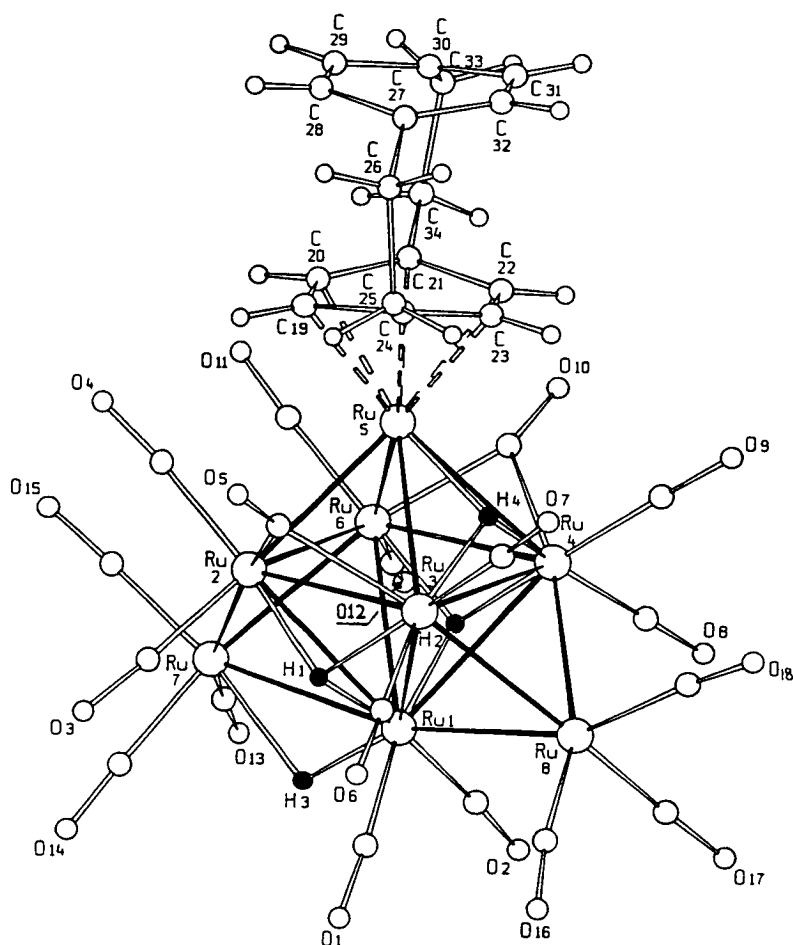
Figure 4.2.5i: The solid-state molecular structure of $Ru_8(\mu\text{-}H)_4(CO)_{18}(\eta^6\text{-}C_{16}H_{16})$ **27**, showing the atomic labelling scheme; the C atoms of the CO groups bear the same numbering as the corresponding O atoms. Relevant bond distances (Å): Ru(1)-Ru(2) 3.044(3), Ru(1)-Ru(3) 2.976(3), Ru(1)-Ru(4) 2.986(3), Ru(1)-Ru(6) 3.046(3), Ru(1)-Ru(7) 3.059(3), Ru(1)-Ru(8) 2.799(3), Ru(2)-Ru(3) 2.805(3), Ru(2)-Ru(5) 2.790(3), Ru(2)-Ru(6) 2.792(3), Ru(2)-Ru(7) 2.767(3), Ru(3)-Ru(4) 2.972(3), Ru(3)-Ru(5) 2.858(3), Ru(3)-Ru(8) 2.752(3), Ru(4)-Ru(5) 2.931(3), Ru(4)-Ru(6) 2.784(3), Ru(4)-Ru(8) 2.748(3), Ru(5)-Ru(6) 2.820(3), Ru(6)-Ru(7) 2.823(3), mean $Ru\text{-}C(CO_{terminal})$ 1.87(2), mean $Ru\text{-}C(CO_{bridging})$ 2.15(2), mean C-O 1.15(2), Ru(5)-C(19) 2.27(2), Ru(5)-C(20) 2.21(2), Ru(5)-C(21) 2.40(2), Ru(5)-C(22) 2.24(2), Ru(5)-C(23) 2.20(1), Ru(5)-C(24) 2.37(2), C(19)-C(20) 1.41(2), C(19)-C(24) 1.54(2), C(20)-C(21) 1.41(2), C(21)-C(22) 1.47(2), C(21)-C(34) 1.45(2), C(22)-C(23) 1.42(2), C(23)-C(24) 1.35(2), C(24)-C(25) 1.49(2), C(25)-C(26) 1.62(2), C(26)-C(27) 1.51(2), C(27)-C(28) 1.45(2), C(27)-C(32) 1.39(2), C(28)-C(29) 1.40(2), C(29)-C(30) 1.36(2), C(30)-C(31) 1.36(2), C(30)-C(33) 1.53(2), C(31)-C(32) 1.35(2), C(33)-C(34) 1.56(2), mean H(1)-Ru 1.86(2)[a], mean H(2)-Ru 1.78(2)[b], mean H(4)-Ru 1.78(2)[b], H(3)-Ru(1) 1.71(2)[a], H(3)-Ru(7) 2.14(2).[b] [a] Experimental value; [b] hydride position calculated with XHYDEX.[72]

pseudo m-symmetry of the molecule, as shown in Figure 4.2.5ii. In order to obey the PSEPT, 110 valence electrons are required for an octanuclear cluster with this metal atom topology. This electron count is achieved from the eighteen carbonyl groups, the six-electron donating benzene moiety and the four electrons formally donated by the hydride ligands.
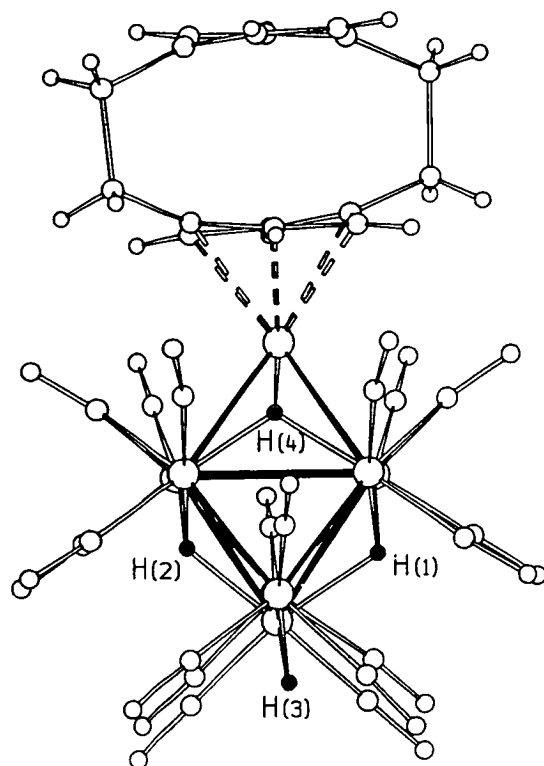
Figure 4.2.5ii: The molecular structure of $Ru_8(\mu\text{-}H)_4(CO)_{18}(\eta^6\text{-}C_{16}H_{16})$ **27**, showing the *pseudo*-mirror plane.

4.3 The Relationship Between Compounds 23 - 27

The previous section described the thermolytic reaction of $Ru_3(CO)_{12}$ **14** and [2.2]paracyclophane in octane, which resulted in the isolation of a range of clusters with nuclearities of three, six and eight, that contained four different types of metal polyhedra. A series of separate experiments are now described which establish that a clear relationship exists between these clusters; this series of reactions are summarised in Scheme 4.3.1.

On heating $Ru_3(CO)_9(\mu_3\text{-}\eta^2\text{:}\eta^2\text{:}\eta^2\text{-}C_{16}H_{16})$ **23** in octane with an equimolar quantity of $Ru_3(CO)_{12}$ **14**, both the open cluster, $Ru_6C(CO)_{15}(\mu_3\text{-}\eta^1\text{:}\eta^2\text{:}\eta^2\text{-}C_{16}H_{16}\text{-}\mu_2\text{-}O)$ **24**, and the octahedral carbido species, $Ru_6C(CO)_{14}(\mu_3\text{-}\eta^2\text{:}\eta^2\text{:}\eta^2\text{-}C_{16}H_{16})$ **25**, are observed. Furthermore, the thermolysis of compound **24** in octane, or its pyrolysis in a gas cell, yields cluster **25** and CO_2 almost quantitatively. The infrared spectrum of the gaseous products from the solid-state pyrolysis of **24** show strong absorptions at 2359 and 2342 cm^{-1} which are characteristic of CO_2, and also peaks at 2170 and 2120 cm^{-1} typical of CO, therefore suggesting that cluster decomposition occurs. The resulting solid residue consists mainly of ruthenium metal, however spot t.l.c. and infrared spectroscopy show that the soluble fraction comprises of **25** with small traces of the unreacted starting material
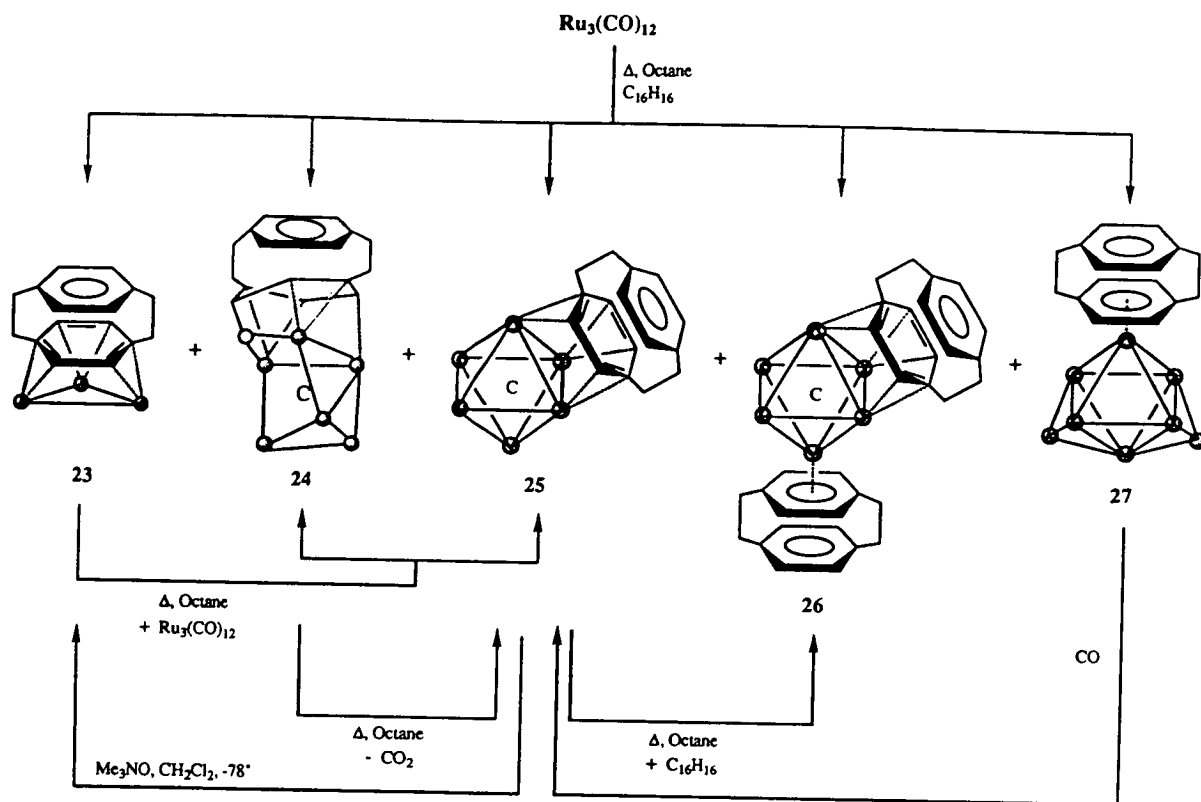
Scheme 4.3.1: The relationship between compounds **23-27**.

24. Hence, it follows that $Ru_6C(CO)_{15}(\mu_3-\eta^1:\eta^2:\eta^2-C_{16}H_{16}-\mu_2-O)$ **24** is a key intermediate compound on route to the carbido-cluster $Ru_6C(CO)_{14}(\mu_3-\eta^2:\eta^2:\eta^2-C_{16}H_{16})$ **25**, merely requiring the loss of CO_2 and a rearrangement of the hexaruthenium polyhedron. This complex is a rare example of a molecular system containing both the carbido- and oxo- ligand of a carbonyl group (which has been cleaved during the build-up from a triruthenium to a hexaruthenium cluster) trapped within a metal cluster framework. In the conversion of **24** to **25** it is thought that the unused lone pair on the O-atom attacks the C-atom of a second carbonyl group resulting in the expulsion of CO_2. This process yields the appropriate number of carbonyl ligands found in **25** (*i.e.* 14), and hence a simultaneous rearrangement of the metal framework would afford the octahedral carbido-cluster (Equation 1). The mechanisms involved in carbide formation are discussed in more detail in the following section.

Equation 1:

$$Ru_6C(CO)_{15}(\mu_3-\eta^1:\eta^2:\eta^2-C_{16}H_{16}-\mu_2-O) \quad \rightarrow \quad Ru_6C(CO)_{14}(\mu_3-\eta^2:\eta^2:\eta^2-C_{16}H_{16}) \quad + \quad CO_2$$

$$\textbf{24}\textbf{25}$$
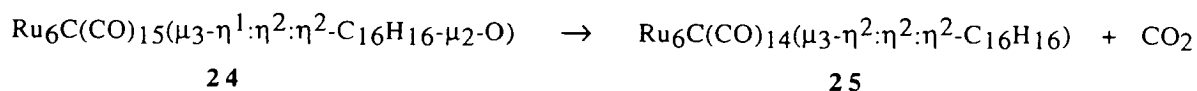
Not surprisingly, the thermolysis of $Ru_6C(CO)_{14}(\mu_3-\eta^2:\eta^2:\eta^2-C_{16}H_{16})$ **25** with an excess of [2.2]paracyclophane in octane yields $Ru_6C(CO)_{11}(\eta^6-C_{16}H_{16})(\mu_3-\eta^2:\eta^2:\eta^2-C_{16}H_{16})$ **26**, where three carbonyl ligands have been displaced by the second paracyclophane moiety. It is also possible to convert **25** back into $Ru_3(CO)_9(\mu_3-\eta^2:\eta^2:\eta^2-C_{16}H_{16})$ **23** by degradation of the cluster core using a large excess of the oxidative decarbonylation reagent trimethylamine *N*-oxide in dichloromethane only. The use of Me_3NO as a reagent to bring about cluster degradation has not been employed before, however, it can be envisaged that the removal of a significant number of carbonyl ligands (by oxidation to CO_2) would render the metal cluster unit unstable and, hence, result in a decrease of cluster nuclearity. Degradation reactions of this sort clearly offer considerable potential in a number of other related compounds, and are discussed again in Chapter five.

The octaruthenium cluster, $Ru_8(\mu-H)_4(CO)_{18}(\eta^6-C_{16}H_{16})$ **27**, has been found to react with a steady stream of CO in dichloromethane at room temperature, producing $Ru_3(CO)_{12}$ **14** and $Ru_6C(CO)_{14}(\mu_3-\eta^2:\eta^2:\eta^2-C_{16}H_{16})$ **25** quantitatively. Whilst it is quite easy to envisage that the $Ru_3(CO)_{12}$ may be derived from a recombination of the ruthenium carbonyl fragments generated from the degradative carbonylation of the two capping ruthenium atoms attached to the octahedral cage, the formation of $Ru_6C(CO)_{14}(\mu_3-\eta^2:\eta^2:\eta^2-C_{16}H_{16})$ **25** is less easy to visualise. Clearly the migration of the cyclophane moiety from a terminal position to a face-capping site is required (a process quite common in these systems),[70c,73] but the entrapment of a carbido atom into the octahedral cavity is also necessary. Thus, the octahedron must somehow open up and undergo such a transformation that upon cleavage of a carbonyl ligand, the octahedron reforms with an encapsulated carbido-atom. The mechanism by which this process occurs is not fully understood, however a possible reaction intermediate has been isolated in low yield and will be discussed in due course.

A similar situation has been seen to arise in the reaction of $[Ru_6(CO)_{18}]^{2-}$ with trifluoromethanesulphonic (triflic) anhydride, which results in the chemical cleavage of a coordinated carbonyl ligand to produce $Ru_6C(CO)_{17}$.[74] The proposed mechanism of this reaction is illustrated in Scheme 4.3.2, and is considered to involve the addition of the strongly electrophilic $[CF_3SO_2]^+$ cation to the oxygen of a μ_3 carbonyl ligand attached to $[Ru_6(CO)_{18}]^{2-}$, thus yielding a monoanionic intermediate. The excellent leaving ability of the triflate as an anion results in the spontaneous cleavage of the C-O bond to give the neutral $Ru_6C(CO)_{17}$ molecule containing a tricoordinate surface bound carbide. This species is expected to be unstable with respect to the interstitial complex, and consequently the structure undergoes a core rearrangement to encapsulate the newly formed carbide within the octahedron framework.

$[Ru_6(CO)_{18}]^{2-}$ $Ru_6C(CO)_{17}$
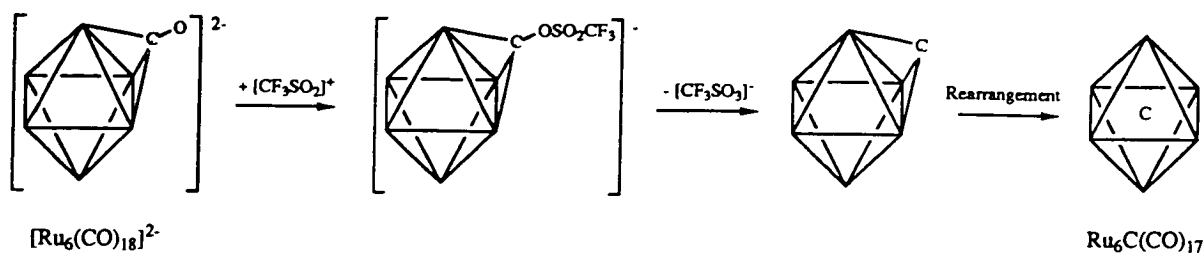
Scheme 4.3.2: The proposed mechanism for the cleavage of a carbonyl C-O bond by trifluoromethanesulphonic anhydride.

4.4 Carbide Formation in Ruthenium Carbonyl Clusters

In 1962 the discovery of $Fe_5C(CO)_{15}$, by Dahl and coworkers, provided the first example of a transition metal carbido-cluster.[75] The subsequent synthesis and structure determination of the hexanuclear cluster dianion, $[Fe_6C(CO)_{16}]^{2-}$,[76] and the tetranuclear species $Fe_4C(CO)_{13}$,[77] provided the first homologous series of carbido-clusters; from the hexanuclear cluster containing completely encapsulated carbon, to the tetranuclear example in which the carbido-ligand is physically and electronically exposed and proves to be a considerably reactive centre (see Figure 4.4.1).[78]

$[Fe_4C(CO)_{13}]$ $[Fe_5C(CO)_{15}]$ $[Fe_6C(CO)_{16}]^{2-}$
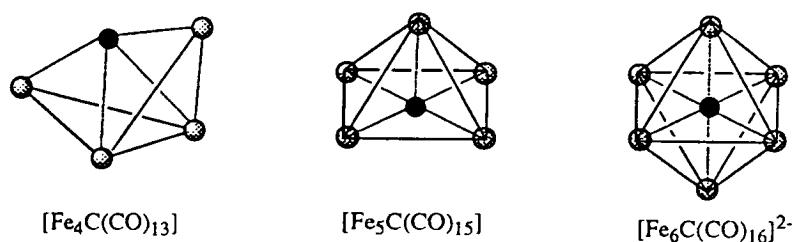
Figure 4.4.1: The metal core structures of the tetra-, penta- and hexairon carbido-clusters.

The chemistry and structural diversity exhibited by the carbido-clusters of ruthenium surpasses that of iron, with nuclearities of four, $Ru_4C(CO)_{13}$;[79] five, $Ru_5C(CO)_{15}$;[80] six, $Ru_6C(CO)_{17}$;[64] and ten, $[Ru_{10}C_2(CO)_{24}]^{2-}$ and $[Ru_{10}C(CO)_{24}]^{2-}$ [81,82] known. Osmium also forms a large number of carbido-clusters with nuclearities ranging from between five and eleven, with the notable exception of six and nine (although a species characterised as $Os_6C(CO)_{17}$ has been isolated on one occasion in minute amounts),[83] these being; $Os_5C(CO)_{15}$,[80,84] $Os_7(\mu-H)_2C(CO)_{19}$,[85] $Os_8C(CO)_{21}$,[84] $[Os_{10}C(CO)_{24}]^{2-}$ [86] and $[Os_{11}C(CO)_{27}]^{2-}$.[87] Significantly, no Os_4C clusters have been characterised to date.

149

The synthesis and unique reactivity of these carbido-clusters have been studied extensively, and although it is not intended to give a full account of their chemistry it should be noted that the carbido-ligand only exhibits reactivity in M_4C systems (even though partially exposed in the square-based pyramidal $M_5C(CO)_{15}$ clusters). The presence of a carbido-ligand tends to confer considerable stability on the cluster framework so that during substitution reactions the cluster unit usually remains intact, or at least its rearrangement is restricted.[88] As a result, carbido clusters are useful materials for systematic organometallic studies merely behaving as a site for coordination and reaction of ligands, without actively participating in the process.

Apart from synthesis, structure and reactivity, the widespread interest in carbido-clusters also provoked studies into the origin of the carbido-atom. Work with isotopically enriched ^{13}CO has enabled workers to confirm that, in the case of the iron-triad carbido-clusters, the source of the isolated C-atom is *via* the thermally induced cleavage of a coordinated carbonyl ligand, (whereas the majority of the carbido-clusters of the cobalt sub-group are synthesised using halomethanes which act as an external source of carbon).[89] Thus, the use of ^{13}C enriched $Fe(CO)_5$ in the synthesis of $[Fe_6C(CO)_{16}]^{2-}$ results in encapsulation of ^{13}C as the carbido-ligand, as evidenced from ^{13}C NMR spectroscopy.[77b] Likewise, ^{13}C enriched $Ru_3(CO)_{12}$ produces $[Ru_6C(CO)_{16}]^{2-}$ containing ^{13}C at its centre,[90] and $[Os_{10}C(CO)_{24}]^{2-}$ with a ^{13}C carbido atom is synthesised from ^{13}CO enriched $Os_3(CO)_{12}$.[91] In the synthesis of $Ru_6C(CO)_{17}$, from the pyrolysis of $Ru_3(CO)_{12}$, carbon dioxide can be detected in the gaseous products of the reaction, therefore suggesting that the cluster unit brings about carbonyl disproportionation, with the elimination of CO_2 and the formation of a carbido-atom (Equation 2).[92]

Equation 2: $2CO \rightarrow {}'C' + CO_2$

The only known example of an iron triad cluster where the carbido-atom is derived from a source other than a carbonyl ligand is in the pyrolysis of $Ru_6(CO)_{15}(CNBu^t)(\eta^5\text{-}CNBu^t)$ to produce $Ru_6C(CO)_{16}(CNBu^t)$. In this example the isonitrile ligand is the source of the carbido-atom, as shown by ^{13}C labelling studies.[93]

The relevance that these discoveries bore on the dissociative adsorption of CO on metal surfaces and the subsequent reactivity of the resulting surface carbido species were immediately recognised by surface scientists as being pivotal processes in hydrocarbon formation reactions such as the Fischer-Tropsch synthesis.[94] The observed proton induced reduction of CO in the conversion of $[HFe_4(CO)_{13}]^-$ to $HFe_4(CO)_{12}(\eta^2\text{-}CH)$[78b] provided a homogeneous parallel to the activation of CO on a Ni surface, whereby the CO is cleaved

producing an active surface carbide which is subsequently reduced.[95] The precise method by which the C-O bond cleavage occurred on the surface was, however, at that time a matter of some debate.

Protonation of the dianionic tetrahedral cluster $[Fe_4(CO)_{13}]^{2-}$ yields the butterfly cluster $[HFe_4(CO)_{13}]^-$.[96] A single crystal X-ray diffraction analysis of this cluster reveals a molecular structure in which a butterfly arrangement of the four iron atoms supports a four electron donating μ_4-η^2 coordinated carbonyl ligand, in which the C-O bond is lengthened significantly. The μ_3-C-O bond in $[Fe_4(CO)_{13}]^{2-}$ is 1.20 Å, which lengthens to 1.26 Å on formation of the μ_4-η^2-CO in $[HFe_4(CO)_{13}]^-$, therefore suggesting that the cluster unit activates the CO moiety by interaction of both the C and O-atoms simultaneously with several metal atoms, thus weakening the C-O bond and increasing the nucleophilicity of the carbonyl oxygen. Reaction with a second equivalent of acid results in protonation of the unique carbonyl oxygen forming a μ_4-η^2-COH moiety,[97] which activates the carbonyl ligand even further by an increased lengthening of the C-O bond. Further protonation results in cleavage of the C-O bond, with the loss of water and the formation of the carbido-cluster $[HFe_4C(CO)_{12}]^-$, and this then reacts with additional H^+ to finally produce the $HFe_4(CO)_{12}(\eta^2$-CH) cluster, which contains a μ_4-η^2 methylidyne ligand (see Scheme 4.4.1).[78b]
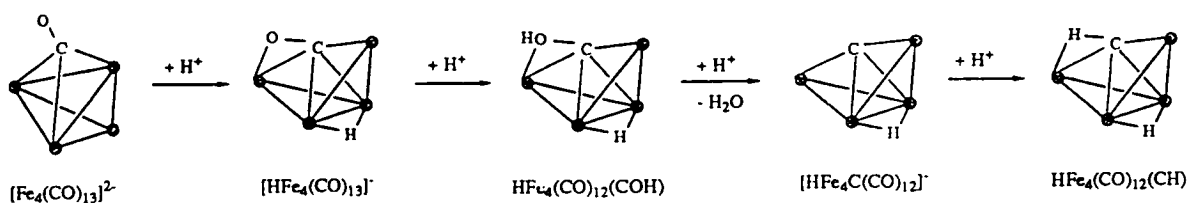
Scheme 4.4.1: The proton induced reduction of CO in $[Fe_4(CO)_{13}]^{2-}$.

The observation that the cleavage of CO was greatly facilitated by coordination through both the C and O-atoms was soon realised by surface scientists who shortly afterwards showed that metal surfaces such as Cr, Fe and Ru could also accommodate carbon monoxide in a 'side-on' manner.[98] The *di-hapto* coordination mode was found to stretch and weaken the C-O bond on the metal surface, with cleavage generally being observed at around 300K resulting in the formation of surface bound carbide and oxide ligands. This carbide is readily transformed into methane in the presence of hydrogen, whereas the oxygen is removed from the metal surface as water in the presence of H_2, and as CO_2 in the presence of CO. The disproportionation of CO to C and CO_2 on a metal surface is called the Boudouard reaction,[94a,99] and is similar to the process observed in

metal carbonyl chemistry where upon pyrolysis or thermolysis the oxygen appears to be transferred to an adjacently bound terminal carbonyl ligand by nucleophilic attack on the strongly electrophilic carbon; CO_2 is evolved and carbido-clusters are generated.

Recently, Chisholm *et al* reported a tetratungsten cluster which provided the first example of a molecular system containing both the carbide and oxide ligands of a cleaved carbonyl.[99] The cluster $W_4(\mu_4\text{-}C)(O)(OiPr)_{12}$ contains both a carbido-atom bonded to four tungsten atoms in a butterfly arrangement, and an oxo-atom bonded to two of the tungsten atoms. The reactivity of a CO molecule bridging metal atoms in tungsten clusters of this type has been compared to that of a CO molecule adsorbed on a Mo(110) metal surface; both react with dissociation to give carbido and oxido ligands bonded to neighbouring metal centres.[100]

The cleavage of CO in cluster compounds therefore has many obvious parallels with CO cleavage on a metal surface, but there is also one important difference. Uptake of CO by a metal surface is always easier than the C-O bond cleavage reaction, which is presumably because the atoms of a metal surface are more unsaturated and receptive to ligand (Lewis base) uptake. In metal clusters, however, there are likely to be a number of significant rearrangements or reactions that have to occur prior to Lewis base uptake, although once the CO ligand adopts a bridging position with both the carbon and oxygen atoms interacting with the metal unit, the C-O bond is so activated that cleavage can occur quite readily, requiring little more than a skeletal rearrangement of the cluster framework.

To summarise, carbido-atoms may be introduced into metal clusters of the iron-triad by the thermally induced cleavage of a coordinated carbonyl ligand. Carbon dioxide is usually detected as a by-product from these reactions, indicating that the disproportionation of two carbonyl groups takes place. It is apparent that C-O bond cleavage occurs more readily if the carbonyl ligand is coordinated in a *di-hapto* manner,[99,101] however, for this to occur carbonyls must be initially lost in order to bring about an unsaturated cluster unit and thereby open up the coordination sites required for activation of a CO ligand in this 'side-on' manner. The multi-hapto coordination of a carbonyl ligand leads to a considerable elongation and weakening of the C-O bond (evidenced by C-O stretching frequencies, and bond lengths), therefore making cleavage relatively facile. Additionally, this coordination mode increases the nucleophilicity of the carbonyl oxygen enabling either protonation, if in the presence of acid as with $[HFe_4(CO)_{13}]^-$, or more commonly attack at the electrophilic carbon of a neighbouring terminal carbonyl. In the latter situation, one might expect to form an ester-type intermediate which then breaksdown into CO_2 and the observed cluster carbide. This mechanism of C-O bond cleavage is similar to that proposed by Deeming, which involves the combination of the oxygen nucleophilicity of a highly bridging carbonyl with the carbon electrophilicity of a terminal carbonyl (see Scheme 4.4.2).[102]
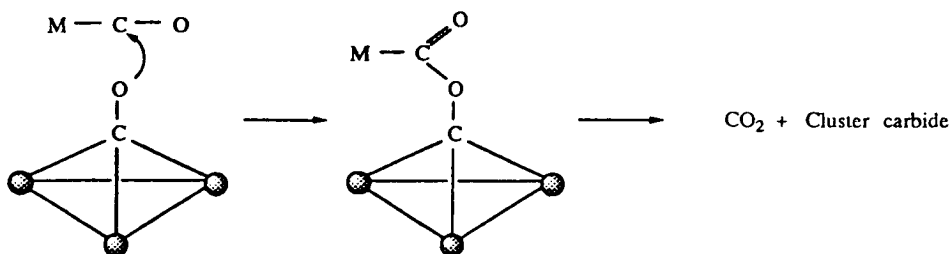
Scheme 4.4.2: A proposed mechanism for CO bond cleavage.

Clusters containing *di-hapto* carbonyl ligands are quite rare, however one example has recently been isolated which has proven to be an important intermediate in the formation of a hexaruthenium carbido-cluster. This cluster system was first introduced in Chapter three and involves the thermolysis of $Ru_3(CO)_{12}$ in heptane-mesitylene to yield the complex $Ru_6C(CO)_{14}(\eta^6\text{-}C_6H_3Me_3)$, together with the two clusters $Ru_6(\mu_4\text{-}\eta^2\text{-}CO)_2(CO)_{13}(\eta^6\text{-}C_6H_3Me_3)$ and $HRu_6(\mu_4\text{-}\eta^2\text{-}CO)(CO)_{13}(\mu_2\text{-}\eta^1\text{:}\eta^6\text{-}C_6H_3Me_2CH_2)$.[103] Furthermore, the thermolysis of $Ru_6(\mu_4\text{-}\eta^2\text{-}CO)_2(CO)_{13}(\eta^6\text{-}C_6H_3Me_3)$ in mesitylene, results in its conversion to $Ru_6C(CO)_{14}(\eta^6\text{-}C_6H_3Me_3)$ and $HRu_6(\mu_4\text{-}\eta^2\text{-}CO)(CO)_{13}(\mu_2\text{-}\eta^1\text{:}\eta^6\text{-}C_6H_3Me_2CH_2)$ in equal yields, together with CO_2. It can therefore be envisaged that the mechanism of carbide formation is *inter*molecular in this case, and involves the cleavage of one of the η^2-CO ligands of $Ru_6(\mu_4\text{-}\eta^2\text{-}CO)_2(CO)_{13}(\eta^6\text{-}C_6H_3Me_3)$ *via* the nucleophilic attack of its oxygen on a terminal carbonyl of a second cluster molecule. Elimination of CO_2 from this intermediate would generate a carbide coordinated to the first cluster, which could then undergo rearrangement to encapsulate the newly formed carbido-atom and so produce the complex $Ru_6C(CO)_{14}(\eta^6\text{-}C_6H_3Me_3)$.

It is believed that the open cluster, $Ru_6C(CO)_{15}(\mu_3\text{-}\eta^1\text{:}\eta^2\text{:}\eta^2\text{-}C_{16}H_{16}\text{-}\mu_2\text{-}O)$ **24**, described in this work represents the following stage of the reaction mechanism, *i.e.* after the C-O bond cleavage of a *di-hapto* carbonyl ligand has occurred, but before the oxygen atom has been expelled from the cluster as CO_2. The proposed mechanism differs slightly to those described above in that the nucleophilic oxygen attacks a ring carbon of a cyclophane moiety within the same molecule, instead of the C-atom of a terminal carbonyl on a second molecule. This is easy to envisage since coordination at a metal centre induces electrophilicity into the cyclophane ring carbons, therefore making them more susceptible to attack by the carbonyl oxygen. As a result, the weak C-O bond undergoes cleavage producing the observed intermediate $Ru_6C(CO)_{15}(\mu_3\text{-}\eta^1\text{:}\eta^2\text{:}\eta^2\text{-}C_{16}H_{16}\text{-}\mu_2\text{-}O)$ **24**. Since the cluster has a particularly open geometric framework, an *intra*molecular mechanism for its conversion to $Ru_6C(CO)_{14}(\mu_3\text{-}\eta^2\text{:}\eta^2\text{:}\eta^2\text{-}C_{16}H_{16})$ **25** can be envisaged whereby the lone pair on the oxygen attacks the carbon of a terminal carbonyl, so generating CO_2 which is

rapidly expelled from the cluster core. The cluster would then contain 14 CO ligands (the number present in **25**) and rearrangement of the metal atom network, together with a simultaneous movement of the carbide and carbonyl ligands, could take place producing the 86 electron octahedral cluster, **25**. The stability of the octahedrally encapsulated carbido-atom in this system, together with the production of CO_2 undoubtedly contribute to the driving force for the C-O cleavage process described.

The cluster $Ru_6C(CO)_{15}(\mu_3-\eta^1:\eta^2:\eta^2-C_{16}H_{16}-\mu_2-O)$ **24** has provided another example of a molecular system containing both the carbido and oxo ligands of a cleaved carbonyl. It has demonstrated that the O-atom of the activated CO may be transferred to a coordinated organo-group, and provides an alternative view of the generation of oxygen containing organic substrates. The transfer of the same oxygen to a carbonyl, which in turn leads to the reduction of the organic is also of some interest. This work emphasises the danger of a simplistic view of CO cleavage, and leads to the conclusion that in cluster chemistry at least, such reactivities may be *intra* rather than *inter*molecular.

4.5 Octaruthenium Clusters Containing Carbon Monoxide in a Unique Coordination Mode

When the thermolysis of $Ru_3(CO)_{12}$ **14** and [2.2]paracyclophane is carried out in heptane as opposed to octane, a similar range of products are obtained with enhanced yields of $Ru_3(CO)_9(\mu_3-\eta^2:\eta^2:\eta^2-C_{16}H_{16})$ **23** and $Ru_6C(CO)_{15}(\mu_3-\eta^1:\eta^2:\eta^2-C_{16}H_{16}-\mu_2-O)$ **24**. These slightly less aggressive conditions, however, also allow the isolation, in low yield, of two additional products which were not observed from the octane reaction. These new compounds have been characterised on the basis of the customary spectroscopic techniques and single crystal X-ray diffraction analyses as $Ru_8(\mu-H)_2(\mu_6-\eta^2-CO)(CO)_{19}(\eta^6-C_{16}H_{16})$ **28** and $Ru_8(\mu_6-\eta^2-CO)(\mu_4-\eta^2-CO)(CO)_{18}(\eta^6-C_{16}H_{16})$ **29**. The solution infrared spectra of the two clusters in the CO stretching region are complex reflecting their low molecular symmetry; both clusters give rise to similar spectra with adsorptions present in the terminal carbonyl region only (between ~2100 and 1930 cm^{-1}). The mass spectra show distinct parent peaks at 1580 (calc. 1579) and 1576 (calc. 1577) amu for **28** and **29**, respectively, together with peaks corresponding to the sequential loss of several CO groups. The ^1H NMR spectrum has been recorded for compound **28** only, due to the insufficient quantities of **29** available, and exhibits signals at δ values of 6.89, 4.40, 3.38, -11.67 and -15.37 ppm, with relative intensities of 4:4:8:1:1. The two signals at δ 6.89 and 4.40 ppm appear as singlets and may be attributed to the four C-H protons of the unattached and coordinated cyclophane rings, respectively. The frequency at which this latter resonance occurs is comparable to that observed for $Ru_8(\mu-H)_4(CO)_{18}(\eta^6-C_{16}H_{16})$ **27** (δ 4.51 ppm) and

hence, suggests that the cyclophane moiety is bound in an η^6 manner. The protons in the -CH_2-CH_2- linkages give rise to the signal at δ 3.38 ppm which appears to be of essentially singlet character. This is unusual since the bridge protons in related paracyclophane clusters generally give rise to two multiplet resonances (typically of AA'BB' character) which can be attributed to the two pairs of CH_2 protons adjacent to and furthest from the coordinated ring. Cooling the sample to 213 K does not appear to have any effect on this signal, and while the precise mechanism by which the CH_2 group protons equilibrate has not been established, it can be envisaged that the ring is not only undergoing rapid rotation about its plane, but may also undergo some form of tumbling motion. The signals at δ -11.67 and -15.37 ppm are both singlet resonances and correspond to the two hydride ligands.

The molecular structures of compounds **28** and **29** have been determined by single crystal X-ray diffraction analyses, with both sets of crystals grown from toluene solutions at -25°C. Although closely related, the two molecular structures are discussed separately and that of compound **28** is shown in Figures 4.5.1(a) and (b) together with some relevant structural parameters.

Compound **28** contains a highly unusual 'open' framework of the eight ruthenium atoms. The metal geometry is best described as a square based pyramid in which two adjacent basal edges are bridged by ruthenium atoms [Ru(6) and Ru(8)]. These two atoms are then fused, and this edge is itself bridged by the final ruthenium atom [Ru(7)]. It would appear that this metal atom topology is the first of its type, and is structurally comparable to an edge-bridged *nido*dodecahedron (see Scheme 4.5.1). In terms of simple electron counting arguments, such a polyhedron should contain 116 valence shell electrons, which is, indeed, the number observed in compound **28**.

(a)   (b)   (c)
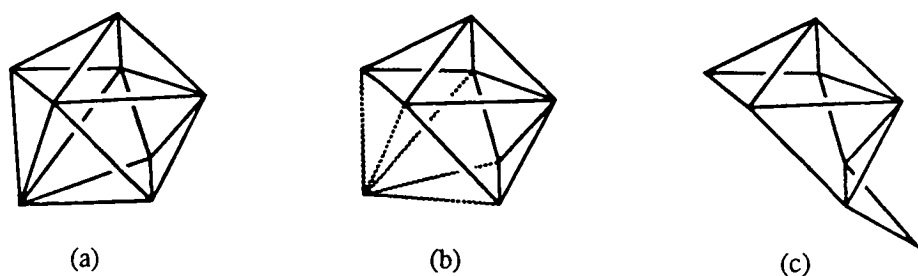
Scheme 4.5.1: (a) Dodecahedron, (b) *Nido*dodecahedron and (c) Edge-bridged *nido*dodecahedron.
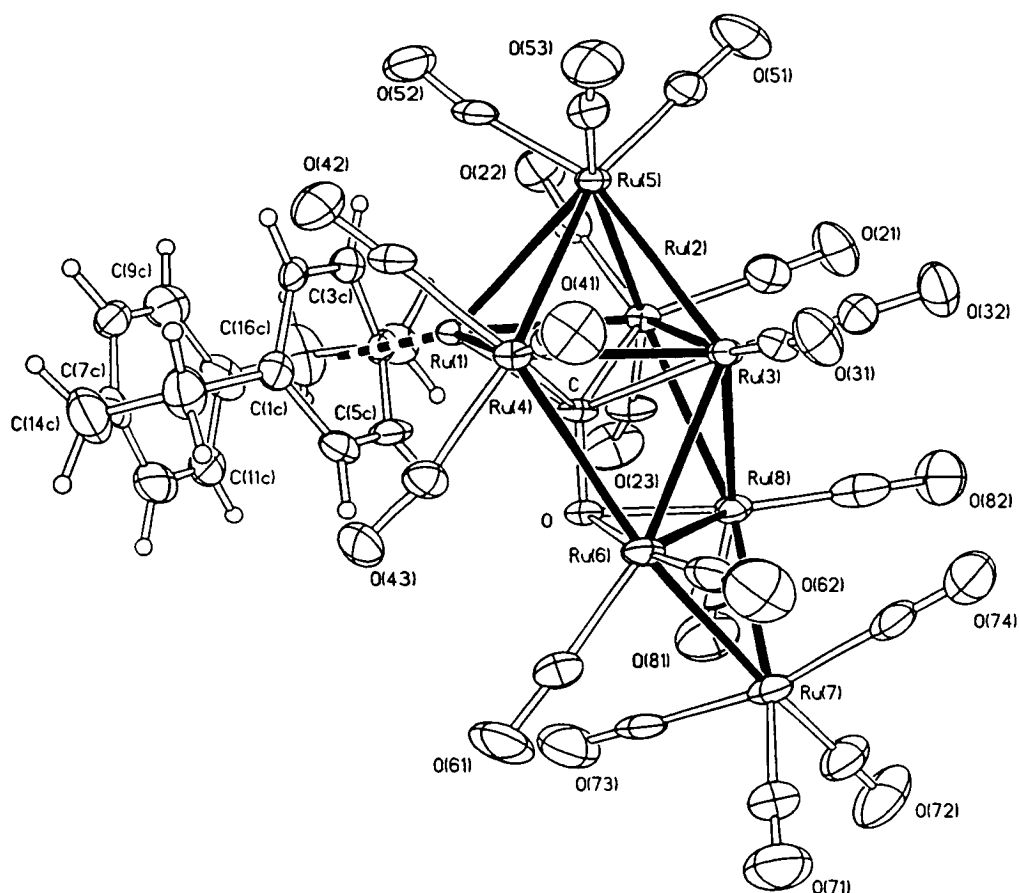
Figure 4.5.1(a): The solid-state molecular structure of $Ru_8(\mu-H)_2(\mu_6-\eta^2-CO)(CO)_{19}(\eta^6-C_{16}H_{16})$ **28**, showing the atomic labelling scheme; the C atoms of the CO groups bear the same numbering as the corresponding O atoms. Relevant bond distances (Å) and angles (°): Ru(1)-Ru(2) 2.691(2), Ru(1)-Ru(4) 2.684(2), Ru(1)-Ru(5) 2.9322(14), Ru(2)-Ru(3) 2.810(2), Ru(2)-Ru(5) 2.828(2), Ru(2)-Ru(8) 2.931(2), Ru(3)-Ru(4) 2.821(2), Ru(3)-Ru(5) 2.8618(14), Ru(3)-Ru(6) 2.850(2), Ru(3)-Ru(8) 2.882(2), Ru(4)-Ru(5) 2.834(2), Ru(4)-Ru(6) 2.983(2), Ru(6)-Ru(7) 2.768(2), Ru(6)-Ru(8) 3.019(2), Ru(7)-Ru(8) 2.773(2), Ru(1)-C 2.042(9), Ru(2)-C 2.170(9), Ru(3)-C 2.280(9), Ru(4)-C 2.197(9), Ru(6)-C 2.662(9), Ru(6)-O 2.149(7), Ru(8)-O 2.125(6), C-O 1.378(11), Ru-C(mean CO) 1.90, C-O(mean CO) 1.14, Ru(1)-C(1C) 2.399(10), Ru(1)-C(2C) 2.261(10), Ru(1)-C(3C) 2.247(10), Ru(1)-C(4C) 2.379(10), Ru(1)-C(5C) 2.157(10), Ru(1)-C(6C) 2.167(10), C(1C)-C(2C) 1.410(14), C(1C)-C(6C) 1.413(14), C(1C)-C(13C) 1.51(2), C(2C)-C(3C) 1.419(14), C(3C)-C(4C) 1.411(14), C(4C)-C(5C) 1.407(14), C(4C)-C(15C) 1.489(14), C(5C)-C(6C) 1.39(2), C(7C)-C(8C) 1.39(2), C(7C)-C(12C) 1.39(2), C(7C)-C(14C) 1.52(2), C(8C)-C(9C) 1.39(2), C(9C)-C(10C) 1.40(2), C(10C)-C(11C) 1.39(2), C(10C)-C(16C) 1.48(2), C(11C)-C(12C) 1.35(2), C(13C)-C(14C) 1.56(2), C(15C)-C(16C) 1.59(2), Ru(1)-C-Ru(2) 79.4(3), Ru(1)-C-Ru(4) 78.5(3), Ru(2)-C-Ru(3) 78.3(3), Ru(3)-C-Ru(4) 78.1(3), Ru(1)-C-O 121.2(6), Ru(2)-C-O 117.5(6), Ru(3)-C-O 109.8(6), Ru(4)-C-O 117.1(6), C-O-Ru(6) 95.5(5), C-O-Ru(8) 95.2(5), Ru(6)-O-Ru(8) 89.9(2).
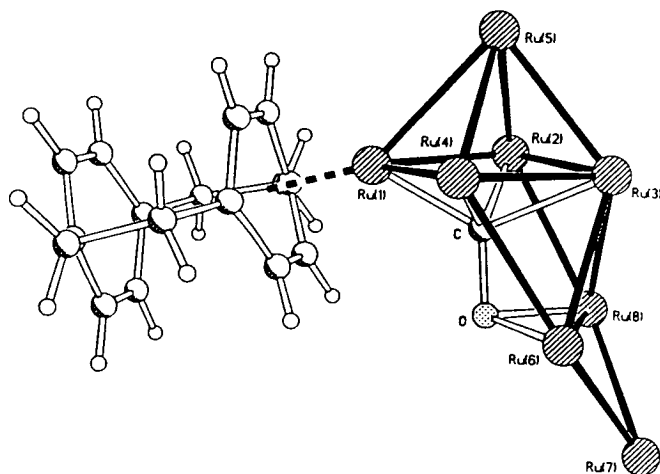
Figure 4.5.1(b): The central cluster framework of **28**, with the terminal carbonyl
ligands omitted for clarity.

It is also worth noting that this metal framework may be derived from a bicapped
octahedron by effectively cleaving three Ru-Ru edges, and the addition of three electron
pairs to the 110 already present would also result in the observed electron count of 116.
(see Scheme 4.5.2).

(a)   (b)
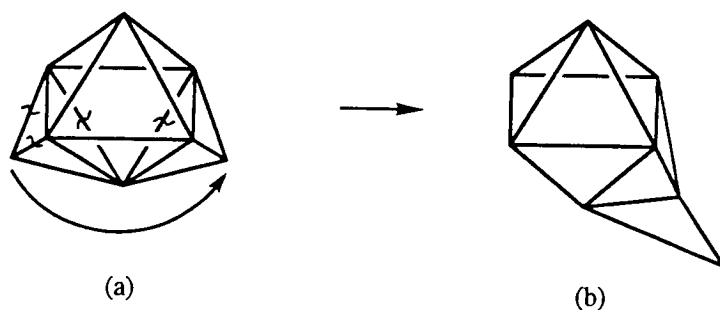
Scheme 4.5.2: The conversion of a bicapped octahedron into an edge-bridged *nido*dodecahedron by the
effective cleavage of three Ru-Ru edges.

The whole metal framework is heavily distorted with Ru-Ru distances varying
considerably in the range 2.684(2) to 3.019(2) Å. The cyclophane ligand is terminally
bound to the only basal vertex of the square pyramid not involved in edge-bridging
[Ru(1)]. The bound ring appears to keep the boat-shaped geometry that is typical of
cyclophanes in this coordination mode, however the centre of this ring does not sit directly
above the metal atom to which it is attached, but is instead slightly displaced towards one
side, as reflected by the variation observed in the Ru-C(ring) bond distances [Ru(1)-C(1C)
2.399(10), Ru(1)-C(2C) 2.261(10), Ru(1)-C(3C) 2.247(10), Ru(1)-C(4C) 2.379(10),
Ru(1)-C(5C) 2.157(10), Ru(1)-C(6C) 2.167(10) Å]. The bound cyclophane ring also

appears to be tilted in such a way that two of the four essentially coplanar C-atoms lie closer to the metal [C(5C) and C(6C)] than the other two [C(2C) and C(3C)]. The *di-hapto* carbonyl ligand sits in a central cavity where it bridges six metal atoms; the carbon coordinating to the four square pyramidal basal rutheniums, and the oxygen to the two fused edge-bridging ruthenium atoms. The carbon atom is displaced below the plane of the four rutheniums by 0.97 Å and is off-centred with respect to the middle of the square base, being shifted slightly towards the cyclophane-bound Ru atom [Ru(1)-C 2.042(9) *vs.* an average of 2.22(1) Å]. The C-O ligand acts as a six electron donor, and it appears that compounds **28** and **29** provide the first examples of a carbonyl coordinated in such a μ_6-η^2 fashion, with the bond length of 1.378(11) Å possibly being the longest C-O distance recorded for a carbon monoxide ligand by crystallographic techniques. The only other known example of a six electron donating carbonyl ligand is found in the triniobium cluster, $(Cp)_3Nb_3(CO)_7$; the length of the C-O bond in this molecule being 1.30 Å.[104] The remaining nineteen carbonyls are all terminal and essentially linear. They are distributed between the seven ruthenium atoms not involved in cyclophane coordination with two carbonyls attached to Ru(3), Ru(6) and Ru(8), three carbonyls situated on Ru(2), Ru(4) and Ru(5), and four carbonyls bonded to the unique atom Ru(7). The two hydride ligands were not located experimentally.

The solid-state structure of **29** is illustrated in Figure 4.5.2(a) and (b), accompanied by selected bond lengths and angles. The molecular structure is very similar to that of **28**, however the two hydride ligands and a terminal carbonyl have been replaced by a second *di-hapto* CO ligand, thus maintaining the required electron count of 116. This four electron donating, μ_4-η^2 carbonyl ligand is situated in the butterfly site created by the ruthenium atoms (3), (6), (7) and (8).

The ruthenium atom framework of **29** is the same as that described for **28**. The Ru-Ru bond lengths range from 2.693(2) to 3.126(2) Å, with the longest edge being that connecting the two hinge atoms of the butterfly unit which is spanned by the μ_4-η^2 carbonyl ligand [Ru(6)-Ru(8)]. As in **28**, the cyclophane ligand is bonded in a terminal fashion to the only basal vertex of the square pyramid not involved in edge-bridging [Ru(1)], and the coordinated ring again adopts a boat-shaped conformation. In this example, the C_6 ring appears to sit centrally over Ru(1), however, it is again tilted in the manner described for **28** with two of the four coplanar C-atoms lying close to the metal [Ru(1)-C(5C) 2.158(5), Ru(1)-C(6C) 2.158(5) Å], while the other two are slightly further away [Ru(1)-C(2C) 2.249(5), Ru(1)-C(3C) 2.251(5) Å]. Due to the cyclophanes boat-shaped conformation, the two *para* bridgehead carbon atoms of the bound ring exhibit an even longer bonding interaction with the metal centre [Ru(1)-C(1C) 2.371(5) and Ru(1)-C(4C) 2.367(5) Å]. As in **28**, the carbon atom of the μ_6-η^2 carbonyl ligand is off-centred
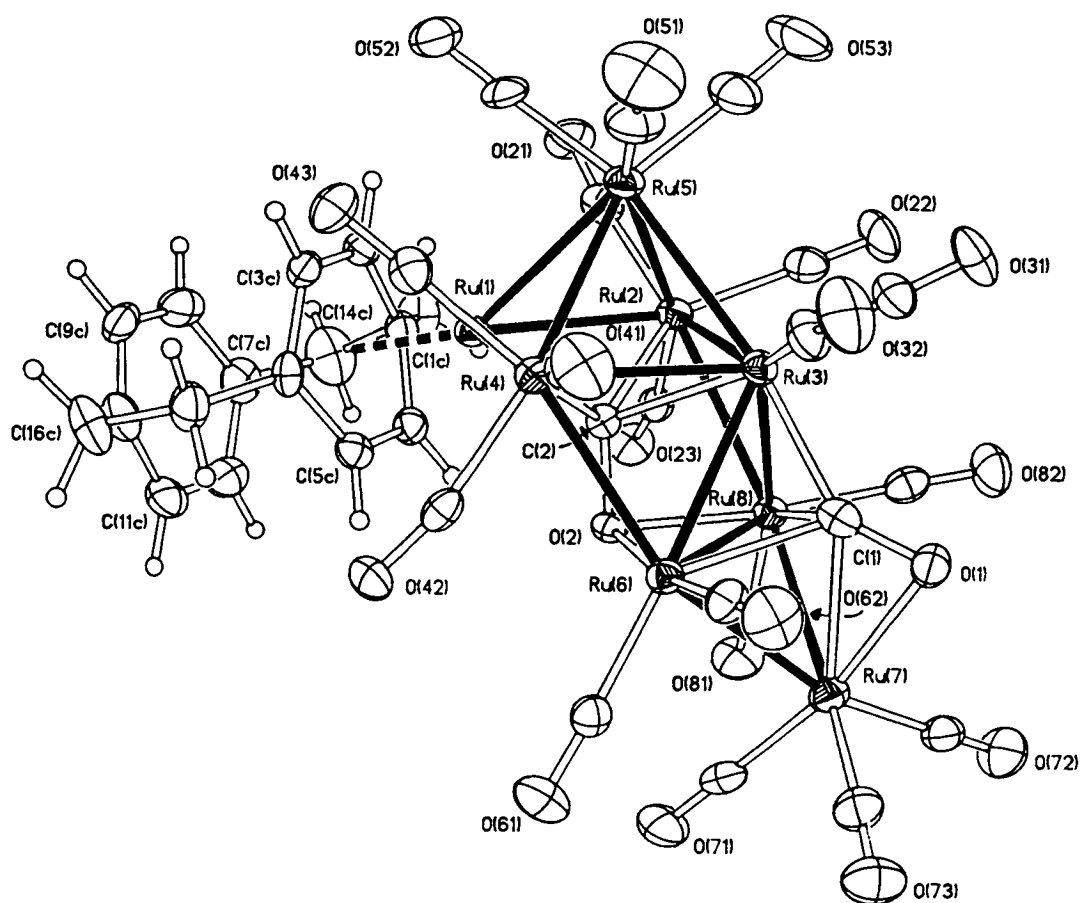
Figure 4.5.2(a): The solid-state molecular structure of $Ru_8(\mu_6\text{-}\eta^2\text{-}CO)(\mu_4\text{-}\eta^2\text{-}CO)(CO)_{18}(\eta^6\text{-}C_{16}H_{16})$ **29**, showing the atomic labelling scheme; the C atoms of the CO groups bear the same numbering as the corresponding O atoms. Relevant bond distances (Å) and angles (°): Ru(1)-Ru(2) 2.695(2), Ru(1)-Ru(4) 2.693(2), Ru(1)-Ru(5) 2.913(2), Ru(2)-Ru(3) 2.785(2), Ru(2)-Ru(5) 2.815(2), Ru(2)-Ru(8) 2.833(2), Ru(3)-Ru(4) 2.793(2), Ru(3)-Ru(5) 2.769(2), Ru(3)-Ru(6) 2.788(2), Ru(3)-Ru(8) 2.795(2), Ru(4)-Ru(5) 2.814(2), Ru(4)-Ru(6) 2.839(2), Ru(6)-Ru(7) 2.758(2), Ru(6)-Ru(8) 3.126(2), Ru(7)-Ru(8) 2.753(2), Ru(3)-C(1) 2.036(6), Ru(6)-C(1) 2.242(6), Ru(7)-C(1) 2.265(6), Ru(7)-O(1) 2.190(4), Ru(8)-C(1) 2.244(6), C(1)-O(1) 1.230(7), Ru(1)-C(2) 2.047(5), Ru(2)-C(2) 2.199(5), Ru(3)-C(2) 2.230(5), Ru(4)-C(2) 2.187(5), Ru(6)-C(2) 2.598(5), Ru(6)-O(2) 2.148(3), Ru(8)-O(2) 2.147(4), C(2)-O(2) 1.355(6), Ru-C(mean CO) 1.897(6), C-O(mean CO) 1.139(7), Ru(1)-C(1C) 2.371(5), Ru(1)-C(2C) 2.249(5), Ru(1)-C(3C) 2.251(5), Ru(1)-C(4C) 2.367(5), Ru(1)-C(5C) 2.158(5), Ru(1)-C(6C) 2.158(5), C(1C)-C(2C) 1.409(7), C(1C)-C(6C) 1.414(8), C(1C)-C(13C) 1.502(8), C(2C)-C(3C) 1.416(8), C(3C)-C(4C) 1.392(8), C(4C)-C(5C) 1.412(7), C(4C)-C(15C) 1.508(7), C(5C)-C(6C) 1.409(7), C(7C)-C(8C) 1.380(9), C(7C)-C(12C) 1.400(9), C(7C)-C(14C) 1.524(9), C(8C)-C(9C) 1.369(9), C(9C)-C(10C) 1.392(9), C(10C)-C(11C) 1.393(9), C(10C)-C(16C) 1.497(9), C(11C)-C(12C) 1.378(9), C(13C)-C(14C) 1.571(8), C(15C)-C(16C) 1.571(8), Ru(1)-C(2)-Ru(2) 78.7(2), Ru(1)-C(2)-Ru(4) 78.9(2), Ru(2)-C(2)-Ru(3) 77.9(2), Ru(3)-C(2)-Ru(4) 78.4(2), Ru(1)-C(2)-O(2) 122.0(3), Ru(2)-C(2)-O(2) 116.8(3), Ru(3)-C(2)-O(2) 109.8(3), Ru(4)-C(2)-O(2) 117.1(3), C(2)-O(2)-Ru(6) 93.0(3), C(2)-O(2)-Ru(8) 93.2(3), Ru(6)-O(2)-Ru(8) 93.38(14).

with respect to the square base, and is shifted towards the cyclophane-bound ruthenium atom [2.047(5) Å *vs.* a mean value of 2.205(5) Å]. It is also displaced beneath the basal plane by 0.97 Å; the same distance observed in **28**. The π-bonded $\mu_4\text{-}\eta^2$ carbonyl ligand

occupies the Ru_4 butterfly site, with the C atom interacting with the two 'hinge' [Ru(6) and Ru(8)] and one 'wing-tip' [Ru(3)] ruthenium atoms through σ bonds, and with the other wing-tip atom [Ru(7)] *via* a C-O π interaction. Although not as long as the μ_6-η^2 C-O bond length of 1.355(6) Å, the μ_4-η^2 C-O bond is considerably lengthened with respect to the terminally coordinated ligands [C(1)-O(1) 1.230(7) *vs.* a mean value of 1.139(7) Å]; an effect which may be attributed to electron donation from the C-O π-bond, and increased electron density in the CO π^* orbital due to the d_π-p_π bonding from three metals.
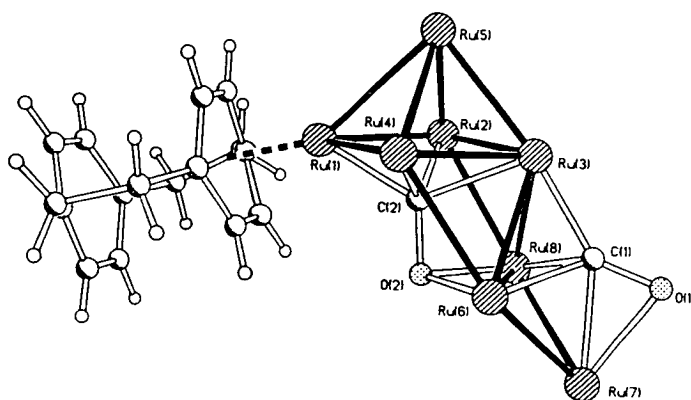
Figure 4.5.2(b): The central cluster framework of **29**, with the terminal carbonyls omitted for clarity.

These two clusters are thought to provide examples of a unique and previously unobserved coordination mode for carbon monoxide (*i.e.* μ_6-η^2-CO). As already noted, when coordinated in a 'side-on' manner the interaction with several metal atoms considerably weakens the C-O bond. Since the carbonyl group interacts with six metal atoms in this case, the bond should be very weak and therefore very active to cleavage. This is evident in the C-O bond lengths observed [1.378(11) and 1.355(6) Å for **28** and **29**, respectively] and should also be apparent from the infrared stretching frequencies which are very sensitive to small changes in the C-O bond order. However, the infrared spectrum of **28**, recorded in KBr, failed to show any peaks in the region 1600 to 1000 cm^{-1} which could be confidently attributed to the υ_{CO} mode of the μ_6-η^2 carbonyl ligand; possibly because such a vibration would be very broad and very weak. The solid-state infrared spectrum of **29** was not recorded due to an insufficient amount of material.

Section 4.3 described how the non-carbido bicapped octahedral cluster, $Ru_8(\mu$-$H)_4(CO)_{18}(\eta^6$-$C_{16}H_{16})$ **27**, undergoes reaction with CO to produce the octahedral carbido-cluster $Ru_6C(CO)_{14}(\mu_3$-η^2:η^2:η^2-$C_{16}H_{16})$ **25** and $Ru_3(CO)_{12}$ **14** in high yield. Clearly during this reaction the metal core of the precursor compound not only undergoes a

reduction in nuclearity, but must also endure a substantial polyhedral rearrangement in order to accommodate the carbido-atom. Although there is no direct evidence, it is possible that **28**, with its unusually open metal framework and elongated *di-hapto* carbonyl ligand, may represent the type of intermediate formed during this process (see Scheme 4.5.3).
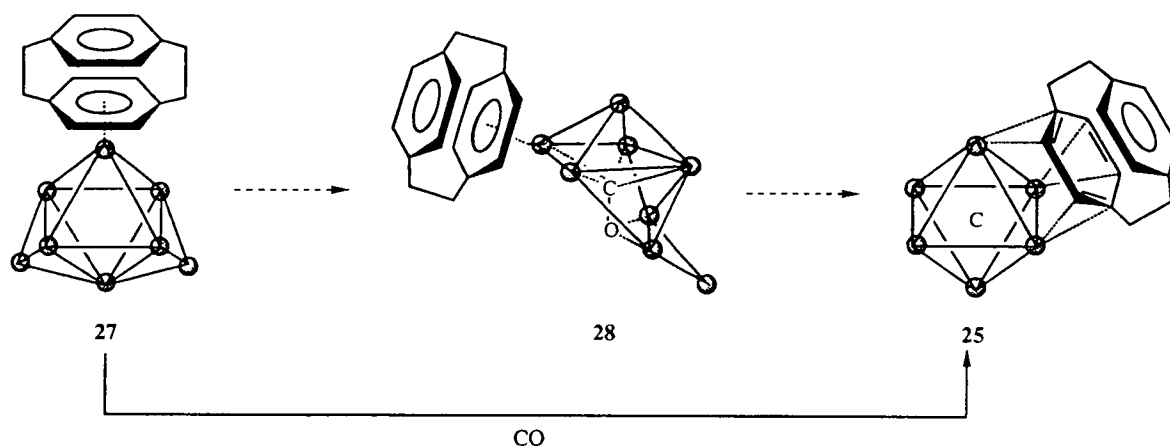
Scheme 4.5.3: The conversion of $Ru_8(\mu\text{-}H)_4(CO)_{18}(\eta^6\text{-}C_{16}H_{16})$ **27** into $Ru_6C(CO)_{14}(\mu_3\text{-}\eta^2\text{:}\eta^2\text{:}\eta^2\text{-}C_{16}H_{16})$ **25**, showing **28** as a possible reaction intermediate.

From an inspection of the molecular structure of **28** it can be speculated that cleavage of the C-O bond (by loss of the O-atom as CO_2) would cause the resulting carbide atom to be pulled up into the plane of the four ruthenium atoms to which it is attached, and therefore be within bonding distance of the apical metal atom [Ru(5)]. It should also be noted that there is a significant interaction between the carbon atom and Ru(6) [Ru(6)-C 2.662(9) Å], and hence it is possible that upon C-O bond cleavage the movement of the carbide atom towards Ru(5) would also result in a simultaneous movement of Ru(6) into a position such that the ruthenium atoms (1) - (6) form an octahedron. Clearly Ru(7) and Ru(8) must somehow be cleaved [which may then undergo recombination to form $Ru_3(CO)_{12}$], and the formation of several Ru-Ru bonds is also required for the generation of a *closo*-octahedron. The cyclophane moiety must undergo migration from a terminal to a facial position, although this process is not entirely unexpected since the reaction of $[Ru_5C(CO)_{14}]^{2-}$ with $[Ru(\eta^6\text{-}C_{16}H_{16})(MeCN)_3]^{2+}$ results in $Ru_6C(CO)_{14}(\mu_3\text{-}\eta^2\text{:}\eta^2\text{:}\eta^2\text{-}C_{16}H_{16})$ **25**, where a similar migration has occurred.[105]

Whilst a precise method for the formation of the hexanuclear cluster, $Ru_6C(CO)_{14}(\mu_3\text{-}\eta^2\text{:}\eta^2\text{:}\eta^2\text{-}C_{16}H_{16})$ **25**, has been postulated, the reaction may also be viewed as simply involving the generation of the pentanuclear-cyclophane cluster, $Ru_5C(CO)_{12}(C_{16}H_{16})$, and $Ru_3(CO)_{12}$ **14**, which may then recombine to produce **25**. It

has been found that heating the related parent cluster, $Ru_5C(CO)_{15}$, with $Ru_3(CO)_{12}$ results in the formation of $Ru_6C(CO)_{17}$, and therefore a similar process may take place within the cyclophane system.

Compound **29** is even more unusual due to the presence of a second *di-hapto* carbonyl ligand within the same molecule. However, whereas the μ_6-η^2 CO is unique to these compounds, the μ_4-η^2 carbonyl, while still uncommon, is being found in the butterfly sites of an increasing number of cluster compounds.[96,103] It is possible that compound **29** may also represent an intermediate complex in the aforementioned transformation, but the mechanism by which the octahedral cluster **25** forms is less obvious.

It should be pointed out that at no stage during the transformation of $Ru_8(\mu$-$H)_4(CO)_{18}(\eta^6$-$C_{16}H_{16})$ **27** to $Ru_6C(CO)_{14}(\mu_3$-η^2:η^2:η^2-$C_{16}H_{16})$ **25** are either of the open octaruthenium clusters, **28** and **29**, observed. Also, an initial attempt to convert **28** into **25** by the action of heat or treatment with CO has been unsuccessful. Further attempts and additional chemical investigations which may confirm the speculative mechanisms proposed have, unfortunately, been restricted by the very small amounts of **28** and **29** isolated.

4.6   A ^1H NMR Study of Transition Metal [2.2]paracyclophane Complexes

NMR spectroscopy can be used to provide an interesting insight into the nature of the transition metal-cyclophane interaction, and information as to how the magnetic environment of the cyclophane moiety is affected by the metal centre. ^1H NMR spectra of metal cyclophane complexes are ideally suited to give details concerning the fundamental changes that occur during metal complexation with respect to changes in ring current and charge density at each aromatic deck. When trying to interpret the ^1H NMR spectra of metal complexes containing the [2.2]paracyclophane moiety, it is necessary to first consider the spectrum of the free ligand itself. Since one benzene deck sits directly above the opposite deck, the magnetic environment of [2.2]paracyclophane is quite complex and the chemical shift of the aromatic protons cannot be accurately approximated by reference to its simple arene analogue, *p*-xylene. The aromatic protons of [2.2]paracyclophane appear at δ 6.47 ppm, whereas those of *p*-xylene are at δ 7.05 ppm, and this shift to lower frequency of 0.58 ppm is a result of shielding from the opposite aromatic ring.[33]

When [2.2]paracyclophane is converted into a metal complex, the aromatic protons of the complexed benzene deck are shifted to lower frequency (see Table 4.6 for some examples), and this effect is very similar to the upfield shifts observed for the aromatic

protons of simple arenes when complexed with transition metals.[54b] The shift of these protons during complexation is undoubtedly a combination of effects such as a rehybridisation of the bound aromatic ring carbons, a loss of ring current, the direct effect of the magnetic anisotropy of the metal atoms, and changes in electron density.[33] It is apparent, however, that upon complexation the aromatic protons of the unbound cyclophane deck also show a shift in value, this time to higher frequency. The distance of these protons from the metal is sufficiently great that direct metal anisotropy effects from the metal should be negligible, and the two obvious effects causing this down field shift involve a loss of ring current in the bound aromatic ring, which causes a decrease in shielding on the opposite deck, and also a loss of electron density in the free aromatic ring due to the electron withdrawal by the metal atom bound to the opposite deck. Unfortunately, since the two benzene decks sit directly over one another in [2.2]paracyclophane, there is no simple method available to confirm the relative importance of these two effects. However, in the case of *anti*-[2.2]metacyclophane such a dissection is possible since there is only partial overlap between the two benzene rings (see Figure 4.6).
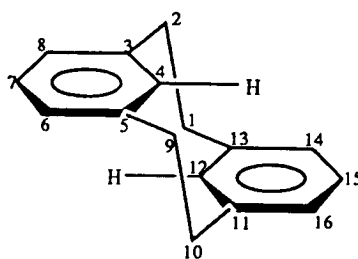
Fig. 4.6: *anti*-[2.2]metacyclophane.

The ^{1}H NMR spectrum of free *anti*-[2.2]metacyclophane shows that the chemical shifts of the internal protons [on C(4) and C(12), δ 4.24 ppm] are strongly shielded by the ring current in the opposite deck, and are influenced to a lesser extent by other factors such as electron density. On the other hand, the end aromatic protons [on C(6), C(7), C(8), C(14), C(15) and C(16)] show an AB_2 pattern that is essentially the same in chemical shift and multiplicity as *m*-xylene [in the range δ 7.08 - 7.28 ppm], and therefore seem to be primarily influenced by electron density, and little affected by changes in the ring current at the opposite deck. Metal complexation of *anti*-[2.2]metacyclophane leads to a normal shift to lower frequency for the AB_2 pattern of the C(6), C(7) and C(8) protons of the metal complexed ring, and as expected the AB_2 pattern of the C(14), C(15) and C(16) protons of the free benzene deck shift to higher frequency; this effect being largely due to a change in charge density as the result of electron transfer to the opposite complexed benzene deck.

However, the signal due to the internal proton at C(12) of the free benzene deck appears at a much higher frequency than those of C(14), C(15) and C(16), and this additional shift to higher frequency must be due to a decreased ring current in the metal-complexed benzene deck.[33]

From these results it may be assumed that for [2.2]paracyclophane the magnetic effects of the unbound ring due to metal complexation at the opposite deck are from both electron-withdrawal and loss of ring current in the metal-bound deck, with other effects such as the direct metal anisotropy of the metal atom or changes in geometry being relatively small.

Table 4.6: ^{1}H NMR values (ppm) of some [2.2]paracyclophane-ruthenium cluster compounds. The values for the free ligand are reported for comparative purposes.

	Free Ring	Bound Ring	Δ
[2.2]paracyclophane - $C_{16}H_{16}$[a]	δ 6.47	δ 6.47	0
$Ru_3(CO)_9(\mu_3\text{-}\eta^2\text{:}\eta^2\text{:}\eta^2\text{-}C_{16}H_{16})$[b] **23**	δ 7.22	δ 3.76	3.46
$Ru_6C(CO)_{14}(\mu_3\text{-}\eta^2\text{:}\eta^2\text{:}\eta^2\text{-}C_{16}H_{16})$[b] **25**	δ 7.44	δ 3.40	4.04
$Ru_8(\mu\text{-}H)_4(CO)_{18}(\eta^6\text{-}C_{16}H_{16})$[b] **27**	δ 6.78	δ 4.51	2.27
$Ru_8(\mu\text{-}H)_2(\mu_6\text{-}\eta^2\text{-}CO)(CO)_{19}(\eta^6\text{-}C_{16}H_{16})$[b] **28**	δ 6.89	δ 4.40	2.49

[a] Values taken from reference 33, [b] Values taken from this work.

Δ = Difference in chemical shifts between the free and coordinated ring protons (ppm).

The ^{1}H NMR chemical shift values (for the ring protons only) for some of the cyclophane-cluster complexes described throughout this chapter are shown in Table 4.6, together with the values of the free ligand for comparison. From the table it is apparent that the difference in chemical shift between the protons of the free and coordinated rings (Δ) is greater when the cyclophane is facially bound than when it is bonded in an η^6 terminal fashion. This is thought to arise because the interaction with three metal atoms of a cluster face causes a greater reduction in ring current, a greater rehybridisation of the bound ring carbons, and also a greater direct effect on the cyclophane from the magnetic anisotropy of the metals. The results also show that for a particular bonding type, namely the face-capping coordination mode, the difference in chemical shift varies as a function of cluster size [3.46 *vs.* 4.04 ppm for **23** and **25**, respectively] and although great care should always be exercised in any correlation of this type, it is reasonable to assume that these changes in shift reflect a change in the electron withdrawing ability of the cluster as its nuclearity is increased. Unfortunately, since no tri- or hexanuclear clusters with η^6 ligands, or even mononuclear Ru(0) cyclophane complexes, are available there is no series of compounds on which to make a similar comparison for cyclophane in the terminal bonding

mode. However, it is likely that the same effects would be observed, especially since benzene has been shown to exhibit a similar behaviour when coordinated in an η^6 fashion to clusters of differing nuclearity (see Chapter three). It therefore appears that ^{1}H NMR spectroscopy is a far more sensitive probe of the electron density on the cluster surface in these systems than, for example, the change in CO stretching vibrations in the infrared spectra.

4.7 Further Reactions

Many attempts to react $Ru_3(CO)_9(\mu_3-\eta^2:\eta^2:\eta^2-C_{16}H_{16})$ **23** further in order to obtain the cluster-cyclophane-cluster or cyclophane-cluster-cyclophane sandwich complexes depicted in Figure 4.7 have been unsuccessful. Synthetic routes have included the thermolysis of **23** with either a quantitative amount of $Ru_3(CO)_{12}$ or with excess [2.2]paracyclophane, respectively, both of which lead to cluster build-up and the formation of $Ru_6C(CO)_{14}(\mu_3-\eta^2:\eta^2:\eta^2-C_{16}H_{16})$ **25**. The chemical activation of **23** using Me_3NO in the presence of [2.2]paracyclophane only leads to cluster decomposition, as do attempts to prepare the *bis*(acetonitrile) derivative, $Ru_3(CO)_7(MeCN)_2(\mu_3-\eta^2:\eta^2:\eta^2-C_{16}H_{16})$, followed by treatment with the cyclophane ligand. Tetrahydro[2.2]paracyclophane[106] has been employed in an attempt to prepare $Ru_3(CO)_9$-[2.2]paracyclophane-$Ru_3(CO)_9$, however, upon coordination of the ligand to one Ru_3 unit, both rings aromatise forming $Ru_3(CO)_9(\mu_3-\eta^2:\eta^2:\eta^2-C_{16}H_{16})$ **23** and therefore preventing coordination to a second cluster. Also, attempts to react $Ru_3(CO)_{10}(MeCN)_2$ with **23** in the hope of displacing the labile MeCN ligands thereby leaving vacant coordination sites on the Ru_3 cluster for attack by the free aromatic ring of **23**, again leads to starting materials and decomposition products only.
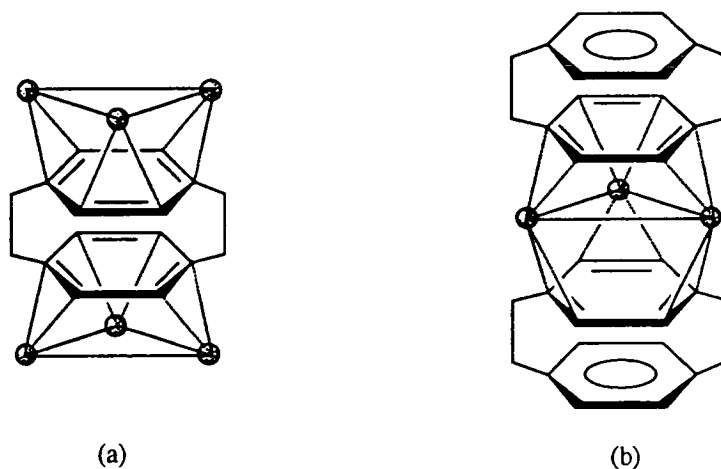

(a)   (b)

Figure 4.7: The (a) $Ru_3(CO)_9$-[2.2]paracyclophane-$Ru_3(CO)_9$ and (b) [2.2]paracyclophane-$Ru_3(CO)_6$-[2.2]paracyclophane sandwich complexes.

It is believed that sandwich complexes of type (a) have yet to be observed because upon coordination to one metal unit the uncoordinated ring is deactivated towards further reaction. This is due to the electron withdrawing character of the metal cluster exerting its influence on both the aromatic ring to which it is coordinated and on the second aromatic nucleus, (as evidenced by ^{1}H NMR). This effect may be overcome by increasing the distance between the rings so that they can both behave as independent units and so form *bis*(complexes). The synthesis of $Ru_3(CO)_6(\mu_3-\eta^2:\eta^2:\eta^2-C_{16}H_{16})_2$ has not been possible owing to the difficulty in removing subsequent carbonyl groups from $Ru_3(CO)_9(\mu_3-\eta^2:\eta^2:\eta^2-C_{16}H_{16})$ **23** without causing extensive decomposition. Since three CO ligands from the parent cluster, $Ru_3(CO)_{12}$, have already been replaced by the weaker π-acid cyclophane ligand in **23** the cluster is electron rich, and therefore removal of further carbonyls would render the cluster unstable and eventually lead to breakdown. It may also be that as more electron density is dispersed onto the remaining nine CO ligands of **23** they become less susceptible to nucleophilic attack, and hence Me_3NO becomes less capable of oxidatively decarbonylating the cluster. This latter effect is reflected by the difference in wavenumber between the main carbonyl stretches in the infrared spectra of the parent cluster, $Ru_3(CO)_{12}$, and those of compound **23**. The infrared spectrum of $Ru_3(CO)_{12}$ shows strong stretches at (υ_{CO}) 2061 and 2029 cm^{-1}, whereas the strongest stretch in the cyclophane species **23** lies at 2024 cm^{-1} indicating a marked increase in back bonding from the metal d-orbitals to the π^* orbitals of the CO ligand.

4.8 Concluding Remarks

[2.2]paracyclophane was initially employed as a ligand with the intention of producing sandwich complexes and precursor sub-units for organometallic cluster polymers. While these objectives have yet to be achieved, many fascinating features have emerged that have previously been unnoticed in the analogous arene chemistry [arene = benzene, toluene, xylene and mesitylene]. Firstly, although paracyclophane has been found to bond in a terminal fashion, it seems to prefer adopting the facial coordination mode, especially in the hexanuclear carbido-cluster $Ru_6C(CO)_{14}(\mu_3-\eta^2:\eta^2:\eta^2-C_{16}H_{16})$ **25**; the reasons for which are unclear but are thought to be essentially electronic in origin. When a second paracyclophane moiety is introduced onto the cluster unit, however, it adopts a terminal site, so preventing the formation of a *bis*(facial) sandwich complex, and showing that the factors which govern the bonding modes adopted by arenes on the cluster surface are still a long way from being fully understood. Secondly, some interesting reaction intermediates have been isolated which shed further light on the mechanisms involved in carbide formation, and bear some relevance to the Fischer-Tropsch reaction that occurs on a metal

surface. The isolation of compounds $Ru_8(\mu\text{-}H)_2(\mu_6\text{-}\eta^2\text{-}CO)(CO)_{19}(\eta^6\text{-}C_{16}H_{16})$ **28** and $Ru_8(\mu_6\text{-}\eta^2\text{-}CO)(\mu_4\text{-}\eta^2\text{-}CO)(CO)_{18}(\eta^6\text{-}C_{16}H_{16})$ **29** not only provide a unique metal framework, but also a new coordination mode for CO in which the ligand bridges six metal atoms and contains a C-O bond length of 1.378(11) Å; possibly the longest observed to date in a cluster compound. Finally ^{1}H NMR has proved a useful and sensitive probe for determining the electron density available for bonding on the cluster surface.

The possibility of forming organometallic dimers and polymers is still a realistic proposition, especially if cyclophane ligands with longer bridges or additional benzene rings are employed. Nonetheless, this work, with its diverse metal frameworks and unique metal-cyclophane interactions, has hopefully demonstrated the potential that cyclophanes have as π-ligands in cluster chemistry, and that as quoted by Cram back in 1970 "the wealth of wondrous chemistry of these beautifully symmetrical compounds, with their bent and battered benzene rings, will be complete only when chemists tire of tinkering with them." [5]

4.9　References

1.　Brown, C.J.; Farthing, A.C.; *Nature (London)*, **1949**, *164*, 915.
2.　Cram, D.J.; Steinberg, H.; *J. Am. Chem. Soc.*, **1951**, *73*, 5691.
3.　Vögtle, F.; Neumann, P.; *Tetrahedron*, **1970**, *26*, 5847.
4.　Kleinschroth, J.; Hopf, H.; *Angew. Chem. Int. Ed. Engl.*, **1982**, *21*, 469.
5.　Cram, D.J.; Cram, J.M.; *Acc. Chem. Res.*, **1971**, *4*, 204.
6.　Boekelheide, V.; *Acc. Chem. Res.*, **1980**, *13*, 65.
7.　Vögtle, F.; *Angew. Chem. Int. Ed. Engl.*, **1969**, *8*, 274.
8.　Boekelheide, V.; Hollins, R.A.; *J. Am. Chem. Soc.*, **1970**, *92*, 3512.
9.　Truesdale, E.A.; Cram, D.J.; *J. Am. Chem. Soc.*, **1973**, *95*, 5825.
10.　Gray, R.; Boekelheide, V.; *Angew. Chem. Int. Ed. Engl.*, **1975**, *14*, 107.
11.　Gilb, W.; Menke, K.; Hopf, H.; *Angew. Chem. Int. Ed. Engl.*, **1977**, *16*, 191.
12.　Kleinschroth, J.; Hopf, H.; *Angew. Chem. Int. Ed. Engl.*, **1979**, *18*, 329.
13.　Schirch, P.F.T.; Boekelheide, V.; *J. Am. Chem. Soc.*, **1979**, *101*, 3125.
14.　Sekine, Y.; Brown, M.; Boekelheide, V.; *J. Am. Chem. Soc.*, **1979**, *101*, 3126.
15.　Brown, C.J.; *J. Chem. Soc.*, **1953**, 3265.
16.　Lonsdale, K.; Milledge, J.J.; Rao, K.V.K.; *Proc. Roy. Soc.*, **1960**, *A255*, 82.
17.　Bekoe, A.D.; Trueblood, K.N.; *Abst. Am. Cryst. Assoc.*, **1964**, *J12*, 87.
18.　Bernstein, J.; Trueblood, K.N.; Hope, H.; *Acta Cryst.*, **1972**, *B28*, 1733.
19.　Gantzel, P.K.; Trueblood, K.N.; *Acta Cryst.*, **1965**, *18*, 958.
20.　(a) Boyd, R.H.; *Tetrahedron*, **1966**, *22*, 119; (b) Shieh, C.; McNally, D.C.; Boyd, R.H.; *Tetrahedron*, **1969**, *25*, 3653.
21.　Hanson, A.W.; *Acta Cryst.*, Sect. B, **1972**, *28*, 2287.
22.　Hanson, A.W.; *Acta Cryst.*, Sect. B, **1977**, *33*, 2003.
23.　Sekine, Y.; Boekelheide, V.; *J. Am. Chem. Soc.*, **1981**, *103*, 1777.
24.　(a) Lindner, H.J.; *Tetrahedron*, **1976**, *32*, 753; (b) Nishiyama, K.; Sakujama, M.; Saki, S.; Horita, H.; Otsubo, T.; Misumi, S.; *Tetrahedron Lett.*, **1977**, 3739.
25.　Sheehan, M.; Cram, D.J.; *J. Am. Chem. Soc.*, **1969**, *91*, 3553.
26.　(a) Vögtle, F.; Hohner, G.; *Top. Curr. Chem.*, **1978**, *1*, 74; (b) Vögtle, F.; *Cyclophane Chemistry*, Wiley, **1993**.
27.　Nakazaki, M.; Yamamoto, Y.; Miura, Y.; *J. Org. Chem.*, **1978**, *43*, 1041.
28.　Bodwell, G.; Ernst, L.; Haenel, M.W.; Hopf, H.; *Angew. Chem. Int. Ed. Engl.*, **1989**, *28*, 455.
29.　Tobe, Y.; Kawaguchi, M.; Kakiuchi, K.; Naemura, K.; *J. Am. Chem. Soc.*, **1993**, *115*, 1173.
30.　Misumi, S.; Otsubo, T.; *Acc. Chem. Res.*, **1978**, *11*, 251.
31.　Umemoto, T.; Otsubo, T.; Misumi, S.; *Tetrahedron Lett.*, **1974**, 1573.
32.　(a) Norinder, U.; Tanner, D.; Wennerström, O.; *Tetrahedron Lett.*, **1983**, *24*, 5411; (b) Pierre, J.L.; Baret, P.; Chautemps, P.; Armand, M.; *J. Am. Chem. Soc.*, **1981**, *103*, 2986.
33.　Laganis, E.D.; Voegeli, R.H.; Swann, R.T.; Finke, R.G.; Hopf, H.; Boekelheide, V.; *Organometallics*, **1982**, *11*, 1415.
34.　Kang, H.C.; Hanson, A.W.; Eaton, B.; Boekelheide, V.; *J. Am. Chem. Soc.*, **1985**, *107*, 1979.
35.　(a) Diederich, F.; *Angew. Chem. Int. Ed. Engl.*, **1988**, *27*, 362; (b) Seel, C.; Vögtle, F.; *Angew. Chem. Int. Ed. Engl.*, **1992**, *31*, 528.
36.　Chan, C.W.; Wong, H.N.C.; *J. Am. Chem. Soc.*, **1985**, *107*, 4790.
37.　Reiser, O.; Reichow, S.; de Meijere, A.; *Angew. Chem. Int. Ed. Engl.*, **1987**, *26*, 1277.
38.　Psiorz, M.; Hopf, H.; *Angew. Chem. Int. Ed. Engl.*, **1982**, *21*, 623.
39.　Hopf, H.; Mlynek, C.; *J. Org. Chem.*, **1990**, *55*, 1361.
40.　Sakurai, H.; Hoshi, S.; Kamiya, A.; Hosomi, A.; Kabuto, C.; *Chem. Lett.*, **1986**, 1781.
41.　Gleiter, R.; Schäfer, W.; Krennrich, G.; Sakurai, H.; *J. Am. Chem. Soc.*, **1988**, *110*, 4117.

42. Sekiguchi, A.; Yatabe, T.; Kabuto, C.; Sakurai, H.; *Angew. Chem. Int. Ed. Engl.*, **1989**, *28*, 757.

43. Cram, D.J.; Wilkinson, D.I.; *J. Am. Chem. Soc.*, **1960**, *82*, 5721.

44. Kai, Y.; Yasuoka, N.; Kasai, N.; *Acta Cryst.*, **1978**, *B34*, 2840.

45. Elschenbroich, C.; Möckel, R.; Zenneck, U.; *Angew. Chem. Int. Ed. Engl.*, **1978**, *17*, 531.

46. Förster, E.; Albrecht, G.; Durselen, W.; Kurras, E.; *J. Organomet. Chem.*, **1969**, *19*, 215.

47. Koray, A.R.; Ziegler, M.L.; Blank, N.E.; Haenel, M.W.; *Tetrahedron Lett.*, **1979**, 2465.

48. Blank, N.E.; Haenel, M.W.; Koray, A.R.; Weidenhammer, K.; Ziegler, M.L.; *Acta Cryst.*, **1980**, *B36*, 2054.

49. Morosin, B.; *Acta Cryst.*, **1974**, *B30*, 838.

50. Elschenbroich, C.; Hurley, J.; Massa, W.; Baum, G.; *Angew. Chem. Int. Ed. Engl.*, **1988**, *27*, 684.

51. Ohno, H.; Horita, H.; Otsubo, T.; Sakata, Y.; Misumi, S.; *Tetrahedron Lett.*, **1977**, 265.

52. Oike, H.; Kai, Y.; Miki, K.; Tanaka, N.; Kasai, N.; *Bull. Chem. Soc. Jpn.*, **1987**, *60*, 1993.

53. Swann, R.T.; Hanson, A.W.; Boekelheide, V.; *J. Am. Chem. Soc.*, **1986**, *108*, 3324.

54. (a) Bennett, M.A.; Matheson, T.W.; *J. Organomet. Chem.*, **1979**, *175*, 87; (b) Bennett, M.A.; Matheson, T.W.; Robertson, G.B.; Smith, A.K.; Tucker, P.A.; *Inorg. Chem.*, **1980**, *19*, 1014.

55. Laganis, E.D.; Finke, R.G.; Boekelheide, V.; *Tetrahedron Lett.*, **1980**, *21*, 4405.

56. (a) Darrensbourg, M.Y.; Muetterties, E.L.; *J. Am. Chem. Soc.*, **1978**, *100*, 7425; (b) Huttner, G.; Lange, S.; *Acta Cryst.*, **1972**, *28*, 2049.

57. Finke, R.G.; Voegeli, R.H.; Laganis, E.D.; Boekelheide, V.; *Organometallics*, **1983**, *2*, 347.

58. Voegeli, R.H.; Kang, H.C.; Finke, R.G.; Boekelheide, V.; *J. Am. Chem. Soc.*, **1986**, *108*, 7010.

59. Plitzko, K.D.; Rapko, B.; Gollas, B.; Wehrle, G.; Weakley, T.; Pierce, D.T.; Geiger, W.E.; Haddon, R.C.; Boekelheide, V.; *J. Am. Chem. Soc.*, **1990**, *112*, 6545.

60. Adams, C.M.; Holt, E.M.; *Organometallics*, **1990**, *9*, 980.

61. Lindner, E.; Wassing, W.; Fawzi, R.; Steimann, M.; *Angew. Chem. Int. Ed. Engl.*, **1994**, *33*, 321.

62. Wilkinson, G.; Rosenblum, M.; Whiting, M.C.; Woodward, R.B.; *J. Am. Chem. Soc.*, **1952**, *74*, 2125.

63. Braga, D.; Dyson, P.; Grepioni, F.; Johnson, B.F.G.; *Chem. Rev.*, **1994**, *94*, 1585.

64. (a) Johnson, B.F.G.; Johnston, R.D.; Lewis, J.; *J. Chem. Soc., Chem. Comm.*, **1967**, 1057; (b) Johnson, B.F.G.; Johnston, R.D.; Lewis, J.; *J. Chem. Soc. (A)*, **1968**, 2865.

65. (a) Johnson, B.F.G.; Lewis, J.; Martinelli, M.; Wright, A.H.; Braga, D.; Grepioni, F.; *J. Chem. Soc., Chem. Comm.*, **1990**, 364; (b) Braga, D.; Grepioni, F.; Johnson, B.F.G.; Lewis, J.; Housecroft, C.E.; Martinelli, M.; *Organometallics*, **1991**, *10*, 1260.

66. (a) Sirigu, A.; Bianchi, M.; Benedetti, E.; *J. Chem. Soc., Chem. Comm.*, **1969**, 596; (b) Braga, D.; Grepioni, F.; Dyson, P.J.; Johnson, B.F.G.; Frediani, P.; Bianchi, M.; Piacento, F.; *J. Chem. Soc., Dalton Trans.*, **1992**, 2565.

67. Braga, D.; Grepioni, F.; Parisini, E.; Johnson, B.F.G.; Martin, C.M.; Nairn, J.G.M.; Lewis, J.; Martinelli, M.; *J. Chem. Soc., Dalton Trans.*, **1993**, 1891.

68. Braga, D.; Grepioni, F.; Parisini, E.; Dyson, P.J.; Blake, A.J.; Johnson, B.F.G.; *J. Chem. Soc., Dalton Trans.*, **1993**, 2951.

69. Owen, S.M.; *Polyhedron*, **1988**, *7*, 253, and references cited therein.

70. (a) Gomez-Sal, M.P.; Johnson, B.F.G.; Lewis, J.; Raithby, P.R.; Wright, A.H.; *J. Chem. Soc., Chem. Comm.*, **1985**, 1682; (b) Dyson, P.J.; Johnson, B.F.G.; Lewis, J.; Martinelli, M.; Braga, D.; Grepioni, F.; *J. Am. Chem. Soc.*, **1993**, *115*, 9062; (c) Dyson, P.J.; Johnson, B.F.G.; Reed, D.; Braga, D.; Grepioni, F.; Parisini, E.; *J. Chem. Soc., Dalton Trans.*, **1993**, 2817.

71. Braga, D.; Grepioni, F.; Sabatino, P.; Dyson, P.J.; Johnson, B.F.G.; Lewis, J.; Bailey, P.J.; Raithby, P.R.; Stalke, D.; *J. Chem. Soc., Dalton Trans.*, **1993**, 985.

72. Orpen, A.G.; XHYDEX, A Program for Locating Hydrides, Bristol University, **1980**; See also Orpen, A.G.; *J. Chem. Soc., Dalton Trans.*, **1980**, 2509.

73. Braga, D.; Grepioni, F.; Parisini, E.; Dyson, P.J.; Johnson, B.F.G.; Reed, D.; Shepherd, D.S.; Bailey, P.J.; Lewis, J.; *J. Organomet. Chem.*, **1993**, *462*, 301.

74. Bailey, P.J.; *J. Organomet. Chem.*, **1991**, *420*, C21.

75. Braye, E.H.; Dahl, L.F.; Hübel, W.; Wampler, D.L.; *J. Am. Chem. Soc.*, **1962**, *84*, 4633.

76. (a) Churchill, M.R.; Wormald, J.; Knight, J.; Mays, M.J.; *J. Am. Chem. Soc.*, **1971**, *93*, 3073; (b) Churchill, M.R.; Wormald, J.; *J. Chem. Soc., Dalton Trans.*, **1974**, 2410.

77. (a) Bradley, J.S.; Ansell, G.B.; Hill, E.W.; *J. Am. Chem. Soc.*, **1979**, *101*, 7417; (b) Bradley, J.S.; Ansell, G.B.; Leonowicz, M.E.; Hill, E.W.; *J. Am. Chem. Soc.*, **1981**, *103*, 4968.

78. (a) Holt, E.M.; Whitmire, K.H.; Shriver, D.F.; *J. Am. Chem. Soc.*, **1982**, *104*, 5621; (b) Holt, E.M.; Whitmire, K.H.; Shriver, D.F.; *J. Organomet. Chem.*, **1981**, *213*, 125.

79. Cowie, A.G.; Johnson, B.F.G.; Lewis, J.; Raithby, P.R.; *J. Organomet. Chem.*, **1986**, *306*, C63.

80. Eady, C.R.; Johnson, B.F.G.; Lewis, J.; Matheson, T.; *J. Organomet. Chem.*, **1975**, *57*, C82.

81. Hayward, C.M.T.; Shapely, J.R.; Churchill, M.R.; Bueno, C.; Rheingold, M.R.; *J. Am. Chem. Soc.*, **1982**, *120*, 7347.

82. Bailey, P.J.; Johnson, B.F.G.; Lewis, J.; McPartlin, M.; Powell, H.R.; *J. Organomet. Chem.*, **1989**, *377*, C17.

83. Hayward, C.M.T.; Shapely, J.R.; *Inorg. Chem.*, **1982**, *21*, 3816.

84. Eady, C.R.; Johnson, B.F.G.; Lewis, J.; *J. Chem. Soc., Dalton Trans.*, **1975**, 2606.

85. Eady, C.R.; Johnson, B.F.G.; Lewis, J.; *J. Organomet. Chem.*, **1973**, *57*, C84.

86. Jackson, P.F.; Johnson, B.F.G.; Lewis, J.; McPartlin, M.; Nelson, W.J.H.; *J. Chem. Soc., Chem. Comm.*, **1981**, 224.

87. Braga, D.; Hendrick, K.; Johnson, B.F.G.; Lewis, J.; McPartlin, M.; Nelson, W.J.H.; Sirioni, A.; Vargas, M.D.; *J. Chem. Soc., Chem. Comm.*, **1985**, 1132.

88. For example: Bradley, J.S.; *Adv. Organomet. Chem.*, **1983**, *22*, 1.

89. (a) Albano, V.G.; Sansoni, M.; Chini, P.; Martinengo, S.; *J. Chem. Soc., Dalton Trans.*, **1973**, 651; (b) Albano, V.G.; Sansoni, M.; Chini, P.; Martinengo, S.; Strumolo, D.; *J. Chem. Soc., Chem. Comm.*, **1972**, 299.

90. Bradley, J.S.; Hill, E.W.; Ansell, G.B.; *J. Organomet. Chem.*, **1980**, *184*, C33.

91. Drake, S.R.; Johnson, B.F.G.; Lewis, J.; *J. Chem. Soc., Dalton Trans.*, **1988**, 1517.

92. (a) Eady, C.R.; Johnson, B.F.G.; Lewis, J.; *J. Organomet. Chem.*, **1972**, *39*, 329; (b) Johnson, B.F.G.; Lewis, J.; Wong, K.; McPartlin, M.; *J. Organomet. Chem.*, **1980**, *185*, C17.

93. Adams, R.D.; Mathur, P.; Segmüller, B.E.; *Organometallics*, **1983**, *2*, 1258.

94. (a) Herrmann, W.A.; *Angew. Chem. Int. Ed. Engl.*, **1982**, *21*, 117; (b) Muetterties, E.L.; Stein, J.; *Chem. Rev.*, **1979**, *79*, 479.

95. Ho, S.V.; Harriot, P.; *J. Catal.*, **1980**, *64*, 272.

96. Manassero, M.; Sansoni, M.; Longoni, G.; *J. Chem. Soc., Chem. Comm.*, **1976**, 919.

97. (a) Whitmire, K.; Shriver, D.F.; *J. Am. Chem. Soc.*, **1980**, *102*, 1456; (b) Whitmire, K.; Shriver, D.F.; *J. Am. Chem. Soc.*, **1981**, *103*, 6754.

98. (a) Shinn, N.D.; Madley, T.E.; *J. Chem. Phys.*, **1985**, *83*, 5928; (b) Moon, D.W.; Bernasek, S.L.; Dwyer, D.J.; Gland, J.L.; *J. Am. Chem. Soc.*, **1985**, *107*, 4364; (c) Hoffmann, F.M.; de Paola, R.A.; *Surf. Sci.*, **1985**, *154*, L261.

99. Chisholm, M.H.; Hammond, C.E.; Johnston, V.J.; Streib, W.E.; Huffman, J.C.; *J. Am. Chem. Soc.*, **1992**, *114*, 7056.

100. Gates, B.C.; *Angew. Chem. Int. Ed. Engl.*, **1993**, *32*, 228.

101. Muetterties, E.L.; *Bull. Soc. Chim. Belg.*, **1975**, *84*, 959; *ibid* **1976**, *85*, 451.

102. Deeming, A.J.; in *Transition Metal Clusters*, Ed. Johnson, B.F.G.; Wiley, New York, **1980**.

103. (a) Anson, C.E.; Bailey, P.J.; Conole, G.; Johnson, B.F.G.; Lewis, J.; McPartlin, M.; Powell, H.R.; *J. Chem. Soc., Chem. Comm.*, **1989**, 442; (b) Bailey, P.J.; Duer, M.J.; Johnson, B.F.G.; Lewis, J.; Conole, G.; McPartlin, M.; Powell, H.R.; Anson, C.E.; *J. Organomet. Chem.*, **1990**, *383*, 441.

104. (a) Herrmann, W.A.; Ziegler, M.L.; Windenhammer, K.; Biersack, H.; *Angew. Chem. Int. Ed. Engl.*, **1979**, *18*, 960; (b) Herrmann, W.A.; Biersack, H.; Ziegler, M.L.; Windenhammer, K.; Siegel, R.; Rehder, D.; *J. Am. Chem. Soc.*, **1981**, *103*, 1692.

105. Dyson, P.J.; *Personal Communication.*

106. Zahn, T.; Ziegler, M.L.; *Acta Cryst.*, **1986**, *C42*, 494.

Chapter Five

The Reactivity of Some [2.2]Paracyclophane Clusters of Ruthenium

This chapter commences with a brief résumé outlining the reactivity of arene carbonyl clusters, especially $Os_3(CO)_9(\mu_3-\eta^2:\eta^2:\eta^2-C_6H_6)$, towards nucleophilic addition and carbonyl substitution. Following this a series of reactions performed on the trinuclear and hexanuclear-carbido cyclophane clusters, $Ru_3(CO)_9(\mu_3-\eta^2:\eta^2:\eta^2-C_{16}H_{16})$ **23** and $Ru_6C(CO)_{14}(\mu_3-\eta^2:\eta^2:\eta^2-C_{16}H_{16})$ **25**, are detailed. This study involves a new type of reaction in which the clusters undergo a *controlled* degradation by reaction with Me_3NO only, and by this method a diruthenium complex with a $\mu_2-\eta^3:\eta^3$ bridging cyclophane moiety has been produced which serves as an excellent model for a proposed intermediate in arene migration, and also has some relevance to the chemisorption of benzene on the metal surface. Carbonyl substitution by acetylenes and phosphines is also examined, and a comparison between chemical and thermal activation techniques is critically assessed. A highly unusual by-product, *viz.* $Ru_2(CO)_6(\{\mu_2-\eta^1:\eta^2-C_2Ph_2\}_2-CO)$, has been isolated which is thought to be the first example of a complex in which two acetylene units are linked by a carbonyl group, and a mechanism for its formation is proposed. The synergic nature of [2.2]paracyclophane is demonstrated by its application as an effective electronic probe in recognising changes in coordination mode, cluster nuclearity and the presence of additional ligands, as assessed by ^1H NMR spectroscopy. Two complexes have been isolated in which the [2.2]paracyclophane moiety adopts a coordination mode previously unobserved in arene cluster chemistry. These bonding modes have been established in the solid-state as $\mu_3-\eta^1:\eta^2:\eta^2$ in $Ru_4(CO)_9(\eta^4-C_6H_8)(\mu_3-C_{16}H_{16})$ and *pseudo* $\mu_3-\eta^1:\eta^1:\eta^1$ in $Ru_6C(CO)_{12}(\mu_2-\eta^2:\eta^2-C_6H_8)(\mu_3-C_{16}H_{16})$, the latter of which is comparable to an adsorption mode of benzene on a metal surface. Lastly, two isomeric butterfly clusters containing [2.2]paracyclophane in the terminal and facial coordination modes are described and compared with the analogous benzene system.

5.1 An Introduction

Detailed studies of the reactivity of arene carbonyl clusters has mainly centred on the trinuclear benzene clusters, $M_3(CO)_9(\mu_3-\eta^2:\eta^2:\eta^2-C_6H_6)$ (M = Ru, Os), with particular emphasis paid to the osmium complex owing to its increased stability over the ruthenium analogue.[1] These reactions fall into two main categories; namely, substitution reactions on the metal framework, and nucleophilic attack at the benzene ring.

The substitution reactions generally involve activation of the cluster by replacing CO with a "labile" ligand, typically acetonitrile, followed by subsequent displacement of this ligand for an appropriate group; a technique which is well documented throughout transition metal carbonyl chemistry. For example, the activated benzene cluster, $Os_3(CO)_8(MeCN)(\mu_3-\eta^2:\eta^2:\eta^2-C_6H_6)$, can be isolated from the reaction of equimolar quantities of $Os_3(CO)_9(\mu_3-\eta^2:\eta^2:\eta^2-C_6H_6)$ and Me_3NO in acetonitrile. Two-electron donor ligands L (*e.g.* L = CO, PR_3, alkenes *etc.*) readily displace the labile MeCN group forming derivatives of the type $Os_3(CO)_8(L)(\mu_3-\eta^2:\eta^2:\eta^2-C_6H_6)$ which retain the face-capping benzene ligand.[2,3] Alternatively, the acetonitrile intermediate may be by-passed and direct CO substitution may occur either by using Me_3NO in a non-coordinating solvent containing the appropriate ligand, or simply by thermolysis in the presence of excess ligand.

Apart from substitution reactions at the cluster framework, the reactivity of the μ_3 benzene ligand in this triosmium complex has also been probed.[4] The ability of certain transition-metal centres to activate normally unreactive π-hydrocarbons towards nucleophilic attack is well known,[5] and it has been illustrated, for example, that metal clusters exert a powerful electron withdrawing influence on an arene ligand when coordinated in a face-capping bonding mode.[4] This enhances the acidity of the arene hydrogens and thus, activates the ring towards nucleophilic addition as opposed to the characteristic electrophilic substitution reactions that "free" benzene undergoes. The complex $Os_3(CO)_9(\mu_3-\eta^2:\eta^2:\eta^2-C_6H_6)$ reacts rapidly with good hydride donors (*e.g.* $Li(BHEt_3)$ or $[NEt_4][BH_4]$) in tetrahydrofuran at -78°C, affording the anionic, triply-bridging cyclohexadienyl cluster, $[Os_3(CO)_9(\mu_3-\eta^1:\eta^2:\eta^2-C_6H_7)]^-$, stabilised as the $[N(PPh_3)_2]^+$ salt. Abstraction of a hydride from this anionic cluster is possible by treatment with $[Ph_3C][BF_4]$ in dichloromethane at -78°C, regenerating the benzene cluster, $Os_3(CO)_9(\mu_3-\eta^2:\eta^2:\eta^2-C_6H_6)$.[1] Alternatively, the anionic complex can be protonated with $HBF_4.Et_2O$ to produce the neutral hydrido-dienyl complex, $Os_3(\mu-H)(CO)_9(\mu_3-\eta^1:\eta^2:\eta^2-C_6H_7)$. Treatment of this dienyl cluster with $[Ph_3C][BF_4]$ yields the cationic benzene complex, $[Os_3(\mu-H)(CO)_9(\mu_3-\eta^2:\eta^2:\eta^2-C_6H_6)]^+$,[6] which can also be generated from $Os_3(CO)_9(\mu_3-\eta^2:\eta^2:\eta^2-C_6H_6)$ by treatment with $HBF_4.Et_2O$.[4] This latter reaction can be reversed, and treatment with DBU (1,8-diazabicyclo[5.4.0]undeca-7-ene) abstracts a proton from the cationic cluster, $[Os_3(\mu-H)(CO)_9(\mu_3-\eta^2:\eta^2:\eta^2-C_6H_6)]^+$, to produce the original neutral benzene cluster, $Os_3(CO)_9(\mu_3-\eta^2:\eta^2:\eta^2-C_6H_6)$.[6]

$Os_3(CO)_9(\mu_3-\eta^2:\eta^2:\eta^2-C_6H_6)$ also undergoes reaction with methyl- or phenyl-lithium in tetrahydrofuran at -78°C, affording the functionalised cyclohexadienyl complexes, $[Os_3(CO)_9(\mu_3-\eta^1:\eta^2:\eta^2-C_6H_6R)]^-$ (R=Me or Ph), as a result of *exo*-addition which can be isolated as the $[N(PPh_3)_2]^+$ salts. Further treatment using $HBF_4.Et_2O$ results in protonation, yielding the neutral edge-bridging hydrido cluster, $Os_3(\mu-H)(CO)_9(\mu_3-$

$\eta^1:\eta^2:\eta^2$-C$_6$H$_6$R). The functionalised anionic cyclohexadienyl complexes also react cleanly with electrophiles such as [Au(PEt$_3$)]$^+$ to afford the species Os$_3$(CO)$_9${Au(PEt$_3$)}(μ_3-$\eta^1:\eta^2:\eta^2$-C$_6$H$_6$R) (R=Me and Ph) in which electrophilic attack of the gold phosphine cation occurs at the metal triangle.[4]

This series of reactions are summarised in Scheme 5.1, and demonstrate that the reactivity of the face-capping arene ligand in cluster compounds towards nucleophilic addition is remarkably similar to that of the η^6 arene ligand in mononuclear complexes.
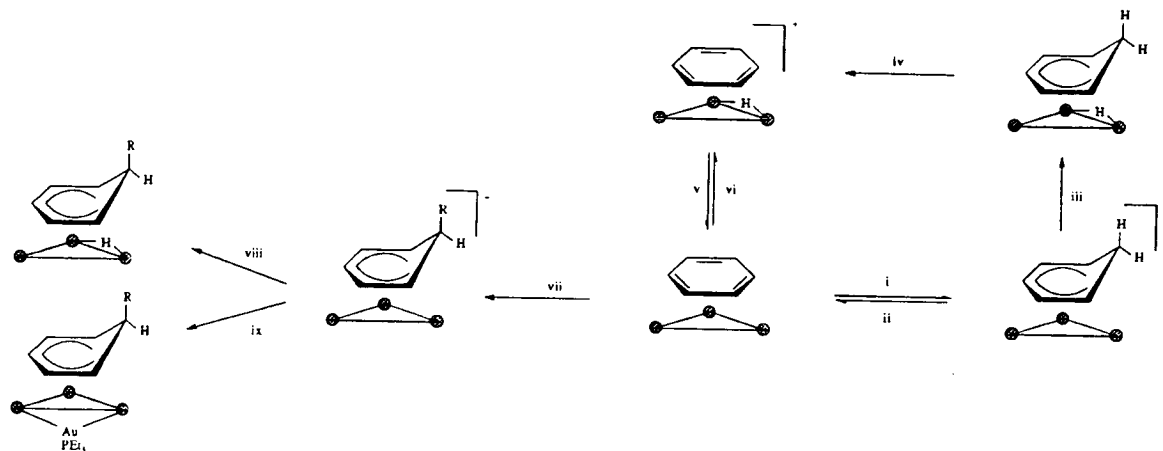
Scheme 5.1: The reactivity of the μ_3-benzene ligand in Os$_3$(CO)$_9$(μ_3-$\eta^2:\eta^2:\eta^2$-C$_6$H$_6$): (i) Li(BHEt$_3$) or [NEt$_4$][BH$_4$]; (ii) [Ph$_3$C][BF$_4$]; (iii) HBF$_4$.Et$_2$O; (iv) [Ph$_3$C][BF$_4$]; (v) HBF$_4$.Et$_2$O; vi) DBU; (vii) LiMe or LiPh; (viii) HBF$_4$.Et$_2$O; (ix) [Au(PEt$_3$)]$^+$.

In contrast, [2.2]paracyclophane has been shown to display only a very limited reactivity towards nucleophiles when coordinated to a mononuclear transition metal centre.[7] The reactivity and size of paracyclophane make it an effective 'blocking agent', exerting steric as opposed to kinetic control over reaction products.[8] Indeed, even poorly electrophilic arenes such as hexamethylbenzene display a significant reactivity towards nucleophiles when complexed with metal-paracyclophane fragments.[7] It has been established that single nucleophilic additions readily occur at the arene ligands in a range of complexes of formula [Ru(η^6-arene)(η^6-[2.2]paracyclophane)]$^{2+}$, however, paracyclophane may also direct double nucleophilic additions onto other arenes when coordinated to the same metal centre. For example, the action of the reducing agent Red-Al on the cations [Ru(η^6-arene)(η^6-[2.2]paracyclophane)]$^{2+}$ (arene = C$_6$H$_6$ and C$_6$Me$_6$) results in the formation of the ruthenium(0) 1,3-diene compound [Ru(η^4-C$_6$H$_8$)(η^6-C$_{16}$H$_{16}$)] and the 1,4-diene compound [Ru(η^4-C$_6$Me$_6$H$_2$)(η^6-C$_{16}$H$_{16}$)], respectively.[9]

These reactions differ to those in which double nucleophilic addition to $[Ru(\eta^6\text{-arene})_2]^{2+}$ cations give $[Ru(\text{cyclohexadienyl})_2]^{2+}$ species.[10]

The reactivity of the [2.2]paracyclophane ligand has yet to be examined when complexed to a metal cluster, however, several CO substitution reactions at the metal framework of the trinuclear and hexanuclear-carbido cyclophane clusters, $Ru_3(CO)_9(\mu_3\text{-}\eta^2\text{:}\eta^2\text{:}\eta^2\text{-}C_{16}H_{16})$ **23** and $Ru_6C(CO)_{14}(\mu_3\text{-}\eta^2\text{:}\eta^2\text{:}\eta^2\text{-}C_6H_6)$ **25**, have been carried out. The products from these reactions are described in the following text and comparisons are made to the analogous benzene chemistry where appropriate.

5.2 Degradative Reactions using Me₃NO: The Molecular Structure of $Ru_2(CO)_6(\mu_2\text{-}\eta^3\text{:}\eta^3\text{-}C_{16}H_{16})$ 30

Trimethylamine *N*-oxide has been used extensively as an oxidative decarbonylation reagent (removing CO as CO_2) throughout the work described in the preceding chapters. This reagent can be used in combination with a coordinating solvent, typically acetonitrile, which may be displaced by the appropriate ligand in a subsequent step (see Chapter two), or alternatively, Me₃NO may be used in a non-coordinating solvent containing the appropriate ligand so that direct substitution takes place (see Chapters two and three). It is believed that employing Me₃NO as a reagent to bring about cluster degradation has not been previously recognised, and when reacted with a cluster in a non-coordinating solvent it can be envisaged that the loss of CO results in the formation of an unstable, unsaturated cluster unit which, if in the absence of an appropriate ligand, may lead to the *controlled degradation* of the parent compound.

Chapter four describes how the reaction of $Ru_6C(CO)_{14}(\mu_3\text{-}\eta^2\text{:}\eta^2\text{:}\eta^2\text{-}C_{16}H_{16})$ **25** with a large excess of Me₃NO in dichloromethane affords the trinuclear cluster, $Ru_3(CO)_9(\mu_3\text{-}\eta^2\text{:}\eta^2\text{:}\eta^2\text{-}C_{16}H_{16})$ **23**, in modest yield. In a similar fashion, three molecular equivalents of Me₃NO in dichloromethane are added dropwise to a solution of **23**, also in dichloromethane, at -78°C. Slowly warming to room temperature results in the formation of a dinuclear species, $Ru_2(CO)_6(\mu_2\text{-}\eta^3\text{:}\eta^3\text{-}C_{16}H_{16})$ **30**, which can be isolated from the reaction mixture by t.l.c. using a solution of dichloromethane-hexane (2:3, v/v) as eluent. These reactions are illustrated in Scheme 5.2.1.

The molecular formula of **30** was initially proposed as $Ru_2(CO)_6(\mu_2\text{-}\eta^3\text{:}\eta^3\text{-}C_{16}H_{16})$ on evidence provided by mass, infrared and ¹H NMR spectroscopy. The mass spectrum exhibits a strong parent peak at m/z 579 (calc. 579) followed by the loss of six carbonyl groups in succession. The infrared spectrum is devoid of bands in the carbonyl bridging region, only showing peaks between 2060 and 1950 cm⁻¹ that are typical of terminally bonded CO, and the ¹H NMR spectrum in $CDCl_3$ exhibits signals at δ 7.06 (s),

3.59 (s), 2.93 (m) and 2.56 (m) ppm with equal relative intensities; this pattern being consistent with the presence of a coordinated paracyclophane moiety. The singlet
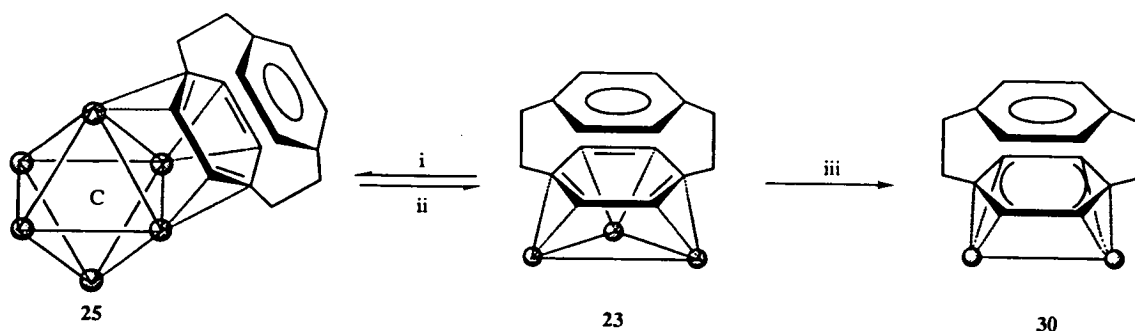
Scheme 5.2.1: Reactions of 23 involving a change in nuclearity. Reagents and conditions; (i) Δ, $Ru_3(CO)_{12}$/octane, (ii) 10 mol. eq. Me_3NO/CH_2Cl_2, (iii) 3 mol. eq. Me_3NO/CH_2Cl_2.

resonances at δ 7.06 and 3.59 ppm can be attributed to the four aromatic protons of the unattached and coordinated rings, respectively, and as emphasised in Chapter four, these signals are again shifted to higher and lower frequency than the degenerate aromatic C-H proton signal found in the free ligand (δ 6.47 ppm). It is interesting to note that the difference between these two singlets (3.47 ppm) is greater than that observed for an η^6 bound cyclophane ligand [*cf.* 2.27 ppm for $Ru_8(\mu\text{-}H)_4(CO)_{18}(\eta^6\text{-}C_{16}H_{16})$ 27], but is similar to that found when cyclophane coordinates facially [*cf.* 3.46 ppm in $Ru_3(CO)_9(\mu_3\text{-}\eta^2:\eta^2:\eta^2\text{-}C_{16}H_{16})$ 23 and 4.04 ppm for $Ru_6C(CO)_{14}(\mu_3\text{-}\eta^2:\eta^2:\eta^2\text{-}C_{16}H_{16})$ 25], thus suggesting interaction of the cyclophane with both metal atoms. The remaining two resonances, observed at δ 2.93 and 2.56 ppm, are multiplets showing typical AA'BB' couplings which can be associated with the bridging CH_2 protons.

The formulation of $Ru_2(CO)_6(\mu_2\text{-}\eta^3:\eta^3\text{-}C_{16}H_{16})$ 30 from spectroscopic data was verified by a single crystal X-ray diffraction analysis, using a crystal grown by vapour diffusion from dichloromethane-pentane at room temperature. The solid-state structure of 30 is shown in Figure 5.2.1, accompanied by some relevant structural parameters.

The most important feature of this molecule is the manner in which the paracyclophane moiety bridges the two metal centres, with each ruthenium atom interacting with three carbon atoms of the bonded ring. A close examination of this $\mu_2\text{-}\eta^3:\eta^3$ interaction reveals that the coordinated ring adopts a boat conformation with an angle between the two enyl-planes defined by C(1C)-C(6C)-C(5C) and C(2C)-C(3C)-C(4C) of 56°. A similar bonding mode has previously been observed in the dirhodium complex, $Rh_2(Cp)_2(\mu_2\text{-}\eta^3:\eta^3\text{-}C_6H_6)$,[11] which also exhibits deviations from planarity towards a boat-shaped conformation, with the angle of 53° between the two η^3-enyl planes of the benzene unit being of a similar magnitude to that found in 30. Although the rings in free [2.2]paracyclophane already adopt a boat conformation, the angle between the two enyl

planes is only 23°,[12] thus indicating a dramatic change upon coordination to the dimetallic unit; a feature which is rather unusual for aromatic systems. It would appear from these observations that significant deviations from planarity and hence different hybridisation states of the ring C-atoms are essential for an efficient overlap between the metal and ligand orbitals, which is necessary for a stable $\eta^3:\eta^3$ interaction between the organic ring and the two metal atoms. In this connection it is also worth noting that the mean C-C bond lengths of the enyl sections of the ring, *viz.* C(1C)-C(6C), C(5C)-C(6C), C(2C)-C(3C) and C(3C)-C(4C) are shorter than the C-C bonds linking the two enyl units, *viz.* C(1C)-C(2C) and C(4C)-C(5C) [mean 1.414(10) *vs.* 1.484(10) Å, respectively], (see Figure 5.2.2). In the free [2.2]paracyclophane ligand, and the unattached ring in $Ru_2(CO)_6(\mu_2\text{-}\eta^3:\eta^3\text{-}C_{16}H_{16})$ **30** there is no recognisable pattern of long and short C-C bond lengths; the mean distance in the rings being 1.385 Å and 1.390(11) Å, respectively.
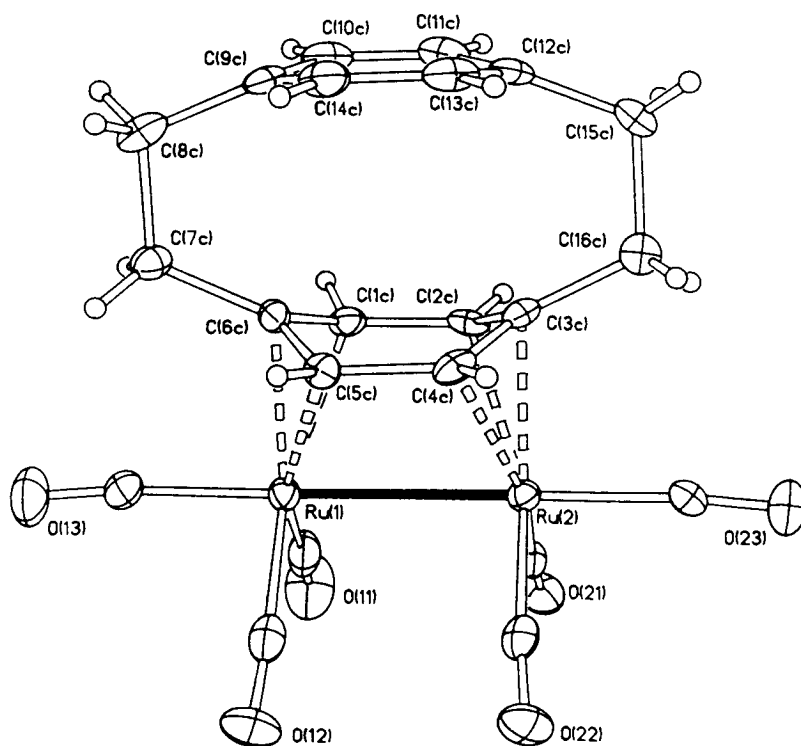
Figure 5.2.1: The molecular structure of $Ru_2(CO)_6(\mu_2\text{-}\eta^3:\eta^3\text{-}C_{16}H_{16})$ **30** in the solid-state. The C-atoms of the CO ligands bear the same numbering as the corresponding O-atoms. Principal bond parameters (Å) are: Ru(1)-Ru(2) 2.838(3), mean Ru-C(CO) 1.916, mean C-O(CO) 1.145, Ru(1)-C(1C) 2.264(7), Ru(1)-C(5C) 2.295(7), Ru(1)-C(6C) 2.191(7), Ru(2)-C(2C) 2.278(7), Ru(2)-C(3C) 2.187(7), Ru(2)-C(4C) 2.253(7), C(1C)-C(2C) 1.481(10), C(1C)-C(6C) 1.437(10), C(2C)-C(3C) 1.399(10), C(3C)-C(4C) 1.412(10), C(3C)-C(16C) 1.541(10), C(4C)-C(5C) 1.486(10), C(5C)-C(6C) 1.408(10), C(6C)-C(7C) 1.529(10), C(7C)-C(8C) 1.569(10), C(8C)-C(9C) 1.505(11), C(9C)-C(10C) 1.393(11), C(9C)-C(14C) 1.398(11), C(10C)-C(11C) 1.380(12), C(11C)-C(12C) 1.408(11), C(12C)-C(13C) 1.389(11), C(12C)-C(15C) 1.498(11), C(13C)-C(14C) 1.372(11), C(15C)-C(16C) 1.564(10).
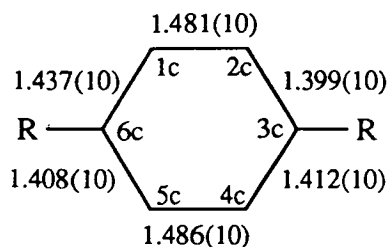
Figure 5.2.2: Plan view of the coordinated ring showing the distribution of bond lengths: C-C bonds within the enyl-groups are shorter than those linking the two enyl-units.

The high quality of the low temperature data collected in this X-ray analysis has enabled location of the ring hydrogens, and in the coordinated ring all four hydrogen atoms are observed to bend out of the plane defined by C(1C), C(2C), C(4C) and C(5C) and away from the ruthenium atoms by a mean displacement of 0.20(8) Å. This bending of the arene C-H bonds either towards or away from the metal unit has been observed on numerous occasions.[13] It can be ascribed to a reorientation of the ring π orbitals in order to achieve maximum overlap with suitable metal orbitals, and a similar bending has been rationalised in terms of molecular orbital theory.[14]

The distortions described above for the coordinated cyclophane ring are not observed in the unattached ring. Infact they are slightly reversed, with the ring approaching planarity and the angle between the two enyl planes of 18° being less than in the free ligand itself (*cf.* 23°). Also the hydrogen atoms lie in the plane defined by C(10C), C(11C), C(13C) and C(14C) [mean deviation = 0.05(8) Å]. An interpretation of the variations in structural features between the two rings of the cyclophane moiety is not easy but, as previously pointed out by ^{1}H NMR, suggests that they act in synchrony with an increased boat-shaped deformation in one ring resulting in the second ring becoming more planar.

The central carbon atoms of the enyl units, C(3C) and C(6C), lie almost directly above the two ruthenium atoms, and their Ru-C distances of 2.187(7) and 2.191(7) Å respectively, are notably shorter than the remaining four bonds [mean 2.273(7) Å]. The metal-metal bond length is 2.838(3) Å, and each ruthenium atom also carries one axial and two equatorial terminal carbonyl ligands. Compound **30** contains 34 valence shell electrons and is therefore consistent with the EAN rule.

There are several examples in arene carbonyl clusters of ruthenium and osmium where the arene ligand undergoes migration, either reversibly or irreversibly, from a facial to a terminal site or *vice-versa*,[15] or even from one η^6 site to another [as in the square-pyramidal cluster $Ru_5C(CO)_{12}(C_6H_6)$ where the benzene migrates from the apical η^6 position to an η^6 site on a basal ruthenium atom],[16] and such migrations can be initiated by thermal, photochemical or chemical influences. Although the precise mechanisms by which

these isomerisations occur has not been established, kinetic analyses have confirmed, in the case of $Ru_5C(CO)_{12}(C_6H_6)$, that the process is non-dissociative and takes place *via* an *intra*molecular reaction mechanism.[17] It is possible that these migrations may occur *via* arene slippage from a terminal η^6 position onto a M-M edge and then either across onto a trimetallic face or onto an alternative single metal atom, and such slippages would also require the simultaneous concerted movement of the carbonyl ligands. As yet a reaction transition state or intermediate in these isomerisations has not been isolated, however the possibility that a μ_2-η^3:η^3 type interaction occurs between the arene and a M-M edge of the cluster unit is easily envisaged and seems a reasonable explanation. To date, the edge-bridged *bis*(allyl) bonding mode has not been observed in a cluster complex, however the isolation of $Ru_2(CO)_6(\mu_2$-η^3:η^3-$C_{16}H_{16})$ **30** provides an excellent model for this proposed migratory intermediate (see Scheme 5.2.2).

η^6 $\qquad\qquad$ μ_2-η^3:η^3 $\qquad\qquad$ μ_3-η^2:η^2:η^2
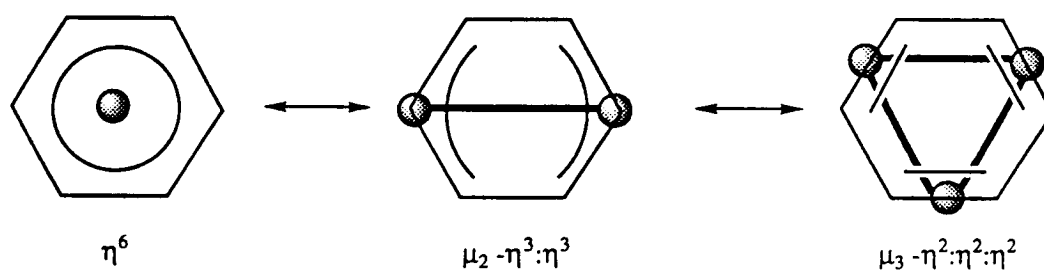
Scheme 5.2.2: The proposed migration of benzene on a cluster surface from a terminal site to a face-capping position and *vice-versa*, *via* an edge-bridging μ_2-η^3:η^3 intermediate.

The complex $Ru_2(CO)_6(\mu_2$-η^3:η^3-$C_{16}H_{16})$ **30** also provides an attractive model for the established surface chemistry of benzene. As described in the introductory chapter, benzene has been observed on a close packed, atomically flat metal surface in a variety of adsorption sites; one of which is the so-called 'bridge' site, having two-fold local symmetry (C_{2v}).[18] This bridge site is occupied by benzene molecules on a number of metal surfaces, and has a similar bonding type to that observed in compound **30**. However, whereas in **30**, the two ruthenium atoms are eclipsed by carbon atoms thus adopting a μ_2-η^3:η^3 coordination mode with four short and two long C-C bonds, on the Pd(111),[19] Rh(111),[20] and Pt(111),[21a] crystal faces, in the presence of coadsorbed CO, the two metal atoms are generally eclipsed by C-C bonds, hence resulting in essentially two short and four long C-C bonds and more of a μ_2-η^2:η^2 interaction. Figure 5.2.3 (a) illustrates this bonding situation for the Pt(111)/2C_6H_6/4CO metal surface, however the relatively large error bars of $\pm$ 0.15 Å associated with the C-C bonds of the chemisorbed ring must be kept in mind, and therefore the differences in bond length may not be of any real significance. This bonding

situation is therefore not directly comparable to that observed in the dinuclear complex **30**, and a 'bridge' site of this type has yet to be established in a cluster compound. Recently, the surface structure of benzene in a disordered monolayer on Pt(111) has been established [note that the chemisorbed benzene layer remains disordered in the absence of coadsorbed CO] and displays a bonding interaction which is accurately modelled by that found in $Ru_2(CO)_6(\mu_2\text{-}\eta^3\text{:}\eta^3\text{-}C_{16}H_{16})$ **30**,[21b] *i.e.* two *para* carbon-atoms of the benzene ring sit directly above two surface metal atoms, resulting in these two carbons being situated closer to the metal surface than the other four. There is also evidence to suggest that the benzene buckles to assume a boat-like configuration, and it appears that there are essentially four short and two long C-C bonds within the ring [1.45 *vs.* 1.63 Å] which is reminiscent of the $\mu_2\text{-}\eta^3\text{:}\eta^3$ interaction, although as before, large error bars must be considered. This situation is illustrated in Figure 5.2.3 (b).
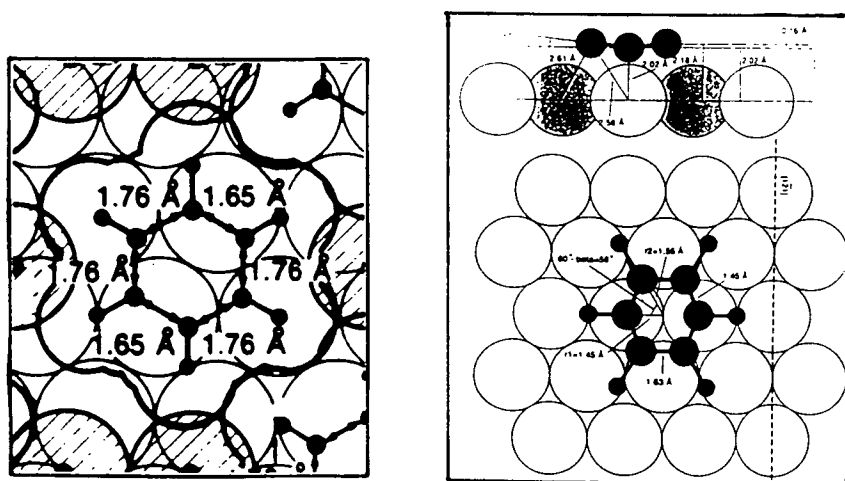
Figure 5.2.3: The surface structure of benzene on the Pt(111) crystal face: (a) when coadsorbed with CO that induces ordering, and (b) in the absence of coadsorbed CO which causes disordering.

The coordination mode present in **30** therefore serves as a molecular model for the chemisorption of benzene at a bridge site, and is postulated as a transition state in the migration of arenes on the cluster surface. The migration of benzene across a metal surface is important with respect to catalysis, however, little is known about the mechanisms involved in such processes and therefore this $\mu_2\text{-}\eta^3\text{:}\eta^3$ type interaction may prove useful in future work.

It is clear from this discussion that attack by Me_3NO on $Ru_3(CO)_9(\mu_3\text{-}\eta^2\text{:}\eta^2\text{:}\eta^2\text{-}C_{16}H_{16})$ **23** selectively removes one Ru moiety from the triangular cluster. Although it is difficult to monitor the reaction pathway of this degradative process, it would appear that

attack of the Me$_3$NO occurs selectively at the same Ru(CO)$_3$ site. This concept certainly raises interesting synthetic possibilities since the scope and applicability of the reaction are very general and could be employed in the *controlled* degradation of a whole range of other cluster systems.

5.3   Reaction with Alkynes: The Molecular Structures of Ru$_3$(CO)$_7$(μ_3-η^1:η^2:η^1-C$_2$Ph$_2$)(η^6-C$_{16}$H$_{16}$) 31 and Ru$_2$(CO)$_6$({μ_2-η^1:η^2-C$_2$Ph$_2$}$_2$-CO) 33

On reaction with alkynes, the benzene cluster M$_3$(CO)$_9$(μ_3-η^2:η^2:η^2-C$_6$H$_6$) (M = Ru, Os) yields compounds in which the benzene has undergone migration from a face-capping to a terminal site and the alkyne adopts the facial position. The only difference between the corresponding reactions of the ruthenium and osmium derivatives is that in the case of the ruthenium complex, a carbonyl group is inserted between the alkyne ligand and the metal atom carrying the benzene moiety, [see Figures 5.3 (a) and (b), respectively].[22]

As already outlined, the triosmium benzene cluster, Os$_3$(CO)$_9$(μ_3-η^2:η^2:η^2-C$_6$H$_6$), readily undergoes reaction with Me$_3$NO in the presence of MeCN to produce the activated species Os$_3$(CO)$_8$(MeCN)(μ_3-η^2:η^2:η^2-C$_6$H$_6$), in which the labile acetonitrile ligand is easily displaced by two electron donors to afford complexes of the type Os$_3$(CO)$_8$(L)(μ_3-η^2:η^2:η^2-C$_6$H$_6$).[2] Substitution of MeCN with ethylene or styrene affords π-bound alkene complexes of formula Os$_3$(CO)$_8$(η^2-CH$_2$.CHR)(μ_3-η^2:η^2:η^2-C$_6$H$_6$) (R = H and Ph). The molecular structure of the ethylene derivative has been established by X-ray diffraction and is based upon that of Os$_3$(CO)$_9$(μ_3-η^2:η^2:η^2-C$_6$H$_6$) with an equatorial carbonyl group being replaced by a symmetrically coordinated ethylene molecule which is slightly displaced from the metal plane towards the benzene ring. Variable temperature ^{1}H and ^{13}C NMR, and ^{13}C 2D-exchange spectroscopy show that Os$_3$(CO)$_8$(η^2-CH$_2$CH$_2$)(μ_3-η^2:η^2:η^2-C$_6$H$_6$) undergoes five fluxional processes in solution.[3,23] The two tricarbonyl units undergo localised 'turnstile' rotation; a trigonal-twist process allows movement of the alkene between equatorial sites within the Os(CO)$_2$(CH$_2$CH$_2$) unit; a Cramer-type alkene rotation also occurs about the Os-(C$_2$H$_4$) axis; and lastly a 1,2-ring hopping motion permutes the nuclei of the μ_3 benzene ligand. These rearrangements are all *intra*molecular and in combination have been described as 'helicopter-like' motions.

Os$_3$(CO)$_8$(η^2-CH$_2$CH$_2$)(μ_3-η^2:η^2:η^2-C$_6$H$_6$) may undergo further reaction with Me$_3$NO-MeCN to produce the activated cluster, Os$_3$(CO)$_7$(MeCN)(η^2-CH$_2$CH$_2$)(μ_3-η^2:η^2:η^2-C$_6$H$_6$). This activated species readily reacts with alkynes (C$_2$RR') in dichloromethane at room temperature to yield complexes of the formula Os$_3$(CO)$_7$(μ_3-η^1:η^2:η^1-RC$_2$R')(η^6-C$_6$H$_6$) (R=R'=H, Ph or Me; R=H, R'=Ph; R=Me, R'=Et) in which the benzene is now bonded to a single osmium atom.[22,24] In contrast, the analogous ruthenium

compound, $Ru_3(CO)_9(\mu_3-\eta^2:\eta^2:\eta^2-C_6H_6)$, reacts directly with similar alkynes by heating in dichloromethane under reflux to yield $Ru_3(CO)_7(\mu_3-\eta^2-RC_2R'CO)(\eta^6-C_6H_6)$ in which both benzene migration and carbonyl insertion has occurred.[22]

When the hexaruthenium-carbido benzene cluster $Ru_6C(CO)_{14}(\eta^6-C_6H_6)$ is treated with alkynes, by direct chemical activation with two molecular equivalents of Me_3NO in the presence of the alkyne, the benzene maintains its terminal position with the alkyne once again adopting a facial position [see Figure 5.3(c)].[25] No carbonyl insertion is observed in this case.
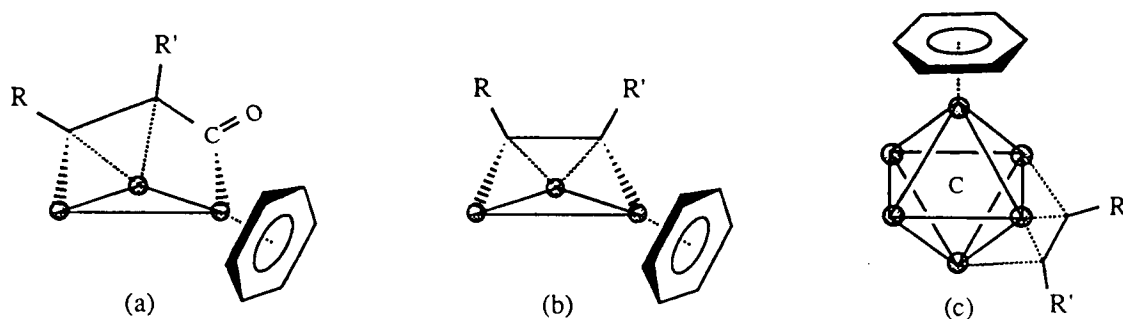
Figure 5.3: (a) $Ru_3(CO)_7(\mu_3-\eta^2-RC_2R'CO)(\eta^6-C_6H_6)$, (b) $Os_3(CO)_7(\mu_3-\eta^2-RC_2R')(\eta^6-C_6H_6)$, and (c) $Ru_6C(CO)_{12}(\mu_3-\eta^2-RC_2R')(\eta^6-C_6H_6)$.

Similar reactions have been pursued using the [2.2]paracyclophane compounds $Ru_3(CO)_9(\mu_3-\eta^2:\eta^2:\eta^2-C_{16}H_{16})$ **23** and $Ru_6C(CO)_{14}(\mu_3-\eta^2:\eta^2:\eta^2-C_{16}H_{16})$ **25**, and while the chemistry resembles that of the $M_3(CO)_9(\mu_3-\eta^2:\eta^2:\eta^2-C_6H_6)$ (M = Ru, Os) systems, significant differences are also observed.

5.3.1 Reaction of $Ru_3(CO)_9(\mu_3-\eta^2:\eta^2:\eta^2-C_{16}H_{16})$ 23 with diphenylacetylene

The cluster $Ru_3(CO)_9(\mu_3-\eta^2:\eta^2:\eta^2-C_{16}H_{16})$ **23** reacts with diphenylacetylene under two sets of conditions with the same major product, $Ru_3(CO)_7(\mu_3-\eta^1:\eta^2:\eta^1-C_2Ph_2)(\eta^6-C_{16}H_{16})$ **31**, being formed in each case. The two reaction types involve thermal and chemical activation, *i.e.* by heating **23** in dichloromethane under reflux in the presence of diphenylacetylene, and also by treatment of **23** with two molecular equivalents of Me_3NO in the presence of diphenylacetylene at -78°C, followed by warming to room temperature. In the thermal reaction two additional products, namely $Ru_3(CO)_7(\mu_3-\eta^2-PhC_2PhCO)(\eta^6-C_{16}H_{16})$ **32** and $Ru_2(CO)_6(\{\mu_2-\eta^1:\eta^2-C_2Ph_2\}_2-CO)$ **33** have also been isolated (see Scheme 5.3.1i). It has been found that the relative yields of compounds **31** - **33** produced

during the reaction depend critically on the thermolysis time, with the diruthenium complex **33** being formed in highest yields when the longest reaction period is employed. Cluster **32** is not observed under such conditions and is only present in low yield on heating for a relatively short period. Since $Ru_3(CO)_7(\mu_3\text{-}\eta^2\text{-}PhC_2PhCO)(\eta^6\text{-}C_{16}H_{16})$ **32** is a minor product of the reaction it has been characterised only from a comparison of its infrared spectrum with that observed for the benzene analogue, $Ru_3(CO)_7(\mu_3\text{-}\eta^2\text{-}PhC_2PhCO)(\eta^6\text{-}C_6H_6)$, which has been characterised crystallographically.[22] Their spectra are almost identical in both profile and wavenumber and, hence, it may be assumed that the compounds are isostructural and that a carbonyl has inserted between one of the C-atoms of the alkyne and a metal atom of the cluster.
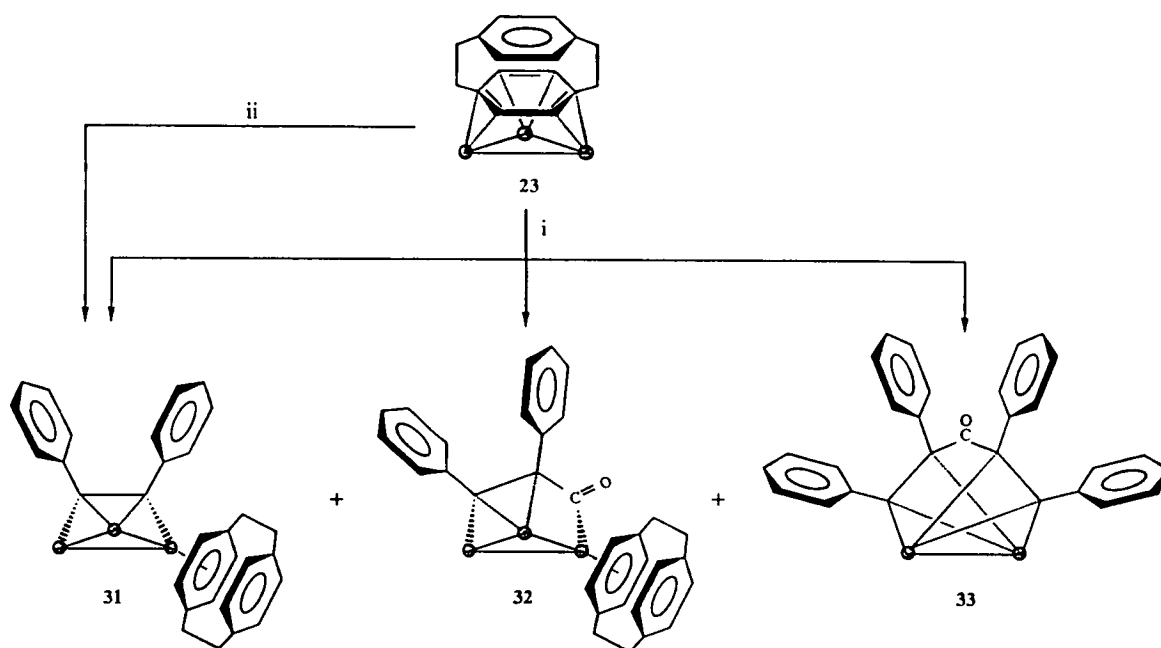
Scheme 5.3.1i: Reactions of **23** with diphenylacetylene. Reagents and conditions:
(i) Δ, C_2Ph_2/CH_2Cl_2, (ii) 2 mol. eq. $Me_3NO/C_2Ph_2/CH_2Cl_2$.

The same method of characterisation was used for compound **31** in the first instance; *i.e.* a comparison of its infrared spectrum (υ_{CO}) with that of the related osmium benzene species, $Os_3(CO)_7(\mu_3\text{-}\eta^1\text{:}\eta^2\text{:}\eta^1\text{-}C_2Me_2)(\eta^6\text{-}C_6H_6)$.[22,24] Again the two spectra show a clear similarity and hence, formulation of **31** as $Ru_3(CO)_7(\mu_3\text{-}\eta^1\text{:}\eta^2\text{:}\eta^1\text{-}C_2Ph_2)(\eta^6\text{-}C_{16}H_{16})$ could be assumed. This formulation was substantiated by mass and ^1H NMR spectroscopy. The mass spectrum contains a parent ion at 885 (calc. 886) which is followed by the sequential loss of seven CO groups. The ^1H NMR spectrum exhibits a multiple resonance between δ 7.09 and 6.75 ppm which may be assigned to the phenyl protons of

the acetylene ligand. The ring protons of the uncoordinated cyclophane ring give rise to a singlet at δ 6.72 ppm while those on the bound ring produce two multiplets at δ 5.29 and 4.60 ppm. The chemical shifts of these latter coordinated ring protons are at a significantly higher frequency than those of the parent compound, $Ru_3(CO)_9(\mu_3-\eta^2:\eta^2:\eta^2-C_{16}H_{16})$ **23** (δ 3.76 ppm), thus suggesting the presence of a terminal cyclophane moiety. Likewise, the CH_2 groups neighbouring the unattached ring produce one multiplet centred at δ 3.12 ppm, with two multiplets at δ 2.72 and 2.55 ppm for those adjacent to the coordinated ring. The relative intensities of the aforementioned signals are correct for their proposed assignments, and the solution structure is in complete agreement with the structure observed in the solid-state.

The molecular structure of **31** in the solid-state has been established by a single crystal X-ray diffraction analysis on a crystal grown from a toluene solution at -25°C, and is shown in Figure 5.3.1i, together with the principal structural parameters.

The three ruthenium atoms in **31** define a triangle, with the edge carrying the bridging carbonyl [Ru(2)-Ru(3)] being significantly longer than the other two [2.8006(13) *vs.* 2.6969(13) and 2.6957(12) Å, respectively]. The diphenylacetylene ligand straddles the face of the ruthenium triangle and donates four electrons to the cluster unit *via* one π and two σ interactions. The distances between the acetylene carbons and the ruthenium atoms are Ru(1)-C(1a) 2.237(9), Ru(1)-C(2a) 2.216(9), Ru(2)-C(2a) 2.294(9) and Ru(3)-C(1a) 2.108(9) Å and, hence, the σ interaction involving the metal to which the paracyclophane moiety is attached [Ru(2)] is longer than the other σ interaction [$\Delta = 0.186$ Å]. In contrast, the carbonyl ligand which asymmetrically bridges the same two metals, Ru(2) and Ru(3), has a shorter distance to the metal carrying the paracyclophane ligand [Ru(2)-C(21) 1.894(10) *versus* Ru(3)-C(21) 2.384(11), $\Delta = 0.490$ Å]. The unsaturated bond, C(1a)-C(2a), in the acetylene ligand is no longer of triple bond character and its length of 1.409(13) Å is more representative of a double bond. The non-linearity of the acetylene introduced upon coordination is also apparent with the angles between C(2a)-C(1a)-C(3a) and C(1a)-C(2a)-C(9a) of 124.2(8) and 125.9(8)°, respectively, showing a clear sp^2 pattern. The cyclophane unit is bonded to Ru(2) in an η^6 fashion. The bonded ring maintains the boat-shaped conformation present in the free ligand,[12] with the four coplanar C-atoms [C(1c), C(2c), C(4c) and C(5c)] lying closer to Ru(2) [mean = 2.258(10) Å] than the two bridgehead carbons C(3c) and C(6c), [mean = 2.403(9) Å]. The angle between the two enyl planes defined by C(1c)-C(5c)-C(6c) and C(2c)-C(4c)-C(3c) is 23.9(12)°, which is the same, to within errors, as that observed in the free paracyclophane molecule. The angle between the enyl planes of the unattached ring [defined by C(9c)-C(10c)-C(14c) and C(11c)-C(12c)-C(13c)] also remains unperturbed from that of the free ligand. The remaining six carbonyl ligands are all terminal and essentially linear, and are distributed

equally between the two ruthenium atoms not involved in coordination with the cyclophane moiety. The complex $Ru_3(CO)_7(\mu_3-\eta^1:\eta^2:\eta^1-C_2Ph_2)(\eta^6-C_{16}H_{16})$ **31** contains a total of 48 valence shell electrons, which makes it consistent with the EAN rule.
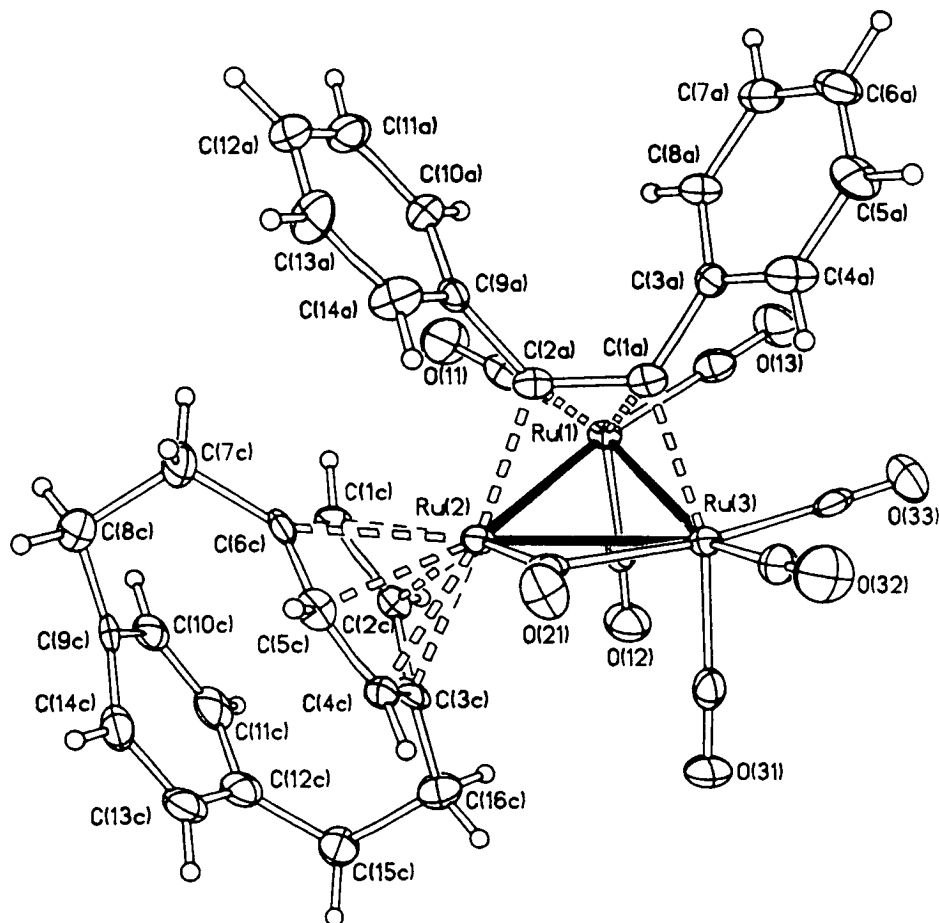
Figure 5.3.1i: The molecular structure of $Ru_3(CO)_7(\mu_3-\eta^1:\eta^2:\eta^1-C_2Ph_2)(\eta^6-C_{16}H_{16})$ **31** in the solid-state. The C-atoms of the CO ligands bear the same numbering as the corresponding O-atoms. Principal bond lengths (Å) are: Ru(1)-Ru(2) 2.6969(13), Ru(1)-Ru(3) 2.6957(12), Ru(2)-Ru(3) 2.8006(13), mean Ru-$C_{(CO)}$ 1.910, mean C-$O_{(CO)}$ 1.150, Ru(2)-C(1C) 2.246(9), Ru(2)-C(2C) 2.294(9), Ru(2)-C(3C) 2.403(9), Ru(2)-C(4C) 2.241(9), Ru(2)-C(5C) 2.251(10), Ru(2)-C(6C) 2.403(9), C(1C)-C(2C) 1.417(14), C(1C)-C(6C) 1.380(14), C(2C)-C(3C) 1.408(13), C(3C)-C(4C) 1.415(14), C(3C)-C(16C) 1.497(14), C(4C)-C(5C) 1.394(14), C(5C)-C(6C) 1.405(14), C(6C)-C(7C) 1.496(14), C(7C)-C(8C) 1.601(14), C(8C)-C(9C) 1.519(14), C(9C)-C(10C) 1.40(2), C(9C)-C(14C) 1.385(14), C(10C)-C(11C) 1.39(2), C(11C)-C(12C) 1.39(2), C(12C)-C(13C) 1.38(2), C(12C)-C(15C) 1.52(2), C(13C)-C(14C) 1.38(2), C(15C)-C(16C) 1.582(14), Ru(1)-C(1A) 2.237(9), Ru(1)-C(2A) 2.216(9), Ru(2)-C(2A) 2.294(9), Ru(3)-C(1A) 2.108(9), C(1A)-C(2A) 1.409(13), C(1A)-C(3A) 1.482(13), C(2A)-C(9A) 1.480(13), mean C-$C_{(phenyls)}$ 1.39.

The characterisation of compound **33** as $Ru_2(CO)_6(\{\mu_2\text{-}\eta^1\text{:}\eta^2\text{-}C_2Ph_2\}_2\text{-}CO)$ was less forthcoming due to its highly unusual and unexpected nature, and both spectroscopic and crystallographic analyses were required. Apart from the characteristic stretches between 2090 and 2028 cm^{-1} indicative of terminal carbonyl ligands, both the solution and solid-state infrared spectra of **33** contain a strong C-O stretch at 1672 cm^{-1} which can be ascribed to a ketonic C-O bond. The mass spectrum exhibits the expected parent peak at 756 (calc. 755) followed by a complicated fragmentation pattern, and the ^1H NMR spectrum simply comprises of two multiplets of equal relative intensities at δ 7.26 and 7.14 ppm, characteristic of two phenyl groups in different chemical environments. The above data is consistent with the structure obtained in the solid-state from a single crystal X-ray diffraction study, using a crystal grown by vapour diffusion from dichloromethane-pentane at room temperature. The molecular structure is not of high quality due to the poor crystals obtained, even after repeated attempts. However, due to the unusual nature of the molecule,
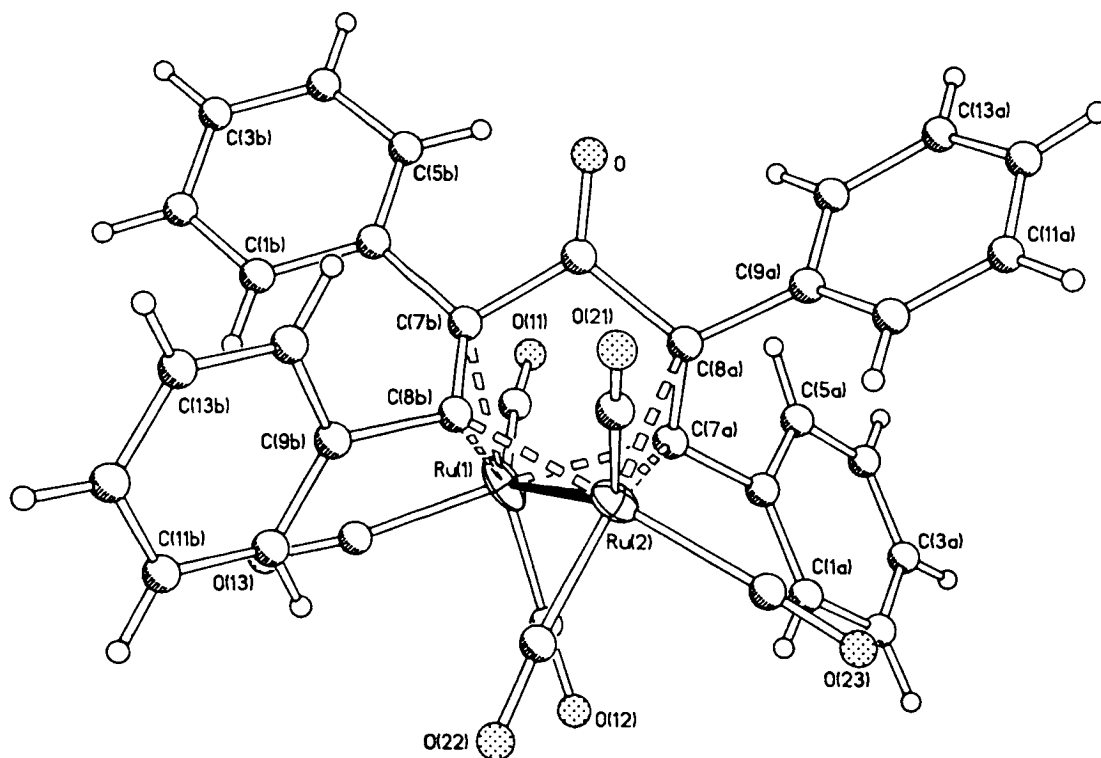
Figure 5.3.1ii: The molecular structure of $Ru_2(CO)_6(\{\mu_2\text{-}\eta^1\text{:}\eta^2\text{-}C_2Ph_2\}_2\text{-}CO)$ **33** in the solid-state. The C-atoms of the CO ligands bear the same numbering as the corresponding O-atoms. Principal bond parameters ($\mathring{A}$) are: Ru(1)-Ru(2) 2.751(3), mean Ru-$C_{(CO)}$ 1.90, mean C-$O_{(CO)}$ 1.16, Ru(1)-C(7A) 2.07(2), Ru(1)-C(7B) 2.23(2), Ru(1)-C(8B) 2.17(2), Ru(2)-C(7A) 2.24(2), Ru(2)-C(8A) 2.27(2), Ru(2)-C(8B) 2.06(2), C(7A)-C(8A) 1.44(3), C(7B)-C(8B) 1.31(3), C(8A)-C 1.54(3), C(7B)-C 1.55(3), C-O 1.20(2), C(6A)-C(7A) 1.48(3), C(8A)-C(9A) 1.54(3), C(6B)-C(7B) 1.57(3), C(8B)-C(9B) 1.60(3), mean C-$C_{(phenyls)}$ 1.38.

and since spectroscopic data and microanalytical results [Found (Calc.): C 55.75 (55.70), H 2.70 (2.67) %] are in good agreement with the established structure, it is felt that the gross features are worth describing, although caution must be taken in reading too much into the actual bond lengths obtained.

The molecular structure of **33** is illustrated in Figure 5.3.1ii, together with relevant bond parameters. The two diphenylacetylene units are linked through a carbonyl group and each of the alkyne moieties bonds to the ruthenium dimer *via* one π and one σ-interaction, thereby providing the two metals with a total of six electrons. Apart from this, each metal atom also carries three terminal carbonyl groups, and with the Ru-Ru bond each metal has an electron count of 18, and hence the EAN rule is obeyed.

It is believed that the formation of the ketone in this molecule *via* CO-insertion is unprecedented, and a possible mechanism for the reactions involved has been proposed. $Ru_3(CO)_7(\mu_3-\eta^1:\eta^2:\eta^1-C_2Ph_2)(\eta^6-C_{16}H_{16})$ **31** is thought to be produced *via* the same reaction mechanism in both the thermal reaction and that utilising Me_3NO under ambient conditions. It can be envisaged that the replacement of two carbonyl ligands for the four electron donating acetylene occurs at the same ruthenium atom with the alkyne initially coordinating to a single metal atom. Migration of this ligand to two metals and then finally onto the trimetallic face is considered to follow, together with a simultaneous and contra-movement of the paracyclophane ligand from the metal face to a single metal atom *via* a M-M edge, thereby forming **31**. During the thermolytic reaction it can be reasonably assumed that the compound $Ru_3(CO)_7(\mu_3-\eta^2-PhC_2PhCO)(\eta^6-C_6H_6)$ **32** may be derived from **31** by the insertion of a CO group into one of the two Ru-C σ interactions. Carbonyl insertion is a common feature of alkyl-metal complexes and has been observed in a number of carbonyl cluster reactions with alkynes.[26] A second possibility would be the attack of the diphenylacetylene reactant on the C-atom of a terminally bound CO ligand in the parent cluster. The formation of compound $Ru_2(CO)_6(\{\mu_2-\eta^1:\eta^2-C_2Ph_2\}_2-CO)$ **33** clearly involves a reduction in cluster nuclearity. Previous thermolytic reactions have shown that products involving both cluster build-up and cluster degradation are common occurrences in reactions of this type, and it can therefore be speculated that the action of heat on $Ru_3(CO)_7(\mu_3-\eta^2-PhC_2PhCO)(\eta^6-C_6H_6)$ **32** causes cleavage of the weakened M-C$_{(inserted}$ $_{CO)}$ bond and loss of the metal atom bearing the cyclophane ligand. It is difficult to visualise the precise mechanism by which this process occurs, however it is clear that the addition of a second diphenylacetylene molecule to the C-atom of the inserted carbonyl and to the diruthenium unit would result in **33**. The fact that **32** is a minor product which is only observed when the thermolysis period is short, and that the yield of **33** is enhanced as the reaction time is lengthened, goes some way to confirm that **33** is at least derived from **32** even if the exact mechanistic pathway by which it is formed is unclear. The proposed

mechanism involved in the formation of **31, 32** and **33** from $Ru_3(CO)_9(\mu_3-\eta^2:\eta^2:\eta^2-C_{16}H_{16})$ **23** is illustrated in Scheme 5.3.1ii.
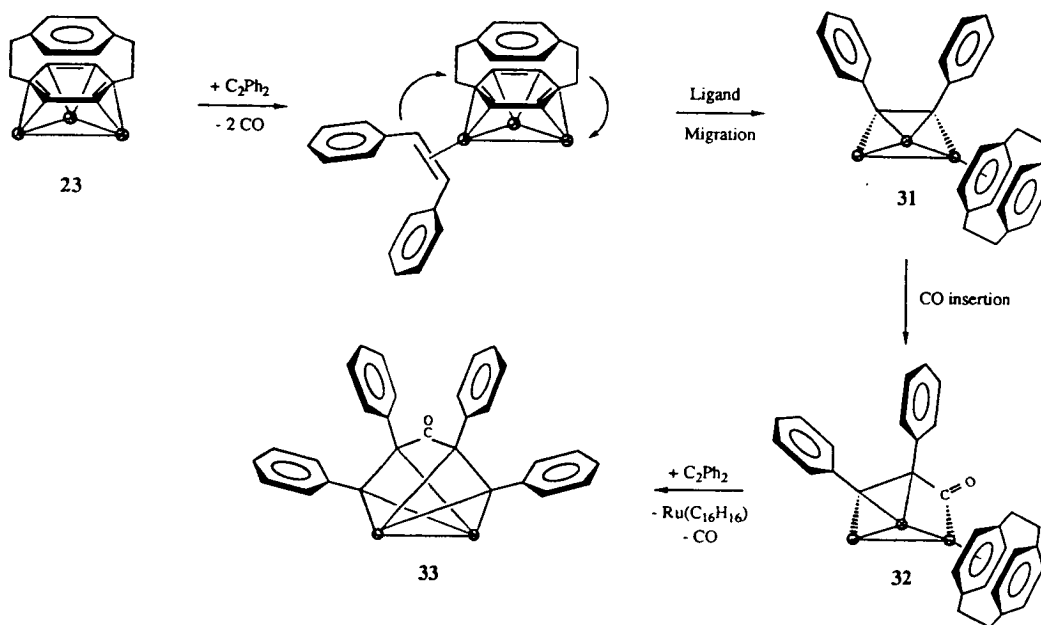
Scheme 5.3.1ii: A possible mechanism for the formation of **31, 32** and **33** from the thermolytic reaction between $Ru_3(CO)_9(\mu_3-\eta^2:\eta^2:\eta^2-C_{16}H_{16})$ **23** and diphenylacetylene.

5.3.2 Reaction of $Ru_6C(CO)_{14}(\mu_3-\eta^2:\eta^2:\eta^2-C_{16}H_{16})$ with alkynes

Although not directly part of this work, the action of two equivalents of Me_3NO on a dichloromethane solution of $Ru_6C(CO)_{14}(\mu_3-\eta^2:\eta^2:\eta^2-C_{16}H_{16})$ **25** containing excess alkyne (alkyne = but-2-yne and diphenylacetylene) has been found to produce $Ru_6C(CO)_{12}(\mu_3-\eta^1:\eta^2:\eta^1-RC_2R')(\mu_3-\eta^2:\eta^2:\eta^2-C_{16}H_{16})$, in which the cyclophane moiety has maintained its facial position, with the alkyne adopting the face directly opposite, (see Figure 5.3.2).[25] The thermolysis of **25** with excess acetylene in dichloromethane over a prolonged period results in the same product *albeit* in lower yield, and in neither reaction has there been any trace of the apical isomer, *i.e.* $Ru_6C(CO)_{12}(\mu_3-\eta^1:\eta^2:\eta^1-RC_2R')(\eta^6-C_{16}H_{16})$. Hence, in contrast to the trinuclear species, it is apparent that cyclophane migration does not occur. This provides further evidence for the cyclophane's unusual preference to coordinate to the Ru_6C octahedron in a facial manner, and also demonstrates that the larger polyhedron is capable of accommodating both ligands in their preferred facial coordination sites. If the Ru_3 derivative were to contain both ligands bonded in a facial

manner they would obviously have to coordinate to opposite sides of the same triangle; a feature which appears to be disfavoured by the cluster unit, resulting in rearrangement and migration.
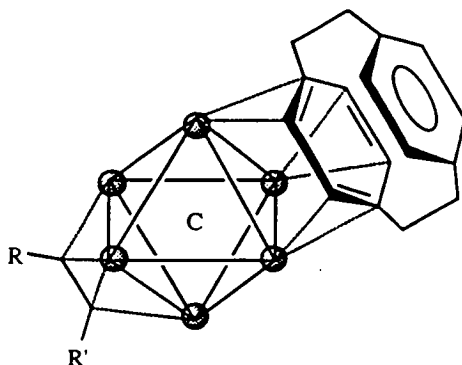
Figure 5.3.2: $Ru_6C(CO)_{12}(\mu_3-\eta^1:\eta^2:\eta^1-RC_2R')(\mu_3-\eta^2:\eta^2:\eta^2-C_{16}H_{16})$.

5.4 Reaction with Phosphines: The Molecular Structures of $Ru_3(CO)_8(PPh_3)(\mu_3-\eta^2:\eta^2:\eta^2-C_{16}H_{16})$ 34 and $Ru_6C(CO)_{13}(PPh_3)(\mu_3-\eta^2:\eta^2:\eta^2-C_{16}H_{16})$ 35

Reaction of the triosmium benzene cluster, $Os_3(CO)_9(\mu_3-\eta^2:\eta^2:\eta^2-C_6H_6)$, with phosphines results in compounds where the face-capping benzene ligand is retained and phosphine substitution occurs at an equatorial site.[2] This carbonyl substitution reaction proceeds rather inefficiently when thermally promoted, and therefore a carbonyl ligand is initially displaced by acetonitrile using Me_3NO, and this more labile group is then subsequently replaced by the desired phosphine ligand. The analogous substitution chemistry has not been developed for the triruthenium-benzene cluster, owing to its relative instability to this type of reaction.

It was of interest to examine the substitution chemistry of $Ru_3(CO)_9(\mu_3-\eta^2:\eta^2:\eta^2-C_{16}H_{16})$ 23 and $Ru_6C(CO)_{14}(\mu_3-\eta^2:\eta^2:\eta^2-C_{16}H_{16})$ 25 with phosphines firstly to confirm that the paracyclophane ligands retain their facial coordination modes, and secondly to see whether the phosphine ligand has an effect on the ^{1}H NMR spectra of these compounds. It has been established that in the ^{1}H NMR spectra of cyclophane-clusters the frequency of the coordinated ring protons decreases from the value observed for free cyclophane whilst that of the unattached ring protons increases in value. The extent of these shifts is difficult to rationalise but it would appear that they can be directly related to the electron density associated with the cluster and hence, the substitution of a carbonyl ligand for a phosphine may influence these parameters, and shed further light on this intriguing phenomenon.

5.4.1 Reaction of $Ru_3(CO)_9(\mu_3\text{-}\eta^2\text{:}\eta^2\text{:}\eta^2\text{-}C_{16}H_{16})$ 23 with triphenylphosphine

$Ru_3(CO)_9(\mu_3\text{-}\eta^2\text{:}\eta^2\text{:}\eta^2\text{-}C_{16}H_{16})$ 23 readily undergoes substitution reactions in which one carbonyl group can be replaced by a phosphine ligand. This can be achieved using Me_3NO which removes CO leaving a vacant coordination site on the cluster to which the two electron donating phosphine ligand may attach. Alternatively, heating compound 23 to reflux in tetrahydrofuran containing excess phosphine for a few hours affords the same product. When triphenylphosphine is used, a red product is obtained in good yield, which has been characterised by spectroscopic means as $Ru_3(CO)_8(PPh_3)(\mu_3\text{-}\eta^2\text{:}\eta^2\text{:}\eta^2\text{-}C_{16}H_{16})$ 34 (see scheme 5.4.1).
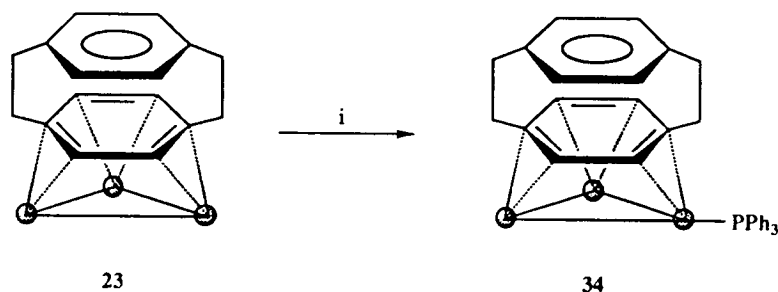
Scheme 5.4.1: Reaction of 23 with triphenylphosphine. Reagents and conditions; (i) 1 mol. eq. $Me_3NO/PPh_3/CH_2Cl_2$ or Δ, PPh_3/thf.

The infrared spectrum of $Ru_3(CO)_8(PPh_3)(\mu_3\text{-}\eta^2\text{:}\eta^2\text{:}\eta^2\text{-}C_{16}H_{16})$ 34 shows peaks in the terminal CO stretching region between 2049 and 1975 cm^{-1}, with the main peaks arising at lower wavenumbers than those found in the parent compound 23. This effect is usual when a carbonyl is replaced by a poorer π-acidic phosphine ligand. The mass spectrum of 34 exhibits a strong molecular ion at 735 (calc. 997) amu which corresponds to the weight of the cluster without the phosphine unit. The ^{31}P NMR spectrum of 34 contains one signal at δ 38.01 ppm which is readily assignable to the phosphorous atom of the PPh_3 fragment. The ^1H NMR spectrum is more complicated, but is nonetheless readily assigned. It consists of five resonances at δ 7.40, 7.32, 3.12, 2.95 and 2.41 ppm with relative intensities 15:4:4:4:4. The first signal centred at δ 7.40 ppm is a multiplet and corresponds to the protons of the three phenyl rings attached to the phosphine ligand. The remaining signals are derived from the cyclophane unit; the singlet resonance at δ 7.32 ppm can be attributed to the C-H protons of the unbound ring whilst a multiplet at δ 3.12 ppm is associated with the coordinated ring protons. The chemical shift of these latter protons is at very low frequency, thus suggesting the cyclophane has maintained its facial coordination mode. The final two signals are multiplets corresponding to the protons in the $-CH_2CH_2-$ bridges. This data is entirely consistent with the molecular structure of compound 34

observed in the solid-state, which has been established by a single crystal X-ray diffraction analysis on a crystal grown by the slow evaporation of a dichloromethane-hexane solution at room temperature, and is illustrated in Figure 5.4.1 together with relevant bond distances.
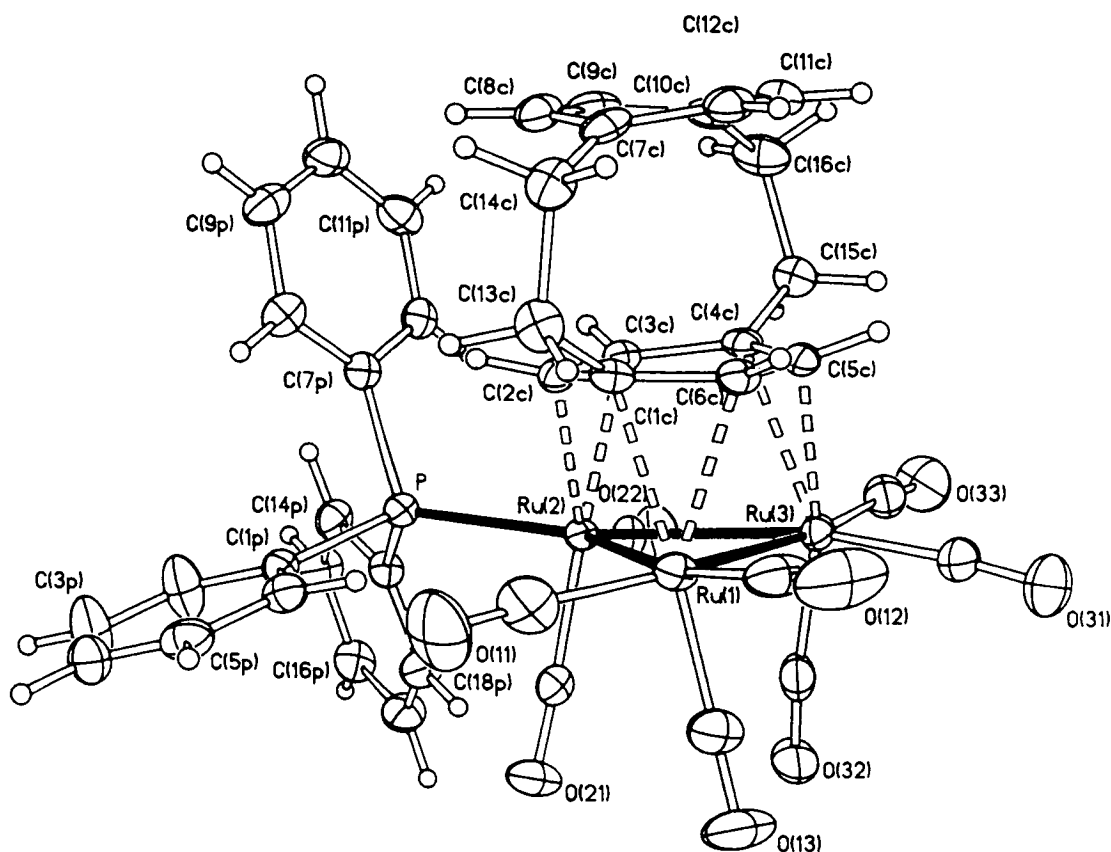
Figure 5.4.1: The molecular structure of $Ru_3(CO)_8(PPh_3)(\mu_3\text{-}\eta^2\text{:}\eta^2\text{:}\eta^2\text{-}C_{16}H_{16})$ **34** in the solid-state. The C-atoms of the CO ligands bear the same numbering as the corresponding O-atoms. Principal bond parameters (Å) are: Ru(1)-Ru(2) 2.905(2), Ru(1)-Ru(3) 2.840(2), Ru(2)-Ru(3) 2.830(2), mean Ru-C$_{(CO)}$ 1.89, mean C-O$_{(CO)}$ 1.145, Ru(1)-C(1C) 2.305(4), Ru(1)-C(6C) 2.313(4), Ru(2)-C(2C) 2.309(4), Ru(2)-C(3C) 2.227(4), Ru(3)-C(4C) 2.451(4), Ru(3)-C(5C) 2.268(4), C(1C)-C(2C) 1.461(5), C(1C)-C(6C) 1.407(5), C(1C)-C(13C) 1.532(5), C(2C)-C(3C) 1.419(5), C(3C)-C(4C) 1.450(5), C(4C)-C(5C) 1.399(5), C(4C)-C(15C) 1.517(5), C(5C)-C(6C) 1.440(5), C(7C)-C(8C) 1.399(5), C(7C)-C(14C) 1.499(5), C(8C)-C(9C) 1.382(6), C(8C)-C(12C) 1.389(6), C(9C)-C(10C) 1.394(6), C(10C)-C(11C) 1.399(6), C(10C)-C(16C) 1.505(6). C(11C)-C(12C) 1.385(6), C(13C)-C(14C) 1.562(6), C(15C)-C(16C) 1.571(5), Ru(2)-P 2.351(2), P-C(1P) 1.828(4), P-C(7P) 1.820(4), P-C(13P) 1.846(3), mean C-C$_{(phenyls)}$ 1.38.

The structure constitutes a triangular array of ruthenium atoms which is capped on one side by a μ_3-η^2:η^2:η^2 paracyclophane ligand. Ru(1) and Ru(3) also bear tricarbonyl units, while Ru(2) carries two carbonyl ligands and an equatorially disposed triphenylphosphine moiety. The molecular structure contains 48 electrons and is thus consistent with the EAN rule. The coordinated ring is flattened somewhat in comparison to free paracyclophane such that the dihedral angle between the two planes defined by C(1c)-C(2c)-C(6c) and C(3c)-C(4C)-C(5c) is 15.7(5)° [*cf.* free paracyclophane 23°].[12] However, the unattached ring is more contorted towards a boat-shaped conformation with an angle between the enyl planes defined by C(7c)-C(12c)-C(8c) and C(9c)-C(11c)-C(10c) of 24.2(4)°. Hence, the distortions found in the cyclophane ligand of **34** are the opposite to those observed in $Ru_2(CO)_6(\mu_2$-η^3:η^3-$C_6H_6)$ **30**, where the bound cyclophane ring has a more pronounced boat-shape than the free ligand and the uncoordinated ring is more planar. The PPh_3 unit occupies an equatorial site, although slightly displaced above the ruthenium triangular plane [*viz.* 0.236(1)°]. The structure of **34** is analogous to the triosmium-benzene species, $Os_3(CO)_8(PPh_3)(\mu_3$-η^2:η^2:η^2-$C_6H_6)$, which exhibits the same gross structural features.[2] Unlike other complexes containing face-capping paracyclophane ligands, the ring adopts an approximately staggered conformation over the triruthenium face. This is reflected in the Ru-C(ring) bond distances which vary only slightly [Ru(1)-C(1c) 2.305(3), Ru(1)-C(6c) 2.313(3), Ru(2)-C(2c) 2.309(3), Ru(2)-C(3c) 2.227(3), Ru(3)-C(4c) 2.451(3) and Ru(3)-C(5c) 2.268(3) Å].

In the parent cluster compound, $M_3(CO)_{12}$ (M = Ru, Os), substitution of CO by tertiary phosphines invariably occurs at an equatorial site.[27] This preference for equatorial substitution can be accounted for in steric terms, and simple calculations on $Os_3(CO)_{12-x}L_x$ systems have shown that equatorial sites, in compounds with an approximately anticuboctahedral structure of ligands, are less sterically hindered than axial sites.[28] In contrast, when CNR groups are employed the substituting ligand can occupy either an axial or equatorial site depending on the steric requirements of the R group, and MeCN predominantly coordinates axially.[27,28] In $M_3(CO)_{12}$ (M = Ru, Os) the axial carbonyl ligands are more weakly bound, with slightly longer axial M-C distances than equatorial ones being observed [*e.g.* the mean M-CO$_{(ax)}$ = 1.942(4), 1.95(1) *vs.* the mean M-CO$_{(eq)}$ = 1.921(5), 1.91(1) Å for Ru and Os, respectively].[29,30] In $M_3(CO)_{12-x}(MeCN)_x$, however, the axial CO ligands *trans* to the acetonitrile ligands have the shortest M-C bond lengths, and are therefore more strongly bound. This is observed in the complexes, $Os_3(CO)_{12-x}(MeCN)_x$ (x = 1, 2), which have been characterised by X-ray diffraction,[31] and axial nitrile ligation therefore appears to significantly enhance π-backbonding to *trans*-related carbonyls by virtue of the good σ-donor / poor π-acceptor properties of the N-based ligand when compared to CO.

These arguments explain, in terms of both steric and electronic effects, the reasons for equatorial substitution of CO by a tertiary phosphine ligand in complexes of the type $M_3(CO)_9(\mu_3-\eta^2:\eta^2:\eta^2$-arene). Although the molecular structure of $Ru_3(CO)_9(\mu_3-\eta^2:\eta^2:\eta^2-C_{16}H_{16})$ **23** has not been established, it is expected to be very similar to that of the analogous benzene complex, $Ru_3(CO)_9(\mu_3-\eta^2:\eta^2:\eta^2-C_6H_6)$, which has been characterised by X-ray diffraction and indeed shows that the axial CO ligands contain slightly shorter Ru-C distances than the equatorial ones.[13a] This concept is indicative of the lower π-acidity of the μ_3 benzene ligand relative to an axial tricarbonyl ligand set, which in turn increases the π back-donation over the ligands *trans* to the benzene double bonds, and so increases the preference for equatorial substitution of a carbonyl ligand by the entering phosphine.

5.4.2   Reaction of $Ru_6C(CO)_{14}(\mu_3-\eta^2:\eta^2:\eta^2-C_{16}H_{16})$ 25 with phosphines

Reaction of the hexanuclear-carbido cluster, $Ru_6C(CO)_{14}(\mu_3-\eta^2:\eta^2:\eta^2-C_{16}H_{16})$ **25**, with one molecular equivalent of trimethylamine *N*-oxide in the presence of excess triphenylphosphine produces $Ru_6C(CO)_{13}(PPh_3)(\mu_3-\eta^2:\eta^2:\eta^2-C_{16}H_{16})$ **35** in high yield. The same product is also obtained in moderate yield from the thermolysis of **25** with PPh_3 in tetrahydrofuran for 1 hour. This product can be isolated from the crude reaction mixture by chromatography on silica using a dichloromethane-hexane (3:7, v/v) solution as eluent.

The infrared spectrum of $Ru_6C(CO)_{13}(PPh_3)(\mu_3-\eta^2:\eta^2:\eta^2-C_{16}H_{16})$ **35** shows typical terminal CO stretches between 2050 and 1955 cm^{-1}, with the main peaks again arising at lower wavenumbers than in the parent compound, $Ru_6C(CO)_{14}(\mu_3-\eta^2:\eta^2:\eta^2-C_{16}H_{16})$ **25**. A bridging CO stretch is also observed at 1802 cm^{-1}. The mass spectrum exhibits a parent peak at 1452 (calc. 1453) amu, followed by peaks corresponding to the loss of the triphenylphosphine fragment and several carbonyl groups in succession. The ^1H NMR spectrum shows three multiplet resonances centred at δ values of 7.5, 3.4 and 3.0 ppm with approximate relative intensities of 5:2:1. Although the assignment of this spectrum is not immediately apparent, it is nonetheless relatively straightforward. The signal at δ 7.5 ppm consists of the phenyl ring protons which partially obscure the singlet resonance derived from the ring protons of the uncoordinated cyclophane group at δ 7.43 ppm. The multiplets at δ 3.4 and 3.0 ppm can be assigned to the -CH$_2$CH$_2$- bridges of the ring system, the former containing the singlet derived from the ring protons of the coordinated ring, the value of this being δ 3.38 ppm which is typical for a facially coordinated cyclophane ligand. The precise assignment of the -CH$_2$CH$_2$- linkages can only be speculated, and it is thought that the pair closest to the bound ring are those at the lower frequency. The ^{31}P NMR spectrum consists of a singlet resonance at δ 43.5 ppm.

In a similar reaction to that described above employing chemical activation, the more basic tricyclohexylphosphine ligand has also been introduced into cluster **25**, thereby producing the new derivative, $Ru_6C(CO)_{13}(PCy_3)(\mu_3-\eta^2:\eta^2:\eta^2-C_{16}H_{16})$ **36**. This compound was initially characterised by a comparison of the carbonyl stretching frequencies in its infrared spectrum with those of the triphenylphosphine analogue **35**. The two spectra have identical profiles, with the peaks in **36** being shifted to slightly lower wavenumber as would be expected for the more basic phosphine. The mass spectrum is also similar to that of **35** with a parent peak found at 1470 (calc. 1471) amu, and the next lowest ion corresponding to the loss of the tricyclohexylphosphine moiety, followed by the loss of several carbonyl groups in succession. The ^{31}P NMR spectrum contains one singlet resonance at δ 55.5 ppm. The ^1H NMR contains six signals at δ 7.36, 3.33, 3.22, 2.93, 1.80 and 1.31 ppm. The former four signals are of equal relative intensities with the signals at δ 7.36 and 3.22 ppm both being singlet resonances which correspond to the C-H ring protons of the uncoordinated and coordinated rings, respectively. The signals at δ 3.33 and 2.93 ppm are multiplets which are derived from the $-CH_2CH_2-$ bridges, while the protons associated with the tricyclohexyl groups give rise to two complex multiplet resonances centred at δ 1.80 and 1.31 ppm which in total integrate approximately to the required 33 protons.

A single crystal X-ray diffraction analysis has been carried out on the triphenylphosphine derivative, $Ru_6C(CO)_{13}(PPh_3)(\mu_3-\eta^2:\eta^2:\eta^2-C_{16}H_{16})$ **35**, using a crystal grown by vapour diffusion at room temperature with dichloromethane-pentane. The molecular structure of **35** is illustrated in Figure 5.4.2 together with principal bond lengths. The metal atom core consists of the same octahedral framework encapsulating a carbide atom that was observed in the precursor starting material, $Ru_6C(CO)_{14}(\mu_3-\eta^2:\eta^2:\eta^2-C_{16}H_{16})$ **25**. The Ru-Ru bonds are comparable with those in **25** [Ru-Ru bond lengths range from 2.798(2)-3.070(2) Å in **35** and from 2.794(1)-2.990(1) Å in **25**], the shortest bond in each case representing the edge bridged by the μ_2-CO ligand. The interstitial carbide atom is centrally disposed within the cluster octahedron, with Ru-C(carbide) bond lengths ranging from 2.031(8) to 2.092(8) Å, and a mean value of 2.055(8) Å [*cf.* range 2.001(8)-2.080(8), mean 2.051(8) Å in **25**]. The triphenylphosphine fragment is coordinated to a ruthenium atom not involved in cyclophane substitution *via* a typical interaction, Ru(4)-P(1) 2.399(3) Å, and the bond parameters within the PPh_3 ligand do not show any abnormalities. The most interesting feature of this molecule is the cyclophane moiety and the triangular face to which it is attached. As in $Ru_3(CO)_8(PPh_3)(\mu_3-\eta^2:\eta^2:\eta^2-C_{16}H_{16})$ **34**, the mid-points of the C=C bonds in **35** essentially eclipse the ruthenium atoms, which is generally the favoured orientation for face-capping arene groups. However, in **25** this is not the case and alternate C-atoms of the C_6 ring move from a more staggered towards a near eclipsed position above the ruthenium atoms of the cluster face. The remaining features of the cyclophane entity in

35 are comparable to those in 25, and upon coordination to the trimetallic face, the bound ring flattens out whilst the unattached ring maintains the boat-shaped conformation present in the free ligand. Both clusters contain 86 valence electrons and are therefore consistent with the PSEPT.
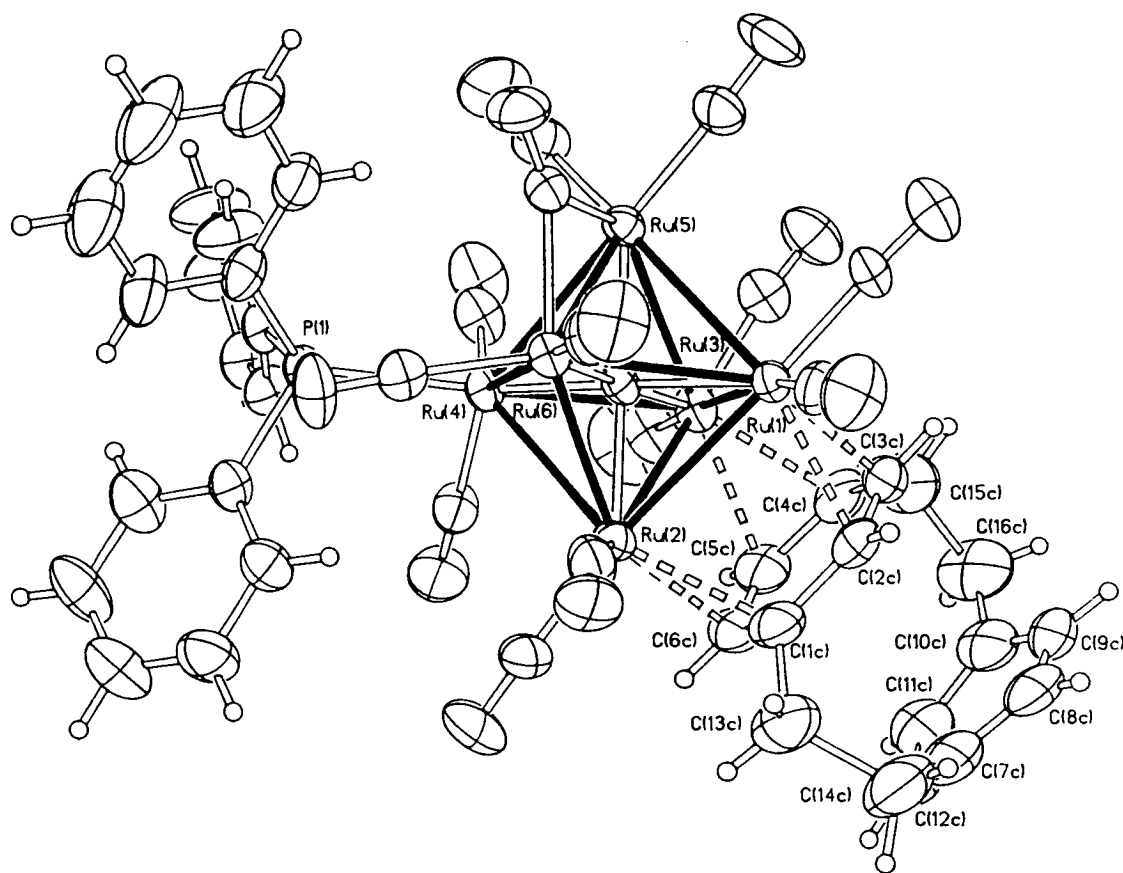
Figure 5.4.2: The molecular structure of $Ru_6C(CO)_{13}(PPh_3)(\mu_3-\eta^2:\eta^2:\eta^2-C_{16}H_{16})$ 35 in the solid-state. The C-atoms of the CO ligands bear the same numbering as the corresponding O-atoms. Principal bond parameters (Å) are: Ru(1)-Ru(2) 2.8397(13), Ru(1)-Ru(3) 2.803(2), Ru(1)-Ru(5) 2.896(2), Ru(1)-Ru(6) 2.8913(14), Ru(2)-Ru(3) 2.967(2), Ru(2)-Ru(4) 2.950(2), Ru(2)-Ru(6) 2.848(2), Ru(3)-Ru(4) 2.8645(14), Ru(3)-Ru(5) 3.004(2), Ru(4)-Ru(5) 2.9321(14), Ru(4)-Ru(6) 3.070(2), Ru(5)-Ru(6) 2.798(2), Ru(1)-C(1) 2.053(8), Ru(2)-C(1) 2.049(8), Ru(3)-C(1) 2.031(8), Ru(4)-C(1) 2.049(8), Ru(5)-C(1) 2.054(8), Ru(6)-C(1) 2.092(8), Ru(5)-C(53) 2.060(9), Ru(6)-C(53) 2.067(9), C(53)-O(53) 1.163(11), mean Ru-C$_{(terminal\ CO)}$ 1.883(11), mean C-O$_{(terminal\ CO)}$ 1.138(13), Ru(1)-C(2C) 2.293(9), Ru(1)-C(3C) 2.303(9), Ru(2)-C(1C) 2.268(11), Ru(2)-C(6C) 2.236(10), Ru(3)-C(4C) 2.216(10), Ru(3)-C(5C) 2.322(10), C(1C)-C(2C) 1.44(2), C(1C)-C(6C) 1.36(2), C(1C)-C(13C) 1.53(2), C(2C)-C(3C) 1.412(14), C(3C)-C(4C) 1.49(2), C(4C)-C(5C) 1.42(2), C(4C)-C(15C) 1.53(2), C(5C)-C(6C) 1.42(2), C(7C)-C(8C) 1.36(2), C(7C)-C(12C) 1.32(2), C(7C)-C(14C) 1.50(2), C(8C)-C(9C) 1.38(2), C(9C)-C(10) 1.39(2), C(10C)-C(11C) 1.42(2), C(10C)-C(16C) 1.46(2), C(11C)-C(12C) 1.37(2), C(13C)-C(14C) 1.57(2), C(15C)-C(16C) 1.56(2), Ru(4)-P(1) 2.399(3), P(1)-C(1P) 1.835(10), P(1)-C(7P) 1.833(9), P(1)-C(13P) 1.821(10), mean C-C$_{(phenyls)}$ 1.37(2).

5.4.3   A ^{1}H NMR Study of Phosphine Containing Cyclophane Clusters

To briefly reiterate on the ^{1}H NMR discussion of Chapter four, it is apparent that upon metal complexation, the degenerate resonance at δ 6.47 ppm, attributed to the aromatic ring protons of the free [2.2]paracyclophane moiety, splits into two signals with the protons of the bound cyclophane deck experiencing a significant shift to lower frequency, while those of the uncomplexed ring shift to higher frequency. This observation may be taken to indicate a type of synergic bonding; firstly between the bound ring and the cluster, and secondly a concomitant interaction between the two rings. The large shielding effect experienced by the complexed cyclophane ring appears to be a general phenomenon in both the ^{1}H and ^{13}C NMR spectra of any classical, cyclic, aromatic system in which all ring carbons are involved in π-bonding to a metal.[32] Although the source of this large shielding increase is poorly understood, it is variously attributed to quenching of the ring current effect, metal-ligand bond anisotropy, the changes in hybridisation of the ring carbons associated with the use of π-orbitals for bonding with metal d-orbitals, and changes in electron density, since a reduction in C-C π-bond order can account for changes in chemical shift as well as bond lengthening.[32,33] It is clear that no single explanation can account for such shifts, and instead they seem to arise from a combination of the above effects to differing degrees. Chapter four also describes how the protons of a cyclophane ring bonded in the facial μ_3-η^2:η^2:η^2 coordination mode give rise to a resonance in the ^{1}H NMR spectrum at significantly lower frequency than those of a terminal η^6 cyclophane, this effect being attributed to the enhanced effects of the ring interacting directly with three metal atoms as opposed to one. This shielding effect may also be attributed to the size of the cluster, with a greater shielding experienced as the nuclearity of the cluster is increased.

Hence, a comparison of the ^{1}H NMR spectra of the phosphine complexes $Ru_3(CO)_8(PPh_3)(\mu_3$-η^2:η^2:η^2-$C_{16}H_{16})$ **34**, $Ru_6C(CO)_{13}(PPh_3)(\mu_3$-$\eta^2$:$\eta^2$:$\eta^2$-$C_{16}H_{16})$ **35** and $Ru_6C(CO)_{13}(PCy_3)(\mu_3$-$\eta^2$:$\eta^2$:$\eta^2$-$C_{16}H_{16})$ **36**, with those of the parent starting materials $Ru_3(CO)_9(\mu_3$-η^2:η^2:η^2-$C_{16}H_{16})$ **23** and $Ru_6C(CO)_{14}(\mu_3$-η^2:η^2:η^2-$C_{16}H_{16})$ **25** is worth considering, bearing in mind the unusual ability of the [2.2]paracyclophane moiety to probe the electron density available on the cluster surface for bonding. Table 5.4.3 lists the chemical shifts of the C-H ring protons in the compounds described in this section, together with those of the parent cyclophane compounds. A triosmium benzene complex and its phosphine derivative are also listed for comparison.

Replacement of carbonyls on a cluster by more basic phosphine ligands should increase the electron density on the central cluster unit. A comparison of the chemical shift values of the parent clusters with their phosphine derivatives shows that this trend is observed, with the addition of a phosphine ligand generally increasing Δ (the difference in shift between the unattached and coordinated ring protons), and always causing a shift of the bound ring to lower frequency. This may also be compared to the triosmium benzene

Table 5.4.3: The ^{1}H NMR values (ppm) of free [2.2]paracyclophane, some [2.2]paracyclophane-phosphine-ruthenium cluster compounds, their precursor materials, and the analogous triosmium-benzene clusters are listed.

	Free Ring	Bound Ring	Δ
[2.2]paracyclophane - $C_{16}H_{16}$[a]	δ 6.47	–	–
$Ru_3(CO)_9(\mu_3\text{-}\eta^2\text{:}\eta^2\text{:}\eta^2\text{-}C_{16}H_{16})$[b] 23	δ 7.22	δ 3.76	3.46
$Ru_3(CO)_8(PPh_3)(\mu_3\text{-}\eta^2\text{:}\eta^2\text{:}\eta^2\text{-}C_{16}H_{16})$[b] 34	δ 7.32	δ 3.12	4.20
$Ru_6C(CO)_{14}(\mu_3\text{-}\eta^2\text{:}\eta^2\text{:}\eta^2\text{-}C_{16}H_{16})$[b] 25	δ 7.44	δ 3.40	4.04
$Ru_6C(CO)_{13}(PPh_3)(\mu_3\text{-}\eta^2\text{:}\eta^2\text{:}\eta^2\text{-}C_{16}H_{16})$[b] 35	δ 7.43	δ 3.38	4.05
$Ru_6C(CO)_{13}(PCy_3)(\mu_3\text{-}\eta^2\text{:}\eta^2\text{:}\eta^2\text{-}C_{16}H_{16})$[b] 36	δ 7.36	δ 3.22	4.14
$Os_3(CO)_9(\mu_3\text{-}\eta^2\text{:}\eta^2\text{:}\eta^2\text{-}C_6H_6)$[c]	–	δ 4.42	–
$Os_3(CO)_8(PPh_3)(\mu_3\text{-}\eta^2\text{:}\eta^2\text{:}\eta^2\text{-}C_6H_6)$[c]	–	δ 3.87	–

[a,c] Values taken from reference 34 and 2 respectively, [b] Values taken from this work.

Δ = Difference in chemical shifts between the free and coordinated ring protons (ppm).

cluster, $Os_3(CO)_9(\mu_3\text{-}\eta^2\text{:}\eta^2\text{:}\eta^2\text{-}C_6H_6)$, in which the chemical shift of the benzene ring protons is reduced in frequency from δ 4.42 to 3.87 ppm upon substitution of one carbonyl group for a triphenylphosphine ligand.[2]

The coordination of a μ_3 arene over a trimetallic face is thought to involve a type of synergic bonding by which the arene accepts π-electron density from the metal through back donation into empty π*-orbitals of the bound ring, as well as interacting *via* the conventional ligand-to-metal π-donation. Capitalisation of both the electron density donation and acceptance by benzene frontier orbitals in this synergic fashion has been observed for the μ_3 benzene ligand in the complex $Os_3(CO)_9(\mu_3\text{-}\eta^2\text{:}\eta^2\text{:}\eta^2\text{-}C_6H_6)$ [by modelling the cluster with its triruthenium analogue][2,13a] and also in the hypothetical model complex $(CpCo)_3(\mu_3\text{-}\eta^2\text{:}\eta^2\text{:}\eta^2\text{-}C_6H_6)$.[13b] Fenske-Hall quantum chemical calculations have been performed on these two clusters and both sets of results illustrate that the bonding of the benzene ring to the metal triangle may be described in terms of the Dewar-Chatt-Duncanson approach applicable to an alkene interacting with a single transition metal in low oxidation state.[35] Thus, the main bonding interactions in the molecules amount to ring-to-metal π-donation from the filled e_{1g} orbitals (HOMO) on the benzene into the vacant 2e acceptor orbitals (LUMO) of the cluster fragment, accompanied by π-back donation to the benzene e_{2u} (LUMO) orbitals from a high-lying cluster based molecular orbital set (1e). Both interactions weaken the π-bonding observed in the benzene, which results in a significant lengthening of the C-C bonds.

The metal-to-arene back-bonding interaction is thought to play a part in the large chemical shifts to lower frequency that are experienced in the NMR spectra of arene-metal cluster compounds when compared to those of the free ligands. Firstly, an increase in π-

electron density at the ring leads to substantial shielding of the carbon nuclei,[36] and secondly the π-back donation results in an increase in p-character for the ring carbons which should again lead to increased shielding of both ^{1}H and ^{13}C nuclei.[37] These factors also partially account for the differences in shielding between terminally and facially bound arenes, and changes of chemical shifts with cluster nuclearity, with the larger degree of shielding observed for the μ_3 ligand reflecting a greater π-acidity for benzene when bonded in this fashion. This effect is also apparent from infrared spectroscopic studies which indicate that υ_{C-H} modes for the terminal and face-capping ligands occur at significantly different energies.[2] For example, in the *bis*(benzene) cluster $Ru_6C(CO)_{11}(\eta^6\text{-}C_6H_6)(\mu_3\text{-}\eta^2:\eta^2:\eta^2\text{-}C_6H_6)$ vibrational modes of a_1/e symmetry for μ_1 and μ_3 benzene are seen at 3125/3118 and 3100/3065 cm^{-1}, respectively, suggesting a more extensive rehybridisation ($sp^2 \to sp^3$) of the face-capping carbons as a consequence of increased π-acceptance from the cluster in the face-capping mode.

Although no investigations of this type have been carried out on the cyclophane clusters $Ru_3(CO)_9(\mu_3\text{-}\eta^2:\eta^2:\eta^2\text{-}C_{16}H_{16})$ **23** and $Ru_6C(CO)_{14}(\mu_3\text{-}\eta^2:\eta^2:\eta^2\text{-}C_{16}H_{16})$ **25**, the principal bonding interactions are expected to closely resemble those described above. Therefore when a carbonyl is replaced by a more basic phosphine ligand the electron density associated with the cluster framework is increased. This in turn causes a stronger back-bonding interaction, which results in an enhanced shielding effect and hence chemical shifts of the coordinated ring protons arise at lower frequencies (see Table 5.4.3). It is also apparent that the effect of the phosphine is far more noticeable, in terms of these shift values, on the trinuclear cluster than on the hexanuclear cluster. The bound ring protons of $Ru_3(CO)_9(\mu_3\text{-}\eta^2:\eta^2:\eta^2\text{-}C_{16}H_{16})$ **23** give rise to a singlet resonance at δ 3.76 ppm, while those in the phosphine derivative $Ru_3(CO)_8(PPh_3)(\mu_3\text{-}\eta^2:\eta^2:\eta^2\text{-}C_{16}H_{16})$ **34** appear at δ 3.12 ppm [Δ = 0.64 ppm], whereas in the hexanuclear clusters $Ru_6C(CO)_{14}(\mu_3\text{-}\eta^2:\eta^2:\eta^2\text{-}C_{16}H_{16})$ **25** and $Ru_6C(CO)_{13}(PPh_3)(\mu_3\text{-}\eta^2:\eta^2:\eta^2\text{-}C_{16}H_{16})$ **35**, the corresponding signals arise at δ 3.40 and 3.38 ppm respectively [Δ = 0.02 ppm]. This is not totally unexpected since the additional electron density from the phosphine ligand is spread over three metal atoms as oppose to six, and also there are less carbonyl ligands present in the molecule onto which this extra electron density may be dispersed. One last feature worth noting is that when a more basic phosphine is employed, such as PCy_3 in the cluster $Ru_6C(CO)_{13}(PCy_3)(\mu_3\text{-}\eta^2:\eta^2:\eta^2\text{-}C_{16}H_{16})$ **36**, the situation is again enhanced [Δ = 0.18 ppm] illustrating that only slight changes in electron density on the cluster can lead to distinct changes in the ^{1}H NMR spectra.

Unfortunately this study has been limited to a small number of complexes, and only ^{1}H NMR spectra have been considered. Therefore a detailed comparison cannot be discussed, although from the results attained it is apparent that the [2.2]paracyclophane

ligand, which is considered a poor π-acid ligand especially when compared to CO, is a net electron acceptor from the metal. This capability is enhanced upon coordination in the facial mode, as is evidenced by an increase in $sp^2 \rightarrow sp^3$ hybridisation. Once again it seems that ^1H NMR spectroscopy may be used as a probe of the electron density on the cluster surface, not only by recognising when CO has been substituted by a phosphine ligand, but also noting the difference between the basicity of the phosphines employed. The decrease in the chemical shift of the coordinated ring together with the simultaneous increase of the chemical shift in the uncoordinated ring is consistent with a through space synergic interaction in the [2.2]paracyclophane; first between the bound ring and the cluster, and secondly a concomitant interaction between the two rings.

5.5   Reaction with Cyclohexa-1,3-diene: The Molecular Structures of $Ru_4(CO)_9(\eta^4\text{-}C_6H_8)(\mu_3\text{-}\eta^1:\eta^2:\eta^2\text{-}C_{16}H_{16})$ 37 and $Ru_6C(CO)_{12}(\mu_2\text{-}\eta^2:\eta^2\text{-}C_6H_8)(\mu_3\text{-}\eta^2:\eta^2:\eta^2\text{-}C_{16}H_{16})$ 38

The cyclophane clusters $Ru_3(CO)_9(\mu_3\text{-}\eta^2:\eta^2:\eta^2\text{-}C_{16}H_{16})$ 23 and $Ru_6C(CO)_{14}(\mu_3\text{-}\eta^2:\eta^2:\eta^2\text{-}C_{16}H_{16})$ 25 have been examined with attention focused on their reactivity towards Me_3NO only, alkynes, and phosphines. This series of reactions have been shown to yield a wide variety of complexes, both structurally and electronically, and hence it was decided to extend the range of derivatives and see how the complexes react with cyclohexa-1,3-diene.

A dichloromethane solution of the related triosmium cluster, $Os_3(CO)_9(\mu_3\text{-}\eta^2:\eta^2:\eta^2\text{-}C_6H_6)$, has been found to undergo reaction with two molecular equivalents of Me_3NO at -78°C in the presence of excess cyclohexa-1,3-diene producing the benzene-diene cluster, $Os_3(CO)_7(\eta^4\text{-}C_6H_8)(\mu_3\text{-}\eta^2:\eta^2:\eta^2\text{-}C_6H_6)$, in high yield, where the benzene ligand retains its facial coordination mode. Further reaction with trityl tetrafluoroborate, [Ph$_3$C][BF$_4$], in dichloromethane followed by treatment with the non-nucleophilic base DBU (DBU = 1,8-diazabicyclo[5.4.0]undeca-7-ene) results in the formation of the *bis*(benzene) cluster, $Os_3(CO)_6(\eta^6\text{-}C_6H_6)(\mu_3\text{-}\eta^2:\eta^2:\eta^2\text{-}C_6H_6)$, which contains benzene ligands in both the facial and terminal coordination modes.[38] The addition of trityl presumably abstracts a hydride from the diene moiety thereby affording a cationic intermediate containing a C_6H_7 ring, and then DBU removes a proton, thus generating a second C_6H_6 ring. This reaction sequence is illustrated in scheme 5.5i. In contrast, the analogous triruthenium benzene cluster does not undergo a similar reaction, with all attempts to activate the complex further leading to extensive cluster decomposition. This once again illustrates the relative instability of the ruthenium cluster when compared with its osmium analogue.
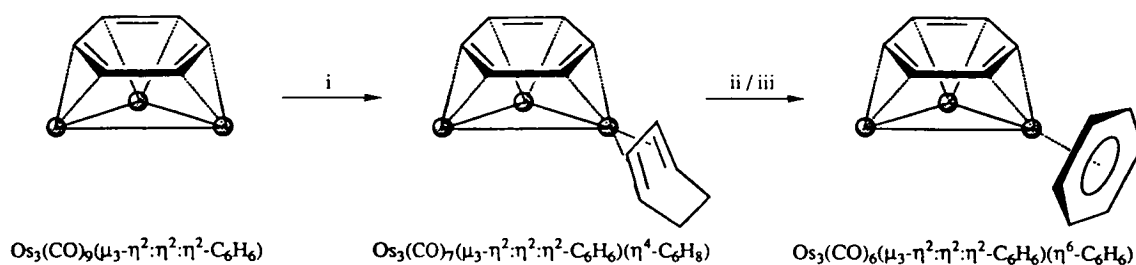
Scheme 5.5i: The reaction of $Os_3(CO)_9(\mu_3\text{-}\eta^2\text{:}\eta^2\text{:}\eta^2\text{-}C_6H_6)$ with Me_3NO and cyclohexa-1,3-diene. (i) 2 mol. equiv. $Me_3NO/1,3\text{-}C_6H_8/CH_2Cl_2/\text{-}78°C$, (ii) $[Ph_3C][BF_4]/CH_2Cl_2$, (iii) DBU/CH_2Cl_2.

The hexaruthenium benzene cluster, $Ru_6C(CO)_{14}(\eta^6\text{-}C_6H_6)$, on the other hand, has been found to undergo reaction with Me_3NO and cyclohexa-1,3-diene to give two benzene-diene isomers, $Ru_6C(CO)_{12}(\mu_2\text{-}\eta^2\text{:}\eta^2\text{-}C_6H_8)(\mu_3\text{-}\eta^2\text{:}\eta^2\text{:}\eta^2\text{-}C_6H_6)$ and $Ru_6C(CO)_{12}(\mu_2\text{-}\eta^2\text{:}\eta^2\text{-}C_6H_8)(\eta^6\text{-}C_6H_6)$, together with the *bis*(benzene) species, $Ru_6C(CO)_{11}(\eta^6\text{-}C_6H_6)(\mu_3\text{-}\eta^2\text{:}\eta^2\text{:}\eta^2\text{-}C_6H_6)$.[39] The former benzene-diene complex may be converted into the latter by heating in hexane, the process requiring the migration of the benzene from a facial to a terminal coordination mode. The *bis*(benzene) cluster can also be generated from either of the benzene-diene isomers by the addition of a second aliquot of Me_3NO, or alternatively *via* the cationic benzene-dienyl intermediate, $[Ru_6C(CO)_{11}(\eta^6\text{-}C_6H_6)(\mu_3\text{-}$
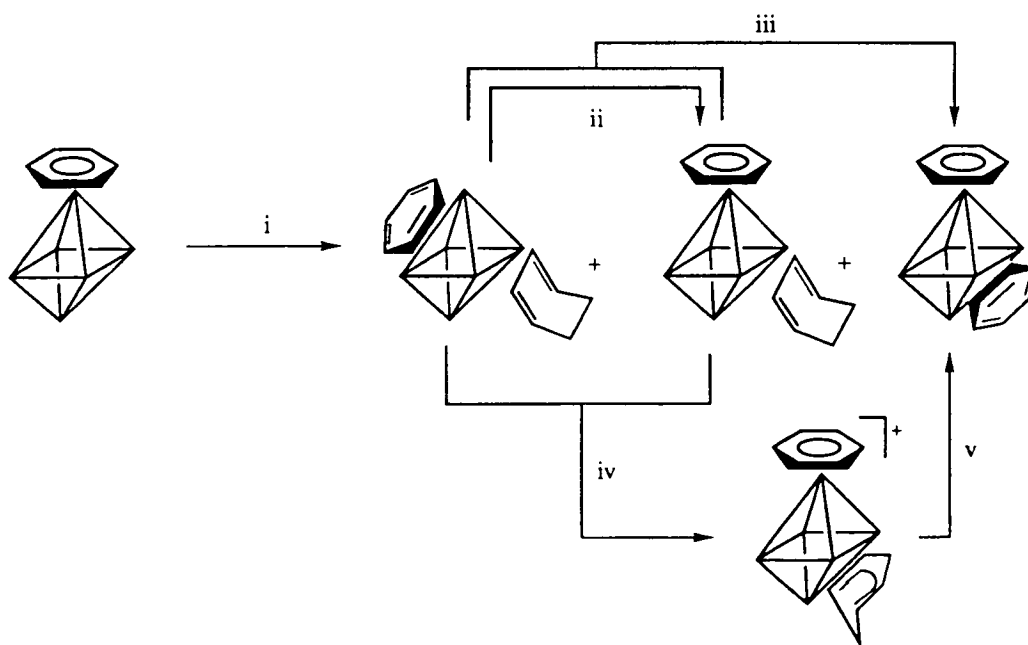
Scheme 5.5ii: The reaction of $Ru_6C(CO)_{14}(\eta^6\text{-}C_6H_6)$ with Me_3NO and cyclohexa-1,3-diene. (i) 3 mol. equiv. $Me_3NO/1,3\text{-}C_6H_8/CH_2Cl_2/\text{-}78°C$, (ii) Δ, hexane, (iii) 1 mol. equiv. $Me_3NO/CH_2Cl_2/\text{-}78°C$, (iv) $[Ph_3C][BF_4]/CH_2Cl_2$, (v) DBU/CH_2Cl_2.

$\eta^1{:}\eta^2{:}\eta^2\text{-}C_6H_7)]^+$, formed by the abstraction of H⁻ upon reaction with Ph_3C^+. This cationic species then reacts with the non-coordinating base DBU to afford $Ru_6C(CO)_{11}(\eta^6\text{-}C_6H_6)(\mu_3\text{-}\eta^2{:}\eta^2{:}\eta^2\text{-}C_6H_6)$, as summarised in scheme 5.5ii.

The two cyclophane clusters, $Ru_3(CO)_9(\mu_3\text{-}\eta^2{:}\eta^2{:}\eta^2\text{-}C_{16}H_{16})$ **23** and $Ru_6C(CO)_{14}(\mu_3\text{-}\eta^2{:}\eta^2{:}\eta^2\text{-}C_{16}H_{16})$ **25**, have been subjected to similar reaction conditions as those described for the triosmium and hexaruthenium benzene clusters, and have yielded two highly unusual products.

5.5.1 Reaction of $Ru_3(CO)_9(\mu_3\text{-}\eta^2{:}\eta^2{:}\eta^2\text{-}C_{16}H_{16})$ 23 with cyclohexa-1,3-diene

To a solution of $Ru_3(CO)_9(\mu_3\text{-}\eta^2{:}\eta^2{:}\eta^2\text{-}C_{16}H_{16})$ **23** in dichloromethane containing an excess of cyclohexa-1,3-diene at -78°C, 2.2 molecular equivalents of Me_3NO, also in dichloromethane, were added dropwise. The solution was stirred at -78°C for twenty minutes and then allowed to slowly warm to room temperature where it was stirred for a further three hours. The products were extracted from the reaction mixture by t.l.c., using a dichloromethane-hexane solution (3:7, v/v) as eluent, which resulted in the isolation, in modest yield, of the yellow starting material **23** and a new orange complex, $Ru_4(CO)_9(\eta^4\text{-}C_6H_8)(\mu_3\text{-}C_{16}H_{16})$ **37** (see Scheme 5.5.1).
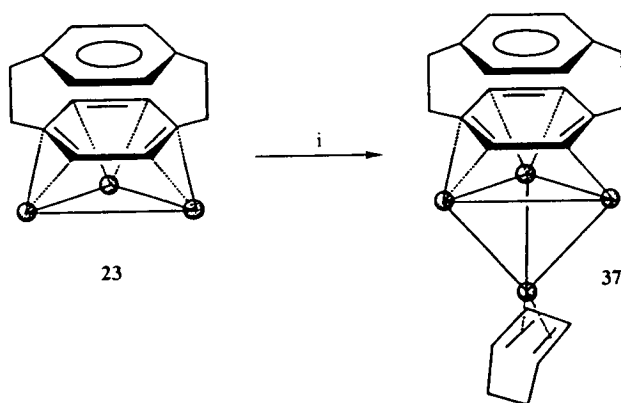
Scheme 5.5.1: The reaction of $Ru_3(CO)_9(\mu_3\text{-}\eta^2{:}\eta^2{:}\eta^2\text{-}C_{16}H_{16})$ 23 with Me_3NO and cyclohexa-1,3-diene: (i) 2.5 mol. equiv. $Me_3NO/1,3\text{-}C_6H_8/CH_2Cl_2/\text{-}78°C$.

Characterisation of $Ru_4(CO)_9(\eta^4\text{-}C_6H_8)(\mu_3\text{-}C_{16}H_{16})$ **37** was initially based on spectroscopic evidence. The infrared spectrum shows peaks (υ_{CO}) between 2038 and 1795 cm^{-1} which are indicative of both terminal and bridging carbonyl ligands. The mass spectrum exhibits a parent peak at 945 (calc. 946) amu followed by peaks corresponding to

the loss of nine CO ligands; the largest peak being at 862 amu which corresponds to the loss of three CO groups. The ^{1}H NMR spectrum of **37** contains eight signals at δ 7.48 (s, 4H), 5.75 (m, 2H), 4.54 (m, 2H), 3.32 (m, 4H), 3.26 (s, 4H), 2.47 (m, 4H), 2.12 (m, 2H) and 1.88 (m, 2H). The resonances at δ 7.48, 3.32, 3.26 and 2.47 are derived from the [2.2]paracyclophane moiety, with the first and third corresponding to the aromatic protons of the unattached and coordinated rings, respectively, and the remaining two from the CH_2CH_2 bridges. These signals are typical for a μ_3-η^2:η^2:η^2 paracyclophane system, with the chemical shift of the bound ring protons (δ 3.26 ppm) being comparable to that of similar clusters containing a facial cyclophane ligand. The remaining signals may be assigned to the cyclohexa-1,3-diene ring, with those at δ 5.75 and 4.54 ppm being associated with the olefinic protons of the diene, and those at δ 2.12 and 1.88 ppm corresponding to the aliphatic ring protons.

Crystals of **37** suitable for a single crystal X-ray analysis were grown from a solution of dichloromethane layered with octane after standing for several days at room temperature. The molecular structure of **37** is shown in Figure 5.5.1i together with relevant bond parameters.

The metal framework in **37** consists of a tetrahedron of ruthenium atoms with Ru-Ru bond distances ranging from 2.780(2) - 2.897(2) Å. Three edges of the tetrahedron are asymmetrically bridged by μ_2 carbonyl ligands, and these edges are shorter than the remaining three which make up the triangular face capped by the cyclophane moiety [mean 2.815(2) *vs.* 2.872(3) Å]. Of the nine carbonyl ligands three form the aforementioned bridging interactions, while the other six are terminal and evenly distributed amongst the three ruthenium atoms involved in cyclophane substitution. The most interesting feature of this compound is the presence of the [2.2]paracyclophane ligand which bonds to the cluster face defined by Ru(1)-Ru(2)-Ru(4) in a highly unusual manner more reminiscent of a μ_3 cyclohexadienyl ring. In addition, a cyclohexa-1,3-diene moiety is coordinated solely to Ru(3) in an η^4 manner.

An alternative view of the bound cyclophane C_6 ring and the triruthenium section of the cluster to which it is attached is presented in Figure 5.5.1ii(a). As mentioned above, the bonding is closely related to that observed in the facially bound cyclohexadienyl ring of $Ru_3(\mu$-H)$(CO)_9(\mu_3$-η^1:η^2:η^2-$C_6H_7)$,[40] which is illustrated in Figure 5.5.1ii(b) for comparison. In the cluster $Ru_4(CO)_9(\eta^4$-$C_6H_8)(\mu_3$-η^1:η^2:η^2-$C_{16}H_{16})$ **37**, Ru(1) interacts strongly with C(4c) [2.115(9) Å], with much weaker interactions being formed with both C(3c) and C(5c) [2.538(9) and 2.505(10) Å, respectively]. Consequently, C(4c) is only considered to donate a single electron to Ru(1), forming an η^1 bond. Two pairs of electrons are thought to be formally donated to Ru(2) and Ru(4) through the η^2 C=C bonds; each interaction consisting of one long and one short bond, *viz.* Ru(2)-C(5c) 2.478(9), Ru(2)-C(6c) 2.184(8) and Ru(4)-C(3c) 2.482(9), Ru(4)-C(2c) 2.184(8) Å. Whilst the η^1:η^2:η^2

Figure 5.5.1i: The molecular structure of $Ru_4(CO)_9(\eta^4\text{-}C_6H_8)(\mu_3\text{-}\eta^1{:}\eta^2{:}\eta^2\text{-}C_{16}H_{16})$ **37** in the solid-state showing the atomic labelling scheme. The C-atoms of the CO ligands bear the same numbering as the corresponding O-atoms. Relevant bond distances (Å) include: Ru(1)-Ru(2) 2.869(3), Ru(1)-Ru(3) 2.843(2), Ru(1)-Ru(4) 2.850(2), Ru(2)-Ru(3) 2.821(2), Ru(2)-Ru(4) 2.897(2), Ru(3)-Ru(4) 2.780(2), Ru(1)-C(31) 2.303(10), Ru(3)-C(31) 1.965(10), C(31)-O(31) 1.165(11), Ru(2)-C(33) 2.020(11), Ru(3)-C(33) 2.144(9), C(33)-O(33) 1.175(12), Ru(3)-C(32) 2.108(10), Ru(4)-C(32) 2.035(10), C(32)-O(32) 1.193(11), mean Ru-C$_{(terminal\ CO)}$ 1.891(12), mean C-O$_{(terminal\ CO)}$ 1.149(11), Ru(1)-C(3c) 2.538(9), Ru(1)-C(4c) 2.115(9), Ru(1)-C(5c) 2.506(8), Ru(2)-C(5c) 2.478(9), Ru(2)-C(6c) 2.187(8), Ru(4)-C(2c) 2.184(8), Ru(4)-C(3c) 2.482(9), C(1c)-C(2c) 1.428(13), C(1c)-C(6c) 1.402(13), C(1c)-C(13c) 1.497(14), C(2c)-C(3c) 1.442(13), C(3c)-C(4c) 1.444(12), C(4c)-C(5c) 1.461(13), C(4c)-C(15c) 1.545(13), C(5c)-C(6c) 1.440(13), C(7c)-C(8c) 1.389(13), C(7c)-C(12c) 1.405(14), C(7c)-C(14c) 1.51(2), C(8c)-C(9c) 1.385(14), C(9c)-C(10c) 1.382(14), C(10c)-C(11c) 1.41(2), C(10c)-C(16c) 1.46(2), C(11c)-C(12c) 1.38(2), C(13c)-C(14c) 1.538(14), C(15c)-C(16c) 1.572(14), Ru(3)-C(1d) 2.301(9), Ru(3)-C(2d) 2.222(10), Ru(3)-C(3d) 2.149(9), Ru(3)-C(4d) 2.222(8), C(1d)-C(2d) 1.38(2), C(1d)-C(6d) 1.521(12), C(2d)-C(3d) 1.440(13), C(3d)-C(4d) 1.431(14), C(4d)-C(5d) 1.49(2), C(5d)-C(6d) 1.534(14).

nomenclature has been ascribed to the bonding mode observed, an alternative description could also be used in which the ring forms an η^3 interaction with Ru(1) and two η^1 interactions with Ru(2) and Ru(4). The distances of 2.73 and 2.80 Å that are observed for Ru(2)···C(1c) and Ru(4)···C(1c), respectively, show little, if any, interaction between C(1c) and the metal framework.

203

(a)   (b)

Figure 5.5.1ii: Comparative views of the metal-ring interaction in
(a) $Ru_4(CO)_9(\eta^4\text{-}C_6H_8)(\mu_3\text{-}\eta^1\text{:}\eta^2\text{:}\eta^2\text{-}C_{16}H_{16})$ **37** and (b) $Ru_3(\mu\text{-}H)(CO)_9(\mu_3\text{-}\eta^1\text{:}\eta^2\text{:}\eta^2\text{-}C_6H_7)$.

In $Ru_4(CO)_9(\eta^4\text{-}C_6H_8)(\mu_3\text{-}\eta^1\text{:}\eta^2\text{:}\eta^2\text{-}C_{16}H_{16})$ **37**, the boat-shaped deviation from planarity observed in the free [2.2]paracyclophane ligand is only observed for one of the enyl-units of the bound ring; the angle between the planes of the central rectangle and the triangular ends defined by C(2c)-C(1c)-C(6c) and C(5c)-C(4c)-C(3c) being 1(1) and 17(1)°, respectively [*cf.* 12.6° for the comparable angle in the free molecule]. Hence, the angle of the unit which may be described as involving an η^3 interaction has increased dramatically, while the other has decreased to such an extent that it is almost planar. This may be compared with the situation found in $Ru_2(CO)_6(\mu_2\text{-}\eta^3\text{:}\eta^3\text{-}C_{16}H_{16})$ **30**, which contains two η^3 type interactions both of which deviate from planarity quite considerably (see Section 5.2). Whilst it is possible that a H-atom is connected to C(1c) thereby turning the ligand into a dienyl system, the approximate sp^2 hybridisation of this C-atom tends to rule out this possibility, as does the ^1H NMR spectrum.

A valence electron count of 60 is required for a tetrahedral cluster to fulfil the EAN rule, and hence with the cyclophane ligand only donating five electrons the cluster is one electron deficient. It was therefore anticipated that a hydride would bridge the Ru(2)-Ru(4) edge, as observed in the analogous position in the dienyl species $Ru_3(\mu\text{-}H)(CO)_9(\mu_3\text{-}\eta^1\text{:}\eta^2\text{:}\eta^2\text{-}C_6H_7)$,[40] especially since this is the longest Ru-Ru bond [2.897(2) Å] of the cluster framework. However, a hydride has not been observed by ^1H NMR spectroscopy or directly located in the crystal structure.

In contrast to the solid-state structure, the ^1H NMR spectrum of $Ru_4(CO)_9(\eta^4\text{-}C_6H_8)(\mu_3\text{-}C_{16}H_{16})$ **37** indicates that the cyclophane ligand behaves as a six electron donor,

exhibiting four signals in a pattern which is typical of that observed when [2.2]paracyclophane coordinates to a cluster in the μ_3-η^2:η^2:η^2 mode. The singlet resonance of the coordinated C-H ring protons at δ 3.26 ppm would not be anticipated from the bonding observed in the solid-state, and it is therefore possible that the ring is undergoing some type of dynamical behaviour in solution which equilibrates all the C-H resonances. A solution IR spectrum of the actual crystal used for the X-ray data collection is identical to that of the bulk solution, which suggests that the solid-state structure represents a conformation encountered in solution during rotation, merely frozen out by packing forces. The following section points out an unusual near-eclipsed *pseudo* μ_3-η^1:η^1:η^1 coordination mode of the cyclophane ligand and these two orientations, combined with the conventional μ_3-η^2:η^2:η^2 mode, provide possible snapshots of the position of the ligand as it rotates over the metal face.

The increase in nuclearity observed during the formation of $Ru_4(CO)_9(\eta^4$-$C_6H_8)(\mu_3$-$C_{16}H_{16})$ **37** from $Ru_3(CO)_9(\mu_3$-η^2:η^2:η^2-$C_{16}H_{16})$ **23** is not entirely unexpected. The reaction of **23** with Me_3NO only and with diphenylacetylene has previously resulted in dinuclear products, thus illustrating that fragmentation is a common feature of this type of reaction. Hence, it can be envisaged that in the presence of cyclohexa-1,3-diene, fragmentation of **23** is followed by recombination to form a tetranuclear cluster incorporating the diene ligand. A similar type of reaction is observed when $Rh_4(CO)_{12}$ is treated with two equivalents of Me_3NO in the presence of $1,3$-C_6H_8, and instead of the anticipated tetrarhodium product, an increase in cluster nuclearity results in the formation of $Rh_6(CO)_{14}(\eta^4$-$C_6H_8)$.[41] However, there is a greater propensity for rhodium carbonyl clusters to undergo cluster build-up than there is for ruthenium.[42]

5.5.2 Reaction of $Ru_6C(CO)_{14}(\mu_3$-η^2:η^2:η^2-$C_{16}H_{16})$ 25 with cyclohexa-1,3-diene

The [2.2]paracyclophane cluster, $Ru_6C(CO)_{14}(\mu_3$-η^2:η^2:η^2-$C_{16}H_{16})$ **25**, has been found to undergo reaction with cyclohexa-1,3-diene by chemical activation using Me_3NO. This procedure is similar to that just described except that a much shorter reaction time, *viz.* 30 minutes, is used. The mixed cyclophane-diene complex, $Ru_6C(CO)_{12}(\mu_2$-η^2:η^2-$C_6H_8)(\mu_3$-η^2:η^2:η^2-$C_{16}H_{16})$ **38**, can be isolated by t.l.c., using a dichloromethane-hexane (2:3, v/v) solution as eluent.

Compound **38** was characterised initially from a comparison of its infrared spectrum with that of the benzene-diene cluster $Ru_6C(CO)_{12}(\mu_2$-η^2:η^2-$C_6H_8)(\mu_3$-η^2:η^2:η^2-$C_6H_6)$.[39] The symmetry of the υ_{CO} stretches in the two spectra are virtually identical, merely shifted to slightly lower wavenumbers in that of **38**. The mass spectrum is also in good agreement with the formulation of **38** as $Ru_6C(CO)_{12}(\mu_2$-η^2:η^2-$C_6H_8)(\mu_3$-η^2:η^2:η^2-$C_{16}H_{16})$ with a strong parent peak at 1242 (calc. 1243) followed by peaks corresponding to the sequential

loss of twelve carbonyl groups in succession. The ^{1}H NMR spectrum is very complicated; twelve signals would be predicted for such a compound, *i.e.* four from the paracyclophane moiety and eight from the diene unit. However, additional signals appear to be present which suggests the possibility of isomers in solution. Unfortunately, problems associated with the poor solubility of crystalline material has hampered further spectroscopic studies.

The molecular structure of **38** has been established by a single crystal X-ray analysis on a crystal grown from a dichloromethane-hexane solution at -25°C, and is shown in Figure 5.5.2i together with relevant structural details. The cluster framework comprises of an octahedral array of ruthenium atoms encapsulating a carbide atom which sits approximately in the centre of the cavity. The Ru-Ru bond lengths range from 2.778(3) to 3.036(3) Å, which is comparable to the values observed in $Ru_6C(CO)_{14}(\mu_3\text{-}\eta^2\text{:}\eta^2\text{:}\eta^2\text{-}C_{16}H_{16})$ **25** and $Ru_6C(CO)_{11}(\eta^6\text{-}C_{16}H_{16})(\mu_3\text{-}\eta^2\text{:}\eta^2\text{:}\eta^2\text{-}C_{16}H_{16})$ **26**, with the shortest edge being that bridged by the μ_2 CO ligand [Ru(5)-Ru(6)]. The paracyclophane ligand is facially bound, as in **25** and **26**, and again the bound ring flattens out whilst the uncoordinated ring retains its boat-shaped conformation. The cyclohexa-1,3-diene ligand adopts the usual edge-bridging $\mu_2\text{-}\eta^2\text{:}\eta^2$ coordination mode found in all the 1,3-C_6H_8 derivatives of the hexanuclear cluster $Ru_6C(CO)_{17}$,[39] and spans an edge opposite to the paracyclophane-bound cluster face. The cluster contains a total of 86 valence electrons and is therefore consistent with the PSEPT of electron counting.

Apart from these general features, the coordination of the paracyclophane ligand deserves further comment, and is discussed in relation to $Ru_6C(CO)_{14}(\mu_3\text{-}\eta^2\text{:}\eta^2\text{:}\eta^2\text{-}C_{16}H_{16})$ **25** and $Ru_6C(CO)_{11}(\eta^6\text{-}C_{16}H_{16})(\mu_3\text{-}\eta^2\text{:}\eta^2\text{:}\eta^2\text{-}C_{16}H_{16})$ **26**, which were introduced in Chapter four. The structures of **25**, **26** and **38** offer the opportunity to study the coordination of paracyclophane in different crystalline environments, and the μ_3 rings in each complex show a differing degree of torsion with respect to the underlying Ru_3 fragments. This is reflected in the value of the Ru-C distances which alternate in length around the ring, the difference increasing in the order **26** < **25** < **38**, with mean Ru-C distances of 2.23(2) *vs.* 2.33(2) ($\Delta = 0.10$) in **26**, 2.20(1) *vs.* 2.37(1) ($\Delta = 0.17$) in **25** and 2.17(3) *vs.* 2.45(3) Å ($\Delta = 0.28$ Å) in **38**. The fact that on going from **26** to **25** and then to **38** the short Ru-C separation becomes progressively shorter, while the long Ru-C distance increases, clearly indicates that the separation between the ring and the metal triangle is retained, while the ligand rotates from a near staggered configuration of the ring carbon atoms with respect to the Ru-atoms towards a conformation where alternate C-atoms nearly eclipse the Ru-atoms. These orientations are represented in Figure 5.5.2ii.
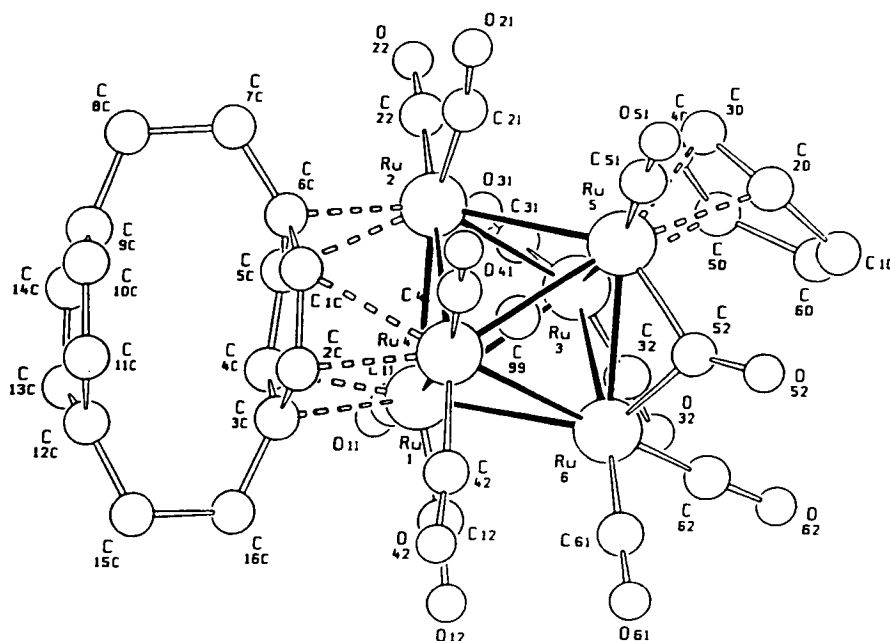
Figure 5.5.2i: The solid-state molecular structure of $Ru_6C(CO)_{12}(\mu_2-\eta^2:\eta^2-C_6H_8)(\mu_3-\eta^2:\eta^2:\eta^2-C_{16}H_{16})$ **38**, showing the atomic labelling scheme; the C atoms of the CO groups bear the same numbering as the corresponding O atoms. Relevant bond distances ($\mathring{A}$): Ru(1)-Ru(2) 2.922(3), Ru(1)-Ru(3) 2.821(3), Ru(1)-Ru(4) 2.848(2), Ru(1)-Ru(6) 3.036(3), Ru(2)-Ru(3) 2.908(2), Ru(2)-Ru(4) 2.844(3), Ru(2)-Ru(5) 2.929(3), Ru(3)-Ru(5) 2.908(2), Ru(3)-Ru(6) 3.007(3), Ru(4)-Ru(5) 2.952(3), Ru(4)-Ru(6) 2.878(2), Ru(5)-Ru(6) 2.778(3), Ru(1)-C 2.06(2), Ru(2)-C 2.06(2), Ru(3)-C 2.02(2), Ru(4)-C 2.05(2), Ru(5)-C 2.03(2), Ru(6)-C 2.10(2), Ru(1)-C(3C) 2.49(2), Ru(1)-C(4C) 2.21(2), Ru(1)-C(5C) 2.70(2), Ru(2)-C(1C) 2.70(2), Ru(2)-C(5C) 2.41(2), Ru(2)-C(6C) 2.14(2), Ru(4)-C(1C) 2.44(2), Ru(4)-C(2C) 2.15(2), C(1C)-C(2C) 1.41(3), C(1C)-C(6C) 1.44(3), C(2C)-C(3C) 1.43(3), C(3C)-C(4C) 1.42(3), C(3C)-C(16C) 1.45(3), C(4C)-C(5C) 1.43(3), C(5C)-C(6C) 1.43(3), C(6C)-C(7C) 1.50(3), C(7C)-C(8C) 1.53(3), C(8C)-C(9C) 1.47(3), C(9C)-C(10C) 1.44(3), C(9C)-C(14C) 1.32(3), C(10C)-C(11C) 1.37(3), C(11C)-C(12C) 1.41(3), C(12C)-C(13C) 1.40(3), C(12C)-C(15C) 1.48(3), C(13C)-C(14C) 1.43(3), C(15C)-C(16C) 1.57(3), Ru(3)-C(4D) 2.36(3), Ru(3)-C(5D) 2.28(2), Ru(5)-C(2D) 2.26(2), Ru(5)-C(3D) 2.23(2), C(1D)-C(2D) 1.54(3), C(1D)-C(6D) 1.55(4), C(2D)-C(3D) 1.37(3), C(3D)-C(4D) 1.50(3), C(4D)-C(5D) 1.33(3), C(5D)-C(6D) 1.54(4).

The comparative analysis of compounds **25, 26** and **38** offers an important indication that the face-capping interaction is highly deformable. This is not so evident when the ligand is benzene which is almost completely embedded within the ligand shell, but becomes more pronounced with the bulky paracyclophane ligand which protrudes

207

from the cluster surface. It is difficult to explain these differences in terms of electronic influences because by simply replacing two of the carbonyl groups on **25** by a cyclohexa-1,3-diene moiety, as in **38**, the most dramatic effect in the orientation of the ring over the triruthenium face has occurred. Also *intra*molecular steric arguments seem of little consequence, since the section of the cluster to which the ring is bound is virtually unperturbed in the three complexes being studied. It therefore seems reasonable to attribute the differences to the effect that extra molecular forces have on the molecules embedded in their crystalline field. Hence, although both the initial factors must make some contribution, it is thought that crystal packing forces probably dominate.
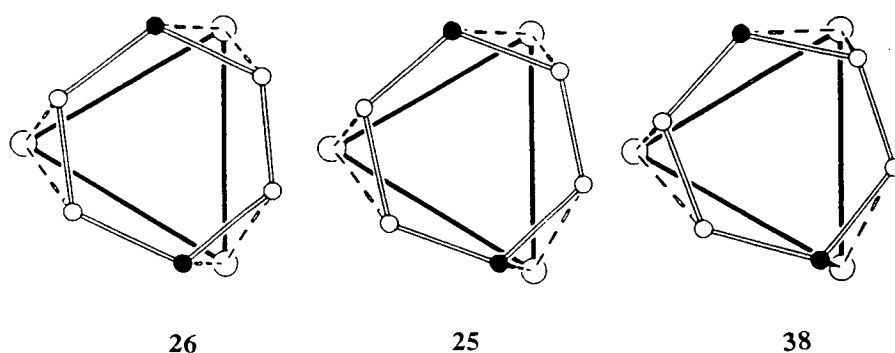
Figure 5.5.2ii: Comparative projections of the [2.2]paracyclophane-coordination planes in **26, 25** and **38** showing the progression from near-eclipsing to near-staggering of the C=C midpoints over the Ru atoms. The remaining portions of the clusters and of the ligands have been omitted for clarity. Filled C-atoms are those connected to the CH_2CH_2 bridges.

A detailed and systematic study of the molecular structures possessed by **25, 26** and **38** has therefore shown that the $C_{16}H_{16}$ moiety undergoes significant distortions on coordination, giving rise to a variation in coordination mode from the nearly perfectly staggered to the nearly eclipsed conformation of the ring with respect to the underlying triangular cluster face. The compound $Ru_6C(CO)_{12}(\mu_2-\eta^2:\eta^2-C_6H_8)(\mu_3-\eta^2:\eta^2:\eta^2-C_{16}H_{16})$ **38** also has some relevance to the chemisorption of benzene on the metal surface. The coordination of the *pseudo* $\mu_3-\eta^1:\eta^1:\eta^1$ cyclophane ligand in this complex is comparable to the structure observed for chemisorbed benzene at a 'hollow' $[C_{3v}(\sigma_v)]$ site on a Rh(111) surface, which has been stabilised by the coadsorption of sodium [Rh(111)/ C_6H_6/Na] and is considered to be a transition state in arene rotation on the metal surface.[43]

5.6   **Reaction of $Ru_4(CO)_{12}(\mu_4\text{-}\eta^1\text{:}\eta^1\text{:}\eta^2\text{:}\eta^2\text{-}C_6H_8)$ with [2.2]paracyclophane: The Molecular Structures of $Ru_4(CO)_9(\mu_4\text{-}\eta^1\text{:}\eta^1\text{:}\eta^2\text{:}\eta^2\text{-}C_6H_8)(\eta^6\text{-}C_{16}H_{16})$ 39 and $Ru_4(CO)_9(\mu_4\text{-}\eta^1\text{:}\eta^1\text{:}\eta^2\text{:}\eta^2\text{-}C_6H_8)(\mu_3\text{-}\eta^2\text{:}\eta^2\text{:}\eta^2\text{-}C_{16}H_{16})$ 40**

Chapter three described the synthesis and structural characterisation of a number of tetraruthenium butterfly clusters containing both cyclohexyne and benzene ligands, and it was demonstrated that two isomeric forms of the cluster $Ru_4(CO)_9(\mu_4\text{-}\eta^1\text{:}\eta^1\text{:}\eta^2\text{:}\eta^2\text{-}C_6H_8)(\eta^6\text{-}C_6H_6)$ [*i.e.* where the benzene moiety occupies either a hinge or a wing-tip ruthenium atom] could undergo interconversion. In an attempt to repeat this chemistry using [2.2]paracyclophane as opposed to benzene, an octane solution of the butterfly cluster, $Ru_4(CO)_{12}(\mu_4\text{-}\eta^1\text{:}\eta^1\text{:}\eta^2\text{:}\eta^2\text{-}C_6H_8)$ 15, containing excess [2.2]paracyclophane was heated to reflux for 4 hours. Two products were extracted from the reaction mixture by t.l.c. using dichloromethane-hexane (2:3, v/v) as eluent, and were characterised as $Ru_4(CO)_9(\mu_4\text{-}\eta^1\text{:}\eta^1\text{:}\eta^2\text{:}\eta^2\text{-}C_6H_8)(\eta^6\text{-}C_{16}H_{16})$ 39 and $Ru_4(CO)_9(\mu_4\text{-}\eta^1\text{:}\eta^1\text{:}\eta^2\text{:}\eta^2\text{-}C_6H_8)(\mu_3\text{-}\eta^2\text{:}\eta^2\text{:}\eta^2\text{-}C_{16}H_{16})$ 40. The addition of three molecular equivalents of Me_3NO to the reaction mixture during reflux was found to improve the yield of the products.

Characterisation of compounds 39 and 40 was based, in the first instance, on spectroscopic evidence. Compound 39 was immediately recognised as $Ru_4(CO)_9(\mu_4\text{-}\eta^1\text{:}\eta^1\text{:}\eta^2\text{:}\eta^2\text{-}C_6H_8)(\eta^6\text{-}C_{16}H_{16})$ from its infrared spectrum which closely resembles, both in profile and wavenumber, that of the analogous benzene compound, $Ru_4(CO)_9(\mu_4\text{-}\eta^1\text{:}\eta^1\text{:}\eta^2\text{:}\eta^2\text{-}C_6H_8)(\eta^6\text{-}C_6H_6)$ 16. The benzene ligand in 16 coordinates to a 'hinge' ruthenium atom and therefore it is reasonable to assume that the cyclophane moiety in 39 bonds at an analogous hinge site. It was noted, however, that the infrared spectrum of compound 40 is not comparable to that of the alternative η^6 'wing-tip' benzene isomer, 17. Both compounds 39 and 40 exhibit the same strong molecular ion in the mass spectrum at 946 (calc. 946) amu, together with peaks corresponding to the loss of several carbonyl groups, and it therefore appeared that the two compounds were isomeric. The ^1H NMR spectrum of $Ru_4(CO)_9(\mu_4\text{-}\eta^1\text{:}\eta^1\text{:}\eta^2\text{:}\eta^2\text{-}C_6H_8)(\eta^6\text{-}C_{16}H_{16})$ 39 is quite complicated since some of the signals overlap, however the paracyclophane unit gives rise to three signals; singlet resonances of equal relative intensity at δ 6.80 and 4.34 ppm for the C-H protons of the uncoordinated and coordinated rings, respectively, and one multiplet centred at δ 3.2 ppm which integrates appropriately for all eight of the protons in the $-CH_2CH_2-$ bridges. The value of δ 4.34 ppm for the bound ring C-H protons is as would be expected for a cyclophane moiety coordinated in a terminal fashion. The cyclohexyne ring protons produce three multiplet resonances centred at δ 3.29, 2.88 and 1.70 ppm with relative intensities of 1:1:2, which are directly comparable to those signals observed in the spectrum of the analogous benzene cluster, 16 (see Chapter three). The ^1H NMR spectrum of $Ru_4(CO)_9(\mu_4\text{-}\eta^1\text{:}\eta^1\text{:}\eta^2\text{:}\eta^2\text{-}C_6H_8)(\mu_3\text{-}\eta^2\text{:}\eta^2\text{:}\eta^2\text{-}C_{16}H_{16})$ 40 contains six resonances of equal relative intensity, four of which can be attributed to the cyclophane moiety and the

remaining two to the cyclohexyne unit. Singlet resonances at δ 7.21 and 3.16 ppm result from the ring C-H protons of the uncoordinated and coordinated rings, respectively. The latter value is lower than that found in **39** and is comparable to that observed in $Ru_4(CO)_9(\eta^4\text{-}C_6H_8)(\mu_3\text{-}C_{16}H_{16})$ **37** (δ 3.26 ppm) therefore suggesting the presence of a facially coordinated ligand. Multiplet signals at δ 3.17 and 2.56 ppm can be assigned to the $-CH_2CH_2-$ bridges of the cyclophane ring system, the former corresponding to the CH_2 protons furthest from the coordinated ring and the latter to those closest. The cyclohexyne entity produces two multiplet resonances centred at δ 3.77 and 1.90 ppm, which is similar to that observed for **39**.

The molecular structures of $Ru_4(CO)_9(\mu_4\text{-}\eta^1\text{:}\eta^1\text{:}\eta^2\text{:}\eta^2\text{-}C_6H_8)(\eta^6\text{-}C_{16}H_{16})$ **39** and $Ru_4(CO)_9(\mu_4\text{-}\eta^1\text{:}\eta^1\text{:}\eta^2\text{:}\eta^2\text{-}C_6H_8)(\mu_3\text{-}\eta^2\text{:}\eta^2\text{:}\eta^2\text{-}C_{16}H_{16})$ **40** have been established in the solid-state by single crystal X-ray diffraction analyses, and are illustrated in Figures 5.6.1 and 5.6.2, respectively, together with relevant bond parameters. Suitable crystals of **39** were grown from a solution of dichloromethane-octane by slow evaporation, whilst crystals of **40** were obtained by vapour diffusion from dichloromethane-pentane at room temperature. The molecular structure of **40** is of poor quality due to the compound crystallising with four independent molecules per asymmetric unit as well as in the presence of disordered solvent. Further attempts to recrystallise using a different solvent have been unsuccessful, however, because the molecule represents the first example of a butterfly cluster containing an arene ligand in the $\mu_3\text{-}\eta^2\text{:}\eta^2\text{:}\eta^2$ coordination mode, and since spectroscopic data are in good agreement with the established structure, it is felt that the gross features of the structure are worth describing, although caution must be taken in reading too much into the actual bond parameters observed.

The two compounds **39** and **40** are isomeric with the complex $Ru_4(CO)_9(\eta^4\text{-}C_6H_8)(\mu_3\text{-}C_{16}H_{16})$ **37**, however, structurally the clusters are very different; the four ruthenium atoms in **39** and **40** adopt a butterfly geometry rather than a tetrahedron, and the C_6H_8 ligand represents a cyclohexyne ligand rather than a cyclohexa-1,3-diene moiety. In both clusters **39** and **40** the skeletal framework, which consists of the four ruthenium atoms and the two carbon atoms of the cyclohexyne group that are bonded to the cluster, can be described in terms of a *pseudo closo*-octahedron. The cyclohexyne ligand formally contributes six electrons to the metal framework (as opposed to four from the cyclohexa-1,3-diene moiety in **37**), thereby providing the butterfly cluster with the additional electron pair required to obtain a count of 62 and, thus, fulfil the EAN rule.

The Ru-Ru bond lengths in $Ru_4(CO)_9(\mu_4\text{-}\eta^1\text{:}\eta^1\text{:}\eta^2\text{:}\eta^2\text{-}C_6H_8)(\eta^6\text{-}C_{16}H_{16})$ **39** range from 2.634(2) to 2.843(2) Å and are rather unusual in that the two shortest edges correspond to those linking the hinge atom bearing the cyclophane moiety, Ru(4), to the two wing-tip ruthenium atoms [Ru(1)-Ru(4) 2.634(2), Ru(3)-Ru(4) 2.636(2) Å *vs.* Ru(1)-

Ru(2) 2.712(2), Ru(2)-Ru(3) 2.727(2) Å]. This metal atom distribution is analogous to that found in the isostructural complex, $Ru_4(CO)_9(\mu_4-\eta^1:\eta^1:\eta^2:\eta^2-C_6H_8)(\eta^6-C_6H_6)$ **16**, but differs to that observed in the parent butterfly cluster, $Ru_4(CO)_{12}(\mu_4-\eta^1:\eta^1:\eta^2:\eta^2-C_6H_8)$ **15**, in which all four hinge-wing-tip distances are approximately equal [range 2.721(2) to 2.743(2) Å]. This resulting contraction may again be attributed to the less efficient π-accepting capability of the cyclophane ligand with respect to the tricarbonyl unit,
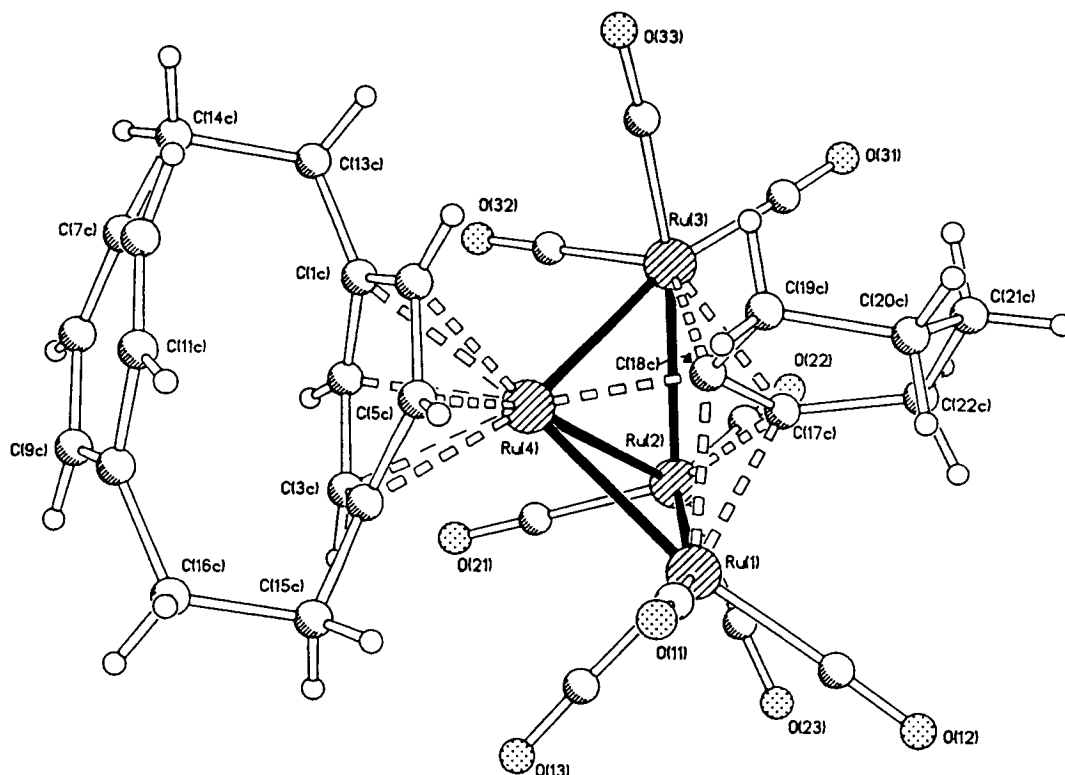
Figure 5.6.1: The molecular structure of $Ru_4(CO)_9(\mu_4-\eta^1:\eta^1:\eta^2:\eta^2-C_6H_8)(\eta^6-C_{16}H_{16})$ **39** in the solid-state showing the atomic labelling scheme. The C-atoms of the CO ligands bear the same numbering as the corresponding O-atoms. Relevant bond distances (Å) include: Ru(1)-Ru(2) 2.712(2), Ru(1)-Ru(4) 2.634(2), Ru(2)-Ru(3) 2.727(2), Ru(2)-Ru(4) 2.843(2), Ru(3)-Ru(4) 2.636(2), mean Ru-C(CO) 1.90(2), mean C-O 1.15(2), Ru(4)-C(1c) 2.369(14), Ru(4)-C(2c) 2.226(14), Ru(4)-C(3c) 2.24(2), Ru(4)-C(4c) 2.364(14), Ru(4)-C(5c) 2.18(2), Ru(4)-C(6c) 2.168(14), C(1c)-C(2c) 1.37(2), C(1c)-C(6c) 1.38(2), C(1c)-C(13c) 1.52(2), C(2c)-C(3c) 1.41(2), C(3c)-C(4c) 1.40(2), C(4c)-C(5c) 1.41(2), C(4c)-C(15c) 1.53(2), C(5c)-C(6c) 1.43(2), C(7c)-C(8c) 1.37(2), C(7c)-C(12c) 1.37(2), C(7c)-C(14c) 1.50(2), C(8c)-C(9c) 1.38(2), C(9c)-C(10c) 1.37(2), C(10c)-C(11c) 1.42(2), C(10c)-C(16c) 1.53(2), C(11c)-C(12c) 1.31(2), C(13c)-C(14c) 1.62(2), C(15c)-C(16c) 1.54(2), Ru(1)-C(17c) 2.296(14), Ru(1)-C(18c) 2.219(13), Ru(2)-C(17c) 2.126(14), Ru(3)-C(17c) 2.250(13), Ru(3)-C(18c) 2.236(13), Ru(4)-C(18c) 2.073(14), C(17c)-C(18c) 1.44(2), C(17c)-C(22c) 1.56(2), C(18c)-C(19c) 1.55(2), C(19c)-C(20c) 1.54(2), C(20c)-C(21c) 1.51(2), C(21c)-C(22c) 1.49(2).

which results in a slight increase of bonding electron density on Ru(4). In common with other butterfly clusters,[44] the Ru-Ru edge connecting the two hinge atoms [Ru(2)-Ru(4)] is significantly longer than the others [2.843(2) *vs.* mean 2.729(2) Å], and is comparable to that found in the starting material **15** [2.849(3) Å].

The cyclohexyne unit lies between the wings of the butterfly with its alkyne C-C bond disposed parallel to the butterfly hinge. The alkyne bonds to all four metal atoms, donating six electrons to the cluster *via* two σ-interactions with the hinge atoms and two π-interactions with the wing-tip rutheniums. This ligand is also slightly displaced towards Ru(4), with the hinge-to-ring distances being Ru(4)-C(18c) 2.073(14) and Ru(2)-C(17c) 2.126(14) Å. This situation may be compared to that observed in the hexaruthenium-carbido system, in which the carbide atom in clusters of the formula $Ru_6C(CO)_{14}(\eta^6$-arene) is always displaced towards the Ru-atom bearing the arene ligand.[15,45] The multiple bond of the cyclohexyne ring is short in comparison to the other C-C bonds of the ring [1.44(2) *vs.* a mean value of 1.53(2) Å], however it is considerably lengthened when compared to that present in the free ligand.[26] The [2.2]paracyclophane moiety is coordinated in a terminal fashion to Ru(4) *via* four short and two long interactions. Once again, the ring is not planar but again adopts a boat-shaped configuration with the four approximately coplanar C-atoms [C(2c), C(3c), C(5c) and C(6c)] lying closer to Ru(4) [mean = 2.20(2) Å] than the two *para*-carbons to which the aliphatic bridges attach [C(1c) and C(4c), mean = 2.37(2) Å]. The angle between the two enyl planes defined by C(2c)-C(1c)-C(6c) and C(3c)-C(4c)-C(5c) and the central rectangle are 18(1) and 15(2)°, respectively, which are similar to the angle observed in the free [2.2]paracyclophane molecule, *viz.* 12.6°,[12] *albeit* slightly larger. The angle between the enyl planes in the unattached ring defined by C(7c)-C(8c)-C(12c) and C(9c)-C(10c)-C(11c) are 11(2)° which is relatively unperturbed from that of the free molecule. The nine carbonyl ligands are all terminal and are evenly distributed between the three ruthenium atoms not involved in cyclophane substitution.

The molecular structure of $Ru_4(CO)_9(\mu_4$-η^1:η^1:η^2:η^2-$C_6H_8)(\mu_3$-η^2:η^2:η^2-$C_{16}H_{16})$ **40** is very similar to that of **39**, the only difference being in the coordination mode adopted by the [2.2]paracyclophane moiety. The four metal atoms again adopt a butterfly arrangement, with the cyclohexyne ligand trapped between the two wings and attached to the cluster *via* a μ_4-η^1:η^1:η^2:η^2 interaction. The cyclophane in this instance is coordinated to the outside of one of the triangular wings [Ru(1)-Ru(2)-Ru(3)] in a facial μ_3-η^2:η^2:η^2 manner, and it is believed that this is the first example of a butterfly cluster containing a face-capping arene ligand. Two terminal carbonyl ligands are situated on each of the ruthenium atoms to which the cyclophane moiety coordinates, whilst the remaining ruthenium atom carries a tricarbonyl unit.
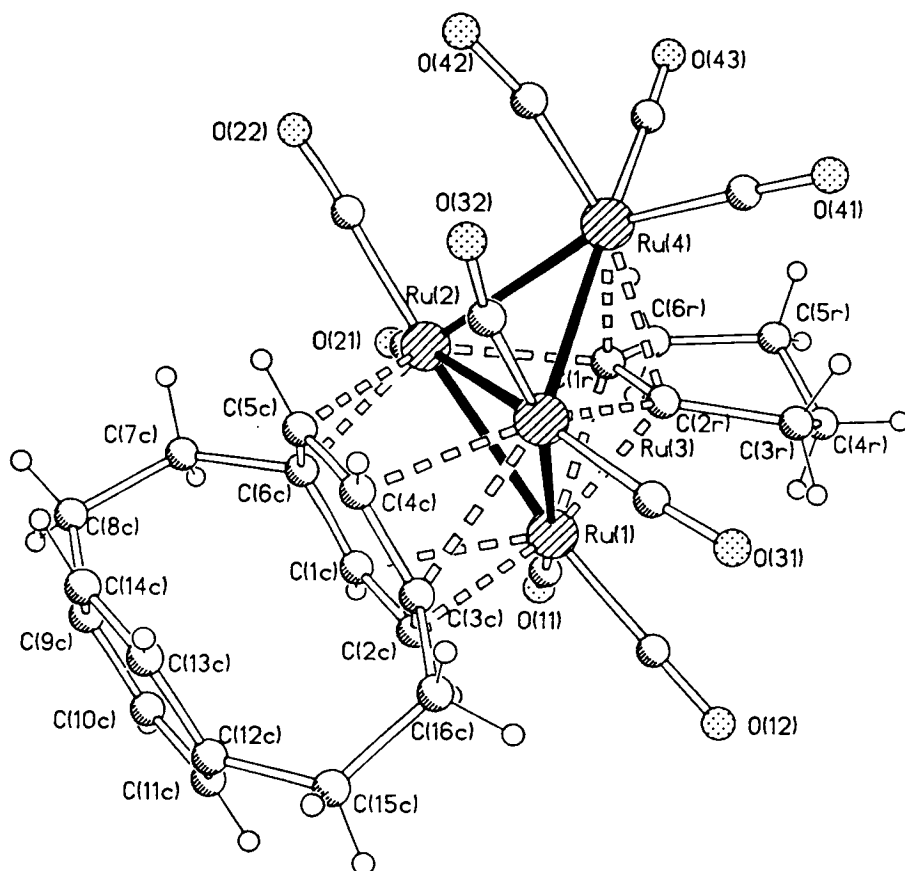
Figure 5.6.2: The molecular structure of $Ru_4(CO)_9(\mu_4-\eta^1:\eta^1:\eta^2:\eta^2-C_6H_8)(\mu_3-\eta^2:\eta^2:\eta^2-C_{16}H_{16})$ **40** in the solid-state showing the atomic labelling scheme. The C-atoms of the CO ligands bear the same numbering as the corresponding O-atoms. Relevant bond distances (Å) include: Ru(1)-Ru(2) 2.732(4), Ru(1)-Ru(3) 2.731(4), Ru(2)-Ru(3) 2.823(4), Ru(2)-Ru(4) 2.767(4), Ru(3)-Ru(4) 2.679(4), mean Ru-C(CO) 1.863(17), mean C-O 1.163(18), Ru(1)-C(1C) 2.340(24), Ru(1)-C(2C) 2.185(25), Ru(2)-C(5C) 2.361(26), Ru(2)-C(6C) 2.105(27), Ru(3)-C(3C) 2.411(26), Ru(3)-C(4C) 2.173(28), C(3C)-C(16C) 1.544(40), C(6C)-C(7C) 1.603(49), C(7C)-C(8C) 1.580(70), C(8C)-C(9C) 1.545(62), C(12C)-C(15C) 1.574(56), C(15C)-C(16C) 1.502(60), all other C-C(cyclophane) distances are fixed at 1.390 Å, Ru(1)-C(1R) 2.236(44), Ru(1)-C(2R) 2.161(36), Ru(2)-C(1R) 2.216(45), Ru(3)-C(2R) 2.174(36), Ru(4)-C(1R) 2.253(43), Ru(4)-C(2R) 2.233(36), C(1R)-C(2R) 1.384(55), C(1R)-C(6R) 1.488(59), C(2R)-C(3R) 1.582(53), C(3R)-C(4R) 1.529(57), C(4R)-C(5R) 1.441(61), C(5R)-C(6R) 1.503(61).

It has been found that the hinge-isomer, $Ru_4(CO)_9(\mu_4-\eta^1:\eta^1:\eta^2:\eta^2-C_6H_8)(\eta^6-C_{16}H_{16})$ **39**, slowly converts into the facial-isomer, $Ru_4(CO)_9(\mu_4-\eta^1:\eta^1:\eta^2:\eta^2-C_6H_8)(\mu_3-\eta^2:\eta^2:\eta^2-C_{16}H_{16})$ **40**, on standing in solution at room temperature. Alternatively, **39** can be converted quantitatively into **40** by simply heating a dichloromethane solution under reflux for two hours. The hinge-isomer **39** is therefore considered to be the kinetic product from

the thermolysis reaction since it undergoes isomerisation *via* migration of the [2.2]paracyclophane unit to the facial position, thereby affording the thermodynamic product, **40**. This process is not reversible, and again illustrates the unusual nature of [2.2]paracyclophane with its preference to coordinate in a facial manner. This is in contrast to that observed for most arenes where the terminal bonding site is predominant. This series of reactions is illustrated by Scheme 5.6.
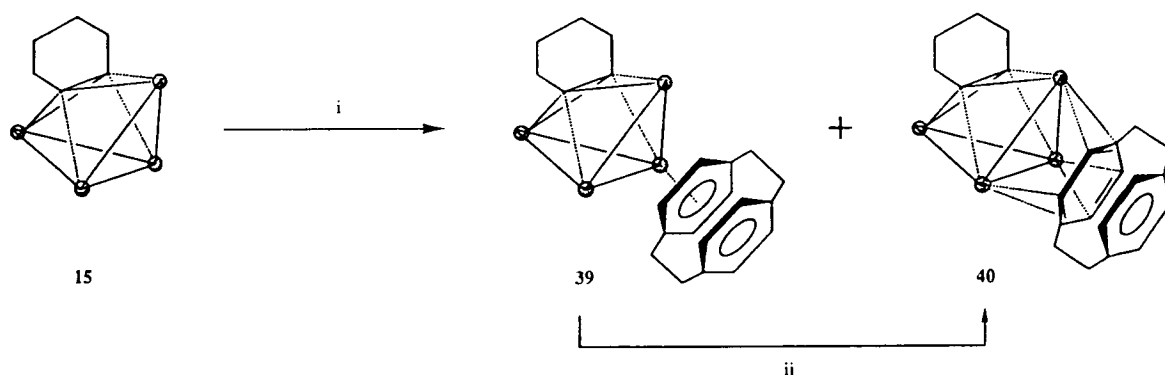
Scheme 5.6: Reaction of $Ru_4(CO)_{12}(\mu_4-\eta^1:\eta^1:\eta^2:\eta^2-C_6H_8)$ **15** with [2.2]paracyclophane; i) Δ, octane/$C_{16}H_{16}$/3 mol. eq. Me_3NO, ii) Δ, CH_2Cl_2.

5.7 Concluding Remarks

Various ways of manipulating the triruthenium and hexaruthenium cyclophane clusters $Ru_3(CO)_9(\mu_3-\eta^2:\eta^2:\eta^2-C_{16}H_{16})$ **23** and $Ru_6C(CO)_{14}(\mu_3-\eta^2:\eta^2:\eta^2-C_{16}H_{16})$ **25** have been illustrated in a series of reactions which employ either thermolytic action or chemical initiation using Me_3NO. Whilst very different products are obtained from these reactions in the absence of a ligand, when a suitable ligand is employed both thermolysis and chemical activation tend to result in formation of the same compounds, although the chemical activation method is generally more selective and yields are higher. The series of reactions described throughout this chapter are summarised in Scheme 5.7 and show a wide and diverse range of products. Some of these reactions have been employed in the analogous benzene compounds, $M_3(CO)_9(\mu_3-\eta^2:\eta^2:\eta^2-C_6H_6)$ (M = Ru, Os) and $Ru_6C(CO)_{14}(\eta^6-C_6H_6)$ and, where appropriate, comparisons have been made. One of the most interesting features of this work is the isolation of products formed by either cluster degradation or a recombination of fragments, which result in cluster nuclearities that are both smaller and larger than the precursor starting material (a feature which has yet to be observed in the

analogous benzene chemistry). Also, [2.2]paracyclophane has been found to bond to the cluster framework in a number of ways which have not been noted in the corresponding benzene complexes; for example the edge-bridging mode (μ_2-η^3:η^3), and the facial coordination modes in which the ring is near-eclipsed (μ_3-η^1:η^1:η^1) in one example and
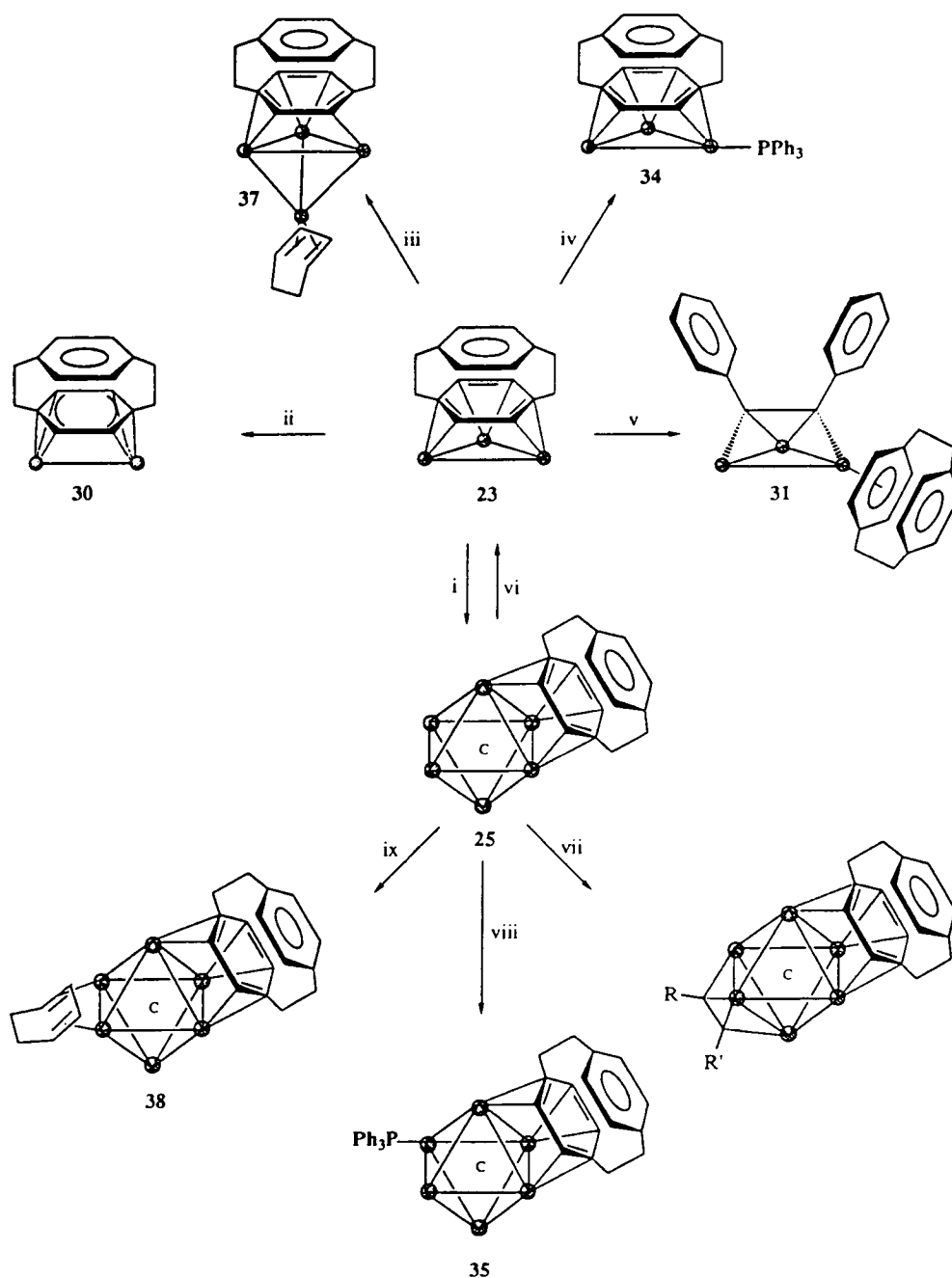
Scheme 5.7: A summary of the reactions of $Ru_3(CO)_9(\mu_3$-η^2:η^2:η^2-$C_{16}H_{16})$ **23** and $Ru_6C(CO)_{14}(\mu_3$-η^2:η^2:η^2-$C_{16}H_{16})$ **25** described throughout the chapter. i) Δ, octane/$Ru_3(CO)_{12}$, ii) 3 mol. eq. Me_3NO, iii) 2 mol. eq. $Me_3NO/1,3$-C_6H_8, iv) 1 mol. eq. Me_3NO/PPh_3 or Δ, thf/PPh_3, v) 2 mol. eq. Me_3NO/C_2Ph_2 or Δ, CH_2Cl_2/C_2Ph_2, vi) Excess Me_3NO, vii) 2 mol. eq. Me_3NO/alkyne, viii) 1 mol. eq. Me_3NO/PPh_3 or Δ, thf/PPh_3, ix) 2 mol. eq. $Me_3NO/1,3$-C_6H_8.

involves only five of the six ring carbon atoms (μ_3-η^1:η^2:η^2) in another. These new coordination modes are thought to represent model intermediates for both the migration and the rotation of arene ligands on a metal cluster, and can also be compared to the chemisorption of benzene on a metal surface. Once again ^{1}H NMR spectroscopy has proved to be a useful tool for qualitatively assessing the electron density available on the cluster framework for bonding, especially in the phosphine containing derivatives, and this chapter also illustrates the first example of a butterfly cluster containing an arene ligand in the μ_3-η^2:η^2:η^2 face-capping coordination mode.

5.8   References

1.   Dyson, P.J.; Johnson, B.F.G.; *Transition Met. Chem.*, **1993**, *18*, 539.

2.   Gallop, M.A.; Gomez-Sal, M.P.; Housecroft, C.E.; Johnson, B.F.G.; Lewis, J.; Owen, S.M.; Raithby, P.R.; Wright, A.H.; *J. Am. Chem. Soc.*, **1992**, *114*, 2502.

3.   Gallop, M.A.; Johnson, B.F.G.; Lewis, J.; Raithby, P.R.; *J. Chem. Soc., Chem. Comm.*, **1987**, 1809.

4.   Gallop, M.A.; Johnson, B.F.G.; Lewis, J.; Wright, A.H.; *J. Chem. Soc., Dalton Trans.*, **1989**, 481.

5.   Kane-Maguire, L.A.P.; Honig, E.D.; Sweigart, D.A.; *Chem. Rev.*, **1984**, *84*, 525.

6.   Gomez-Sal, M.P.; Johnson, B.F.G.; Lewis, J.; Raithby, P.R.; Wright, A.H.; *J. Chem. Soc., Chem. Comm.*, **1985**, 1162.

7.   (a) Steed, J.W.; Tocher, D.A.; *J. Organomet. Chem.*, **1991**, *412*, C37; (b) Elsegood, M.R.J.; Steed, J.W.; Tocher, D.A.; *J. Chem. Soc., Dalton Trans.*, **1992**, 1797.

8.   Davies, S.G.; Green, M.L.H.; Mingos, D.M.P.; *Tetrahedron*, **1978**, *34*, 3047.

9.   Swann, R.T.; Hanson, A.W.; Boekelheide, V.; *J. Am. Chem. Soc.*, **1986**, *108*, 3324.

10.   (a) Jones, D.; Pratt, L.; Wilkinson, G.; *J. Chem. Soc.*, **1962**, 4458; (b) Rybinskaya, M.I.; Kaganovitch, V.S.; Kudinov, A.R.; *J. Organomet. Chem.*, **1982**, *235*, 215.

11.   Müller, J.; Gaede, P.E.; Qiao, K.; *Angew. Chem. Int. Ed. Engl.*, **1993**, *32*, 1697.

12.   Bernstein, J.; Trueblood, K.N.; Hope, H.; *Acta Cryst.*, **1972**, *B28*, 1733.

13.   See for example: (a) Braga, D.; Grepioni, F.; Johnson, B.F.G.; Lewis, J.; Housecroft, C.E.; Martinelli, M.; *Organometallics*, **1991**, *10*, 1260; (b) Wadepohl, H.; Zhu, L.; *J. Organomet. Chem.*, **1989**, *376*, 115.

14.   Elian, M.; Chen, M.L.; Mingos, D.M.P.; Hoffmann, R.; *Inorg. Chem.*, **1976**, *15*, 1148.

15.   (a) Braga, D.; Grepioni, F.; Righi, S.; Dyson, P.J.; Johnson, B.F.G.; Bailey, P.J.; Lewis, J.; *Organometallics*, **1992**, *11*, 4042; (b) Dyson, P.J.; Johnson, B.F.G.; Reed, D.; Braga, D.; Grepioni, F.; Parisini, E.; *J. Chem. Soc., Dalton Trans.*, **1993**, 2817, and references cited therein.

16.   Braga, D.; Grepioni, F.; Sabatino, P.; Dyson, P.J.; Johnson, B.F.G.; Lewis, J.; Bailey, P.J.; Raithby, P.R.; Stalke, D.; *J. Chem. Soc., Dalton Trans.*, **1993**, 985.

17.   Dyson, P.J.; Johnson, B.F.G.; Braga, D.; *Inorg. Chim. Acta*, **1994**, *222*, 229.

18.   (a) Wadepohl, H.; Büchner, K.; Herrmann, M.; Pritzkow, H.; *Organometallics*, **1991**, *10*, 861; (b) Wadepohl, H.; *Angew. Chem. Int. Ed. Engl.*, **1992**, *31*, 247.

19.   Wadill, G.D.; Kesmodel, L.L.; *Phys. Rev.*, **1985**, *B31*, 4940.

20.   Van Hove, M.A.; Lin, R.F.; Somorjai, G.A.; *J. Am. Chem. Soc.*, **1986**, *108*, 2532.

21.   (a) Lin, R.F.; Blackman, G.S.; Van Hove, M.A.; Somorjai, G.A.; *Acta Cryst. Sect. B*, **1987**, *43*, 368; (b) Somorjai, G.A.; *Introduction to Surface Chemistry and Catalysis*, Wiley, New York, **1994**.

22.   Braga, D.; Grepioni, F.; Johnson, B.F.G.; Parisini, E.; Martinelli, M.; Gallop, M.A.; Lewis, J.; *J. Chem. Soc., Dalton Trans.*, **1992**, 807.

23.   (a) Gallop, M.A.; Johnson, B.F.G.; Keeler, J.; Lewis, J.; Heyes, S.J.; Dobson, C.M.; *J. Am. Chem. Soc.*, **1992**, *114*, 2510; (b) Heyes, S.J.; Gallop, M.A.; Johnson, B.F.G.; Lewis, J.; Dobson, C.M.; *Inorg. Chem.*, **1991**, *30*, 3850.

24.   Braga, D.; Grepioni, F.; Johnson, B.F.G.; Lewis, J.; Martinelli, M.; Gallop, M.A.; *J Chem. Soc., Chem. Comm.*, **1990**, 53.

25.   Johnson, B.F.G.; Mallors, R.L.; The University of Edinburgh, **1994**, *unpublished results*.

26.   Raithby, P.R.; Rosales, M.J.; *Adv. Inorg. Chem. & Radiochem.*, **1985**, *29*, 169.

27.   Deeming, A.J.; *Adv. Organomet. Chem.*, **1986**, *26*, 1.

28. Johnson, B.F.G.; Lewis, J.; Pippard, D.A.; *J. Chem. Soc., Dalton Trans.*, **1981**, 407.

29. Churchill, M.R.; Hollander, F.J.; Hutchinson, J.P.; *Inorg. Chem.*, **1977**, *16*, 2655.

30. Churchill, M.R.; DeBoer, B.G.; *Inorg. Chem.*, **1977**, *16*, 878.

31. Dawson, P.A.; Johnson, B.F.G.; Lewis, J.; Puga, J.; Raithby, P.R.; Rosales, M.J.; *J. Chem. Soc., Dalton Trans.*, **1982**, 233.

32. Graves, V.; Lagowski, J.J.; *J. Organomet. Chem.*, **1976**, *120*, 397 and references cited therein.

33. (a) Thoennes, D.J.; Wilkins, C.L.; Trahanovsky, W.S.; *J. Magn. Resonance*, **1974**, *13*, 18; (b) Farnell, L.F.; Randell, E.W.; Rosenberg, E.; *J. Chem. Soc., Chem. Comm.*, **1971**, 1078; (c) Langer, E.; Lehner, H.; *J. Organomet. Chem.*, **1979**, *173*, 47.

34. Laganis, E.D.; Voegeli, R.H.; Swann, R.T.; Finke, R.G.; Hopf, H.; Boekelheide, V.; *Organometallics*, **1982**, *11*, 1415.

35. Greaves, E.O.; Lock, C.J.L.; Maitlis, P.M.; *Can. J. Chem.*, **1968**, *46*, 3880 and references cited therein.

36. Olah, G.A.; Mateescu, G.D.; *J. Am. Chem. Soc.*, **1970**, *92*, 1430.

37. Mann, B.E.; Taylor, B.F.; '*13C N.M.R. Data for Organometallic Compounds*', Academic Press, London, **1981**.

38. Ingham, S.L.; Johnson, B.F.G.; Nairn, J.G.M.; *J. Chem. Soc., Chem. Comm.*, **1995**, 189.

39. Dyson, P.J.; Johnson, B.F.G.; Lewis, J.; Martinelli, M.; Braga, D.; Grepioni, F.; *J. Am. Chem. Soc.*, **1993**, *115*, 9062.

40. Braga, D.; Grepioni, F.; Parisini, E.; Johnson, B.F.G.; Martin, C.M.; Nairn, J.G.M.; Lewis, J.; Martinelli, M.; *J. Chem. Soc., Dalton Trans.*, **1993**, 1891.

41. Dyson, P.J.; Ingham, S.L.; Blake, A.J.; Johnson, B.F.G.; *J. Chem. Soc., Dalton Trans.*, submitted for publication.

42. Chini, P.; Longoni, G.; Albano, V.G.; *Adv. Organomet. Chem.*, **1976**, *14*, 285 and references cited therein.

43. Rosina, G.; Rangelov, G.; Bertel, E.; Saalfeld, H.; Netzer, F.P.; *Chem. Phys. Lett.*, **1987**, 140, 200.

44. Sapa, E.; Tiripicchio, A.; Carty, A.J.; Toogood, G.E.; *Prog. Inorg. Chem.*, **1987**, *35*, 437.

45. Braga, D.; Grepioni, F.; Johnson, B.F.G.; Chen, H.; Lewis, J.; *J. Chem. Soc., Dalton Trans.*, **1991**, 2559.

Chapter Six

Experimental

6.1 General Synthetic and Analytical Techniques

Synthetic procedures

All reactions were carried out with the exclusion of air under an atmosphere of dried nitrogen, using freshly distilled solvents. Autoclave reactions were carried out in a magnetically stirred Burghoff (250 ml) autoclave fitted with a PTFE liner. $Ru_3(CO)_{12}$ and $Os_4(\mu-H)_4(CO)_{12}$ were prepared by the literature procedures,[1,2] while $Os_3(CO)_{12}$ was purchased from Oxkem. Trimethylamine N-oxide (Me_3NO), purchased from Aldrich Chemicals as the dihydrate, was dried initially by a Dean and Stark distillation in benzene, followed by sublimation prior to reaction. All other chemicals were used as supplied, without further purification, unless otherwise stated. Cyclohexa-1,3-diene (C_6H_8) and cyclohexene (C_6H_{10}) were purchased from Aldrich Chemicals, and [2.2]paracyclophane was bought from Fluka Chemicals. Percentage yields are given on the basis of Ru or Os content.

Separations

The reaction mixtures obtained were separated chromatographically on silica. Thin layer chromatography (t.l.c.) was carried out using glass plates (20 cm x 20 cm) supplied by Merck, coated with a 0.25 cm layer of silica gel 60 F_{254}. Column chromatography was carried out using a 50 cm (2 cm id) glass column with a 250 ml solvent reservoir and a facility for nitrogen pressurisation. 60 mesh silica gel, supplied by Fluka, was used as the packing material. Eluents were mixed from standard laboratory grade solvents.

Crystallisations

Wherever possible, the spectroscopic and analytical data for all compounds were obtained from crystalline samples. Single crystals of high quality were required for the collection of X-ray diffraction data.

A number of different techniques were used in the growth of crystalline material including slow evaporation from a dichloromethane-hexane or toluene solution, vapour diffusion using dichloromethane-pentane, layering with dichloromethane-hexane/octane or at reduced temperatures (-25°C) from dichloromethane-hexane or toluene solutions. The method employed in the production of single crystals suitable for X-ray diffraction will be specified in the text where appropriate.

Infrared spectroscopy

Solution infrared spectra were recorded in dichloromethane (unless stated to the contrary) in NaCl cells (0.5 mm path length) supplied by Specac Ltd., while solid state spectra were obtained from pressed KBr discs. All spectra were recorded on a Perkin-Elmer 1710 Series fourier transform spectrometer, calibrated with carbon dioxide.

Mass spectroscopy

Fast atom bombardment (FAB) mass spectra were obtained on a Kratos MS50TC spectrometer. The instrument was run in positive mode, using CsI as calibrant. Samples were dissolved in a minimum amount of acetone prior to addition of the matrix liquid.

NMR spectroscopy

^{1}H, ^{13}C and ^{31}P NMR spectra were recorded on Bruker WH 200, 250 and AM 360 fourier transform spectrometers. All spectra described herein were recorded in deuterated solvents, $CDCl_3$ in most instances, and referenced to internal TMS. The conditions for homonuclear nOe and decoupling experiments will be quoted in the text where necessary, as will those for the more elaborate NMR techniques used.

Single crystal X-ray diffraction analysis

All X-ray measurements were collected on an Enraf-Nonius CAD4 or Stoë Stadi-4-circle-diffractometer equipped with a graphite monochromator (Mo Kα radiation, $\lambda = 0.71073$ Å). An Oxford Cryosystems device was used for data collection at low temperature.[3] The relevant crystal data, data collection and structure solution and refinement parameters are presented in the text where appropriate. All calculations were performed using the crystallographic programs SHELXS86,[4] SHELX76,[5] and SHELXL93.[6] Molecular geometry calculations utilised CALC,[7] and figures were produced using either SHELXTL PC,[8] or SCHAKAL88.[9] When metal hydride ligands could not be located by direct experiment they were positioned using the program XHYDEX.[10] This program employs a 'potential-energy' technique in order to define the most likely site for a hydride ligand to adopt in a cluster. Optimum positions are found for each postulated hydride site by minimisation of the potential energy of the *intra*molecular non-bonded interactions involving the hydride. The resultant potential energy enables a quantitative comparison to be made of the various possible hydride locations on the cluster.

6.2   Experimental Details for Chapter Two

Preparation of Os₄(μ-H)₄(CO)₁₀(MeCN)₂ 2

In a similar manner to that described in the literature procedure,[11] the compound $Os_4(\mu$-$H)_4(CO)_{12}$ **1** (100 mg) was suspended in acetonitrile (50 ml), and two molar equivalents of Me_3NO (14 mg) in acetonitrile (20 ml) were added dropwise at room temperature, to gradually produce a yellow-orange solution. The reaction was complete in 1 hour, as indicated by IR spectroscopy, and the solution was filtered rapidly through silica gel to remove any excess Me_3NO and decomposition material present. The solvent was removed *in vacuo* and the orange solid obtained was characterised by IR spectroscopy as $Os_4(\mu$-$H)_4(CO)_{10}(MeCN)_2$ **2** (95%). Due to the sensitivity of this material, it was used *in situ* without further purification.

Spectroscopic data for **2**: IR (MeCN): υ_{CO} 2080w, 2051m, 2020s, 1998vs, 1983s, 1944w cm^{-1}.

Reaction of Os₄(μ-H)₄(CO)₁₀(MeCN)₂ 2 with cyclohexa-1,3-diene

An excess of cyclohexa-1,3-diene (2 ml) was added to a solution of $Os_4(\mu$-$H)_4(CO)_{10}(MeCN)_2$ **2** (92 mg) in dichloromethane (50 ml). The mixture was stirred at room temperature for 6 hours and the reaction monitored by IR spectroscopy. The solvent was removed under reduced pressure and the residue separated by t.l.c. using dichloromethane-hexane (1:3, v/v) as eluent. A number of bands were produced, including four in reasonable yield which were extracted into dichloromethane and characterised spectroscopically as $Os_4(\mu$-$H)_3(CO)_{11}(\mu_2$-η^1:η^2-$C_6H_9)$ **3** (orange, 12%), $Os_4(\mu$-$H)_2(CO)_{11}(\eta^4$-$C_6H_8)$ **5** (orange, 15%), $Os_4(\mu$-$H)_2(CO)_{12}(\eta^2$-$C_6H_8)$ **4** (green, 8%) and $Os_4(\mu$-$H)_2(CO)_{10}(\eta^6$-$C_6H_6)$ **6** (orange, 28%), in order of elution. Single crystals of **5** suitable for an X-ray diffraction analysis were grown from a toluene solution at -25°C.

Spectroscopic data for **3**: IR (Hexane): υ_{CO} 2098w, 2066vs, 2051s, 2037s, 2022s, 2010vs, 1995m, 1985m, 1954w cm^{-1}, (CH₂Cl₂): υ_{CO} 2098m, 2084w, 2066vs, 2049s, 2034s, 2002m br, 1978w cm^{-1}; ^{1}H NMR (CDCl₃): δ 4.19 (m, 1H), 3.33 (m, 2H), 2.75 (m, 1H), 2.50 (m, 1H), 1.65 (m, 2H), 1.30 (m, 2H), -15.17 (s, 1H), -19.25 (s, 1H), -20.74 (s, 1H) ppm; MS: M$^+$ = 1154 (calc. 1153) amu.

Spectroscopic data for **4**: IR (Hexane): υ_{CO} 2080m, 2060w, 2038vs, 2021s, 1995m, 1984w, 1956w, 1880w cm^{-1}, (CH₂Cl₂): υ_{CO} 2090w, 2077m, 2058m, 2032vs, 2017s, 1987m br, 1952w cm^{-1}; ^{1}H NMR (CDCl₃): δ 4.95 (m, 2H), 3.26 (m, 1H), 3.06 (m, 1H), 2.45 (m, 1H), 1.82 (m, 1H), 1.28 (m, 1H), 1.11 (m, 1H), -19.62 (br s, 2H) ppm; MS: M$^+$ = 1179 (calc. 1178) amu.

Spectroscopic data for **5**: IR (Hexane): υ_{CO} 2092w, 2069s, 2049s, 2012s, 1998m, 1850vw cm^{-1}, (CH₂Cl₂): υ_{CO} 2092m, 2066vs, 2044s, 2008s, 1842w cm^{-1}; ^{1}H NMR (CDCl₃): δ 5.58 (m, 2H), 3.96 (m, 2H), 2.02 (m, 4H), -19.70 (br s, 2H) ppm; MS: M$^+$ = 1150 (calc. 1151) amu. Analytical data, Found (Calc.): C 17.82 (17.77), H 0.93 (0.87) %.

Crystal data and measurement details for **5**: Formula $C_{17}H_{10}O_{11}Os_4$, M = 1151.0, T = 150(1) K, monoclinic, space group $P 2_1/n$, a = 8.4465(22), b = 13.852(3), c = 18.259(6) Å, β = 93.837(24)°, U = 2131 Å^3, Z = 4, D_c = 3.586 g cm^{-3}, μ(Mo–Kα) = 23.863 mm^{-1}, F(000) = 2016, orange column, 0.54 x 0.35 x 0.31 mm, $2\theta_{max}$ 45°, 3657 unique data collected, 2585 reflections with F $\geq$ 4σ(F) used in all calculations, R = 0.0350, R' = 0.0490, S = 1.066 for 290 parameters.

Spectroscopic data for **6**: IR (Hexane): υ_{CO} 2083w, 2063m, 2037s, 2005m, 1997m, 1956w cm^{-1}, (CH$_2$Cl$_2$): υ_{CO} 2082m, 2060s, 2033s, 1993s br, 1959w, cm^{-1}; ^{1}H NMR (CDCl$_3$): δ 5.95 (s, 6H), -19.04 (br s, 1H), -20.70 (br s, 1H) ppm; MS: M$^+$ = 1120 (calc. 1120) amu.

Reaction of Os₄(μ-H)₄(CO)₁₂ 1 with cyclohexa-1,3-diene and Me₃N O

The compound Os$_4$(μ-H)$_4$(CO)$_{12}$ **1** (100 mg) was dissolved in dichloromethane (100 ml), an excess of cyclohexa-1,3-diene (2 ml) was added and the solution cooled to -78°C. A solution of Me$_3$NO (22 mg, 3.2 mol. equiv.) in dichloromethane (20 ml) was added dropwise over a 30 minute period. The reaction mixture was allowed to warm to room temperature where it was stirred for a further hour. The solvent was removed *in vacuo* and the products separated by t.l.c. using a dichloromethane-hexane (1:3, v/v) solution as eluent, which resulted in the isolation of the same four products as the previous reaction, *i.e.* Os$_4$(μ-H)$_3$(CO)$_{11}$(μ_2-η^1:η^2-C$_6$H$_9$) **3** (12%), Os$_4$(μ-H)$_2$(CO)$_{11}$(η^4-C$_6$H$_8$) **5** (15%), Os$_4$(μ-H)$_2$(CO)$_{12}$(η^2-C$_6$H$_8$) **4** (6%) and Os$_4$(μ-H)$_2$(CO)$_{10}$(η^6-C$_6$H$_6$) **6** (24%).

Thermolysis of Os₄(μ-H)₂(CO)₁₂(η²-C₆H₈) 4 in hexane

The complex Os$_4$(μ-H)$_2$(CO)$_{12}$(η^2-C$_6$H$_8$) **4** (15 mg) was suspended in hexane (20 ml) and heated to reflux for 3 hours. The solvent was removed *in vacuo* and purification by t.l.c., using dichloromethane-hexane (1:3, v/v) as eluent, yielded two compounds characterised by IR spectroscopy as the starting material, Os$_4$(μ-H)$_2$(CO)$_{12}$(η^2-C$_6$H$_8$) **4** (32%), and Os$_4$(μ-H)$_2$(CO)$_{11}$(η^4-C$_6$H$_8$) **5** (10%).

Thermolysis of Os₄(μ-H)₂(CO)₁₁(η⁴-C₆H₈) 5 in hexane

The complex Os$_4$(μ-H)$_2$(CO)$_{11}$(η^4-C$_6$H$_8$) **5** (20 mg) was suspended in hexane (30 ml) and heated to reflux for 3 hours. The solvent was removed *in vacuo* and purification by t.l.c. using dichloromethane-hexane (3:7, v/v) as eluent resulted in two compounds, the first of which was characterised spectroscopically as starting material, Os$_4$(μ-H)$_2$(CO)$_{11}$(η^4-C$_6$H$_8$) **5** (35%), and the second as Os$_4$(μ-H)$_2$(CO)$_{10}$(η^6-C$_6$H$_6$) **6** (12%). Decomposition was also observed.

Reaction of Os₄(μ-H)₂(CO)₁₀(η⁶-C₆H₆) 6 with cyclohexa-1,3-diene and Me₃N O

Me$_3$NO (3.2 mol. equiv., 4.3 mg) in dichloromethane (10 ml) was added dropwise to a dichloromethane solution (30 ml) of Os$_4$(μ-H)$_2$(CO)$_{10}$(η^6-C$_6$H$_6$) **6** (20 mg) at -78°C,

containing excess cyclohexa-1,3-diene (2 ml). The solution was allowed to warm to room temperature (1 hour) after which it was stirred for a further 30 mins. during which the colour of the solution turned from orange to deep red. The solvent was removed *in vacuo*, and the residue chromatographed using dichloromethane-hexane (1:3, v/v) as eluent, affording three major bands. In order of elution, they were characterised by spectroscopic methods as starting material $Os_4(\mu-H)_2(CO)_{10}(\eta^6-C_6H_6)$ **6** (orange, 25%), $Os_4(CO)_9(\eta^6-C_6H_6)(\eta^4-C_6H_8)$ **7** (red, 20%) and $Os_4(\mu-H)_2(CO)_8(\eta^6-C_6H_6)(\eta^4-C_6H_8)$ **8** (orange, 25%). Crystals of **8** were grown from the slow evaporation of a CDCl$_3$ solution at room temperature.

Spectroscopic data for **7**: IR (CH$_2$Cl$_2$): υ_{CO} 2080w, 2055s, 2018vs, 1976m, 1949w, 1850w, cm^{-1}; ^{1}H NMR (CDCl$_3$): δ 5.75 (s, 6H), 5.46 (m, 1H), 5.37 (m, 1H), 4.49 (m, 1H), 3.58 (m, 1H), 2.36 and 2.12 (m, 2H), 1.95 and 1.84 (m, 2H) ppm; MS: M$^+$ = 1170 (calc. 1170) amu.

Spectroscopic data for **8**: IR (Hexane): υ_{CO} 2068s, 2049m, 2036s, 2021m, 1996vs, 1987s, 1880w cm^{-1}, (CH$_2$Cl$_2$): υ_{CO} 2064vs, 2047m, 2022s, 1984vs br, 1942w, 1845w cm^{-1}; ^{1}H NMR (CDCl$_3$): δ 5.74 (s, 6H), 5.04 (m, 2H), 3.55 (m 2H), 2.16 (m, 2H), 1.67 (m, 2H), -15.72 (br s, 1H), -19.44 (br s, 1H) ppm; MS: M$^+$ = 1144 (calc. 1145) amu. Analytical data, Found (Calc.): C 21.26 (20.96), H 1.48 (1.40) %. Crystal data and measurement details for **8**: Formula C$_{20}$H$_{16}$O$_8$Os$_4$, M = 1145.10, T = 298(1) K, triclinic, space group P -1, a = 8.4267(14), b = 8.7464(17), c = 15.871(6) Å, α = 84.924(18), β = 77.617(12), γ = 75.525(10)°, U = 1105.5 Å^3, Z = 2, D_c = 3.440 g cm^{-3}, μ(Mo–Kα) = 22.995 mm^{-1}, F(000) = 1008, red plate, 0.198 x 0.185 x 0.060 mm, 2θ$_{max}$ 45°, 4369 unique data collected, 2622 reflections with F ≥ 4σ(F) used in all calculations, R = 0.0493, R' = 0.0609, S = 0.938 for 189 parameters.

Reaction of $Os_4(\mu-H)_2(CO)_{10}(\eta^6-C_6H_6)$ 6 with benzene and Me$_3$N O

$Os_4(\mu-H)_2(CO)_{10}(\eta^6-C_6H_6)$ **6** (30 mg) was dissolved in dichloromethane-acetone-benzene (30: 5: 5 ml, respectively) and cooled to -78°C. A solution of Me$_3$NO (6.4 mg, 3.2 mol. equiv.) in dichloromethane (10 ml) was added dropwise to the reaction mixture over a 10 minute period, and the solution was allowed to warm to room temperature (1 hour) during which time the colour of the solution darkened. The solvent was removed under reduced pressure and the residue was subjected to t.l.c. eluting with dichloromethane-hexane (3:7, v/v). Two orange bands were obtained and characterised as starting material, $Os_4(\mu-H)_2(CO)_{10}(\eta^6-C_6H_6)$ **6** (22%), and $Os_4(CO)_8(\eta^6-C_6H_6)_2$ **9** (14%).

Spectroscopic data for **9**: IR (CH$_2$Cl$_2$): υ_{CO} 2059w, 2050m, 2032m, 2017m, 1988vs, 1833m cm^{-1}; ^{1}H NMR (CDCl$_3$): δ 5.75 (s, 12H) ppm; MS: M$^+$ = 1140 (calc. 1140) amu.

Thermolysis of $Os_4(\mu-H)_4(CO)_{10}(MeCN)_2$ 2 with cyclohexa-1,3-diene in dichloromethane

The compound $Os_4(\mu-H)_4(CO)_{10}(MeCN)_2$ **2** (95 mg) in dichloromethane (50 ml) containing an excess of cyclohexa-1,3-diene (2 ml) was heated to reflux for 18 hours. IR

spectroscopy indicated complete consumption of starting material after this time. The solvent was removed under reduced pressure and the products separated by t.l.c. using a solution of dichloromethane-hexane (1:3, v/v) as eluent. Several bands were obtained, which in order of elution were extracted and characterised spectroscopically as $Os_4(\mu$-$H)_3(CO)_{11}(\mu_2$-η^1:η^2-$C_6H_9)$ **3** (orange, 8%), $Os_4(\mu$-$H)(CO)_{10}(\eta^3$-$C_6H_9)(\mu_3$-η^1:η^1:η^2-$C_6H_8)$ **10** (orange, 5%), $Os_4(\mu$-$H)_2(CO)_{11}(\eta^4$-$C_6H_8)$ **5** (orange, 8%), $Os_5(\mu$-$H)_2(CO)_{13}(\eta^4$-$C_6H_8)$ **12** (orange, 6%), $Os_4(\mu$-$H)_2(CO)_{10}(\eta^6$-$C_6H_5C_6H_9)$ **11** (orange, 6%), $Os_4(\mu$-$H)_2(CO)_{12}(\eta^2$-$C_6H_8)$ **4** (green, 4%), $Os_4(\mu$-$H)_2(CO)_{10}(\eta^6$-$C_6H_6)$ **6** (orange, 18%) and $Os_4(CO)_9(\eta^6$-$C_6H_6)(\eta^4$-$C_6H_8)$ **7** (red, 10%), respectively. Crystallisation of **10** and **11** was achieved from toluene solutions at -25°C, and crystals of **12** were grown using the vapour diffusion method from a dichloromethane-pentane solvent system at room temperature.

Spectroscopic data for **10**: IR (Hexane): υ_{CO} 2099w, 2086s, 2059vs, 2042vs, 2024m, 2012vs, 1990w, 1973m, 1960w, 1947w cm^{-1}; (CH_2Cl_2): υ_{CO} 2098w, 2085m, 2059s, 2038vs, 2000m, 1966w cm^{-1}; ^1H NMR $(CDCl_3)$: δ 5.62 (m, 1H), 4.06 (m, 1H), 3.47 (m, 2H), 3.06 (m, 1H), 2.90 (m, 1H), 2.64 (m, 2H), 2.05 (m, 3H), 1.84 (m, 2H), 1.67 (m, 1H), 1.50 (m, 2H), 1.18 (m, 1H), -22.0 (s, 1H) ppm; MS: M^+ = 1202 (calc. 1203) amu.

Crystal data and measurement details for **10**: Formula $C_{22}H_{18}O_{10}Os_4$, M = 1203.16, T = 150(1) K, monoclinic, space group $P\,2_1/n$, a = 9.442(3), b = 16.900(5), c = 15.555(5) Å, β = 97.45(3)°, U = 2461.2 $Å^3$, Z = 4, D_c = 3.247 g cm^{-3}, $\mu(Mo-K\alpha)$ = 19.867 mm^{-1}, $F(000)$ = 2136, orange plate crystal 0.39 x 0.35 x 0.05 mm, $2\theta_{max}$ 45°, wR_2 (on F^2, all data) = 0.1748, R_1 [on F, for 2993 unique reflections with I > $2\sigma(I)$] = 0.0597, 3127 collected reflections, 3127 unique reflections used in the refinement, S (on F^2) = 1.026.

Spectroscopic data for **11**: IR (Hexane): υ_{CO} 2083m, 2062s, 2036vs, 2022w, 2004m, 1995s, 1955m, 1797w cm^{-1}; (CH_2Cl_2): υ_{CO} 2082s, 2060vs, 2032vs, 1994s br, 1958m, 1786w br cm^{-1}; ^1H NMR $(CDCl_3)$: δ 5.84 (m, 5H), 3.58 (m, 2H), 1.99 (m, 7H), -19.09 (s, 1H) and -20.45 (s, 1H) ppm; MS: M^+ = 1202 (calc. 1201) amu.

Crystal data and measurement details for **11**: Formula $C_{22}H_{16}O_{10}Os_4$, M = 1201.15, T = 293(1) K, monoclinic, space group $P\,2_1/n$, a = 9.018(2), b = 25.198(4), c = 11.336(2) Å, β = 95.11(2)°, U = 2565.9(8) $Å^3$, Z = 4, D_c = 3.109 g cm^{-3}, $\mu(Mo-K\alpha)$ = 19.797 mm^{-1}, $F(000)$ = 2128, dark red needle 0.51 x 0.12 x 0.10 mm, $2\theta_{max}$ 45°, wR_2 (on F^2, all data) = 0.1719, R_1 [on F, for I > $2\sigma(I)$] = 0.0590, 3365 collected reflections, 3364 unique reflections used in the refinement, S (on F^2) = 1.052.

Spectroscopic data for **12**: IR (CH_2Cl_2): υ_{CO} 2085w, 2065s, 2050m, 2030m, 2018vs, 1983m, 1940w cm^{-1}; MS: M^+ = 1397 (calc. 1397) amu.

Crystal data and measurement details for **12**: Formula $C_{19}H_{10}O_{13}Os_5$, M = 1397.27, T = 150(1) K, triclinic, space group P-1, a = 9.394(10), b = 16.149(13), c = 17.257(18) Å, α = 105.41(7), β = 97.58(9), γ = 93.30(7)°, U = 2490 $Å^3$, Z = 4, D_c = 3.727 g cm^{-3}, $\mu(Mo-K\alpha)$ = 24.532 mm^{-1}, $F(000)$ = 2432, red lath crystal, 0.15 x 0.05 x 0.005 mm, $2\theta_{max}$ 45°, wR_2 (on F^2, all data) = 0.3830, R_1 [on F, for I > $2\sigma(I)$] = 0.1033, 7109 collected reflections, 6419 unique reflections used in the refinement, S (on F^2) = 0.913.

Thermolysis of Os₄(μ-H)₃(CO)₁₁(μ₂-η¹:η²-C₆H₉) 3 in octane

The complex $Os_4(\mu\text{-H})_3(CO)_{11}(\mu_2\text{-}\eta^1\text{:}\eta^2\text{-}C_6H_9)$ **3** (25 mg) was suspended in octane (30 ml) and heated to reflux for a 2 hour period. The solvent was removed *in vacuo* and purification by t.l.c. using dichloromethane-hexane (1:3, v/v) as eluent resulted in two compounds, the first of which was characterised as starting material, $Os_4(\mu\text{-H})_3(CO)_{11}(\mu_2\text{-}\eta^1\text{:}\eta^2\text{-}C_6H_9)$ **3** (orange, 24%), and the second as $Os_4(\mu\text{-H})_2(CO)_{11}(\mu_2\text{-}\eta^1\text{:}\eta^2\text{:}\eta^1\text{-}C_6H_8)$ **13** (orange, 18%).

Spectroscopic data for **13**: IR (Hexane): υ_{CO} 2099m, 2068vs, 2057s, 2021vs, 2016s, 2005m, 1994w, 1980w, 1960m cm⁻¹; (CH₂Cl₂): υ_{CO} 2098m, 2067vs, 2056s, 2017s br, 2003m, 1979w, 1960w cm⁻¹; ¹H NMR (CDCl₃): δ 3.18 (m, 4H), 1.76 (m, 4H), -10.46 (s, 1H), -21.53 (s, 1H) ppm; MS: M⁺ = 1151 (calc. 1151) amu.

6.3 Experimental Details for Chapter Three

Thermolysis of Ru₃(CO)₁₂ 14 with cyclohexa-1,3-diene in octane

The compound $Ru_3(CO)_{12}$ **14** (250 mg) in octane (30 ml) containing cyclohexa-1,3-diene (5 drops) was heated to reflux for 1 h, during which time the solution darkened quite substantially. Excess cyclohexa-1,3-diene (2 ml) was added, and the reaction mixture was returned to a vigorous reflux for a further 3 h. The reaction was monitored by spot t.l.c. which indicated complete consumption of starting material after this time. The solvent was removed *in vacuo* and the products separated by column chromatography, using a solution of dichloromethane-hexane (3:7, v/v) as eluent. Four main bands, in order of elution, were isolated and characterised by spectroscopy as $Ru_4(CO)_{12}(\mu_4\text{-}\eta^1\text{:}\eta^1\text{:}\eta^2\text{:}\eta^2\text{-}C_6H_8)$ **15** (red, 28%), $Ru_4(CO)_9(\mu_4\text{-}\eta^1\text{:}\eta^1\text{:}\eta^2\text{:}\eta^2\text{-}C_6H_8)(\eta^6\text{-}C_6H_6)$ **16** (red, hinge isomer, 14%), $Ru_4(CO)_9(\mu_4\text{-}\eta^1\text{:}\eta^1\text{:}\eta^2\text{:}\eta^2\text{-}C_6H_8)(\eta^6\text{-}C_6H_6)$ **17** (purple, wing-tip isomer, 8%) and the known compound $Ru_6C(CO)_{14}(\eta^6\text{-}C_6H_6)]$ **18** (brown, 22%). Crystals of **15** and **16** were nucleated from toluene at -25°C over a prolonged period, whilst crystallisation of **17** was achieved by the slow evaporation of a dichloromethane-hexane solution.

Spectroscopic data for **15**: IR (CH₂Cl₂) : υ_{CO} 2091w, 2064s, 2034vs, 2009m, 1968w sh cm⁻¹; ¹H NMR (CDCl₃): δ 3.35 (m, 4H), 1.82 (m, 4H) ppm; MS: M⁺ = 821 (calc. 821) amu; Analytical data, Found (Calc.): C 26.28 (26.34), H 0.89 (0.98) %.
Crystal data and measurement details for **15**: Formula $C_{18}H_8O_{12}Ru_4$, M = 820.5, T = 150(1) K, monoclinic, space group $P\,2_1/c$, a = 9.779(8), b = 22.163(14), c = 10.069(6) Å, β = 90.23(9)°, U = 2182(3) Å³, Z = 4, μ(Mo–Kα) = 27.79 mm⁻¹, $F(000)$ = 1552, deep red block, 0.39 x 0.27 x 0.19 mm, $2\theta_{max}$ 50°, wR_2 (on F^2, all data) = 0.0658, R_1 [on F, for 3408 unique reflections with $I > 2\sigma(I)$] = 0.0238, 4528 collected reflections, 4323 unique reflections used in the refinement, S (on F^2) = 1.205.

Spectroscopic data for **16**: IR (CH_2Cl_2): υ_{CO} 2060m, 2035vs, 2010s, 1981s, 1969m sh, 1924w cm^{-1}; ^1H NMR ($CDCl_3$): δ 5.52 (s, 6H), 3.27 (m, 4H), 1.82 (m, 4H) ppm; MS: M$^+$ = 815 (calc. 815) amu; Analytical data, Found (Calc.): C 30.99 (30.96), H 1.47 (1.72) %.

Crystal data and measurement details for **16**: Formula $C_{21}H_{14}O_9Ru_4$, M = 814.5, T = 296(1) K, monoclinic, space group $P\,2_1/c$, a = 10.010(3), b = 15.532(4), c = 15.384(4) Å, β = 93.50(2)°, U = 2378(1) Å^3, Z = 4, μ(Mo–Kα) = 23.29 mm^{-1}, $F(000)$ = 1552, $2\theta_{max}$ 60°, wR_2 (on F^2, all data) = 0.0748, R_1 [on F, for 3464 unique reflections with $I > 2\sigma(I)$] = 0.0277, 3693 collected reflections, 3575 unique reflections used in the refinement, S (on F^2) = 1.214.

Spectroscopic data for **17**: IR (CH_2Cl_2): υ_{CO} 2065s, 2022s, 2009vs, 1993w sh, 1958m cm^{-1}; ^1H NMR ($CDCl_3$): δ 5.67 (s, 6H), 3.37 (m, 4H), 1.80 (m, 4H) ppm; MS: M$^+$ = 816 (calc. 815) amu; Analytical data, Found (Calc.): C 31.06 (30.96), H 1.50 (1.72) %.

Crystal data and measurement details for **17**: Formula $C_{21}H_{14}O_9Ru_4$, M = 814.5, T = 150(1) K, monoclinic, space group $P\,2_1/c$, a = 16.655(3), b = 15.709(3), c = 17.831(4) Å, β = 91.44(3)°, U = 4664(2) Å^3, Z = 8, μ(Mo–Kα) = 25.91 mm^{-1}, $F(000)$ = 3104, red plate, 0.43 x 0.31 x 0.11 mm, $2\theta_{max}$ 50°, wR_2 (on F^2, all data) = 0.2563, R_1 [on F, for 4973 unique reflections with $I > 2\sigma(I)$] = 0.0706, 8969 collected reflections, 8969 unique reflections used in the refinement, S (on F^2) = 1.207.

Spectroscopic data for **18**: IR (CH_2Cl_2): υ_{CO} 2078m, 2026vs, 1816w br cm^{-1}; ^1H NMR ($CDCl_3$): δ 5.56 (s, 6H) ppm; MS: M$^+$ = 1088 (calc. 1089) amu.

Thermolysis of $Ru_4(CO)_{12}(\mu_4\text{-}\eta^1{:}\eta^1{:}\eta^2{:}\eta^2\text{-}C_6H_8)$ **15** with cyclohexa-1,3-diene in octane

Cyclohexa-1,3-diene (1 ml) was added to a solution of compound **15** (50 mg) in octane (25 ml) and heated to reflux for 3 h. The solvent was removed under reduced pressure and the residue purified by t.l.c. using a dichloromethane-hexane (3:7, v/v) solution as eluent. Several bands were obtained in low yield, of which the major product was isolated and characterised as $Ru_4(CO)_9(\mu_4\text{-}\eta^1{:}\eta^1{:}\eta^2{:}\eta^2\text{-}C_6H_8)(\eta^6\text{-}C_6H_6)$ **16** (hinge isomer, 18%).

Reaction of $Ru_4(CO)_{12}(\mu_4\text{-}\eta^1{:}\eta^1{:}\eta^2{:}\eta^2\text{-}C_6H_8)$ **15** with cyclohexa-1,3-diene and Me_3NO

The compound $Ru_4(CO)_{12}(\mu_4\text{-}\eta^1{:}\eta^1{:}\eta^2{:}\eta^2\text{-}C_6H_8)$ **15** (50 mg) was dissolved in dichloromethane (50 ml), an excess of cyclohexa-1,3-diene (1-2 ml) was added and the solution cooled to -78°C. A solution of Me_3NO (15 mg, 3.2 mol. equiv.) in dichloromethane (20 ml) was added dropwise over a 10 minute period. The reaction mixture was allowed to warm to room temperature where it was stirred for a further hour. The solvent was removed under reduced pressure and the products separated by t.l.c. using dichloromethane-hexane (3:7, v/v) as eluent. Four products were extracted which, in order of elution, were characterised spectroscopically as $Ru_3(CO)_8(\mu_3\text{-}\eta^1{:}\eta^2{:}\eta^1\text{-}C_6H_8)(\eta^4\text{-}C_6H_8)$ **20** (yellow, 16%), $Ru_4(CO)_9(\mu_4\text{-}\eta^1{:}\eta^1{:}\eta^2{:}\eta^2\text{-}C_6H_8)(\eta^6\text{-}C_6H_6)$ **16** (red, 4%), $Ru_4(CO)_9(\mu_4\text{-}\eta^1{:}\eta^1{:}\eta^2{:}\eta^2\text{-}C_6H_8)(\eta^6\text{-}C_6H_6)$ **17** (purple, 25%) and $Ru_4(CO)_8(\mu_4\text{-}\eta^1{:}\eta^1{:}\eta^2{:}\eta^2\text{-}C_6H_8)(\eta^4\text{-}C_6H_8)_2$ **19** (orange, 14%). Crystals of **19** were grown from the slow evaporation of a dichloromethane-hexane solution at room temperature.

Spectroscopic data for **19**: IR (CH$_2$Cl$_2$): υ_{CO} 2055vs, 2031s, 2020m, 1979s br, 1838s br cm^{-1}; ^{1}H NMR (CDCl$_3$): δ 5.02 (m, 4H), 3.40 (m, 4H), 2.54 (br s, 4H), 2.31 (d; 11.5 Hz, 4H), 1.54 (d; 11.5 Hz, 4H), 1.24 (br s, 4H) ppm; MS: M$^+$ = 868 (calc. 869) amu.

Crystal data and measurement details for **19**: Formula C$_{26}$H$_{24}$O$_8$Ru$_4$, M = 868.73, T = 150(1) K, monoclinic, space group $P\,2_1/c$, a = 9.699(3), b = 15.588(5), c = 17.061(6) Å, β = 91.13(6)°, U = 2578.9(14) Å^3, Z = 4, D_c = 2.237 g cm^{-3}, μ(Mo–Kα) = 2.347 mm^{-1}, F(000) = 1680, dark red tablet, 0.38 x 0.38 x 0.19 mm, 2θ$_{max}$ 50°, wR_2 (on F^2, all data) = 0.0734, R_1 [on F, for 4552 unique reflections with $I > 2\sigma(I)$] = 0.0283, 4681 collected reflections, 4552 unique reflections used in the refinement, S (on F^2) = 1.124.

Spectroscopic data for **20**: IR (CH$_2$Cl$_2$): υ_{CO} 2077s, 2041vs, 2017m, 1998m, 1987w sh, 1878m, 1839m cm^{-1}; ^{1}H NMR (CDCl$_3$): δ 4.91 (m, 2H), 3.34 (m, 2H) range 2.83 - 1.73 (m, 12H) ppm; MS: M$^+$ = 688 (calc. 688) amu.

The interconversion of isomers 16 and 17

A solution of Ru$_4$(CO)$_9$(μ$_4$-η^1:η^1:η^2:η^2-C$_6$H$_8$)(η^6-C$_6$H$_6$) **17** (10 mg) in octane (30 ml) was heated under reflux for 2 h. During this time the colour of the solution changed from purple to red, and IR spectroscopy indicated complete consumption of the starting material to Ru$_4$(CO)$_9$(μ$_4$-η^1:η^1:η^2:η^2-C$_6$H$_8$)(η^6-C$_6$H$_6$) **16** (> 90%). This was confirmed by spot t.l.c. which showed no other products present, and that only a small amount of decomposition had taken place during the reaction. However on standing at room temperature, a dichloromethane solution of **16** reverts slowly back to **17**, as evidenced by IR spectroscopy and spot t.l.c.

The photolysis of Ru$_4$(CO)$_9$(μ$_4$-η^1:η^1:η^2:η^2-C$_6$H$_8$)(η^6-C$_6$H$_6$) 16

A solution of Ru$_4$(CO)$_9$(μ$_4$-η^1:η^1:η^2:η^2-C$_6$H$_8$)(η^6-C$_6$H$_6$) **16** (10 mg) in hexane (30 ml) was irradiated for a ten minute period using filtered light (> 300 nm) from a water-cooled 125 watt medium pressure mercury arc lamp. During this time a colour change from red to purple was observed, and both IR spectroscopy and spot t.l.c. indicated that isomerisation from the hinge isomer, **16**, to the wing-tip isomer, **17**, had occurred quantitatively.

Thermolysis of Ru$_3$(CO)$_{12}$ 14 with cyclohexene in octane

The compound Ru$_3$(CO)$_{12}$ **14** (250 mg) was suspended in octane (30 ml) and excess cyclohexene (2 ml) was added. The reaction mixture was heated to reflux for 6 h during which time the solution darkened quite substantially. The reaction was monitored by spot t.l.c. which indicated complete consumption of starting material after this time. The solvent was removed *in vacuo* and the products separated by t.l.c., eluting with a solution of dichloromethane-hexane (3:7, v/v). Several bands were isolated and characterised by spectroscopy, in order of elution, as Ru$_4$(CO)$_{12}$(μ$_4$-η^1:η^1:η^2:η^2-C$_6$H$_8$) **15** (red, 18%), Ru$_4$(CO)$_9$(μ$_4$-η^1:η^1:η^2:η^2-C$_6$H$_8$)(η^6-C$_6$H$_6$) **16** (red, 8%), Ru$_6$(μ$_3$-H)(μ$_4$-η^2-CO)$_2$(CO)$_{13}$(η^5-C$_5$H$_4$Me) **21** (brown, 12%) Ru$_4$(CO)$_9$(μ$_4$-η^1:η^1:η^2:η^2-C$_6$H$_8$)(η^6-C$_6$H$_6$)

17 (purple, 4%), $Ru_8(\mu\text{-}H)_4(CO)_{18}(\eta^6\text{-}C_6H_6)$ **22** (brown, 14%) and the known compound $Ru_6C(CO)_{14}(\eta^6\text{-}C_6H_6)$ **18** (brown, 18%). Crystals of **21** and **22** were grown from toluene at -25°C over several days, and from the slow evaporation of a dichloromethane-hexane solution at room temperature, respectively.

Spectroscopic data for **21**: IR (CH_2Cl_2): υ_{co} 2093w, 2080m, 2066vs, 2034m, 2022m, 1965w, 1920w cm^{-1}; (KBr disc): υ_{co} 1431s, 1388m cm^{-1}; ^{1}H NMR (CDCl$_3$): δ 5.44 (m, 2H), 5.31 (m, 2H), 2.10 (s, 3H), -17.81 (s, 1H) ppm; MS: M$^+$ = 1106 (calc. 1107) amu.

Crystal data and measurement details for **21**: Formula $C_{21}H_8O_{15}Ru_6$, M = 1106.69, T = 150(1) K, monoclinic, space group $P2_1/m$, a = 9.910(3), b = 16.963(4), c = 24.936(9) Å, β = 100.26(3)°, U = 4125(2) Å^3, Z = 6, D_c = 2.673 g cm^{-3}, μ(Mo–Kα) = 3.284 mm^{-1}, F(000) = 3108, dark red tablet, 0.12 x 0.31 x 0.39 mm, $2\theta_{max}$ 50°, wR_2 (on F^2, all data) = 0.1134, R_1 [on F, for 5185 unique reflections with $I > 2\sigma(I)$] = 0.0409, 6648 collected reflections, 6282 unique reflections used in the refinement, S (on F^2) = 1.128.

Spectroscopic data for **22**: IR (CH_2Cl_2): υ_{co} 2091m, 2080m, 2066vs, 2031s, 2006w sh, 1966w, 1922w, 1823 cm^{-1}; ^{1}H NMR (CDCl$_3$): δ 5.40 (s, 6H), -17.80 (s, 2H), -19.26 (s br, 2H) ppm; MS: M$^+$ = 1394 (calc. 1394) amu.

Crystal data and measurement details for **22**: Formula $C_{24}H_{10}O_{18}Ru_8$, M = 1394.89, T = 293(2) K, monoclinic, space group $P2_1/n$, a = 15.930(7), b = 12.909(5), c = 16.43(2) Å, β = 95.51(6)°, U = 3363.1 Å^3, Z = 4, D_c = 2.78 g cm^{-3}, μ(Mo–Kα) = 3.281 mm^{-1}, F(000) = 2600, crystal size 0.12 x 0.15 x 0.14 mm, $2\theta_{max}$ 50°, wR_2 (on F^2, all data) = 0.0658, R_1 [on F, for 4687 unique reflections with $I > 2\sigma(I)$] = 0.0222, 6401 collected reflections, 5869 unique reflections used in the refinement, S (on F^2) = 1.04.

Thermolysis of $Ru_6(\mu_3\text{-}H)(\mu_4\text{-}\eta^2\text{-}CO)_2(CO)_{13}(\eta^5\text{-}C_5H_4Me)$ 21

The compound $Ru_6(\mu_3\text{-}H)(\mu_4\text{-}\eta^2\text{-}CO)_2(CO)_{13}(\eta^5\text{-}C_5H_4Me)$ **21** (10 mg) was suspended in solvent (20 ml) (solvent = hexane, heptane) and heated to reflux for 8 h. The reactions were monitored by IR spectroscopy and spot t.l.c., both of which indicated that no reaction had occurred, and that only starting material remained.

Thermolysis of $Ru_6(\mu_3\text{-}H)(\mu_4\text{-}\eta^2\text{-}CO)_2(CO)_{13}(\eta^5\text{-}C_5H_4Me)$ 21 in high-boiling solvents

The compound $Ru_6(\mu_3\text{-}H)(\mu_4\text{-}\eta^2\text{-}CO)_2(CO)_{13}(\eta^5\text{-}C_5H_4Me)$ **21** (10 mg) was suspended in solvent (20 ml) (solvent = toluene, octane and mesitylene) and heated to reflux for 30 minutes. IR spectroscopy and spot t.l.c. indicated that extensive decomposition had occurred, with no products resulting.

6.4 Experimental Details for Chapter Four

Thermolysis of $Ru_3(CO)_{12}$ 14 with [2.2]paracyclophane in octane

A suspension of $Ru_3(CO)_{12}$ **14** (500 mg) in octane (30 ml) containing a large excess of [2.2]paracyclophane (200 mg) was heated to reflux for between 1 and 5 h. Five products were formed from the reaction; their distribution being dependant on the time of the thermolysis. In each case, the solvent was removed from the reaction solution under reduced pressure, and the products separated by column chromatography, using a solution of dichloromethane-hexane (3:7, v/v) as eluent. In order of elution, the products were characterised by spectroscopy as $Ru_3(CO)_9(\mu_3-\eta^2:\eta^2:\eta^2-C_{16}H_{16})$ **23** (yellow), $Ru_8(\mu-H)_4(CO)_{18}(\eta^6-C_{16}H_{16})$ **27** (brown), $Ru_6C(CO)_{14}(\mu_3-\eta^2:\eta^2:\eta^2-C_{16}H_{16})$ **25** (red), $Ru_6C(CO)_{15}(\mu_3-\eta^1:\eta^2:\eta^2-C_{16}H_{16}-\mu_2-O)$ **24** (purple), together with small amounts of a closely related isomer **24a**, and $Ru_6C(CO)_{11}(\mu_3-\eta^2:\eta^2:\eta^2-C_{16}H_{16})(\eta^6-C_{16}H_{16})$ **26** (brown). Short reaction periods produce mostly **23**, with optimum yields of **24**, while longer reaction times afford mostly **25**, with increased quantities of **26** and **27**. Reaction times and typical corresponding yields are as follows:

> 1 h: **23** (35%), **24** (10%), **24a** (2%), and **25** (22%).
>
> 3 h: **23** (14%), **24** (4%), **25** (30%), **26** (6%) and **27** (4%).
>
> 5 h: **23** (5%), **25** (16%), **26** (12%) and **27** (10%).

Crystals of **24, 25, 26,** and **27** suitable for X-ray diffraction analyses were grown from toluene at -25°C (**24** and **27**), and from the slow evaporation of dichloromethane-hexane at room temperature (**25** and **26**).

Spectroscopic data for **23**: IR (CH_2Cl_2): υ_{CO} 2067s, 2024vs, 1993m, 1980m, 1959w sh cm^{-1}; ^1H NMR ($CDCl_3$): δ 7.22 (s, 4H), 3.76 (s, 4H), 3.23 (m, 4H), 2.67 (m, 4H) ppm; ^{13}C NMR ($CDCl_3$): δ 197.6 (9 CO), 138.5 (2 q), 132.1 (4 CH), 76.0 (2 q), 54.7 (4 CH), 40.7 (2 CH_2), 35.2 (2 CH_2) ppm; MS: M^+ = 763 (calc. 764) amu; Analytical data, Found (Calc.): C 41.12 (39.32), H 2.31 (2.10) %.

Spectroscopic data for **24**: IR (CH_2Cl_2): υ_{CO} 2085m, 2053s, 2037vs, 2016m, 2008m, 1968w, 1866w cm^{-1}; ^1H NMR ($CDCl_3$): δ 7.79 (d,d; 7.9, 1.6 Hz; 1H); 7.46 (d,d; 7.9, 1.6 Hz; 2H); 7.05 (d,d; 7.9, 1.6 Hz; 1H); 5.91 (d,d; 6.2, 2.1 Hz; 1H); 4.18 (d,d; 5.8, 1.6 Hz; 1H); 4.08 (d,d; 6.2, 1.6 Hz; 1H); 3.78 (d,d; 5.8, 2.1 Hz; 1H); 3.68 (d,d,d; 14.0, 8.8, 1.6 Hz; 1H); 3.2-3.5 (overlapping multiplets; 3H); 2.95 (d,t; 13.6, 8.6 Hz; 1H); 2.4-2.55 (overlapping multiplets; 2H); 1.64 (d,d,d; 13.8, 9.7, 7.8 Hz; 1H) ppm; ^{13}C NMR ($CDCl_3$) ([2.2]paracyclophane resonances only): δ 138.2 (q), 136.9 (q), 133.8 (CH), 133.6 (CH), 133.4 (CH), 130.1 (CH), 109.2 (q), 88.3 (CH), 74.4 (CH), 65.1 (q), 47.4 (CH), 39.8 (CH_2), 35.8 (CH_2), 34.6 (CH_2), 34.3 (CH_2), 21.6 (CH) ppm; MS: M^+ = 1262 (calc. 1263) amu; Analytical data, Found (Calc.): C 30.03 (30.43), H 1.32 (1.28) %.

Crystal data and measurement details for **24**: Formula $C_{33}H_{18}O_{16}Ru_6Cl_2$, M = 1347.8, T = 150(1) K, orthorhombic, space group $Pca2_1$, a = 18.270(4), b = 10.432(6), c = 19.825(6) Å, U = 3781(2) Å^3, Z = 4, μ(Mo–Kα) = 2.368 cm^{-1}, $F(000)$ = 2568, red tablet, 0.19 x 0.23 x 0.04 mm, $2\theta_{max}$ 45°, wR_2 (on F^2, all data) = 0.1168, R_1 [on F, for 2162 unique reflections with $I > 2\sigma(I)$] = 0.0543, 2849 collected reflections, 2581 unique reflections used in the refinement, S (on F^2) = 1.052

Spectroscopic data for **24a**: IR (CH_2Cl_2): υ_{CO} 2085s, 2053s, 2037vs, 2016m, 2008m, 1968w, 1869w cm^{-1}; ^1H NMR ($CDCl_3$): δ 7.84 (d,d; 7.9, 1.6 Hz; 1H); 7.52 (d,d; 7.8, 1.8 Hz; 1H); 7.42 (d,d; 7.9, 1.6 Hz; 1H); 7.12 (d,d; 7.9, 1.8 Hz; 1H); 5.94 (d,d; 6.9, 1.8 Hz; 1H); 4.42 (d,d; 5.9, 1.8 Hz; 1H); 4.35 (d,d; 5.9, 1.7 Hz; 1H); *ca.* 3.5 (overlapping signals; 2H); 3.40 (d,d; 6.9, 1.7 Hz; 1H); *ca.* 3.2 (overlapping multiplets; 2H); *ca.* 2.75 (overlapping multiplets; 2H); 2.16 (d,t; 14.8, 9.5 Hz; 1H); 1.69 (d,t; 13.9, 9.2 Hz; 1H) ppm; MS: M^+ = 1263 (calc. 1263) amu.

Spectroscopic data for **25**: IR (CH_2Cl_2): υ_{CO} 2076w, 2039s, 2024vs, 1982w br, 1940w br, 1814w br cm^{-1}; ^1H NMR ($CDCl_3$): δ 7.44 (s, 4H), 3.43 (m, 4H), 3.40 (s, 4H), 2.98 (m, 4H) ppm; MS: M^+ = 1219 (calc. 1219) amu; Analytical data, Found (Calc.): C 30.51 (30.54), H 1.38 (1.31) %.
Crystal data and measurement details for **25**: Formula $C_{31}H_{16}O_{14}Ru_6$, M = 1218.81, T = 150(1) K, triclinic, space group P-1, a = 10.193(3), b = 10.311(3), c = 16.377(5) Å, α = 88.45(2), β = 87.52(2), γ = 72.48(2)°, U = 1638 Å^3, Z = 2, μ(Mo–Kα) = 27.2 cm^{-1}, F(000) = 1156, $2\theta_{max}$ 45°, R [on F, for 3594 unique reflections with $I > 2\sigma(I)$] = 0.044, R' = 0.056, 5607 collected reflections, 4026 unique reflections used in the refinement, S (on F^2) = 1.04.

Spectroscopic data for **26**: IR (CH_2Cl_2): υ_{CO} 2031s, 1995vs, 1944w, 1786w br cm^{-1}; MS: M^+ = 1344 (calc. 1343) amu; Analytical data, Found (Calc.): C 39.44 (39.35), H 2.43 (2.40) %.
Crystal data and measurement details for **26**: Formula $C_{44}H_{32}O_{11}Ru_6$, M = 1343.12, T = 150(1) K, monoclinic, space group P $2_1/a$, a = 19.295(23), b = 10.487(19), c = 20.19(4) Å, β = 93.74(14)°, U = 4076.7 Å^3, Z = 4, μ(Mo–Kα) = 2.05 mm^{-1}, F(000) = 2592, crystal size 0.28 x 0.28 x 0.28 mm, $2\theta_{max}$ 45°, wR_2 (on F^2, all data) = 0.2532, R_1 [on F, $I > 2\sigma(I)$] = 0.0678, 5609 collected reflections, 5152 unique reflections used in the refinement, S (on F^2) = 1.044.

Spectroscopic data for **27**: IR (CH_2Cl_2): υ_{CO} 2088m, 2063s, 2028vs, 2001w sh, 1874w cm^{-1}; ^1H NMR ($CDCl_3$): δ 6.78 (s, 4H), 4.51 (s, 4H), 3.18 (m, 4H), 2.85 (m, 4H), -17.80 (s, 2H), -19.40 (s br, 2H) ppm; MS: M^+ = 1524 (calc. 1525) amu.
Crystal data and measurement details for **27**: Formula $C_{41}H_{28}O_{18}Ru_8$, M = 1617.2, T = 298(1) K, triclinic, space group P-1, a = 11.087(7), b = 14.047(7), c = 16.090(9) Å, α = 80.68(6), β = 72.11(7), γ = 72.91(4)°, U = 2272 Å^3, Z = 2, D_c = 2.36 g cm^{-3}, μ(Mo–Kα) = 26.58 cm^{-1}, F(000) = 1540, $2\theta_{max}$ 54°, wR_2 (on F, all data) = 0.1169, R_1 [on F, for 2266 unique reflections with $I > 2\sigma(I)$] = 0.0455, 10726 collected reflections, 7506 unique reflections used in the refinement, S (on F^2) = 1.42.

Thermolysis of $Ru_3(CO)_9(\mu_3-\eta^2:\eta^2:\eta^2-C_{16}H_{16})$ 23 with $Ru_3(CO)_{12}$ 14 in octane

The compound $Ru_3(CO)_9(\mu_3-\eta^2:\eta^2:\eta^2-C_{16}H_{16})$ **23** (50 mg) was suspended in octane (30 ml) and $Ru_3(CO)_{12}$ **14** (42 mg, 1 mol. equiv.) added. The reaction mixture was heated to reflux for 3 h, during which time the colour of the solution darkened from orange to deep red. Monitoring the reaction by spot t.l.c. indicated that 3 h was an optimum time in which the balance between remaining starting material and decomposition products was achieved. The solvent was removed *in vacuo* and the residue purified by t.l.c. using a solution of dichloromethane-hexane (3:7, v/v) as eluent. Apart from the remaining starting material **23** (12%), two bands; one red and one purple, were isolated and characterised by spectroscopy as $Ru_6C(CO)_{14}(\mu_3-\eta^2:\eta^2:\eta^2-C_{16}H_{16})$ **25** (26%) and $Ru_6C(CO)_{15}(\mu_3-\eta^1:\eta^2:\eta^2-C_{16}H_{16}-\mu_2-O)$ **24** (8%), respectively.

Thermolysis of $Ru_6C(CO)_{15}(\mu_3-\eta^1:\eta^2:\eta^2-C_{16}H_{16}-\mu_2-O)$ 24 in octane

The compound $Ru_6C(CO)_{15}(\mu_3-\eta^1:\eta^2:\eta^2-C_{16}H_{16}-\mu_2-O)$ 24 (10 mg) was heated to reflux in octane (20 ml) for 3 hours. During this time the reaction was monitored by IR spectroscopy which indicated the complete consumption of starting material. The solvent was removed under reduced pressure and the product extracted by t.l.c. using a solution of dichloromethane-hexane (3:7, v/v) as eluent. The major red band was collected and characterised by IR and mass spectroscopy as $Ru_6C(CO)_{14}(\mu_3-\eta^2:\eta^2:\eta^2-C_{16}H_{16})$ 25 (90%).

Solid State Pyrolysis of $Ru_6C(CO)_{15}(\mu_3-\eta^1:\eta^2:\eta^2-C_{16}H_{16}-\mu_2-O)$ 24

The compound $Ru_6C(CO)_{15}(\mu_3-\eta^1:\eta^2:\eta^2-C_{16}H_{16}-\mu_2-O)$ 24 (10 mg) was placed in a bulb attached to the base of an IR gas cell (NaCl windows, 10 cm path length). The cell was evacuated, sealed, and placed in the spectrometer where a background was recorded. The bulb containing the compound was heated to *ca.* 200°C for 2 mins. and a second IR spectrum recorded. The IR spectrum of the gaseous products showed strong absorptions at 2359 and 2342 cm^{-1}, clearly illustrating that CO_2 had evolved, and further heating of the bulb also led to peaks at 2170 and 2120 cm^{-1} which are typical of CO, therefore suggesting cluster decomposition. The remaining solid residue was dissolved in dichloromethane and characterised by IR and mass spectroscopy as $Ru_6C(CO)_{14}(\mu_3-\eta^2:\eta^2:\eta^2-C_{16}H_{16})$ 25.

Thermolysis of $Ru_6C(CO)_{14}(\mu_3-\eta^2:\eta^2:\eta^2-C_{16}H_{16})$ 25 with [2.2]para-cyclophane in octane

The compound $Ru_6C(CO)_{14}(\mu_3-\eta^2:\eta^2:\eta^2-C_{16}H_{16})$ 25 (30 mg) was suspended in octane and excess [2.2]paracyclophane (10 mg) added. The reaction mixture was heated to reflux for a 4 h period, during which the reaction was monitored by IR spectroscopy and spot t.l.c. The solvent was removed *in vacuo* and the products separated by t.l.c., eluting with a solution of dichloromethane-hexane (3:7, v/v). Decomposition was observed together with the isolation of two bands; one red and the other brown. These products were collected and characterised by IR and mass spectroscopy as the starting material, 25 (15%), and $Ru_6C(CO)_{11}(\mu_3-\eta^2:\eta^2:\eta^2-C_{16}H_{16})(\eta^6-C_{16}H_{16})$ 26 (22%).

Reaction of $Ru_6C(CO)_{14}(\mu_3-\eta^2:\eta^2:\eta^2-C_{16}H_{16})$ 25 with Me_3NO

The compound $Ru_6C(CO)_{14}(\mu_3-\eta^2:\eta^2:\eta^2-C_{16}H_{16})$ 25 (20 mg) was dissolved in dichloromethane (20 ml) and cooled to -78°C. To this solution a ten fold excess of Me_3NO (12 mg) in dichloromethane (4 ml) was added dropwise. The reaction mixture was allowed to warm to room temperature (1h), where it was stirred for a further 30 minutes. The solvent was removed *in vacuo*, and the residue subjected to t.l.c., eluting with a dichloromethane-hexane (4:6, v/v) solution. The major yellow product was characterised

spectroscopically as $Ru_3(CO)_9(\mu_3\text{-}\eta^2\text{:}\eta^2\text{:}\eta^2\text{-}C_{16}H_{16})$ **23** (24%). Extensive decomposition was also observed.

Reaction of $Ru_8(\mu\text{-}H)_4(CO)_{18}(\eta^6\text{-}C_{16}H_{16})$ 27 with CO

A steady stream of CO was bubbled through a room temperature solution of $Ru_8(\mu\text{-}H)_4(CO)_{18}(\eta^6\text{-}C_{16}H_{16})$ **27** (30 mg) in dichloromethane (20 ml) for 5 minutes. The CO source was removed, the solvent removed *in vacuo* and the products isolated by t.l.c. eluting with a dichloromethane-hexane (3:7, v/v) solution. Two products were extracted and characterised spectroscopically as $Ru_3(CO)_{12}$ **14** (30%) and $Ru_6C(CO)_{14}(\mu_3\text{-}\eta^2\text{:}\eta^2\text{:}\eta^2\text{-}C_{16}H_{16})$ **25** (62%).

Thermolysis of $Ru_3(CO)_{12}$ 14 with [2.2]paracyclophane in heptane

A suspension of $Ru_3(CO)_{12}$ **14** (250 mg) in heptane (30 ml) containing a large excess of [2.2]paracyclophane (100 mg) was heated to reflux. The reaction was monitored by spot t.l.c., and after a period of 3 h the reaction was stopped and the solvent removed under reduced pressure. The products were separated by t.l.c., using a solution of dichloromethane-hexane (3:7, v/v) as eluent. In order of elution, the products were characterised by spectroscopy as $Ru_3(CO)_9(\mu_3\text{-}\eta^2\text{:}\eta^2\text{:}\eta^2\text{-}C_{16}H_{16})$ **23** (yellow, 32%), $Ru_8(\mu\text{-}H)_2(\mu_6\text{-}\eta^2\text{-}CO)(CO)_{19}(\eta^6\text{-}C_{16}H_{16})$ **28** (purple, 2%), $Ru_8(\mu_6\text{-}\eta^2\text{-}CO)(\mu_4\text{-}\eta^2\text{-}CO)(CO)_{18}(\eta^6\text{-}C_{16}H_{16})$ **29** (purple, ~1%), $Ru_6C(CO)_{14}(\mu_3\text{-}\eta^2\text{:}\eta^2\text{:}\eta^2\text{-}C_{16}H_{16})$ **25** (red, 18%) and $Ru_6C(CO)_{15}(\mu_3\text{-}\eta^1\text{:}\eta^2\text{:}\eta^2\text{-}C_{16}H_{16}\text{-}\mu_2\text{-}O)$ **24** (purple, 12%). Crystals of **28** and **29**, suitable for X-ray diffraction analysis, were grown from toluene solutions at -25°C.

Spectroscopic data for **28**: IR (CH_2Cl_2): υ_{CO} 2101m, 2062s, 2034vs, 1984w, 1957w cm^{-1}; ^1H NMR ($CDCl_3$): δ 6.89 (s, 4H), 4.40 (s, 4H), 3.38 (br s, 8H), -11.67 (s, 1H), -15.37 (s, 1H) ppm; MS: M$^+$ = 1580 (calc. 1579) amu.

Crystal data and measurement details for **28**: Formula $C_{57}H_{42}O_{20}Ru_8$ (including three molecules of toluene solvate), M = 1855.47, T = 150(2) K, monoclinic, space group $P\,2_1/n$, a = 14.088(6), b = 25.134(12), c = 17.834(8) Å, β = 109.54(5)°, U = 5951(5) Å^3, Z = 4, D_c = 2.071 g cm^{-3}, μ(Mo–Kα) = 1.845 mm^{-1}, $F(000)$ = 3584, dark red column, 0.85 x 0.58 x 0.38 mm, $2\theta_{max}$ 45°, wR_2 (on F^2, all data) = 0.1315, R_1 [on F, for 5946 unique reflections with $I > 2\sigma(I)$] = 0.0496, 8622 collected reflections, 7725 unique reflections used in the refinement, S (on F^2) = 1.072.

Spectroscopic data for **29**: IR (CH_2Cl_2): υ_{CO} 2100w, 2089m, 2060s, 2036vs, 2017s, 1983m, 1934w cm^{-1}; MS: M$^+$ = 1576 (calc. 1577) amu.

Crystal data and measurement details for **29**: Formula $C_{46.5}H_{28}O_{20}Ru_8$ (including 1.5 toluene molecules), M = 1715.25, T = 150(2) K, triclinic, space group P-1, a = 13.084(8), b = 13.200(7), c = 15.382(10) Å, α = 74.72(5), β = 89.76(4), γ = 80.37(5)°, U = 2524(3) Å^3, Z = 2, D_c = 2.257 g cm^{-3}, μ(Mo–Kα) = 2.402 mm^{-1}, $F(000)$ = 1638, dark red lath, 0.47 x 0.15 x 0.078 mm, $2\theta_{max}$ 50°, wR_2 (on F^2, all data) = 0.0672, R_1 [on F, for $I > 2\sigma(I)$] = 0.0310, 9804 collected reflections, 8903 unique reflections used in the refinement, S (on F^2) = 1.093.

Thermolysis of $Ru_3(CO)_9(\mu_3\text{-}\eta^2\text{:}\eta^2\text{:}\eta^2\text{-}C_{16}H_{16})$ 23 with [2.2]para-cyclophane in octane

The compound $Ru_3(CO)_9(\mu_3\text{-}\eta^2\text{:}\eta^2\text{:}\eta^2\text{-}C_{16}H_{16})$ **23** (25 mg) was suspended in octane (30 ml) and excess [2.2]paracyclophane (~15 mg) added. The reaction mixture was heated to reflux for 3 h, after which the solvent was removed *in vacuo* and the residue purified by t.l.c. using a solution of dichloromethane-hexane (3:7, v/v) as eluent. Decomposition products were observed together with unreacted starting material **23** (16%), and a small amount of $Ru_6C(CO)_{14}(\mu_3\text{-}\eta^2\text{:}\eta^2\text{:}\eta^2\text{-}C_{16}H_{16})$ **25** (10%), as evidenced by IR spectroscopy.

Reaction of $Ru_3(CO)_9(\mu_3\text{-}\eta^2\text{:}\eta^2\text{:}\eta^2\text{-}C_{16}H_{16})$ 23 with Me_3NO in the presence of [2.2]paracyclophane

The compounds $Ru_3(CO)_9(\mu_3\text{-}\eta^2\text{:}\eta^2\text{:}\eta^2\text{-}C_{16}H_{16})$ **23** (30 mg) and [2.2]paracyclophane (12 mg, 1.5 mol. equiv.) were dissolved in dichloromethane (20 ml), and cooled to -78°C. A solution of Me_3NO (9 mg, 3.2 mol. equiv.) in dichloromethane (10 ml) was added in a dropwise fashion, after which the reaction mixture was allowed to warm to room temperature (1 h) where it was stirred for a further 30 minutes. The solvent was removed *in vacuo*, and the residue subjected to t.l.c., eluting with a dichloromethane-hexane (1:4, v/v) solution. Extensive decomposition was observed with only a small amount of the starting material, $Ru_3(CO)_9(\mu_3\text{-}\eta^2\text{:}\eta^2\text{:}\eta^2\text{-}C_{16}H_{16})$ **23** (8%), remaining.

Attempted Preparation of $Ru_3(CO)_7(\mu_3\text{-}\eta^2\text{:}\eta^2\text{:}\eta^2\text{-}C_{16}H_{16})(MeCN)_2$, and Subsequent Reaction with [2.2]paracyclophane

The compound $Ru_3(CO)_9(\mu_3\text{-}\eta^2\text{:}\eta^2\text{:}\eta^2\text{-}C_{16}H_{16})$ **23** (50 mg) was dissolved in acetonitrile-dichloromethane (40:10 ml, respectively) and cooled to -78°C. A solution of Me_3NO (10 mg, 2.1 mol. equiv.) in acetonitrile (10 ml) was added dropwise to the solution over a 20 minute period, and the reaction mixture was allowed to slowly warm to room temperature, where it was stirred for a further 30 minutes. The solution was filtered through silica gel to remove any excess Me_3NO and the large amount of decomposition products observed, and the solvent was removed *in vacuo*. The yellow-brown solid obtained was not isolated or characterised, but used directly in the subsequent reaction with [2.2]paracyclophane.

This yellow-brown solid (~ 25 mg) was dissolved in dichloromethane (30 ml) and excess [2.2]paracyclophane (12 mg) added. The solution was stirred at room temperature for a period of 3 hours, with the reaction being monitored by spot t.l.c. and IR spectroscopy. The solvent was removed under reduced pressure, and the residue subjected to t.l.c. using dichloromethane-hexane (4:6, v/v) as eluent. A small amount of the starting material, **23** (14%), was recovered from the reaction.

Reaction of $Ru_3(CO)_{12}$ 14 with Me_3NO in the presence of tetrahydro[2.2]paracyclophane

Tetrahydro[2.2]paracyclophane was prepared from the Birch reduction of [2.2]paracyclophane, using the synthetic procedure described in the literature.[12]

The compounds $Ru_3(CO)_{12}$ **14** (50 mg) and tetrahydro[2.2]paracyclophane (17 mg, 0.5 mol. equiv.) were dissolved in dichloromethane (60 ml) and the solution cooled to -78°C. A solution of Me_3NO (18 mg, 3.1 mol. equiv.) in dichloromethane (20 ml) was added dropwise over a 30 minute period, and the reaction mixture was allowed to warm to room temperature where it was stirred for a further hour. The solvent was removed *in vacuo* and the products separated by t.l.c. using a dichloromethane-hexane (3:7, v/v) as eluent. Two yellow bands were obtained which, in order of elution, were characterised spectroscopically as the starting material, $Ru_3(CO)_{12}$ **14** (26%), and $Ru_3(CO)_9(\mu_3$-η^2:η^2:η^2-$C_{16}H_{16})$ **23** (38%).

Preparation of $Ru_3(CO)_{10}(MeCN)_2$ and reaction with $Ru_3(CO)_9(\mu_3$-η^2:η^2:η^2-$C_{16}H_{16})$ - Attempted Preparation of $[Ru_3(CO)_9]_2(C_{16}H_{16})$

The compound $Ru_3(CO)_{10}(MeCN)_2$ was prepared according to the literature procedure.[13] Once complete, the solution was filtered through silica gel to remove any excess Me_3NO and decomposition material, and the solvent was removed under reduced pressure. The orange solid obtained was characterised by IR spectroscopy (90%), and it was used *in situ* in subsequent reactions without further purification, due to its sensitivity.

Spectroscopic data for $Ru_3(CO)_{10}(MeCN)_2$: IR (MeCN): υ_{co} 2086w, 2017s, 1998vs, 1951m br cm^{-1}; (THF): υ_{co} 2086w, 2055sh, 2018vs, 1999s, 1987sh, 1954m cm^{-1}.

A solution of $Ru_3(CO)_{10}(MeCN)_2$ (90 mg) and $Ru_3(CO)_9(\mu_3$-η^2:η^2:η^2-$C_{16}H_{16})$ **23** (105 mg, 1 mol. equiv.) in solvent (70 ml) (solvent = dichloromethane, hexane and octane) was heated to reflux for a period of 3 h. The reactions were monitored by spot t.l.c. and IR spectroscopy and, in each case, both indicated that extensive decomposition had occurred. The solvent was removed *in vacuo*, and the residue purified by t.l.c. using a dichloromethane-hexane (3:7, v/v) solution as eluent. When dichloromethane and hexane were used as solvent, the only product observed was a small amount of starting material **23** (10%). However, when octane was used as solvent, two bands were isolated and characterised, in order of elution, as the starting material **23** (5%) and $Ru_6C(CO)_{14}(\mu_3$-η^2:η^2:η^2-$C_{16}H_{16})$ **25** (8%).

6.5   Experimental Details for Chapter Five

The clusters $Ru_4(CO)_{12}(\mu_4-\eta^1:\eta^1:\eta^2:\eta^2-C_6H_8)$ **15**, $Ru_3(CO)_9(\mu_3-\eta^2:\eta^2:\eta^2-C_{16}H_{16})$ **23** and $Ru_6C(CO)_{14}(\mu_3-\eta^2:\eta^2:\eta^2-C_{16}H_{16})$ **25** were prepared according to the methods outlined in sections 6.3 and 6.4.

Reaction of $Ru_3(CO)_9(\mu_3-\eta^2:\eta^2:\eta^2-C_{16}H_{16})$ 23 with Me_3NO

To a solution of $Ru_3(CO)_9(\mu_3-\eta^2:\eta^2:\eta^2-C_{16}H_{16})$ **23** (50 mg) in dichloromethane (20 ml) at -78°C, a three fold excess of Me_3NO (16 mg) in dichloromethane was added dropwise over a 15 minute period. The reaction mixture was allowed to warm to room temperature where it was stirred for a further 30 minutes. The solvent was removed under reduced pressure and extraction of the products by t.l.c., using a solution of dichloromethane-hexane (2:3, v/v) as eluent, revealed two yellow bands which were characterised spectroscopically, in order of elution, as the new cluster complex $Ru_2(CO)_6(\mu_2-\eta^3:\eta^3-C_{16}H_{16})$ **30** (yellow, 16%) and starting material **23** (22%). Crystals of **30**, suitable for a single crystal X-ray diffraction analysis, were grown by vapour diffusion from dichloromethane-pentane at room temperature.

Spectroscopic data for **30**: IR (CH_2Cl_2): υ_{co} 2060s, 2022vs, 1993s, 1950w sh cm^{-1}; ^1H NMR $(CDCl_3)$: δ 7.06 (s, 4H), 3.59 (s, 4H), 2.93 (m, 4H) and 2.56 (m, 4H) ppm; MS: M^+ = 579 (calc. 579) amu.
Crystal data and measurement details for **30**: Formula $C_{22}H_{16}O_6Ru_2$, M = 578.5, T = 150(1) K, monoclinic, space group $P 2_1/n$, a = 9.183(10), b = 21.912(10), c = 10.366(10) Å, β = 106.84(4)°, U = 1996(3) $Å^3$, Z = 4, D_c = 1.925 g cm^{-3}, μ(Mo–Kα) = 1.550 mm^{-1}, F(000) = 1136, yellow column, 0.30 x 0.15 x 0.10 mm, $2\theta_{max}$ 45°, wR_2 (on F^2, all data) = 0.1301, R_1 [on F, for $I > 2\sigma(I)$] = 0.0363, 2605 collected reflections, 2563 unique reflections used in the refinement, S (on F^2) = 1.063.

Thermolysis of $Ru_3(CO)_9(\mu_3-\eta^2:\eta^2:\eta^2-C_{16}H_{16})$ 23 with diphenylacetylene in dichloromethane

The compound $Ru_3(CO)_9(\mu_3-\eta^2:\eta^2:\eta^2-C_{16}H_{16})$ **23** (50 mg) was dissolved in dichloromethane (30 ml) and an excess of diphenylacetylene (~25 mg) added. The reaction mixture was heated to reflux for 18 h, after which time the solvent was removed *in vacuo*, and the products separated by t.l.c., eluting with a solution of dichloromethane-hexane (3:7, v/v). Four bands were extracted from the t.l.c. plate which, in order of elution, were characterised spectroscopically as starting material **23** (yellow, 20%), $Ru_3(CO)_7(\mu_3-\eta^1:\eta^1:\eta^2-C_2Ph_2)(\eta^6-C_{16}H_{16})$ **31** (orange, 16%), $Ru_3(CO)_7(\mu_3-\eta^2-PhC_2PhCO)(\eta^6-C_{16}H_{16})$ **32** (orange, 2%) and $Ru_2(CO)_6(\{\mu_2-\eta^1:\eta^2-C_2Ph_2\}_2-CO)$ **33** (yellow, 12%). Increasing the reaction time does not improve the total yields of compounds **31, 32** and **33**, instead there is an increase in the amount of decomposition material produced. Crystals of **31** and **33** suitable for a single crystal X-ray diffraction study were grown from toluene

at -25°C over a period of several days, and from dichloromethane-pentane by vapour diffusion at room temperature, respectively.

Spectroscopic data for **31**: IR (CH$_2$Cl$_2$): υ_{CO} 2056s, 2020vs, 1982s, 1958w sh, 1923w cm^{-1}; ^{1}H NMR (CDCl$_3$): δ 6.92 (m, 10H), 6.72 (s, 4H), 5.29 (m, 2H), 4.60 (m, 2H), 3.12 (m, 4H), 2.72 (m, 2H), 2.55 (m, 2H) ppm; MS: M$^+$ = 885 (calc. 886) amu; Analytical data, Found (Calc.): C 50.23 (50.17), H 3.04 (2.96) %.

Crystal data and measurement details for **31**: Formula C$_{38.75}$Cl$_{3.50}$H$_{26}$O$_7$Ru$_3$ (including disordered dichloromethane solvate), M = 1030.88, T = 150(1) K, monoclinic, space group $P\,2_1/c$, a = 15.408(4), b = 10.127(3), c = 25.289(9) Å, β = 105.65(2)°, U = 3800(2) Å^3, Z = 4, D_c = 1.802 g cm^{-3}, μ(Mo–Kα) = 1.472 mm^{-1}, $F(000)$ = 2024, dark red column, 0.48 x 0.10 x 0.10 mm, 2θ$_{max}$ 45°, wR_2 (on F^2, all data) = 0.1631, R_1 [on F, for I > 2σ(I)] = 0.0443, 5649 collected reflections, 4898 unique reflections used in the refinement, S (on F^2) = 1.066.

Spectroscopic data for **32**: IR (CH$_2$Cl$_2$): υ_{CO} 2065s, 2032vs, 1993s cm^{-1}.

Spectroscopic data for **33**: IR (CH$_2$Cl$_2$): υ_{CO} 2090m, 2069vs, 2028s, 1672m cm^{-1}; ^{1}H NMR (CDCl$_3$): δ 7.26 (m, 10H), 7.14 (m, 10H) ppm; MS: M$^+$ = 756 (calc. 755) amu; Analytical data, Found (Calc.): C 55.75 (55.70), H 2.70 (2.67) %.

Crystal data and measurement details for **33**: Formula C$_{35}$H$_{20}$O$_7$Ru$_2$, M = 754.65, T = 150(1) K, monoclinic, space group $P\,2_1/n$, a = 11.96(1), b = 10.58(1), c = 24.05(2) Å, β = 104.21(8)°, U = 2950(5) Å^3, Z = 4, D_c = 1.699 g cm^{-3}, μ(Mo–Kα) = 1.074 mm^{-1}, $F(000)$ = 1496, yellow lath, 0.18 x 0.27 x 0.35 mm, 2θ$_{max}$ 45°, wR_2 (on F^2, all data) = 0.2716, R_1 [on F, for I > 2σ(I)] = 0.1028, 3658 collected reflections, 3497 unique reflections used in the refinement, S (on F^2) = 1.110.

Reaction of Ru$_3$(CO)$_9$(μ$_3$-η^2:η^2:η^2-C$_{16}$H$_{16}$) 23 with diphenylacetylene and Me$_3$NO

Diphenylacetylene (~15 mg) and the compound Ru$_3$(CO)$_9$(μ$_3$-η^2:η^2:η^2-C$_{16}$H$_{16}$) **23** (30 mg) were dissolved in dichloromethane (30 ml) and the solution cooled to -78°C. A solution of Me$_3$NO (7 mg, 2.2 mol. equiv.) in dichloromethane (10 ml) was added dropwise over a 15 minute period. The reaction mixture was allowed to warm to room temperature over a period of 1 h, and then stirred for a further hour. The solvent was removed under reduced pressure and the products extracted by t.l.c., using a dichloromethane-hexane (3:7, v/v) solution as eluent. The major product was characterised spectroscopically as Ru$_3$(CO)$_7$(μ$_3$-η^1:η^2:η^1-C$_2$Ph$_2$)(η^6-C$_{16}$H$_{16}$) **31** (orange, 28%).

Thermolysis of Ru$_3$(CO)$_9$(μ$_3$-η^2:η^2:η^2-C$_{16}$H$_{16}$) 23 in tetrahydrofuran with triphenylphosphine

The compound Ru$_3$(CO)$_9$(μ$_3$-η^2:η^2:η^2-C$_{16}$H$_{16}$) **23** (30 mg) was dissolved in tetrahydrofuran (30 ml) and an excess of triphenylphosphine (~20 mg) was added. The reaction mixture was heated to reflux for 3 h, after which time the solvent was removed under reduced pressure and the products separated by t.l.c., eluting with a solution of dichloromethane-hexane (4:6, v/v). The major band was extracted and characterised

spectroscopically as $Ru_3(CO)_8(PPh_3)(\mu_3-\eta^2:\eta^2:\eta^2-C_{16}H_{16})$ **34** (red, 18%). Crystals of **34** suitable for a single crystal X-ray analysis were grown at room temperature from the slow evaporation of a dichloromethane-hexane solution.

Spectroscopic data for **34**: IR (CH_2Cl_2): υ_{CO} 2049s, 2012s, 1986vs, 1975s sh cm^{-1}; ^1H NMR $(CDCl_3)$: δ 7.40 (m, 15H), 7.32 (s, 4H), 3.12 (m, 4H), 2.95 (m, 4H), 2.41 (m, 4H) ppm; ^{31}P NMR $(CDCl_3)$: δ 38.01 (s) ppm; MS: M^+ = 735 (calc. 997) amu. Analytical data, Found (Calc.): C 52.95 (52.17), H 3.34 (3.23) %.

Crystal data and measurement details for **34**: Formula $C_{42}H_{31}O_8PRu_3$, M = 997.85, T = 150(1) K, monoclinic, space group $P\,2_1/n$, a = 14.421(12), b = 16.265(10), c = 16.273(15) Å, β = 100.66(12)°, U = 3751(5) Å^3, Z = 4, D_c = 1.767 g cm^{-3}, $\mu(Mo-K\alpha)$ = 1.289 mm^{-1}, $F(000)$ = 1976, red block, 0.50 x 0.38 x 0.38 mm, $2\theta_{max}$ 50°, wR_2 (on F^2, all data) = 0.0730, R_1 [on F, for $I > 2\sigma(I)$] = 0.0269, 7698 collected reflections, 6578 unique reflections used in the refinement, S (on F^2) = 1.146.

Reaction of $Ru_3(CO)_9(\mu_3-\eta^2:\eta^2:\eta^2-C_{16}H_{16})$ 23 with triphenylphosphine and Me_3NO

The compounds $Ru_3(CO)_9(\mu_3-\eta^2:\eta^2:\eta^2-C_{16}H_{16})$ **23** (50 mg) and triphenylphosphine (35 mg) were dissolved in dichloromethane (30 ml) and cooled to -78°C. To this solution a 1.1 molar equivalent of Me_3NO (5 mg) in dichloromethane (10 ml) was added dropwise. The solution was then allowed to warm to room temperature over a 1 h period, which was accompanied by a colour change from yellow to brown. The solvent was removed under vacuum and the brown residue subjected to t.l.c. using a solution of dichloromethane-hexane (3:7, v/v) as eluent. A single product was isolated and characterised as $Ru_3(CO)_8(PPh_3)(\mu_3-\eta^2:\eta^2:\eta^2-C_{16}H_{16})$ **34** (red, 64%) by spectroscopy.

Thermolysis of $Ru_6C(CO)_{14}(\mu_3-\eta^2:\eta^2:\eta^2-C_{16}H_{16})$ 25 in tetrahydrofuran with triphenylphosphine

The compound $Ru_6C(CO)_{14}(\mu_3-\eta^2:\eta^2:\eta^2-C_{16}H_{16})$ **25** (50 mg) was dissolved in tetrahydrofuran (30 ml) and an excess of triphenylphosphine (20 mg) added. The reaction mixture was heated to reflux for 1 h, after which time the solvent was removed under reduced pressure and the products separated by t.l.c., eluting with a solution of dichloromethane-hexane (3:7, v/v). The major product was extracted and characterised spectroscopically as $Ru_6C(CO)_{13}(PPh_3)(\mu_3-\eta^2:\eta^2:\eta^2-C_{16}H_{16})$ **35** (red, 18%). Crystals of **35**, suitable for a single crystal X-ray analysis, were nucleated from dichloromethane-pentane at room temperature by vapour diffusion.

Spectroscopic data for **35**: IR (CH_2Cl_2): υ_{CO} 2050m, 2014vs, 1998s sh, 1967w, 1955w, 1802m br cm^{-1}; ^1H NMR $(CDCl_3)$: δ 7.5 (m, 15H), 7.43 (s, 4H), 3.4 (m, 4H), 3.38 (s,4H), 3.0 (m, 4H) ppm; ^{31}P NMR $(CDCl_3)$: δ 43.5 (s) ppm; MS: M^+ = 1452 (calc. 1453) amu.

Crystal data and measurement details for **35**: Formula $C_{48}H_{31}O_{13}PRu_6$, M = 1453.12, T = 277(2) K, triclinic, space group $P-1$, a = 11.740(5), b = 12.928(5), c = 18.369(7) Å, α = 78.26(2), β = 74.38(3), γ = 84.48(3)°, U = 2626(2) Å^3, Z = 2, D_c = 1.838 g cm^{-3}, $\mu(Mo-K\alpha)$ = 1.770 mm^{-1}, $F(000)$ = 1404, deep

red tablet, 0.54 x 0.35 x 0.19 mm, $2\theta_{max}$ 45°, wR_2 (on F^2, all data) = 0.1603, R_1 [on F, for $I > 2\sigma(I)$] = 0.0430, 6838 collected reflections, 6836 unique reflections used in the refinement, S (on F^2) = 1.090.

Reaction of $Ru_6C(CO)_{14}(\mu_3\text{-}\eta^2\text{:}\eta^2\text{:}\eta^2\text{-}C_{16}H_{16})$ 25 with PX_3 (X= Ph and Cy) and Me_3NO

The compounds $Ru_6C(CO)_{14}(\mu_3\text{-}\eta^2\text{:}\eta^2\text{:}\eta^2\text{-}C_{16}H_{16})$ **25** (50 mg) and triphenylphosphine (20 mg) were dissolved in dichloromethane (40 ml) and the solution cooled to -78°C. Me_3NO (4 mg, 1.2 mol. equiv.) in dichloromethane (10 ml) was added dropwise to this solution over a 15 minute period. The solution was allowed to warm to room temperature, where it was stirred for a further hour. The solvent was removed under reduced pressure and the product extracted from the brown residue by t.l.c. using a solution of dichloromethane-hexane (1:3, v/v) as eluent. The major product was extracted and characterised as $Ru_6C(CO)_{13}(PPh_3)(\mu_3\text{-}\eta^2\text{:}\eta^2\text{:}\eta^2\text{-}C_{16}H_{16})$ **35** (47%) by spectroscopic techniques. The tricyclohexylphosphine analogue, $Ru_6C(CO)_{13}(PCy_3)(\mu_3\text{-}\eta^2\text{:}\eta^2\text{:}\eta^2\text{-}C_{16}H_{16})$ **36**, was prepared and isolated (red, 43%) in an analogous manner.

Spectroscopic data for **36**: IR (CH_2Cl_2): υ_{CO} 2046m, 2010vs, 1994s sh, 1959w, 1944w, 1802 m br cm^{-1}; ^1H NMR ($CDCl_3$): δ 7.36 (s, 4H), 3.33 (m, 4H), 3.22 (s, 4H), 2.93 (m, 4H), 1.80 - 1.31 (m, 33H) ppm; ^{31}P NMR ($CDCl_3$): δ 55.5 (s) ppm; MS: M^+ = 1470 (calc. 1471) amu.

Reaction of $Ru_3(CO)_9(\mu_3\text{-}\eta^2\text{:}\eta^2\text{:}\eta^2\text{-}C_{16}H_{16})$ 23 with cyclohexa-1,3-diene and Me_3NO

Me_3NO (11 mg, 2.2 mol. equiv.) in dichloromethane (20 ml) was added dropwise to a solution of $Ru_3(CO)_9(\mu_3\text{-}\eta^2\text{:}\eta^2\text{:}\eta^2\text{-}C_{16}H_{16})$ **23** (50 mg) in dichloromethane (40 ml) containing excess cyclohexa-1,3-diene (2 ml) at -78°C. The solution was allowed to warm to room temperature (1 h) where it was stirred for a further 3 h during which the colour of the solution darkened. The solvent was removed *in vacuo* and the residue chromatographed by t.l.c. using a dichloromethane-hexane (3:7, v/v) solution as eluent. Two main products were observed which, in order of elution, were characterised by spectroscopy as starting material **23** (yellow, 25%), and $Ru_4(CO)_9(\eta^4\text{-}C_6H_8)(\mu_3\text{-}C_{16}H_{16})$ **37** (orange, 10%). Crystals of **37** suitable for a single crystal X-ray diffraction study were grown from a solution of dichloromethane layered with octane after standing for several days at room temperature.

Spectroscopic data for **37**: IR (CH_2Cl_2): υ_{CO} 2038m, 2014vs, 2005vs, 1973m, 1952m, 1852m, 1795m cm^{-1}; ^1H NMR ($CDCl_3$): δ 7.48 (s, 4H), 5.75 (m, 2H), 4.54 (m, 2H), 3.32 (m, 4H), 3.26 (s, 4H), 2.47 (m, 4H), 2.12 (m, 2H), 1.88 (m, 2H) ppm; MS: M^+ = 945 (calc. 946) amu.
Crystal data and measurement details for **37**: Formula $C_{31}H_{24}O_9Ru_4$, M = 944.78, T = 150(1) K, monoclinic, space group $P 2_1/n$, a = 9.224(6), b = 9.775(4), c = 16.638(11) Å, β = 98.59(7)°, U = 1483(2) $Å^3$, Z = 2, D_c = 2.115 g cm^{-3}, μ(Mo-Kα) = 2.053 mm^{-1}, $F(000)$ = 916, deep red lath, 0.08 x 0.12 x 0.31 mm, $2\theta_{max}$ 45°, wR_2 (on F^2, all data) = 0.0533, R_1 [on F, for 1923 unique reflections with $I >$

$2\sigma(I)] = 0.0235$, 4893 collected reflections, 2065 unique reflections used in the refinement, S (on F^2) = 1.041.

Reaction of $Ru_6C(CO)_{14}(\mu_3\text{-}\eta^2\text{:}\eta^2\text{:}\eta^2\text{-}C_{16}H_{16})$ 25 with cyclohexa-1,3-diene and Me_3NO

The compound $Ru_6C(CO)_{14}(\mu_3\text{-}\eta^2\text{:}\eta^2\text{:}\eta^2\text{-}C_{16}H_{16})$ **25** (50 mg) was dissolved in dichloromethane (40 ml) containing an excess of cyclohexa-1,3-diene (2 ml) and cooled to -78°C. A solution of Me_3NO (6 mg, 2.1 mol. equiv.) in dichloromethane (10 ml) was added dropwise, and the reaction mixture allowed to slowly warm to room temperature. After a 30 minute period, IR spectroscopy indicated that the reaction had reached completion. The solvent was removed *in vacuo* and the products isolated by t.l.c. using a dichloromethane-hexane (2:3, v/v) solution as eluent. The major band was extracted and characterised spectroscopically as $Ru_6C(CO)_{12}(\mu_2\text{-}\eta^2\text{:}\eta^2\text{-}C_6H_8)(\mu_3\text{-}\eta^2\text{:}\eta^2\text{:}\eta^2\text{-}C_{16}H_{16})$ **38** (orange, 28%). Crystals of **38**, suitable for a single crystal X-ray analysis, were grown from a dichloromethane-hexane solution at -25°C.

Spectroscopic data for **38**: IR (CH_2Cl_2): υ_{CO} 2015vs, 2005s sh, 1893w br, 1786w br cm^{-1}; MS: M$^+$ = 1242 (calc. 1243) amu. Analytical data, Found (Calc.): C 33.02 (33.82), H 2.07 (1.95) %.
Crystal data and measurement details for **38**: Formula $C_{35}H_{24}O_{12}Ru_6$, $M = 1242.96$, T = 293(1) K, monoclinic, space group $P2_1/a$, $a = 19.819(10)$, $b = 9.887(5)$, $c = 20.864(10)$ Å, $\beta = 111.78(4)°$, $U = 3796.5$ Å^3, $Z = 4$, μ(Mo–Kα) = 2.20 mm^{-1}, $F(000) = 2376$, crystal size 0.41 x 0.03 x 0.25 mm, $2\theta_{max}$ 45°, wR_2 (on F^2, all data) = 0.2048, R_1 [on F, for $I > 2\sigma(I)$] = 0.0623, 5032 collected reflections, 4890 unique reflections used in the refinement, S (on F^2) = 1.049.

Thermolysis of $Ru_4(CO)_{12}(\mu_4\text{-}\eta^1\text{:}\eta^1\text{:}\eta^2\text{:}\eta^2\text{-}C_6H_8)$ 15 with [2.2]paracyclophane in octane

The compound $Ru_4(CO)_{12}(\mu_4\text{-}\eta^1\text{:}\eta^1\text{:}\eta^2\text{:}\eta^2\text{-}C_6H_8)$ **15** (30 mg) in octane (30 ml) containing an excess of [2.2]paracyclophane (15 mg) was heated to reflux for 4 h. Monitoring the reaction by spot t.l.c. indicated that this was an optimum time in which the balance between remaining starting material and decomposition products was achieved. The solvent was removed *in vacuo*, and the residue purified by t.l.c., eluting with a dichloromethane-hexane (2:3, v/v) solution. Together with unreacted starting material, **15** (red, 18%), two products were obtained and characterised by spectroscopy as $Ru_4(CO)_9(\mu_4\text{-}\eta^1\text{:}\eta^1\text{:}\eta^2\text{:}\eta^2\text{-}C_6H_8)(\eta^6\text{-}C_{16}H_{16})$ **39** (red, 14%) and $Ru_4(CO)_9(\mu_4\text{-}\eta^1\text{:}\eta^1\text{:}\eta^2\text{:}\eta^2\text{-}C_6H_8)(\mu_3\text{-}\eta^2\text{:}\eta^2\text{:}\eta^2\text{-}C_{16}H_{16})$ **40** (brown, 18%), respectively. A large amount of decomposition was also experienced. Crystals of **39**, suitable for an X-ray diffraction analysis, were grown from a solution of dichloromethane-octane by slow evaporation, whilst crystals of **40** were obtained by vapour diffusion from dichloromethane-pentane at room temperature.

Spectroscopic data for **39**: IR (CH$_2$Cl$_2$): υ_{CO} 2069w, 2055m, 2030vs, 2004s, 1977s, 1960sh cm^{-1}; ^{1}H NMR (CDCl$_3$): δ 6.80 (s, 4H), 4.34 (s, 4H), 3.29 (m, 2H), 3.2 (m, 8H), 2.88 (m, 2H), 1.7 (m, 4H) ppm; MS: M$^+$ = 946 (calc. 946) amu.

Crystal data and measurement details for **39**: Formula C$_{31}$H$_{24}$O$_9$Ru$_4$, M = 944.78, T = 298(1) K, monoclinic, space group $P2_1/a$, a = 10.419(2), b = 18.787(3), c = 15.589(3) Å, β = 94.92(3)°, U = 3043.9(9) Å^3, Z = 4, D_c = 2.064 g cm^{-3}, μ(Mo–Kα) = 2.003 mm^{-1}, F(000) = 1832, red tablet, 0.06 x 0.16 x 0.16 mm, 2θ_{max} 40°, wR_2 (on F^2, all data) = 0.0959, R_1 [on F, for 1940 unique reflections with I > 2σ(I)] = 0.0487, 3614 collected reflections, 2806 unique reflections used in the refinement, S (on F^2) = 1.102.

Spectroscopic data for **40**: IR (CH$_2$Cl$_2$): υ_{CO} 2071m, 2030m, 2002vs, 1978m sh, 1937w cm^{-1}; ^{1}H NMR (CDCl$_3$): δ 7.21 (s, 4H), 3.77 (m, 4H), 3.17 (m, 4H), 3.16 (s, 4H), 2.56 (m, 4H), 1.90 (m, 4H) ppm; MS: M$^+$ = 946 (calc. 946) amu.

Crystal data and measurement details for **40**: Formula C$_{31}$ClH$_{24}$O$_9$Ru$_4$, M = 980.23, T = 298(1) K, monoclinic, space group $P2_1/c$, a = 10.984(2), b = 75.71(3), c = 15.295(3) Å, β = 91.73(2)°, U = 12714(6) Å^3, Z = 16, D_c = 2.048 g cm^{-3}, μ(Mo–Kα) = 2.001 mm^{-1}, F(000) = 7600, dark red lath, 0.54 x 0.31 x 0.12 mm, 2θ_{max} 45°, wR_2 (on F^2, all data) = 0.5159, R_1 [on F, for I > 2σ(I)] = 0.1218, 15678 collected reflections, 15158 unique reflections used in the refinement, S (on F^2) = 1.099.

Thermolysis of Ru$_4$(CO)$_{12}$(μ_4-η^1:η^1:η^2:η^2-C$_6$H$_8$) 15 with [2.2]paracyclophane and Me$_3$NO in octane

The compound Ru$_4$(CO)$_{12}$(μ_4-η^1:η^1:η^2:η^2-C$_6$H$_8$) **15** (50 mg) was suspended in octane (30 ml), and excess [2.2]paracyclophane (25 mg) and Me$_3$NO (15 mg, 3.2 mol. equiv.) were added. The reaction mixture was heated to reflux for 4 h, by which stage IR spectroscopy indicated the complete consumption of starting material. The solvent was removed under reduced pressure and the products separated by t.l.c. using a dichloromethane-hexane (2:3, v/v) solution as eluent. Two major bands were isolated and characterised by spectroscopy as Ru$_4$(CO)$_9$(μ_4-η^1:η^1:η^2:η^2-C$_6$H$_8$)(η^6-C$_{16}$H$_{16}$) **39** (red, 20%) and Ru$_4$(CO)$_9$(μ_4-η^1:η^1:η^2:η^2-C$_6$H$_8$)(μ_3-η^2:η^2:η^2-C$_{16}$H$_{16}$) **40** (brown, 28%), respectively.

Conversion of Ru$_4$(CO)$_9$(μ_4-η^1:η^1:η^2:η^2-C$_6$H$_8$)(η^6-C$_{16}$H$_{16}$) 39 to Ru$_4$(CO)$_9$(μ_4-η^1:η^1:η^2:η^2-C$_6$H$_8$)(μ_3-η^2:η^2:η^2-C$_{16}$H$_{16}$) 40

A solution of Ru$_4$(CO)$_9$(μ_4-η^1:η^1:η^2:η^2-C$_6$H$_8$)(η^6-C$_{16}$H$_{16}$) **39** (10 mg) in dichloromethane (20 ml) was heated to reflux for 2 hours. IR spectroscopy and spot t.l.c. indicated that complete conversion to Ru$_4$(CO)$_9$(μ_4-η^1:η^1:η^2:η^2-C$_6$H$_8$)(μ_3-η^2:η^2:η^2-C$_{16}$H$_{16}$) **40** had taken place.

6.6 References

1. Eady, C.R.; Jackson, P.F.; Johnson, B.F.G.; Lewis, J.; Malatesta, M.C.; McPartlin, M.; Nelson, W.J.H.; *J. Chem. Soc., Dalton Trans.*, **1980**, 383.

2. Zuccaro, C.; Pamploni, G.; Calderazzo, F.; *Inorg. Syn.*, *26*, 293.

3. Cosier, J.; Glazer, A.M.; *J. Appl. Crystallogr.*, **1986**, *19*, 105.

4. Sheldrick, G.M.; SHELXS 86, Program for crystal structure solution, *Acta Crystallogr., Sect. A*, **1990**, *46*, 467.

5. Sheldrick, G.M.; SHELX 76, Program for crystal structure refinement, University of Cambridge, U.K., **1976**.

6. Sheldrick, G.M.; SHELXL 93, Program for crystal structure refinement, University of Göttingen, Germany, **1993**.

7. Gould, R.O.; Taylor, P.; CALC, Program for molecular geometry calculations, University of Edinburgh, U.K., **1985**.

8. Sheldrick, G.M.; SHELXTL PC, University of Göttingen and Siemens Analytical X-Ray Instruments, Madison, **1990**.

9. Keller, E.; SCHAKAL 93, Graphical representation of molecular models, University of Freiburg, Germany, **1993**.

10. Orpen, A.G.; XHYDEX, A Program for Locating Hydrides, Bristol University, **1980**; see also Orpen, A.G.; *J. Chem. Soc., Dalton Trans.*, **1980**, 2509.

11. Chen, H.; Johnson, B.F.G.; Lewis, J.; Braga, D.; Grepioni, F.; Parisini, E.; *J. Chem. Soc., Dalton Trans.*, **1991**, 215.

12. Marshall, J.L.; Song, B-H.; *J. Org. Chem.*, **1974**, *39*, 1342.

13. Foulds, G.A.; Johnson, B.F.G.; Lewis, J.; *J. Organomet. Chem.*, **1985**, *296*, 147.